

Draft
Final Report (Vol. I)

**Soil Treatability Pilot Studies To Design And Model
Soil Aquifer Treatment Systems**

to
**American Water Works Association Research Foundation
Water Environmental Research Foundation
National Water Research Institute
Salt River Project
City of Tucson
U. S. Dept. of Agriculture Water Conservation Research Laboratory
City of Phoenix
City of Scottsdale
City of Glendale
City of Mesa
City of Youngstown
City of Tempe**

by
**Arizona State University
University of Arizona
University of Colorado**

*H. BOWLER
US WATER CONSER.
LABORATORY -*

*CO 699 585-94
AWWARF*

Feb. 1, 1996

CONTENTS

LIST OF TABLES.....	9
LIST OF FIGURES	16
EXECUTIVE SUMMARY.....	34
CHAPTER 1. INTRODUCTION.....	1-1
Background.	1-1
Soil Aquifer Treatment Versus Conventional Technologies for Waster Reclamation.	1-8
Research Objectives.	1-10
Research Plan.....	1-11
Fundamentals of SAT Systems	1-14
References	1-20
CHAPTER 2. EXPERIMENTAL METHODS AND PROCEDURES	2-1
Column Design and Operation.....	2-1
ASU-91st Avenue 3 Meter Columns.....	2-1
UA-1 meter, 2 meter and Schmutzdecke Columns	2-6
Wet/Dry Cycles, Ponding Depths and Infiltration Rates	2-6
Soils.....	2-10
Soil Types and Characteristics	2-10
Effluent Types and Characteristics.....	2-11
Arizona State University.....	2-11
University of Arizona	2-11
University of Colorado	2-12
Summary.....	2-13
Procedures	2-14
BDOC (Bench Scale Bioreactors).....	2-14
Ozonation	2-16
Chlorination/Chloramination.....	2-17
Azide Inactivation	2-18

DOC Fractionation (UF and XAD-8).....	2-18
Analytical Methods	2-19
Quality Control and Quality Assurance.....	2-23
Replication.....	2-23
Interlab Comparison	2-25
 CHAPTER 3. HYDRAULICS.....	 3-1
Introduction and Background.....	3-1
Results of Laboratory Column Tests.....	3-2
Description of Soil Types	3-2
Water and Air Permeability Tests.....	3-3
Arizona State University Laboratory “Clean Water” Column Studies.....	3-4
Arizona State University Large Column Studies	3-38
University of Arizona Laboratory Column Studies	3-52
Results of Field Tests	3-61
Greeley and Hansen Field Percolation Basins	3-61
Small Scale Field Percolation Tests.....	3-71
Numerical Simulation of Field Infiltration	3-81
Summary and Discussion of Soil Hydrological Properties from Field and Column Studies	3-100
Infiltration Rate and Hydraulic Conductivity	3-100
Hydraulic Parameters	3-101
Clogging Layer Studies	3-102
Clogging Layer Model.....	3-102
Hydraulic Conductivity and Consolidation Tests	3-106
Relationship Between Column and Prototype Hydraulics.....	3-121
References	3-123
Appendix	3-126
 CHAPTER 4. THE FATE OF RESIDUAL WASTEWATER ORGANICS DURING SOIL AQUIFER TREATMENT	 4-1
Overview-Introduction to the Experimental Design	4-1

Hypotheses.....	4-1
Column Studies: Independent Variables.....	4-2
Dependent Variables.....	4-2
Summary of Experimental Methods and Objectives	4-4
Reactor Design and Operation.....	4-4
Summary of Research Objectives with Respect to Organics Removals	4-9
Results and Discussion	4-10
Column Maturation	4-10
Effect of Soil Type	4-22
Effects of Differences in Above-ground Treatment Process on Post-SAT	
Effluent Quality	4-38
Depthwise Measurements of Organic Parameters During SAT Simulations	4-52
Comparison of Intact and Repacked Soil Column Performance.....	4-56
Biochemical and Abiotic Contributions to Overall SAT Performance	4-59
Nature of Organic Compounds that Survive SAT Simulation.....	4-63
Discussion.....	4-70
 CHAPTER 5. NITROGEN TRANSFORMATIONS.....	 5-1
Introduction	5-1
Nitrogen Removal in Previous SAT System.....	5-2
Removal/Transformation Mechanisms of Nitrogen.....	5-6
Research Methodology.....	5-9
Column Design and Operation.....	5-9
Wet/Dry Cycles, Ponding Depths and Infiltration rates.....	5-14
Soil Type and Characteristics.....	5-18
Effluent Type and Characteristics	5-19
Overview of ASU and U of A SAT Results	5-21
ASU 91st Avenue Columns	5-21
U of A Column Study.....	5-29
Results and Discussion	5-33

Comparison of Effluent Types	5-33
Comparison of Soil Types	5-35
Comparison of Wet/Dry Schedules	5-35
Mass Balance Summary.....	5-41
Adsorption and Breakthrough of Ammonia.....	5-50
Oxygen Depletion and Reaeration.....	5-62
Evidence of Denitrification	5-62
Effects of Ozonation on Effluent.....	5-66
Biotic Tests for Nitrification and Denitrification.....	5-66
References	5-70
Appendix	5-71
 CHAPTER 6. MICROBIOLOGY	 6-1
General Experimental Procedures	6-1
Schmutzdecke Column Results	6-1
One Meter Column Results.....	6-3
Schmutzdecke Column Results.....	6-5
Virus Removal	6-5
Dependence of Bacteriophage Removal on Flow Rate	6-12
Poliovirus Removal	6-12
Parasite Removal in the Schmutzdecke Columns.....	6-16
One Meter Column Results	6-20
Virus Removal	6-20
Dependence of Bacteriophage Removal on Flow Rate	6-25
Effect of Soil Profile Length on Virus Removal	6-25
Poliovirus Removal	6-28
Removal of Bacteriophage from Primary Effluent	6-28
Cryptosporidium Removal in the One Meter Columns	6-32
Pathogen Migration in Simulated Rainfall Flushing Events.....	6-35
Virus Desorption in the Rainwater Infiltration Experiments.....	6-35

Cryptosporidium Elution in the Rainfall Experiments	6-42
Work in Progress.....	6-42
Conclusions.....	6-44
Microbiology References	6-48
 CHAPTER 7. EFFECTS OF ENVIRONMENTAL VARIABLES-TEMPERATURE AND OXYGEN EFFECTS ON SAT PERFORMANCE IN COLUMN REACTORS.....	
Temperature Studies	7-1
Oxygen Studies	7-2
Aeration Studies	7-5
Algal Studies	7-16
 CHAPTER 8. SOIL AQUIFER TREATMENT STUDIES IN FILTERED PRIMARY EFFLUENT	
Introduction	8-1
Materials and Methods	8-2
Soil Characteristics	8-2
Effluent Characterization and Filtration.....	8-2
Preliminary Biodegradability Studies.....	8-5
Experimental Setup	8-6
Analytical Techniques.....	8-14
Results	8-19
Hydraulics	8-20
Major Ions and Some Metals	8-25
DOC and UVA ₂₅₄ and Effect of Oxygen Levels.....	8-25
Turbidity	8-29
Nitrogen.....	8-29
Phosphorus	8-32
Total and Fecal Coliforms.....	8-34

Bacteriophages	8-38
Discussion.....	8-41
Hydraulics	8-41
DOC and Humic Substances (UVA ₂₅₄)	8-42
Phosphorus	8-48
Total and Fecal Coliforms and Bacteriophages.....	8-49
Conclusions and Recommendations	8-50
References	8-52
 CHAPTER 9. GROUNDWATER MOUNDING CONTROL	9-1
Overview	9-1
Purpose.....	9-1
Problem Statement	9-2
Recharge-Aquifer System Description	9-3
Overview of Optimization Model Formulation.....	9-5
Girinski Potential Transformation and Sensitivity.....	9-9
Overview of Solution Schemes.....	9-10
Optimal Withdrawal Policy.....	9-12
Optimal Energy Based Model.....	9-22
Optimal Well Location	9-23
Summary.....	9-26
References	9-26
 CHAPTER 10. DESIGN AND OPERATION OF SAT SYSTEMS	10-1
Development of Simulator.....	10-1
Introduction	10-1
Mathematical Statement of NITRINFIL	10-3
Numerical Solution.....	10-13
Parameter Calibration	10-13
Conclusions.....	10-31

Development of Optimizer	10-34
Introduction	10-34
Operation of SAT Systems	10-35
Mathematical Formulation of Optimization Model	10-36
Interface of SALQR with Modified HYDRUS	10-38
Convergence Procedure.....	10-41
Application Examples	10-43
Conclusions.....	10-51
The Optimal Operation of SAT Systems: SALQR-NITRINFIL Interfacing.....	10-55
Consideration on Nitrogen and Organics Removal During Operation of SAT Systems ..	10-55
Mathematical Description of the Optimization Model	10-55
SALQR- NITRINFIL Interfacing	10-57
Application Example	10-60
Conclusions.....	10-62
Operation of SAT Systems Considering Parameter Uncertainty	10-68
Introduction	10-68
Interface SALQR with MSTs.....	10-68
Uncertainties in the SAT Systems.....	10-71
Uncertainty Analysis of Unsaturated Hydraulic Conductivity	10-74
Chance-Constrained SAT Operation Model.....	10-82
Model Applications	10-86
Operation of SAT Systems Under Heterogeneity of Soil Properties	10-92
Introduction	10-92
Heterogeneous Hydraulic Conductivity Field	10-92
Generation of Random Hydraulic Conductivity Field	10-95
Monte Carlo SAT Management Model.....	10-97
Model Application and Post Monte Carlo Analysis	10-100
References	10-108
Appendix	10-115
A: NITRINFIL User's Manual	10-115

B: SALQR Algorithm.....	10-135
C: SALQR User's Guide	10-140
D: Derivative Calculations for SALQR Interfaced with HYDRUS	10-149
E: Derivative Calculations for SALQR Interfaced with NITRINFIL	10-153
 CHAPTER 11 SUMMARY AND CONCLUSIONS	11-1
Overview	11-1
Hydraulics	11-2
Effect of Clogging	11-3
Effect of Water depth	11-4
Effect of Wet/Dry Cycle Times.....	11-4
Expect Infiltration Rates	11-5
Organics.....	11-5
Nitrogen.....	11-7
Pathogens	11-9
Model Development and Optimization.....	11-9
Groundwater Mound Control	11-10
SAT Design and Operations Recommendations	11-12
SAT Pretreatment Requirements	11-12
SAT Soil Requirements	11-13
SAT Design Criteria	11-15
Design and Operational Implications.....	11-16
 APPENDIX GLOSSARY	A-1

FIGURES

1.1 An SAT system consists of five major components: (1) pipelines that carry the treated effluent from the wastewater treatment plat to the SAT system; (2) percolation basins where treated effluent infiltrates into the ground; (3) the soil immediately below the infiltration basins (vadose zone); (4) the aquifer where water is stored for a long duration; and (5) the recovery wells where water is pumped from the aquifer for potable and non-potable reuse.....	1-2
1.2 Soil aquifer treatment system dynamics.....	1-5
1.3 Universities' research interaction	1-12
1.4 Processes related to operation of SAT system	1-15
1.5 Prior to SAT, the air spaces are void and allow for infiltration of water	1-16
1.6 After SAT the air space become filled with biofilm, algae, and SS. In addition, a mat of algae can cover the surface greatly reducing infiltration rate	1-18
1.7 Flowdiagram of the nitrogen cycle in SAT system	1-19
2.x Top section of pilot scale columns	2-2
2.x Weir Detail of pilot scale columns	2-4
2.x Bottom section of pilot scale columns.....	2-5
3.1 Air permeability for SAT soils	3-5
3.2 Column infiltration apparatus.....	3-7
3.3 Degree of saturation profile for Agua Fria soil column.....	3-9
3.4 Degree of saturation profile for Sweetwater soil column.....	3-10
3.5 Degree of saturation profile for South Pond soil column.....	3-11
3.6 Degree of saturation profile for North Pond soil column.....	3-12
3.7 Degree of saturation profile for Ag. Field soil column.....	3-13
3.8 Soil suction profile for Ag. Field clay (wetting at 48 cm)	3-17
3.9 Agua Fria soil column infiltration.....	3-22
3.10 Agua Fria soil column infiltration (ponding depth=1 cm, t=85 sec.).....	3-23

3.11 Agua Fria soil column infiltration.....	3-24
3.12 Sweetwater soil column infiltration.....	3-25
3.13 Sweetwater soil column infiltration (ponding depth=15 cm, t=7 min.).....	3-26
3.14 Sweetwater soil column infiltration.....	3-27
3.15 South Pond soil column infiltration.....	3-28
3.16 South Pond soil column infiltration (ponding depth=15 cm, t=175 min.).....	3-29
3.17 South Pond soil column infiltration.....	3-30
3.18 North Pond soil column infiltration.....	3-31
3.19 North Pond soil column infiltration (ponding depth=15 cm, t=170 min.).....	3-32
3.20 North Pond soil column infiltration.....	3-33
3.21 Ag. Field soil column infiltration.....	3-34
3.22 Ag. Field soil column infiltration (ponding depth =15 cm, t=146 hour).....	3-35
3.23 Ag. Field soil column infiltration.....	3-36
3.24 South Pond soil column infiltration (bounded).....	3-39
3.25 South Pond soil column infiltration (bounded, ponding depth=15 cm, t=120 min.).....	3-40
3.26 North Pond soil column infiltration (bounded).....	3-41
3.27 North Pond soil column infiltration (bounded, ponding depth=15 cm, t=175 min.).....	3-42
3.28 Cumulative infiltration loads for North Pond silt columns (#1, #3, #50 and Agr. clay columns (#7, #8).....	3-43
3.29 Average infiltration rates for cycles 1-39 (column #1, soil type: North Pond silt, Effluent type: chlorinated denitrified).....	3-44
3.30 Average infiltration rates for cycles 1-39 (column #3, soil type: North Pond silt, Effluent type: dechlorinated denitrified).....	3-45
3.31 Average infiltration rates for cycles 1-39(column #5, soil type: North Pond silt, Effluent type: chlorinated secondary.....	3-46
3.32 Average infiltration rates for cycles 1-14(column #7, soil type: Ag. Field clay, Effluent type: chlorinated denitrified).....	3-48
3.33 Average infiltration rates for cycles 1-14(column #8, soil type:Ag. Field clay, Effluent type: dechlorinated denitrified).....	3-49
3.34 Typical infiltration rates as a function of time during a 7-day wetting period	

for columns containing repacked Agua Fria sand, Sweetwater sandy loam, and North Pond silt. Data shown were collected after development of surface clogging layers	3-54
3.35 Typical daily measurements of metric potential as a function of soil depth for 1-meter columns containing repacked Agua Fria sand during a 7-day wetting period. Data shown were collected after development of surface clogging layers	3-56
3.36 Cumulative hydraulic loading as a function of wet cycle for columns containing repacked Agua Fria sand, Sweetwater sandy loam, and North pond silt during the first 25 wetting periods	3-57
3.37 Typical daily measurements of metric potential as a function of soil depth for 1-meter columns containing repacked Sweetwater sandy loam during a 7-day wetting period. Data shown were collected after development of surface clogging layers	3-59
3.38 South percolation test site daily infiltration rates	3-62
3.39 North percolation test site daily infiltration rates	3-63
3-40 Plan view of North and South Basins	3-65
3.41 North Pond neutron moisture profile	3-67
3.42 South Pond neutron moisture profile	3-68
3.43 Graphical representation of the boring logs	3-70
3.44 Plane view of field percolation test pond	3-72
3.45 North Pond field percolation test (central point, diameter=101 cm, water depth=13 cm)	3-74
3.46 North Pond field percolation test (central point, drying process)	3-75
3.47 North Pond field percolation test (edge point, diameter=101 cm, water depth=13 cm)	3-76
3.48 North Pond field percolation test (edge point, drying process)	3-77
3.49 North Pond field percolation test (50 cm from pond, diameter=101 cm, water depth=13 cm)	3-78
3.50 North Pond field percolation test (50 cm from pond, drying process)	3-79
3.51 Field percolation test (ponding depth=12 cm, diameter=100 cm)	3-80

3.52 Simulation domain and boundary condition.....	3-82
3.53 North Pond field percolation (Central point, diameter=101 cm, water depth=13 cm)	3-83
3.54 North Pond field percolation (Central point, diameter=10 cm, water depth=12 cm, t=8 hours)	3-84
3.55 Wetting front position (North Pond soil, t=8 h)	3-85
3.56 Wetting front position (Sweetwater soil, t=12 min.).....	3-86
3.57 Wetting front position (Ag. Field clay, t=180 h).....	3-87
3.58 Axisymmetric simulation for North Pond soil (pond size effect)	3-89
3.59 Axisymmetric simulation for Sweetwater soil (pond size effect)	3-90
3.60 1-D simulation of North Pond soil with clay lenses (position of lense= 2 m, ponding depth=1 cm)	3-93
3.62 1-D simulation of Sweetwater soil with clay lenses (position of lense= 2 m, ponding depth=1 cm)	3-94
3.63 1-D simulation of North Pond soil with clay lenses (thickness of clay=20cm, ponding depth=1 cm)	3-95
3.64 1-D simulation of Sweetwater soil with clay lenses (thickness of clay=10cm, ponding depth=1 cm)	3-96
3.65 Cross-section of simulation domain	3-97
3.66 2-D simulation of North Pond soil with discontinues clay lense.....	3-98
3.67 2-D simulation of Sweetwater soil with discontinuous clay lense.....	3-99
3.68 Clogging layer schematic	3-104
3.69 Flow for hypothesized clogging layer flow model	3-107
3.70 CRS consolidation on SAT soils.....	3-117
3.71 Incrementally loaded consolidation mixed culture algae	3-119
4.1 Influent and effluent levels of dissolved organic carbon and ultraviolet-absorbing material as functions of cycle # in a one-meter (UA) column (#3) containing Agua Fria sand. The column was fed effluent from the Roger Road Wastewater Treatment in Tucson	4-12
4.2 Influent and effluent levels of dissolved organic carbon and ultraviolet-absorbing	

material as functions of cycle # in a one-meter (UA) column (#7) containing Agua Fria sand. The column was fed secondary effluent from the Roger Road Wastewater Treatment in Tucson	4-13
4.3 Influent and effluent levels of dissolved organic carbon and ultraviolet-absorbing material as functions of cycle # in a one-meter (UA) column (#11) containing Agua Fria sand. The column was fed secondary effluent from the Roger Road Wastewater Treatment in Tucson. Addition of 2.0 mM Na azide was initiated in cycle # 12 and continued throughout the remainder of the record shown. Points represent the arithmetic mean of at least seven measurements during individual cycles. Error bars encompass two standard deviations. Where no error bars are visible, a standard deviation lay within the symbol.....	4-14
4.4 Influent and effluent levels of dissolved organic carbon and ultraviolet-absorbing material as functions of cycle # in a one-meter (UA) column (#5) containing Sweetwater sandy loam. The column was fed secondary effluent from the Roger Road Wastewater Treatment in Tucson. Points represent the arithmetic mean of at least seven measurements during individual cycles. Error bars encompass two standard deviations. Where no error bars are visible, a standard deviation lay within the symbol.....	4-18
4.5 Influent and effluent levels of dissolved organic carbon and ultraviolet-absorbing material as functions of cycle # in a one-meter (UV) column (#9) containing Sweetwater sandy loam. The column was fed secondary effluent from the Roger Road Wastewater Treatment in Tucson. Points represent the arithmetic mean of at least seven measurements during individual cycles. Error bars encompass two standard deviations. Where no error bars are visible, a standard deviation lay within the symbol.....	4-19
4.6 Influent and effluent levels of dissolved organic carbon and ultraviolet-absorbing material as functions of cycle # in a one-meter (UA) column (#13) containing Sweetwater sandy loam. The column was fed secondary effluent from the Roger Road Wastewater Treatment in Tucson.	4-20
4.7 Average effluent concentration of TOC and UV ₂₅₄ in (a) North Pond silt and	

(b) South Pond silt repacked in 2-meter (ASU) columns. Both column received chlorinated secondary effluent from 91st Avenue Wastewater Treatment Plant in Phoenix. Column designation correspond to those provided in Table 4.2.b.....	4-23
4.8 Average effluent concentration of TOC and UV ₂₅₄ in (a) North Pond silt and (b) South Pond silt repacked in 2-meter (ASU) columns. Both column received chlorinated secondary effluent from 91st Avenue Wastewater Treatment Plant in Phoenix. Column designation correspond to those provided in Table 4.2	4-24
4.9 Average effluent concentration of TOC and UV ₂₅₄ in (a) North Pond silt and (b) South Pond silt repacked in 2-meter (ASU) columns. Both column received chlorinated secondary effluent from 91st Avenue Wastewater Treatment Plant in Phoenix. Column designations correspond to those provided in Table 4.2.b	4-25
4.10 Average effluent concentration of TOC and UV ₂₅₄ versus wetting cycle in 2-meter (ASU) columns. Column designation correspond to those provided in Table 4.2.b. Column were fed effluents from 91st Avenue Wastewater Treatment Plant in Phoenix. (a) North Pond silt fed chlorinated secondary effluent. (b) South Pond silt fed chlorinated secondary effluent.....	4-26
4.10 (continued) (c) North Pond silt fed chlorinated secondary effluent. (d) South Pond silt chlorinated secondary effluent.	4-27
4.10 (continued) (e) North Pond silt fed nitrified/denitrified effluent. (f) South Pond silt fed nitrified/denitrified effluent	4-28
4.11 Effluent concentrations of TOC and UV ₂₅₄ versus wetting cycle in 2-meter (ASU) columns packed with Agua Fria sand. Column designation correspond to those assigned in Table 4.2.b. (a) Agua Fria sand fed chlorinated secondary effluent. (b) Agua Fria sand fed nitrified/denitrified effluent.....	4-29
4.11 Effluent concentrations of TOC and UV ₂₅₄ versus wetting cycle in 2-meter (ASU) columns packed with Ag. field clay. Column designation correspond to those assigned in Table 4.2.b. Column were fed effluents from 91st Avenue Wastewater Treatment Plant in Phoenix. (c) Clayey soil fed chlorinated secondary effluent. (d) Clayey soil fed nitrified/denitrified effluent	4-30
4.12 Average influent and effluent concentrations of DOC and UV ₂₅₄ in a one-meter (UA)	

column packed with North Pond silt. The Column received chlorinated secondary effluent from the Roger Road Wastewater Treatment Plant in Tucson. Points represent the arithmetic mean of at least seven measurements during individual cycles. Error bars encompass two standard deviations. Where no error bars are visible, a standard deviation lay within the symbol.	4-35
4.13 Effluent concentration of TOC and UV ₂₅₄ versus wetting cycle in 2-meter (ASU) columns packed with South Pond silt. in (a) North Pond silt and (b) South Pond silt repacked in 2-meter (ASU) columns. Column designation correspond to those assigned in Table 4.2.b. Column were fed effluents from 91st Avenue Wastewater Treatment Plant in Phoenix. (a) South Pond silt fed chlorinated secondary effluent. (b) North Pond silt fed nitrified/denitrified effluent.....	4-37
4.14 Synopsis of simulated SAT and BDOC treatment efficiencies in the removal of DOC, UVA ₂₅₄ , and THMFP in secondary and ozonated-secondary effluents. Reported data are the results of a single intensive study as opposed to data averages. POST-SAT data represent levels of DOC, UVA ₂₅₄ and THMFP in 18-cm schmutzdecke columns. The columns were packed with Sweetwater sandy loam and received secondary effluent from the Roger Road Wastewater Plant in Tucson.....	4-42
4.15 Time-dependent concentrations of DOC in BDOC flasks containing acclimated sands and secondary effluents from the Roger Road Wastewater Plant in Tucson. The ozone dosage was 1 part ozone transferred per part DOC.	4-44
4.16 Summary of treatment efficiencies during simulated SAT (one-meter columns packed with Agua Fria sand) and BDOC tests. Columns received effluent from the Roger Road Wastewater Plant in Tucson. Ozone dosage was 1 part O ₃ transferred per part DOC or carbon.....	4-45
4.17 Effect of acclimation procedure (surface water acclimation versus effluent acclimation) on the performance of “acclimated” bacteria during five-day BDOC tests. Data points on each line represent the results of successive tests.	4-47
4.18 Effect of ozone dose in mg O ₃ transferred per mg DOC on organics removal during the BDOC test procedure. The wastewater designation (T3) is explained in Table 4.10.	4-48

4.19	Effect of ozonation at 1 part O ₃ transferred per part DOC on the biodegradability of dissolved organic residuals in treated wastewaters and a surface water source. Biodegradability was measured in a series of 5-day BDOC tests.	4-49
4.20	Depth-dependent profiles of DOC and UV ₂₅₄ concentrations in a one-meter column (#5) packed with Sweetwater sandy loam. Profiles were measured daily during the week long wet period of cycle # 10.	4-53
4.21	Depth-dependent concentrations of DOC and UV ₂₅₄ in a one-meter column (#5) packed with Sweetwater sandy loam. Profiles were measured daily during the week long wet period of cycle # 11.	4-54
4.22	Influent and effluent concentrations of DOC and UV ₂₅₄ during simulated SAT in a one-meter column containing on intact core Agua Fria sand. Column designations correspond to those in Table 4.2a.....	4-57
4.23	Influent and effluent concentrations of DOC and UV ₂₅₄ during simulated SAT in a one-meter column containing on intact core North Pond silt. Column designations correspond to those in Table 4.2a.....	4-58
4.24	Percent reduction of DOC for Azide-amended (secondary control) and secondary columns. Columns were the short, schmutzdecke reactors. Reductions were influent-to-effluent, over the 6-7 inch reactor depth.	4-61
4.25	Percent reduction of UV ₂₅₄ for Azide-amended (secondary control) and secondary columns. Columns were the short, schmutzdecke reactors. Reductions were influent-to-effluent, over the 6-7 inch reactor depth.....	4-62
5.1	Top section of pilot scale columns	5-11
5.2	Weir detail of pilot scale columns	5-12
5.3	Bottom section of pilot scale columns.....	5-13
5.4	Effluent ammonia and nitrate from a silt (North Pond) column (#1) flooded chlorinated denitrified effluent	5-22
5.5	Effluent ammonia and nitrate from a silt (North Pond) column (#5) flooded chlorinated secondary effluent.....	5-24
5.6	Effluent ammonia and nitrate from a clay(Ag. field) column fed chlorinated denitrified effluent.....	5-25

5.7 Effluent ammonia and nitrate from a sand (Agua Fria) column (#9)	
flooded chlorinated denitrified effluent	5-27
5.8 Effluent ammonia and nitrate from a silt (South Pond) column (#12)	
flooded dechlorinated denitrified effluent.....	5-28
5.9 Ammonia concentration vs. time in Agua Fria sand column #3, cycle 12	5-30
5.10 (Nitrate+nitrite)-N concentration vs. time for Agua Fria sand and	
Sweetwater soil during cycle 13	5-31
5.11 Comparison of flow weighted average effluent nitrate concentrations	
or different effluents fed to (North Pond) columns. Chlorinated denitrified	
and dechlorinated denitrified consistently meet MCL chlorinated secondary	
does meet MCL.	5-34
5.12 Weighted effluent ammonia and nitrate concentrations for #1a silt (North Pond)	
flooded chlorinated denitrified effluent.	5-37
5.13 Weighted effluent ammonia and nitrate concentrations for #3 a silt (North Pond)	
flooded dechlorinated denitrified effluent.....	5-39
5.14 A silt (North Pond) column (#5) flooded with chlorinated secondary effluent.	
Average concentration consistently exceeded the MCL for nitrate.	5-40
5.15 Sweetwater soil column B-1--primary effluent.....	5-44
5.16 Sweetwater soil column B-2--primary effluent.....	5-45
5.17 Sweetwater soil column B-2, cycle 12-16, mass balance summary.	
Fractions next to bars indicate ratio of primary to nitrified secondary	
effluent applied to column. Note that the percentage of n removal	
increases with the percentage of primary effluent applied	5-46
5.18 Agua Fria sand column #3--secondary effluent, mass balance summary.	
Note that only one cycle (cycle 18) exhibited positive nitrogen removal.....	5-49
5.19 Sorption of ammonia within a 2 inch depth in a silt (North Pond) column (#4)	
fed dechlorinated denitrified effluent.....	5-51
5.20 Sorption of ammonia within a 22 inch depth for a silt (North Pond) column (#6)	
fed chlorinated secondary effluent	5-52
5.21 Ammonia breakthrough curves for four types of soils (effluent ammonia=20 mg/L)	5-54

5.22 Ammonia concentration vs. time curve: phase I and II	5-56
5.23 Ammonia concentration and cumulative mass (in-out)	5-58
5.24 Ammonia concentration vs. time in biologically inhibited column.	5-61
5.25 Sweetwater soil column #5--secondary effluent, cycle 13, enlarged view of post-nitrate flush (nitrate+nitrite)-N concentration vs. time.....	5-63
5.26 Percent nitrogen removal as a function of the effluent blend applied to a 1-meter sandy-loam soil column.	5-66
6.1 Removal of indigenous bacteriophage (cumulative influent-cumulative effluent) from primary effluent in an 18-cm Sweetwater sandy loam column for two representative wet periods. Daily percent removal is calculated from daily influent and effluent concentration.....	6-7
6.2 Removal of indigenous bacteriophage (cumulative influent-cumulative effluent) from secondary effluent in two 18-cm Sweetwater sandy loam columns for representative wet periods. Daily percent removal is calculated from daily influent and effluent concentration.....	6-8
6.3 Removal of indigenous bacteriophage (cumulative influent-cumulative effluent) from tertiary effluent in two 18-cm Sweetwater sandy loam columns for representative wet periods. Daily percent removal is calculated from daily influent and effluent concentration.....	6-9
6.4 Removal of indigenous bacteriophage (cumulative influent-cumulative effluent) from ozonated secondary effluent in two 18-cm Sweetwater sandy loam columns for representative wet periods. Daily percent removal is calculated from daily influent and effluent concentration	6-10
6.5 The observed negative correlation between removal of indigenous bacteriophage from tertiary effluent in an 18-cm Sweetwater sandy loam and column flow rate.	6-13
6.6 Observed negative correlation between removal of indigenous bacteriophage and column flow rate from an 18-secondary effluent column ($r^2=0.32$; $P=0.0083$).	6-14
6.7 Observed negative correlation between removal of indigenous bacteriophage and column flow rate from an 18-tertiary effluent column ($r^2=0.56$; $P=6.5 \times 10^{-6}$).	6-15
6.8 (A) Removal of indigenous <i>Giardia</i> cysts and (B) <i>Cryptosporidium</i> oocysts from	

primary effluent in an 18-cm Sweetwater sandy loam column. Average for two wet periods in which Log reduction is calculated from daily influent and effluent concentrations.....	6-17
6.9 (A) Removal of seeded <i>Cryptosporidium</i> oocysts from secondary effluent, and (B) secondary ozonated effluent in an 18-cm Sweetwater sandy loam column. Average for two wet periods in which Log reduction is calculated from daily influent and effluent concentrations	6-18
6.10 (A) Removal of seeded <i>Cryptosporidium</i> oocysts from tertiary effluent in an 18-cm Sweetwater sandy loam column. Average for two wet periods in which Log reduction is calculated from daily influent and effluent concentrations.....	6-19
6.11 Removal of indigenous bacteriophage (cumulative influent-cumulative effluent) from secondary effluent in a 1-cm Agua Fria sand column for two representative cycles. Daily percent removal is calculated from daily influent and effluent concentrations	6-21
6.12 Removal of indigenous bacteriophage (cumulative influent-cumulative effluent) from secondary effluent in a 1-cm Sweetwater sandy loam column for two representative cycles. Daily percent removal is calculated from daily influent and effluent concentrations.....	6-22
6.13 Removal of indigenous bacteriophage (cumulative influent-cumulative effluent) from secondary effluent in a 1-cm North Pond silt column for two representative cycles. Daily percent removal is calculated from daily influent and effluent concentrations	6-23
6.14 Removal of indigenous bacteriophage (cumulative influent-cumulative effluent) from secondary effluent in a azide-inhibited 1-m Agua Fria sand column for two representative cycles. Daily percent removal is calculated from daily influent and effluent concentrations.....	6-26
6.15 Observed negative correlation between removal of indigenous bacteriophage and column flow rate from 1-m Agua Fria sand column ($r^2=0.36$; $P=6.5 \times 10^{-5}$).	6-27
6.16 Removal of poliovirus (cumulative influent-cumulative effluent) from secondary effluent in a 1-m Agua Fria sand column for two representative cycles. Daily	

percent removal is calculated from daily influent and effluent concentrations	6-29
6.17 Removal of indigenous bacteriophage (cumulative influent-cumulative effluent) from primary effluent in a 1-m Sweetwater sandy loam column for one wet period. Daily percent removal is calculated from daily influent and effluent concentrations	6-30
6.18 Removal of indigenous bacteriophage (cumulative influent-cumulative effluent) from primary effluent in a 1-m Sweetwater sandy loam non-ponded column (A) wet period 1 and (B) wet period 2, in which percent removal is calculated from daily influent and effluent concentrations	6-31
6.19 (A) Removal of seeded <i>Cryptosporidium</i> oocysts from secondary effluent in a 1-m Agua Fria sand column, and (B) Sweetwater sandy loam column. Average for two wet periods in which Log reduction is calculated from daily influent and effluent concentrations	6-33
6.20 Removal of indigenous <i>Cryptosporidium</i> oocysts from primary effluent. 1-m (A) Sweetwater sandy loam ponded column for one wet period, and (B) Sweetwater sandy loam non-ponded column for average of two wet periods, in which Log reduction is calculated from daily influent and effluent concentrations	6-34
6.21 (A) Rainfall cycle 1, 1-m Agua Fria sand column. A peak in effluent indigenous bacteriophage concentration is observed to coincide with the breakthrough of low ionic strength (Low CND) artificial rainwater. (B) Enlarged view of the bacteriophage breakthrough in rainfall cycle 1.	6-38
6.22 (A) Enlarged view of rainfall cycle 2, 1-m Agua Fria sand column. No increase in effluent ms-2 bacteriophage concentration is observed to coincide with the breakthrough of high ionic strength, clean water. However, a peak is observed with the low ionic strength artificial rainwater. (B) The MS-2 effluent bacteriophage peak is small relative to the number of bacteriophage removed by the soil (influent-effluent).	6-39
6.23 Rainfall cycle 3, performed with actual local (Tucson) runoff. A peak in effluent in effluent bacteriophage is again observed to coincide with the breakthrough of low ionic strength water.	6-41

7.1 Influent DOC, effluent DOC and % DOC removed over time during wetting periods for column packed with Sweetwater sandy loam soil and modified for temperature control. The column was fed chlorinated/dechlorinated secondary effluent from the Roger Road Wastewater Treatment Plant through the periods shown.....	7-3
7.2 Influent and effluent UVA ₂₅₄ over time during wetting periods for column packed with Sweetwater sandy loam soil and modified for temperature control. The column was fed chlorinated/dechlorinated secondary effluent from the Roger Road Wastewater Treatment Plant	7-4
7.3 Influent DOC, effluent DOC and % DOC removed over time is illustrated a column that is packed with Sweetwater sandy loam soil. During cycle 10 and 11, ponded water in the headspace above the soil surface was aerated to produce near-saturation dissolved oxygen levels. During cycle 12 and 13 the column was operated with no aeration in the ponded water. Influent dissolved oxygen levels were near zero. The column was fed chlorinated/dechlorinated secondary effluent from the Roger Road Wastewater Treatment Plant through the periods shown	7-6
7.4 Influent and effluent UVA ₂₅₄ over time is illustrated for column packed with Sweetwater sandy loam soil. During cycle 10 and 11, ponded water in the headspace above the soil surface was aerated producing near saturation dissolved oxygen levels. During cycle 12 and 13 the column was operated without aeration producing near aero dissolved oxygen	7-7
7.5 Depthwise molecular oxygen partial pressure measurements for Sweetwater column operated with pond aeration. Measure were taken during a typical wet period.	7-8
7.6 Depthwise molecular oxygen partial pressure measurements for Sweetwater column operated without pond aeration.....	7-9
7.7 Influent dissolved oxygen concentrations in a one-meter column containing Sweetwater sandy loam. The column was operated with and without aeration of ponded water in the headspace. Feed water was chlorinated/dechlorinated secondary effluent from Roger Road Wastewater Plant in Tucson.	7-10
7.8 Oxygen content versus soil depth for an unponded sand column (#7) and a ponded Sweetwater soil column (#5) during wet cycle #5. Both column received secondary	

effluent from Roger Road Wastewater Treatment Plant.	7-12
7.9 Depth-dependent profiles of gas-phase molecular oxygen in one-meter column containing Agua Fria sand and Sweetwater sandy Loam. Measurements were taken over the course of 7-day or 11-day drying cycle. Reoxygenation of the columns shown was passive. That is, forced aeration was not employed, and oxygen transport was predominantly due to diffusion.	7-14
7.10 Depth-dependent profiles of gas-phase molecular oxygen in one-meter column containing Agua Fria sand and Sweetwater sandy Loam. air was forced through the column for a brief period once per day during the column drying periods shown. Oxygen measurements were made daily, just prior to the start of forced aeration period.....	7-15
8.1 Primary effluent sand filter. The effluent is applied with the help of peristaltic pumps. Head losses are prevented by blowing air 5 cm below and above the top filter.	8-4
8.2 Concentration of DOC (A) and percent reduction of DOC (B) from a series of five day BDOC experiments (biodegradable dissolved organic carbon) for filtered primary effluent. More than 60% of organic carbon was aerobically degraded during the first 15 hours.....	8-7
8.3 Schematic of 1-m column design (not to scale)	8-8
8.4 Leaching of humic substances (in terms of UV ₂₅₄ absorbances) during 1-m soil column saturation before primary effluent application for columns #1 (A) and #2 (B). Samples were collected at the top of the columns	8-10
8.5 Experimental setup for the 1-m column fed with filtered primary effluent (10: unponded) as opposed to those receiving secondary wastewater (20:constant head).....	8-11
8.6 Bromide breakthrough curves for 1-m soil column # 1 (A) and #2 (B) receiving filtered primary effluent during detention time experiments. Infiltration rates were around 0.14m/day (0.46 ft/day). Detention times varied from 36.75 and 36.5 hours with water contents around 0.22	8-13
8.7 Infiltration rates (A) and matric potential distribution with depth (B) for one of the 1-m soil columns receiving filtered primary effluent. Data correspond to wet cycle #5. Hydraulic load was maintained constant throughout the cycle to avoid	

a rapid oxygen depletion due to water ponding. An incipient clogging layer within the first 5 cm of soil is indicated by the tensiometer readings	8-22
8.8 Infiltration rates (A) and matric potential distribution with depth (B) for one of the 1-m soil columns receiving primary effluent. Data correspond to wet cycle #11. Hydraulic load was still maintained constant during the wet cycle to avoid a rapid oxygen depletion due to water ponding. A better soil acclimation is evidenced by the tensiometer readings.....	8-23
8.9 Cumulative hydraulic loads for 1-m soil column #1 (14 wet cycles) and #2 (8 wet under unponded conditions (A). Cumulative hydraulic loads for 1-m soil column #2 showing the transition from unponded conditions (cycles 1 to 8) into a constant 25-cm hydraulic head (cycle 9-11) (B)	8-24
8.10 Mean column influent and effluent DOC concentrations (A) and UVA-254 absorbances (B) for 1-m soil column #1 as a function of wet cycle number. Apparently, column influent DOC concentration presented seasonal variations possibly related to changes on sewage quality. Error bars indicate one standard deviation from the mean (n=6 to 7). Large error bars are related to leaching of DOC and humic substances during column acclimation.	8-28
8.11 (A) Soil oxygen profiles for 1-m column #2 (wet cycle #4) as a function of depth. Unponded conditions during filtered primary effluent application allowed oxygen supply via diffusion. A gradual depletion of oxygen along all column profile was observed during column acclimation. (B) Soil oxygen profiles as a function of depth for 1-m column #2 during dry cycle #1. A seven-day dry cycle was sufficient for oxygen replenishment near air-saturation levels. Oxygen replenishment was due to diffusion coupled with mass flow.....	8-30
8.12 Mean column influent and effluent turbidities for 1-m soil column fed filtered primary effluent as a function of wet cycle number. Error bars indicated one standard deviation from the mean (n=6 to 7)	8-31
8.13 Leaching of total and reactive phosphorus (as PO ₄ -P) during 1-m soil column saturation before primary effluent application for column B1 (A) and B2(B) Samples were collected at the top of the columns.	8-33

- 8.14 Generalized breakthrough curves for reactive phosphorous from wet cycle 1 through 5 for 1-m soil columns #1 (A) and #2 (B) receiving filtered primary effluent. Recovery of soil sorption capacity between wet cycles could be attributed to the start of a slow-kinetics precipitation phenomenon. Time between wet cycles is not considered..... 8-35
- 8.15 Cumulative rective phosphorus loading from wet cycles 1 through 13 for 1-m soil columns #1 receiving filtered primary effluent. Equality slopes for influent and effluent loads indicated leaching of phosphorus. 8-36
- 8.16 Total and fecal coliforms concentration during three consecutive wet cycles for 1-m soil column #1. Concentration are expressed as logarithm of the most probable number (MPN) per 100 ml of sample. A column effluent concentration below detection limits at the beginning of the wet cycle # 13 is not represented 8-36
- 8.17 (A) Cumulative influent and effluent indigenous bacteriophage and daily percent removal for 1-m soil column #1 receiving filtered primary effluent under unponded conditions (wet cycle 11). (B) Cumulative influent and effluent indigenous bacteriophage and daily percent removal for 1-m soil column # 1 receiving filtered primary effluent under unponded conditions (wet cycle 12). 8-39
- 8.17 (C) Cumulative influent and effluent indigenous bacteriophage and daily percent removal for 1-m soil column #1 receiving filtered primary effluent under ponded conditions (wet cycle..... 8-40
- 8.18 Percentage of DOC (A) and UVA₂₅₄ (B) as a function of cumulative time since start of the experiment for 1-m soil column # 1 for wet cycle 12 to 14, and 11 to 14, respectively. Results from time-series analyses (linear regressions) showed a mean-steady column operation after ten cycles. Time between wet cycle is not considered. 8-44
- 8.19 (A) Depletion of soil oxygen levels at different depths as a function of time for 1-m primary column #2 (wet cycle #4). The oxygen depletion rate (represented by the slopes) was mostly uniform for depths below 12 cm. (B) Oxygen replenishment curves during dry cycle #1 (same column as above) Breakthrough curves were resulted of oxygen replenishment due to a coupled transport

phenomenon (diffusion and mass transport)	8-47
9.1 Nonlinear programming approach with MODFLOW	9-12
9.2 Locations of observation wells-case 1	9-15
9.3 Locations of potential withdrawal wells	9-16
9.4 Locations of observation wells-case 2 and recharge basins	9-19
10.1 Hydraulic boundary conditions (infiltration rate and ponding depth vs. operation conditions)	10-5
10.2 Conceptual model of nitrogen and organics removal mechanisms	10-9
10.3 NITRINFIL program structure	10-14
10.4 ASSRS-NITRINFIL interface flowchart	10-20
10.5 MARQUARDT-NITRINFIL interface flowchart	10-22
10.6 Calibration results on ponding depth on field depth on field silt column	10-23
10.7 Calibration results on infiltration rate on field silt column	10-24
10.8 Curves fitness of parameter calibration on lab silt column	10-24
10.9 Variation of ponding depth via operation schedule	10-27
10.10 Variation of infiltration rate via operation time	10-28
10.11 Variation of outflow rate via operation time	10-28
10.12 Mass balance between inflow and outflow water	10-29
10.13 Nitrogen concentration comparison between monitored and simulated data	10-29
10.14 Monitored and simulated effluent organic carbon	10-30
10.15 Variation of ammonium nitrogen flux via operation cycle	10-30
10.16 Total nitrogen balance via operation cycle	10-31
10.17 Relation of optimizer and simulator	10-40
10.18 Flow chart of the SALQR interfaced with HYDRUS	10-42
10.19 Loading rate, infiltration rate and ponding depth versus operation schedule	10-46
10.20 Flowchart of the SALQR interfaced with NITRINFIL	10-61
10.21 Optimal solution to the experiment problem: the operation schedule	10-64
10.22 Optimal solution to the experiment problem: effluent concentration controlled by the optimizer to be under quality standards (upper bounds)	10-67
10.23 Optimizer-simulator interface	10-70

10.24 The flowchart of SALQR method (Li, 1994)	10-72
10.25 Effect of parameter uncertainty on kuns as a function of suction head for coefficients of variation of 5%	10-79
10.26 Effect of parameter uncertainty on kuns as a function of suction head for coefficients of variation of 10%	10-79
10.27 Fraction of uncertainty due to n , α , and k_s for various suction head.....	10-80
10.28 Fraction of uncertainty due to n , α , and k_s for various suction head.....	10-80
10.29 Fraction of uncertainty due to n , α , and k_s for various suction head.....	10-81
10.30 Fraction of uncertainty due to n , α , and k_s for various suction head.....	10-81
10.31 Fraction of uncertainty due to n , α , and k_s for various suction head.....	10-82
10.32 Fraction of uncertainty due to n , α , and k_s for various suction head.....	10-82
10.33 Overall solution procedure.....	10-84
10.34 Flowchart for chanced-constrained method	10-87
10.35 Results for different uncertainty level of parameters	10-91
10.36 Results for different reliability level.....	10-91
10.37 2-Dimensional log-hydraulic conductivity field.....	10-93
10.38 2-D random field of hydraulic conductivity (variation=0.1)	10-98
10.39 2-D random field of hydraulic conductivity (different realization).....	10-99
10.40 Flowchart of Monte Carlo method.....	10-101
10.41 Wetting time series of Monto Carlo results (30 realizations)	10-104
10.42 Wetting time series of Monto Carlo results (50 realizations)	10-104
10.43 Draining time series of Monte Carlo results (30 realizations).....	10-105
10.44 Draining time series of Monte Carlo results (50 realizations).....	10-105
10.45 Drying time series of Monte Carlo results (30 realizations)	10-106
10.46 Drying time series of Monte Carlo results (50 realizations)	10-106
10.47 Results comparison between Monte Carlo model with deterministic model	10-107



EXECUTIVE SUMMARY

This research project titled "Soil Treatabilities Pilot Studies to Design and Model a Soil Aquifer Treatment System" were performed by a team consisting of faculty and graduate students from Arizona State University, the University of Arizona, and the University of Colorado. It was funded by the cities of Phoenix, Mesa, Scottsdale, Tempe, Glendale and Youngstown, Arizona, the Salt River Project, Tucson Water, the USDA Water Conservation Laboratory, the American Water Works Association Research Foundation (AWWARF), the Water Environment Research Foundation (WERF), and the National Water Resources Institute (NWRI).

The overall objectives of the project has been to study the treatment of wastewater effluent as it percolates through soil and to evaluate means to maximize the treatment efficiency and capacity of **soil aquifer treatment (SAT)** systems. A major portion of the work was devoted to a systematic evaluation of the effects of soil type and effluent pre-treatment on SAT. These two factors along with wet/dry scheduling can control the performance of SAT systems.

The major concerns associated with soil aquifer treatment leading to potable or non-potable reuse of wastewater effluent were identified as organic carbon, nitrogen species, and pathogens. The levels of organic carbon, nitrogen species, and pathogens found in municipal wastewater effluents treated biologically tend to be at levels greater than that found in surface waters and provide serious concerns for reuse. The enforcement of industrial pre-treatment programs has eliminated most concerns over priority pollutants in treated municipal wastewater and priority pollutants were not a focus of this study.

The concerns over organics in treated municipal wastewaters are analogous to the concerns associated with naturally occurring organics in surface waters or groundwaters. One major concern is the reaction of the organics with the commonly used disinfectant chlorine to produce disinfection by-products. Both the removal of organic carbon during soil aquifer treatment and the reactivity of organic residuals with chlorine to form disinfection by-products was studied.

Nitrogen species, in particular nitrate-nitrogen are one of the most common reasons that groundwaters do not meet drinking water standards. Nitrogen can be removed effectively before soil aquifer treatment to ensure compliance with nitrogen standards. Previous studies indicated

that significant transformations of nitrogen occur during soil aquifer treatment provide further removal of nitrogen species. The wastewaters used in this study differed considerably in terms of total concentration and predominant forms of nitrogen present.

The removal of protozoan parasites, bacteria, and viruses during simulated soil aquifer treatment was studied. Pathogenic bacteria and viruses can be present in large numbers in biologically treated wastewater. However, disinfection prior to soil aquifer treatment is effective at deactivating pathogens. In previous field studies involving soil aquifer treatment, infective enteric viruses or enteric bacteria in aquifers that were recharged with wastewater have rarely been found. This study particularly focused on examining the fate of *Cryptosporidium* and Hepatitis A, since these pathogens are of potential concern and very little data on their fate during soil aquifer treatment existed.

The results were used to complement the development of a model to optimize the operation of soil aquifer treatment systems. Several components of the model were developed to aid the decision maker by optimizing removal efficiencies of critical components at different infiltration rates and maximizing the recovery of recharged water while preventing mounding.

The major technical approach to the research consisted of:

- Pilot-scale column studies using soils from the proposed and existing SAT sites. Sets of columns were operated to simulate soil aquifer treatment with five different soils and six different effluent qualities.
- Extensive laboratory studies were used to quantify individual abiotic and biotic removal mechanisms, to determine the effects of preozonation on BDOC (biodegradable dissolved organic carbon), and to investigate the effect of soil compaction on column studies.
- Detailed data analysis were performed to develop monitoring requirements and models for the optimal design and operation of SAT based on relationships between effluent pretreatment levels, soil types, and infiltration rates.

Process performance, removal mechanisms, and monitoring requirements were determined for the following water quality parameters:

- Health-effect-related parameters, including pathogens and DBPs (disinfection-by-products) represented by HAAs and THMs
- Dissolved organic carbon (DOC)
- Nitrogen (Org-N, NH_3 , NO_2^- , NO_3^-)

For the removal of organics, many of the key results can be summarized by one primary observation. Under aerobic conditions, the DOC concentration could be reduced to approximately 4 to 6 mg/L through SAT. This result was independent of the pre-treatment used prior to SAT, independent of soil type, and essentially independent of infiltration rate. Essentially, this corresponds to complete removal of carbonaceous biological oxygen demand (CBOD). Therefore, even primary effluent that was applied slowly to prevent ponding and associated oxygen limitations could produce a post-SAT quality effluent that was similar to the post-SAT quality of denitrified effluent, even though the denitrified effluent contained 80% lower levels of DOC than the primary effluent. Pre-treatment with ozone did not have a significant effect on the 4 to 6 mg/L of DOC levels that proved refractory during SAT, although destruction of compounds contributing to UV absorbance did occur. The refractory level of 4 to 6 mg/L was confirmed by repeated BDOC tests indicating that 4 to 6 mg/L of DOC is refractory to removal over a five day or lower time scale. Well acclimated cultures were capable of reducing DOC levels to 3 mg/L, indicating that greater removal can occur after sufficient acclimation of biological cultures. The removal of DOC was primarily by aerobic biological activity and was sustainable over the two-year time period of the experiment. The removal efficiency of UV_{254} was lower than the removal efficiency of DOC, and the abundance of aromatic humic-type substances in the refractory effluent was confirmed by more detailed investigations into the classes of compounds present. The trihalomethane formation potential (THMFP) of the refractory DOC was also higher than typical organic matter associated with surface waters. Therefore, production of DBP's upon chlorination could be a problem with recovered water. Chloramination demonstrated potential for eliminating problems with THMFP. Most field sites that are affected by SAT have lower levels of DOC (1 to 2 mg/L) indicating that other removal mechanisms for DOC occur in the field that were not observed in this study. Analysis of samples for specific organic compounds in wastewater effluents were consistent with studies of other wastewater

effluents. The presence of compounds such as EDTA (ethylenediamine tetracetic acid) and alkyl-phenol ethoxylates in wastewater effluents could provide indicators of how effective overall DOC removal is in the field when the effects of dilution are uncertain.

The removal of DOC by aerobic conditions influences nitrogen removal in several ways. The removal of DOC creates anoxic conditions in the soil which prevents nitrification during application of water. If the majority of biodegradable DOC is removed under aerobic conditions, there will not be sufficient organic carbon to stimulate denitrification when nitrate is present and anoxic conditions exist.

The major observation for nitrogen was that SAT systems tend to promote nitrification of influent wastewater and transform the majority of influent nitrogen to nitrate. A significant carbon source, anoxic conditions and nitrate-N must be simultaneously available to promote denitrification. Although denitrified effluents contained nitrate-N and biodegradable carbon, the BOD levels were too low to create anoxic conditions. Trickling filter and high-rate activated sludge effluents with influent nitrogen levels ranging from 10 to 40 mg-N/L consistently showed effluent nitrate nitrogen peaks in excess of the MCL of 10 mg-N/L. Attempts to establish denitrifying conditions by manipulating the wetting/drying schedule were not successful. Denitrification was observed when nitrate was blended with primary effluent since sufficient BOD and nitrogen were available to produce anoxic conditions in the column reactors. Unlike the simulations, denitrification has been observed in several field studies of soil aquifer treatment, suggesting that mechanisms for denitrification exist in the vadose zone that are not present in lab or pilot-scale columns. Denitrified effluents that were below the MCL before SAT remained below the MCL when drying cycles were long enough to promote complete nitrification and prevent extended accumulation of ammonia. However, short drying periods during cool weather did not provide complete nitrification, thus allowing ammonia to build up in the soil. Nitrification under warmer conditions lead to increased nitrate-N concentrations that often appear as spikes at the beginning of wetting. This phenomenon was noticed for all effluent pretreatments, including denitrified effluents, and concentration spikes as greater 100 mg/L of nitrate-N can occur when ammonia accumulates at high levels. Overextended wetting could eventually cause ammonia-N to penetrate in the groundwater, particular for coarser grained soils with lower cation exchange capacities. Operation with denitrified effluents should maintain nitrogen levels below the MCL.

Minor deviations above the MCL from nitrate spikes should be mitigated by dispersion and mixing as the nitrate spike approaches the groundwater. Nitrate-N concentration spikes are not a problem after dilution with the rest of the percolating water. Flow weighted average concentrations need to be used to determine the actual impact on the groundwater.

Pathogen removal studies indicated that removal efficiency inversely correlated with flowrate, or directly correlated to detention time. High virus removal efficiencies (>99%) were observed in one-meter of soil after low infiltration rates were induced by the development of a clogging layer. The lowest removal efficiencies (45%) were observed when infiltration rates were high, such as for the removal of bacteriophage in a porous sand that did not have a clogging layer and aerobic biological activity was inhibited in the soil. For virus removal, the general mechanism for removal is sorption and decay. Removal of indigenous bacteriophage ranged from 76% to 96% for flow through one meter of soil. The 76% removal efficiency occurred with a porous sand. In every case, removal efficiencies was lower at the beginning of wet periods when infiltration rates were high and detention times low. The removal of poliovirus across one meter of porous sand was 88-99%, indicating that indigenous bacteriophage are removed less efficiently than poliovirus and that bacteriophage could serve as conservative indicator of virus removal during SAT. Four logs removal of *Cryptosporidium* was routinely observed after passing through one meter, of soil including the porous sand with the highest infiltration rates. Since the removal of pathogens during soil aquifer treatment is dependent on sorption and decay, significant removal of pathogens is expected to continue deeper in the vadose zone. Assuming a first-order decay relationship, if 90% removal of virus occurred during flow through one-meter of soil, then 90% removal would occur in each subsequent meter of soil. Therefore, two meters of soil would remove 99% of viruses and three meters of soil would remove 99.9% of viruses. These high removal rates are not surprising in light of the lack of evidence for enteric viruses in groundwaters recharged by treated wastewaters. Further analysis of data must be done to determine whether a first-order relationship is appropriate.

The hydraulics of SAT systems are affected by many factors including soil type, field spatial variability of soil type, the formation of a surface clogging layer, wetting/drying cycle times for application of the secondary effluent, effluent type, and climatic conditions. Clearly, the maintenance of a reasonable rate of infiltration is of prime importance to the success of any SAT

facility. Further, the hydraulic loading rate relates directly to the land requirements for SAT. Field and laboratory observations indicate that the hydraulics of SAT infiltration basins are controlled to a large extent by the formation of a low conductivity clogging layer on and within the upper few centimeters of the surface soils. Therefore, management of surface and near-surface basin soils through control of wetting and drying cycle times and periodic basin surface scarification is generally required to ensure adequate infiltration rates. Not only is the hydraulic loading rate important from a feasibility/economics standpoint, it also relates to the efficiency of treatment, this is particularly apparent for pathogen removal as evidenced by the dependence of viral removal efficiencies on infiltration rate.

The saturated hydraulic conductivity of soils studied ranged from 0.005 to 250 ft/day (0.0015 to 76 m/day). The clays provided infiltration rates too low for practical SAT. Silts with hydraulic conductivities from 0.1 to 0.6 ft/day (0.03 to 0.18 m/day) tended to have infiltration rates close to the saturated hydraulic conductivity and were not significantly affected by clogging layer development unless drying did not occur between cycles. This observation indicates that the conductivity of the soil was controlling and that the clogging layer conductivity was greater than 0.5 ft/day (0.15 m/day). Soils with higher saturated hydraulic conductivities exhibited more classical behavior with infiltration rates approaching their hydraulic conductivity at the beginning of wetting followed by a rapid decrease in infiltration rate as the clogging layer developed. With denitrified effluent, almost two years were necessary to develop a clogging layer on porous sand while clogging layer developed was rapidly with trickling filter effluent. In most cases, infiltration rates began to decrease in subsequent cycles even though sufficient drying occurred to desiccate the upper clogging layer. After 21 cycles of wetting with effluent, removal of desiccated algae and raking of the surface clogging layer to a depth of about one inch reestablished the original higher infiltration rates in the porous sand column. However, shallow scraping was not effective in reestablishing the rates of infiltration for the Sweetwater column (sandy loam). Removal of the top six inches of soil was required to regenerate hydraulic capacity in the sandy loam columns. Preliminary results indicate that fines migration might explain the development of a deeper clogging layer with the Sweetwater sandy loam.

A program of consolidation and hydraulic conductivity testing has been conducted with the intent of quantifying the mechanical and hydrologic characteristics of the clogging layer and its

individual components. This program includes tests of actual clogging layers, as well as tests of the individual constituents such as soil, algae, wind blown dust and effluent suspended solids. The results indicated that the algae contributed significantly to the reduction in hydraulic loading caused by the formation of the clogging layer. Further, it appears that compression of the algae resulting from seepage gradients can be significant at pond depths in the range of those normally considered for SAT operation. Attempts to control algal development by limiting incident sunlight by 40-60% were not successful indicating that the planting of trees around basins would not prevent algal development.

Column results indicate that a hydraulic loading rate of approximately 0.1 to 0.5 ft/day (0.03 to 0.15 m/day) for the silts and 0.3 to 1 ft/day (0.09 to 0.3 m/day) for the Sweetwater and Agua Fria sands could be maintained, even with effluent infiltration and resultant surface clogging, by controlling the wetting/drying cycles and through periodic surface scarification of the clogging layer (or at worst periodic removal and replacement of the very near-surface soils).

The observed dependence of infiltration rates on water quality was not as significant as originally postulated. This fact represents the robustness of SAT. Organic removal was almost independent of infiltration rate. Very low infiltration rates actually increased DOC levels since algal contributions of organic carbon became significant. Sufficient oxygen and microbial activity was present to remove biodegradable organic carbon in almost all the effluents studied at a wide range of infiltration rates. Nitrogen transformations are dependent on infiltration rate to the extent that the total mass of ammonia adsorbed during wetting depends on the mass loading of ammonia during wetting. Increased drying times can be necessary to add sufficient oxygen during drying to nitrify adsorbed ammonia and prevent a large accumulation of ammonia in the soil. This does represent a limit on infiltration rates since the increased drying times reduce average infiltration rates. For pathogen removal, there is an inverse relationship between infiltration rate and pathogen removal.

The overall results were used to help develop the SAT simulation model NITRINFIL which was used to determine the trade-off between wet/dry cycle times, infiltration rates, and predicted removal efficiencies. The model is a one-dimensional variably saturated flow and interactive multi-component solute transport model for cyclic operation of soil aquifer treatment systems. NITRINFIL is specifically designed to simulate the hydrological, hydraulic, physico-chemical,

biochemical processes during cyclic operation of soil aquifer treatment systems and evaluate the performance of the system under certain operating conditions. NITRINFIL contains sub-models for variably saturated water flow, multi-component solute transport, biochemical degradation, and surface clogging effect. The flow submodel assumes one-dimensional, isothermal flow governed by Darcy's law where the relationships of water content and hydraulic conductivity are defined by van Genuchten equations. The solute transport submodel is based on one-dimensional hydrodynamic dispersion and advective transport where the influent concentration of dissolved oxygen, ammonium nitrogen, nitrate and nitrite nitrogen, biodegradable organic carbon, non-biodegradable organic carbon, are assigned by users. The surface clogging submodel consists of a sedimentation layer and a filtration layer and the concentrations of algae and suspended solids in influent are given by users.

After extensive calibration of soil parameters, the water quality simulation results compared well with field monitoring data for three major pollutants: ammonium nitrogen, nitrite/nitrate nitrogen, and organic carbon. With the exception of nitrate-N peaks, the general trends of the variations are matched. The nitrate-N peaks were difficult to simulate since precise operating times were necessary, however, the magnitude of the peaks was predicted well and the magnitude is more important than the time. Water quality was simulated for 44 operation cycles (480 days) of the pilot scale columns at the 91st Avenue WWTP. The model predicted that denitrification did occur during early cycles. Changes in wet/dry cycle times increased the aeration of the soil system, eliminating the possibilities of denitrification, and influx and outflux nitrogen are almost balanced. The ability to simulate aeration of the soil system is critical since experimental results indicate that SAT performance can be strongly dependent on soil reaeration under certain operating conditions.

The simulation model was coupled with an optimization technique to provide results to a decision maker that are based on desired criteria for SAT. The criteria for designing the optimal operation of soil aquifer treatment system are to maintain a desired infiltration rate while maintaining water quality goals. Mathematically, the problem is to maximize the infiltration subject to constraints describing:

- Subsurface unsaturated flow;

- Ponding and draining processes;
- Clogging effect;
- Biodegradation of nitrogen and organic carbon; and
- Some necessary numerical constraints on SAT operation.

The optimizer, the simulator, and the interface subroutine, are the three primary components of this overall optimization model.

One example of using the model to aid a decision maker was the development of graphs that demonstrate the relationship between infiltration rate, wet/dry cycle times, and removal efficiencies for a specific soil. The infiltration rate was plotted as a function of application periods and drying time. In this manner the decision maker can choose a range of wet/dry cycles that are within the range of infiltration rates used for design. The next step is to observe a plot of organic, nitrogen, or pathogen removal efficiency as a function of application periods and drying time. For the wet/dry cycles that provide the design infiltration rate, the removal efficiencies of specific contaminants can be determined from plots and the most appropriate wet/dry cycle times can be determined along with feasibility. In the present model, decisions would be made primarily on nitrogen or pathogens since organic removal was not a strong function of infiltration rate. The model is primarily based on studies with column simulations that represent near soil surface removal mechanisms. Future results from field work could be used to better adapt the model to field situations where other mechanisms for organic carbon and nitrogen removal are apparent in the deep vadose zone. The present model can also be used to predict the effect of wet/dry cycles on the accumulation of ammonia and magnitude of nitrate spikes. As expected, the model predicts that nitrate peaks are attenuated by dilution as flow occurs deeper in the vadose zone.

A list of engineering implications are presented in Chapter 5 that are based on the results of this study.



CHAPTER 1

INTRODUCTION

BACKGROUND

This research project titled *“Soil Treatabilities Pilot Studies to Design and Model a Soil Aquifer Treatment System”* has been performed by a team consisting of faculty and graduate students from *Arizona State University, the University of Arizona, and the University of Colorado* and is being funded by the cities of *Phoenix, Mesa, Scottsdale, Tempe, Glendale and Youngstown, Arizona, the Salt River Project, Tucson Water, the USDA Water Conservation Laboratory, the American Water Works Association Research Foundation (AWWARF), the Water Environment Research Foundation (WERF), and the National Water Resources Institute (NWRI).*

The overall objective of the project has been to study the treatment of wastewater effluent as it percolates through soil to evaluate means to maximize the treatment efficiency and capacity of **soil aquifer treatment (SAT)** systems (see Figure 1.1).

The major concerns associated with soil aquifer treatment to provide high quality potable or non-potable water from wastewater effluent were identified as organic carbon, nitrogen species, and pathogens. Priority pollutants in biologically treated wastewater from the 91st Avenue Wastewater Treatment Plant in Phoenix, Arizona have satisfied primary drinking water standards since strict industrial pre-treatment requirements were enforced. The levels of organic carbon, nitrogen species, and pathogens found in biologically treated wastewater tend to be at levels greater than that found in surface waters and provide serious concerns for reuse.

The organics in biologically treated wastewaters are analogous to the organics present in surface waters and the major concern is the same concern associated with naturally occurring organics in surface waters or groundwaters. This concern is the reaction of the organics with the commonly used disinfectant chlorine to produce disinfection by-products. Both the removal of organic carbon during soil aquifer treatment and the effect on the formation of disinfection by-products was studied.

Nitrogen species, in particular nitrate-nitrogen are one of the most common reasons that groundwaters do not meet drinking water standards. Nitrogen can be removed effectively before soil

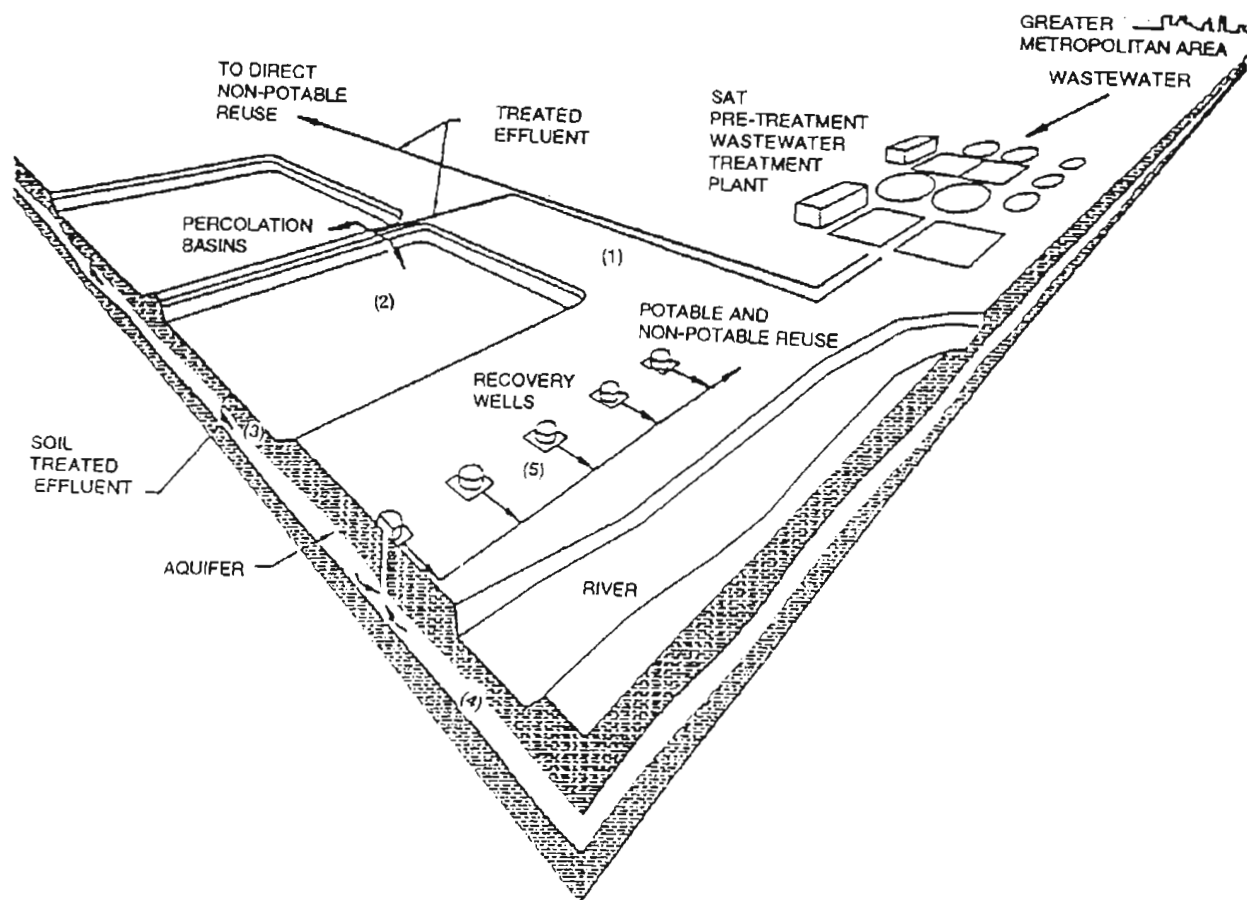


Figure 1.1 An SAT system consists of five major components: (1) pipelines that carry the treated effluent from the wastewater treatment plant to the SAT system; (2) percolation (infiltration) basins where the treated effluent infiltrates into the ground; (3) the soil immediately below the infiltration basins (vadose zone); (4) the aquifer where water is stored for a long duration; and (5) the recovery wells where water is pumped from the aquifer for potable and non-potable reuse.

aquifer treatment to ensure compliance with nitrogen standards. Previous studies had also indicated that significant transformations of nitrogen occur during soil aquifer treatment to provide further removal of nitrogen species. A wide range of nitrogen characteristics in wastewater effluents was studied to determine impacts on nitrogen transformations. Table 1.1 presents the effluents studied and their wide range of characteristics.

Table 1.1

Typical range of water quality parameters (mg/L)

Effluent	Type	BOD	SS	NH ₃ -N	NO _x -N	Total-N	TOC
Phoenix 91st Ave. WWTP Effluent	Dechlorinated Denitrified	3-7	3-7	1.0-3.0	1.0-6.0	4-10	8-10
	Chlorinated Denitrified	3-7	3-7	1.0-3.0	1.0-6.0	4-10	8-10
	High Rate Activated Sludge (Chlorinated)	10-15	10-25	10-30	0-8.0	10-40	13-15
Tucson Roger Road WWTP Effluent	Secondary Trickling Filter*	20-25	20-30	15-25	0-2.0	15-30	15-20
	Tertiary-Pressure Filter	10-15	5-10	15-25	0-2.0	15-30	10-15
	Primary	50-80	60-100	20-35	0-1.0	25-40	40-50

* O₃ secondary effluent was also studied

The removal of all three major classes of pathogens that are of concern when wastewater is reclaimed was studied.. These pathogen studies include parasites, bacteria, and viruses. Pathogenic bacteria and viruses can be present in large numbers in biologically treated wastewater, however, disinfection prior to soil aquifer treatment is effective at eliminating pathogens. During previous studies

on soil aquifer treatment, no enteric viruses or enteric bacteria have been found in aquifers that were recharged with wastewater. This study particularly focused on examining the fate of *Cryptosporidium* during soil aquifer treatment and Hepatitis A, since these two pathogens are of concern and very little data on their fate during soil aquifer treatment existed.

The results were used to complement the development of a model to optimize the operation of soil aquifer treatment systems. Several components of the model were developed to aid the decision maker, optimized the removal of critical components, and to optimized recovery of recharged water and prevent mounding.

What are SAT Systems ?

An SAT system consists of five major components: (1) the pipe line that carries the treated effluent from the wastewater treatment plant; (2) percolation (infiltration) basins where the treated effluent infiltrates into the ground; (3) the soil immediately below the infiltration basins (vadose zone); (4) the aquifer where water is stored for a long duration; and (5) the recovery well where water is pumped from the aquifer for potable or non-potable reuse. A glossary of terms is provided at the end of this report.

Figure 1.2 illustrates the SAT system dynamics which can be described by the inputs of the system, the state of the system, and the outputs of the system. Inputs to the system include the

- soil type
- water quality
- operation of the SAT system
- environment

where each input effects the state of the system. The state of an SAT system includes the

- soil moisture profile within the vadose zone
- level of oxygen
- algal growth
- soil hydraulic conductivity

where the state of the system controls the residence time of water in the vadose zone and the level of microbial activity. Of particular importance is the level of oxygen which is related to the micro-organism distribution and oxygen demanding substrates. Algal growth is related to the clogging layer

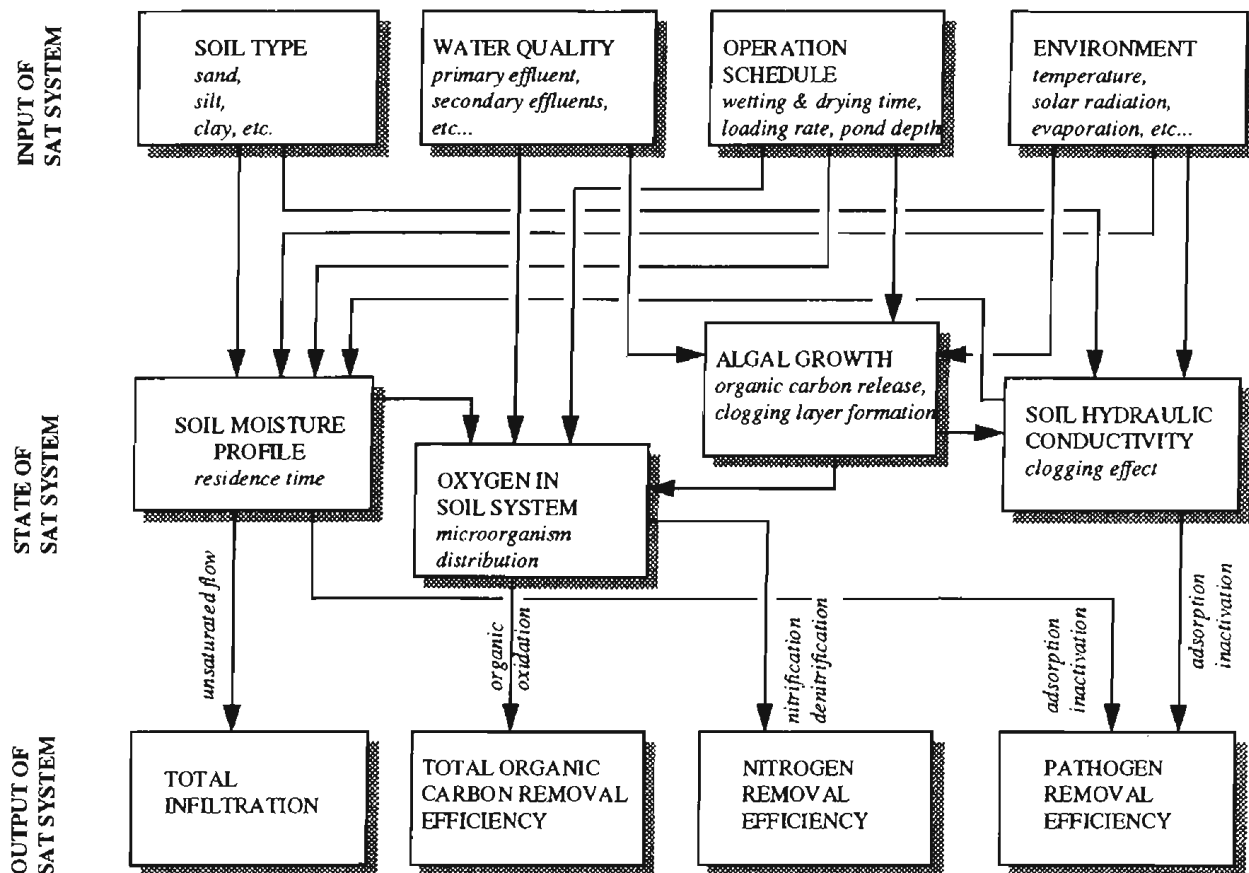


Figure 1.2 Soil aquifer treatment system dynamics

formation on the soil surface and effective soil hydraulic conductivity. The soil moisture is directly affected by inputs: soil type and the environment, and indirectly by the water quality which affects algal growth and the soil hydraulic conductivity. The oxygen in the vadose zone is affected by the soil moisture profile, the water quality of treated effluent, the operation schedule and the algal growth. Algal growth is affected by the water quality of the treated effluent, the operation schedule and the environment. Soil hydraulic conductivity is affected by the algal growth, the soil type, and the environment.

The critical outputs of the system are the total infiltration, the total organic carbon removal efficiency, the nitrogen removal efficiency, and the pathogen removal efficiency. The total organic carbon removal efficiency is primarily affected by the amount of oxygen in the system through the

organic oxidation process. Nitrogen removal efficiency is dependent upon the amount of oxygen and the availability of organic carbon through the nitrification-denitrification process. Pathogen removal efficiency is dependent upon the soil moisture profile and the soil hydraulic conductivity through the adsorption-inactivation process.

The major purification processes occurring in the soil aquifer system are: filtration, chemical precipitation/dissolution, organic biodegradation, nitrification, denitrification, disinfection, ion exchange, and adsorption/desorption. As part of a water reclamation process, Soil Aquifer Treatment (SAT) is a key step to polishing the water. This step provides for (a) mechanical filtration of suspended particles, (b) biological processes (e.g, breakdown of organics, nitrification-denitrification), and (c) physical-chemical retention of inorganic and organic dissolved constituents (e.g. phosphorous, potassium, trace elements), from the biologically treated waste water.

What Has Been Done Before ?

Infiltration basins (SAT systems) are by far the most widely used method for groundwater recharge and municipal waste removal (U.S. EPA, 1991). Because of the economical attractiveness and low cost maintenance, many SAT systems have been installed or are planned to be installed in the United States and other countries throughout the world. Los Angeles County implemented the use of SAT systems for groundwater recharge in the Montbello Forebay in the early 1960s. After over 20 years of operation and extensive study, no measurable impact on groundwater quality or human health could be established (Nellor et al., 1984). Bouwer (1980, 1985) studied SAT systems in the Phoenix metropolitan area with effluents from two different wastewater treatment plants. SAT systems have also been studied and used in Israel (Idelovitch et al, 1980) and in Australia (Ho et al., 1983). Wilson et al. (1995) has studied water quality changes and the fate of disinfection by-products at the Tucson Sweetwater Recharge Site. The largest SAT project to date is presently being considered on Phoenix, Arizona, and is a major focus of this research proposal.

Water reuse can be one of the most important strategies for meeting water quantity objectives in arid and semiarid regions like the southwestern United States. In a number of populous areas, local groundwater supplies are already augmented by treated wastewater that reenter the ground via managed infiltration practices or injection wells. The infiltration of wastewater effluents to

augment local aquifers is accomplished in shallow infiltration basins that are usually constructed in regions with permeable soils. The treated water simply percolates through the soil mantle and unconsolidated sediments, and then the vadose zone, to reach an unconfined aquifer. Although these activities are generally not located in the vicinity of production wells, waters that are added to local aquifers in this manner mix with the native groundwater and are eventually recovered and used again (see Figure 1.1). When recovered waters are used for potable purposes, the practice results in indirect potable reuse.

The managed infiltration of treated wastewater can be used in conjunction with engineered, above-ground wastewater treatment processes to guarantee the public health and to meet water reuse or drinking water quality standards at the point of withdrawal. Among the residual contaminants in treated wastewater that might inhibit the reuse of treated effluent for indirect potable applications are (i) organic constituents that resist degradation by aerobic process during the time frame of above-ground treatment processes (on the order of hours), (ii) nitrogen species that may eventually contribute to dissolved nitrate levels in groundwater, and (iii) pathogens that resist inactivation during above-ground treatment including viruses and protozoan cysts such as those of *Giardia*, and *Cryptosporidium*. The attenuation of these contaminants during infiltration and aquifer storage/transport of effluent that precedes its recovery and reuse is of great practical concern for the protection of the public health.

What This Project is About !

A combination of field testing, laboratory column studies, and computer modeling have been used to synthesize an understanding of SAT and to optimize the hydrological, physical, and biochemical processes involved. The removal mechanisms and their efficiencies have been correlated with various soil characteristics, effluent pretreatment methods, and hydraulic loading rates. Pilot-scale soil column studies have been conducted to analyze removal mechanisms and the long-term fate of wastewater effluent pollutants in SAT systems. Study results have been used to develop an SAT simulation model and an operation optimization model. The sustainability of SAT systems have been evaluated, and potential public health concerns and monitoring requirements have been identified to help ensure that a SAT system does not contribute to the degradation of potable groundwater supplies.

This research project has been designed to determine the water quality improvements during soil-aquifer treatment which include the sum of biological and abiotic processes that affect water quality during infiltration and temporary storage in the ground. The mechanisms of water quality changes during soil aquifer treatment are also of immense interest in as much as biological processes such as the chemical adsorption of wastewater constituents on soil surfaces may eventually exhaust the sorptive capacity of the soil and permit unwanted contaminants to reach points of groundwater withdrawal. Furthermore, there may be compromises between the physical capacity of a soil to transmit percolating waters and the ability of that soil to contribute to the removal of contaminants. Fine-grained soils provide the greatest impediment to water percolation but should facilitate water quality improvements that depend on sorption or the activities of microbial communities that are attached to soils. Determination of the relationships between the degree of above-ground treatment that is provided and the expected efficiencies of SAT for the removal of residuals that persist beyond that treatment are of primary importance. For organic carbon, the primary hypothesis in this area was an expectation that ozonation of wastewater prior to SAT would enhance the biodegradability of organic residuals and improve the efficiencies of SAT for the destruction of persistent organics. The importance of achieving the lowest possible levels of dissolved organics in waters following SAT arise from the potential for development of disinfection by-products such as trihalomethanes from residual organics when such waters are chlorinated prior to their reuse.

SOIL AQUIFER TREATMENT VERSUS CONVENTIONAL TECHNOLOGIES FOR WASTEWATER RECLAMATION

Soil aquifer treatment utilizes natural processes to produce high quality water as opposed to conventional technologies for wastewater reclamation which utilize engineered systems to accomplish the same goals. The source of wastewater available to municipalities for reclamation is most often municipal wastewater that has been treated by biological treatment (secondary treatment) to remove the majority of solids and organic components. Conventional advanced tertiary treatment technologies for reclamation of biologically treated wastewater include chemical addition, sand filtration, activated carbon adsorption, and membrane treatments such as reverse

osmosis. These technologies can be effective but they are expensive, energy intensive, and produce chemical sludges, high strength wastewaters, along with other by-product solid wastes. With enough energy and money almost any water can be used to produce high quality water, but the cost and associated wastes produced make such applications prohibitive.

Soil aquifer treatment primarily uses biological processes that naturally occur in soils to produce high quality water and recharge groundwater supplies. In general, the quality of groundwater tends to be much better than surface waters because as water percolates from the surface to the groundwater table, a variety of natural processes improve water quality. Another analogy is bank infiltration which is commonly used in Europe to improve the quality of surface waters by pumping river water through the ground to utilize natural biological process before the water is treated for use as a drinking water source. After biologically treated municipal wastewater has percolated through several feet of soil, the organic water quality characteristics are comparable to many surface waters. Natural processes continue to improve water quality as the water percolates to the groundwater which may be over 100 feet (30.48 m) below the surface. In some cases, soil aquifer treatment appears to improve the quality of groundwater when the groundwater has been impaired by agricultural contaminants. Contamination from agricultural activities is a common reason groundwaters in Arizona do not meet drinking water standards.

Soil aquifer treatment has the potential to recharge groundwater which provides many benefits not obtained when water is directly reclaimed using conventional technologies. One major benefit is that water may be stored for years in the ground before it is recovered for reuse. Storage of water in the ground is more efficient than surface storage where evaporation and potential exposure to contaminants are serious problems. Water reclaimed by conventional technologies can be directly injected into the groundwater, but the cost and energy requirements are very high. Recharging groundwater through soil aquifer treatment reduces the costs to recover groundwater since groundwater tables rise and the energy necessary to pump the groundwater to the surface is reduced. Water reclaimed by conventional technologies can be used immediately for non-potable uses, however, when the water must be stored, large expensive surface reservoirs must be constructed. Soil aquifer treatment not only holds potential to recharge dwindling groundwater supplies, but also has the potential to improve groundwater quality in many areas.

RESEARCH OBJECTIVES

The main objective of this study has been to develop criteria for the design and operation of SAT systems based on soil characteristics, effluent types, and infiltration rates. The performance of SAT systems were evaluated by studying the components of SAT (see Figure 1.1) in order to maximize the output: total infiltration, total organic carbon removal efficiency, nitrogen removal efficiency, and pathogen removal efficiency. Sustainability has been determined by extensively studying removal mechanisms and quantifying abiotic and biotic removal contributions. Simulation and operation models have been developed for determining the best operation schedule for maximizing infiltration and at the same time considering the other three outputs of the system (see Figure 1.2).

The primary objectives of this study were as follows:

- Demonstrate the feasibility of an SAT system for potable reuse using pilot scale column studies. Water quality has been evaluated by monitoring for nitrogen, TOC (total organic carbon), and pathogens.
- Establish removal mechanism as a function of soil types using five different soils with different particle size distributions. The soil types included a sand, two silts and a clayey soil from the proposed Phoenix SAT site, and a sandy soil with some fines from the Tucson SAT site.
- Determine the effect of effluent pretreatment level on SAT performance using six different effluents including chlorinated-denitrified, dechlorinated-denitrified, and chlorinated secondary effluent from the 91st Avenue WWTP in Phoenix and chlorinated and chlorinated-ozonated secondary effluents, and primary effluent from the Roger Road WWTP in Tucson, Arizona.
- Develop an SAT system simulation model applicable to a variety of soil conditions and effluent pretreatment methods.
- Develop an SAT system operation optimization model.
- Develop methodology for the eventual optimal pumpage for future recovery of water.

Other important objectives of the study were:

- Study the clogging layer to establish detailed profiles of biological and abiotic activities
- Determine the feasibility of ozone dosage pretreatment.

- Study removal of pathogens recognized as high risk, including an evaluation of SAT potential of removing *Cryptosporidium*.
- Identify parameters to be monitored to ensure that sufficient SAT is achieved to protect potable groundwater supplies.
- Study the mechanical and hydraulic properties of clogging layers.

RESEARCH PLAN

Elements of the technical proposal included pilot scale column studies, related field studies, laboratory studies, and development of simulation models and optimal operation models. The research plan has been executed by the team of investigators from Arizona State University (ASU), the University of Arizona (UA), and the University of Colorado, Boulder (UC) illustrated in Figure 1.3.

Personnel from ASU have been responsible for pilot-scale SAT experiments in 8 foot (2.6 m) columns fed with wastewater effluent from the 91st Avenue WWTP, Phoenix, Arizona. Independent variables in pilot-scale work included effluent type, soil type and wet/dry cycle times. This effort comprised a major portion of the backbone of the overall experimental program. Due to the impracticality of initiating field studies with effluent, particular attention was given to investigating the effects of soil reconstruction in the soil column studies and correlating these studies with clean-water field percolation studies. ASU had primary responsibility of compiling the data analyses, developing the simulation model and developing an operational optimization model.

UA investigators operated 3.3 foot-length (1 m) columns fed with secondary chlorinated, and chlorinated-ozonated effluents from Roger Road WWTP in Tucson, Arizona. The columns used soil from the Tucson Sweetwater infiltration site and intact soil cores from the proposed Phoenix SAT site. UA investigators lead in the design and execution of pathogen transport/inactivation experiments. They evaluated SAT removal efficiency of *Cryptosporidium* and Hepatitis A virus and identified potential public health concerns. UA was also responsible for developing an optimization model for determining the optimal pumpage of the aquifer for recovery of water.

- Pilot-scale column studies using soils from the proposed and existing SAT sites. Sets of columns were operated as SAT systems with five different soils and six different effluent qualities.
- Extensive laboratory studies were used to quantify individual abiotic and biotic removal mechanisms, to determine the effects of preozonation on BDOC (biodegradable dissolved organic carbon), and to investigate the effect of soil reconstruction on column studies.
- Detailed data analysis were performed to develop monitoring requirements and models for the optimal design and operation of SAT based on relationships between effluent pretreatment levels, soil types, and infiltration rates.

Process performance, removal mechanisms, and monitoring requirements were determined for the following water quality parameters:

- Health-effect-related parameters, including pathogens and DBPs (disinfection-by-products) represented by HAAs and THMs
- Dissolved organic carbon (DOC)
- Nitrogen (Org-N, NH_3 , NO_2^- , NO_3^-)

The original technical objectives were accomplished by performing the following major tasks:

Task 1 Evaluate Existing Soil Data and Complete Analysis of Proposed SAT Site Soils

Task 2 Construct Columns and Fill with Different Soils

Task 3 Column Operation: Monitoring and Sampling

Subtask 3a Flooding and Drying Cycle Variation

Subtask 3b Routine Monitoring for Basic Water Quality Parameters

Subtask 3c Temporal/Spatial Variation in SAT Efficiency Studies

Subtask 3d Virus Attenuation Studies/Cryptosporidium Removal

Subtask 3e Analysis of Disinfection By-Products

Task 4 Laboratory Soil Column Experiments for Determination of Hydrologic Properties, Effects of Sample Disturbances, and Abiotic Removal Mechanisms

Subtask 4a Determine Hydraulic Parameters

Subtask 4b Determine Effects of Sample Disturbance

Subtask 4c SAT Simulation in Undisturbed Samples

Subtask 4d Determine Breakthrough Curves for TOC And NH_3 For Abiotic Removal Studies

- Task 5 Field Percolation Studies At Proposed Phoenix Sat Site (performed by *Greelea and Hansen*)
- Task 6 Studies on Specific Biological Activities
- Task 7 Fundamental Studies on Clogging Layer Development
- Task 8 Study Accumulation of Abiotically Removed Substances
- Task 9 Data Analysis, Environmental Effects, and SAT Monitoring Needs
- Task 10 Develop an SAT Simulation Model for Design Purposes
- Task 11 Develop an SAT System Operation Optimization Model and an Optimal Pumpage Model
- Task 12 Prepare Final Report

FUNDAMENTALS OF SAT SYSTEMS

The concept of SAT depends on the infiltration of treated wastewater into the soil and percolation through the vadose zone. Improvements in water quality can occur due to many different mechanisms including filtration, biological degradation, physical adsorption, ion exchange and precipitation. This combination of removal processes can be very effective in removing organic compounds, nitrogen, phosphorus, pathogens, suspended solids, and trace metals. Efficiencies of removal for specific water quality constituents are a function of the type of soil, level of pretreatment, and cycle times. The removal of nitrogen, organic compounds, and biochemical oxygen demand(BOD) can be a continuous biological process that is sustainable. Removal of trace metals, phosphorous, and refractory organics by abiotic mechanisms can result in accumulation in the soil and eventual breakthrough. Bouwer (1984) has estimated that accumulation of trace metals and phosphorous could become a problem in future decades.

Previous research has demonstrated that during operation of SAT systems, cyclic flooding and drying of the basins is necessary both to improve infiltration rates and control aerobic/anoxic conditions in the soil. Basins are flooded until infiltration rates decrease due to development of a surface clogging layer. The majority of treatment in SAT systems occurs in the upper strata of soil, near the clogging layer (see Figure 1.4). Therefore, the clogging layer and upper strata of soil are critical to efficient SAT performance. During normal conditions, a cross-section of unsaturated porous medium in Figure 1.5 illustrated that voids consist of water and air. Previous

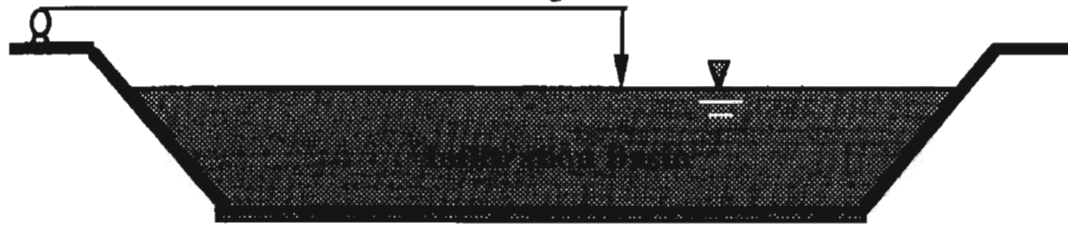
Operational Controls:

Pumping rate

Pumping schedule

(wetting-drying)

Sewage Effluent



Surface Clogging Layer

infiltration

physical clogging

biological clogging



Unsaturated Zone

unsaturated flow

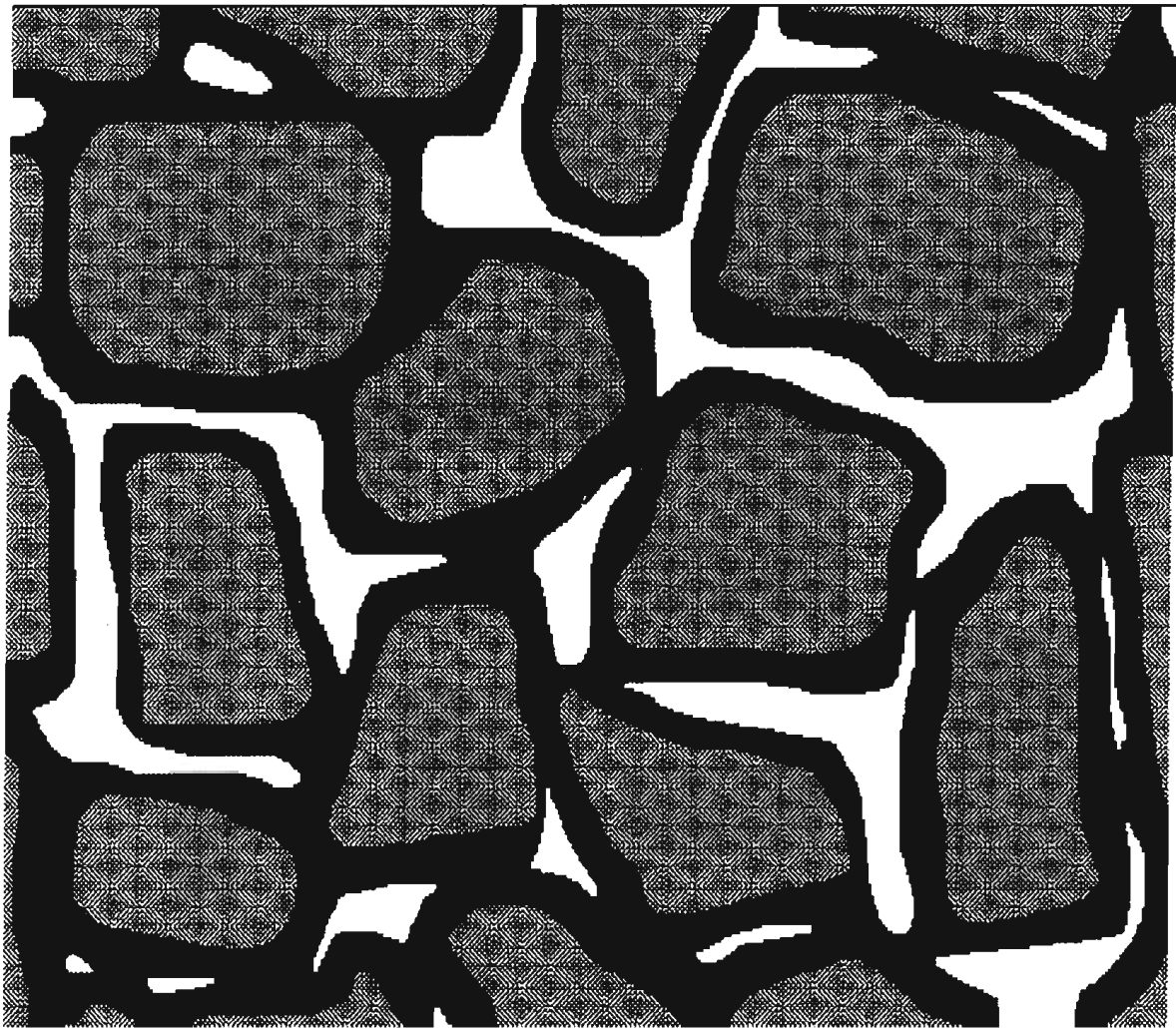
solute transport

biochemical reaction (nitrogen and organics removal)

biological clogging



Figure 1.4 Processes related to operation of SAT system



solid



water



air

Figure 1.5 Prior to SAT, the air spaces are void and allow for infiltration of water

research suggests that a correlation may exist between certain predominate soil characteristics present in the vadose zone (unsaturated zone) and treatment efficiency. However, during the course of operation of soil treatment systems, infiltration of solids and biofilm development in the upper strata results in a clogging layer. Reduced infiltration rates are caused by the accumulation of biofilm, algae, and suspended solids reducing the void space as illustrated in Figure 1.6.

This reduction in infiltration rates adversely affects the operation of SAT systems, and cyclic flooding/drying of the basins is necessary. Basins are flooded for a given duration of time until infiltration rates are reduced. When infiltration rates decrease, flooding of the basin is ceased and the remaining water in the basin is allowed to infiltrate. The soil surface of the basin is allowed to dry and the clogging layer is removed by natural processes, or the soil surface is physically cleaned. Cycle times also influence the presence of oxygen with depth in the vadose zone and the depth of groundwater. Therefore, cycle times are critical to controlling the processes to optimize biological removal (in particular nitrogen removal) and to prevent reduced infiltration rates from groundwater mounding. Almost all research indicates that the upper layer of the vadose zone is where most removal occurs, in particular biological removal which may continue indefinitely, and that the upper layer controls infiltration rates due to the presence of a clogging layer.

The removal of organic carbon and nitrogen in SAT systems (see Figure 1.7) is coupled and the removal mechanisms include adsorption-desorption and biodegradation. During the flooding period, dissolved oxygen in the vadose zone often becomes limited and the primary removal mechanism for organic carbon is adsorption while ammonia is removed by ion exchange. Larger gravel and sands tend to hold larger air pockets which increases aerobic biodegradation of carbon and nitrification of ammonia during flooding. Smaller soils that typically contain more clays and silts have large adsorptive and ion-exchange capacities to remove organic carbon and ammonia. Extremely long flooding time can exhaust the removal capacity for ammonia when insufficient ion-exchange sites for ammonia are present and/or adsorbed organic carbon blocks ion-exchange sites. During drying, the soil in the vadose zone becomes aerobic, however, desiccation of the upper soil layer can decrease biological activity and hinder removal since most removal occurs in the upper soil layer. As the flooding cycle begins again, the nitrate that was produced from nitrification becomes soluble. Denitrification will occur if sufficient organic carbon, and low dissolved oxygen are simultaneously present. Longer flooding cycles and/or the use of primary effluent tend to increase the mass of adsorbed carbon which,

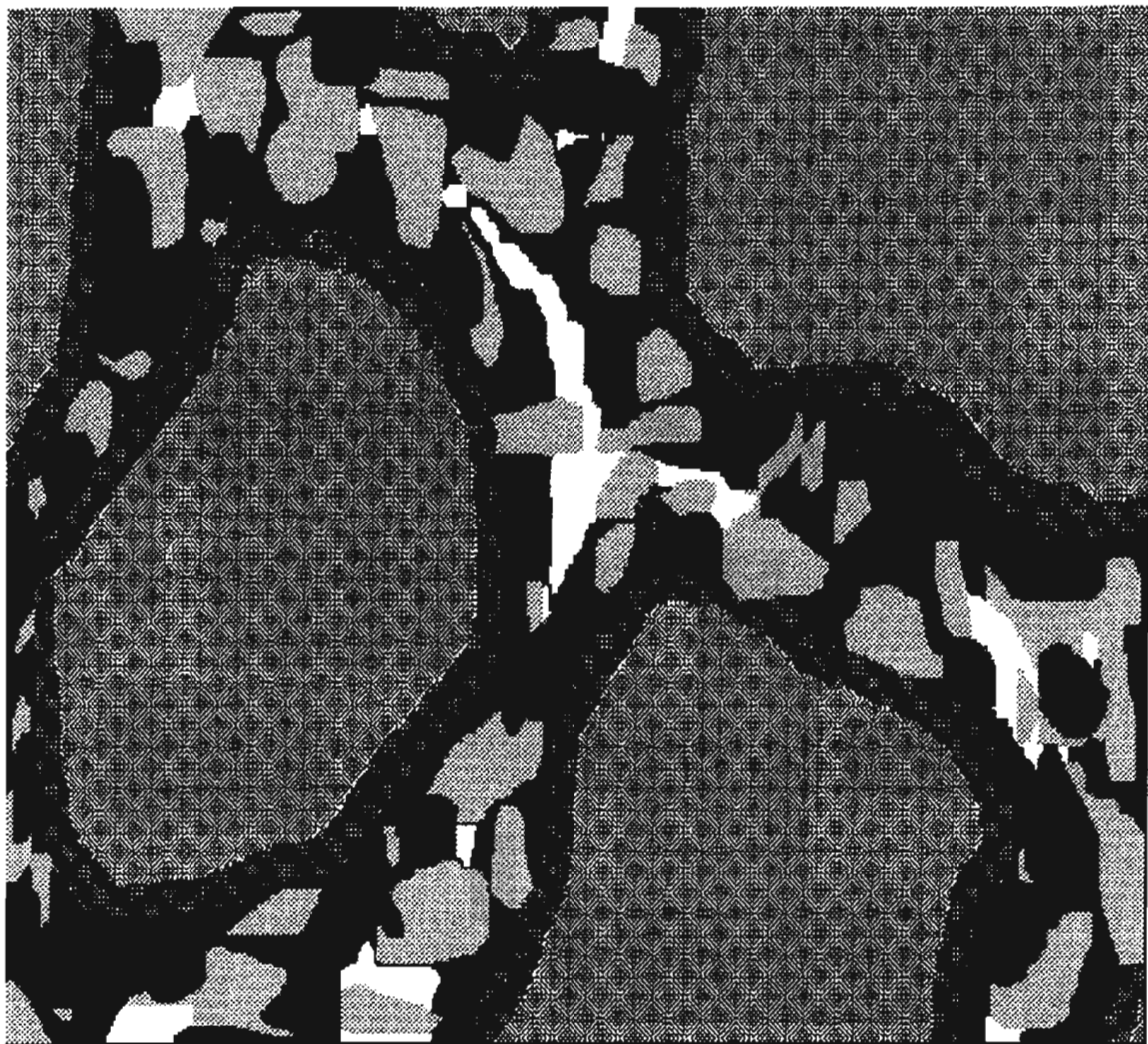


Figure 1.6 After SAT the air spaces become filled with biofilm, algae, and SS. In addition, a mat of algae can cover the surface greatly reducing infiltration rate

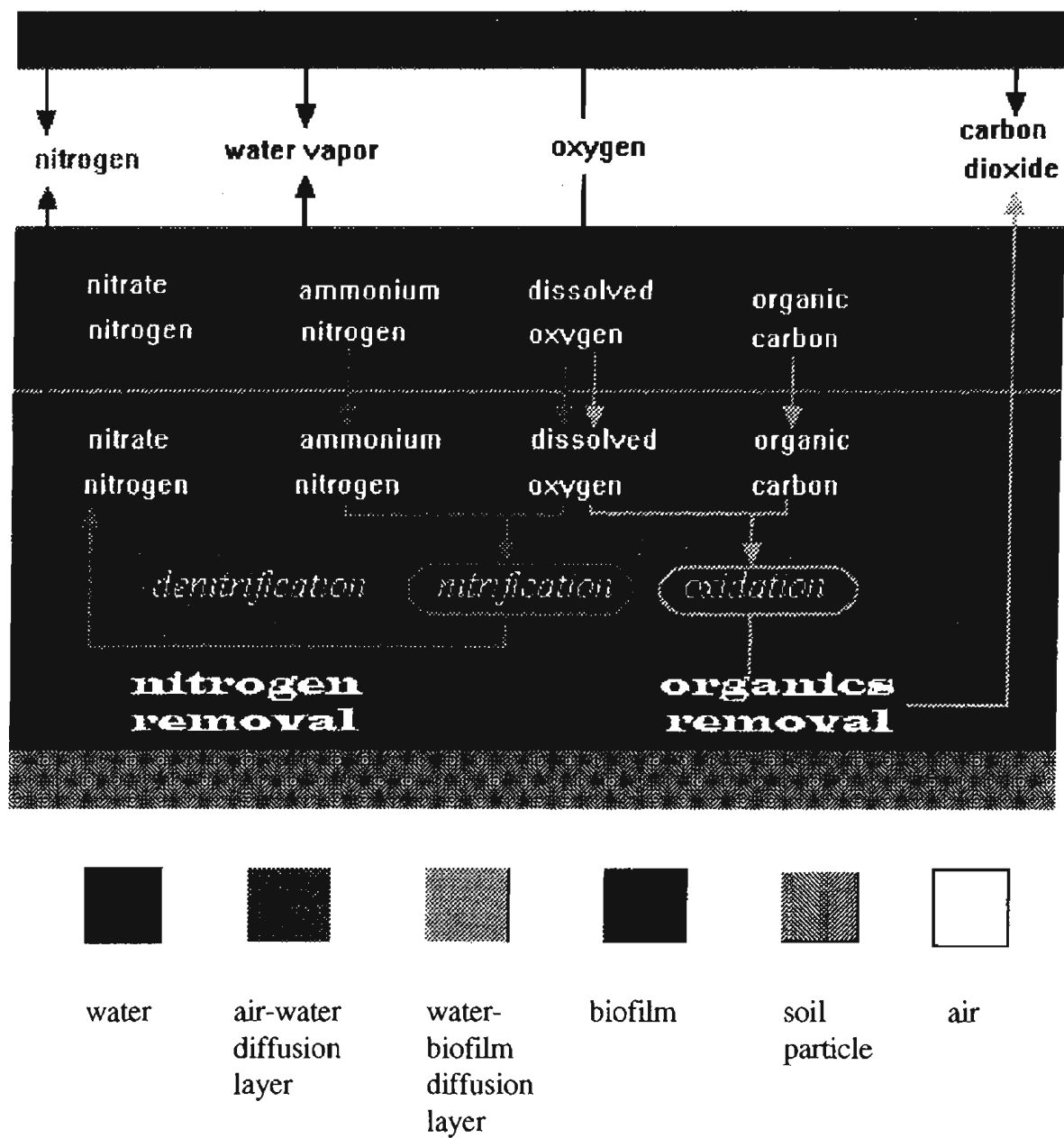


Figure 1.7 Flowdiagram of the nitrogen cycle in SAT system

in turn, can increase total nitrogen removal.

Tremendous efforts have been made in this research project toward unraveling the interactive physical, chemical, and microbiological mysteries of the flow and transport processes in the unsaturated zone. However, these comparatively isolated bodies of current knowledge have not been fully integrated and utilized for simulation/prediction purposes until recently, not to mention the management of the soil aquifer treatment system in a systematic way. The application of comprehensive large-scale SAT system modeling previously was just in the development stage. This research project has made a step forward on a basic understanding of the mechanisms that control the effectiveness of SAT systems and their eventual wide spread usage in the arid and semi-arid regions of the world.

REFERENCES

- Bouwer, H., 1985, Renovation wastewater with rapid infiltration land treatment systems, in: *Artificial Recharge of Groundwater*, T. Asano (ed.), pp.359-395, Butterworth Publishers, Boston, Massachusetts.
- Bouwer, H., R.C. Rice, J.C. Lance, and R.G. Gilbert, 1980, Rapid-infiltration research - the Flushing Meadow Project, Arizona, *Journal Water Pollution Control Federation*, 52(10):2457-2470.
- Ho, G.E., K. Mathew, and P.W.G. Newman, 1983, Water quality improvement of treated wastewater by soil percolation, in: *Proceedings of Seminar, "Water Quality, Its significance in Western Australia"*. Water Research Foundation of Australia, Perth.
- Idelovitch, E., R. Terkeltoub, and M. Michall, 1980, The role groundwater recharge in wastewater reuse: Israel's Dan Region Project. *Journal AWWA*, 72(7):391-400.
- Nellor, M.H., R.B. Baird, and J.R. Smyth, 1984, *Health Effects Study Final Report*. County Sanitation District of Los Angeles County, Whittier, CA.
- U.S. Environmental Protection Agency, 1991, EPA/U.S. *Arid Water Reclamation Reuse Guidelines*.

COLUMN DESIGN AND OPERATION

ASU- 3-meter columns

The design of the pilot scale columns that are in operation at the 91st Avenue waste water treatment plant is summarized in this section. The columns are approximately 2.7 m long, they have a 30.5 cm inside diameter and are comprised of two 1.35 m sections. The top section of the columns is shown in Figure 2.1. The majority of the sampling ports have been located in the top section of the column since most of the removal reactions are expected to occur there. The sampling ports have been used to measure soil suction, redox potential/dissolved oxygen (ORP/DO) and obtain liquid samples. These ports are positioned at depths of 5.0, 10.2, 15.2, 30.5, 61, and 127 cm below the soil surface, with extra ORP/DO ports at depths of 7.6, 12.7, 17.8, and 20.3 cm deep. The tensiometers consist of a ceramic porous cup (1 bar, standard flow) which has been glued into a HDPE elbow fitting. The elbow fitting has been equipped with a plexiglass chamber to hold water and the chamber is sealed by a septum stopper. The liquid sampling ports consist of 0.5 μ or 2 μ stainless steel porous cups tightly fastened into barbed fittings. A vacuum is applied to the barbed end to extract liquid samples. The ORP/DO samplers consist of a tube to male connector with a 0.95 cm diameter, 0.32 cm thick Supelco septum placed inside. The septum allows for penetration into the soil column by the microelectrode used for oxidation-reduction and by syringe used to take liquid samples for dissolved oxygen measurements. The tops of the columns are equipped with overflow weirs, shown in Figure 2.2, to maintain pond depths at 17.8, 33 and 45.7 cm. Effluent that overflows from the weirs is collected in effluent reservoirs and recycled to the column by peristaltic pumps. The bottom section of the columns is shown in Figure 2.3. This bottom section contains one row of sampling ports located at 127 cm below the soil surface.

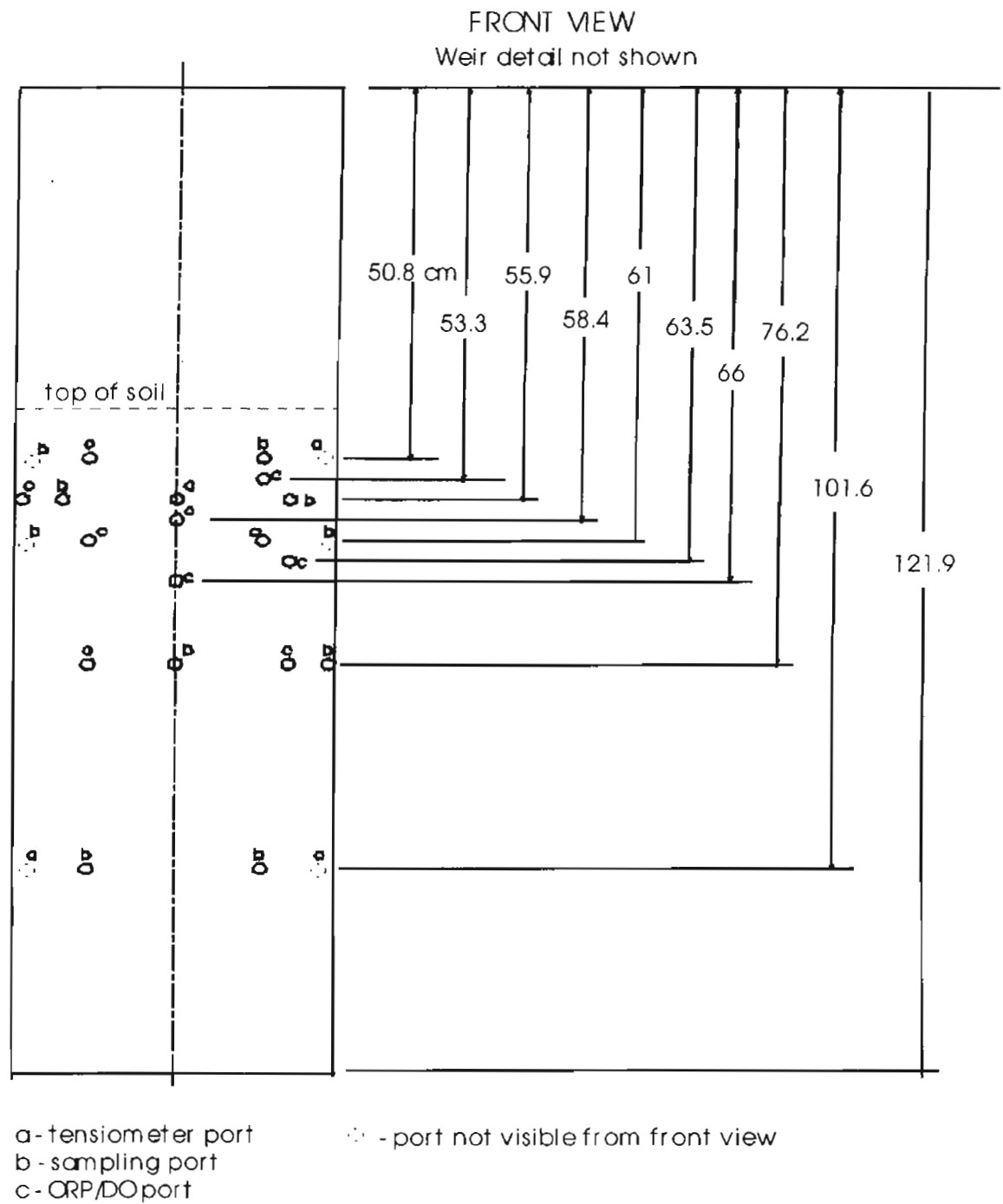
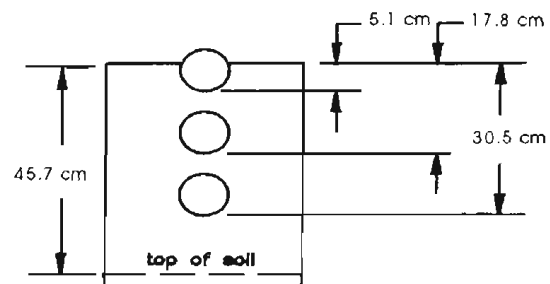
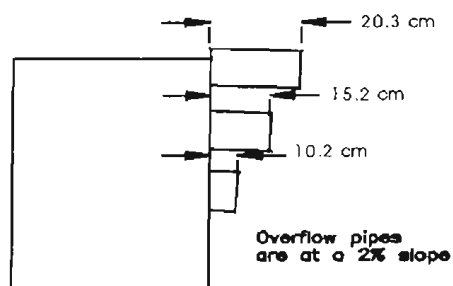


Figure 2.1 Top Section of Pilot Scale Columns



FRONT VIEW



SIDE VIEW

Figure 2.2 Weir Detail of Pilot Scale Columns

Front View

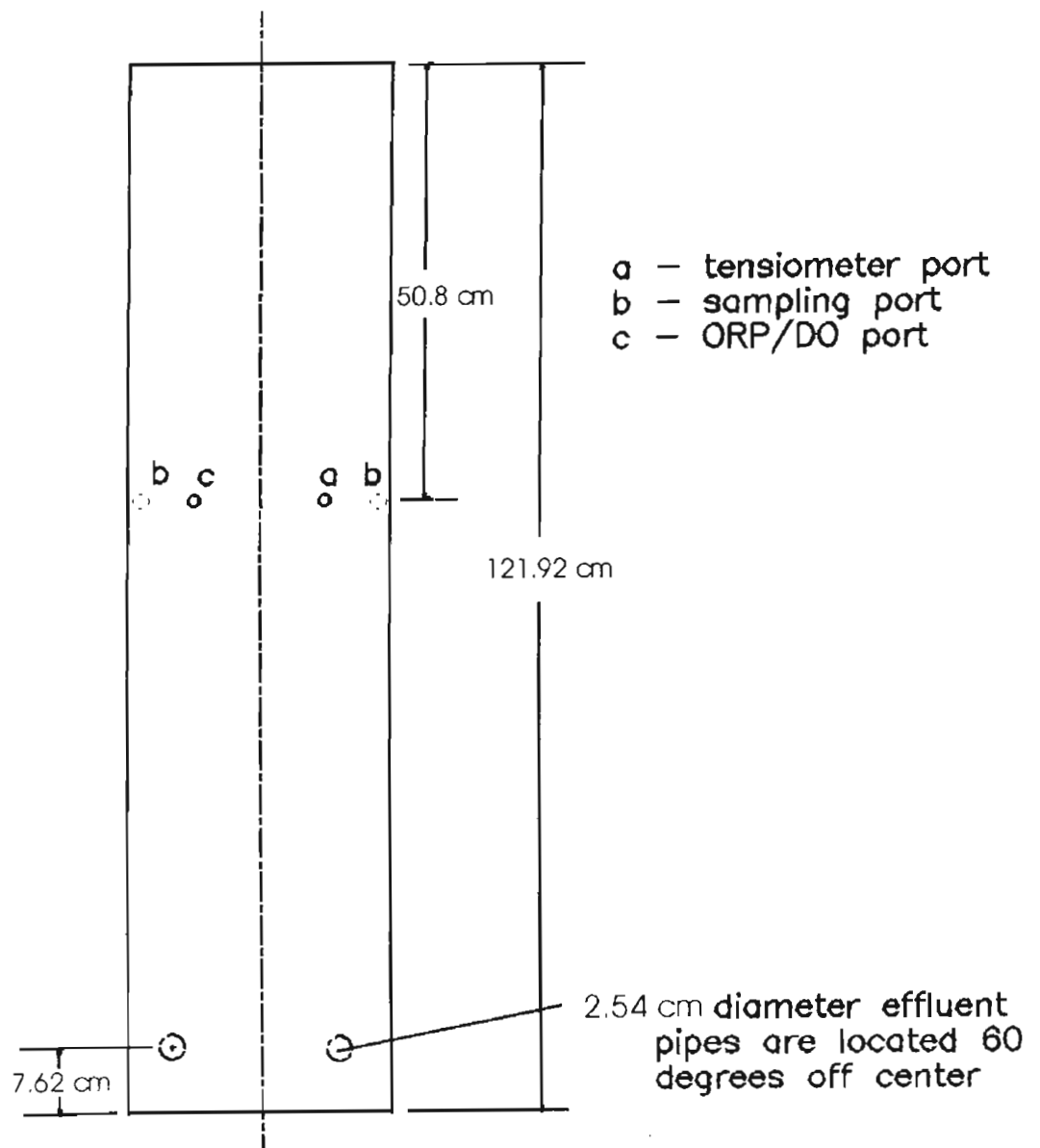


Figure 2.3 Bottom Section of Pilot Scale Columns

Two 15.2 cm long, 2.54 cm O.D. effluent pipes have been welded at 7.6 cm from the column bottom and at 60 degrees off center. These pipes allow for the collection of effluent and maintenance of base boundary conditions. Base boundary conditions are maintained by pulling a slight vacuum on the pipes with the use of a Gast vacuum pump. The base boundary suction was checked periodically by use of a tensicorder. Effluent from the columns was allowed to flow freely or was captured in collection vessels to estimate effluent flow rates. The columns were constructed in two sections to help facilitate the packing of the columns with soil at in-situ densities. The bottom sections were underlain with 0.32 cm neoprene sheets and silicon was applied to obtain a watertight seal. Prior to compaction, six inches of underdrain support medium consisting of silica sand and/or gravel was placed in the bottom of the column. Each underdrain system was designed to prevent movement of the soil into the underdrain without creating resistance to flow greater than each soil's resistance. Compaction of the soil was carried out in four inch lifts to achieve in-situ densities. After compaction, the columns were wrapped with cooling lines and foam rubber insulation to maintain typical in-situ temperatures during the hot summer months.

UA- 0.18 meter, 1 meter, and 2 meter Columns

18-cm Repacked Columns

The design of the schmutzdecke soil columns is shown in Figure 2.4. These columns were 23 cm in length. The soil depth was 18 cm, allowing for 5 cm depth of ponded water within the column. The headspace of each column was sealed from the atmosphere. Effluent was applied to the column headspace via foil-wrapped glass tubing connected to a glass burette, providing a constant hydraulic head (approximately +1.5 ft) to each column. The columns were constructed out of 3.0" inner diameter acrylic tubing with 3/8" sidewalls and were equipped with multiple ports at five soil depths for measurement of soil water tension and soil oxygen content. A wastewater flow schematic for the schmutzdecke columns is shown in Figure 2.5. Effluent was stored in five gallon plastic Nalgene jerricans at 4°C and applied to the columns using peristaltic pumps. Foil-wrapped glass tubing was used to minimize changes in wastewater quality prior to column application.

A total of nine schmutzdecke columns were used. GE Gro-lights were positioned above each column to simulate natural sunlight, promoting development of algae on the soil surface. Integral to each column top plate was a quartz disc (Figure 2.4), allowing the full spectrum of UV-visible light generated by the Gro-lights to impact onto the soil surface. Light exposure was limited by an automatic timer set for 12 hours per day. All 18-cm columns were packed with sieved Sweetwater sandy loam (obtained from Basin #1 at the Sweetwater Underground Storage and Recovery Facility). Bulk density and porosity values for the columns ranged from 1.49 to 1.57 g/cm³ and 0.41 to 0.44, respectively.

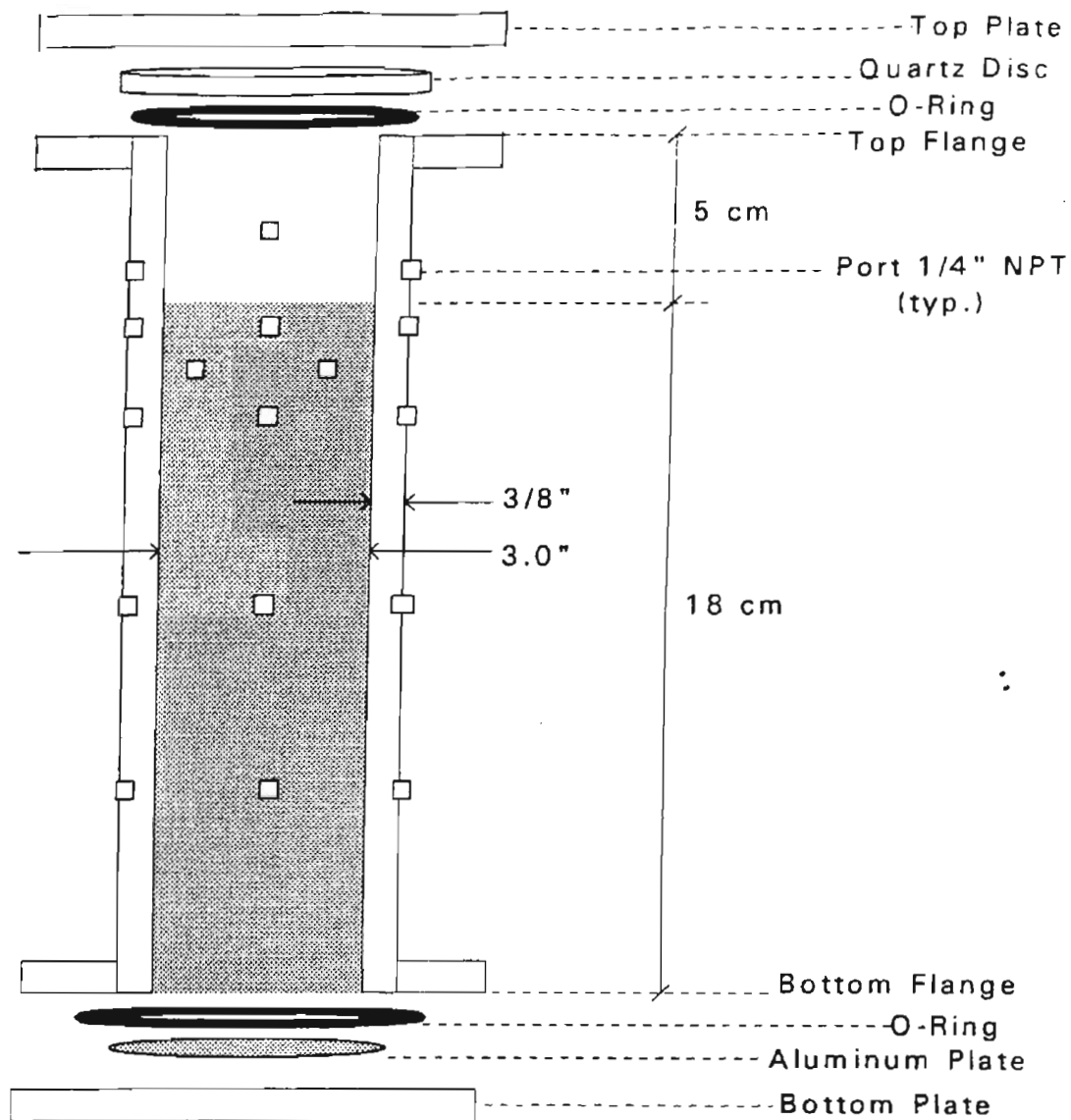


Figure 2.4 Schematic diagram of 18 cm column used for simulating SAT. Total soil depth was 18 cm; total length of column was 23 cm.

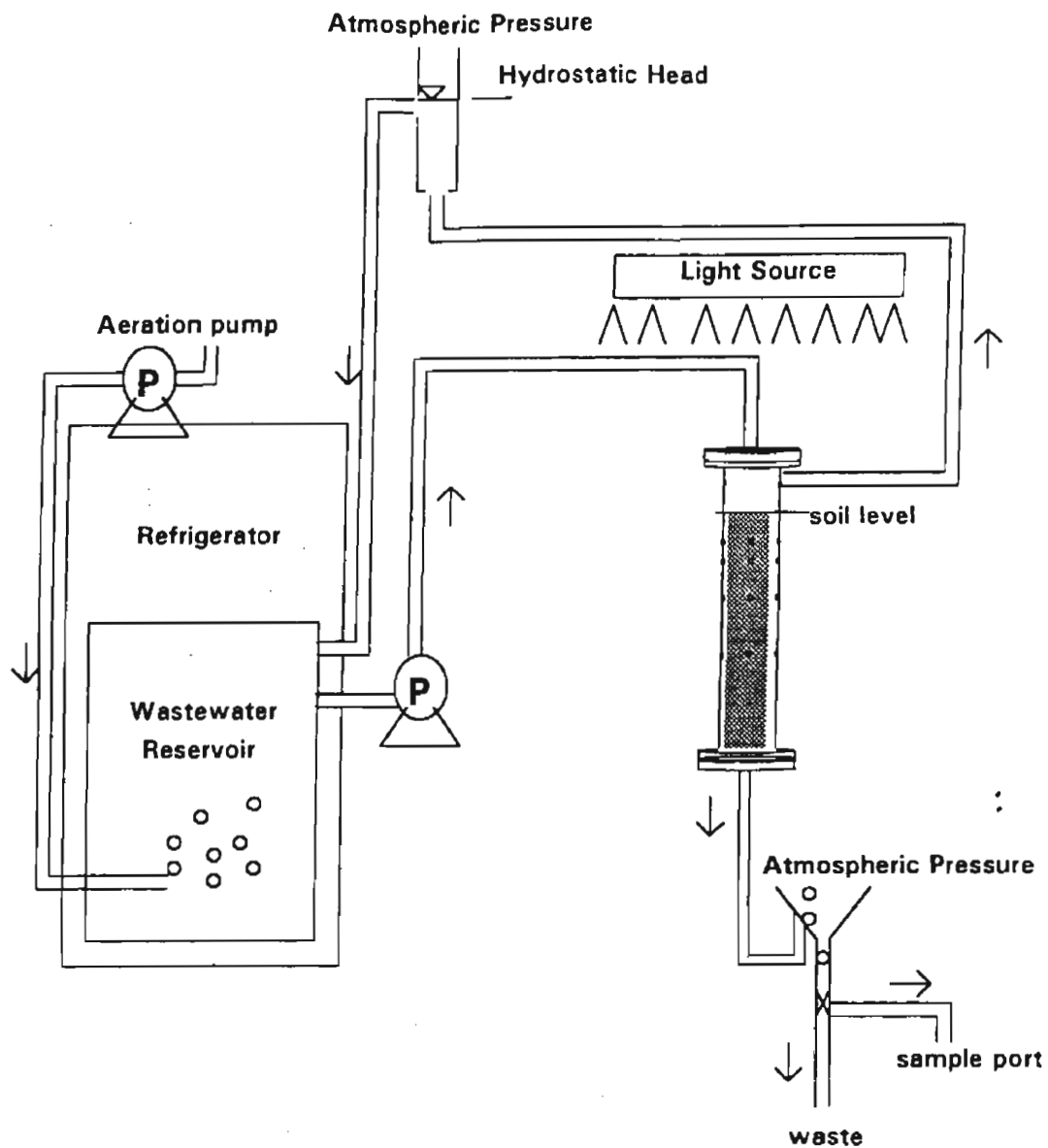


Figure 2.5 Flow schematic for effluent supply to 18-cm columns. Applied hydraulic head was provided by a separate burette for each column. Artificial light (GE Grolight) was applied to the soil surface for 12 hours per day.

1-m Repacked Columns

Figure 2.6 shows the design for the 1-m columns containing repacked sediments. A schematic diagram of the column reactor setup is shown in Figure 2.7. Fourteen 1-meter columns containing either repacked homogenized soils or intact soil cores were used. Columns consisted of 8.62 cm I.D. acrylic tubes with a 0.64 cm wall thickness. Total column length was 130 cm; soil depth was 100 cm leaving a 30 cm headspace for ponding of effluent above the soil surface. Each column was equipped with a series of ports at multiple depths (2, 4, 6, 12, 34, 56, 78, 96, 98 cm) for the measurement of matric potential (via tensiometers), collection of liquid samples, and measurement of molecular oxygen. Tensiometers and liquid samplers consisted of 0.64 cm O.D. stainless steel porous cups (Mott Metallurgical Corp.) that were TIG-welded onto 6.4 cm stainless steel (316 grade) tubes. Pore sizes of the porous cups were 2.0 μm for columns containing Agua Fria sand and Sweetwater sandy loam and 0.5 μm for columns containing North Pond silt. Pore sizes were selected to permit collection of liquid samples using modest suctions, without exceeding the air entry value of each soil type.

The effluent-supply plumbing system used in these experiments was designed to minimize changes in effluent organic quality prior to column application. Peristaltic pumps (Masterflex) and foil-wrapped glass tubing were used to transfer effluent to each column. Before column application, effluent stored in 5-gal. plastic jerricans at 4°C was warmed to 25°C using a water bath (Figure 2.4). Pump speed was set so that a constant head upper boundary condition of 25 cm was maintained in each column, while minimizing over-flow through a weir.

Columns were operated in two-week cycles consisting of 7 days of flooding followed by 7 days of drying. Artificial light sources (VITA-Lite) were used (12 hr per day, timer controlled) to stimulate algal growth in the ponded effluent and on the soil surface (Figure 2.7). An aquarium air pump provided aeration of the ponded effluent during the first half of the experimental period. Artificial aeration was discontinued prior to initiation of nitrogen transformation studies.

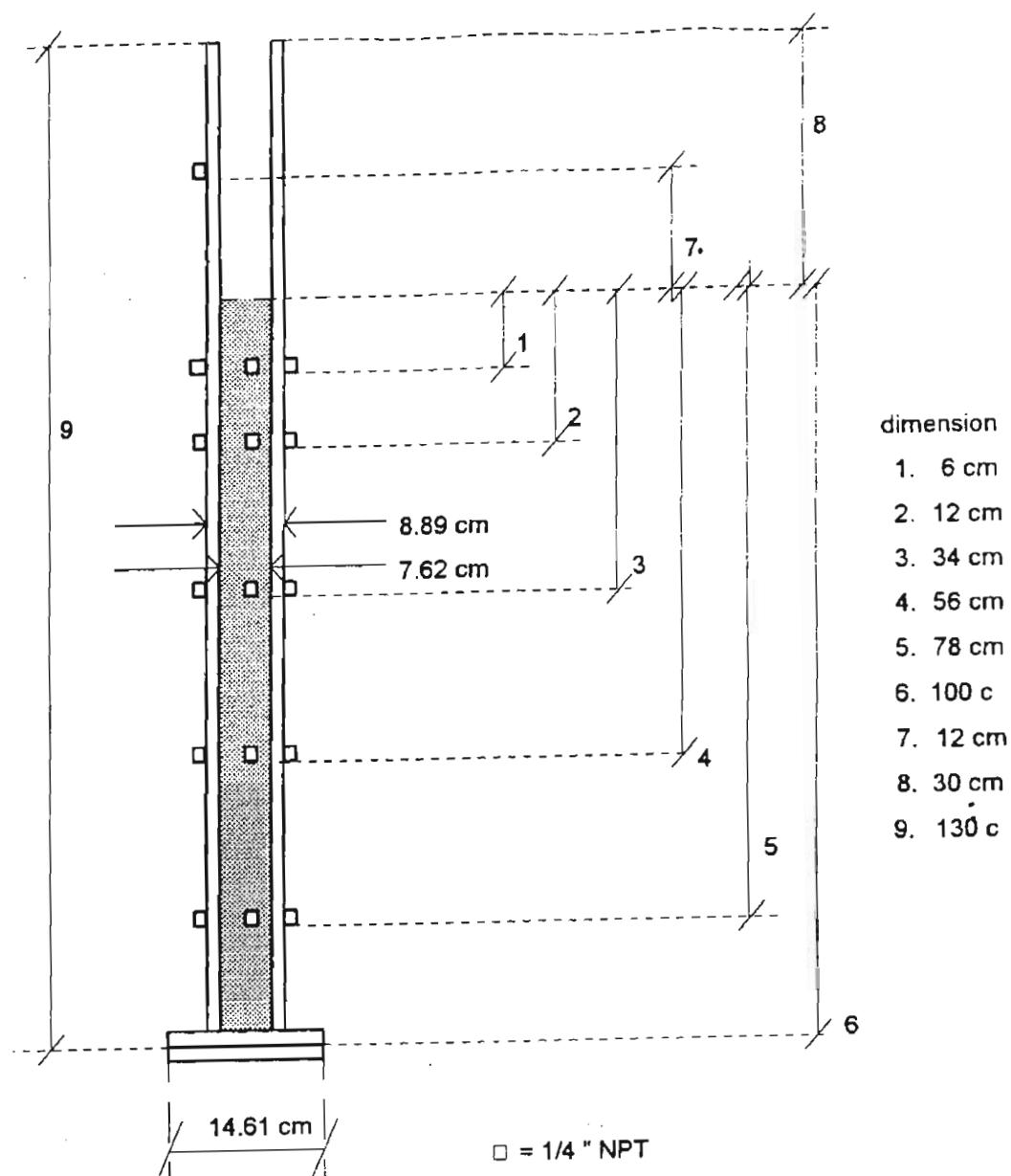


Figure 2.6 Schematic of 1-meter SAT column. Total soil depth was 100 cm. Each level of ports contained a tensiometer, a liquid suction sampler, and a fitting for soil oxygen measurement.

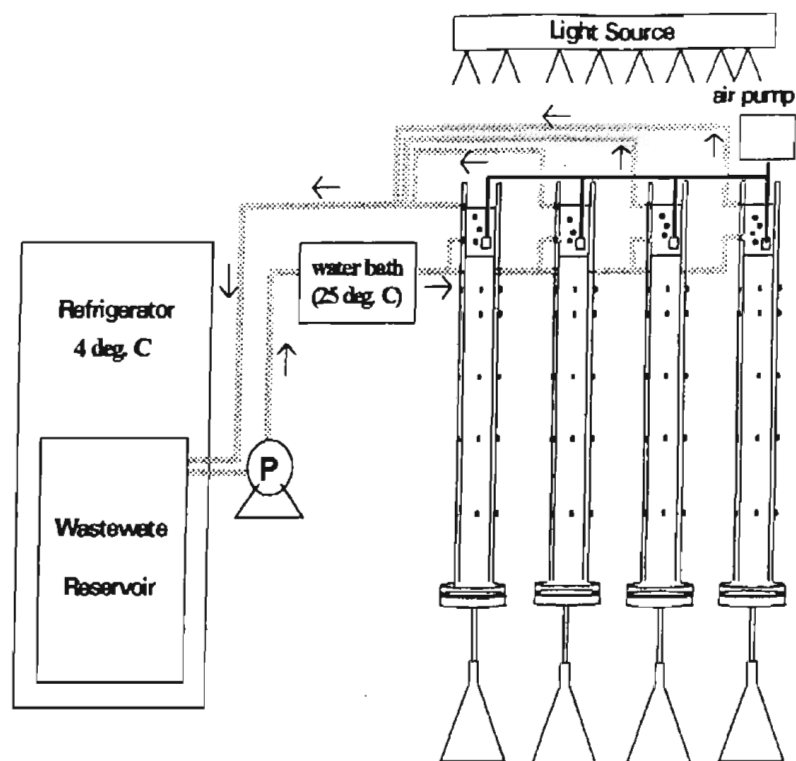


Figure 2.7 Schematic representation of 1-m column reactor setup. Effluent was stored at 4°C and then warmed to 25°C prior to application to the columns. Constant head was maintained using a weir.

1-m Intact Core Columns

Figure 2.8 shows the design of the stainless steel columns used for collection and study of intact soil cores. Three intact soil cores were collected on August 24, 1994; one soil core was collected at each of the three Phoenix area soil sites: North Pond silt, agricultural field clay, and Agua Fria river sand. Intact cores were collected using a drill rig supplied by Envirodrill. Each stainless steel column was driven into the ground using the 140-lb hammer on the drill rig. The columns were then twisted, breaking the soil seal, and hydraulically "jacked" back out of the ground. Cores were obtained at the respective locations where soils were collected for use in the packed column studies conducted by U of A and ASU.

The three intact core columns were equipped with tensiometers, liquid suction samplers, and ports for measurement of soil oxygen content, using predrilled ports designed for this purpose. Problems were encountered during placement of some of these fittings because of large cobbles within the soil cores at locations where ports had been pre-machined in the column wall. Ports blocked by cobbles were sealed with threaded nylon plugs.

2-m Repacked Column

Design details for the two-meter column are shown in Figure 2.9. The 2-m column was packed with Agua Fria sand and operated under similar conditions as the 1-m columns. The additional meter of soil depth allowed for examination of effects due to increased detention time and percolation depth on the removal of organics, transformation of nitrogen species, and removal of pathogens.

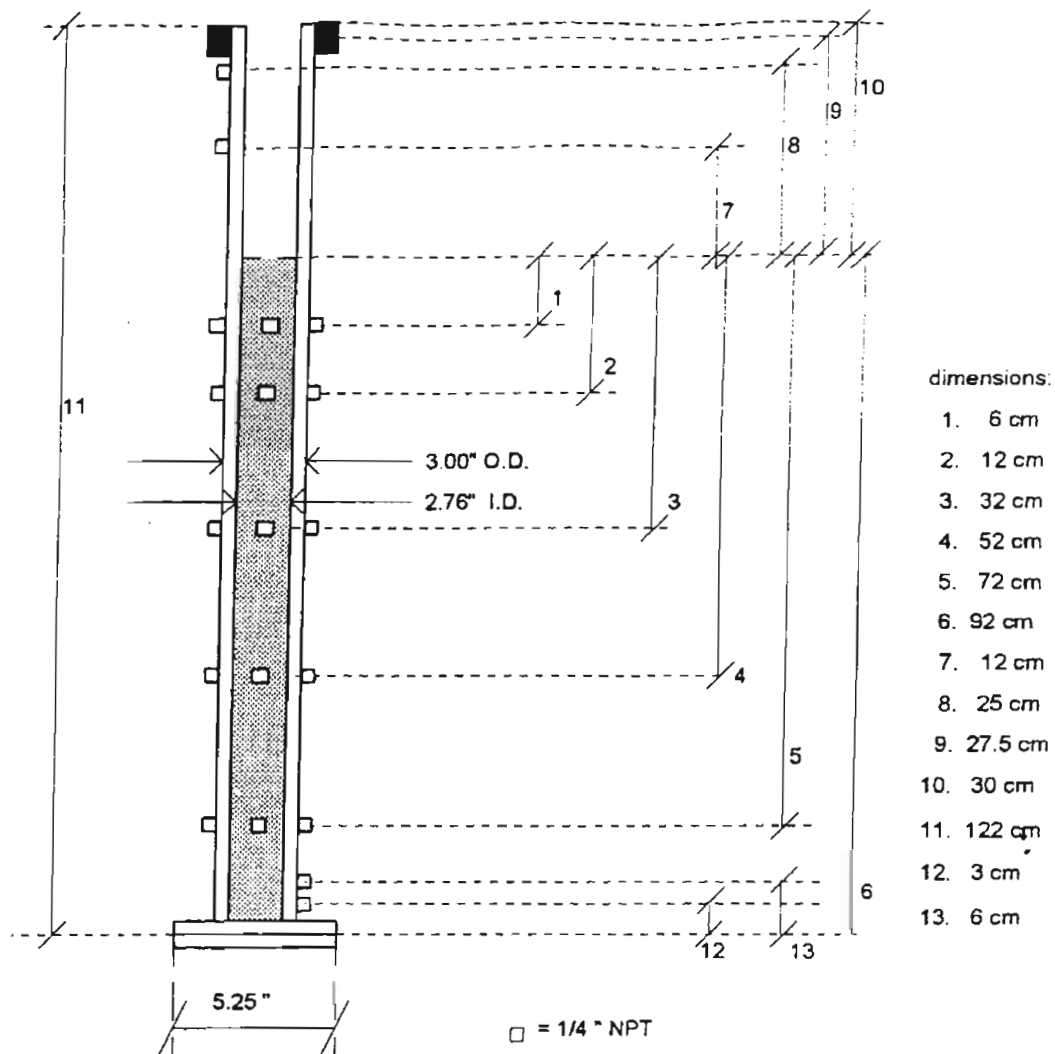


Figure 2.8 Schematic diagram of 1-m stainless steel column used for collection and study of intact soil cores.

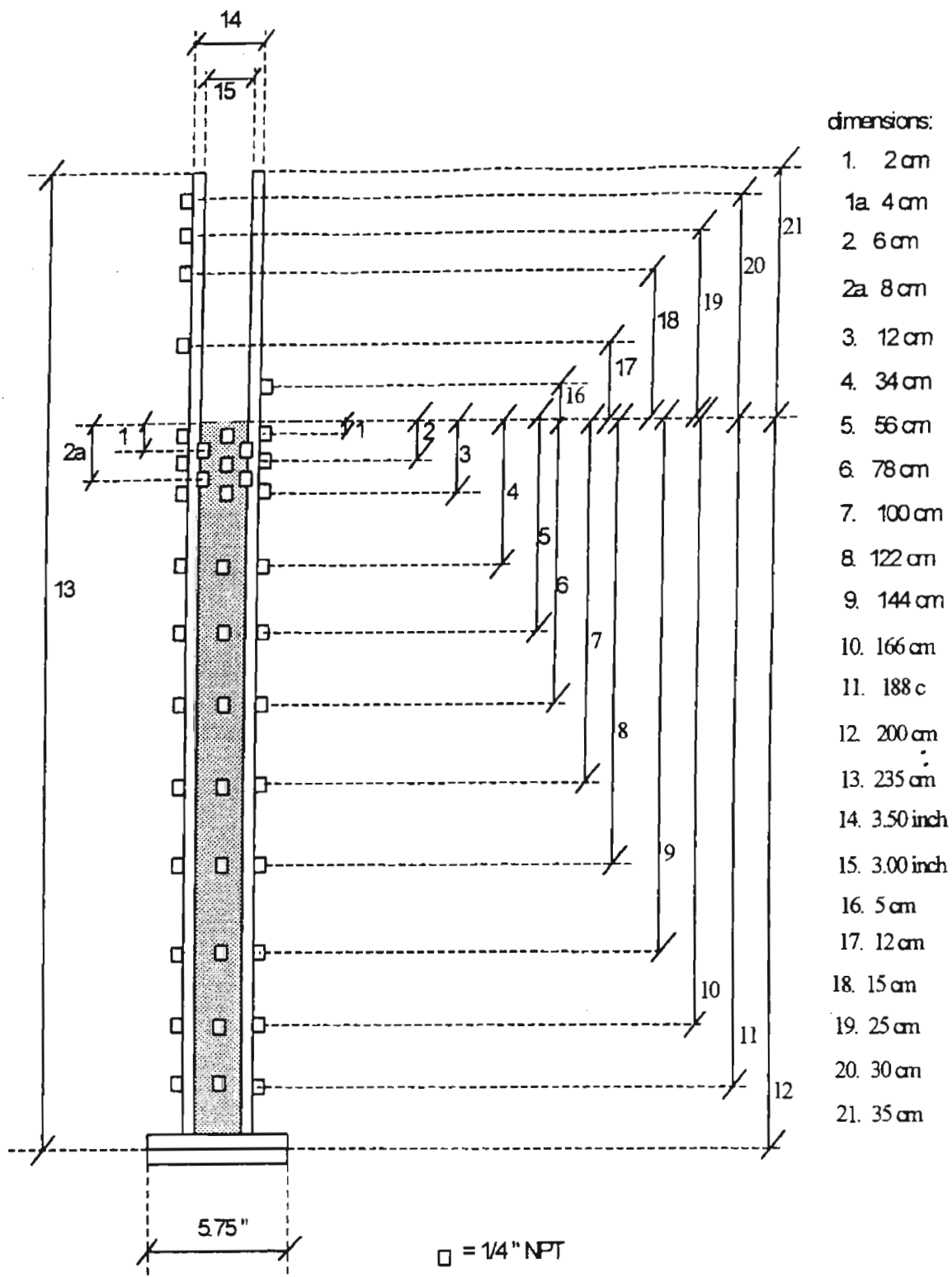


Figure 2.9 Design schematic for 2-m column used for simulating SAT.

Wet/Dry Cycles, Ponding Depths and Infiltration Rates

Arizona State University

This section summarizes the operating conditions for the ASU 91st Avenue Columns. Several operating conditions will be discussed: wetting/drying time, ponding depth, average surface infiltration rate, and base boundary condition.

The columns were operated using variable wetting and drying periods to determine the effect these variables have on the removal of nitrogen, the removal of organic carbon, infiltration rates, and algal growth. The North Pond silts were operated under 4 wetting/drying schedules, the Agua Fria Sand columns were operated under 2 wetting/drying schedules, and the South Pond Silts were operated under only one wetting/drying schedule.

Ponding depth was studied to determine the effect on infiltration and contaminant removal. The North Pond silts used a 17.8 cm ponding depth throughout most of the study, the cycles 48 through 50 were operated at a 17.8 cm pond for the first 7 days of wetting, then at 44.4 cm for the last 5 days of wetting. Cycles 50 onward were operated at 44.4 cm of pond depth. The Ag. Field Clay was operated with a 17.8 cm pond depth until its operation was terminated. The Agua Fria Sand and South Pond Silt columns were not operated under ponded conditions for most of their study periods due to effluent and pumping limitations. From cycles 17 onward the South Pond silt columns were operated under 17.8 cm of pond depth.

Infiltration rates (in cm/day) were not intentionally controlled by the operators (except for the Agua Fria sands and South Pond Silts) but are provided in this section for general information. The infiltration rates for the columns were calculated by taking the total influent volume divided by the total length of the wetting time. Column averages were obtained by averaging the infiltration rates for a particular operating schedule. The infiltration rates of the Agua Fria Sands and South Pond Silts were controlled by the pumping rate. Pumping and effluent limitations led to the inability to achieve ponded conditions.

The base boundary condition was controlled by means of a vacuum pump at the bottoms of the North Pond Silt columns and Ag. Field Clay columns. These columns were operated under 100 cm and 400 cm of suction, respectively.

The following sections summarize these operating conditions in table format for each of the soil types.

North Pond Silt Columns. The North Pond Silt columns were operated under the four wetting/drying schedules summarized in Table 2.1. The length of drying time, length of wetting time, the number of cycles, the time of year the operating schedule occurred, the base boundary condition and the infiltration rates are provided.

Operation of the North Ponds Silts columns began with an operating schedule of 7 days wetting and 7 days drying. Approximately half of the total study period was an acclimation period for the columns. Schedule 2 is a shorter version of Schedule 1 with 3 days wetting and 4 days drying. Note that Schedule 2 in Table 2.1 occurred during the coolest time of the year. The decrease in temperature during this schedule is not only reflected in the decrease in average surface infiltration rate, but in the nitrification results that will be presented in following sections. Schedule 3 added 3 extra days of drying to Schedule 2 to promote nitrification and regain infiltration potentials. Schedule 3 is compounded by the warming weather which also served to increase nitrification and infiltration potentials. The lack of denitrification in the columns prompted Schedule 4 which has a longer wetting time to stimulate denitrification and a sufficiently long drying time to regain infiltration potential.

Table 2.1
Summary of operating conditions for ASU North Pond silt columns
(#1-6)

	Wetting Time	Drying Time	Cycle #s	Dates of Operation	Base Boundary Condition	Average Infiltration Rate cm/day
Schedule 1	7 days	7 days	1-16	May 94 to November 94	0 cm on all columns cycles 1 - 7 100 cm on all columns cycles 8 - 16	18.8 ± 4.9
Schedule 2	3 days	4 days	17-32	November 94 to March 95	100 cm on all columns	12.9 ± 2.0
Schedule 3	3 days	7 days	33-42	March 95 to July 95	100 cm on all columns*	17.1 ± 5.6
Schedule 4	12 days	7 days	43-50	July 95 to December 95	100 cm on #1, #3, and #5 0 cm on #2, #4, and #6	14.8 ± 2.5

* Vacuum system for #2 and #4 started to fail at cycle 38.
Average infiltration rates calculated for one column only - column #2.

Agricultural Field Clay. The two Ag. Field Clay columns (#7 and #8) were operated for 17 cycles (May 1994 to December 1994) under a 17.8 cm ponding depth. The cycle times ranged from 7 to 12 days wetting and 7 days drying. The infiltration rates started at 21.3 cm/day and gradually decreased to 3.0 cm/day by the end of the study.

Agua Fria Sand Columns. The Agua Fria sands (#9 and #10) were operated under two operating schedules: 1) 14 days wetting, 7 days drying and 2) 7 days wetting, 7 days drying. Table 2.2 describes the dates and cycles these schedules occurred as well as the average infiltration rate.

Table 2.2
Summary of operating conditions for the ASU Agua Fria sand columns
(#9 and #10)

	Wetting Time	Drying Time	Cycles	Dates of Operation	Average Infiltration Rate (cm/day)
Cycle 1	14 days	7 days	7-15	August 94 to January 95	250
Cycle 2	7 days	7 days	1-6 16 onward	May 94 to August 94 January 95 - April 95	125-500

South Pond Silt Columns. The South Pond Silt Columns (#11 and #12) began operation in March 1995 and a 7 day wetting/7 day drying schedule has been their only mode of operation. However, these columns have been operated under two ponding depths: no pond and 17.8 cm of pond. The infiltration rate is maintained at xxx to xxx cm/day. Table 2.3 summarizes the operating conditions for the South Pond Silt columns.

Table 2.3
Summary of operating conditions for the ASU South Pond silt columns
(#11 and #12)

	Wetting Time	Drying Time	Cycles	Dates of Operation	Pond Depth (cm)	Average Infiltration Rate (cm/day)
Cycle 1	7 days	7 days	1- 16	May 95 to September 95	0	250
Cycle 2	7 days	7 days	16 onward	September 95 to April 95	17.8	15-250

Needs text and tables summarizing wet/dry cycles, ponding (if any), and infiltration rates (see ASU above)

SOILS

The ASU 91st Avenue columns were packed with four soil types : two silts, a sand, and a clay. The soils were obtained from four sites within the proposed recharge area and are named as follows: Agua Fria sand, North Pond silt, South Pond silt, and Agricultural (Ag.) Field clay. The U of A columns were packed with two soil types: the Agua Fria sand and a soil not from the proposed recharge site, the Sweetwater sand. Table 2.4 provides data on several soil properties for each soil type, as well as the designated ASU and U of A column number.

Table 2.4

Soil properties of ASU 91st Avenue columns and U of A columns

Recompacted								
Soil	Description	USGS	Saturated	Clay	Cation	Total	ASU	U of A
		Designation	Hydraulic	Content	Exchange	Organic	Column	Column
			Conductivity	(% by wt)	Capacity	Content	#	#
			(cm/sec)			(% by wt)		
					(meq/100 g soil)			
Agua Fria Sand	Poorly Graded Sand	SP	N/A	N/A	2.4	.32	#9 #10	
North Pond Silt	Silty Sand	SM	1.8×10^{-4}	3	7.1	1.14	#1, #2, #3, #4, #5, #6	
South Pond Silt	Silty Sand	SM	6.9×10^{-4}	2	6.9	0.97	#11, #12	
Ag. Field Clay	Low Plasticity Clay	CL	3.5×10^{-6}	54	22.3	3.03	#7, #8	
Sweet-water	Poorly Graded / Silty Sand	SP-SM	1.9×10^{-2}	N/A	5.7	0.70		

EFFLUENT TYPES AND CHARACTERISTICS

Arizona State University

Three effluents from the 91st Avenue Wastewater Treatment Plant (WWTP) were applied to the 91st Avenue columns: chlorinated secondary, chlorinated denitrified and dechlorinated denitrified. The chlorinated secondary effluent is biologically treated by activated sludge, while the two denitrified effluents are treated by a nitrifying/denitrifying process. The dechlorinated denitrified effluent was obtained as chlorinated denitrified and was dechlorinated by the ASU students prior to pumping into the columns. Typical influent values for ammonia, nitrate, nitrite (all as nitrogen) and dissolved organic carbon are provided in Table 2.5. Table 2.5 also lists the columns that receive each effluent type.

Table 2.5
Typical influent nitrogen and DOC values for ASU 91st Avenue columns

Effluent	NH ₃ -N (mg/l)	NO ₃ ⁻ -N (mg/l)	NO ₂ ⁻ -N (mg/l)	DOC (mg/l)	Column #
Chlorinated Secondary	10.0 - 30.0	0.0 - 5.0	1.0 - 3.0	13.0 - 15.0	#5 and #6
Chlorinated Denitrified	1.0 - 3.0	1.0 - 5.0	0.1 - 0.8	8.0 - 10.0	#1, #2, #7, #9 and #11
Dechlorinated Denitrified	1.0 - 3.0	1.0 - 5.0	0.1 - 0.8	8.0 - 10.0	#3, #4, #8, #10 and #12

More information needed from ASU regarding 91st Avenue plant; parallel to U of A

University of Arizona

Table 2.6 summarizes the influent nitrogen and DOC values for the effluents studied at the University of Arizona. Primary and secondary effluents were obtained from the Roger Road Wastewater Treatment Plant in Tucson. The secondary wastewater was manually dechlorinated

by U of A students. Ozonation and nitrification of secondary wastewater was also carried out at the University of Arizona.

Table 2.6
Typical influent nitrogen and DOC values for U of A
effluents derived from Roger Road Treatment Plant

Effluent	NH ₃ -N (mg/l)	(NO ₃ ⁻ + NO ₂ ⁻) -N (mg/l)	DOC (mg/l)
Unchlorinated Secondary	9.0 - 24.0	4.0 - 6.0	8 - 15
Ozonated Secondary	12.0 - 22.0	5.0 - 6.0	9 - 16
Nitrified Secondary	0.0 - 0.7	13.0 - 19.0	6 - 9
Primary	20.0 - 28.0	0.0 - 0.4	14 - 42

Roger Road Wastewater Treatment Plant (Tucson, Arizona)

The plant uses two trickling filters (biotowers) for secondary treatment, and has a capacity of 35 MGD. The biotowers use B.F. Goodrich PVC plastic media that is 26 feet in height and 165 feet in diameter. Each tower can treat the plants maximum capacity of 35 MGD. The media is designed to support a naturally growing biofilm that receives its nutrients from clarified primary effluent. Clarified primary is pumped to the top of the biotower and sprayed over the surface with a rotating sprinkler and allowed to trickle down the media surface. Once the effluent reaches the bottom of the biotower, it is further treated with secondary clarifiers. The plant is capable of modifying the feed water to the towers with recycle that mixes part of the secondary treated wastewater with the clarified primary. As with all biological systems, the

quality of the treatment is a function of the influent constituents, concentration and ambient temperature. Colder climatic conditions slow the biotreatment process and both ammonia and organic concentrations are treated less efficiently.

Wastewater Collection and Storage

Clarified secondary wastewater was collected from the Roger Road WWTP in Tucson from the overflow weirs at the secondary clarifiers using a submersible pump and then transferred and stored in twenty-liter Nalgene jerricans. In some cases, the plant's chlorinated product water was used. This water was dechlorinated immediately upon acquisition by adding 10 mL of a 20 g/L sodium thiosulfate solution to each 20-liter jerrican, then transported to the University of Arizona and refrigerated at 4 °C.

University of Colorado

Table 2.7 lists the secondary effluents used and the biological process utilized in the wastewater treatment plant prior to discharge. All effluents were either exposed to activated sludge or a trickling filter; additionally, one effluent was nitrified and denitrified to reduce nitrogen species. The DOC's for these effluents ranged from 8.8 to 17.8 mg/L.

Table 2.7
Secondary effluents studied by the University of Colorado

Secondary Effluent	Location	Biological Process	Average DOC (mg/L)
A1	Boulder, CO	Activated Sludge	10.3
A2	Orange County, CA	Activated Sludge	8.8
A3	Phoenix, AZ	Activated Sludge	9.4
T1	Greeley, CO	Trickling Filter	10.0

T2	Orange County, CA	Trickling Filter	17.8
T3	Roger Road Plant	Trickling Filter	12.9
	Tucson, AZ		
NDN	91st Avenue Plant	Activated Sludge plus	8.8
	Phoenix, AZ	Nitrification/Denitrification	

Upon receipt of the wastewater, residual Cl_2 was measured then dechlorinated with 125% of the stoichiometric concentration of sodium thiosulfate. After thorough mixing, the residual Cl_2 was measured again to assure complete dechlorination. The samples were filtered through 1 μm glass fiber filters (Gelman Sciences Corp., Ann Arbor, MI) to remove suspended solids, and stored at 4°C until utilized.

All pertinent characteristics of Silver Lake source water may be found in MURPHY (1993) as data collected during previous research conducted by Murphy and Dr. Gary Amy, is utilized to compare the biodegradability of surface water NOM with effluent organic matter (EfOM).

Column, Soil and Effluent Summary

Arizona State University

The table below provides a summary of the information presented in the previous sections for each ASU 91st Avenue field column. Soil type, effluent type, base boundary condition, average infiltration rate, and ponding depth are reviewed.

Table 2.8
Summary of ASU 91st Avenue field columns

Column	Soil Type	Effluent Type	Boundary Condition	Avg. Infiltration Rate (cm/day)	Pond Depth (cycle #:cm)
#1	North Pond Silt	Chlorinated Denitrified	-100	15.9	1 - 47:17.8
#2	North Pond Silt	Chlorinated Denitrified	-100		1 - 47:17.8
#3	North Pond Silt	Dechlorinated Denitrified	-100		1 - 47:17.8 48 -:17.8 to 44.4
#4	North Pond Silt	Dechlorinated Denitrified	-100		1 - 47:17.8 48 -:17.8 to 44.4
#5	North Pond Silt	Chlorinated Secondary	-100		1 - 47:17.8 48 -:17.8 to 44.4
#6	North Pond Silt	Chlorinated Secondary	-100		1 - 47:17.8 48 -:17.8 to 44.4
#7	Ag. Field Clay	Chlorinated Denitrified	-400		17.8
#8	Ag. Field Clay	Dechlorinated Denitrified	-400		17.8
#9	Agua Fria Sand	Chlorinated Denitrified	0		0
#10	Agua Fria Sand	Dechlorinated Denitrified	0		0
#11	South Pond Silt	Chlorinated Denitrified	0		1 - 16:0 16 -:17.8
#12	South Pond Silt	Dechlorinated Denitrified	0		1 - 16:0 16 -:17.8

University of Arizona

A similar summary table would be beneficial to the final report

PROCEDURES

BDOC (Bench Scale Bioreactors)

University of Arizona

Biodegradable dissolved organic carbon (BDOC) was determined by separate batch tests conducted in an acclimated sand system. Sixty grams of clean sand was transferred to a 250-mL Erlenmeyer flask. The sand was biologically activated by contact with primary effluent for three days that was continuously agitated to maintain aerobic conditions. This enabled a rapid development of a microbial seed population on the sand. Six reactors were made to improve the precision of the experiment. The reactors were rinsed after each run with a saline solution (0.15M NaCl and 1mM MgCl₂) to remove residual organics. With the microbial population as the only source of degradation, 150 mL of secondary or ozonated secondary effluent was added to the acclimated sand and again placed on the shaker table. Samples (10mL) were taken at time zero and every 24 hours thereafter for five days and analyzed for DOC and ultra-violet light absorbance at 254 nm (UVA₂₅₄). This was replicated for many cycles to ensure that the sand was fully acclimated and that the results were reproducible. Once a steady-state condition was reached, samples were taken on the fifth day only.

University of Colorado

BDOC was measured in both the non-ozonated and ozonated samples. BDOC represents the difference in DOC over a five day period of sample recirculation through sand with a acclimated biofilm, and corresponds to the biodegradable fraction of the bulk DOC.

Two different sources of bacteria were utilized for BDOC experiments. The first were bacteria from a local surface water collected with an in-line sand filter at the intake of the local water utility for a period of thirty days. The second set of bacteria were acclimated onto a sand bed with the source being a combination of a) chlorinated, then dechlorinated, secondary effluent, b) non-chlorinated secondary effluent, and c) soil bacteria taken from a soil sample extracted from a SAT site. The sands containing the biofilms were gently, but thoroughly, washed prior to placement into the reactors. To assure consistency, except for the data regarding the acclimation studies, the data presented represent the wastewater-based BDOC which was solely degraded by the second set of bacteria.

Four of these effluents listed in Table 2.7 were characterized strictly on the basis of BDOC and post-ozonated BDOC at a transferred O₃/DOC dose of 1 mg/mg in an effort to observe the characteristics and/or differences of secondary effluents located in various geographical locations. The remaining three effluents were further studied to observe the effect of ozone dose upon BDOC formation, the kinetics of BDOC removal, the kinetics of nitrification, and the effects of pH as a method to simulate advanced oxidation processes. At this point, pertinent terminology must be defined. For a series of experiments, there were three sampling points: non-ozonated, post-ozonated, and post-biotreated (i.e. the final contents of the BDOC reactor) water. (Hereafter, the BDOC-reactor treated water corresponds to the term *biotreated*).

The BDOC reactors utilized consist of a system of vacuum recirculating glass batch reactors, designed originally by MOGREN et al. (1990). Each reactor consists of a glass container which contains acclimated biofilm on sand, and the sample. The wastewater flows through the sand/biofilm gravitationally and is then reintroduced by suction through a return line. Recirculating flow rates for each reactor are adjustable and flow rates were maintained at approximately 30-40 ml/min allowing complete sample contact with the biofilm every ten minutes. Air is also introduced at the return line to assure aerobic conditions. To minimize the introduction of organic carbon into the system from the feed air, a system of filters is utilized in series. This system consists of a GAC column, a 0.3 μ m hepa filter, and a series of two air scrubbing bottles filled with high purity "Milli-Q" water (Millipore Corp., Bedford, MA). The BDOC data presented from this study represent the mean of BDOC experiments in at least three

reactors which were performed simultaneously. The greatest variation in DOC concentrations in all BDOC experiments was $\pm 8.1\%$.

Ozonation

University of Arizona

Ozone (O_3) was generated with a Griffin ozone generator model GTC1B and measured by a calibrated UV_{254} nm light source. Ozone was produced using medical grade oxygen at a concentration of approximately 30 mg/L O_3 . The secondary effluent was placed in a stirred 20-liter glass carboy reactor then ozone was applied at a rate of 2 liters per minute to the reactor. To obtain the actual mass of ozone transferred to the wastewater, separate feed and reactor off-gas lines were used to measure ozone concentration differences. Mass of ozone applied and exhausted was determined by integrating the product of gas concentration times flow rate over time. The actual O_3 transferred to the wastewater was then obtained by subtracting the mass of O_3 in the exhaust stream from the feed stream. For most applications, the process was continued until O_3 transferred was equal to the DOC in the water on a weight for weight basis.

University of Colorado

Bench scale ozonation was conducted using an OREC (Ozone Science & Equipment Corp., model number O3V5-0, Phoenix, AZ) 110 gram/day ozone generator and a 2.75 liter capacity impeller reactor/contactator. Ozone was generated from high purity oxygen (~5% ozone) and admitted to the reactor in a semi-batch mode (continuous gas admission, static liquid volume). Applied ozone dose (mg/L) was controlled by the mass flow rate into the reactor (mg/L-min) and contact time (min). While experiments were based on transferred ozone dose, both applied and utilized ozone were determined for each experiment in order to ensure the anticipated transfer efficiency (~30%).

Chlorination/Chloramination

University of Arizona

Chlorine Concentration. The THMFP test required an accurate measurement of chlorine (Cl_2) concentration in the solutions used to dose the samples. These solutions (5 to 15 mg/mL approximate) were made from a reagent-grade stock solution of 7.5% sodium hypochlorite (NaOCl). Free chlorine residual was determined via the diethyl-p-phenylene diamine (DPD) colorimetric method utilizing HACH color reagents. The tests were conducted by adding a single HACH powder pillow (DPD) to 25 mL of sample in a cuvette using a HACH DR/2000 Direct Reading Spectrophotometer. The meter will analyze the DPD reaction using a 530nm wavelength and an internal scale calibrated to mg/L Cl_2 . The DPD colorimetric test on the HACH monitor is accurate for chlorine residuals between 0 and 2 mg/L as Cl_2 , so dilutions were made from the chlorine solutions.

Trihalomethane Formation Potential. The trihalomethane formation potential (THMFP) test is designed to measure the maximum potential a water has to form trihalomethane disinfection by-products (DBPs) during chlorination. The concentrations of four trihalomethane (THM) species, chloroform (CHCl_3), dichlorobromomethane (CHCl_2Br), dibromochloromethane (CHBr_2Cl), and bromoform (CHBr_3), were measured using a Hewlett Packard 5794 Gas Chromatograph (GC) equipped with an electron capture detector (ECD) and a HP 7673 auto sampler. A 30-meter DB-624 Megabore capillary column was used for compound separation. Chromatographic data were processed and printed with a Hewlett Packard 3392 reporting integrator.

The wastewater samples and standards were prepared headspace free in acid-washed 40-mL USEPA recommended vials (Supelco) with screw caps and teflon-coated septa. Standards were prepared from a Supelco 2000 $\mu\text{g/L}$ four compound standard, which was diluted to 10 milliliters in methanol (0.2 and 0.4 mg/mL each THM) in a

muffled serum vial with a crimp top. Stock solutions were kept no more than four weeks after initial use or until the presence of an unwanted compound appeared in the chromatographs. Aqueous standards were prepared by injecting between 6 and 50 μ l of stock solution into 40 mL of ultra-pure water. Extraction was then by a pentane separation described later.

In this study, 40 mL of 0.45 μ m filtered sample, one mL potassium phosphate buffer, and a Cl_2 solution made from sodium hypochlorite (NaOCl), was added to the 40-mL vials for twenty-four hours at pH 7, and 20 $^{\circ}\text{C}$. The actual volume in the vial is 42 mL when used headspace free. The buffer was made from KH_2PO_4 (68.1 g/L) and NaOH (11.7 g/L), and the chlorine solutions (5 to 15 mg/mL) were diluted from a 7.5% NaOCl concentrate. The chlorine dose for the samples was calculated to satisfy the ammonia (NH_4^+) derived (theoretical) demand for breakpoint chlorination and to also react with the DOC present in the water. DOC and NH_4^+ (mg/L) were measured prior to the THMFP test to determine the chlorine dose. This dose is 7.6 times the ammonia concentration ($\text{NH}_4^+\text{-N}$) and 5 times the DOC concentration on a mass for mass basis (mg/mg).

THMs from samples and standards were extracted from the aqueous solutions by the liquid-liquid method using a double-syringe technique as outlined in *Standard Methods for the Examination of Water and Wastewater*, 18th ed., section 5710 B, after raising the ionic strength of the solution with the addition of sodium chloride (NaCl). Six grams of NaCl was added to each 40-mL vial to create a salting out effect that would enhance the partitioning of the non-polar contaminants in solution. The non-polar solvent used to extract the THMs from the aqueous phase consisted of four milliliters of THM-free pentane that was injected into the top of the vial, displacing four milliliters of sample from the bottom of the vial through a second needle. The samples and standards were then shaken for one minute to promote the partitioning of THMs into the pentane. After shaking, one mL of pentane was transferred to a Hewlett Packard auto sampler vial, crimped closed, and placed into the auto sampler tray. The column was run at 50 $^{\circ}\text{C}$ and

the retention time for each sample was programmed for 38 minutes based on a retention time of 35 minutes for bromoform.

University of Colorado

The protocol for each sample aliquot involved dosing with free chlorine at a chlorine/DOC ratio (by weight) of 1 mg/mg for simulated distribution system (SDS) and 5 mg/mg for formation potential (FP) and incubation for 24 hours at 20°C. A 0.5 M phosphate buffer was used to maintain pH at 7.5. In the presence of ammonia, the chlorine dose was increased 7.6 times the concentration of ammonia-nitrogen to provide for breakpoint conditions.

The chlorine dosing solutions are prepared from reagent-grade sodium hypochlorite and these solutions are spectrophotometrically analyzed with a Hach Pocket Colorimeter test kit (Cat. No. 46700-00) and occasionally checked with a Hach DR/2000 Spectrophotometer. Both units are based on the DPD titrimetric method (Standard Methods, 1989). The chlorine concentration of the dosing solution is between 1.0-5.0 mg/ml for SDS chlorination and 4.0 to 15.0 mg/ml for FP chlorination, which is about 50 to 100 times the concentration needed in the samples, in order to minimize dilution errors in the reaction vials. Dilution volume is kept less than or equal to 2%, normally around 1 ml in 72 ml. The chlorination experiments are conducted headspace-free in 72 ml glass reaction vials with teflon septa caps. The vials are washed with Alconox and rinsed with tap water followed by a 10:1 nitric acid bath for 24 hours. Upon removal from the acid bath, the vials are rinsed with deionized water followed by Milli-Q water and oven dried. The extraction vials are maintained headspace-free throughout the incubation period. After incubation, the sample is divided into two 30 ml aliquots for THM and HAA analyses and an aliquot of the sample is withdrawn for determination of total and free chlorine residuals (by Hach Pocket Colorimeter DPD method) and estimation of corresponding chlorine demand.

Azide Inactivation

In order to determine the role of aerobic bacterial respiration in effluent renovation, influent wastewater to several columns was poisoned with sodium azide (NaN_3), an aerobic inhibitor. One schmutzdecke column receiving secondary effluent was dedicated for this purpose, with the influent wastewater at a concentration of 5 mM NaN_3 . Azide was applied in dechlorinated secondary effluent to three, 1-meter columns (one Sweetwater sandy loam, one Agua Fria sand, and one North Pond silt) at a concentration of 2 mM NaN_3 .

The efficiency of N_3^- as an inhibitor of aerobic cell activity was determined in past research (Quanrud, et. al, 1996). Oxygen utilization was measured in soil bacteria suspensions from both N_3^- inhibited and non-inhibited soil columns. Although the numbers of culturable bacteria present in the two samples were found to be similar, aerobic respiration was greatly reduced in the N_3^- inhibited soils at the concentration used in this study.

Disposal of column effluent containing sodium azide was conducted according to recommendations from the Hazardous Waste Management Department at the University of Arizona. A cold 5.5% solution of ceric ammonium nitrate ($(\text{NH}_4)_2\text{Ce}(\text{NO}_3)_6$) was slowly added to the effluent, at a ratio of 153 mL solution/1g azide, with sufficient agitation to suspend all solids. Once the chemical reaction was judged to be complete, the mixture was washed down the drain with water.

DOC Fractionation (UF and XAD-8)

University of Arizona

Characterization of waters by molecular size distributions was conducted using Amicon ultrafiltration cells (Amicon Corp., Danvers, MA). Amicon YM-10 (<10,000 AMW), YM-3 (<3,000 AMW), YM-1 (<1,000 AMW), and YC-05 (<500 AMW) ultrafiltration membranes were used. Membranes were prepared before each use according to manufacturer's instruction by pre-soaking each in ultra-pure water for 15

minutes and then rinsing. Membranes were then stored in ultra-pure water at 4 °C for future use.

Each cell was filled with 120 mL of 0.45 µm filtered water, then pressurized at 60 psig with nitrogen gas. The cell stirrer was set at a speed that provided approximately a 10 mL increment of vortex, as measured on the side of the Amicon cell. Permeate was collected in four, 6 mL increments and analyzed for DOC and UVA₂₅₄. A permeation coefficient was calculated according to the model developed by Logan and Jiang (1990) to correct for concentration polarization at the membrane surface. An additional 50 mL of the permeate was collected and used for measurement of THMFP.

University of Colorado

The bulk DOC present at the various sampling points is characterized according to low versus high molecular weight (MW) DOC fractions, and humic (hydrophobic) versus non-humic (hydrophilic) DOC fractions. Molecular weight/size separation was performed using Amicon ultrafiltration YM-1 and YM-10 (apparent molecular weight cutoff equal to 1,000 and 10,000 daltons, respectively) membranes in an Amicon stirred cell (Amicon Corp., Danvers, MA). The humic and non-humic fractions of the effluent DOC were separated by adsorption of the humics onto Amberlite 20 - 40 mesh XAD-8 nonionic resin (Rohm & Haas Company, Philadelphia, PA) in the manner described by LEENHEER (1981).

ANALYTICAL METHODS

Chemical Methods

Arizona State University

Laboratory Methods. The ASU researchers monitored the influent and effluent from the columns for TOC, nitrate, ammonia, nitrite, and phosphorous. The columns were monitored at least three times a week for each of the parameters, while organic nitrogen was monitored

periodically. Column influent samples were taken whenever fresh effluent was obtained and column effluent samples were taken from the sampling tubes at the base of the columns. The effluent from the Agua Fria sand and South Pond silt columns flowed freely from the sampling tubes and this sample was collected in a beaker. The effluent from the Agricultural Field clay columns and the North Pond Silt columns was extracted from the sampling tubes by applying a vacuum for a short period of time (1 - 2 minutes) and collecting the sample in a flask. Column influent and effluent samples were filtered through an 8 μm filter paper and were split into four portions for preservation. One portion was not treated and this was used for UV absorbance. Another portion was treated with sulfuric acid for DOC and ammonia analysis. Another portion was treated with mercuric chloride for nitrate and nitrite analysis. Samples taken for organic nitrogen were not filtered or preserved. Samples for nitrate analysis were frozen while all other bottles were refrigerated at 4 °C.

Nitrate was determined using a Hach Nitrate Ion-Selective Electrode (Model 44560) following the method outlined in Section 4500- NO_3^- D., Standard Methods, 17th Edition. Ammonia was also determined using an electrode, Model 95-12 from Orion, according to Section 4500- NH_3 H. in Standard Methods, 17th Edition. The meters used for the electrode methods were Corning 340 pH/mV meters. Nitrite was determined by an azo dye colorimetric method using Section 4500- NO_2^- B. in Standard Methods, 17th Edition. Photometric measurements for nitrite determination were performed on a Spectronic 20 Spectrophotometer. Organic nitrogen was determined according to the Macro-Kjeldahl method (4500- N_{org} B. in Standard Methods, 17th Edition). This method determines TKN which is the sum of organic and ammonia nitrogen. In the Kjeldahl method, the sample is digested to convert the organic nitrogen to ammonia. After digestion and distillation, the TKN was measured using the ammonia-selective electrode method. To obtain organic nitrogen, the ammonia in the original sample was subtracted from the TKN value.

TOC was determined with a Dohrmann DC-180 Total Organic Carbon Analyzer (Rosemount Analytical/Dohrmann, Santa Clara, CA). This instrument utilizes persulfate in the presence of UV radiation for conversion of organic carbon to carbon dioxide (Method 5310 C. in Standard Methods, 17th Edition). The UV absorbance of samples was measured with a Hewlett Packard 8452A Diode Array Spectrophotometer (Hewlett Packard Co., Palo Alto, CA.). This allowed

for easy determination of the UV absorbance at various wavelengths. UV absorbance was measured at wavelengths of 230, 254, and 270 nm as well as the average absorbance from 230 to 300 nm.

Field Methods. Dissolved oxygen, soil tension and temperature were determined at the ports located along the length of the column. Dissolved oxygen measurements were done on a Microelectrode, Inc. 16-730 Flow-Thru Oxygen Electrode. Approximately 5 ml of sample was extracted from the septum ports using a syringe. The sample in the syringe was then injected into the Flow-Thru Oxygen Electrode and the reading was measured in mV with a VWR Scientific pH and mV meter. Soil suction was determined from the tensiometers using a Soil Measurement Systems Tensiometer and temperature within the columns was determined at the septum ports using a Model No. 8528-20 DigiSense Thermocouple Thermometer from Cole Parmer Instrument Company. A 30.5 cm flexible miniprobe from Cole Parmer Instrument Company was attached to the thermometer and the probe was inserted approximately 3 inches into the soil for temperature readings.

University of Arizona

Influent and effluent samples were collected and analyzed for DOC and UVA_{254} , etc. The column influent samples were collected from influent sample lines. Before sample collection, 20 to 30-mls of water was flushed through the sample line. About 40-mls of column influent was obtained at each sampling period.

Column effluent samples were collected in 50-ml beakers, that were placed below the column during operation. Again, about 40-mls was the standard sample size. Only dissolved organic carbon (DOC) was required, therefore, both influent and effluent samples were filtered in preparation for organic analyses, using 0.45- μ m pore size filters (manufactured by Millipore, Inc.), vacuum flask and pump. The pump pressure was set for 25 inches Hg. Filters were washed between samples by rinsing with about 150-ml of milli-Q water in the "filter wash" vacuum flask. Filtered samples were transferred into a muffled 20-ml scintillation vial. The vials were completely filled with the sample, and aluminum foil was placed over the mouth of

the vial before the plastic cap was placed on the vial. Samples prepared in this manner were refrigerated until the end of the weekly wet period at which time all of the samples were analyzed for organics

DOC analyses were performed using a Shimadzu TOC-5000 Total Carbon Analyzer with autosampler that measured for non-purgable organic carbon (NPOC). NPOC is the removal of inorganic carbon by acid addition and gas sparging. Samples (6mL) were acidified to pH 2 by adding 50 μ l of 2 N HCl and sparged for 4 minutes using ultrapure hydrocarbon-free air. Organic carbon was converted to CO₂ by catalytic combustion at a temperature of 680 °C, and analyzed by a non-dispersive infrared detector. Each sample was then analyzed 5 to 8 times (50 to 100 μ l per injection) in order to achieve a coefficient of variation of ≤ 0.02 . Standards were included during each sample run to calibrate the system response and for blank correction. DOC standards were prepared by dilutions of a 1000 ppm C stock solution. The stock solution was prepared by dissolving 2.125 g of dried reagent-grade potassium hydrogen phthalate in Milli-Q water brought up to 1 liter in a volumetric flask.

Ultra-violet light absorbance analyses at 254 nanometers (UVA₂₅₄) were performed using a Shimadzu UV-160a Spectrophotometer using quartz cuvettes (path length 1 cm). The machine was zeroed with Milli-Q water. Adjustments for pH were not necessary since UVA₂₅₄ is independent of pH in the range 6 to 8 (Edzwald *et al.* 1985).

All pH measurements were performed using a VWR Scientific Standard pH probe connected to a Beckman Φ^{TM} 12pH/ISE meter. Measurements were taken immediately after sample filtration (0.45 μ m). The meter was calibrated daily using two standard buffer solutions (pH values of 4.00 and 7.00) prior to sample measurement.

Turbidity, a measure of the lack of light-transmitting properties of water, is a test used for the indirect characterization of colloidal and suspended matter contents in effluents. Since colloidal and suspended solids prevent light transmission, turbidity is determined by comparing the light scattered by the sample with that of a reference suspension under the same conditions. The standard is a suspension of silica of specified particle size selected, so that a 1.0 mg/l suspension measures 1.0 NTU (nephelometric units). Column influent and effluent turbidities were determined right after sample collection using a Hach Turbidimeter Model 2100A. Having five different NTU ranges (0 to 0.2, 0 to 1.0, 0 to 10.0, 0 to 100.0, and 0 to 1000.0), the

apparatus was calibrated using four Gelex® Secondary Standards (0.77, 6.45, 75.5 and 675 NTU). Sample turbidity was measured using a 25-ml glass cell, after selecting the suitable range for calibration.

Phosphorus concentrations in column influents and effluents were determined by the Ascorbic Acid Method (Standard Methods 1992), modified by the Soil Water and Plant Analysis Laboratory (U of A). A preliminary digestion technique (Persulfate Digestion Method, Standard Methods 1992) was required just for samples tested for total phosphorus.

A) Sample collection and preservation. Column influent and effluent samples (30 - 40 ml) were collected on a daily basis. All samples were kept frozen at -10°C in 50-ml disposable centrifuge tubes until analyzed. All glassware used during analysis was prerinsed with hot diluted hydrochloric acid and Milli-Q water. Use of commercial detergents containing phosphate for cleaning glassware was obviously avoided.

B) Phosphate standards. A 100 ppm stock solution of phosphate-P was prepared by dissolving 0.4394 g of analytical reagent grade (99.9+%) potassium dihydrogen phosphate (KH_2PO_4) (previously oven-dried at 110°C for 4 hours) with 200 ml of Milli-Q water in a 1-liter volumetric flask. The solution was brought to volume with Milli-Q water. From this stock solution, six standards (1.0, 2.0, 4.0, 6.0, 8.0, and 10.0 mg/l of $\text{PO}_4\text{-P}$) were prepared, using Milli-Q water as a blank.

C) Persulfate digestion method. Required reagents were:

- 1) Phenolphthalein indicator aqueous solution,
- 2) Sulfuric acid solution (1 liter of solution contained 300 ml of concentrated H_2SO_4),
- 3) Solid potassium persulfate, $\text{K}_2\text{S}_2\text{O}_8$ and,
- 4) Sodium hydroxide (1 N solution).

A sample size of 10 ml was used for analysis. Samples were amended with 0.2 ml of H_2SO_4 solution was added plus and 0.1 g of $\text{K}_2\text{S}_2\text{O}_8$, then heated for 30 minutes in an autoclave at 121°C and 98 to 137 kPa. Once cooled, samples were neutralized to a faint pink with 1N NaOH using phenolphthalein indicator (0.05 ml) and adjusted to a 20-ml volume with Milli-Q water. Finally, phosphorous concentrations were determined by colorimetry. Blank and standards were carried through the same digestion procedure since a separate calibration curve was necessary for colorimetry.

D) *Ascorbic acid colorimetric method*. Required reagents were:

(1) Molybdate reagent, which consisted of two solutions:

- a) 6.0 g of ammonium molybdate $[(\text{NH}_4)_6\text{Mo}_7\text{O}_{24} \cdot 4\text{H}_2\text{O}]$ in 125 ml of Milli-Q water.
- b) 0.1455 g of antimony potassium tartrate $[\text{K}(\text{SbO}_4)\text{C}_4\text{H}_4\text{O}_6 \cdot 1/2\text{H}_2\text{O}]$ in 500 ml 5 N H_2SO_4 (74 ml of concentrated H_2SO_4 plus Milli-Q water to make up 500 ml).

Both solutions were mixed and brought to 1 liter with Milli-Q water. This reagent was stored in an amber glass bottle and kept refrigerated at 4°C. It was considered stable for one month.

(2) Mixed color developing reagent:

- 1) 0.739 g of ascorbic acid in about 500 ml of Milli-Q water,
- 2) 140 ml of the molybdate reagent prepared as in (1).

Both solutions were mixed and brought to 1 liter with Milli-Q water. This reagent was made fresh daily.

One ml of thoroughly mixed sample or standard was pipetted into a 15-ml capacity test tube, then 9 ml of the mixed color developing reagent was dispensed into the test tube. After mixing for a minimum of 30 minutes but no more than three hours, absorbances of the blank and standards were read in a spectrometer (Hitachi U-2000 Spectrophotometer, Double-beam UV/Vis) at 889.5 nm with 1-cm pathwidth cuvettes, followed by the water samples. A linear relationship between phosphorus concentrations and absorbance was established via regression analysis.

A simple microdiffusion technique modeled after the work of Saghir, et. al. (1993) was used to determine NH_3 - N and $(\text{NO}_3^- + \text{NO}_2^-)$ - N. In this method, a sample is placed in a 1-pint (473-ml) wide-mouth mason jar and NH_4^+ is liberated as NH_3 by the addition of a mild alkali (MgO, magnesium oxide). The liberated NH_3 is then trapped in a boric acid solution contained in a 60-mm (dia.) petri dish suspended from the lid of the mason jar. The NH_3 is allowed to diffuse from the sample to the boric acid trap over a 24 hr+ period. The acid trap is removed and NH_3 - N is then quantitatively determined by titrimetry using 0.0025 M H_2SO_4 . Upon determination of NH_3 - N, Devarda's Alloy is added to the original sample for the purpose of reducing NO_3^- and NO_2^- to NH_4^+ . A fresh boric acid trap and MgO powder are placed in the mason jar and NH_3 is once again liberated, trapped, and titrated with H_2SO_4 as described above.

This yields a value for (nitrate + nitrite) -N. The combined (nitrate + nitrite) -N determination is sufficient for the completion of nitrogen balances as in the case of soil-water samples in which NO_2^- is often assumed negligible or is a minor intermediate species.

The microdiffusion method offers several advantages over other methods for the determination of inorganic N in wastewater. Colorimetric methods are in widespread use but are best suited to drinking water or comparably "clean" samples. Sources such as *Standard Methods* and the Hach Company advise that wastewater samples must be distilled before colorimetric analyses, owing to interferences which may be present. The steam distillation method, as described by Bremner and Shaw (1955), eliminates such interference problems, has the great advantage that it may be used with colored or turbid samples, and provides highly accurate analyses. However, steam distillation is labor intensive and requires an elaborate laboratory setup to run a large volume of samples efficiently. Microdiffusion effectively accomplishes the same goal as steam distillation (i.e. removing NH_4^+ from the sample matrix and trapping it in boric acid for titration), but does so without requiring extensive laboratory setup and expense. In fact, Saghir et al. point out that there should be less chance of interference due to the release of NH_3 from alkali-labile organic compounds (a potential source of minor error when Devarda's Alloy is used) since microdiffusion (unlike steam distillation) is conducted at room temperature. Microdiffusion has been less widely employed than steam distillation both because of the 1-2 day diffusion period and because prior to the paper of Saghir et al., no more than 4-10 mls of sample could be analyzed at a time. With the mason jar reactors, samples ranging from a few mls to 50 mls can be analyzed. Such a size range is useful both for small-volume soil-water samples gathered through suction samplers and for soil extracts which require larger volumes of sample to obtain representative results. It is not necessary to filter samples prior to analysis.

Gas phase samples were withdrawn from the soil column with a 3-cc syringe through a septum-covered sample port. The septa are manufactured by Supelco, Inc. and are 12.5 mm diameter. Molecular oxygen was then measure in the 3-cc gas sample.

Oxygen content was measured using a 16-730 O_2 electrode, manufactured by Microelectrode, Inc. This is a glass electrode surrounded by an oxygen electrolyte solution within the flow-through membrane housing. The electrode was connected to a microelectrode

OM-4 oxygen meter. The oxygen meter is also manufactured by Microelectrode, Inc. . Oxygen measurements were in units of percent oxygen in air or partial pressure.

The oxygen electrode was calibrated for gas samples using humidified air and carbon dioxide or nitrogen. Ambient O₂ levels provided the upper calibration point. Carbon dioxide or nitrogen was used to provide an O₂ free measurement. An Erlenmeyer flask half filled with water was used as the humidification unit. A two-hole rubber stopper with glass tubing was placed in the mouth of the flask to allow the calibrating gas to enter and the humidified gas to exit. The exiting gas flowed through plastic tubing that was connected to the flow-through oxygen electrode. For proper calibration of the electrode, the O₂ free sample was introduced to the probe first. Carbon dioxide was bubbled into the calibrating apparatus and the humidified CO₂ was transmitted to the teflon membrane at the electrode housing. As the gas flowed through the electrode the oxygen meter is set to read 0.0. The gas continues to flow through the membrane in order to insure the reading on the oxygen meter remains stable at 0.0.

Ambient air was used for the second calibration point. The humidification unit for the air is continuously stirred in order to assure equilibrium conditions in the unit. The same procedure was followed for this calibration point as explained before for the O₂ free calibration. That is, ambient air is bubbled into the flask and the humidified gas is passed through the electrode and the oxygen meter is set to read 20.9 and a reading is accepted when the meter demonstrates stability at 20.9 after continued air flow. Once the electrode was satisfactorily calibrated a gas sample was withdrawn from the column and slowly injected into the flow-through electrode. Recorded data represent stable electrode readings obtained while the gas sample was being injected across the electrode membrane.

University of Colorado

DOC measurements were performed after filtration through a pre-rinsed 0.45 µm filter (Millipore Corp., Bedford, MA). These measurements were made using a Shimadzu TOC-5000 low-level analyzer while UV absorbance measurements at 254 nm were completed with a Shimadzu UV-160A UV-visible spectrophotometer using a 1 centimeter quartz cell.

Nitrate (NO_3^-), nitrite (NO_2^-), and phosphate (PO_4^{3-}) were measured by ion chromatography. A Dionex DX-300 with an autosampler and an IonPac AS9-CS column was employed. Through the autosampler, an on-column injection sample volume of 100 μl was utilized. The eluent used was 2mM Na_2CO_3 at 2 ml/min. Total ammonia ($\text{NH}_3 + \text{NH}_4^+$) was measured spectrophotometrically using a Hach DR/2000 Direct Reading Spectrophotometer. Organic nitrogen was deduced by difference upon measurement of Kjeldahl nitrogen via the macro-Kjeldahl method, standard methods 4500-Norg B (GREENBERG et.al., 1992). Total inorganic and organic nitrogen species is reported by addition of all components.

Six of the nine HAA species measured consist of trichloroacetic acid (TCAA), dichloroacetic acid (DCAA), monochloroacetic acid (CAA), dibromoacetic acid (DBAA), monobromoacetic acid (BAA), and bromochloroacetic acid (BCAA). The extraction of haloacetic acids was based on EPA method 552 which involves an acidic, salted medium (Na_2SO_4) extracted with ether (MTBE). The method requires that the samples be acidified to a pH of less than 0.5 (concentrated H_2SO_4) prior to extraction with ether so that the HAAs are not in their dissociated form. Prior to extraction and gas chromatograph analysis, the compounds are derivatized (esterified) with diazomethane to produce methyl ester derivatives which are more amenable to GC analysis.

A Hewlett Packard 5890 gas chromatograph (GC) with an electron capture detector (ECD) was used with a J & W Scientific DB-1 megabore column (cat. no. 125-1032). A HAA chromatogram is shown in Figure 2.10. The GC injector temperature is 180°C with an initial column temperature of 50°C for one minute. After one minute, the temperature is increased at 4°C/min to 102°C. A second increase is used to elevate the temperature to 222°C. The temperature is held at 222°C for five minutes to remove less volatile residue from the column.

The extraction of chloroform (CHCl_3), bromodichloromethane (CHBrCl_2), dibromochloromethane (CHBr_2Cl), and bromoform (CHBr_3) is accomplished by liquid-liquid extraction with MTBE using a modification of EPA method 551. Sodium chloride was used to decrease the solubility of ether in water and to increase the partitioning of THMs into the solvent

phase. The MTBE used contains a fixed amount of chloroform per bottle and is used as an internal standard.

A Hewlett Packard 5890 GC with an ECD was used with a J & W Scientific DB-1 megabore column. A THM and CH chromatogram is shown in Figure 2.11. The GC injector temperature is 120°C with an initial column temperature of 40°C for three minutes. After three minutes, the temperature is increased at 15°C/min. to a temperature of 63°C which is held for 1.5 minutes in order to separate the CHBrCl_2 peak from the chloral hydrate peak. At this point the temperature is increased from 63°C to 100°C at a rate of 15°C/min. and held at 100°C for one minute. During this temperature increase, the remaining peaks (CHBr_2Cl and CHBr_3) pass through the column. From 100°C, a final ramp is used to increase the temperature to 180°C. The column is held at 180°C for two minutes to remove less volatile residue from the column. With some wastewaters, the final time may be increased to five minutes.

Supelco standard solution at 2000 µg/ml are used for the calibration curves. These standards are diluted to 200 µg/ml in five milliliters of methanol. Various solutions ranging from 5 µg/l to 200 µg/l are prepared in 72 ml vials with milli-Q, extracted and analyzed according to the appropriated procedure. Normally, a milli-Q water sample is analyzed as a zero sample in order to determine if residual contaminants in the milli-Q interfere with the calibration. Similarly, 2 or 3 of the samples are independently duplicated to verify calibration results. Figure 2.12 shows a typical calibration curve for dichloroacetic acid. A linear curve fit is forced through zero. Other HAA species are similar with R^2 values ranging from 0.98 to 0.998. Figure 2.13 shows a typical THM linear calibration curve forced through zero for chloroform. Other THM species are also similar with R^2 values ranging from 0.98 to 0.997. Calibration curves are performed on a monthly basis or whenever column conditions are changed.

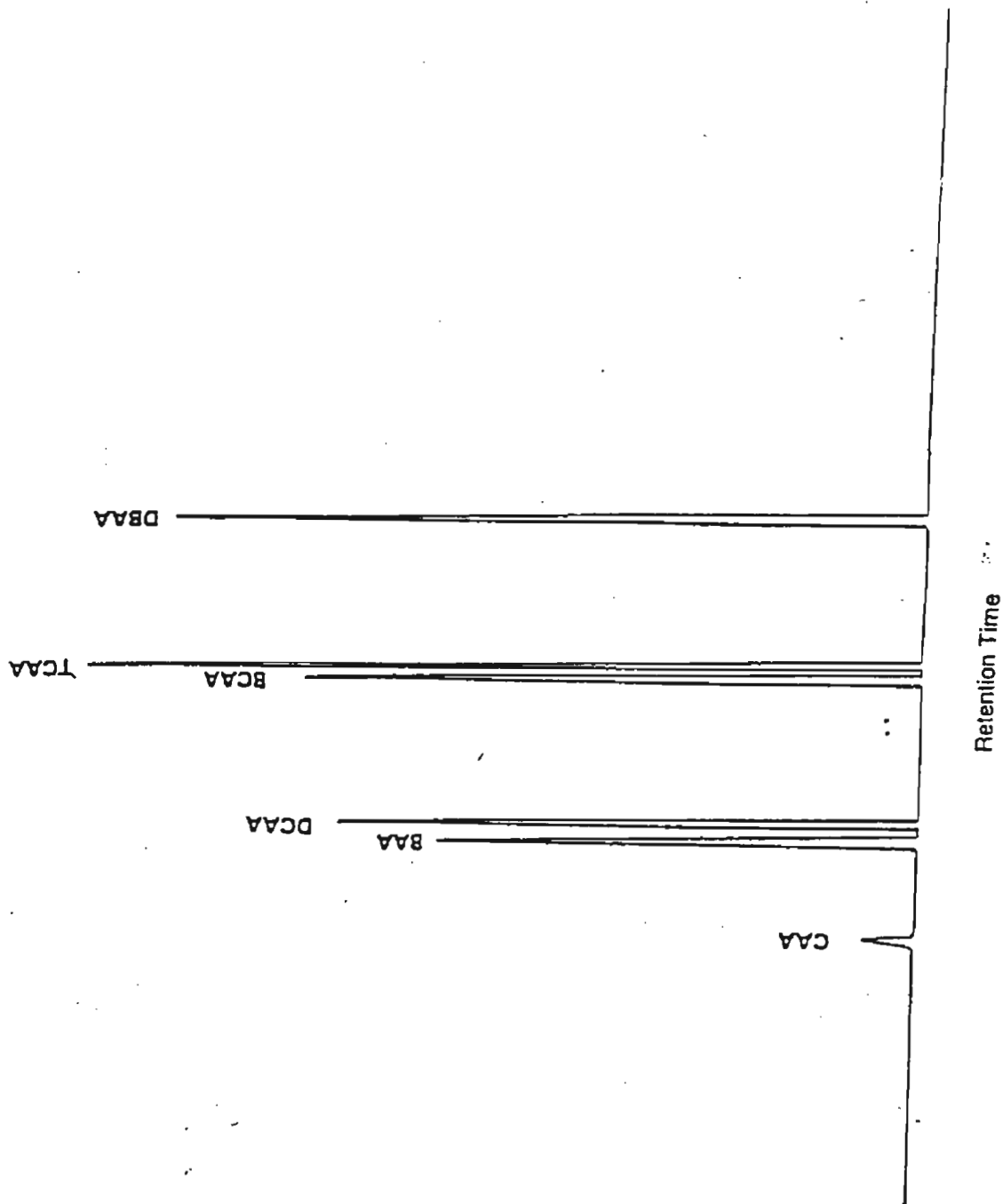
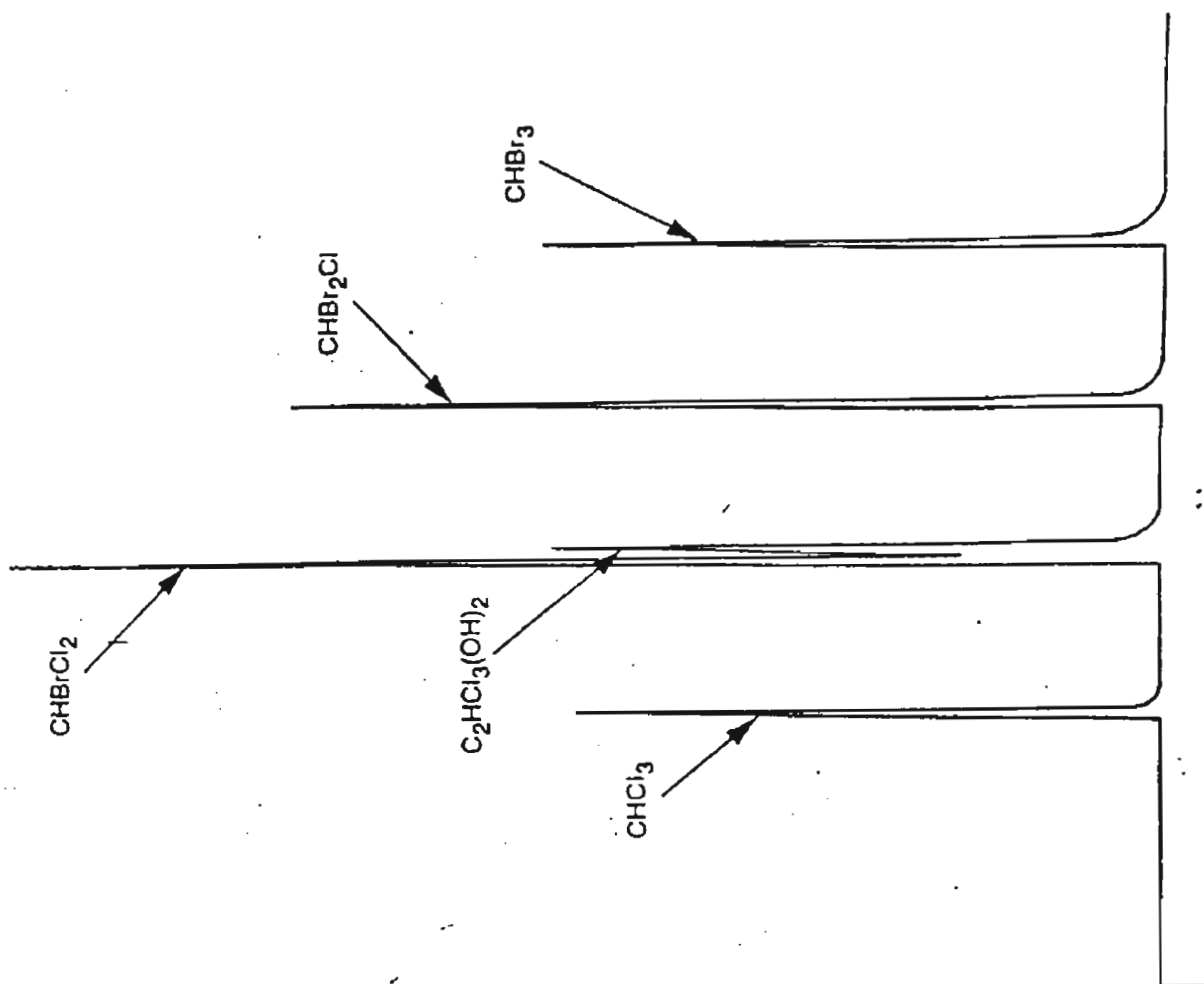


Fig 2.10



Retention Time

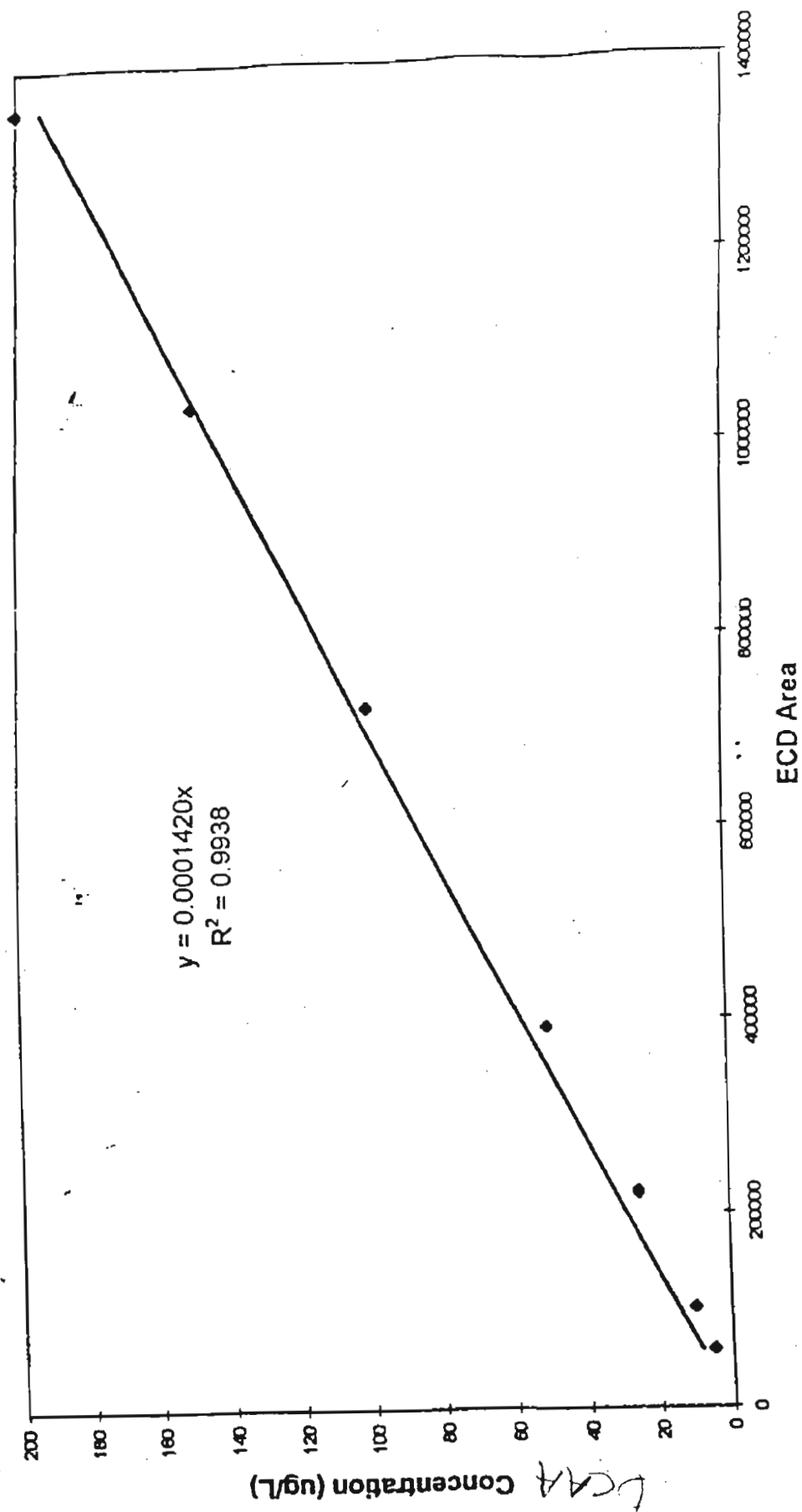
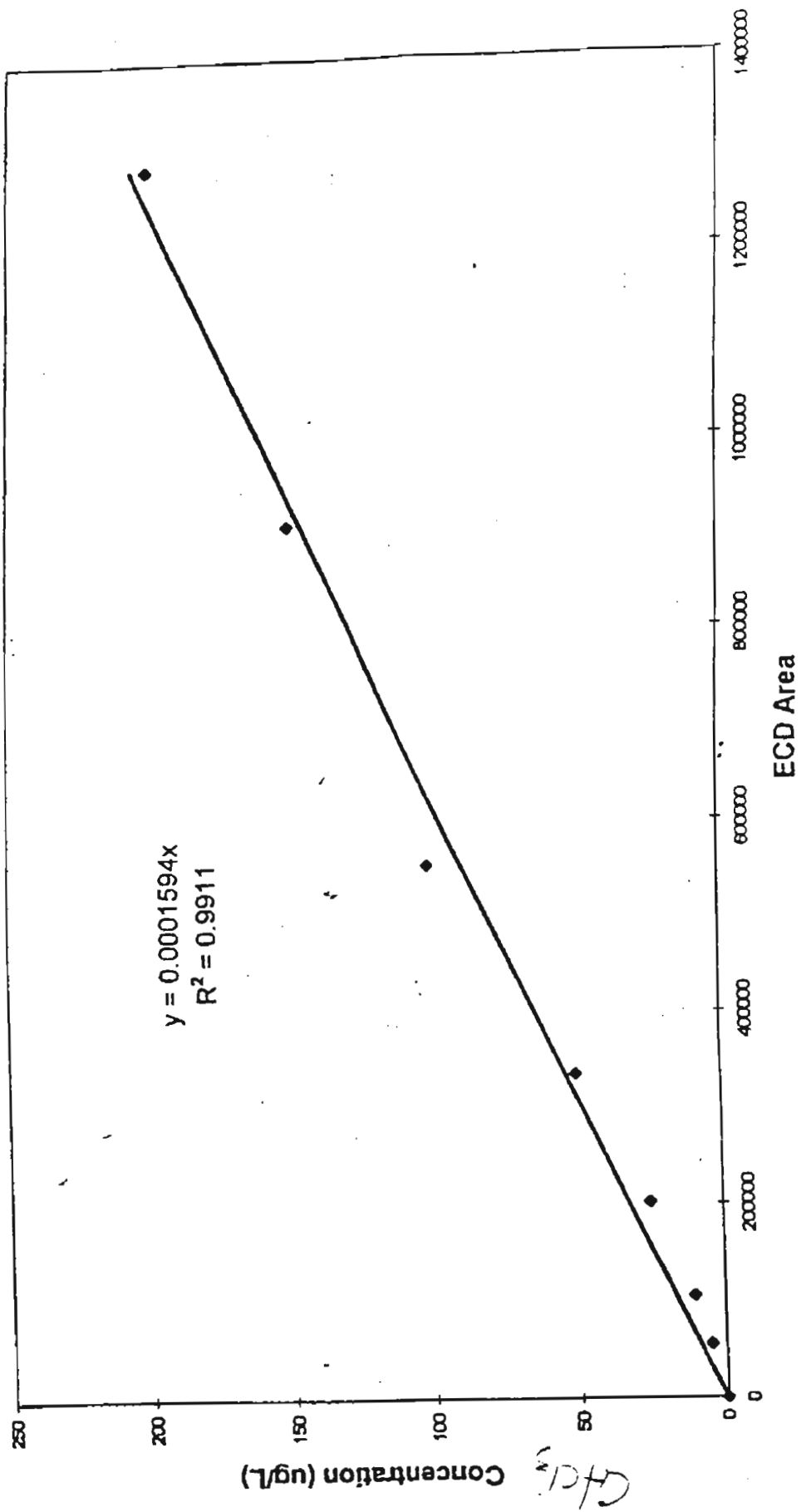


Fig 2.12



70

Ozone by-products, including aldehydes (formaldehyde, acetaldehyde, glyoxal, and methyl glyoxal) and ketoacids (glyoxylic acid, pyruvic acid, and ketomalonic acid), were monitored as chemical surrogates for biodegradability. For the analysis of aldehydes, samples were subjected to PFBHA derivatization then liquid-liquid extraction with hexane prior to injection into a Hewlett Packard 5890 gas chromatograph (GC) utilizing an electron capture detector (ECD) and temperature programming via the method described in SCLIMENTI et al. (1990). For the ketoacids, double derivatization using PFBHA then diazomethane was performed prior to GC analysis (XIE et al., 1992).

Microbiological Methods

Virus measurements

Removal of indigenous or seeded bacteriophage was determined through daily sampling of column influent and effluent over numerous wet cycles for soil columns of different soil types and lengths. Samples were stored from 1 to 3 days at 4° C and then filtered through a 0.22 µm pore size, low protein binding cellulose - acetate Tuffryn membranes (Gelman Sciences, Ann Arbor, MI), that was treated with Tryptic Soy Broth (Difco, Detroit, MI). Filtering the samples removed bacteria that can interfere with visualization of bacteriophage plaques. The filtered samples were then assayed using the plaque forming unit (PFU) method (Adams, 1959), as described below, using *Escherichia coli* (ATCC 15597) as the bacterial host. Bacteriophage were seeded in ozonated effluents due to the disinfecting properties of the ozonation procedure.

Acquisition of viruses. The MS-2 bacteriophages used in the ozonation experiments were obtained from the American Type Culture Collection in Rockville, MD. Poliovirus type 1 Lsc (2ab) was obtained from The Department of Virology, Baylor College of Medicine. Hepatitis A virus was obtained from Dr. Mark Sobsey, Department of Environmental Engineering and Science, The University of North Carolina.

Protocol for bacteriophage assay, the double-agar overlay technique. Material required:

Tris-Buffered Saline solution for dilution of samples:

1600 mL H₂O

63.2 g Trizma Base (Sigma Corporation)

163.6 g NaCl

7.46 g KCl

1.13 g anhydrous Na₂HPO₄

Add 3.6 mL of Tris per test tube.

Bottom agar: Prepare 1.5% Tryptic Soy Agar (TSA) and dispense into petri dishes (Approximately 10 mL/petri dish)

Top Agar: Prepare 1.0% TSA + Tryptic Soy Broth (TSB). Dispense the solution into test tubes, 3 mL per test tube.

Growth media for host bacteria: Prepare TSB, and distribute into test tubes (9mL each). Dispense the remainder in 250 mL flasks (50 mL each).

All the above media must be sterilized in an autoclave for 20 minutes at the time of preparation, and are stored at 4° C until use.

Preparation of Host Bacteria. A 9-mL TSB tube was inoculated with a colony of the host bacterium from a culture petri dish and incubated at 37° C for 18 to 24 hours, at which point the bacteria were in the stationary growth phase. After this incubation period, the suspension was vortexed and inoculated into 50 mL of TSB, and grown at 37° C on a shaker table for 3 to 5 hours. The bacteria must be used between 3 to 5 hours, during their exponential growth phase.

Assay for Bacteriophage. Samples were diluted as necessary to produce bacteriophage concentrations between 30 and 300 PFU per mL. A quantity of 0.4 mL of sample was removed, and added to 3.6 mL of Tris buffer solution. The 1.0% top agar test tubes were then removed from the refrigerator, steamed to liquify, and placed in a 48° C water bath. The 1.5% TSA plates were warmed to room temperature, and the 50 mL of host bacteria was taken from the shaker table incubator.

Each 3 mL top agar tube was inoculated with 1 mL of sample and 1 mL of host bacteria, vortexed and poured onto a 1.5% TSA plate. The plate was swirled carefully to cover the media, and set aside to solidify. Three replicates per sample (or dilution) were assayed. Once all samples had been completed and solidified on the TSA plates, they were inverted and incubated at 37° C overnight. After approximately 24 hours, the bacteriophage were counted by identifying clear "plaques" on the lawn of host bacteria. Only counts within the range of 30 to 300 per mL were considered accurate.

Protocol for the poliovirus plaque assay. Materials required:

A Buffalo Green Monkey (BGM) cell line was maintained and propagated weekly in the laboratory. These cells were used as the animal cell hosts for the assay.

A 4% tissue culture medium supplied nutrients for the BGM cells as they grow. Ingredients of the culture medium are listed here:

- 400 mL 1x Minimum Essential Media (MEM), prepared from MEM Autoclavable Modified Earle's Salts, Irvine Scientific
- 4 mL of 0.893 M Sodium Bicarbonate (15 g NaHCO_3 in 200 mL H_2O)
- 12 mL of 1M hepes
- 16 mL Fetal Bovine Serum
- 1 mL penicillin/streptomycin
- 1 mL kanamycin
- 1 mL mycostatin
- 4 mL glutamine

Overlay Medium is used in the assay to nourish the cells for the incubation period. It is composed of:

- 100 mL 2x MEM (warmed to 37° C)
- 6 mL of 0.893 M Sodium Bicarbonate
- 4 mL Fetal Bovine Serum
- 0.2 mL penicillin/streptomycin
- 0.2 mL kanamycin
- 0.2 mL mycostatin
- 2 mL glutamine
- 100 mL melted 1% agar

Plaque assay procedure for poliovirus. Once the cells have grown into a confluent monolayer on the six - well sterile plastic plates, they can be used in the plaque assay. This usually takes about 5 days from the day they are passed into the wells. Dilutions of the sample must be made in Tris saline buffer solution (Sigma Chemical Co., St. Louis, MO) if the expected sample concentrations will be above 6 per mL. The 4% tissue culture media was poured off of the cells.

Then 0.1 mL of the sample was added to each well, and they were incubated in 5% CO₂ at 37° C for 30 minutes and agitated every 15 minutes to ensure complete coverage of the cells. After this incubation, 3 mL of the overlay medium was added to each cell. The cells were incubated once again in 5% CO₂ at 37° C for 2 days, and then stained with Crystal Violet Dye, which stains the viable cells only. Round, clear spots were designated plaques (dead cells), and counted as PFUs.

Hepatitis A virus assay. The assay for Hepatitis A virus follows a procedure similar to that for poliovirus, with some minor modifications (Enriquez-Enriquez, 1994). A different host cell line was used, Fetal Rhesus Kidney cells, and the incubation period was approximately ten days.

Protocol for parasite assay: Giardia and Cryptosporidium immunofluorescent detection procedure

Materials. Solution A: NaH₂PO₄ (27.6 g), distilled water (1000ml).

Solution B: Na₂HPO₄ (28.42 g), distilled water (1000ml)

Phosphate buffered saline (PBS) solution: Soln. A(20ml), soln. B(105ml), NaCl (8.5g), distilled water (875ml).

Eluting solution: 1% SDS solution(100ml), 1% Tween 80 solution(100ml), PBS(800ml).
10% formalin solution

Sheather's flotation media: Sucrose(500g), distilled water(325ml), liquid phenol(9.7ml).
Specific gravity 1.24.

1° antibody: Monoclonal antibodies specific for *Cryptosporidium* oocysts and *Giardia* cysts were obtained from Meridian Diagnostics Inc. (Cincinnati, OH).

2° antibody: Goat anti-mouse immunoglobulin M(heavy chain) labelled with fluorescein isothiocyanate (FITC) were obtained from Kikegard and Perry Laboratories, Inc. (Gauthersburg, MD).

C. parvum oocysts were obtained from the University of Idaho.

Sample concentration. 1. One liter sample was split between two 750-ml centrifuge bottles. The collection container was rinsed with elution solution and poured into the centrifuge bottles, then centrifuged at 1600 x g for 15 minutes.

2. The centrifuged sample was aspirated down to 20-50 ml without disturbing the pellet. The 750ml bottles were gently swirled to break apart the pellet, then a pipette was used to collect the pellet/supernatant placing it in a 50-ml centrifuge tube. The 750ml centrifuge bottles were rinsed out with elution solution and also pipetted into the 50-ml centrifuge tubes which were centrifuged for 12 minutes to pellet.

3. The new centrifuged sample was aspirated down to 5 ml without disturbing the pellet. At this point four times the pellet size (or if the pellet is 1ml or less, add a minimum of 5 ml 10% formalin) of 10% formalin was added to preserve the sample for later work and to kill the organisms.

Flotation. 4. To remove the formalin, the sample was centrifuged for 10 minutes at 3500 rpm and poured (or aspirated without disturbing the pellet) into the appropriate waste container. Water was added up to the 50 ml mark and centrifuged again, then aspirated down to the pellet.

5. Elution solution was added to bring the volume up to 20 ml. The sample was vortexed to break up the pellet, sonicated for 10 minutes and then gently overlaid on 25 ml of 4/5 Sheather's flotation media. This sample was centrifuged for 12 minutes at 2700 rpm.

6. The top sample was gently aspirated off with a 25-ml pipette, collecting all of the interface and putting it in another tube. Distilled water was added to bring the volume of the new tube with the interface up to 50 ml, and centrifuged for 10 minutes at 3500rpm.

7. The supernatant was aspirated down to 5ml, then the sample was ready for antibody staining.

Antibody Staining. 8. A prewetted (with PBS) pre-filter and a filter for each sample (1.2µm pore size) was placed on the screen of the manifold and held in place with a metal sample holder. Some PBS was added and the vacuum system was turned on to make sure there were no leaks in the system.

9. The 5 ml sample was added with a pipette to the filter membrane and allowed to drain without letting it to dry out.

10. 0.5ml of the 1⁰ antibody was added to each membrane with the filtered sample. The samples were then covered with foil for 30 minutes.

11. Each membrane rinsed with 10ml of PBS before 0.5ml of the 2⁰ antibody was added and the manifold holder was again covered with foil. The samples were allowed to stain for 30 minutes, then each filter was rinsed with 10ml of PBS and drained without letting the membranes dry out.

12. A drop of DABCO/glycerol smeared evenly over a glass slide with a pipette tip. The membrane filter, without the pre-filter was placed face up onto the slide, and another drop of glycerol was placed on the membrane. A glass coverslip was placed on top avoiding air bubbles. The slide was allowed to sit for at least 30 minutes in the refrigerator before reading.

Parasite counting. The slides were inspected using UV-light microscopy at 200x magnification. Based on fluorescence, size and shape (Rose et al. 1988), *Giardia* cysts and *Cryptosporidium* oocysts were identified and counted.

Data Analysis Procedures. All viral assay data compiled from the above plaque assays were expressed in terms of the ratio, C/C_0 , defined as effluent virus concentration divided by the influent concentration. Percentage removal of the virus is then $(1 - C/C_0) \times 100$. This information was computed for each day of the column wet cycles in which virus measurements were made. The total virus removal for a wet period was calculated using the total number of viruses influent to the column ($\sum C_{in} \cdot Q \cdot T$) and total virus coming out of the column ($\sum C_{out} \cdot Q \cdot T$), where C_{in} and C_{out} are the influent and effluent viral concentrations in plaque forming units (pfu) per mL, Q is the average flow rate over the period of interest (usually ~ 24 hours) in mL/min, and T is the time period in minutes.

Removal of indigenous *Giardia* cysts, indigenous *Cryptosporidium* oocysts, and formalin-killed (seeded) *Cryptosporidium* oocysts was determined from daily samples of column influent and effluent during the different wet periods. The samples were analyzed for these

protozoan parasites according to the *Standard Methods for the Examination of Water and Wastewater, 18th Ed (1992)* already described (see above).

Composition of Artificial Rainwater

In order to prepare rainwater for the rainfall experiments in the Agua Fria one-meter sand column, a typical, local rainwater composition was obtained from Brian Barbaris, Department of Atmospheric Sciences, the University of Arizona: per 1 liter of Milli - Q (Millipore filtration system) water:

0.42 mmoles MgSO_4
0.425 mmoles K_2SO_4
0.635 mmoles CaSO_4
0.235 mmoles CaCl_2
0.54 mmoles $\text{NaC}_2\text{H}_3\text{O}_2$
3.07 mmoles NH_4NO_3
1.22 mmoles NaCl
0.56 mmoles HNO_3
0.80 mmoles HCl

The high ionic strength water that was used in the second rainwater experiment was prepared by adding Sea Salts (Sigma Chemical Co, St. Louis, MO) to make the measured conductivity approximately equal to that of secondary effluent, around 900 microsiemens per centimeter (mS/cm).

QUALITY CONTROL AND QUALITY ASSURANCE

Replication

Arizona State University

Detailed text and CV table needed

University of Arizona

Detailed text and CV table needed

University of Colorado

Table 2.9 lists the coefficients of variance (CVs) for the experimental and analytical analyses performed for this study at the University of Colorado. Analytical CVs were based upon reproducibility of data when 10 % of the samples were analyzed in triplicate. These percentages represent the sensitivity of a particular analytical instrument towards a particular water quality parameter; whereas the experimental CVs incorporate the error associated with performing the experiment prior to analysis (i.e., bench scale chlorination, incubation, and extraction within a SDS-THMs experiment).

Table 2.9
Analytical and Experimental Replication Analysis at the University of Colorado

Parameter	Units	C.V. (%) ^a		MDL ^b
		Analytical	Experimental	
TOC (<1um)	mg/L	<2	n/a ^c	0.2
DOC	mg/L	<2	n/a	0.2
BDOC	mg/L	<2	8.1	0.2
UVA ₂₅₄	cm ⁻¹	3.41	n/a	0.001
pH	n/a	0.9	n/a	n/a
Total NH ₃ -N	mg/L	8.45	n/a	0.01
THMs	µg/L	0.78	5.3	0.5
HAA _{6s}	µg/L	2.55	4.2	1.0
Cl ₂ Residual	mg/L	4.0	n/a	0.05

a- Coefficient of variance.

b- Minimum detection limit.

c- not applicable

2.6.2 Interlab Comparison

In addition, Table 2.10 lists the results of a interlaboratory quality control assesment between Arizona State University, The University of Arizona, and the University of Colorado. A sample was taken from the 91st Avenue Plant on January 15, 1996. The sample was filtered with a 0.45 µm filter, frozen, and shipped to the three participating universities.

Table 2.10
Interlaboratory Quality Control

Analysis	ASU	U of A	CU
DOC (mg/L)	np ^a	8.72	9.52
UVA ₂₅₄ (cm ⁻¹)	np	0.121	0.100
NH ₃ -N (mg/L)	1.31	1.74	1.53
NO ₂ ⁻ -N (mg/L)	0.171	np	np
NO ₃ ⁻ -N (mg/L)	1.92	np	np
NO ₂ ⁻ +NO ₃ ⁻ -N (mg/L)	np	2.06	np

a- analysis not performed

References

- Adams, M.H. 1959. *Bacteriophages*. New York: Interscience Publishers, Inc.
- APHA, AWWA, and WPCF. 1992. *Standard Methods for the Examination of Water and Wastewater*. 18th ed. Washington, D.C.: APHA.
- Bremner, J. M., and K. Shaw, 1955. Determination of Ammonia and Nitrate in Soil. *Journal of Agricultural Science* 46:320-328.
- Enriquez-Enriquez, C. 1994. Detection and Survival of Selected Viruses in Water. Ph.D diss., The University of Arizona, Tucson, Az.
- Leenheer, J.A., 1981, Comprehensive Approach to Preparative Isolation and Fractionation of Dissolved Organic Carbon from Natural Waters and Wastewaters, *Environmental Science & Technology*, 15:5:578-587.
- Mogren, E.M.; Scarpino, P. and Summers, R.S., 1990, Measurement of Biodegradable Dissolved Organic Carbon in Drinking Water, In *Proc. of AWWA 1990 Annual Conference*. Cincinnati, Ohio:AWWA.
- Murphy, B. 1993. M.S. thesis, University of Colorado, Boulder, Co.
- Quanrud, David M., R.G. Arnold, L.G. Wilson, H.J. Gordon, D.W. Graham, and G.L. Amy, 1996. Forthcoming. *Journal of Environmental Engineering*
- Saghir, N., R. Mulvaney, and F. Azam, 1993. Determination of Nitrogen by Microdiffusion in Mason Jars., I: Inorganic nitrogen in soil extracts. *Communications in Soil Science and Plant Analysis* 24:1745-1762.
- Sclimenti, 1990

Xie, 1992

2-59

CHAPTER 3

HYDRAULICS

INTRODUCTION AND BACKGROUND

Soil aquifer treatment (SAT) involves the application of secondary effluent through large surface basins to surface or near-surface soils. This effluent infiltrates to an underlying aquifer through the vadose zone as treatment occurs. Field and laboratory observations indicate that the hydraulics of such SAT infiltration basins are affected by many environmental factors including soil type, field spatial variability of soil type, the formation of a surface clogging layer, wetting/drying cycle times for application of the secondary effluent, effluent type, and climatic conditions. Clearly the maintenance of a reasonable rate of infiltration is of prime importance to the success of any SAT facility. Further, the hydraulic loading rate is important because it relates directly to the land requirements for SAT. Field observations indicate that the hydraulics of SAT infiltration basins are controlled to a large extent by the formation of a low conductivity clogging layer on and within the upper few centimeters of the surface soils. Therefore, management of surface and near-surface basin soils through control of wetting and drying cycle times and periodic basin surface scarification is generally required to ensure adequate infiltration rates.

Not only is the hydraulic loading rate important from a feasibility/economics standpoint, it also relates to the efficiency of treatment. For example, although the formation of the basin bottom clogging layer tends to reduce the infiltration rate compared to that of the native soil alone, the clogging layer is beneficial with regard to water quality. The rate of effluent infiltration can affect physical adsorption processes, and the retention time of water in the soil can affect biologically-driven removal mechanisms. In addition, the rate of loading and the length of the wetting and drying cycles affect the degree of wetting and the extent of drying that occurs in the prototype. This means that the optimum rate of loading in consideration of all factors may be somewhat less than the maximum possible loading rate for the soil alone.

The studies described in the following sections address many aspects of the hydraulics of the infiltration and SAT problems using a combination of laboratory and field studies. The studies

include evaluation of the influence of soil type, effluent type, surface clogging material, wetting/drying cycle times, and basin geometry on infiltration rates.

RESULTS OF LABORATORY COLUMN TESTS

Description of Soil Types

One goal of this project is to evaluate the influence of soil type on infiltration rate and treatment efficiency for SAT systems. To achieve that end, five different soil types, covering a wide range of physical, hydrological and chemical characteristics, have been selected for study. Four of them were taken from the vicinity of the proposed SAT site, for disposal of effluent from the 91st Avenue Wastewater Treatment Plant, in Glendale, Arizona. The fifth soil is from the operating Sweetwater Recharge site near the Roger Road Wastewater Treatment Plant in Tucson, Arizona. The specific locations are listed below:

- Agua Fria Soil - Agua Fria River bottom at Camelback Road in Glendale, AZ;
- Sweetwater Soil - Sweetwater Groundwater Recharge Facility in Tucson, AZ;
- South Pond Soil - Southern site for Pilot Percolation Study in Glendale, AZ;
- North Pond Soil - Northern site for Pilot Percolation Study in Glendale, AZ;
- Ag. Field Soil - Agricultural field south of South Pond Site in Glendale, AZ.

In accordance with the Unified Soil Classification System, the soils can be described as: poorly-graded sand or SP (Agua Fria), poorly-graded, silty sand or SP-SM (Sweetwater), silty sands or SM (North and South Pond), and low-plasticity clay or CL (Ag. Field). However herein, they are also referred to as: sand (Agua Fria), sandy-loam (Sweetwater), silts (South and North Pond), and clay (Ag. Field). The characteristics of each soil are fully-described in the Soil Properties Report, which is included as an appendix to this document.

Water and Air Permeability Tests

Hydraulic Conductivity

As a precursor to more complex studies of unsaturated infiltration, an extensive series of saturated hydraulic conductivity tests were performed on each of the five soil types. The tests were conducted in a falling-head type apparatus, and the reported results are the averages of at least two replicates. As detailed in the soils report, target dry densities, that were thought to be representative of field conditions, were selected for each soil type. To provide a better basis for comparisons, the measured conductivity values were adjusted using the Kozeny-Carmen equation if the actual density of a sample differed from the target. The results are summarized in Table 3-1 below.

Table 3-1
Saturated hydraulic conductivity

Soil	Undisturbed Conductivity		Recompacted Conductivity	
	(cm/sec)	(ft/day)	(cm/sec)	(ft/day)
Agua Fria	N/A	N/A	8.4×10^{-2}	238.25
Sweetwater	N/A	N/A	1.9×10^{-2}	53.03
South Pond	1.3×10^{-3}	3.59	6.9×10^{-4}	1.96
North Pond	2.3×10^{-4}	0.65	1.8×10^{-4}	0.50
Ag. Field	3.3×10^{-5}	0.09	3.5×10^{-6}	0.01

Note that for each of the soils with a significant fines content (South Pond, North Pond and Ag. Field), the hydraulic conductivity was measured for both undisturbed and recompacted specimens. The undisturbed specimens were obtained from the near surface using thin-walled Shelby tube samplers. The recompacted samples were prepared in the lab at the target dry density from disturbed bulk samples of the soil. Due to the difficulty in obtaining truly undisturbed samples of granular materials, only tests of recompacted specimens were performed on the Agua Fria and Sweetwater soils. It should be noted that little difference was expected for these two soils, because experience has shown that granular materials are not particularly sensitive to changes in soil structure.

The comparison of results, for the finer grained soils, showed a consistent trend of decreasing hydraulic conductivity with sample disturbance. This can be attributed to changes in the macro-structure of the soil on disturbance and recompaction. Such changes include the breaking of clay clods and the elimination of preferred flow paths that result from shrinkage cracking of the soil and/or the action of plants, burrowing insects and animals. These differences will have to be accounted for in extrapolating the results to field conditions.

Air Permeability

Traditional descriptions of water movement in unsaturated soil neglect the effects of the air phase by assuming that the air is free to escape from the soil. However, if air flow is impeded, a significant reduction in infiltration rate may be observed. As a result, a two phase model may be required to accurately simulate the water flow. In that case, the relationship between air permeability and water degree of saturation is needed to subsequently describe movement in the air phase. To this end, a series of air permeability tests, at different degrees of saturation, were run on each of the five subject soils. The results are illustrated in Figure 3-1.

Arizona State University Laboratory "Clean Water" Column Studies

Laboratory column ponding tests were performed in this study to investigate the degree of saturation profile beyond the wetting front. This investigation was necessary to provide the input data for hydrological parameter estimation. The measurements included inflow infiltration rate, progress of wetting front position, degree of saturation profile, and in some cases, soil suction. In all cases, the soil surface boundary was a constant head boundary. In order to study the effect of air phase flow on water infiltration, the base boundaries included open (vented to atmosphere) and bounded (no air flow).

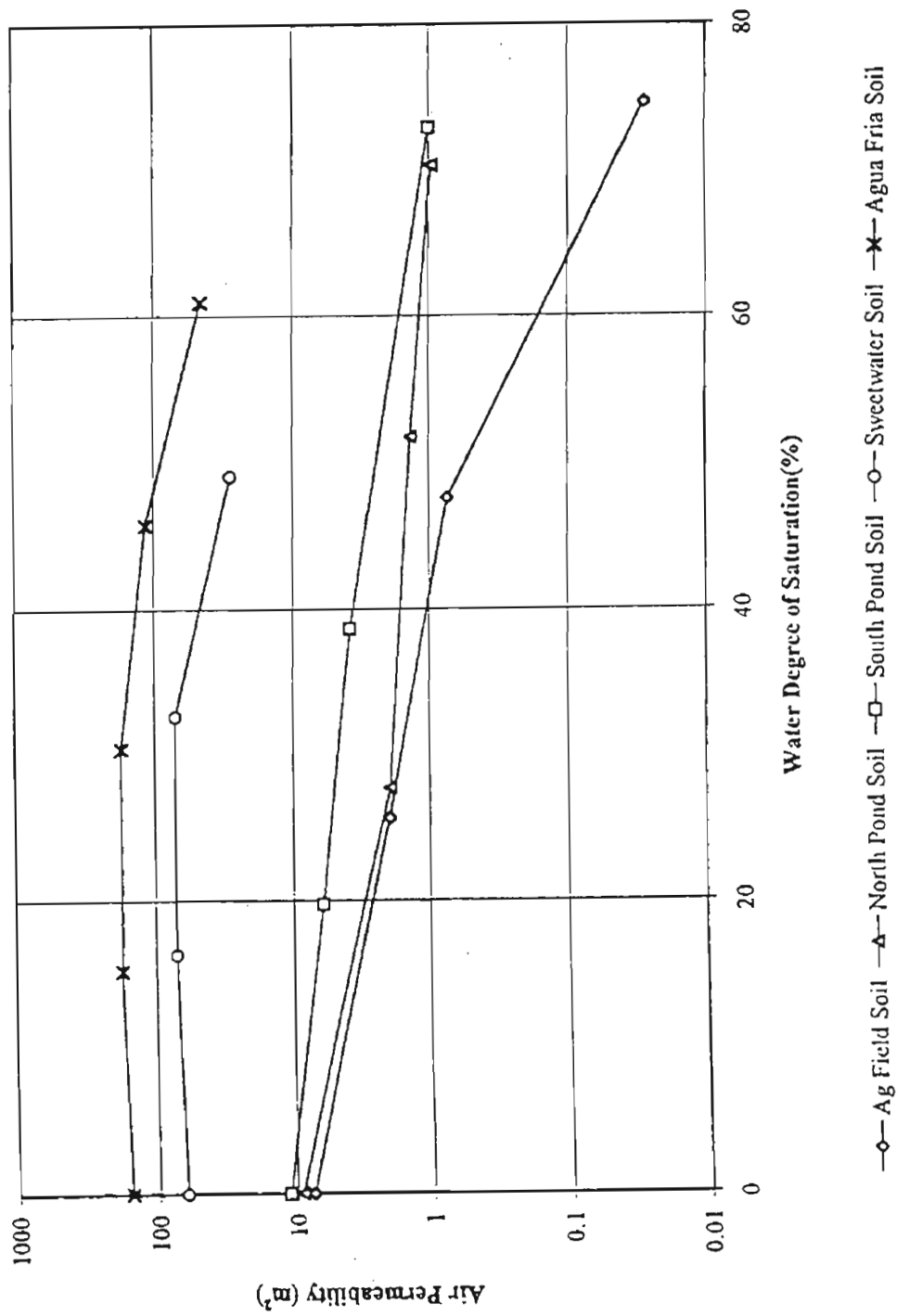


Figure 3-1 Air Permeability for S.A.T. Soils

Test Description

The apparatus consisted of a transparent column with tensiometer and water content sampling ports and a constant head device as shown in Figure 3-2. The columns were made of acrylic cylinders 100 cm high and with a 7.62 cm inside diameter. Along the length of the column, there were two rows of ports to facilitate tensiometer installation and direct soil sampling for water content measurement. In each row, there was a 7.62 cm center to center distance between ports. A Mariot bottle was used to provide constant head for the ponding test while allowing inflow rate measurement. Porous cup tensiometers were used to measure the soil suction. The air entry value for each porous cup was approximately one atmosphere. The tensiometers used were able to measure soil suctions as high as 0.6 atmosphere vacuum. A steel screen was inserted into the bottom of the column to support the filter material. Different types of filter materials were used for different subject soils in order to provide an adequate support for the compacted soil while creating the least possible resistance to water and air flow.

The soils were compacted in several lifts into columns at a target dry density and target molding water content corresponding to average field conditions. Usually 3 inch lifts were adequate to provide uniform compaction. Once the specimen was prepared, the water supply tubing was attached, and the test was begun by removing the stopper in the Mariot bottle and allowing the water to enter the specimen. The wetting front position and the water level in the Mariot bottle was measured at different time intervals. In some instances, the exact location of the wetting front was difficult to define because it did not travel through the soil evenly. In this case, a visual estimation was made of the average position of the wetting front. The test duration varied from several minutes for Agua Fria sand to four weeks for Ag. Field clay. The tensiometer readings were made only for Ag. Field clay. For the other subject soils, the duration of tests was not long enough to provide adequate tensiometer equilibration time.

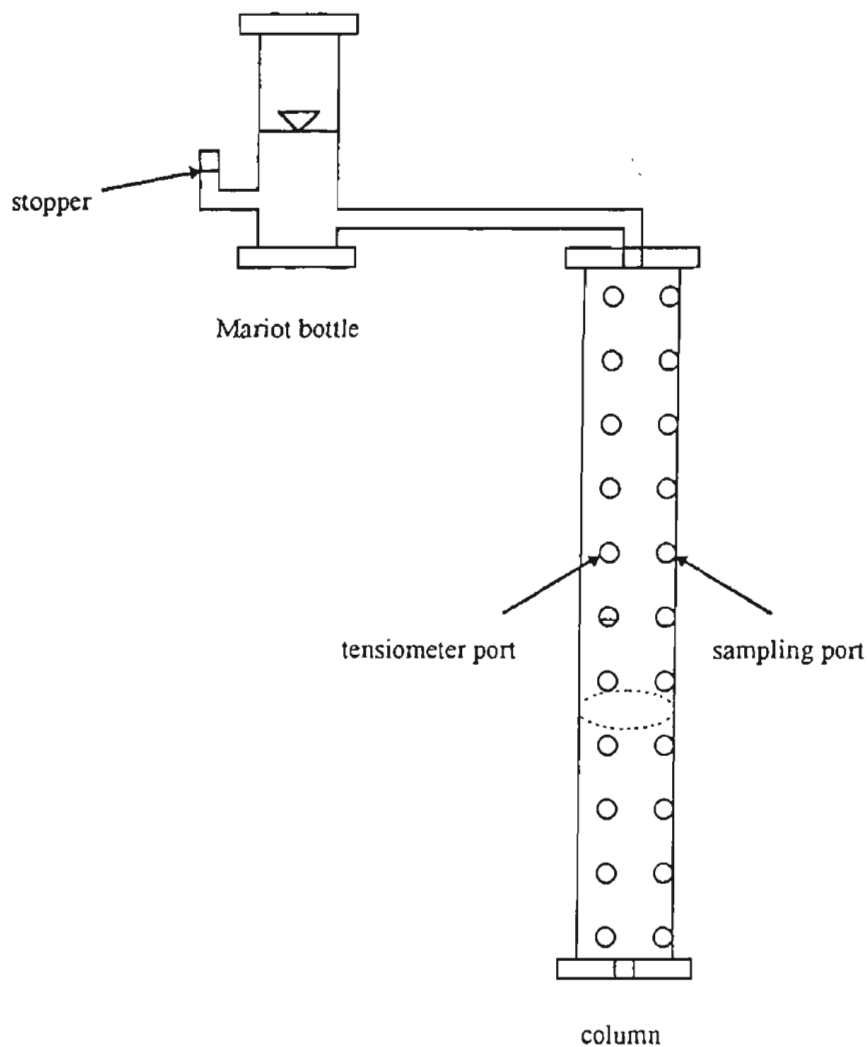


Figure 3-2 Column Infiltration Apparatus

At the end of the infiltration test the water supply was shut off and soil samples were quickly taken from each port. These samples were used to determine the water content and degree of saturation along the profile of the column. It should be noted that direct sampling of sand was a difficult process because the water content changed very quickly after the water supply was terminated.

Experimental Results

Infiltration rate. It has been observed both in laboratory and field tests that the rate at which water infiltrates through the soil surface during ponded infiltration is initially quite large and decreases with increasing time, finally approaching a constant value. This final condition is usually called steady-state infiltration rate. In this column study, the steady state infiltration rate was obtained by measuring the effluent of column infiltration tests. The time needed to reach steady state varied significantly for different soil types -- 30 days for Ag. Field clay, 2 days for silty sand, and 1 to 3 hours for sand. Table 3-2 presents these results for the subject soils.

Table 3-2
Steady state infiltration rate

Soil	Steady State Infiltration Rate	
	(cm/sec)	(ft/day)
Agua Fria	9.2×10^{-2}	260.8
Sweetwater	2.1×10^{-2}	59.5
South Pond	7.8×10^{-4}	2.21
North Pond	2.6×10^{-4}	0.74
Ag. Field	1.96×10^{-6}	0.0056

Compared to the saturated hydraulic conductivity given in Table 3-1 above, the steady state infiltration rates of sand and silty sand are approximately equal to their saturated conductivities. However the steady state infiltration rate of clay is only half of its saturated hydraulic conductivity.

Degree of saturation profiles. Figure 3-3 to Figure 3-7 present the degree of saturation profiles from direct sampling of all the subject soils. In general, the profiles can be divided into four zones similar to those observed by Bodman and Colman (1943). Zone 1: There existed a thin saturation zone in which the degree of saturation approached 100%. The thickness of this zone could not be quantified in this study because of the port spacing for direct sampling. However, it was found that for all soils in this study the thickness of zone 1 was less than 4 cm and may have increased somewhat with time. Zone 2: Immediately below zone 1 was a transmission zone in which the degree of saturation decreased rapidly from saturation to a relative constant value.

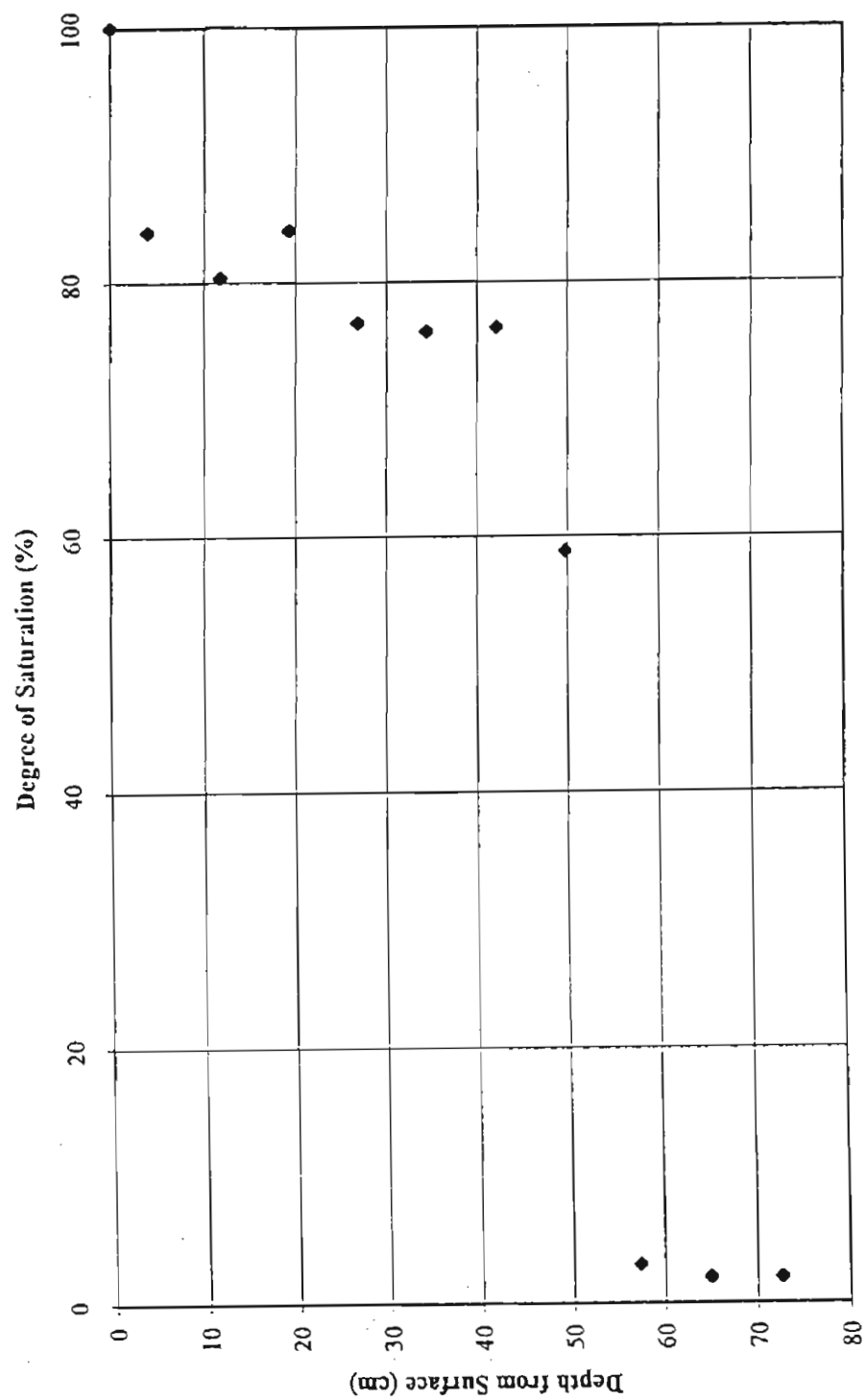


Figure 3-3 Degree of Saturation Profile for Agua Fria Soil Column

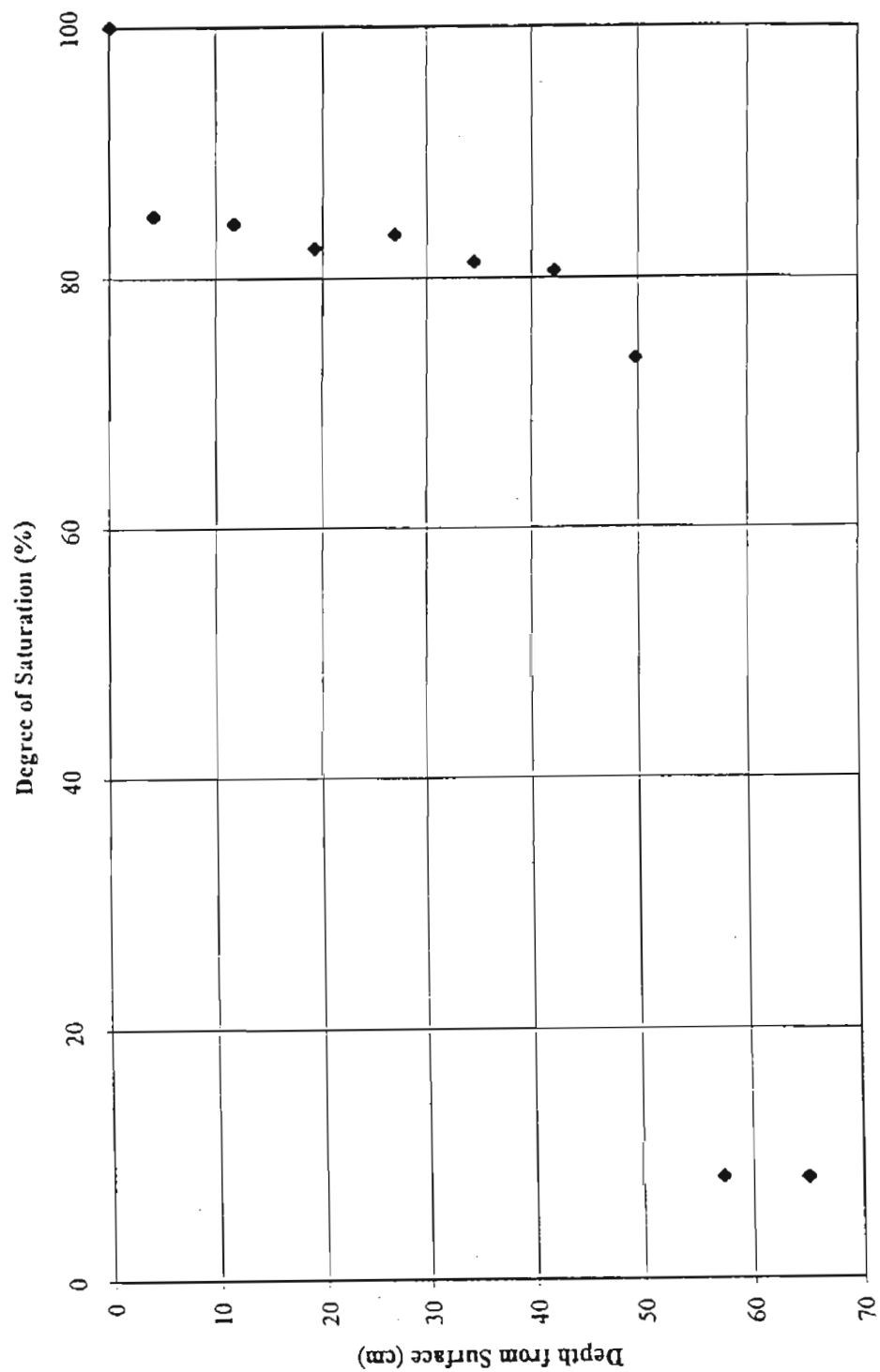


Figure 3-4 Degree of Saturation Profile for Sweetwater Soil Column

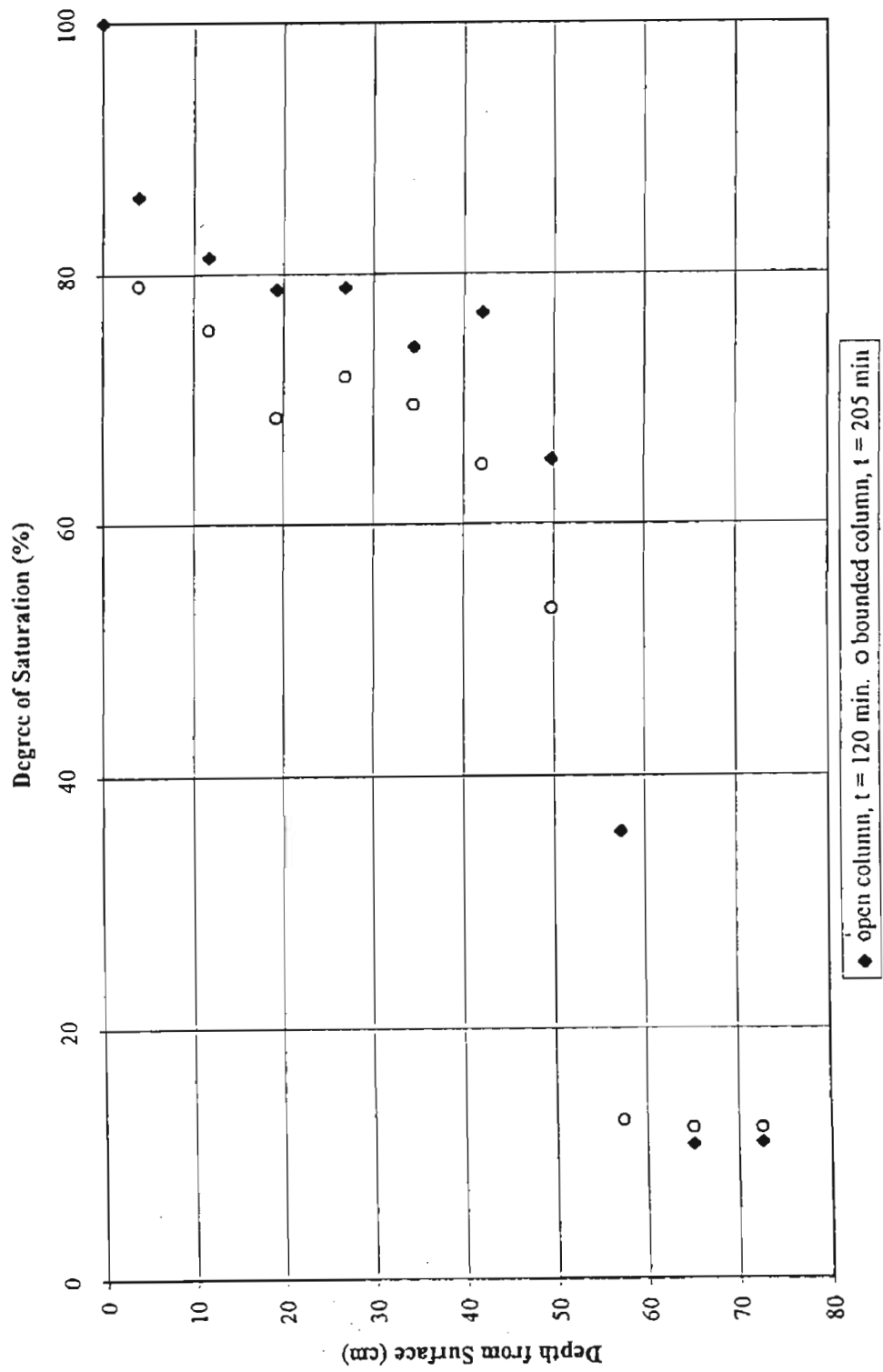


Figure 3-5 Degree of Saturation Profile for South Pond Soil Column

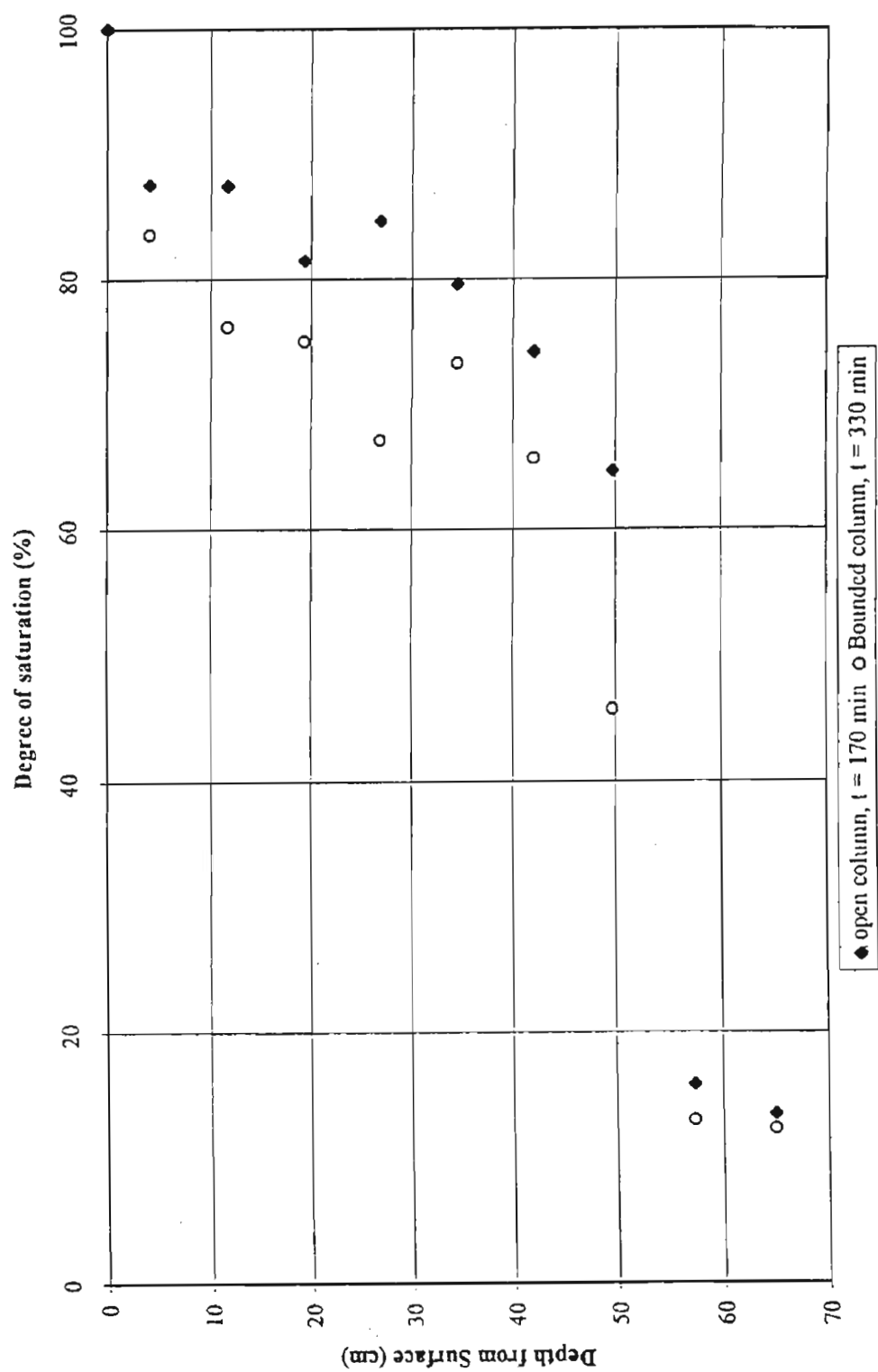


Figure 3-6 Degree of Saturation Profile for North Pond Soil Column

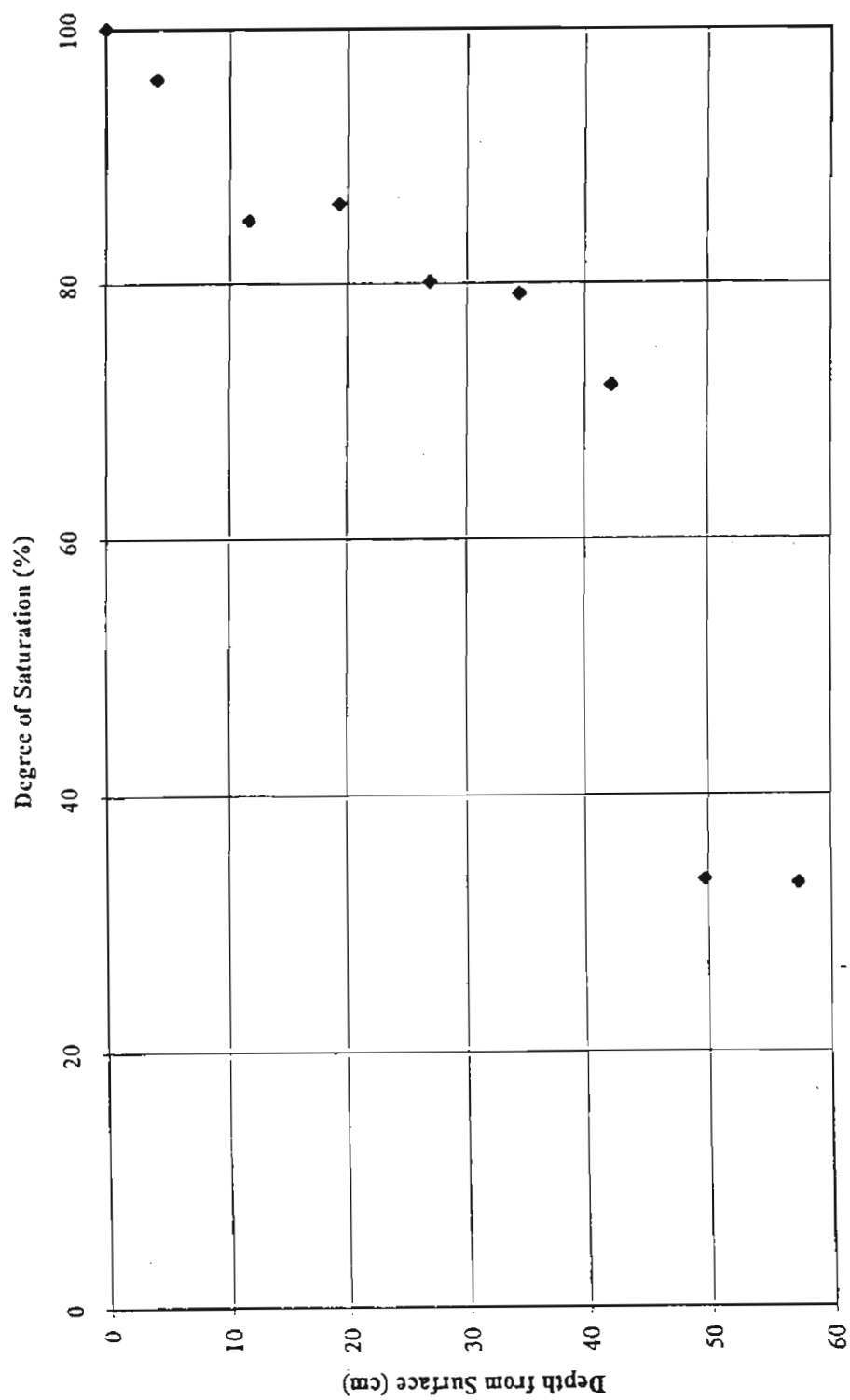


Figure 3-7 Degree of Saturation Profile for Ag. Field Soil Column

Zone 3: This was a zone with a relative constant degree of saturation (70 % to 90 % depending on the soil type and soil density). The thickness of this zone increased with time. Zone 4: Below zone 3 there was another transmission zone or wetting front, in which the degree of saturation decreased rapidly from the relatively constant value described in zone 3 to the initial degree of saturation. The thickness of both transmission zones did not change appreciably throughout the tests.

In order to evaluate the degree of wetting in an average sense, a concept of average degree of saturation behind the wetting front was introduced. The average degree of saturation was calculated from the measured cumulative infiltration and wetting front position instead of direct water content measurements. This avoided the difficulties involved with precisely measuring water content. Assuming at time t the wetting front position is Z_w (cm) from the surface, and the cumulative infiltration is Q (cm). The average gravimetric water content w behind the wetting front can then be calculated from:

$$w = w_i + \frac{Q\rho_w}{Z_w\rho_d} \quad (3-1)$$

where w_i is the initial water content, ρ_d is the soil dry density, and ρ_w is the density of water.

The average degree of saturation S is calculated from the following expression:

$$S = \frac{G_s w}{\frac{G_s \rho_w}{\rho_d} - 1} \quad (3-2)$$

where G_s is the specific gravity of soil solid.

In general, the average degree of saturation was higher at the beginning of the test, and decreased rapidly to an approximately constant value. This phenomenon further verified the existence of zone 3 described above. The constant values for the subject soils are listed in Table 3-3. These results show that the average degree of saturation was well below 100%.

Table 3-3

Average degree of saturation

Soil	Average Degree of Saturation (%)
Agua Fria	87.8
Sweetwater	89.4
South Pond	70.2
North Pond	75.2
Ag. Field	82.5

Empirical fit to measured wetting front velocity. The measured wetting front position versus time can be fitted to a simple parabola using the following expression:

$$Z_w = c_1(K_s t)^{c_2} \quad (3-3)$$

where Z_w is the distance from the surface to the wetting front (cm), K_s is saturated hydraulic conductivity (cm/sec), t is elapsed time since infiltration commenced (sec), and c_1 and c_2 are empirical parameters.

It must be noted that the saturated hydraulic conductivity was introduced into the function to account for the effect of density and initial water content. The parameters c_1 and c_2 for the subject soils are summarized in Table 3-4.

To determine Z_w for a given soil, the percent fines (passing #200 sieve) and saturated hydraulic conductivity tests must be performed. Parameters c_1 and c_2 can then be obtained from Table 3-4 by interpolating or extrapolating from the percent fines data. The progression of the wetting front for a 1-D infiltration can be calculated from Equation 3-3. It must be noted that the results in Table 3-4 were obtained from ponding tests with a 15 cm head. If the ponding depth is much different from 15 cm, the wetting front position obtained from Equation 3-3 should be corrected.

Table 3-4
Wetting front equation parameters

Soil	Percent Fines (< No. 200 Sieve)	C ₁	C ₂
Agua Fria	0.7	11.17	0.752
Sweetwater	5.5	16.38	0.708
South Pond	19.2	22.25	0.569
North Pond	26.9	32.90	0.537
Ag. Field	73.0	37.45	0.433

Soil suction profile. Figure 3-8 presents the soil suction profile obtained from tensiometer readings for Ag. field soil. The measurements were made when the wetting front reached 48 cm below the soil surface. The results qualitatively show that only the upper 5 cm of soil was saturated.

Hydrological Parameters from Inverse Methodology

Numerical simulation for unsaturated flow requires the knowledge of the soil water retention relationship and unsaturated hydraulic conductivity. These relationships have been determined in past studies by direct measurement of soil suction at various water contents and by direct determination of conductivity at various water contents, then selecting the best fit water retention function $\theta(h)$ and unsaturated conductivity function $K(\theta)$ by curve fitting techniques. This direct-determination method has the advantage of being straightforward. However, the measurement of soil suction and unsaturated conductivity are time consuming and involve some measurement difficulties, especially in the measurement of $K(\theta)$. To avoid direct lab or field measurement of $K(\theta)$, some investigators have proposed techniques of predicting $K(\theta)$ from known $\theta(h)$ using models based on pore size distribution (Mualem 1976)(Burdine 1953). Frequently used expressions for the hydraulic conductivity are those developed by Brooks and Corey (1964) and van Genuchten (1980). The expressions developed by van Genuchten are:

$$S_e = \begin{cases} \left(1 + (\alpha h)^n\right)^{-m} & h < 0 \\ 1 & h \geq 0 \end{cases}$$

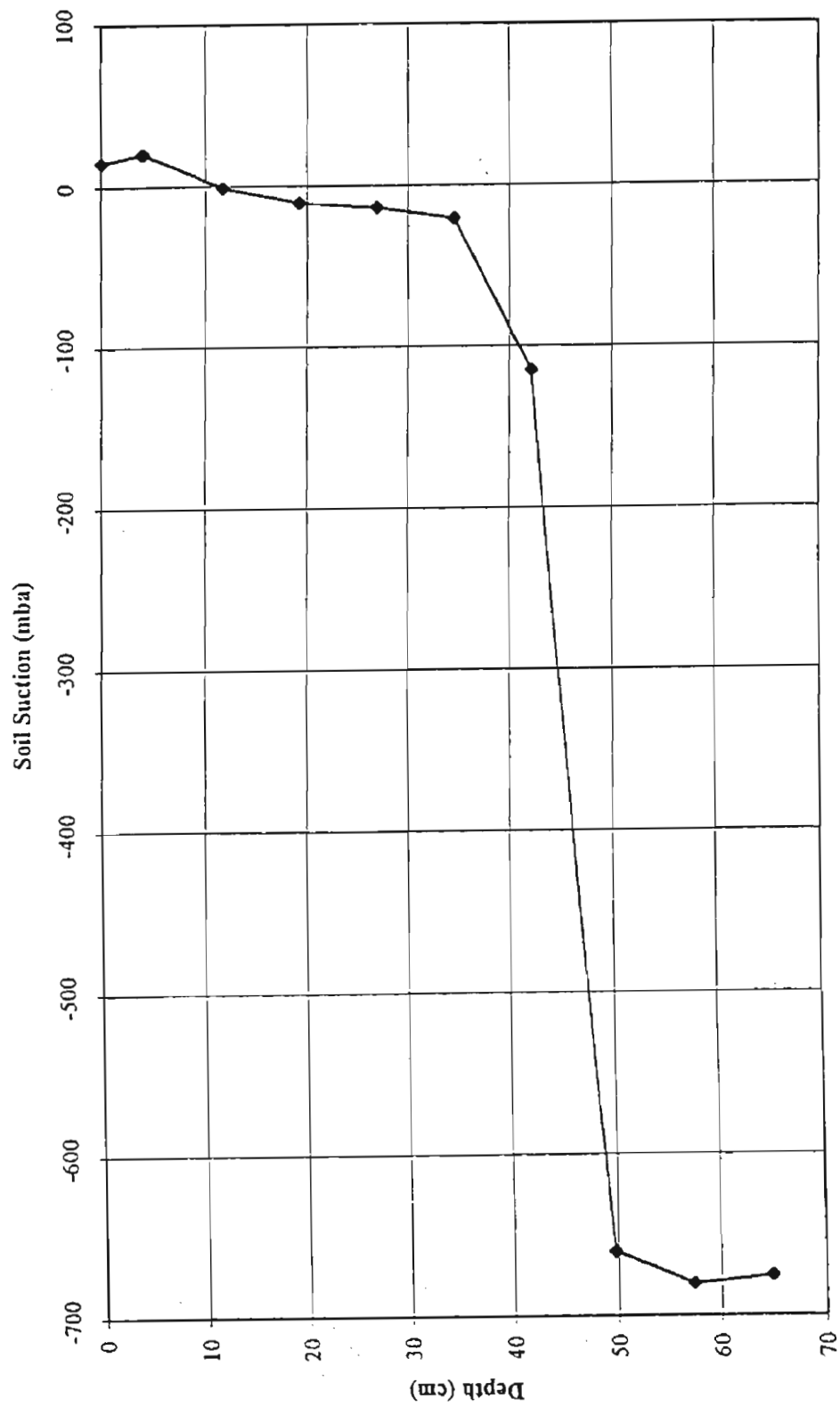


Figure 3-8 Soil Suction Profile for Ag. Field Clay
(wetting front at 48 cm)

$$K = K_s (S_e)^{\frac{1}{\alpha}} \left[1 - \left(1 - (S_e)^{\frac{1}{\alpha}} \right)^m \right]^2$$

where S_e is the effective saturation $= (\theta - \theta_r) / (\theta_s - \theta_r)$, K_s is the saturated hydraulic conductivity, and $m = 1 - 1/n$, α and n are model parameters.

Parameters in the above equations are commonly determined by measuring K_s directly and estimating the remaining parameters by fitting typical water retention functions to the measured (θ, h) data. The disadvantages of such an approach are: (1) time-consuming data collection and (2) the fact that parameters α and n are fitted to (θ, h) only, therefore any inaccuracy in the assumed hydraulic relationships, as well as effect of measurement error are forced into the prediction of $K(h)$. Because of this, the predicted $K(h)$ might sometimes deviate several orders of magnitude from the measured value (Yates et al. 1992). An alternative method would be to use inverse methodology to predict hydraulic properties from lab or field transient flow experiments.

Kool et al (1986) provide a comprehensive review of the available methods for inverse methodology and its application to unsaturated flow problems. Generally, the technique includes assuming the form of the soil water retention and hydraulic conductivity functions with unknown parameters, formulating an objective function to minimize the difference between the observed variables and the response from Richard's equation, and solving the optimization problem to obtain the unknown parameters. The objective function might be formulated as either ordinary least-squares minimization, weighted least-squares minimization, generalized least-squares minimization, or a maximum likelihood problem. The observed variables that might be considered include water content, suction head, or inflow/outflow rate for transient flow experiments. The observed data might be measured from either laboratory or field experiments. The experiment to be back-analyzed can be for the case of drainage or infiltration.

An example of an objective function formulated by a weighted least-squares minimization formulation would be:

$$\min_b O(b) = [q^* - q(b)]^T W [q^* - q(b)] + [b^* - b]^T V [b^* - b]$$

where the objective function $O(b)$ is a function of the model parameters b , $b = \{b_1, \dots, b_m\}^T$; $q^* = \{q_1^*, \dots, q_n^*\}^T$ is the observation vector whose elements represent measured heads, water contents, or fluxes; $q(b) = \{q_1(b), \dots, q_n(b)\}^T$ represents the predicted response for a given parameter vector

\mathbf{b} , \mathbf{b}^* represents direct estimates or measurements of the parameters \mathbf{b} ; \mathbf{W} and \mathbf{V} are symmetric weighting matrices.

In this study, the FLOFIT program (Kool and Parker 1988) was used to estimate the soil hydraulic properties of SAT subject soils by inverse methodology. FLOFIT was developed by Environmental Systems and Technologies, Inc., Blacksburg, Virginia. It is a program for estimating soil hydraulic and transport properties from unsaturated flow and tracer experiments. In solving the inverse problem, FLOFIT works in two stages. The first stage involves computing the model predictions for a given parameter vector by employing an existing unsaturated flow code (e.g. finite element). The second stage involves solving the nonlinear least squares problem followed by computation of the parameter adjustments. This two stage solution procedure continues in an iterative manner until convergence is attained or the specified maximum number of iterations is reached. FLOFIT assumes the unsaturated hydraulic properties, $K(\theta)$ and $\theta(h)$, to be described by the van Genuchten's (1980) parametric model.

Although FLOFIT can be used to estimate parameters θ_r , θ_s , α , n , and K_s simultaneously, it is recommended that some parameters with distinct physical meanings be measured directly. In this study, K_s and θ_s were measured independently, while θ_r was assumed to be the air-dried volumetric water content. The program inputs included the water content profile and cumulative infiltration data from laboratory column infiltration tests. Different weighting was selected for water content and cumulative infiltration, as required. For the studies on the SAT soils, using the "clean" water infiltration tests, the results seemed sensitive to the initial input of the parameters. Therefore, several groups of initial guess parameters were repeated to obtain the best estimates based on the lowest sum of squares. The results of parameter estimations for the SAT subject soils are shown in Table 3-5 below:

Table 3-5
Unsaturated flow parameters from inverse method determination

Soil	θ_r	θ_s	α (cm ⁻¹)	m	n
Agua Fria	0.000	0.427	0.0180	0.889	8.990
Sweetwater	0.000	0.394	0.0178	0.873	7.875
South Pond	0.010	0.394	0.0101	0.602	2.510
North Pond	0.010	0.396	0.0037	0.614	2.590
Ag. Field	0.080	0.427	0.0029	0.425	1.740

Numerical simulation using RETC determined parameters. HYDRUS simulation model (Kool and van Genuchten 1991) was used to simulate the column ponding infiltration so as to examine the hydrological properties given in Table 9 of the Soil Properties Report. These parameters were obtained from measured soil characteristics curves and RETC (van Genuchten 1987) curve fitting program. For the column ponding infiltration test, if the base boundary was vented to the atmosphere, the problem could be considered as a one-dimensional, one-phase fluid flow problem. The grid size was selected as 1 cm, the initial condition was a uniform initial molding water content; and the boundary conditions were as described in Table 3-6.

Table 3-6
Boundary conditions for one phase flow

Boundary	Description	Formula
Upper	constant head	$h_w(0, t) = \text{constant}$
Lower	no flow	$-K_w \left(\frac{\partial h_w}{\partial z} - 1 \right) = 0$

The results, as simulated with RETC-determined parameters, of the inflow infiltration rate, wetting front position, and degree of saturation profile for each of the subject soils are presented in Figure 3-9 to Figure 3-23. These figures also show the 1-D column test results. In general, the rate of infiltration was under-predicted, the degree of saturation behind the wetting front was over-predicted, and the velocity of the wetting front was under-predicted. These errors may have been introduced from many sources. These sources include errors in soil suction and infiltration measurements, numerical errors in simulation, and errors in the assumption of hydrological models. However, the author believes that the most important source is the uncertainty of the hydraulic conductivity.

Unsaturated hydraulic conductivity can be expressed as:

$$K = K_s K_r$$

where K_s is saturated conductivity, and K_r is relative conductivity, which is a function of water content or suction head.

K_r has always been considered to be one of the most highly variable soil parameters that engineers attempt to measure. The scatter for specimens of the same condition may vary by an order of magnitude (Houston et al. 1995).

The relative hydraulic conductivity K_r also varies greatly. Although it is restricted by definition to the range of 0 to 1, the values themselves span several orders of magnitude. This variation in K_r is not independent of the variation in K_s and i (hydraulic gradient). The temptation is strong to seek a single function which can be applied to a wide range of soil types (Mualem 1976, e.g.). However, such a function is not likely to be very appropriate for any particular soil type. The net result is that K_r is typically an additional source of uncertainty and variability. When the soil becomes very dry, i across the wetting front will necessarily become very large, and the corresponding values of K_r must become very small.

Numerical simulation using inverse parameters. The hydraulic parameters obtained by inversion from column infiltration experiments were again input into HYDRUS to examine the agreement between the simulated and experimental results. Theoretically, excellent agreement was expected when the "match" was being made on the same lab test from which the parameters were back-calculated. Figures 3-9 to 3-23 show graphically the position of the wetting front, the soil moisture profile, and the infiltration rate of simulated and experimental data for all of the subject soils. Although very acceptable results were obtained, the simulation over estimated the degree of saturation behind the wetting front. Excellent agreement could only be attained for either wetting front position or infiltration rate by adjusting the weight of input water content and the cumulative infiltration, but not both. This was probably because of the assumption of hydrological functions and the fact that the numerical simulation did not account for the reduction of hydraulic conductivity at the ponding surface.

One dimensional two phase flow simulation. From the column infiltration test, it was found that air phase flow significantly affected the water infiltration rate and wetting front position in the bounded column. Touma and Vauclin (1986) concluded from their lab column experiment and numerical simulation that when air could only escape through the surface, the air compression ahead of the wetting front was the major cause of the reduction in the infiltration rates. In this case, the two-phase approach should be used to simulate water flows for both

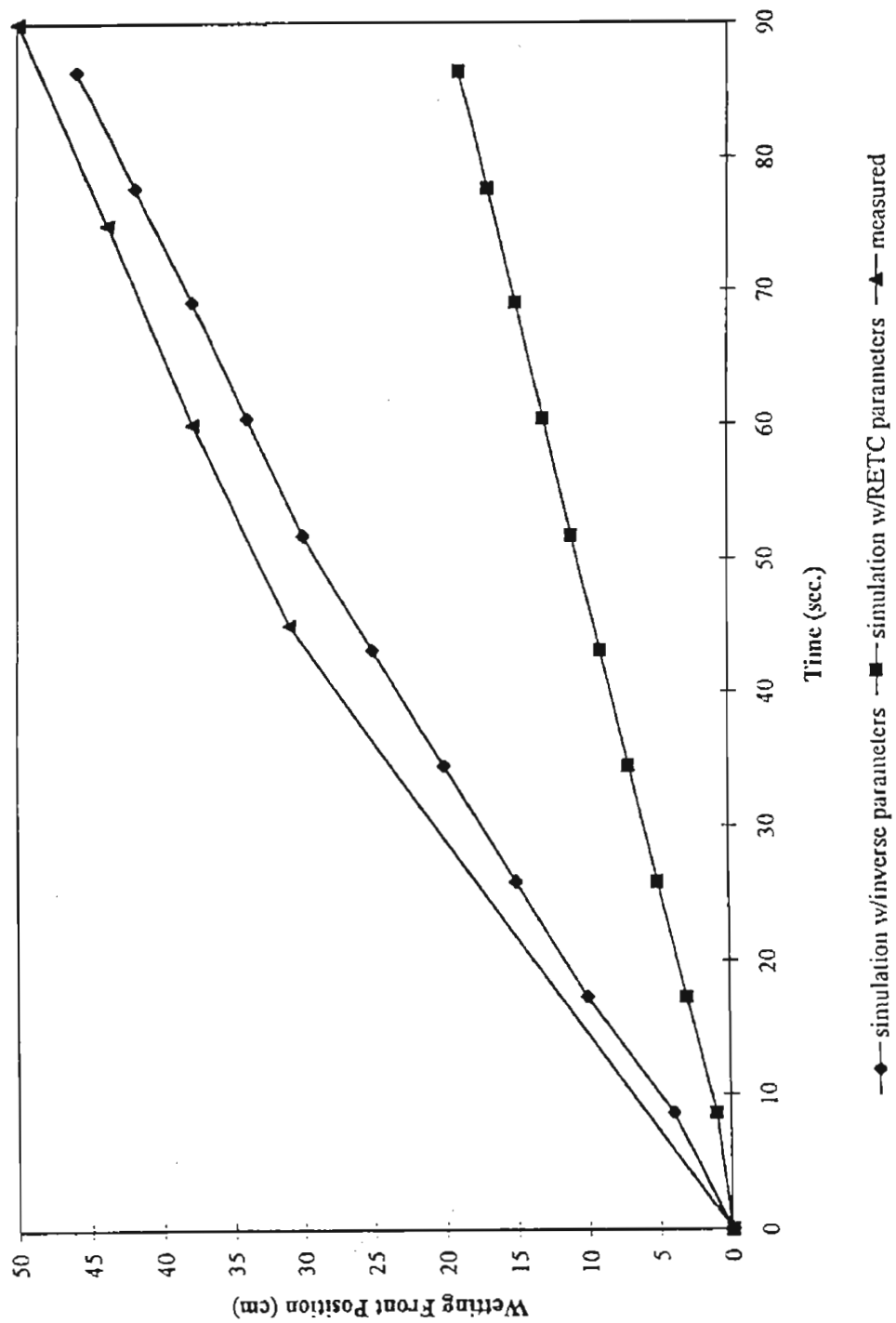


Figure 3-9 Agua Fria Soil Column Infiltration

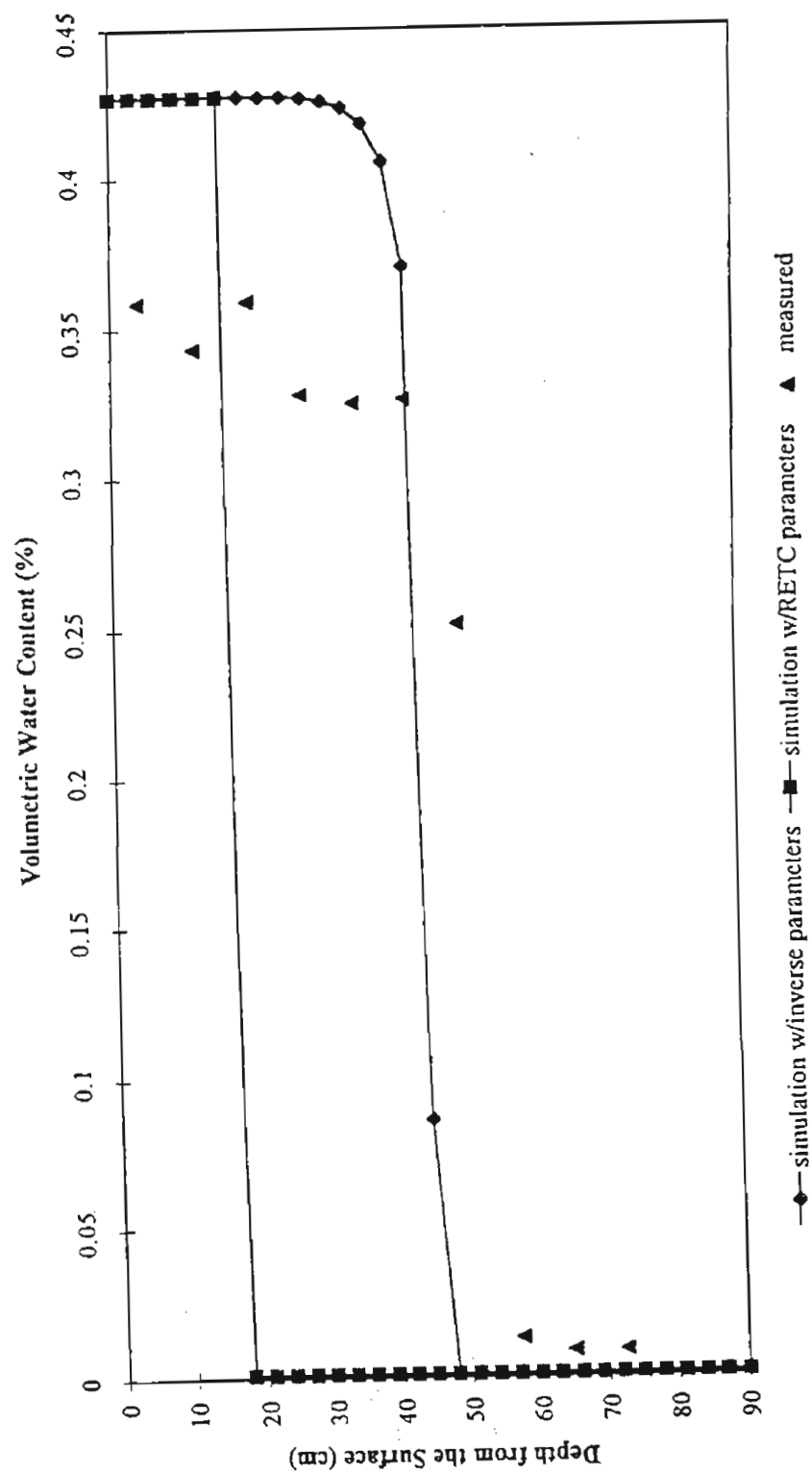


Figure 3-10 Agua Fria Soil Column Infiltration
ponding depth = 1 cm, $t=85$ sec.

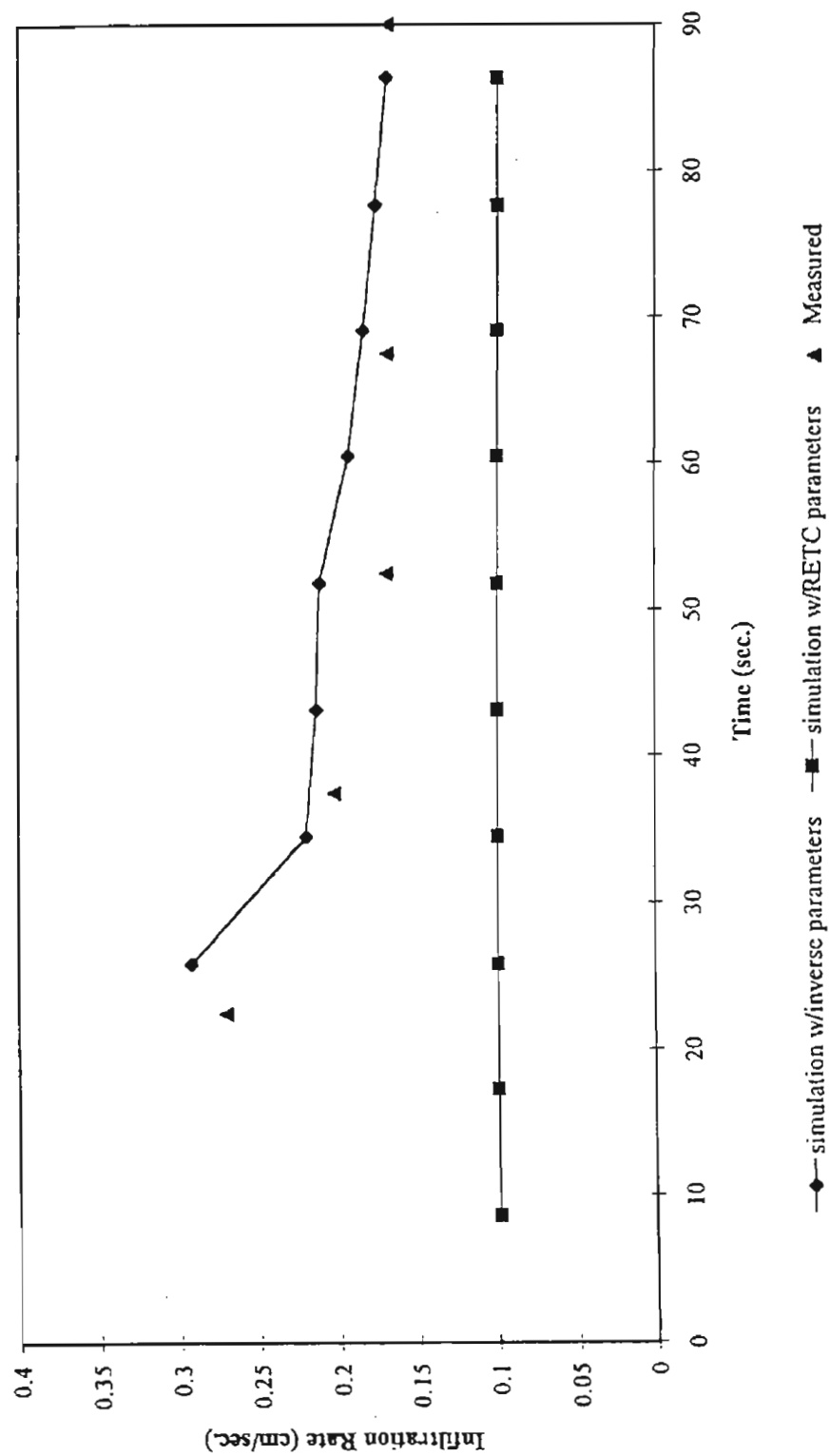


Figure 3-11 Agua Fria Soil Column Infiltration

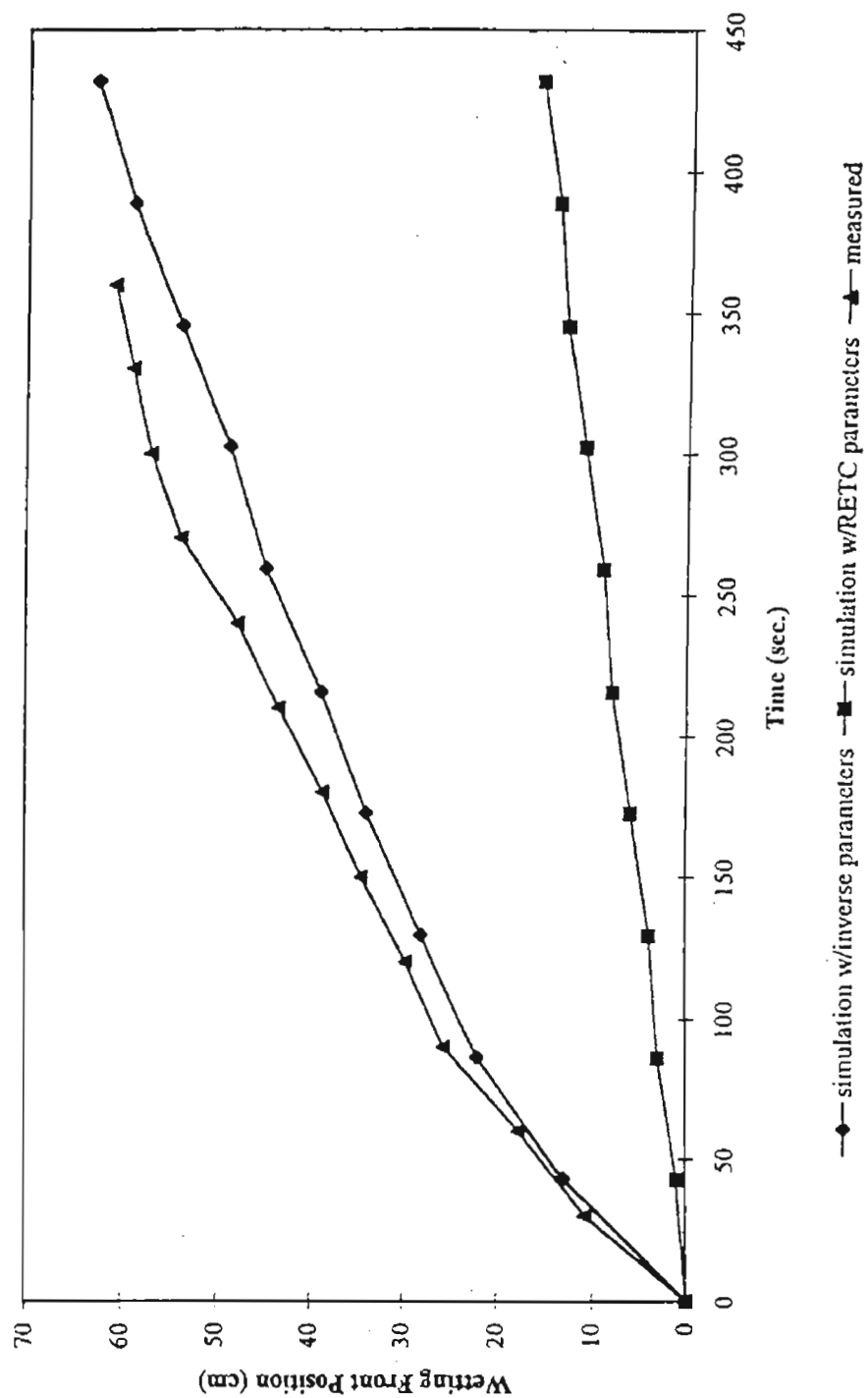


Figure 3-12 Sweetwater Soil Column Infiltration

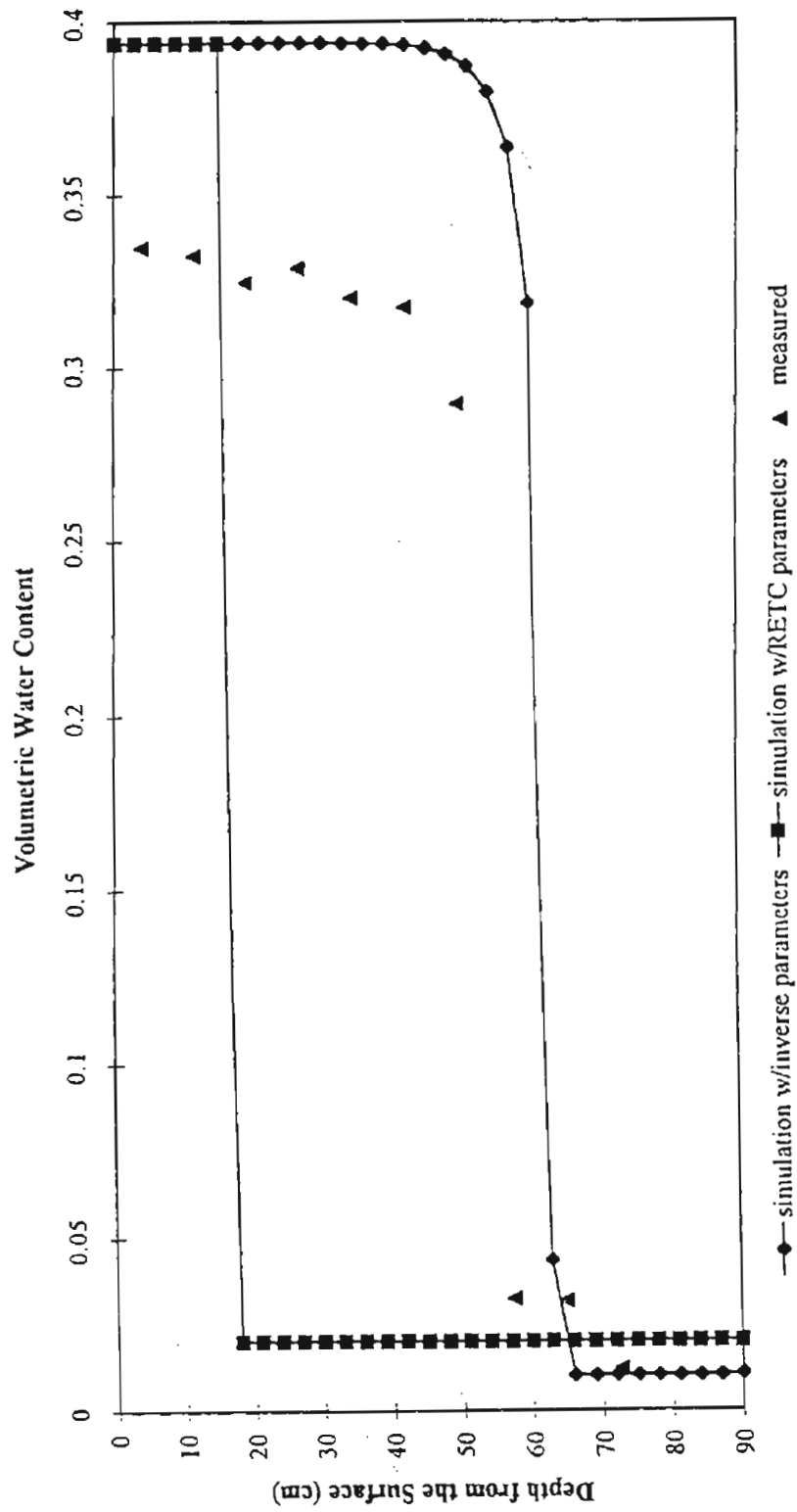


Figure 3-13 Sweewater Soil Column Infiltration
ponding depth=15cm, t=7 min.

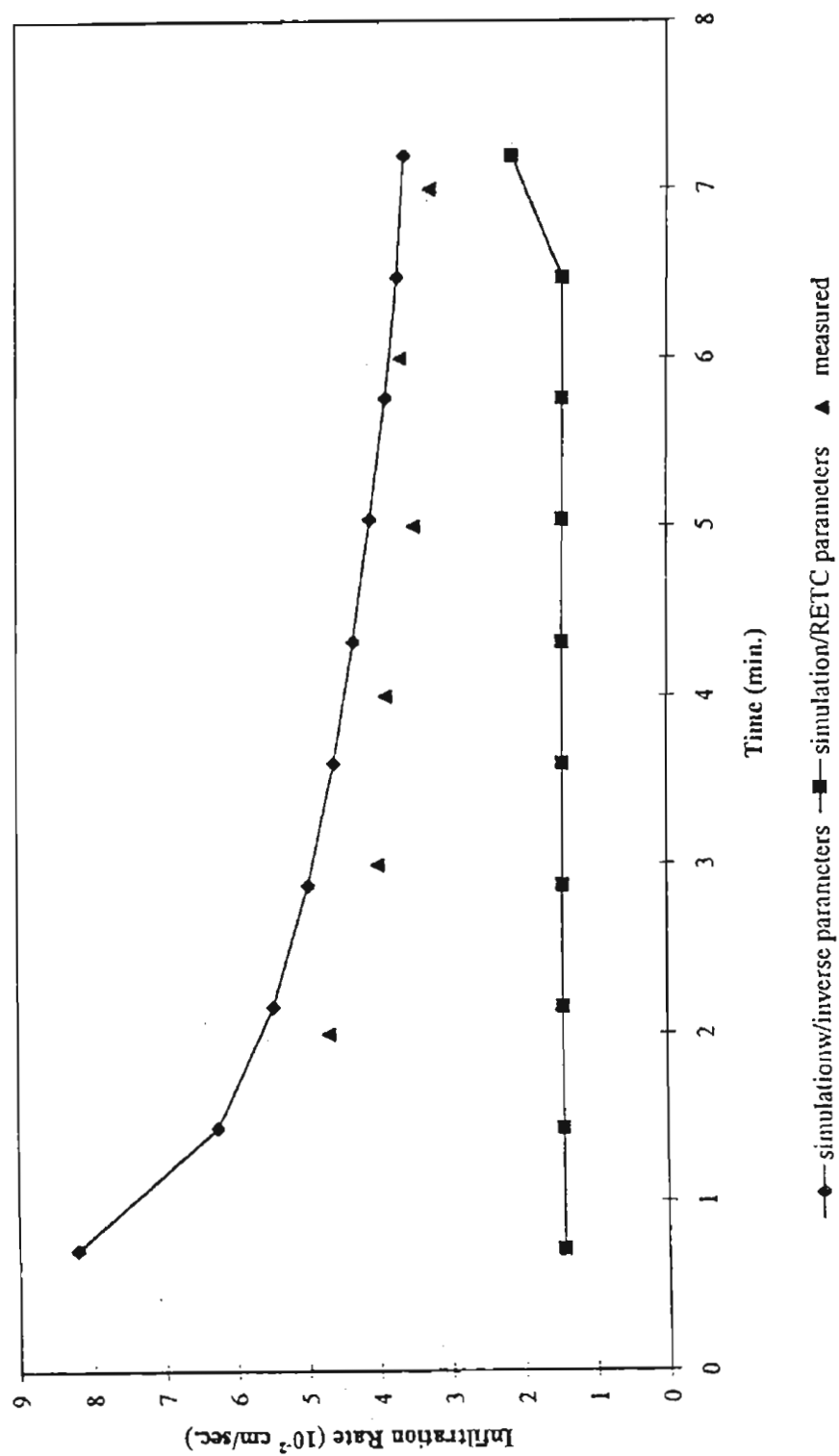


Figure 3-14 Sweetwater Soil Column Infiltration

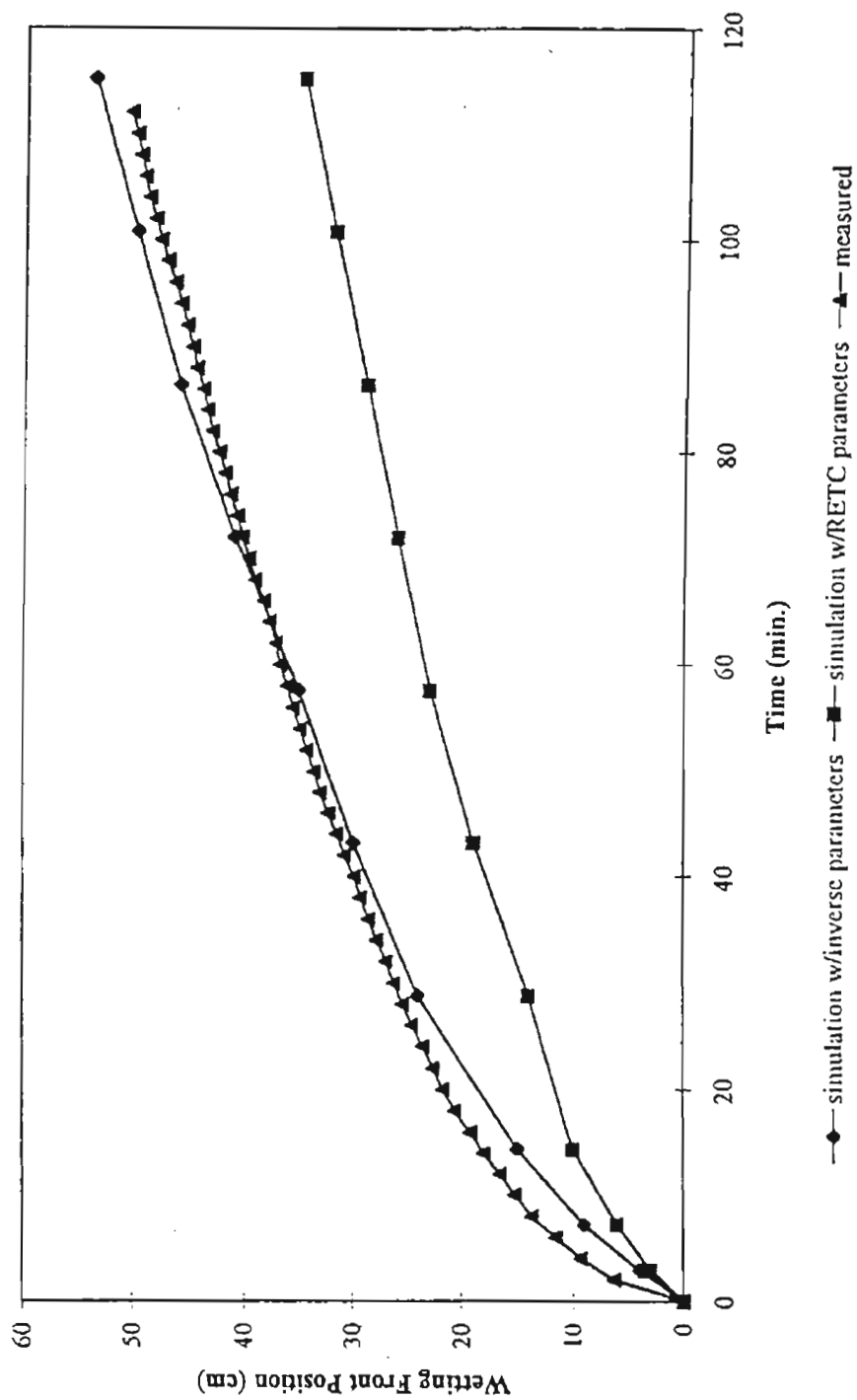


Figure 3-15 South Pond Soil Column Infiltration

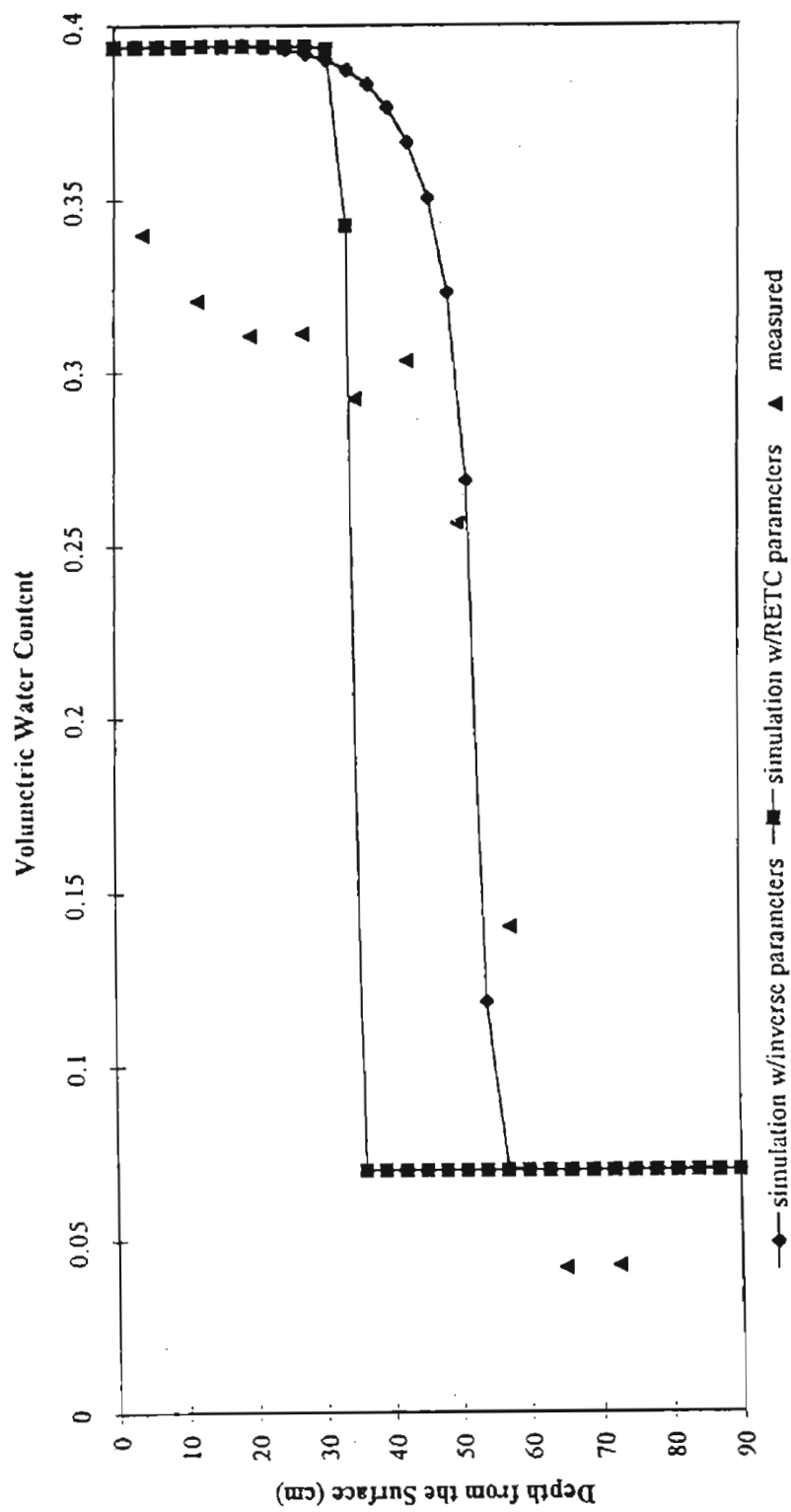


Figure 3-16 South Pond Soil Column Infiltration
ponding depth=15cm, t=175 min.

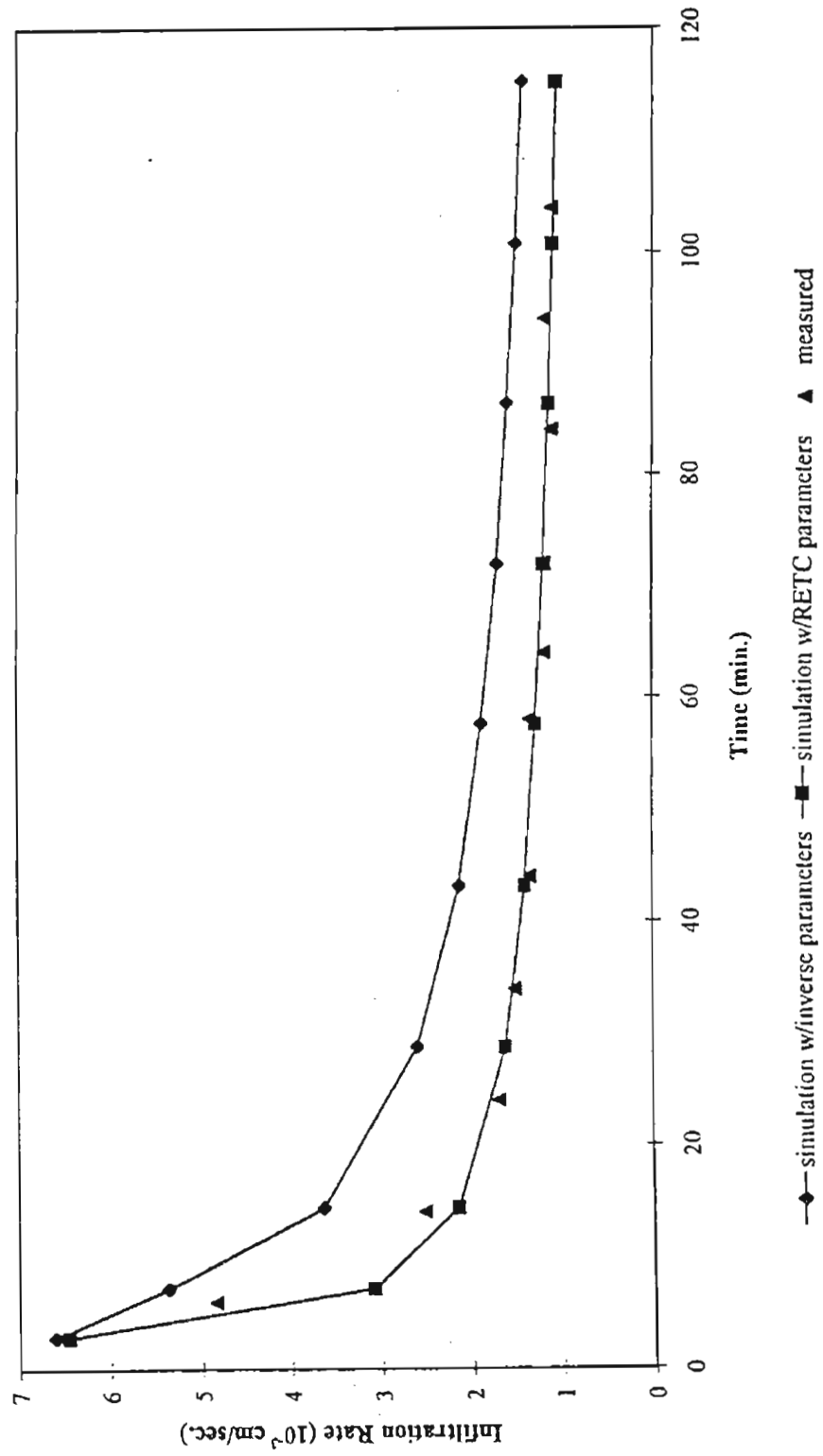


Figure 3-17 South Pond Soil Column Infiltration

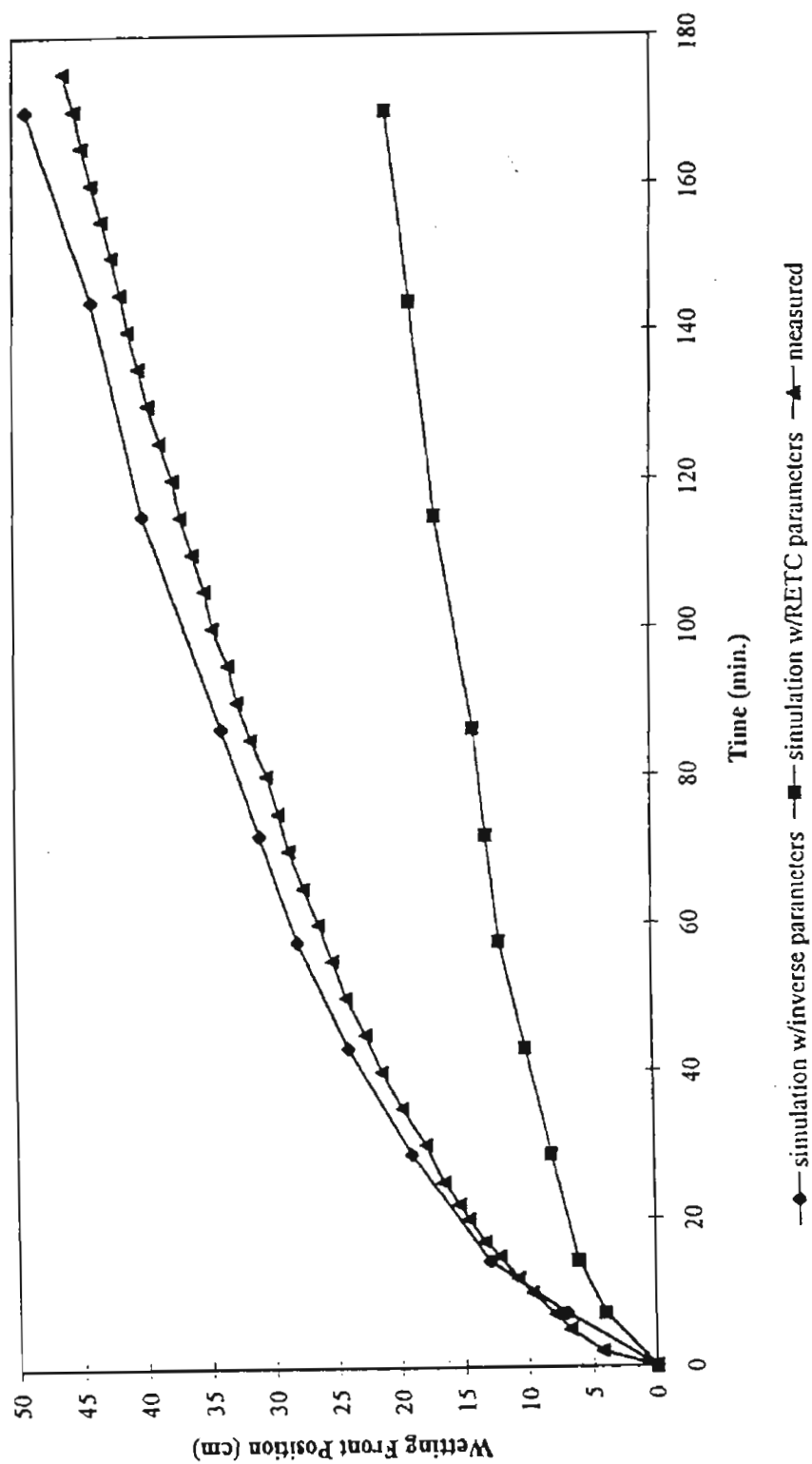


Figure 3-18 North Pond Soil Infiltration

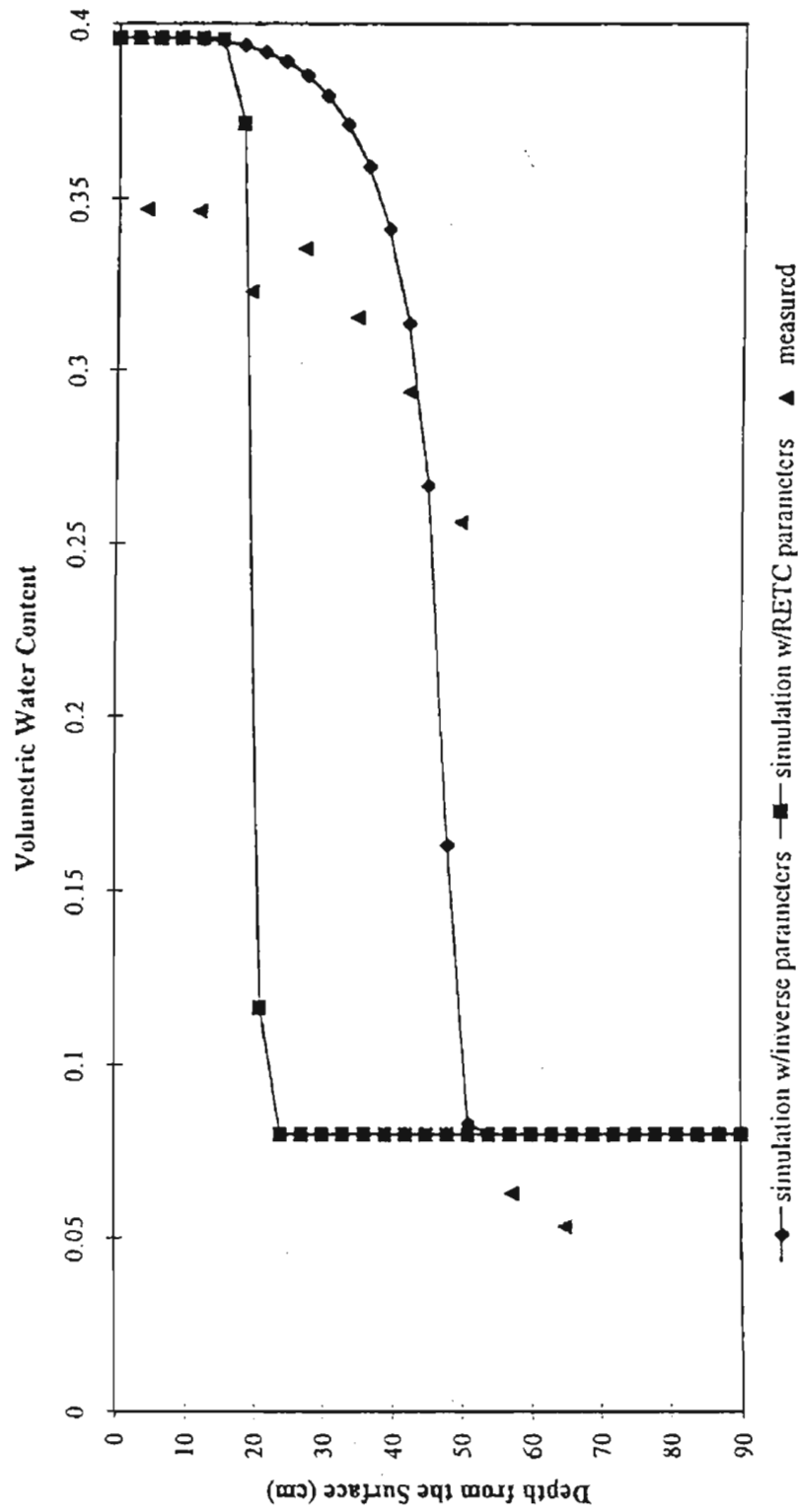


Figure 3-19 North Pond Soil Column Infiltration
ponding depth=15cm, t=170min.

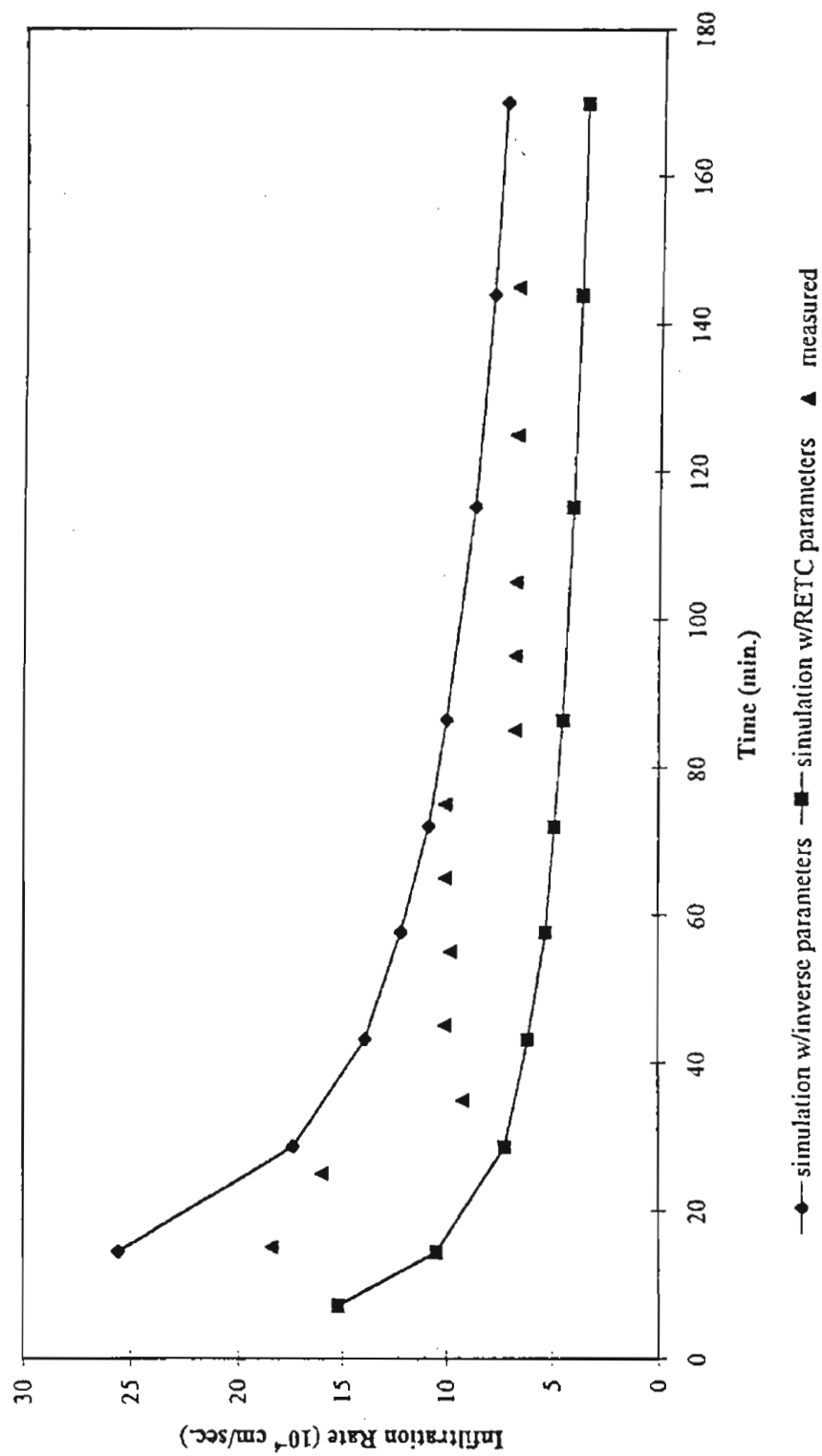


Figure 3-20 North Pond Soil Column Infiltration

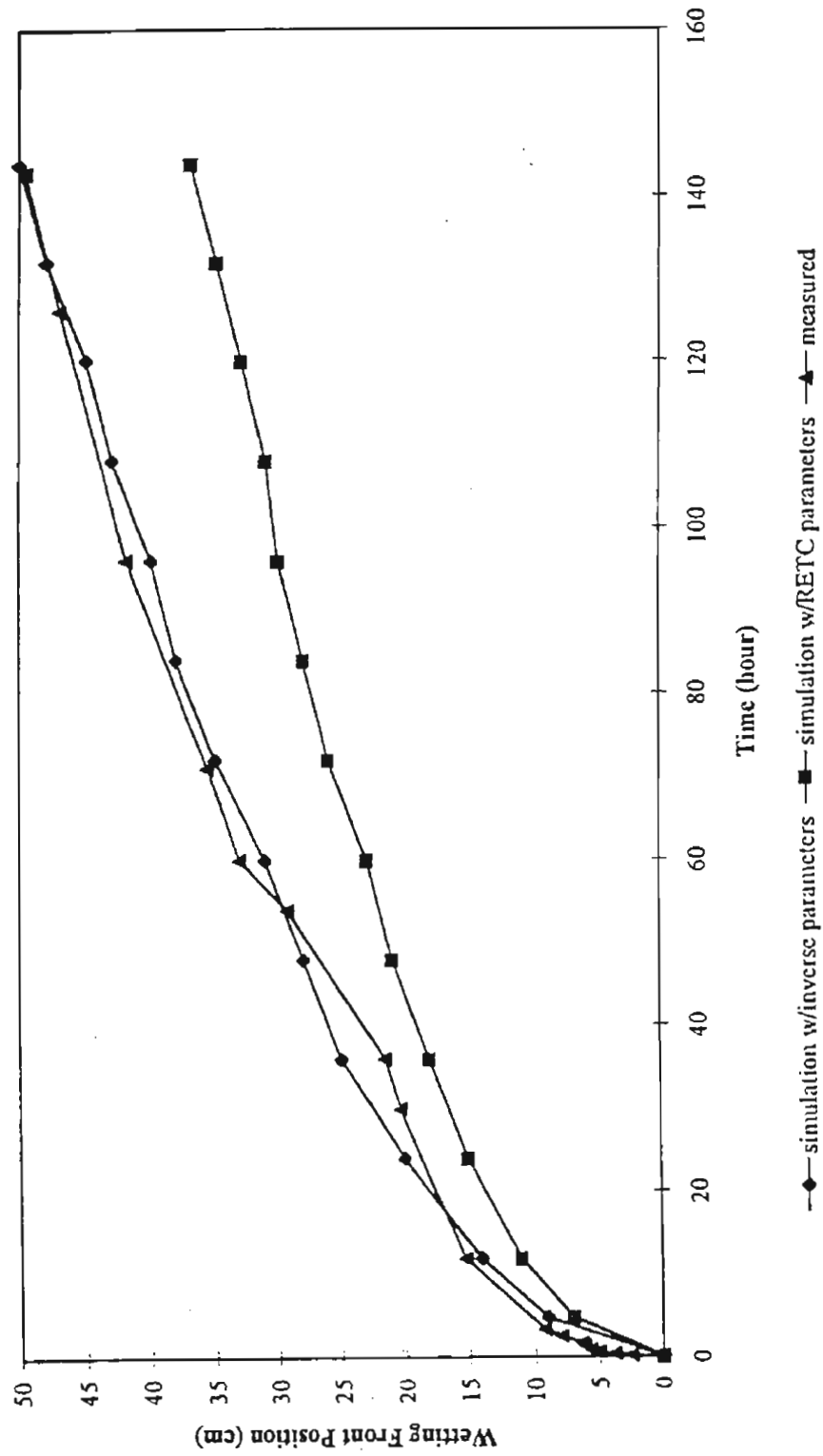


Figure 3-21 Ag. Field Soil Column Infiltration

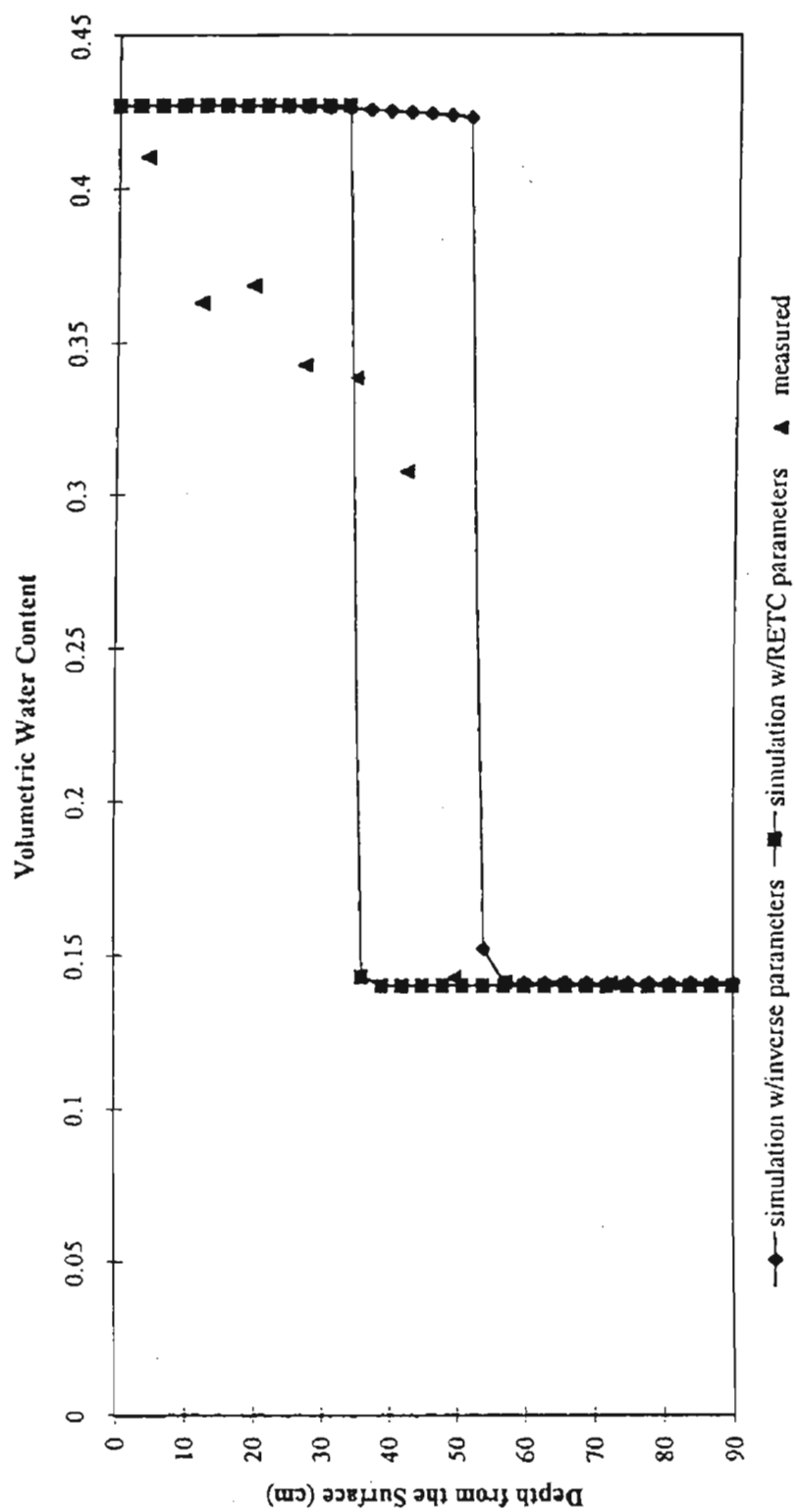


Figure 3-22 Ag. Field Soil Column Infiltration
ponding depth=15cm, t=146 hour

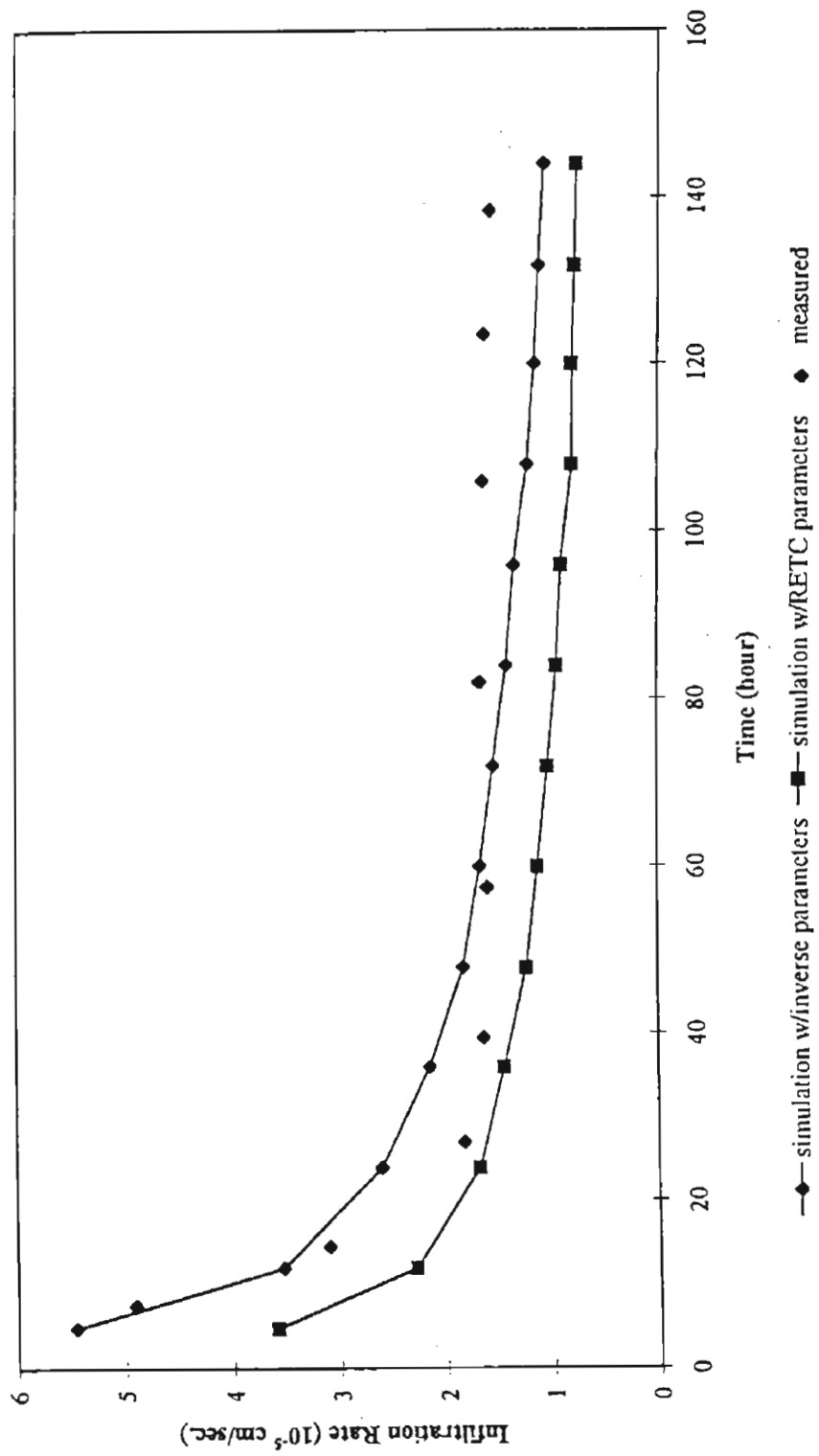


Figure 3-23 Ag. Field Soil Column Infiltration

ponded and flux conditions applied at the soil surface. In this study, a two-phase MSTS (Nichols and White 1993) model was used to simulate ponding infiltration into a bounded column.

The hydraulic parameters used in the two-phase simulation were those given from inverse methodology, as shown in Table 3-5. The relative air permeabilities were determined by fitting the air permeability data presented in the Soil Properties Report to the Touma and Vauclin model (1986). Touma and Vauclin used, for modeling purpose, analytical expressions fitted to experimental data to the air permeability as a function of soil suction head h :

$$K_{ra} = \frac{K_a}{K_{sa}} = \frac{A}{A + h^B} \quad (3-4)$$

where K_{sa} is the air permeability of oven dried soil, and A and B are model parameters.

The parameters A and B can be easily obtained by curve fitting techniques using air permeability test results and a soil water retention relation described above. The results of K_{sa} , A and B for the subject soils are given in Table 3-7.

Table 3-7
Air permeability parameters

Soil	$K_{sa} \text{ (m}^2\text{)}$	A	B
Agua Fria	1.55×10^{-10}	2.54×10^{-5}	-2.65
Sweetwater	6.18×10^{-11}	3.33×10^{-7}	-3.12
South Pond	9.25×10^{-12}	7.19×10^{-6}	-2.19
North Pond	9.18×10^{-12}	7.72×10^{-4}	-0.92
Ag. Field	7.53×10^{-12}	1.90×10^{-6}	-1.37

The boundary conditions are summarized in Table 3-8. The air-entry pressure was selected to be 14 cm of equivalent water head, as estimated by Touma and Vauclin (1986). Therefore, the air pressure at the upper boundary was specified as the pressure equivalent of the water boundary (15 cm) plus the air-entry pressure (14 cm).

Table 3-8

Boundary conditions for two phase flow

Boundary	Description	Formula
Upper Water Phase	constant head	$h_w(0,t) = \text{constant}$
Lower Water Phase	no flow	$-K_w \left(\frac{\partial h_w}{\partial z} - 1 \right) = 0$
Upper Air Phase	constant pressure head	$h_a(0,t) = \text{constant}$
Lower Air Phase	no flow	$-K \left(\frac{\partial h_a}{\partial z} - \frac{\rho_a}{\rho_{ow}} \right) = 0$

Before presenting the results, it should be noted that soil properties were established only from data obtained during open column ponding infiltration. Thus, the numerical simulations for bounded columns might be viewed as predictions and tests of the model by comparing them with the corresponding experimental data.

For the purpose of comparing to the experimental data, the numerical results are reported in Figure 3-24 to Figure 3-27, together with the experimental results. The simulation still over-estimated the degree of saturation behind the wetting front. However, good agreement between simulation and experiment were obtained for the position of the wetting front.

Arizona State University Large Column Studies

Figures 3-29 to 3-31 present the infiltration rates in ft/day for three columns filled with soil obtained from the site of the north basin for the field percolation tests conducted by Greeley and Hansen. Column #1 (1SM - chlorinated denitrified effluent), column #2 (2SM - dechlorinated denitrified effluent), and column #3 (3SM - chlorinated secondary effluent). The other three columns, filled with the North Pond soil, are replicates of the first three columns, and their infiltration rates follow similar patterns to those presented in Figures 3-29 to 3-31. Infiltration rates presented are averages based on readings every two days. All columns have been operated with approximately seven inches of water above the soil surface. These columns have been operated for 46 wetting/drying cycles. Cycles #1 through #16 consisted of either eight day wetting, six day drying periods or seven day wetting, seven day drying periods. Cycles #17 through #32 consisted of three day wetting, four day drying. Cycles #33 through #42 consisted of

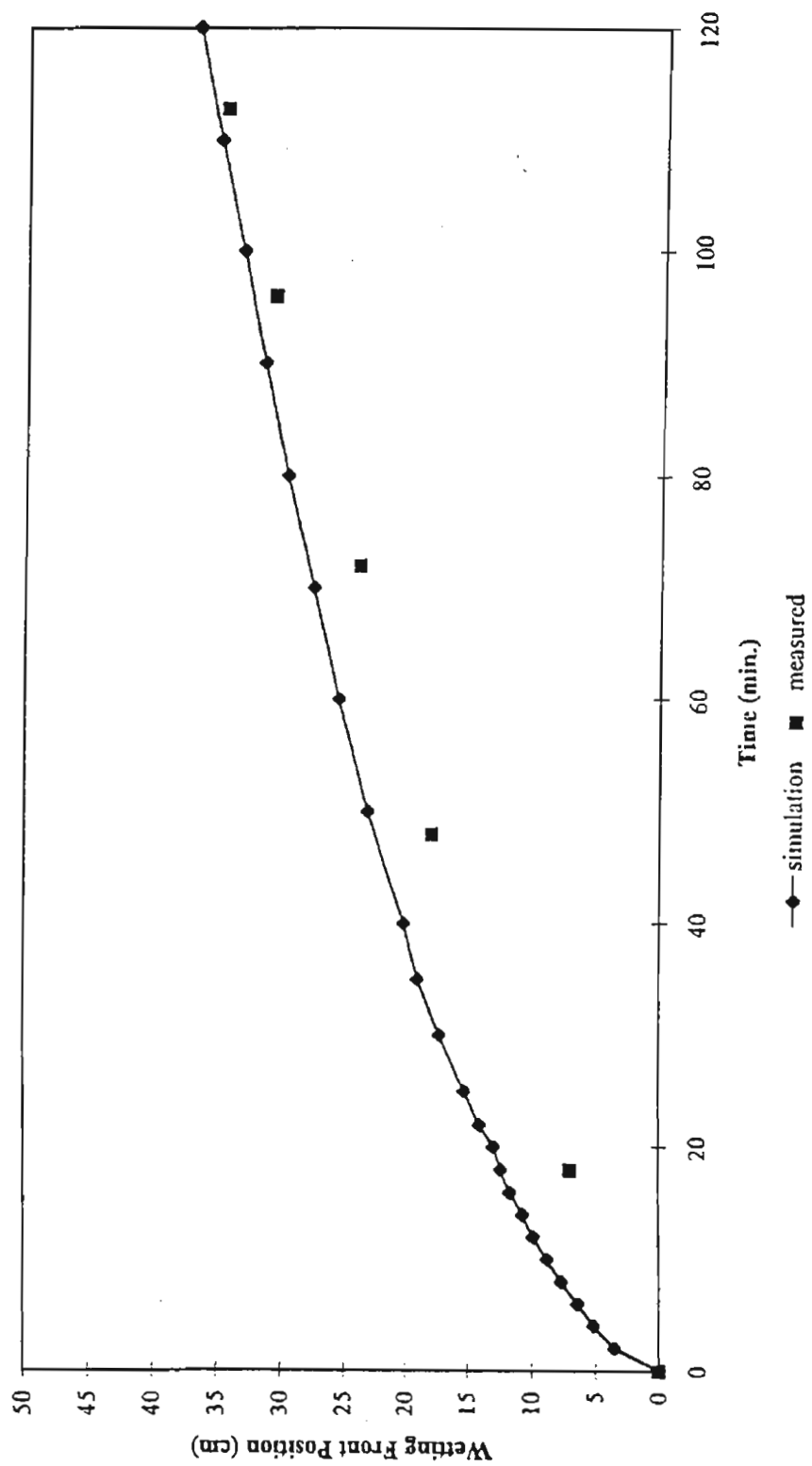


Figure 3-24 South Pond Soil Column Infiltration (bounded)

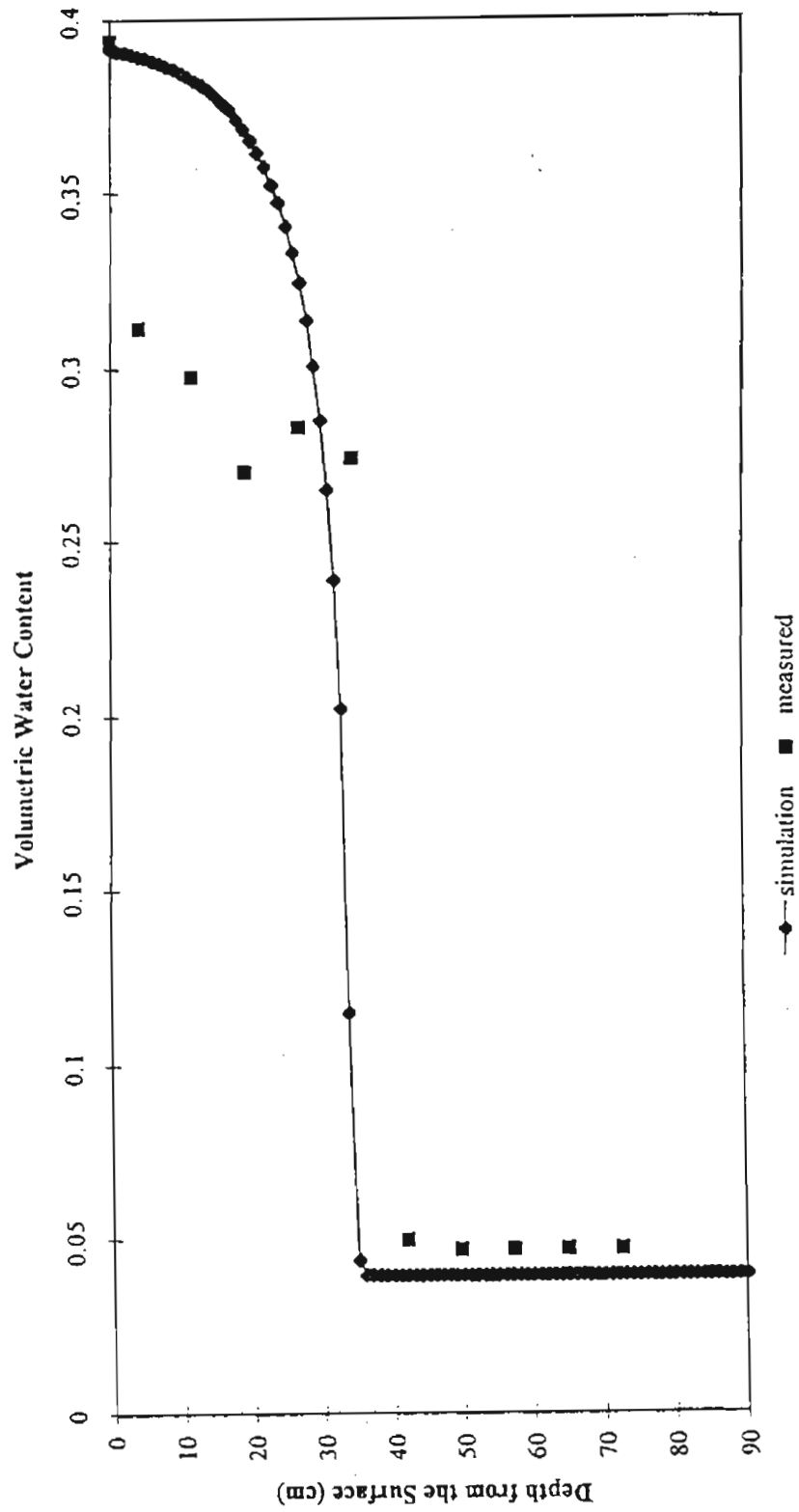


Figure 3-25 South Pond Soil Column Infiltration (bounded)
ponding depth=15cm, $t=120$ min.

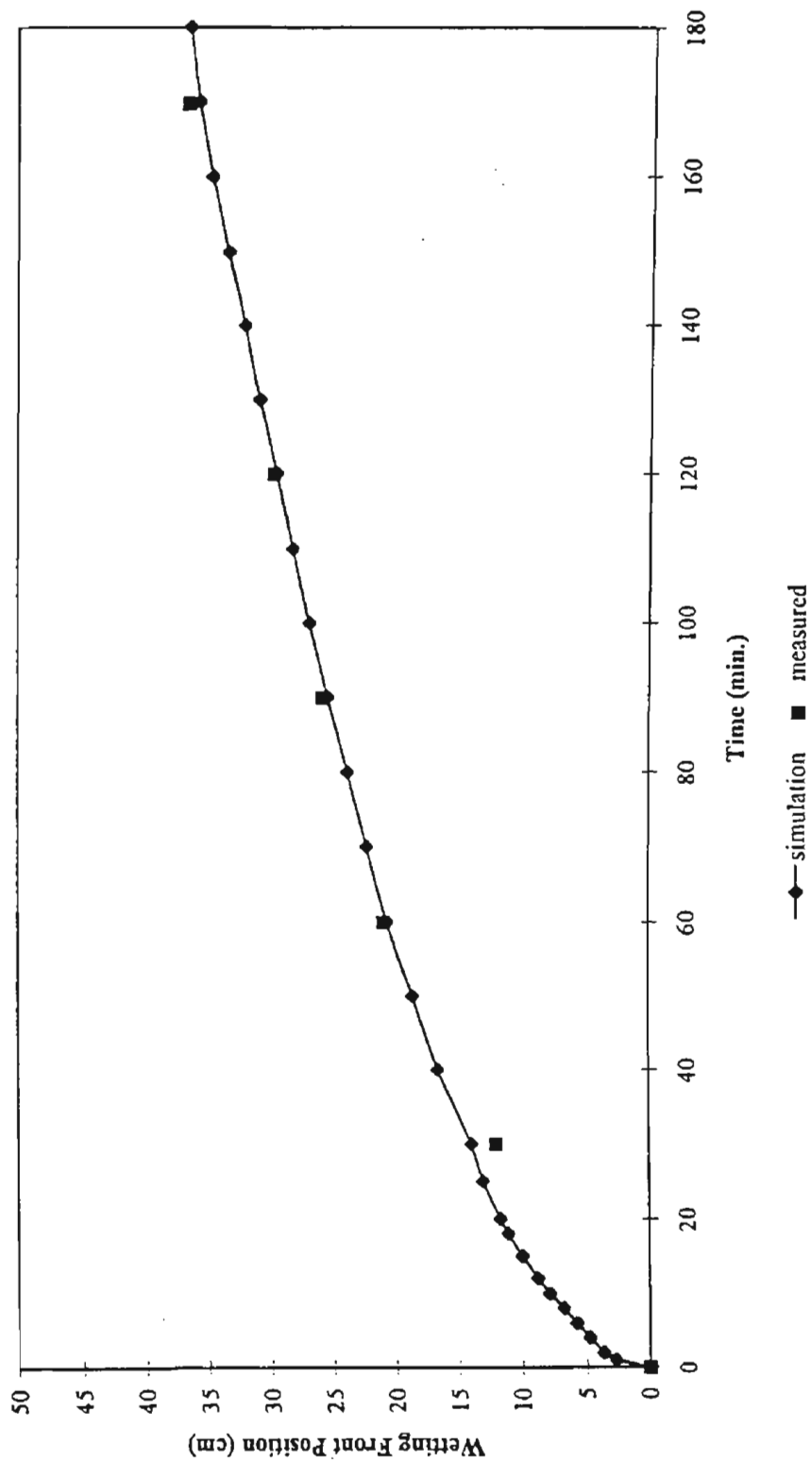


Figure 3-26 North Pond Soil Column Infiltration (bounded)

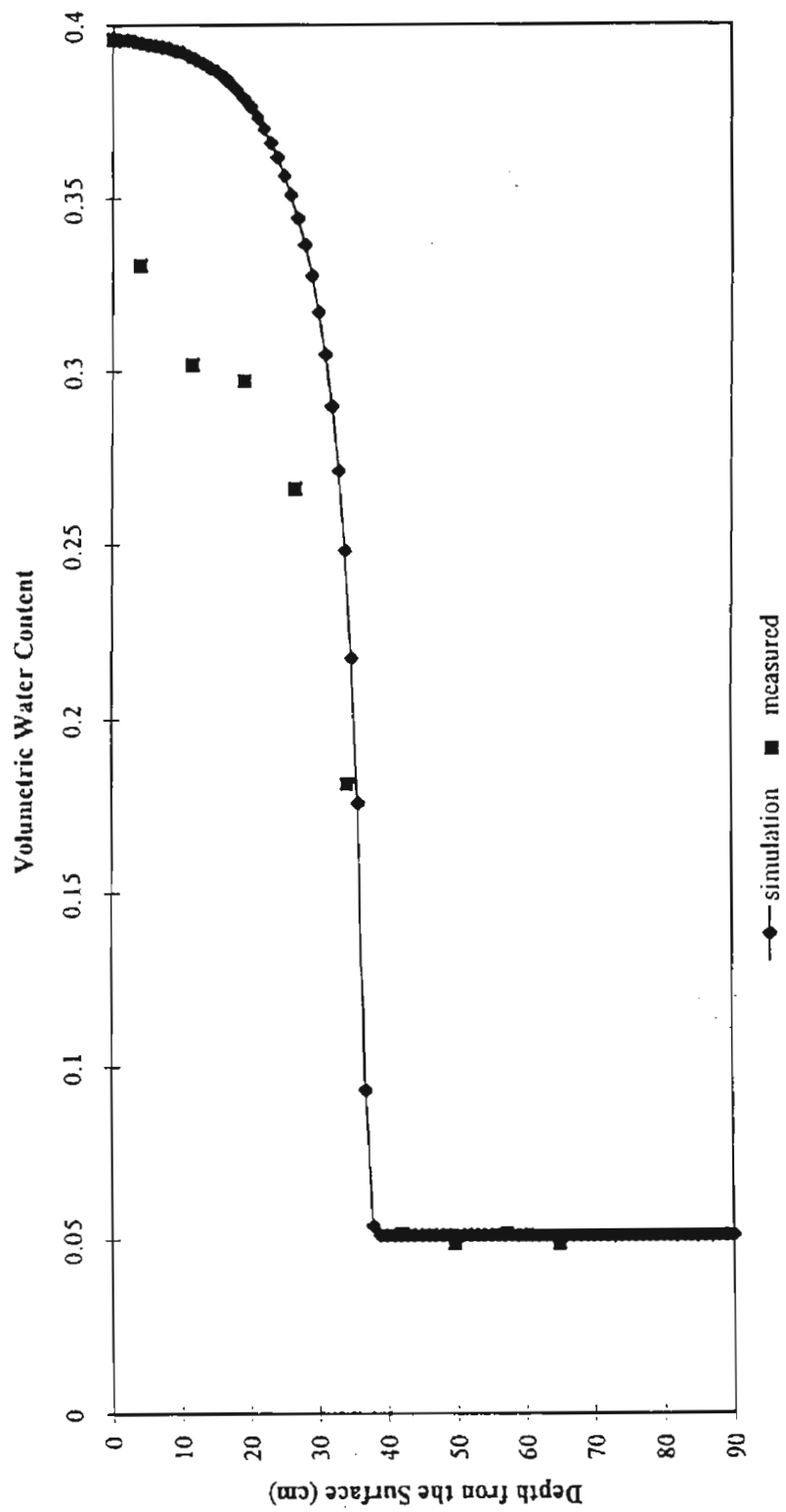


Figure 3-27 North Pond Soil Column Infiltration (bounded)
ponding depth=15cm, t=175 min.

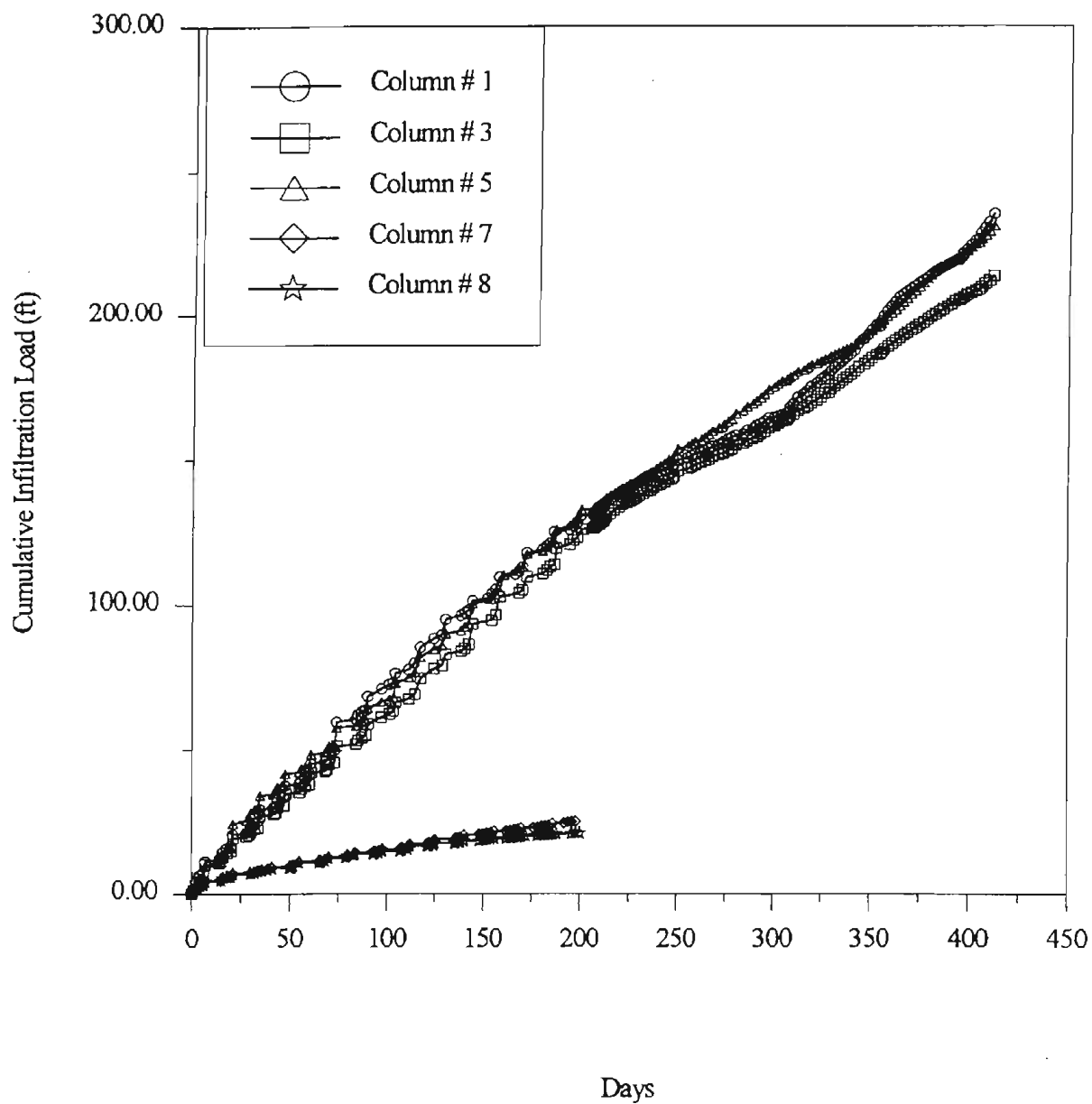


Figure 3.28 Cumulative Infiltration Loads for North Pond Silt Columns (# 1, # 3, # 5) and Agr. Clay Columns (# 7, # 8)

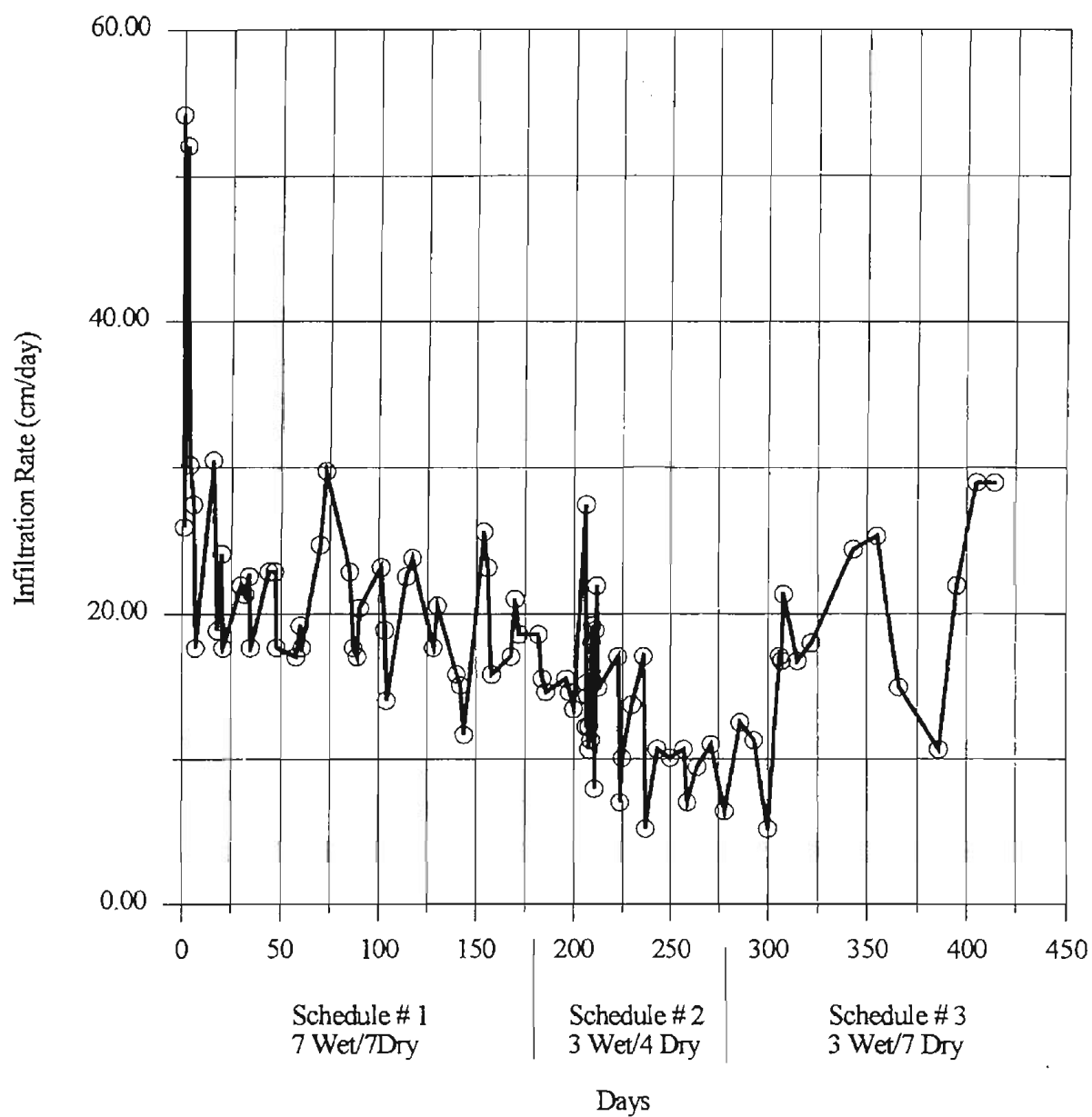


Figure 3.29 Average Infiltration Rates for Cycles 1 - 39
 Column # 1
 Soil type : North Pond Silt
 Effluent Type: Chlorinated Denitrified

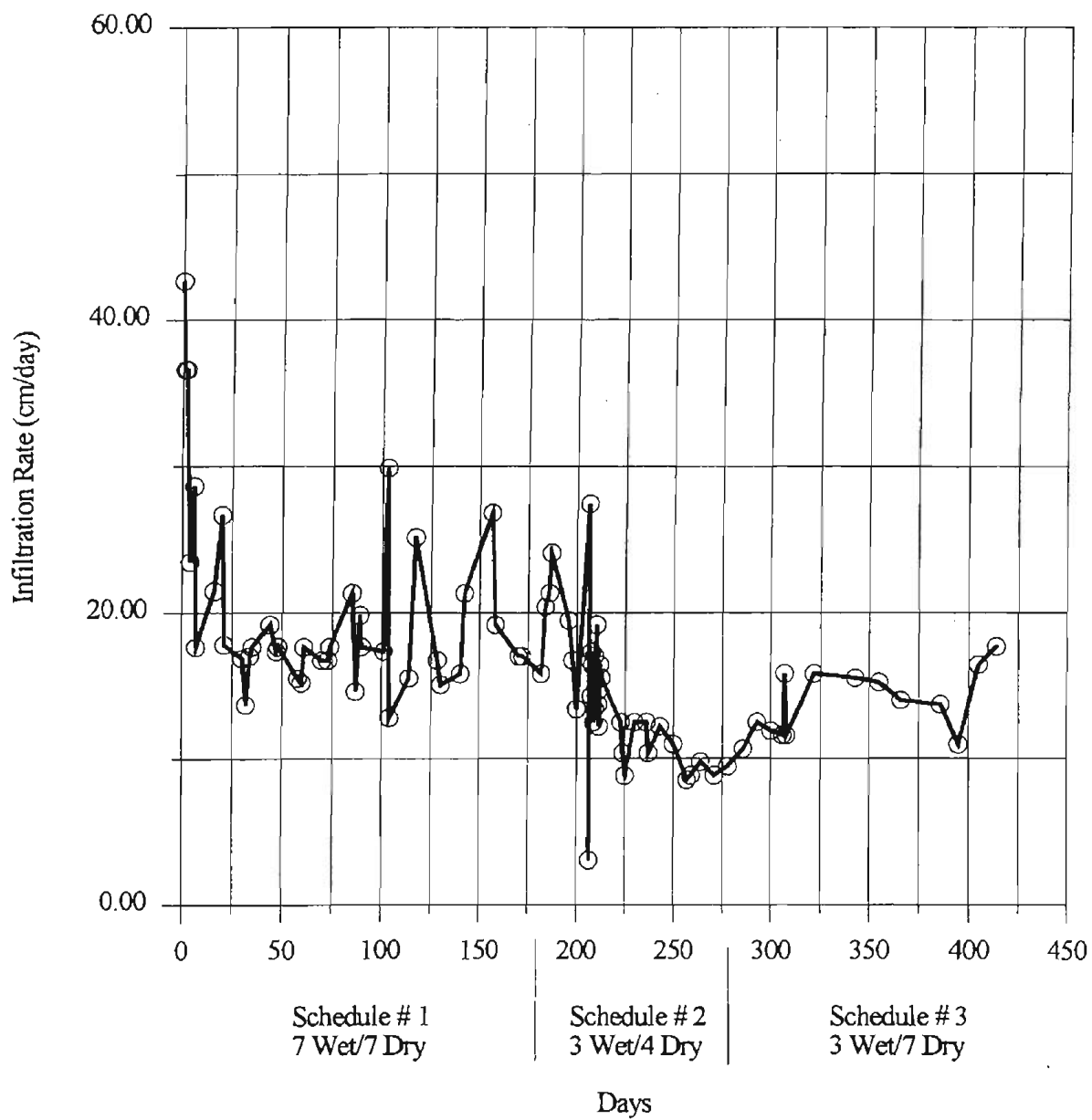


Figure 3.30 Average Infiltration Rates for Cycles 1 - 39
 Column # 3
 Soil type : North Pond Silt
 Effluent Type: Dechlorinated Denitrified

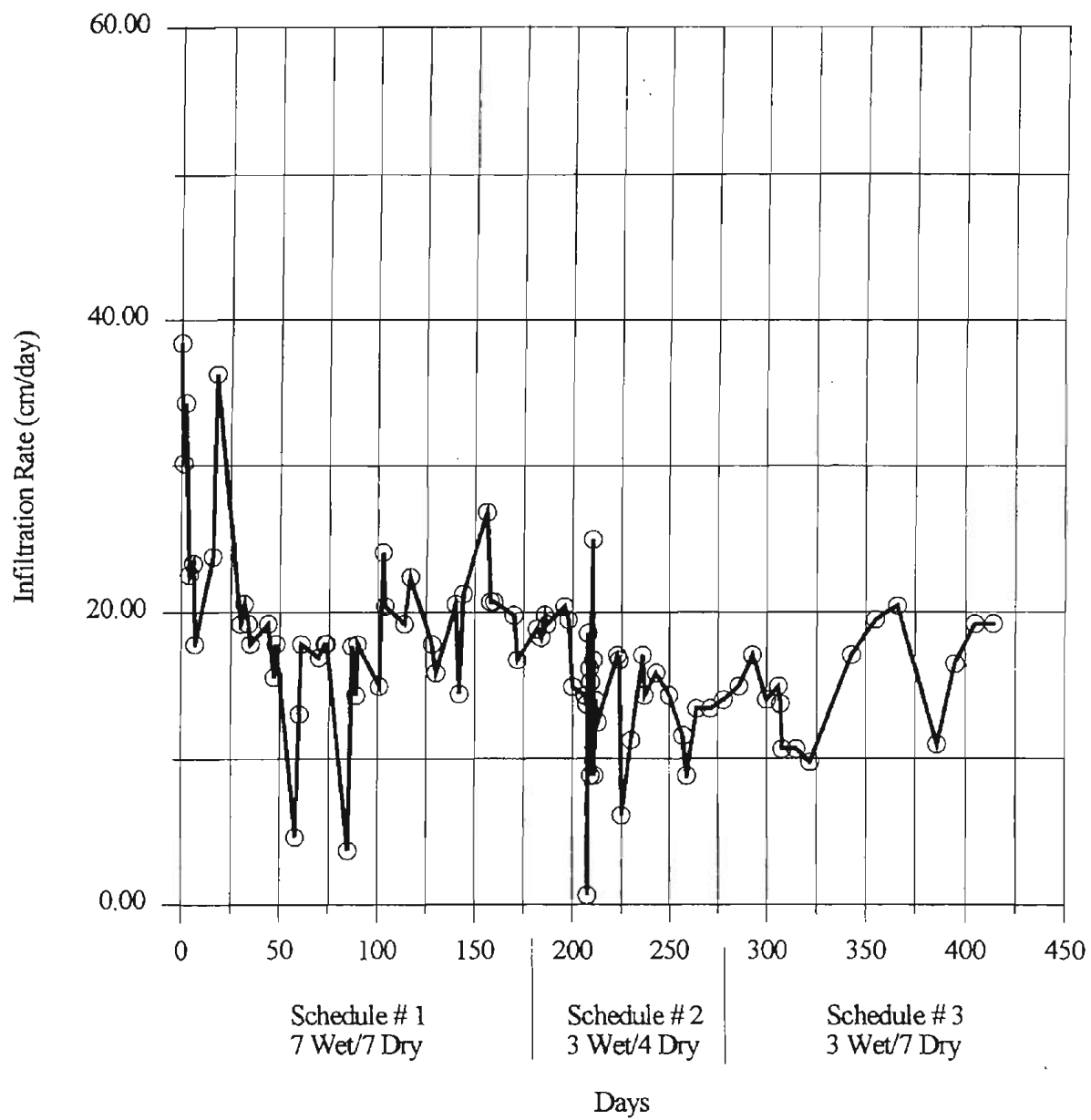


Figure 3.31 Average Infiltration Rates for Cycles 1 - 39
 Column # 5
 Soil type : North Pond Silt
 Effluent Type: Chlorinated Secondary

three day wetting, seven day drying. Cycle #43 until present time consisted of 12 day wetting, 7 day drying, and it takes approximately one day for the remaining water to percolate into the soil at the end of the wetting cycle. During the initial portion of the study, no vacuum was applied to the base of the columns. Therefore, the initial boundary condition simulated an impermeable layer at six feet below the soil surface. Approximately three feet of effluent had typically been applied during a wetting cycle, and the perched layer at the bottom of the column apparently did not affect infiltration rates. Several days of drying were necessary for the perched layer to dissipate. The addition of vacuum at 100 centimeters of water at the base of the silt columns simulated soil suction values that one would expect in the vadose zone. After the addition of vacuum, unsaturated conditions always occurred below the wetted front that develops at the top of the column. Although drying occurs more rapidly throughout the column with the addition of vacuum, drying is not so excessive that it significantly affects infiltration rates. One would expect the initial infiltration rates to be much higher for soils at less than 5 percent moisture content and the infiltration rate should decrease as the moisture content of the soils increases. This was observed at the beginning of this study and has been verified in laboratory studies. One must note that after several days of drying, soil suction values appear to be outside the range of the tensiometers so an exact correlation with moisture content is difficult to make.

Figures 3-32 and 3-33 present the infiltration rate data for the two columns with clayey soil, #7 (1CL - chlorinated denitrified effluent), and #8 (2CL - dechlorinated denitrified effluent). These two columns were operated for 14 cycles. All cycles consisted of eight to twelve days of wetting and eight to nine days of drying. Since the time for water to drain after application of water has taken three to four days, the application time has been reduced to three to four days so that the overall wetting/drying cycle times will be similar to the silts. Similar to the silt columns, applying vacuum did not affect the infiltration rate in the clay columns. Due to their very low infiltration rate, these two columns were taken apart and replaced with the South Pond silt.

Infiltration rates in the Agua Fria sand and the South Pond silt columns have been approximately 6 to 9 ft/day. The capacity of the pumps at the site has not been great enough to supply sufficient flowrate to maintain a constant head (7 inch desired) in the sand and South Pond silt columns.

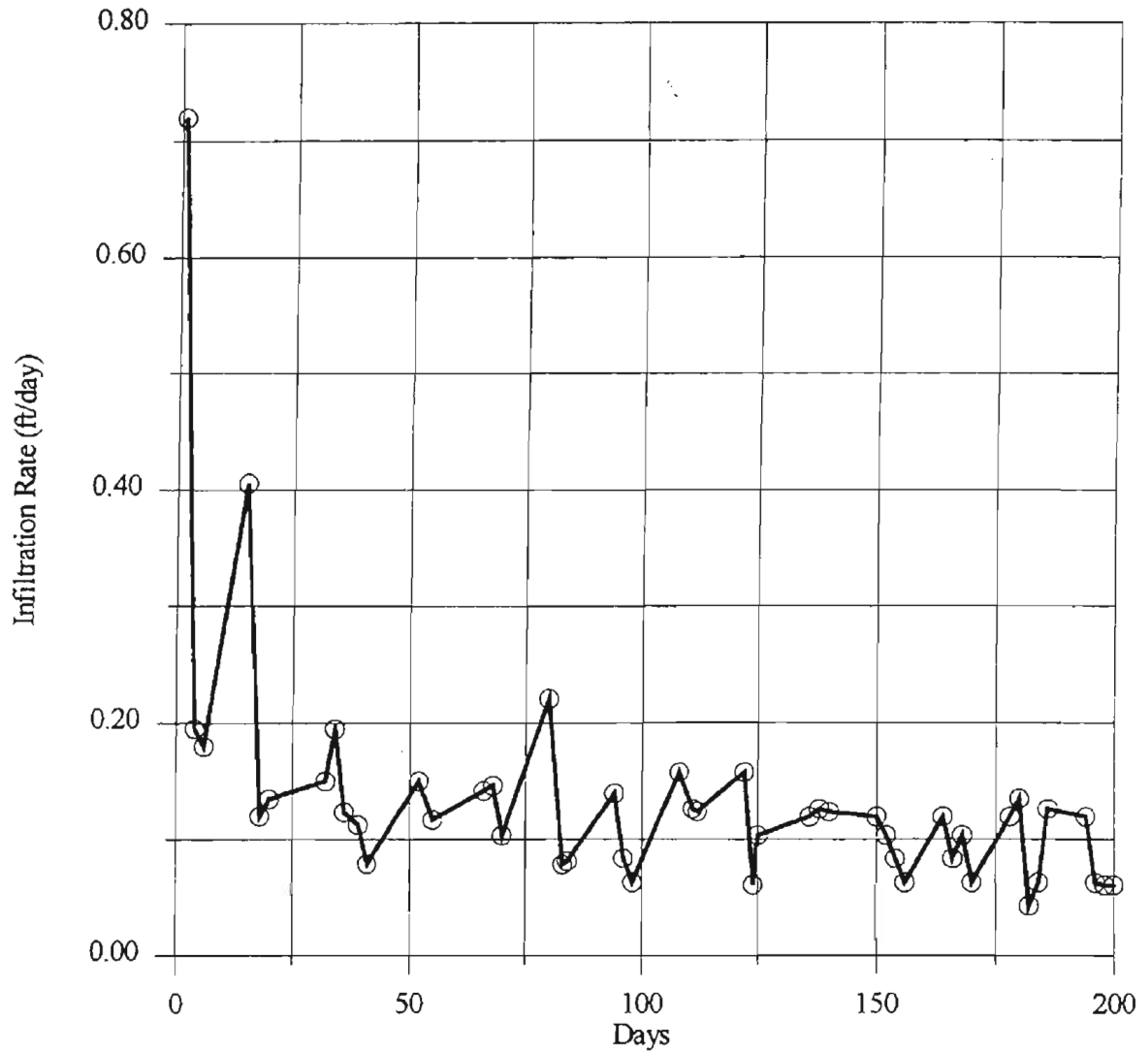


Figure 3.32 Average Infiltration Rates for Cycles 1 - 14
Column # 7
Soil type : Ag. Field Clay
Effluent Type: Chlorinated Denitrified

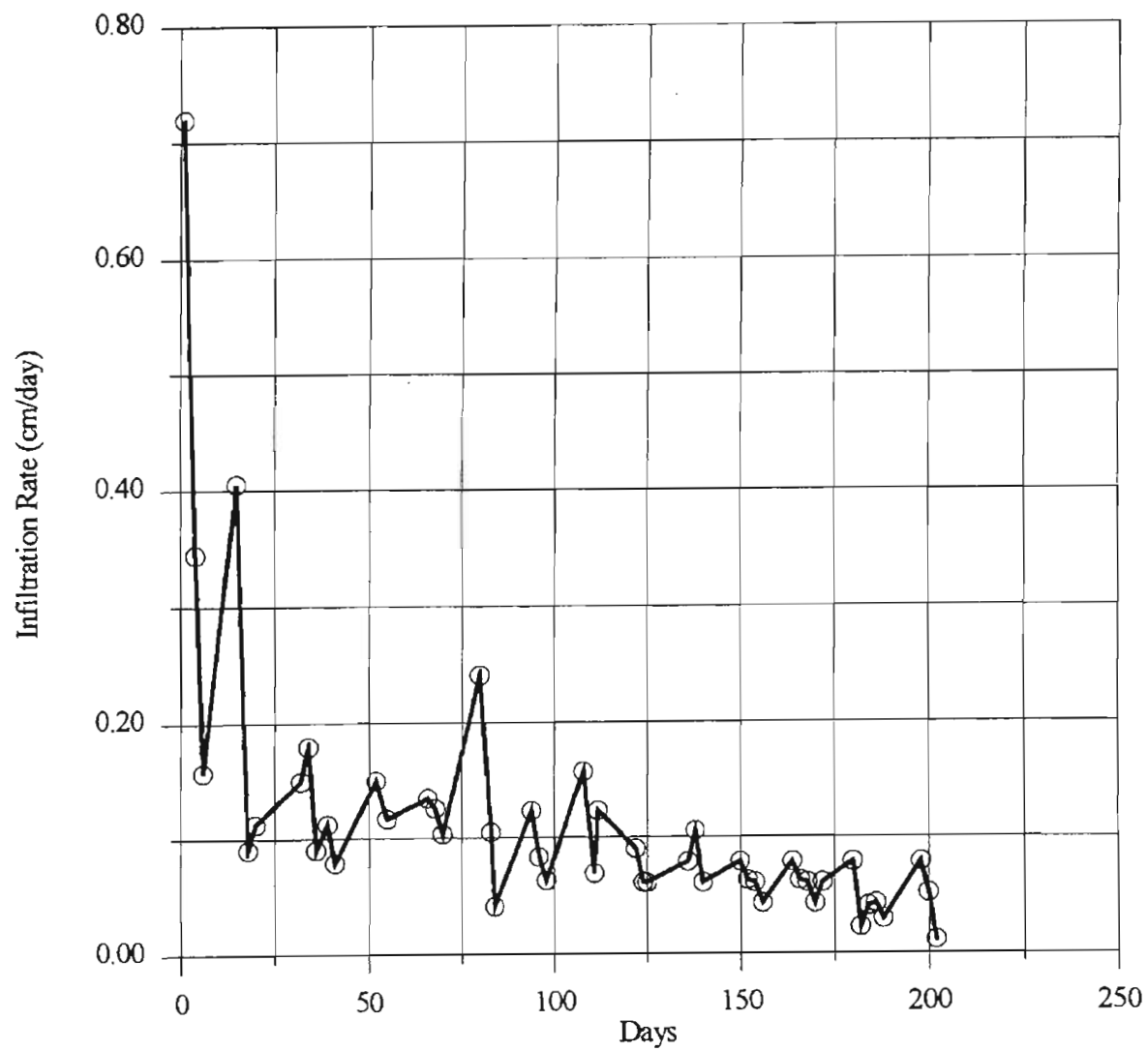


Figure 3.33 Average Infiltration Rates for Cycles 1 - 14
Column # 8
Soil type : Ag. Field Clay
Effluent Type: Dechlorinated Denitrified

Effect of Surface Clogging

North Pond silts. Infiltration rates have steadily decreased as clogging layers have developed with each successive wetting/drying cycle. This trend is pronounced in the first three to four cycles (40 to 50 days) as shown in Figures 3-29 to 3-31. During the first cycle (14 days), initial infiltration rates were 35 to 55 cm/d and infiltration rates decreased to 20 to 25 cm/d by the end of the first cycle.

The clogging layer appears to be a mixture of suspended solids and surface algae growth. The algae begins to grow after two days of wetting and the algal growth is visible through the seven inches of water above the surface. The drying times have been sufficient to cause cracking and peeling of the surface layers. It appears that the clogging layer has become established and is controlling the infiltration rates in the columns.

Infiltration rates have been very consistent in all silt columns. The algae layer was manually removed from column #4 before the fifteenth cycle without any measurable impact on its infiltration rate.

Clays. The development of the clogging layer and infiltration rates have been similar in the columns with clayey soils (Figures 3-32 and 3-33). Infiltration rates have decreased to very low values in both columns and especially #8. Cracking of the clay surface has been observed during drying. Then on wetting, clogging material has been observed to fill these cracks. Diagrams of the cracks have been done to determine if the cracks occur in the same places during each drying cycle. The combination of filling the cracks and swelling of the clays may result in irreversible clogging of the clayey soil columns.

Sands. Although algae covers a portion of the sand surface, it does not clog the pores and reduce the infiltration rate to an extent where it is possible to build up a pond on the surface with the existing pumping rate. In an effort to stimulate clogging layer development, 50 to 200 l of primary effluent has been applied to the columns prior each wetting/drying cycle in the beginning of the study.

Another attempt to stimulate clogging layer development on the sands was made by collecting algae from the effluent channel of Plant 3 at the 91st Avenue Wastewater Treatment

Plant and applying it to the surface of the sands. The introduced algae did not reproduce in the new environment of the column, and no reduction of the infiltration rates was observed.

Effect of Effluent Type

Silts. There has been variation in the development of algae during different times. Environmental factors including both temperature and incident sunlight have changed and most likely have affected algal growth. The differences in the presence of nutrients might have a much more important effect on algal growth. The major difference in nitrogen is that the secondary effluent contains primarily ammonia while the denitrified effluent contains primarily nitrate. Phosphorous concentrations in the secondary effluent are 1 to 2 mg/l higher than phosphorous concentrations in the denitrified effluent (2-5 mg-p/l). Since the differences in phosphorous concentrations are minor, the difference in nitrogen forms is most likely affecting algal growth. One other less plausible explanation is differences in organic carbon compounds. The morphology of algae that grows in columns receiving denitrified effluent is different than the morphology of algae in columns receiving secondary effluent indicating that different species do predominate in different effluent. Generally, the effect of different effluent types on infiltration rates has not been significant.

Clays. The development of the clogging layer and infiltration rates have been similar in both columns with clayey soils. Both surface algae and suspended algae are apparent. The long detention time of water likely eliminates any differences between dechlorinated and chlorinated effluents. The longer detention time also likely enhances the growth of suspended algae which are known to exacerbate clogging layer development.

Sands and South Pond silts. Since the pumping capacity into these columns is much less than the infiltration capacity for the soils in these columns, it is very difficult to detect the effect of effluent type on the infiltration rates.

Effect of Wetting/Drying Cycle Length

The North Pond silt columns were operated under the four wetting/drying schedules summarized in Table 5-4. Figures 3-29 to 3-31 present infiltration data for three different cycle lengths. All of the three figures show a decrease in the infiltration rates during the period of schedule #2, the shortest schedule (3 days wetting and 4 days drying). However, because other environmental factors, like temperature, have also varied for different schedule periods, it is difficult to isolate the effect of cycle length from other factors that might caused the reduction in the infiltration rates.

University of Arizona Laboratory Column Studies

Column studies at the University of Arizona included use of both repacked homogenized soils and intact soil cores. Soils used in the repacked columns were: Agua Fria sand, Sweetwater sandy loam, and North Pond silt. Three columns containing repacked sediments were used for each soil type. In addition, three intact soil cores were collected at the same locations that sediments were obtained for the repacked columns. One 1-meter intact core each of Agua Fria sand, North Pond silt, and Ag. Field clay were used in University of Arizona SAT simulations.

Column hydraulic behavior is reported here organized by soil type. During the course of experiments, all columns received effluent in alternating wetting/drying periods, each of 7 day duration. Length of wetting and drying cycles was not an independent variable in the University of Arizona column studies.

Prior to application of effluent, saturated hydraulic conductivity (K_{sat}) measurements were conducted for most of the columns using a falling-head permeameter test. The following sequence of steps was performed for each column that was tested for K_{sat} :

1. Air was expelled from the soil pore space by applying 60 pore volumes of carbon dioxide to the bottom of the column at a flowrate of 1000 ml/min;
2. The column was slowly saturated from the bottom up over a period of 7-14 days using degassed milli-Q containing 0.01 M CaSO_4 applied at a flowrate of 7-8 cm/day;

3. After visible gas bubbles were eliminated from soil pore space, the K_{sat} test was performed according to the method described in Jury et al. (1991).

In addition to quantifying the initial hydraulic conditions for each soil type, the K_{sat} measurement provides a measure of the degree of uniformity in soil packing between columns containing the same soil type, as well as differences associated with intact cores versus repacked columns. All measurements, shown below in Table 3-9, were obtained using a falling head permeameter test.

Table 3-9

Summary of K_{sat} values for University of Arizona 1-meter SAT columns

Column No.	Soil Type	K_{sat} (cm/sec)	K_{sat} (ft/day)
1	Agua Fria Sand ¹	8.73×10^{-3}	24.7
2	North Pond Silt ¹	5.67×10^{-4}	1.61
2a	Ag. Field Clay ¹	--	--
3	Agua Fria Sand ²	1.63×10^{-1}	462
4	North Pond Silt ²	4.05×10^{-4}	1.15
5	Sweetwater Sandy Loam ²	3.94×10^{-2}	112
7	Agua Fria Sand ²	8.98×10^{-2}	255
8	North Pond Silt ²	7.18×10^{-4}	2.03
9	Sweetwater Sandy Loam ²	2.43×10^{-2}	68.9
11	Agua Fria Sand ²	1.09×10^{-1}	309
12	North Pond Silt ²	--	--
13	Sweetwater Sandy Loam ²	2.04×10^{-2}	57.7

¹ intact core

² repacked sieved soil

Agua Fria Sand

Infiltration rates. Secondary effluent application rates were on the order of 9.0-10.0 ft/day. The columns containing repacked Agua Fria sand (total of 3) developed surface clogging layers after 4-6 cycles of operation, resulting in ponding of effluent above the soil surface and concomitant reductions in infiltration rates. Subsequent to development of clogging layers, infiltration rates averaged around 9.0-10.0 ft/day at the beginning of cycles and decreased to 0.5-1.0 ft/day or less after seven days of operation. A typical plot of infiltration rate as a function of time during a wetting cycle for a column containing Agua Fria sand is given in Figure 3-34.

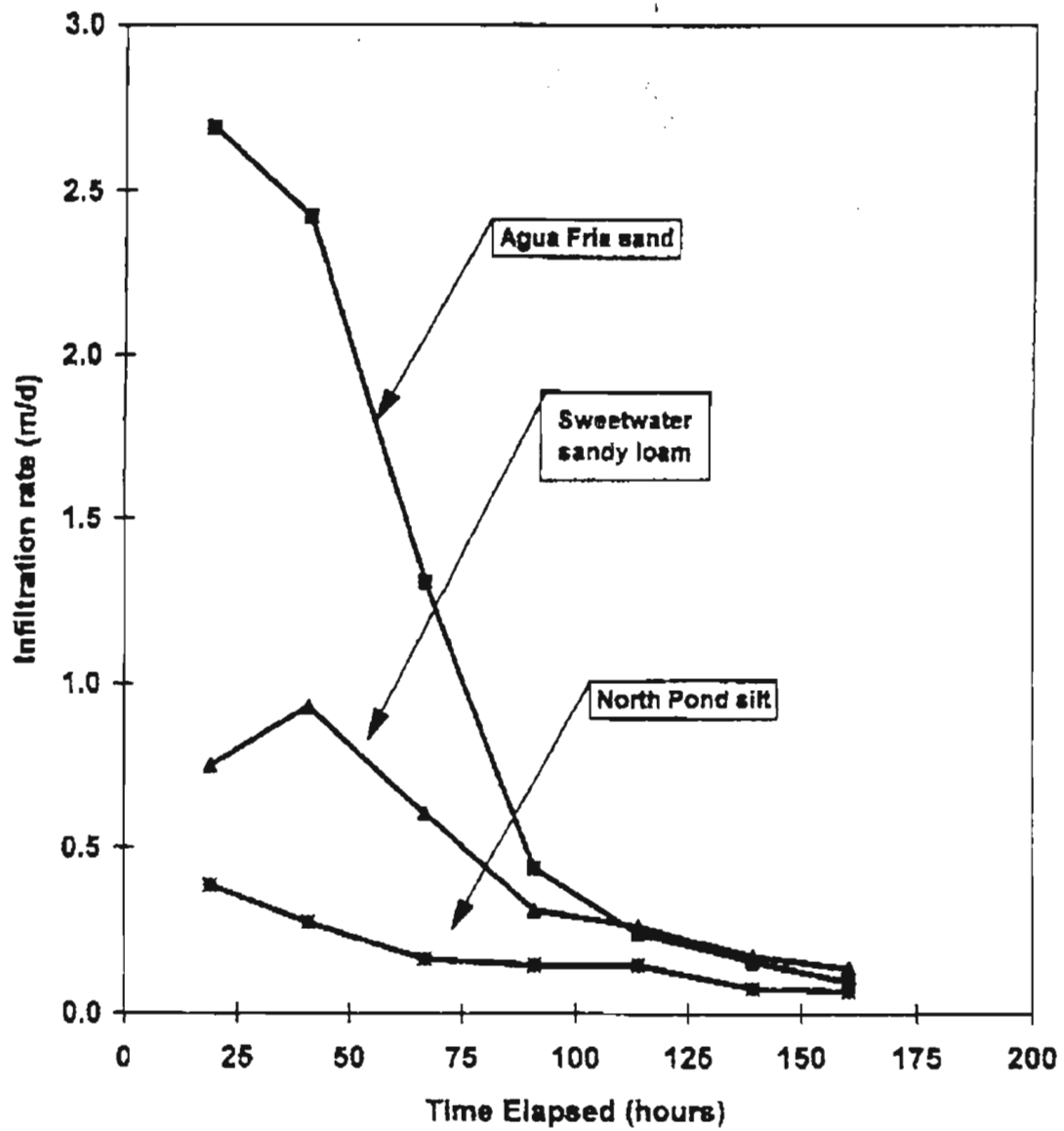


Figure 3-34 Typical infiltration rates as a function of time during a 7-day wetting period for columns containing repacked Agua Fria sand, Sweetwater sandy loam, and North Pond silt. Data shown were collected after development of surface clogging layers.

The 1-meter intact core of Agua Fria sand developed ponded conditions during the first wetting cycle. Infiltration rates for the intact core were lower, averaging 2.0 ft/day at the start of wetting cycles, decreasing to 0.5 ft/day after seven days of operation. Differences in hydraulic behavior between the intact core and the repacked homogenized Agua Fria sediments are believed to be due to the fact that the intact core contained numerous large cobbles, significantly reducing the column pore volume.

Soil suction profiles. A typical plot of matric potential as a function of soil depth is given in Figure 3-35. It is evident that the zone of head loss associated with development of the surface clogging layer (schmutzdecke) occurred within the top 2 centimeters of soil. Below this clogging zone, matric potential did not change as a function of depth, indicating a uniform moisture content profile and suggesting that the surface clogging zone controls the hydraulics of this system. Matric potential profiles for the intact sand core were not obtained; tensiometers could not be installed at the predrilled port locations along the stainless steel sleeve due to blockage by numerous large cobbles.

Effect of surface clogging. After development of surface clogging layers, hydraulic loading rates declined over time (Figure 3-36) in columns containing the Agua Fria sand, suggesting continued development of the surface clogging zones. After approximately 12 wetting periods, hydraulic loading rates for the sand columns approached rates for columns containing the Sweetwater sandy loam.

Effect of surface scarification on infiltration rates. Procedures designed to reestablish column infiltration rates were initiated prior to the beginning of cycle #18. For all three sand columns, the dried algae crust on the soil surface was removed and the soil was raked to a depth of 1 centimeter. Infiltration rates increased during the 18th wetting cycle and then began to decrease again (Figure 3-36). Prior to the start of wetting cycle #21, the surface 2 centimeters of soil in two of the sand columns was stirred using a metal rod to break up the surface clogging zones. Infiltration rates during subsequent wetting periods were significantly higher (Figure 3-36); ponding of effluent did not occur during the course of the following 2 wetting periods. These results suggest that stirring of surface clogging zones is sufficient to reestablish initial hydraulic performance of Agua Fria sand. Hydraulic loading over cycles #21-28 was essentially the same as during the first seven cycles of operation.

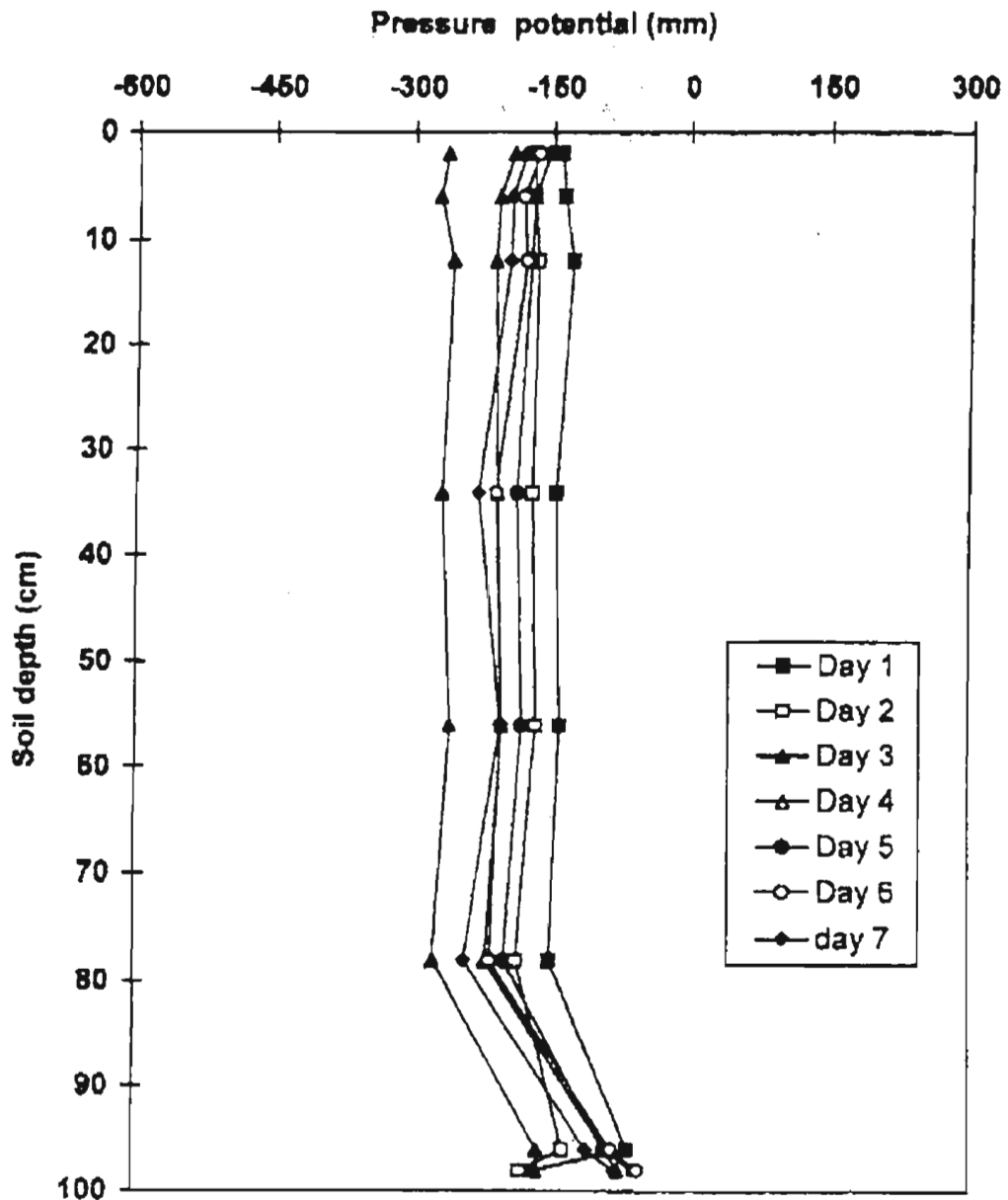


Figure 3-35 Typical daily measurements of matric potential as a function of soil depth for 1-meter columns containing repacked Agua Fria sand during a 7-day wetting period. Data shown were collected after development of surface clogging layers.

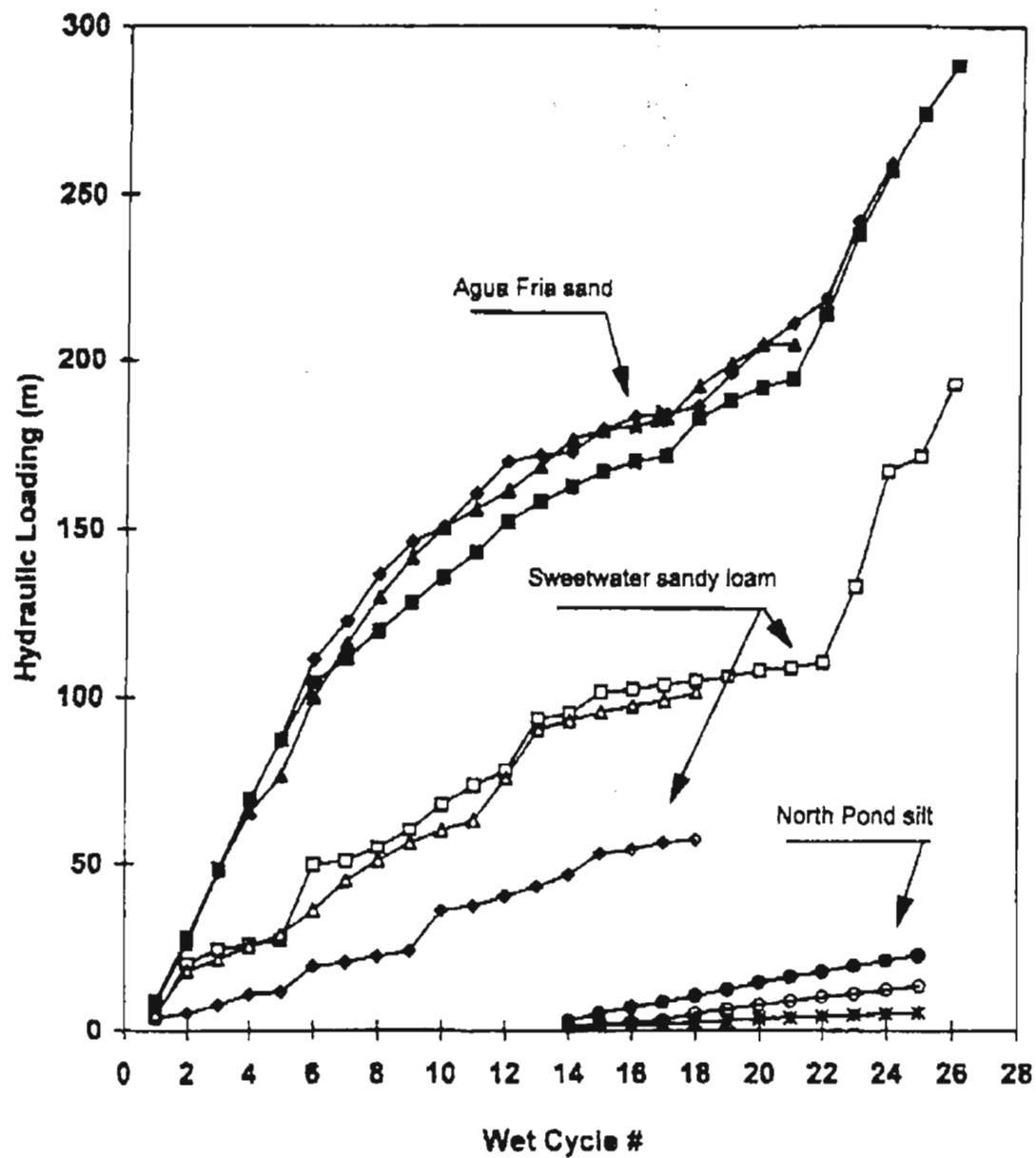


Figure 3-36 Cumulative hydraulic loading as a function of wet cycle for columns containing repacked Agua Fria sand, Sweetwater sandy loam, and North Pond silt during the first 25 wetting periods.

Effect of effluent type. Effluent types applied to columns containing the Agua Fria sand included secondary and ozonated secondary. Ozonated (1:1 O₃ to DOC) secondary effluent was applied to one column containing the Agua Fria sand during wetting cycles #20-28, corresponding the period of re-establishment of infiltration rates due to destruction of surface clogging zones (see above). The column receiving ozonated effluent (Figure 3-36, symbol = black squares) achieved higher hydraulic loading rates during cycles #21-25 than did a parallel column receiving unozonated secondary effluent (Figure 3-36, symbol = black diamonds). The surface clogging zones in both of these columns were destroyed by stirring during cycle #20. It is possible that the ozonation process destroyed a fraction of the suspended solids load in the effluent and that elimination of this fraction delayed the onset of redevelopment of the surface clogging layer, resulting in higher hydraulic loading rates relative to the column that received unozonated effluent.

Sweetwater Sandy Loam

Infiltration rates. The three columns containing repacked Sweetwater sandy loam ponded during the first wetting cycle. Infiltration rates for these columns at the beginning of the first few wetting periods were around 4.5-10.0 ft/day; during subsequent cycles, initial infiltration rates decreased to 1.8-3.6 ft/day, dropping steadily to 0.3-1.0 ft/day after seven days of operation. Figure 3-34 presents a plot of typical infiltration rates as a function of time during a wetting period after development of surface clogging layers. Total hydraulic loading for columns with repacked Sweetwater sandy loam during the first 25 wetting periods is shown in Figure 3-36.

Soil suction profiles. The zone of head loss in columns containing repacked Sweetwater sandy loam occurred within the top 12 cm of soil (Figure 3-37), with the majority of head loss between 6-12 centimeters of depth. Below 12 cm, matric potential was essentially invariant for any given day during a wetting period. Matric potential did change as a function of time within wetting periods and the amount of change was greater than for columns containing the Agua Fria sand. It is possible that production of gas pockets in soil pore spaces by anaerobic bacteria contributed to the change in matric potential below the surface zone of head loss. There appear to be significant differences in the thickness of the zone of clogging layer development for Agua Fria

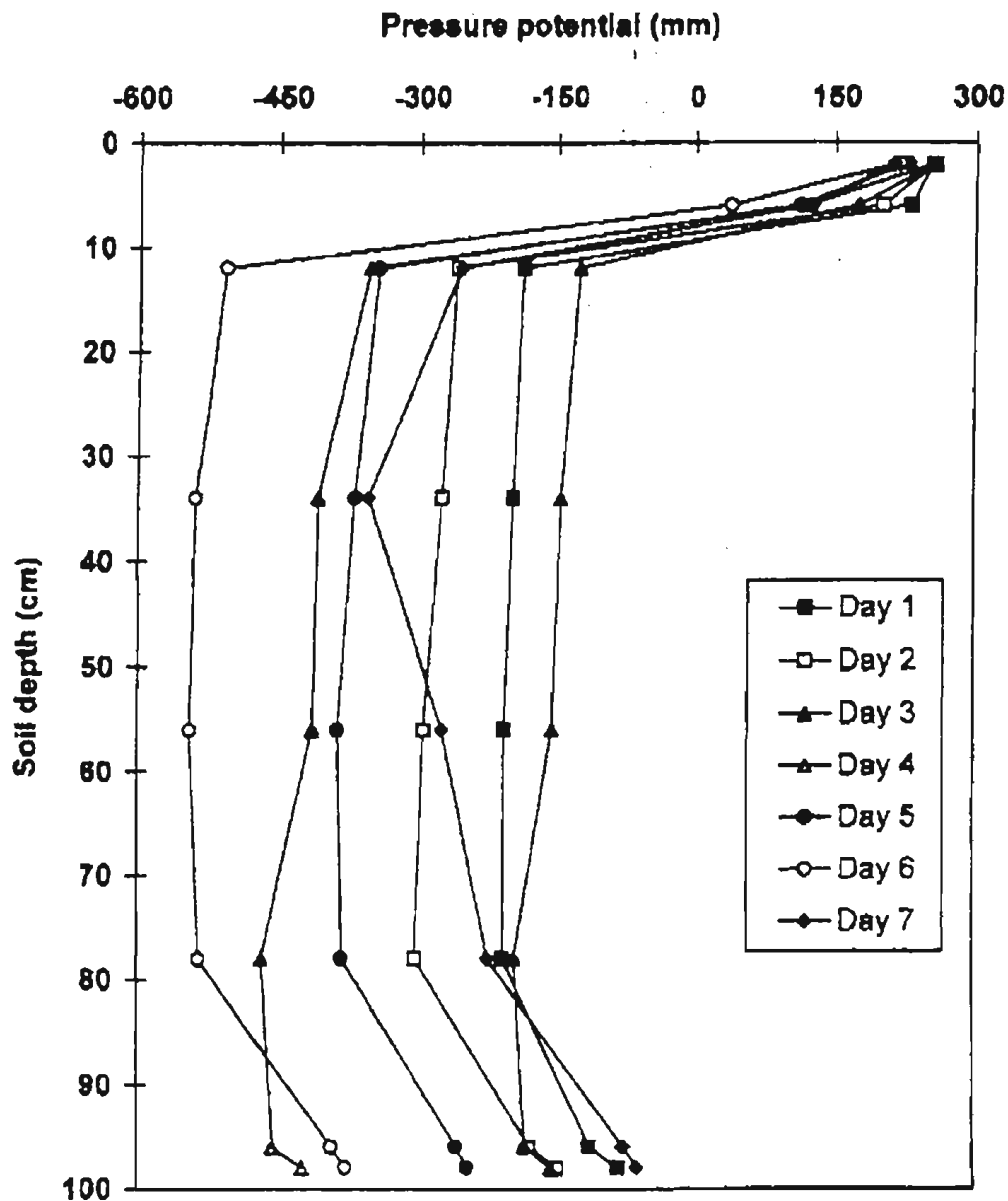


Figure 3-37 Typical daily measurements of matric potential as a function of soil depth for 1-meter columns containing repacked Sweetwater sandy loam during a 7-day wetting period. Data shown were collected after development of surface clogging layers.

sand (2 cm) versus Sweetwater sandy loam (12 cm), suggesting that surface clogging layer development may be related to soil grain size distribution.

Effect of surface scarification on infiltration rates. A sequence of steps were performed on the surface clogging zones in the columns containing the repacked Sweetwater sandy loam to re-establish initial hydraulic loading rates. Prior to the start of wetting cycle #18, the surface mat of dried algae was removed and the first 1 centimeter of soil was broken apart. Prior to the start of cycle #20, the top 6 centimeters of soil were removed and replaced with virgin sediments. Neither of these techniques were successful in re-establishing hydraulic loading rates (Figure 3-36). Prior to the start of cycle #21, the top 12 centimeters of soil was removed and replaced with fresh sediments. Hydraulic loading rates during subsequent cycles were significantly higher, even exceeding rates at the initiation of the study. These results suggest that the zone of clogging occurred deeper in the Sweetwater sandy loam, corresponding to the zone of head loss seen in Figure 3-37.

Effect of effluent type. Effluent qualities applied to columns containing the Sweetwater sandy loam included chlorinated/dechlorinated secondary, nitrified secondary, and filtered primary. Discussion of hydraulic performance of columns receiving nitrified secondary is included in Chapter 5 of this report. Discussion of hydraulic behavior of columns receiving filtered primary is covered in Chapter 8 and will not be reviewed here.

North Pond Silt

Infiltration rates. Three columns containing repacked North Pond silt began operation corresponding to wetting period #14. Ponding occurred on the first day of the first wetting cycle for all silt columns. Infiltration rates for these columns averaged 0.5-1.0 ft/day at the beginning of wetting cycles, decreasing to 0.1-0.5 ft/day after seven days of operation. No significant reductions in hydraulic loading rates over time occurred for these columns (Figure 3-36). It should be noted that a suction of -100 centimeters was applied to the base of all silt columns during wetting periods to maintain a representative moisture content throughout the soil profile. The applied base suction was consistent with procedures used on the 2-meter columns operated by Arizona State University.

The 1-meter intact core of North Pond silt also ponded during the first day of the first wetting cycle. Infiltration rates for the intact core averaged 0.5-0.7 ft/day at the start of wetting cycles, decreasing to 0.2-0.5 ft/day after seven days of operation over the course of five 7-day wetting periods. The intact core was also operated with a -100 centimeter base boundary condition. There were not significant differences in the hydraulic loading rates between the repacked and intact core silt columns.

Soil suction profiles. The columns containing repacked North Pond silt were equipped with tensiometers for measurement of soil matric potential, however, reliable measurements could not be obtained during the course of this study. Therefore, nothing can be said here regarding the zone of head loss and typical soil matric potential profiles for these columns.

RESULTS OF FIELD TESTS

Greeley and Hansen Field Percolation Basins

Two large-scale field tests were conducted by Greeley and Hansen Engineers as pilot percolation studies for the 91st Avenue Wastewater Treatment Plant Reclaimed Water Study. These two test sites are called North Pond site and South Pond site. Each of the two basins was approximately 0.25 acres. The soil profile at both sites is generally described as silty sand and silty sandy grave, with some clayey gravel. The main objective of the large-scale tests was to assess the infiltration performance of the field basins using local groundwater. Infiltration rates were obtained for a series of wetting and drying cycles, and three neutron moisture logging access tubes were installed at each basin, with one piezometer penetrating to the depth of the groundwater.

Infiltration Data

Figure 3-38 and 3-39 show the infiltration rates for several wetting cycles. For the first wetting cycle at the South Pond percolation test site, the infiltration rate are very high upon initial infiltration, and decays to approximately constant value at the end of one month wetting cycle.

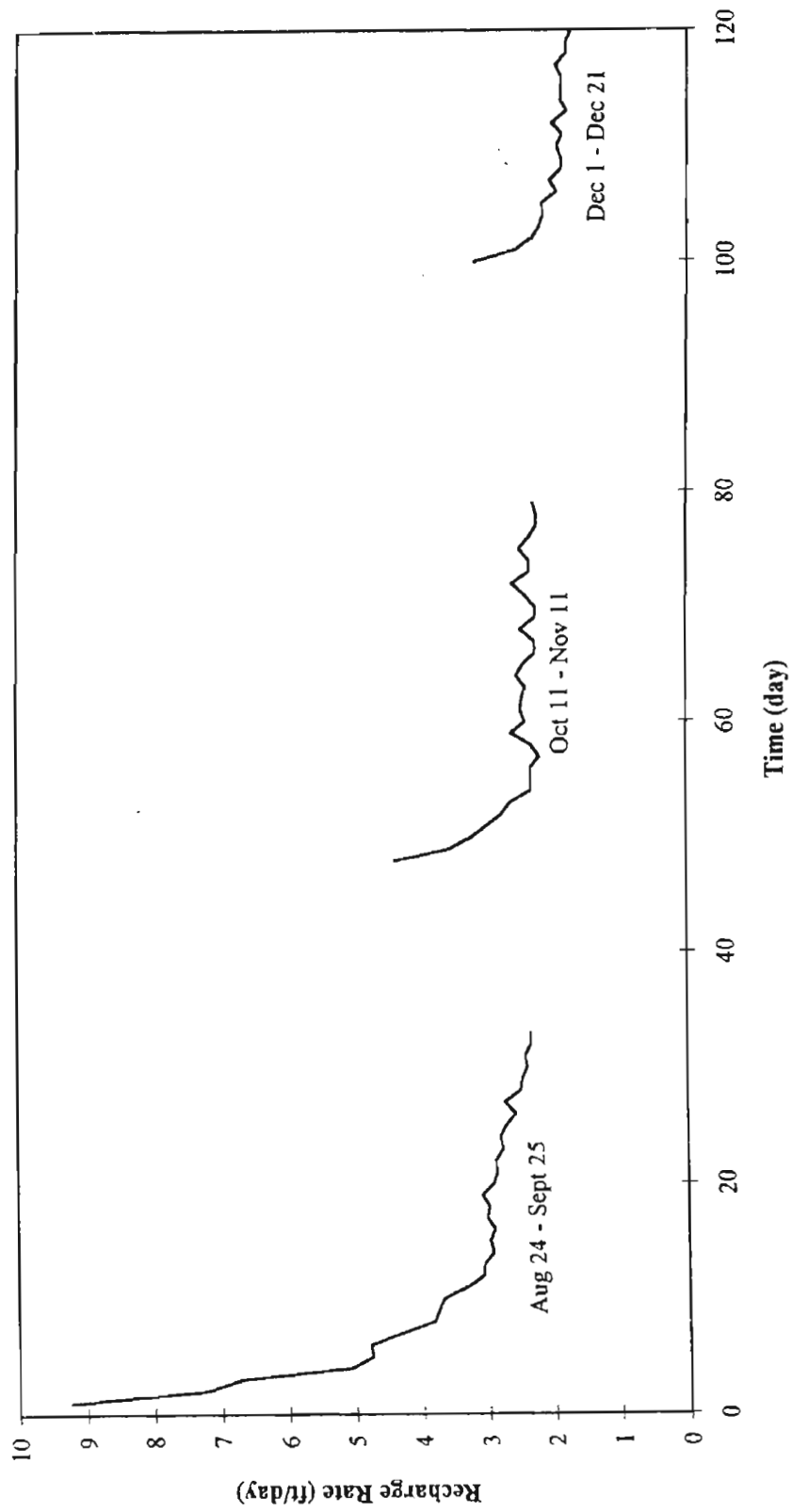


Figure 3-38 South Percolation Test Site
Dialy Infiltration Rates

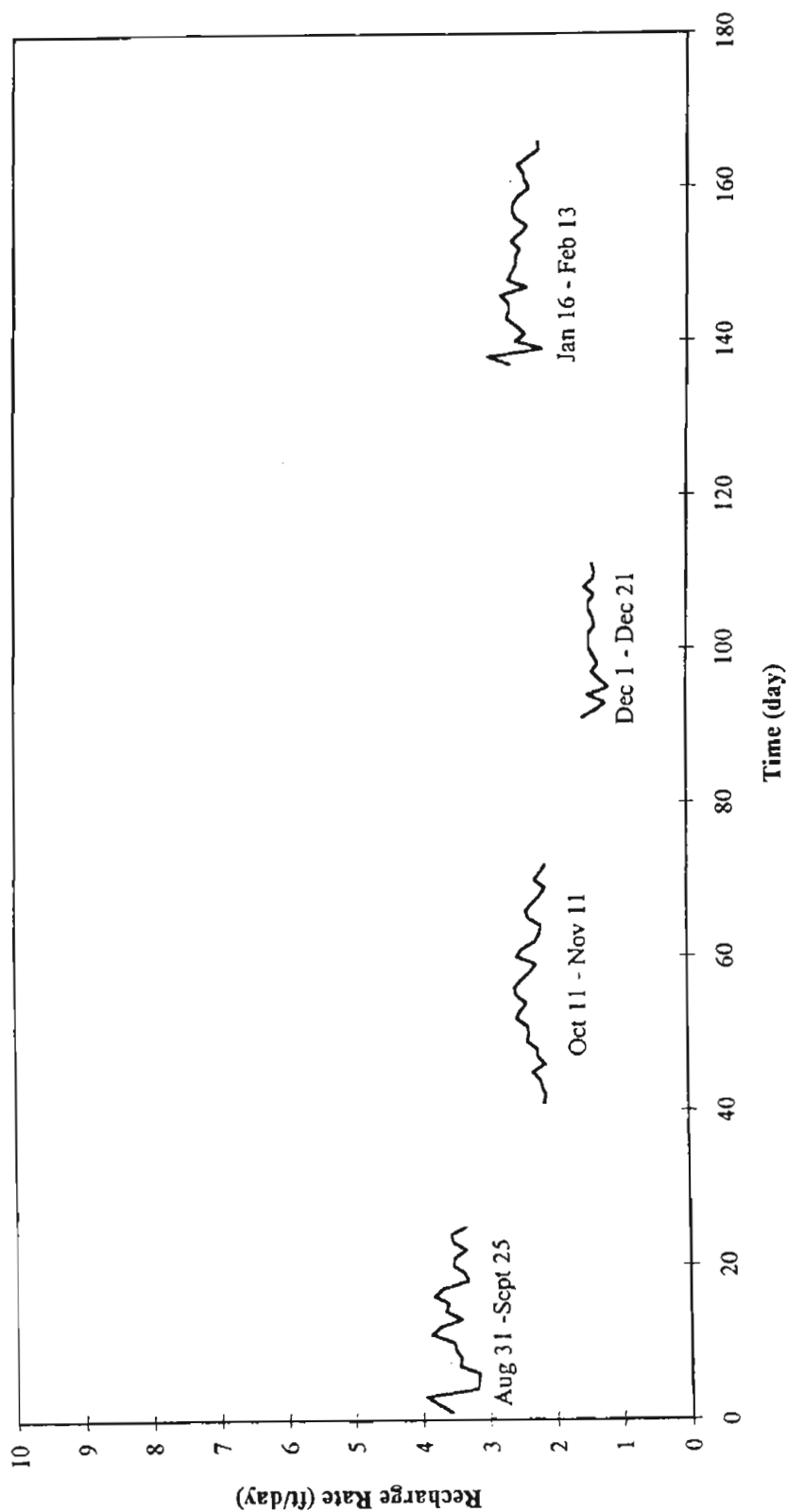


Figure 3-39 North Percolation Test Site
Daily Infiltration Rates

This infiltration response is typical of both laboratory and field infiltration tests. Based on the percolation testing results, the average long-term infiltration rate using groundwater is 2.5 ft/day at each of the two test sites. Neutron logs and piezometer data for the field percolation basins clearly showed that the water was transmitted to the water table, with no perching of water at lower conductivity layers at the North basin site. However, at the South basin location it appears that some lateral movement along a lower-conductivity clayey layer at approximately 20 ft depth occurred. An increased moisture content in this clayey soil likely resulted due to the reduced vertical infiltration rate caused by the lower-conductivity layer. The neutron logs also show that the degree of wetting during infiltration was generally well below 100% for an extended depth below the basin.

Neutron Log Calibration

Knowledge of the moisture content at various depths helps the SAT project researchers to identify the presence of any soil deposit that will impede the downward movement of moisture. It will also indicate whether or not any perched water tables exist beneath the project area. The neutron logs provided by Greeley and Hansen for the North and South Pond sites have been calibrated using direct moisture content measurements performed by ASU. The resulting moisture content-neutron reading curves have been used to predict the moisture content from neutron logs obtained after percolation basin wetting cycles commenced.

Direct moisture content measurements were performed on the field pilot percolation basin sites in August 1993. Samples were obtained at various depths from six boreholes, including a piezometer to the groundwater table at both the north and south test basins. Figure 3-40 is a reproduction of the site plan and indicates the location of the boreholes relative to the test basins. These moisture contents were then correlated to the corresponding neutron logs produced by Greeley and Hansen in August 1993, before any wetting. A linear relationship was assumed between the moisture content and the neutron log readings per Keys and MacCary (1971).

The calibration curves were then used to predict moisture content profiles from neutron logs provided by Greeley and Hansen after the wetting cycle in November 1993. Due to some heterogeneity and linear relationship assumption limitations, quantitative moisture content data is

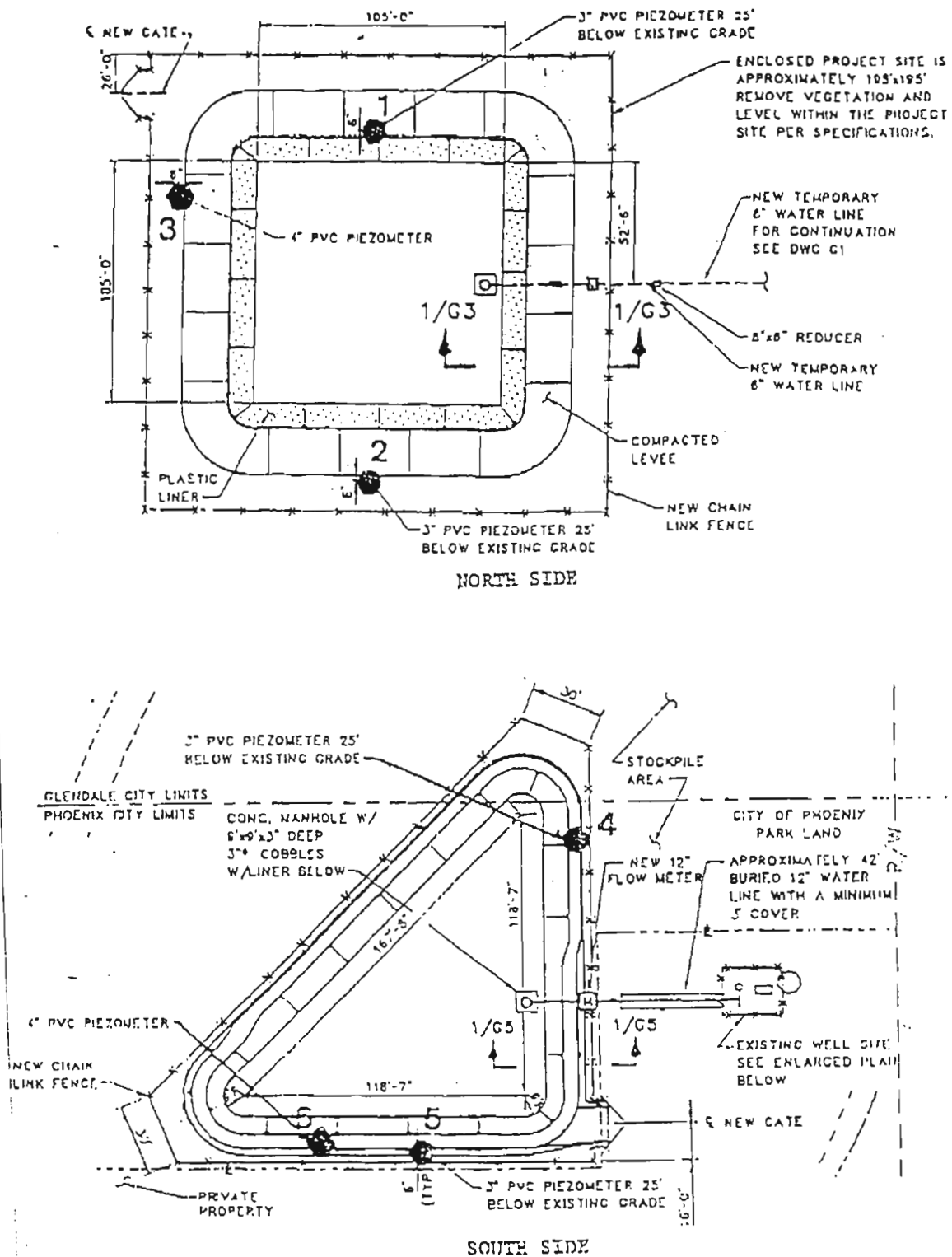


Figure 3-40 Plan View of North and South Basins

difficult to obtain. However, the predicted moisture content values are valid to describe qualitatively the patterns of moisture movement beneath the test basins. Plots of the predicted moisture contents versus depth, after the wetting cycle of November 1993, are presented in Figures 3-41 and 3-42.

Neutron Log Interpretation

Figure 3-41 indicates that no significant increase in moisture content occurred after wetting under the north basin to a depth of about 60 feet. The soil profile in this region consists primarily of low plasticity to non plastic silty sand and sand layers to a depth of 35 feet. Soil between 35 and 60 feet is primarily clayey sandy gravel, clayey sand, sandy clay, silty sand, and sand layers. This region is characterized by its low to medium plasticity. Starting at a depth of 60 feet, the moisture content gradually increases from the base conditions established before wetting. This trend continues until the new depth of the water table is reached. Soil in this region is mainly clayey sands, sandy clay, silty sand, sand, and clayey sandy gravel. Soil deposits from this region exhibit low to medium plasticity. The moderate increase in moisture content in this region might be attributed to a slight increase in the fines content and plasticity. Pronounced increase in the moisture content towards the new water table might also be attributed to the capillary fringe. It is important to note that the groundwater table rose about 20 feet from its original pre-wetting elevation; a fact that indicates high rate of downward movement of water in this vicinity. In conclusion, no soil deposit seems to impede the downward moisture movement at the North Pond site.

Figure 3-42 shows that no significant wetting-induced increase in moisture content occurred under the south basin throughout the entire depth except for the depths between 22 feet and 50 feet. A localized pronounced increase in moisture content takes place in this region. This region coincides with a soil deposit composed of clayey sand and clayey sand/gravel. This deposit possesses medium plasticity, classifying as SC and GC material. Soil deposits overlying and underlying this region exhibit little or no plasticity, and do not show any significant increase in moisture content. The increase in moisture content in the 22 to 50 foot region leads to the conclusion that these soils have significant moisture retaining capability, and relatively low

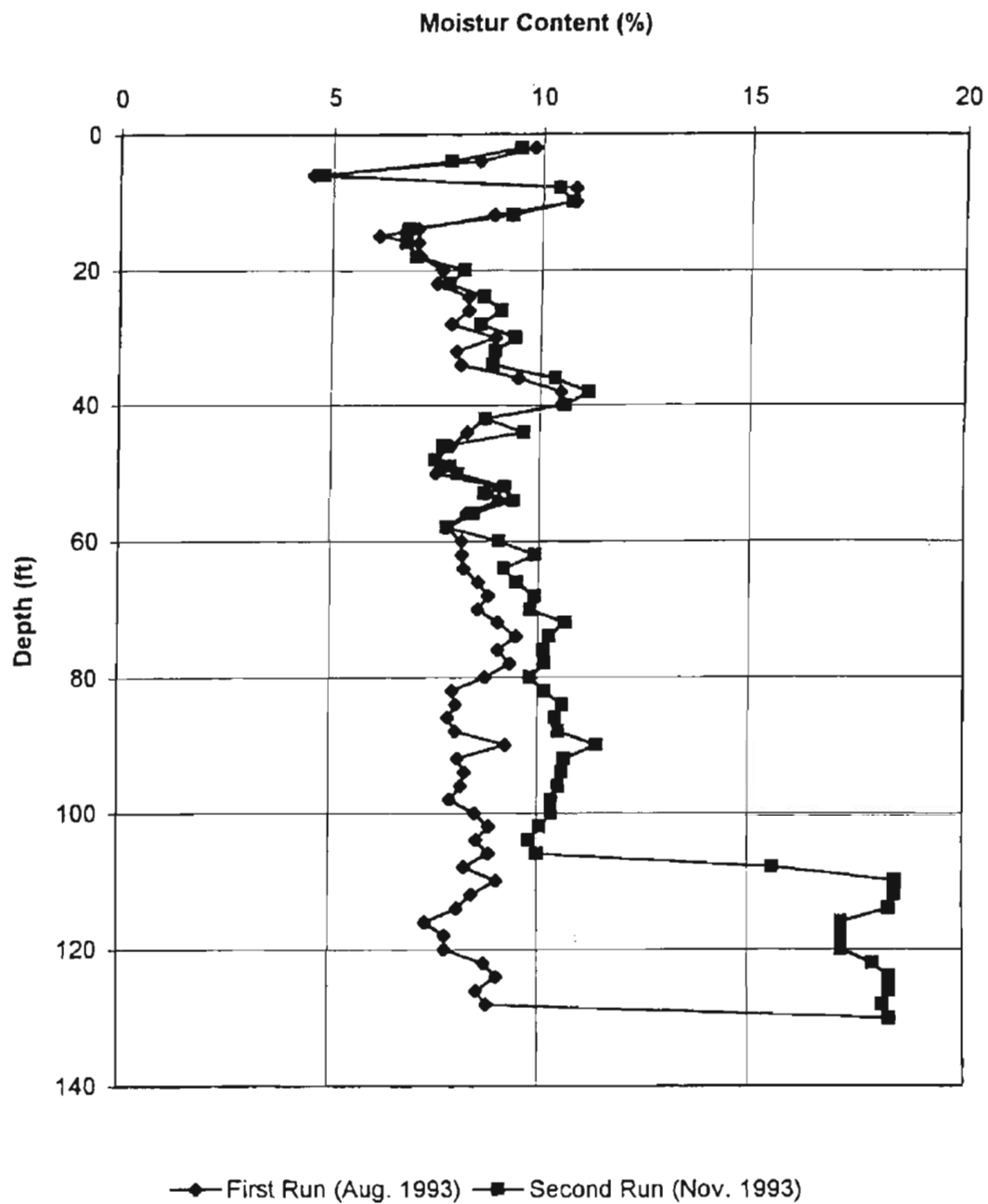


Figure 3-41 North Pond Neutron Moisture Profile

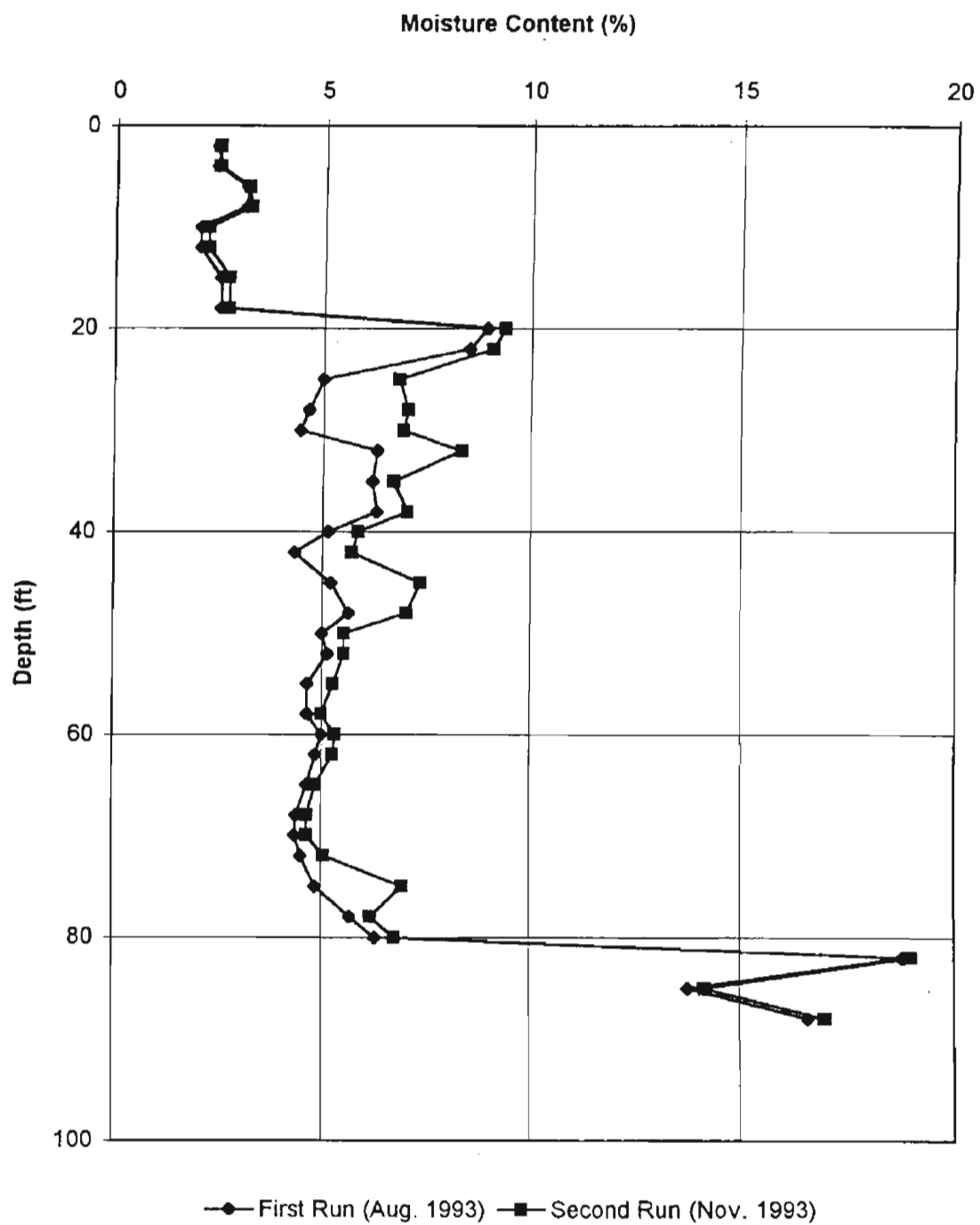


Figure 3-42 South Pond Neutron Moisture Profile

hydraulic conductivity. Therefore, it is believed that this deposit might act as a retarding lens for the downward movement of water and that lateral flow of water might have taken place. This conclusion is supported by the fact that the water table rise due to wetting is minimal, and in fact negligible compared to that of the North Pond, although pumping in the vicinity of the basin could also explain the lack of rise of the water table.

Identification of Potential Problematic Layers

Once it has been established that the material corresponding to the region between 22 to 50 feet is potentially problematic, it is interesting to determine the lateral extent of this layer across the project area. To accomplish this the boring logs produced by SH&B were utilized. These borings are scattered through out the project area. These boring logs characterize the material of interest as being very moist, hard, brown, weakly lime cemented, of medium plasticity clayey sand and gravel with some cobbles. A graphical representation of the findings from the borings is reproduced as Figure 3-43. This material is strongly present in boring logs corresponding to the portion of the project area bounded on the north by the New River bed, on the east by 107th Avenue, on the south by Indian School Road, and on the west by the Agua Fria River bed. It is interesting to note that the south percolation test basin was constructed in the north east corner of this area. This area constitutes more than 25 percent of the total proposed project area. It should be noted that the presence of other potentially problematic materials (such as the surface clay layer) is apparent, however, these surface materials could likely be removed to facilitate the implementation of soil aquifer treatment.

A potentially problematic clayey gravel/clayey sand layer persists over a region compromising about 25 percent of the SAT project area. Material from this layer apparently has low hydraulic conductivity, and might impede the downward movement of water, cause lateral groundwater flow, or perching. Presence of such material may affect many elements of the SAT project, primarily hydraulic loading rates. The potential effects of this layer should be carefully considered before the final location for recharge basins is selected.

FIGURE 3-43

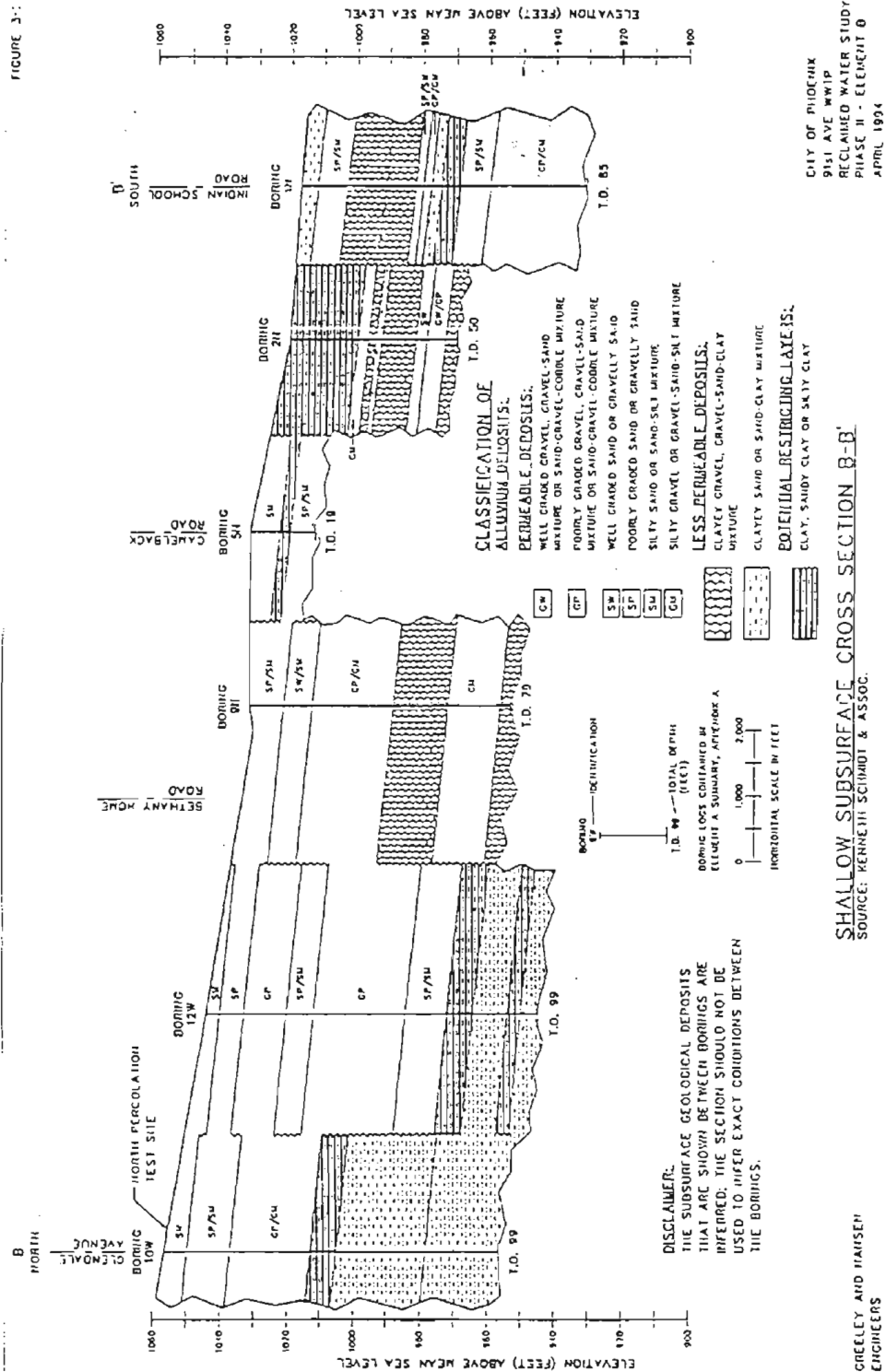


Figure 3-43 Graphical Representation of the Boring Logs

Small-Scale Field Percolation Tests

Some of the largest differences between lab column infiltration tests and in-situ field infiltration tests are soil heterogeneity in the field, sample disturbance, and dimensional effects. The field test is, of course, more practical because it addresses soil heterogeneity and dimensional effects but is not affected by sample disturbance. In this study, small scale field percolation tests were conducted to investigate the differences between lab column tests and field infiltration tests with regard to wetting front progression and degree of wetting. These tests were also performed so as to explore the predictability of results by numerical model using hydrologic parameters back-calculated from lab column tests.

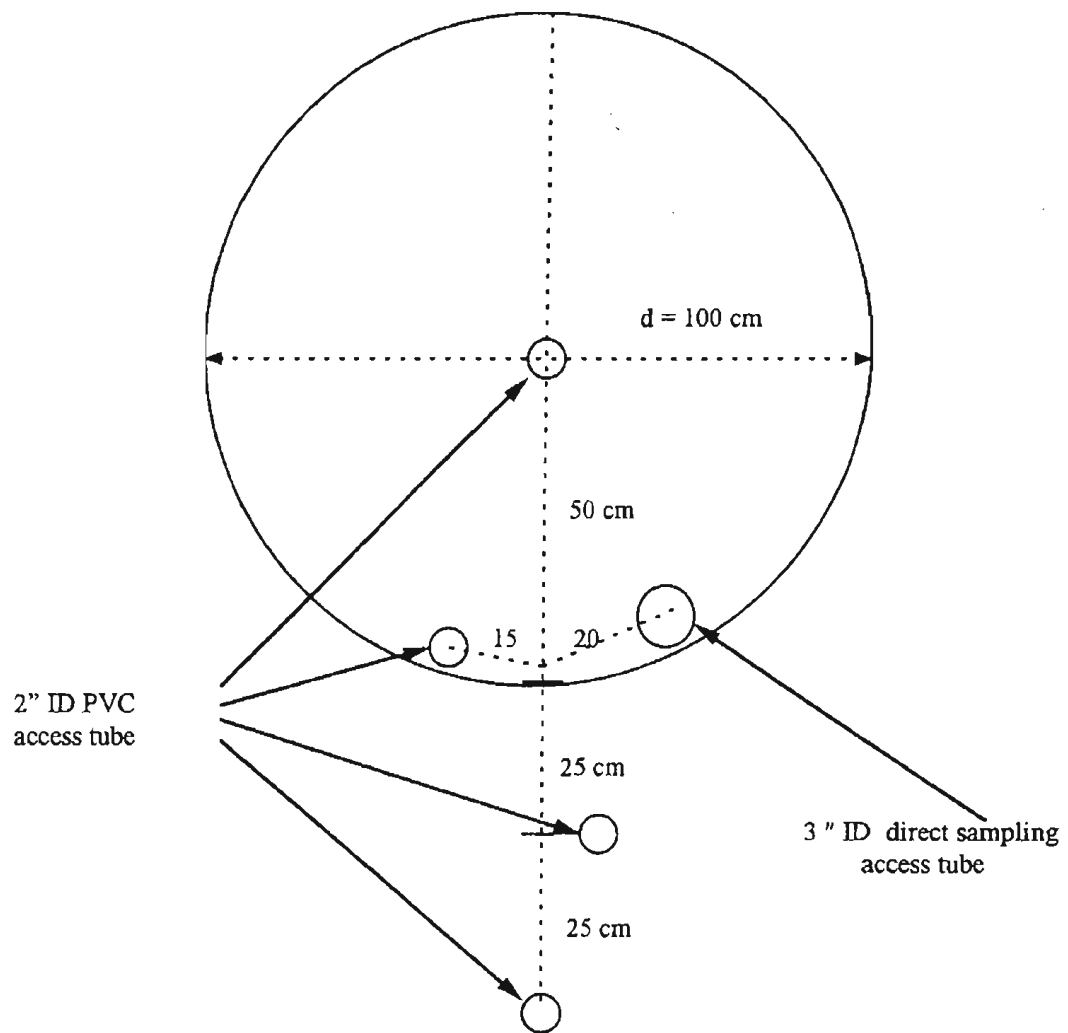
Test Description

The test site was located at the North Percolation Pond site approximately 400 ft south of Glendale Avenue and 1 mile west of 107th Avenue on a tract of undeveloped desert land. From boring logs, the first 16 ft of soil beneath the ground surface consisted of silty sands.

The in-situ moisture contents were measured using a Sentry 200-AP moisture probe, which was the product of Troxler Electronic Laboratories, Inc. This moisture probe measures changes in the dielectric constant of a material. Most solid materials in soil, such as sand, clay, and organic matter have a dielectric constant between 2 and 4. Water however, has a much higher dielectric constant of 78. Thus, measuring the changes in the dielectric constant of a soil sample can determine its moisture content. The Sentry 200-AP moisture probe must be used inside a non-metallic access tube. Two inch, schedule 40 PVC pipe is commonly used. One of the most critical aspects in using the probe successfully is access tube installation. Careful installation can minimize soil disturbance and provide a snug fit between the casing and the soil.

The constant head device used in these tests consisted of a 30 gallon reservoir, a float valve, a float ball, and a 100 cm long staff gauge to measure the water depth inside the reservoir. Using this device, the fluctuation of water depth inside the pond was controlled within 3 mm.

Figure 3-44 shows the test setup. This figure presents the location of direct sampling and the moisture probe access tube. The pond was approximately 100 cm in diameter and 20 cm deep.



Note: direct measurement of initial water content when installing access tubes and direct sampling inside 3" tube provide data for the calibration for Troxler Sentry 200-AP

Figure 3-44 Plane View of Field Percolation Test Pond

The direct water content samples were taken and tested in the lab to calibrate the moisture probe. The data for calibration encompassed the range of moisture content encountered in the test.

The initial water contents were measured at 4 separate access tubes. Moisture probe readings were taken at an interval of 10 cm. The percolation test was then started by introducing water into the pond and maintaining a constant depth using the constant head device described above. The inflow infiltration rate was obtained by measuring the water depth inside the reservoir every 1 hour. The moisture contents were measured at 1, 2, 4, 6, and 8 hours after the beginning of the test. After 8 hours of wetting, the water supply was shut off, and the extra water inside the pond was removed. After this point the drying process began. After drying for 24 hours, the moisture contents were again measured inside the access tubes. This completed the experiment.

Test Results

Figure 3-45 to Figure 3-50 present the moisture profiles during wetting and drying processes. Figure 3-51 presents the infiltration rate versus time. The progress of the wetting front under the center point of the pond was faster than that under the edge point. Table 3-10 gives the wetting front position beneath the center and edge points, together with wetting extent predicted by the empirical fitted equation from 1-D lab column tests. This equation was described in the column test section of this report. The saturated hydraulic conductivity was chosen to be that of an undisturbed sample as given in the soil report. The results show that the progress of the wetting front at the central point was approximately the same as for the 1-D result. After 8 hours of wetting, the vertical and horizontal depth of wetting front was 95 cm and 50 cm respectively.

The degree of saturation behind the wetting front was about 70-80% at both the central point and edge point. These values were similar to those of the lab results.

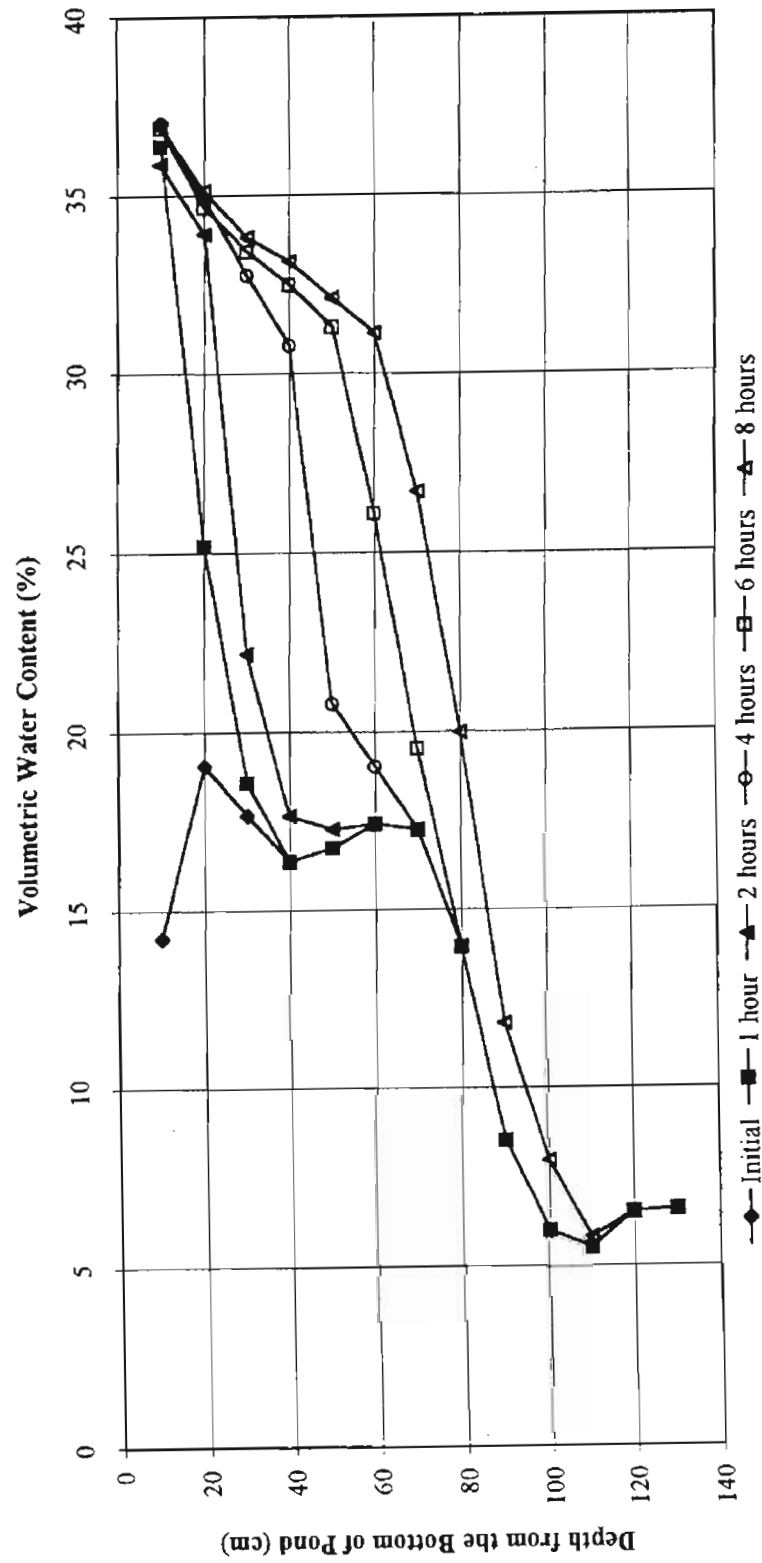


Figure 3-45 North Pond Field Percolation Test (Central Point)

Diameter = 101 cm, Water Depth = 13 cm

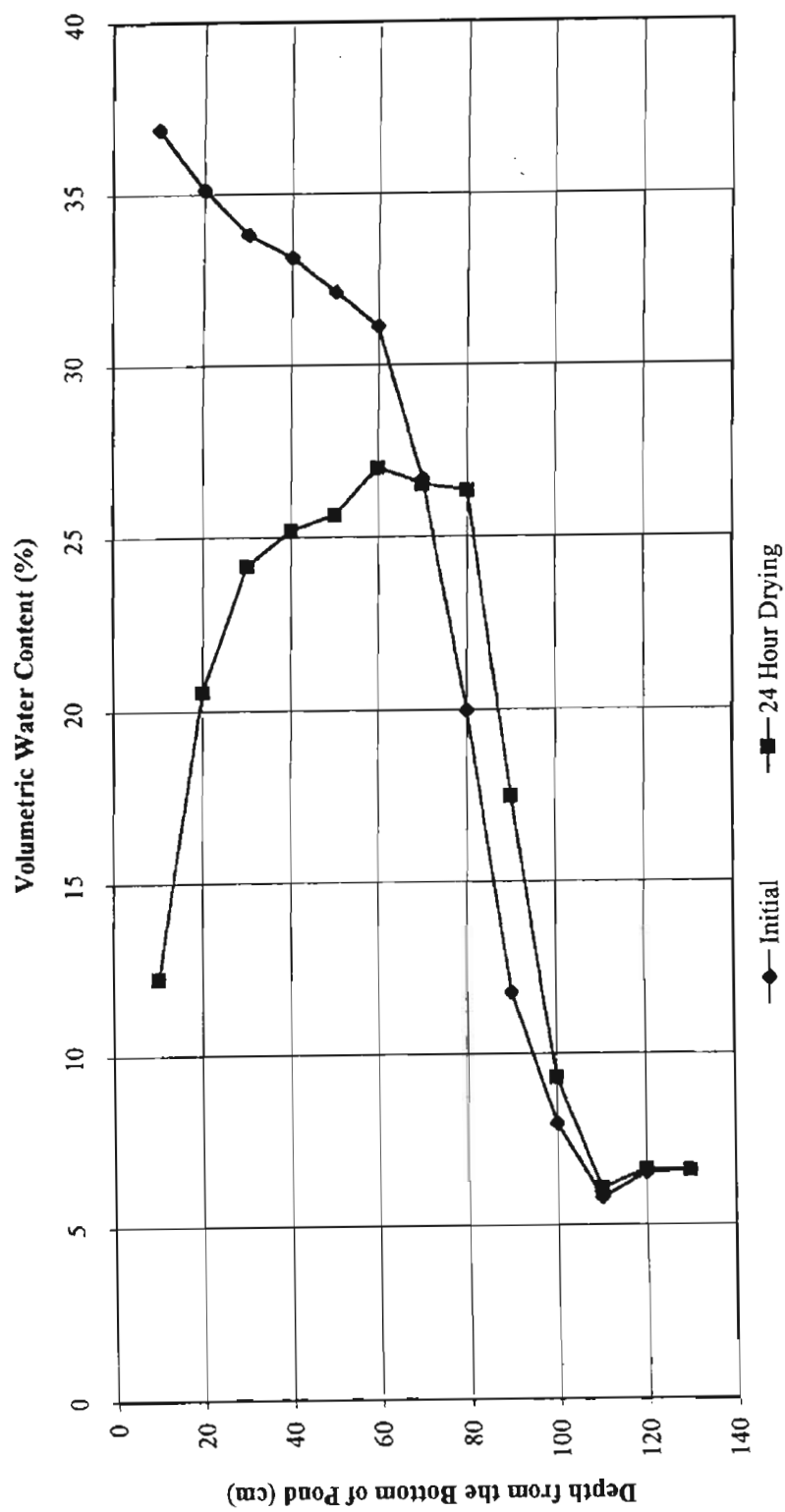


Figure 3-46 North Pond Field Percolation Test (Central Point)
Drying Process

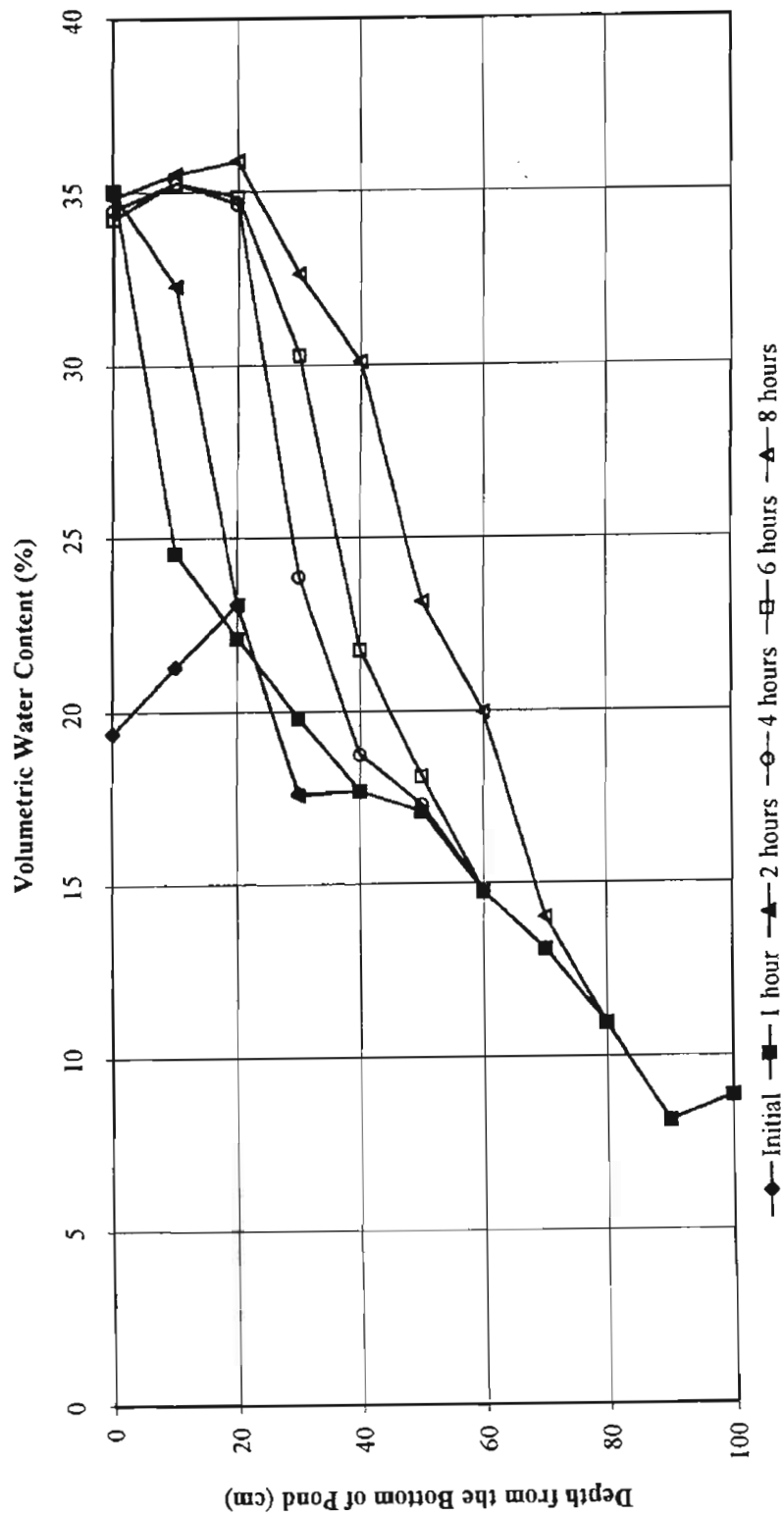


Figure. 3-47 North Pond Field Percolation Test (edge point)

Diameter=101 cm, Water Depth=13 cm

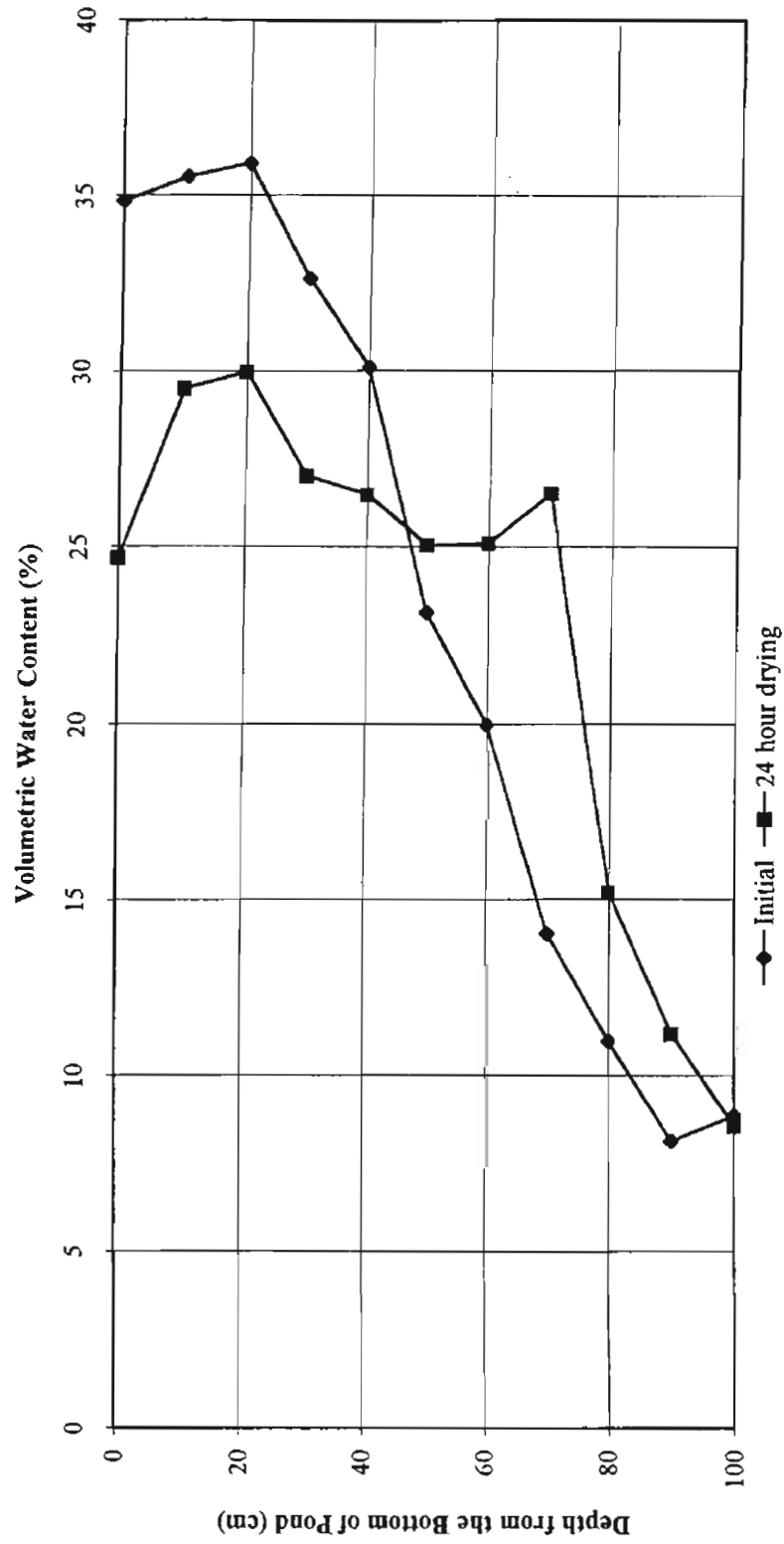


Figure 3-48 North Pond Field Percolation Test (edge point)
Drying Process

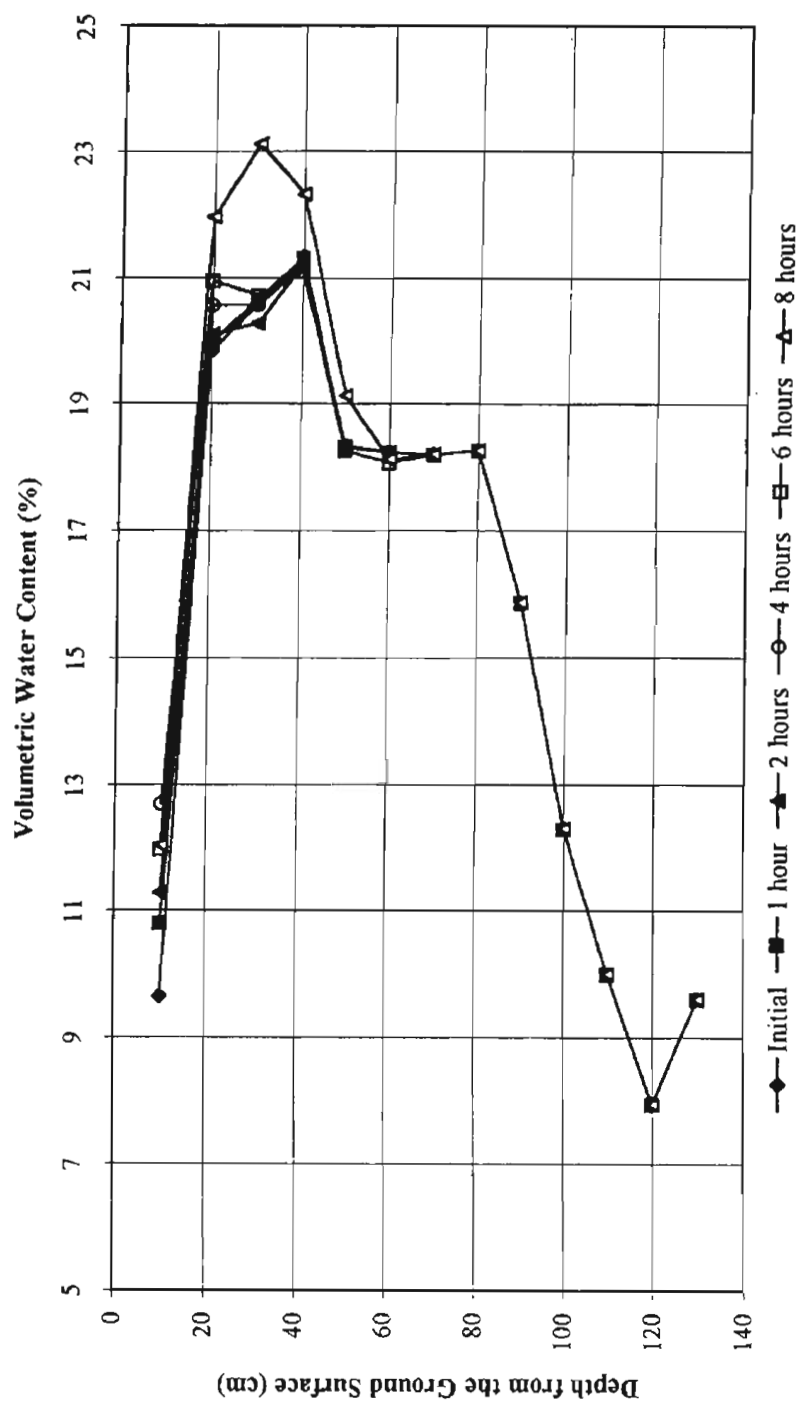


Figure 3-49 North Pond Field Percolation Test (50 cm from pond)
Pond Diameter=101 cm, Water Depth=13cm

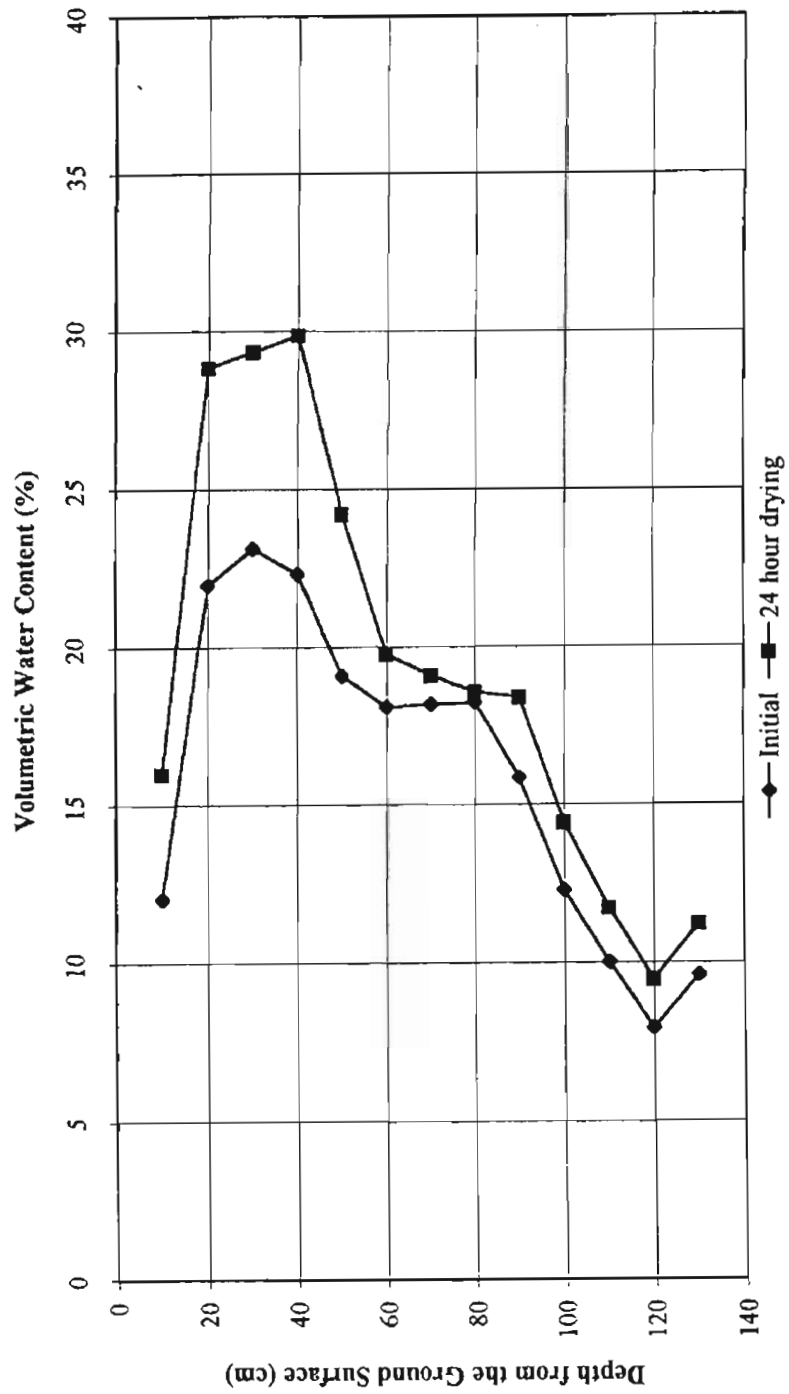


Figure 3-50 North Pond Field Percolation Test (50 cm from pond)
Drying Process

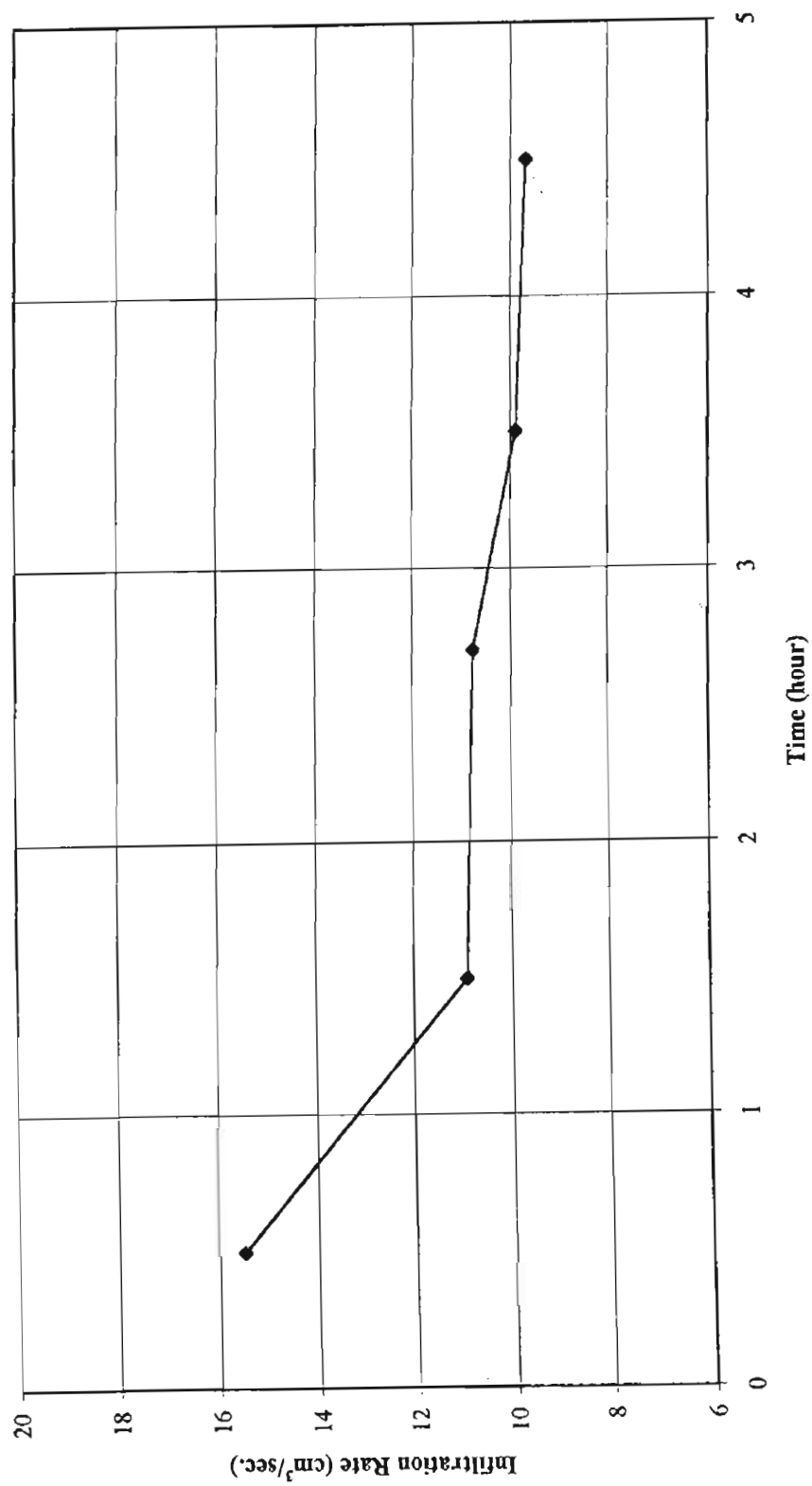


Figure 3-51 Field Percolation Test
Ponding depth = 12 cm, Diameter = 100 cm

Table 3-10
Wetting front position

Time (hour)	Wetting Front Position (cm)		
	Central Point	Edge Point	Predicted
0	0	0	0
1	30	15	29
2	45	20	43
4	65	40	63
6	75	50	78
8	95	70	91

Numerical Simulation of Field Infiltration

Although field percolation test is the most valuable approach to study the performance of field infiltration, large amount of tests cannot be conducted because of its expense. In this study, numerical simulation was performed in order to study several aspects of the field infiltration. These aspects include dimensional effect, soil nonhomogeneity, effect of soil type on the vertical and horizontal wetting extent.

Simulation of Small-Scale Field Percolation Test

MSTS was used to simulate the small-scale field percolation test. The problem was considered to be an axisymmetric problem. The pond diameter was 100 cm and ponding depth was 12 cm. The grid size was selected as 5 cm both in radial and vertical directions. The inverse parameters from the lab infiltration tests were used as the input hydrological parameters, while saturated hydraulic conductivity was selected as that of undisturbed soil samples. The upper boundary inside the pond was constant head. The upper boundary outside the pond and the side boundaries were no-flow boundaries. The bottom boundary was an unit gradient boundary. The initial condition was a uniform moisture content. The simulation domain was 40 m in diameter and 20 m in depth. Figure 3-52 shows the simulation domain and the boundary conditions.

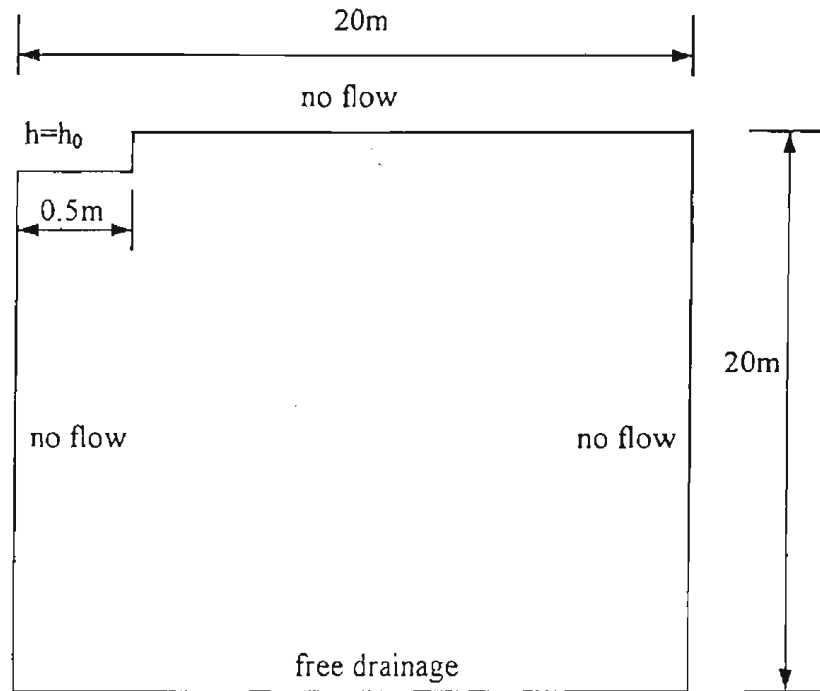


Figure 3-52 Simulation Domain and Boundary Condition

Figure 3-53 and Figure 3-54 present the results of wetting front position and moisture profile for the simulation and experiment. Good agreement was observed for the wetting front position. Again, the simulation over-estimated the degree of saturation behind the wetting front. This result is similar to that of lab column infiltration test. It can be concluded that simulation using hydrological parameters inverse from lab column test can satisfactorily predict the field performance.

The Effect of Soil Type on the Wetting Extent

Axisymmetric simulations were performed on North Pond silty sand, Sweetwater sand and Ag. Field clay. Figure 3-55 to Figure 3-57 show the wetting front progress for different soil types. When infiltration took place into an unsaturated soil, the suction gradients were at first much greater than the gravitational gradient. As the water penetrated deeper and the wetted part of the

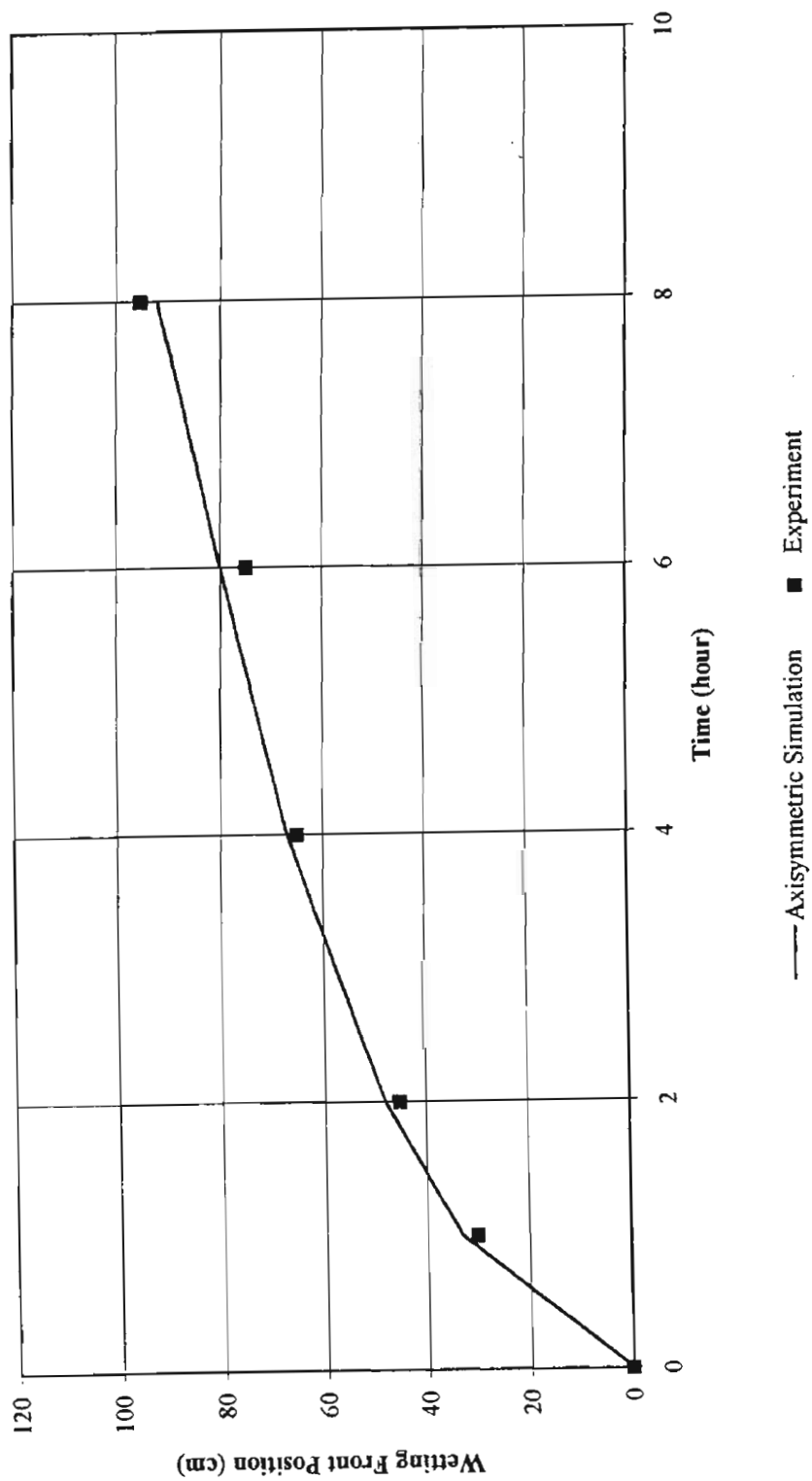


Figure 3-53 North Pond Field Percolation (Central Point)
Diameter = 101 cm, Water Depth = 13 cm

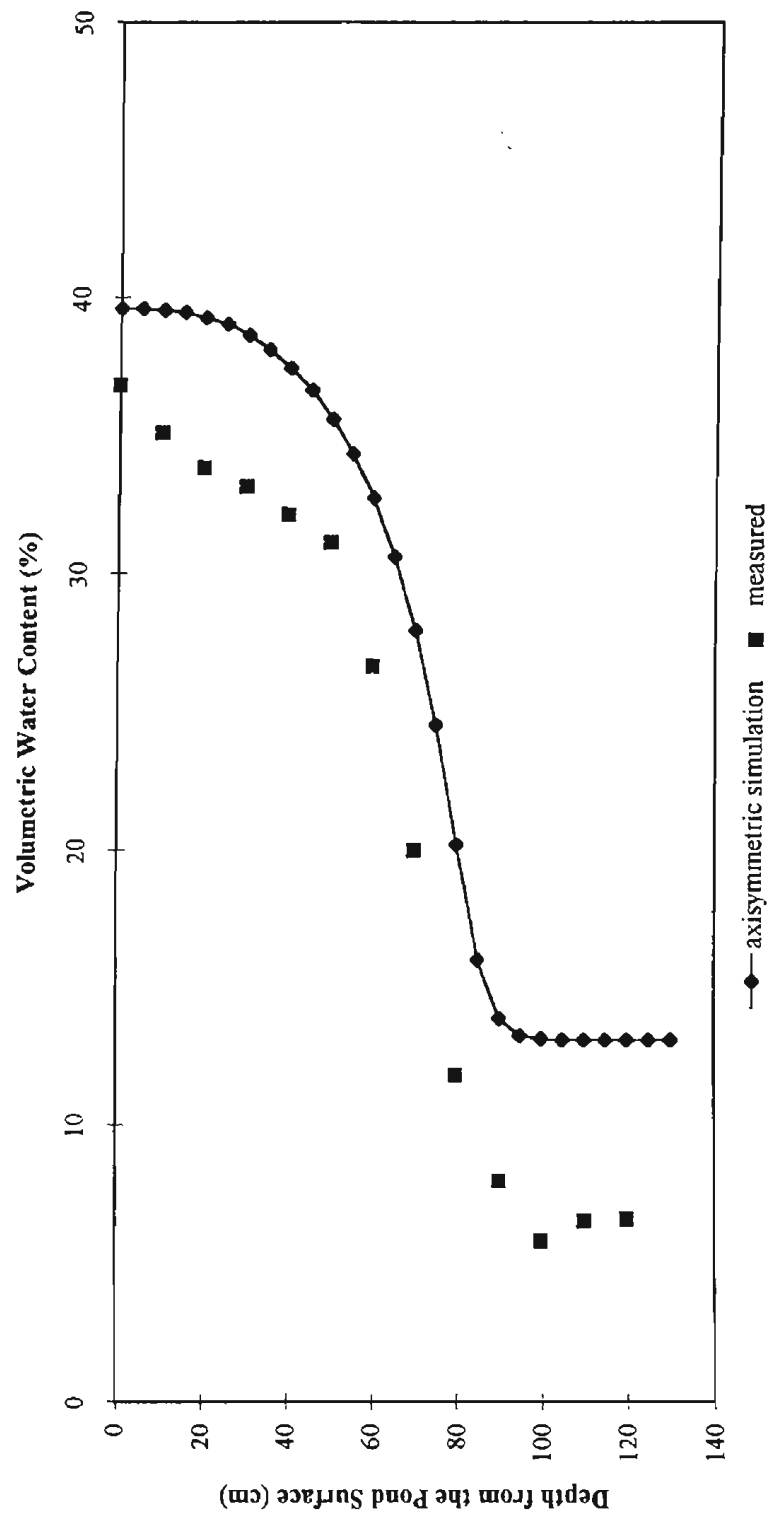


Figure 3-54 North Pond Field Percolation (central Point)
diameter=100cm, water depth=12cm, t=8hours

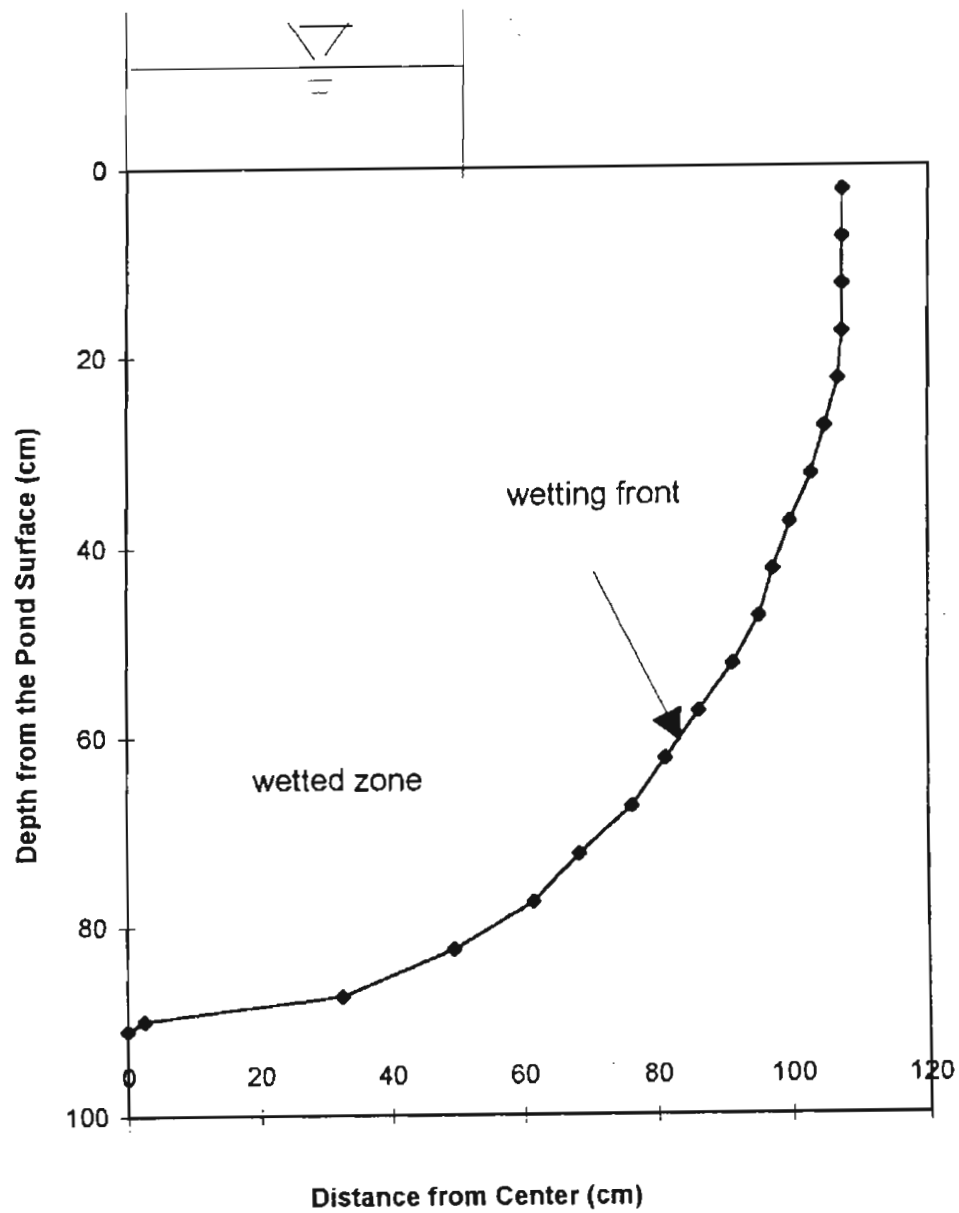


Figure 3-55 Wetting Front Position
North Pond Soil, $t = 8h$

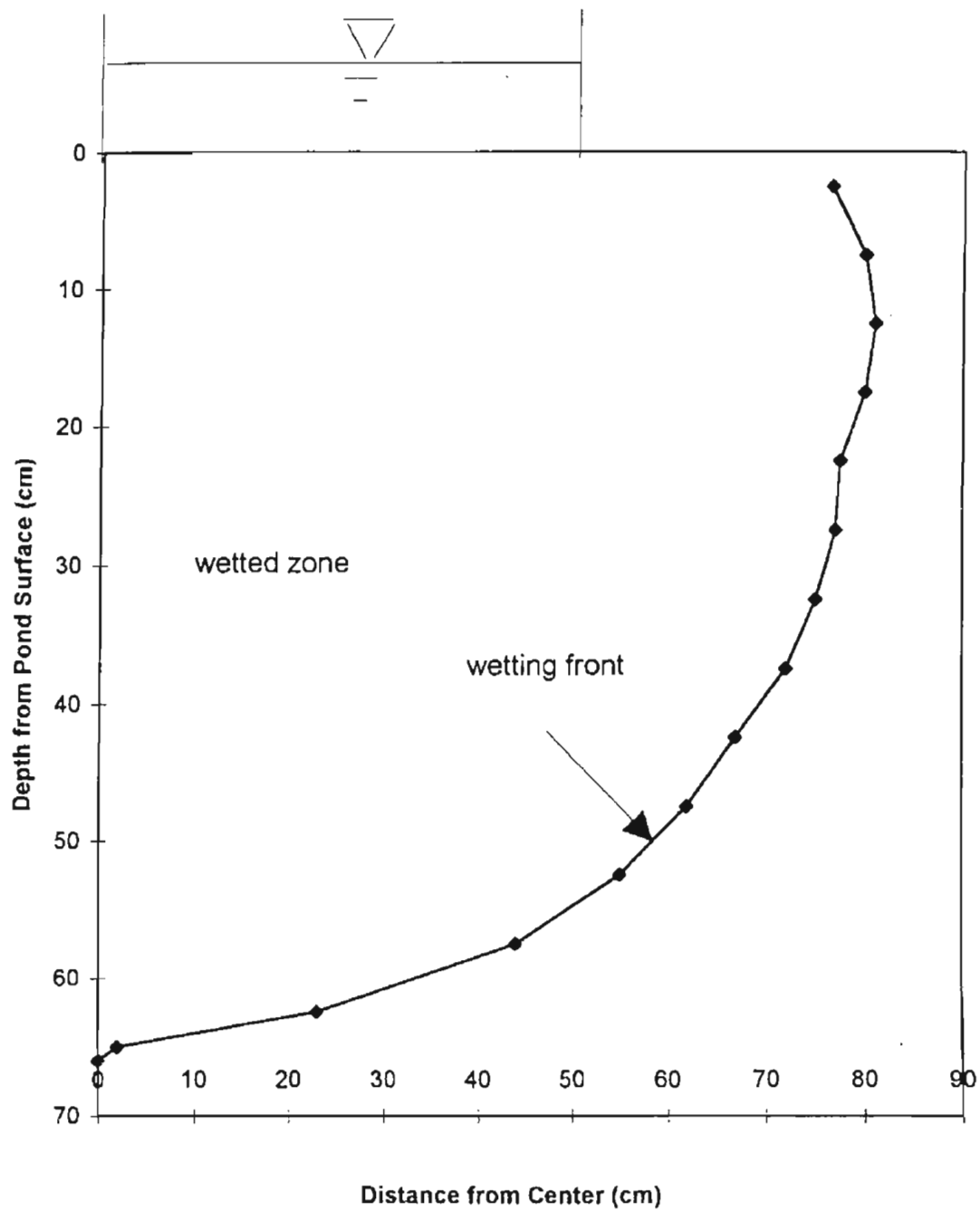


Figure 3-56 Wetting Front Position
Sweetwater Soil, $t=12$ min

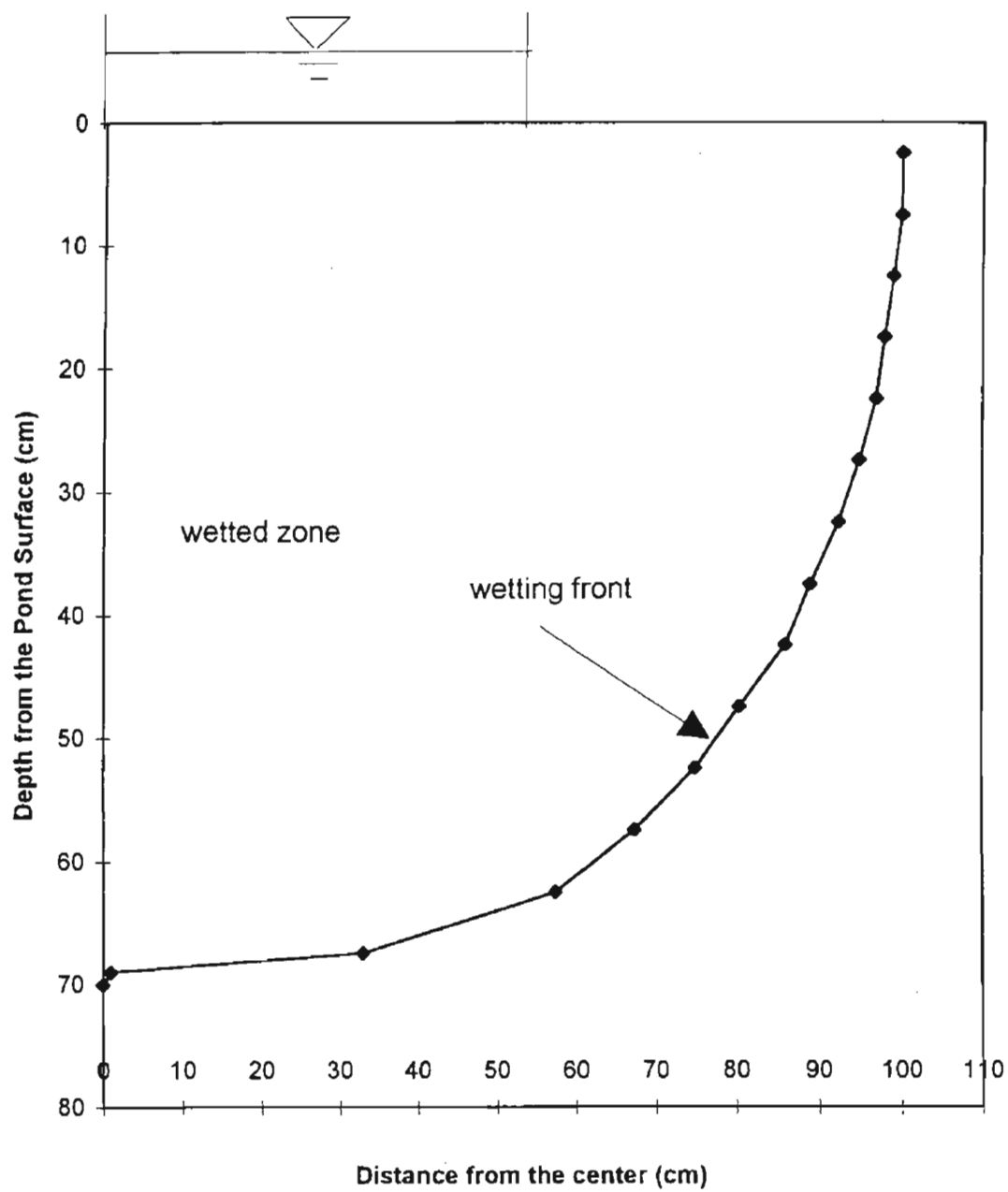


Figure 3-57 Wetting Front Position
Ag. Field clay, $t=180h$

profile lengthened, the average suction gradient decreased. This trend continued until eventually the suction gradient in the upper part of the profile became negligible, leaving the constant gravitational gradient as the only remaining force driving water downward. The more clayey the soil, the more the lateral movement compared to the vertical fluid flow.

The Effect of Pond Size on Infiltration Rate

Axisymmetric numerical simulations were conducted in order to study the effect of the pond size on the infiltration rate. This simulation was important in regard to the interpretation of lab column test results as compared to field results. Theoretically, if pond diameter is large enough, the three dimensional problem can be simplified to a one dimensional problem. The simulation domains, boundary conditions and initial conditions were the same as those described above. Simulation was conducted for 5 different pond diameters-- 0.4 m, 1.0 m, 5.0 m, 10.0 m, and infinite. Soil types were selected as Sweetwater sand, North Pond silty sand and Ag. Field clay. The results were presented in Figure 3-58 to Figure 3-60. Although a steady state was never attained for the entire simulation time, the infiltration rate decreased slightly at the end of the simulation. The infiltration rates q at the end of the simulations were compared in Table 3-11. It could be concluded that if the pond diameter was larger than 10 m, the one dimensional flow assumption was acceptable.

Table 3-11
Pond size effect on infiltration rate

Pond Diameter (m)	North Pond Soil		Sweetwater Soil		Ag. Field Soil	
	q (ft/day)	q/q_{infinite}	q (ft/day)	q/q_{infinite}	q (ft/day)	q/q_{infinite}
0.4	3.58	4.82	2.03×10^2	3.27	6.87×10^{-2}	1.47
1.0	2.15	2.89	1.38×10^2	2.22	5.40×10^{-2}	1.15
5.0	1.16	1.57	0.92×10^2	1.48	5.04×10^{-2}	1.08
10.0	0.85	1.14	0.73×10^2	1.18	4.86×10^{-2}	1.04
infinite	0.74	1.0	0.62×10^2	1.0	4.70×10^{-2}	1.0

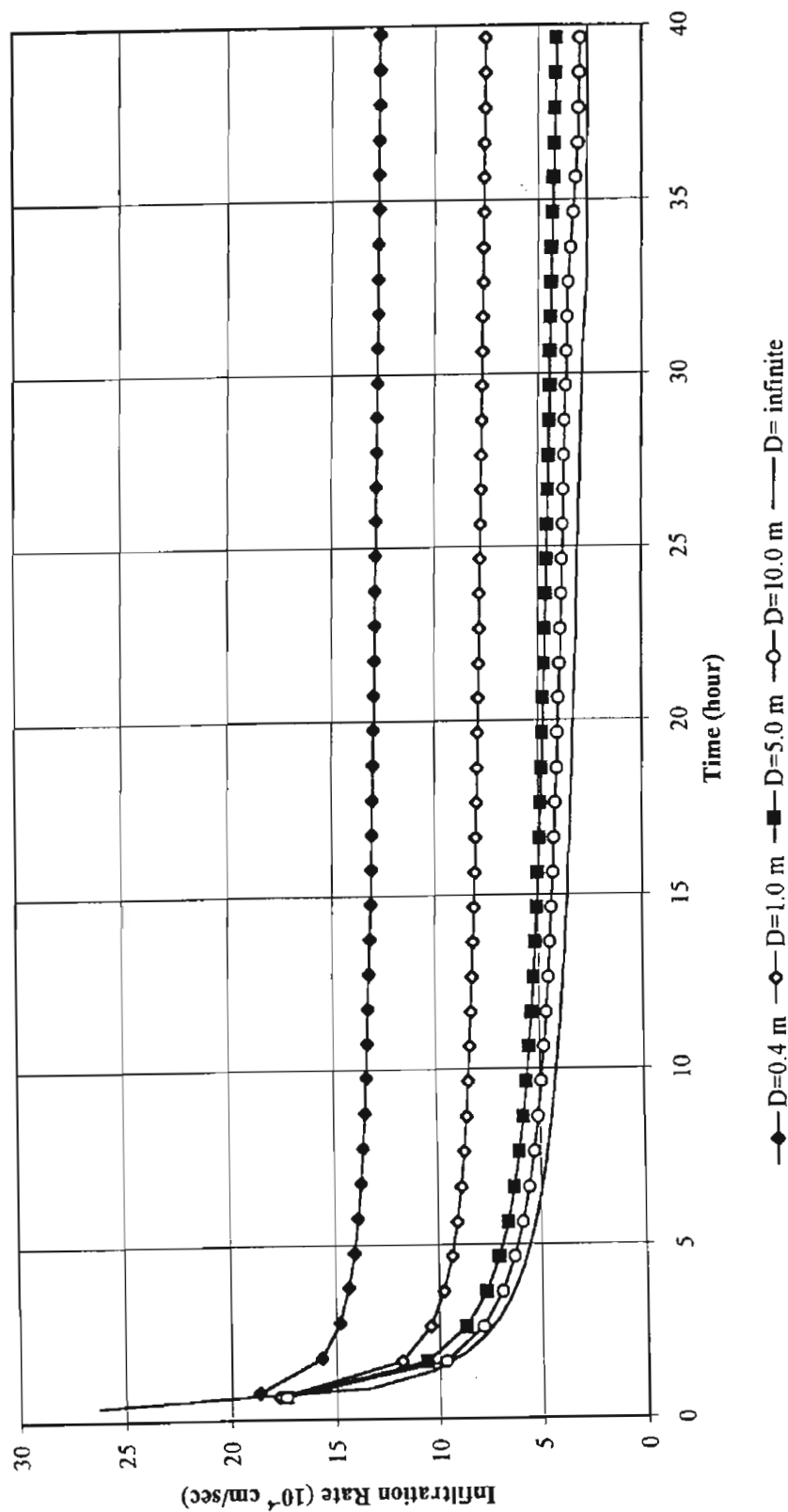


Figure 3-58 Axisymmetric Simulation for North Pond Soil
Pond Size Effect

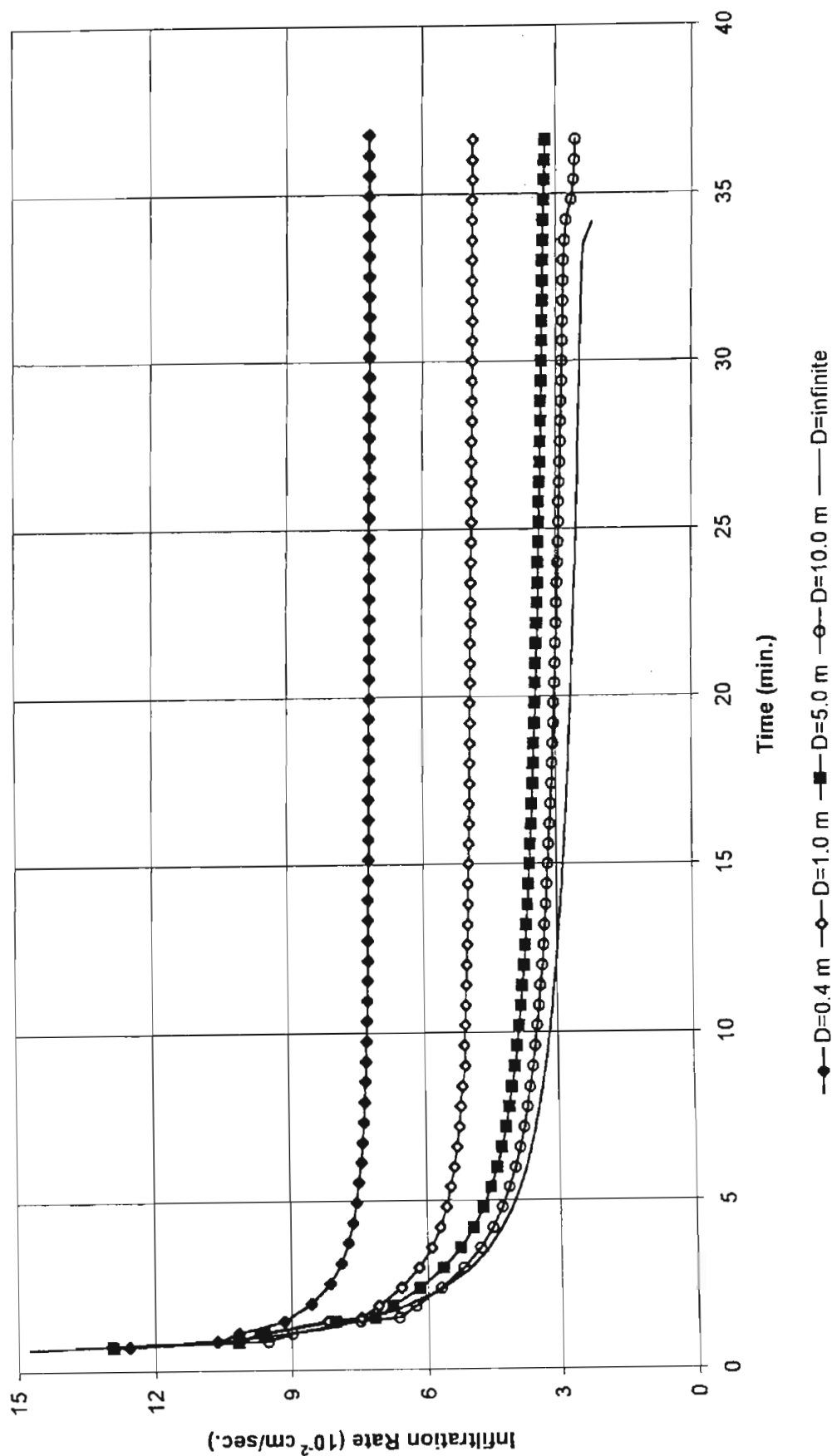


Figure 3-59 Axisymmetric Simulation for Sweetwater Soil
Pond Size Effect

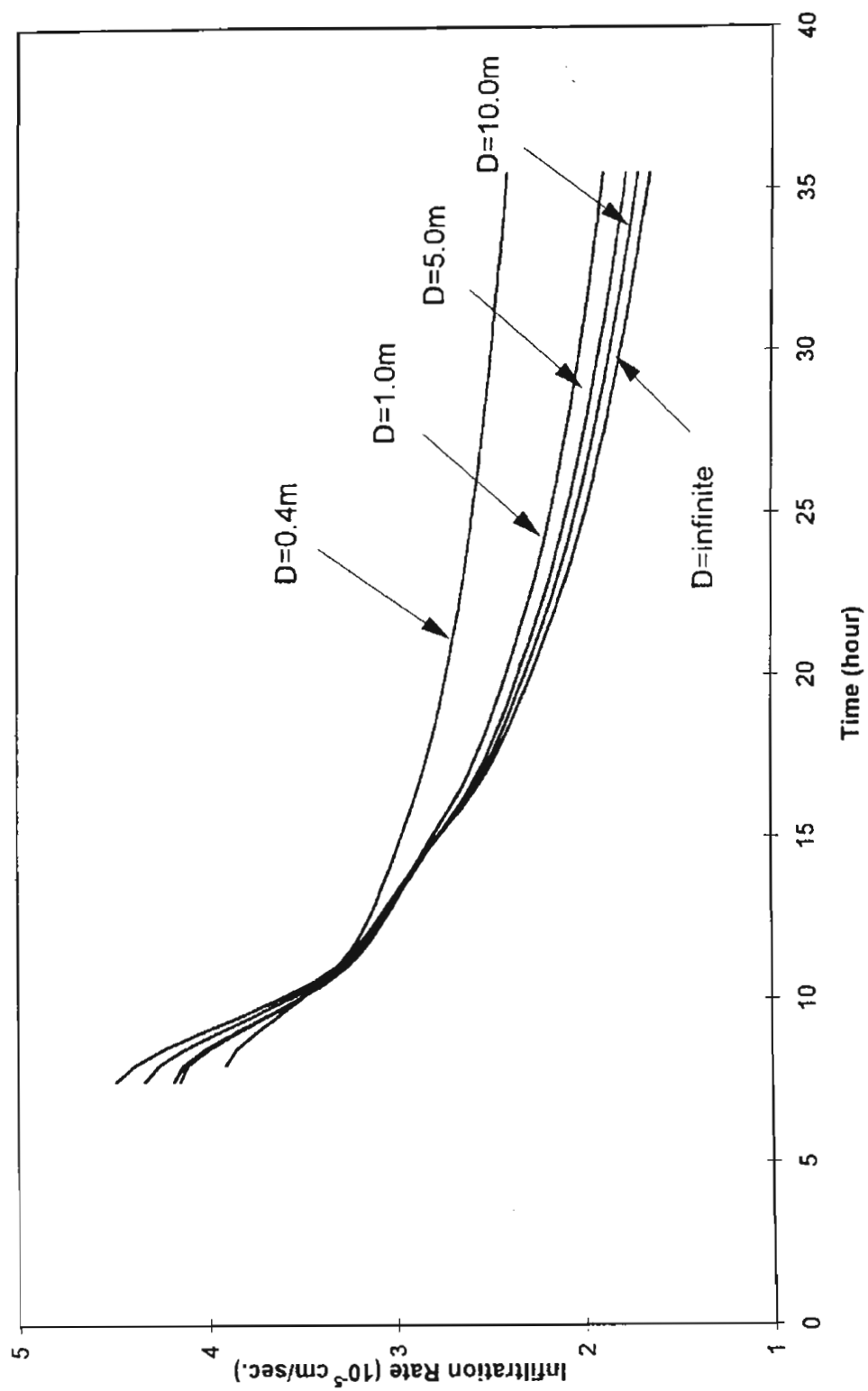


Figure 3-60 Axisymmetric Simulation for Ag. Field Soil
Pond Size Effect

Effect of Soil Nonhomogeneity

In the field situation, it is very common that there exists a clayey layer or a low hydraulic conductivity layer. Infiltration capacity is therefore restricted by this layer. To investigate the effect of this restriction on the steady state infiltration rate, several cases of 1-dimensional and 2-dimensional numerical simulations were performed. Among these were the thickness of the clay layers, the position of the clay layers and lateral extent of the clay layers. The saturated hydraulic conductivities were chosen to be those of recompacted soil samples.

The effect of the thickness of clay layers Figure 3-61 and Figure 3-62 show the steady-state infiltration rate as a function of the thickness of clay layer inside North Pond soil and Sweetwater soil columns. The depth of the soil profile was 10 meters. The surface boundary was 1 cm ponding depth, the bottom boundary was unit gradient. The top of the clay layer was located at 2 meters below the pond surface. The results demonstrated that the larger the thickness of the clay layers, the lower the steady-state infiltration rate. It must be noted that because the ponding depth was small, the steady state infiltration rate from constant ponding infiltration might be viewed as the infiltration rate which didn't produce significant impediments.

The effect of the position of the clay layers Figure 3-63 and Figure 3-64 present the steady-state infiltration rate versus the position of the clay layers inside North Pond soil and Sweetwater soil columns. The thickness of the clay layer was 10 cm. The simulation domain and boundary conditions were the same as above. The results showed that the closer the clay layer to the ponding surface, the lower the steady-state infiltration rate. For the case of North Pond soil, when the 10 cm clay layer was 500 cm below the ponding surface, the steady-state infiltration rate was 1.0×10^{-4} cm/sec compared to 1.8×10^{-4} cm/sec without the existence of the clay layer. For the case of Sweetwater soil, if the 10 cm clay lense was 500 cm below the ponding surface, the infiltration rate was 2.1×10^{-4} cm/sec compared to 1.9×10^{-2} cm/sec without the presence of the clay layer. The impedance of clay layer was more pronounced when the soil, which sandwiched the clay layer was more permeable.

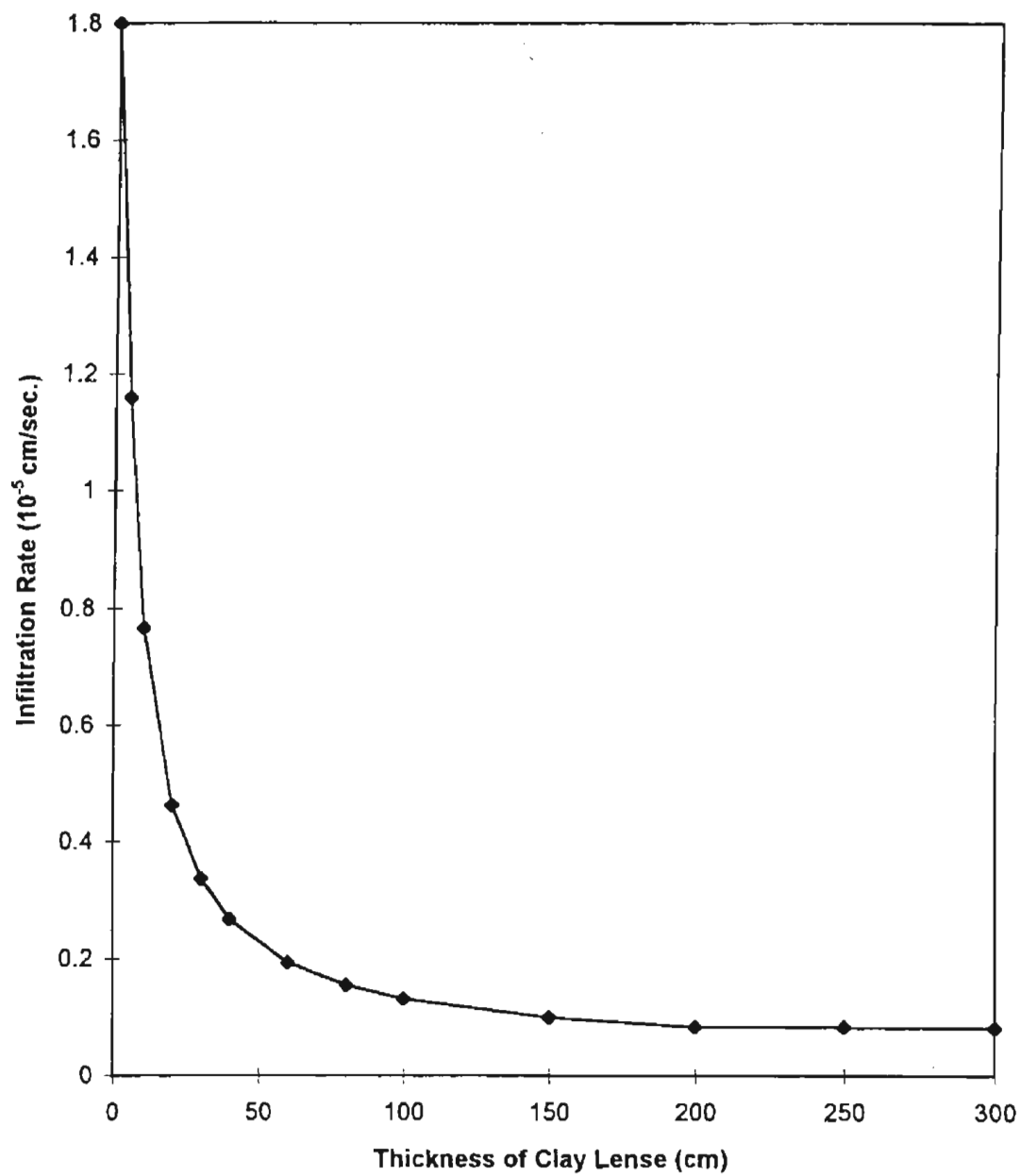


Figure 3-61 1-D Simulation of North Pond Soil with Clay Lenses
position of lense=2 m, ponding depth=1cm

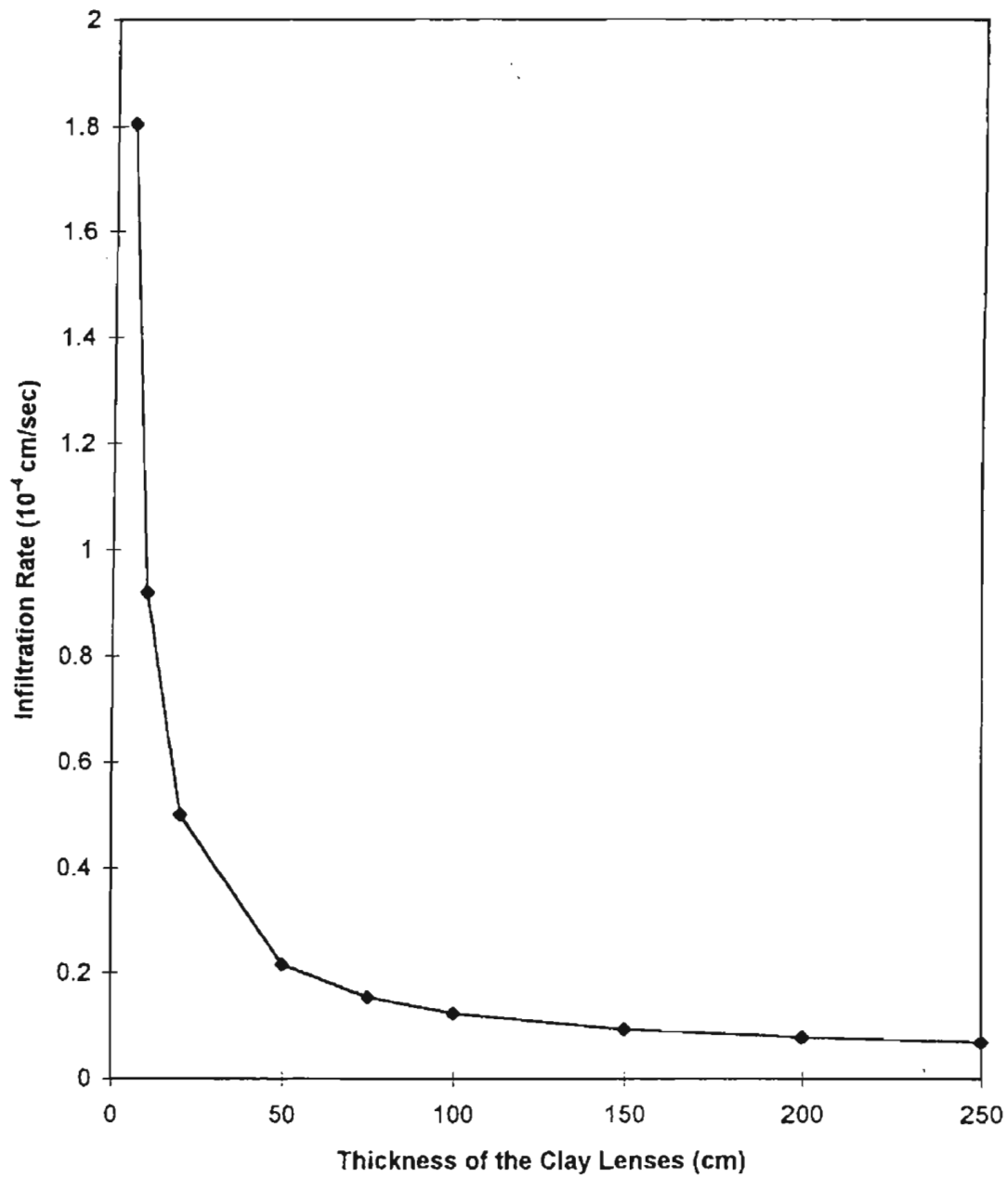


Figure 3-62 1-D Simulation of Sweetwater Soil with Clay Lenses
position of clay=2m, ponding depth=1cm

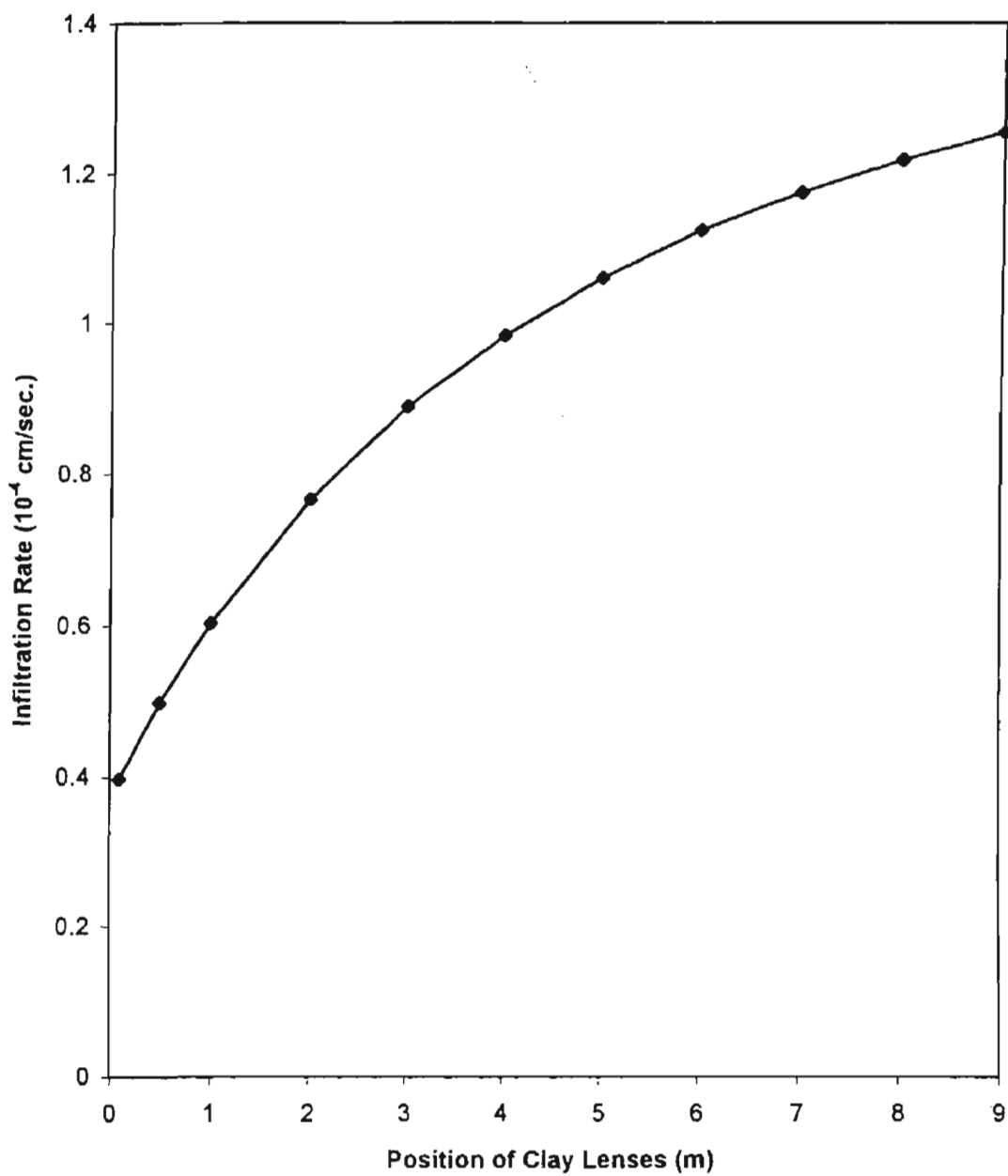


Figure 3-63 1-D Simulation of North Pond Soil with Clay
Lenses
thickness of clay=20 cm, ponding depth=1cm

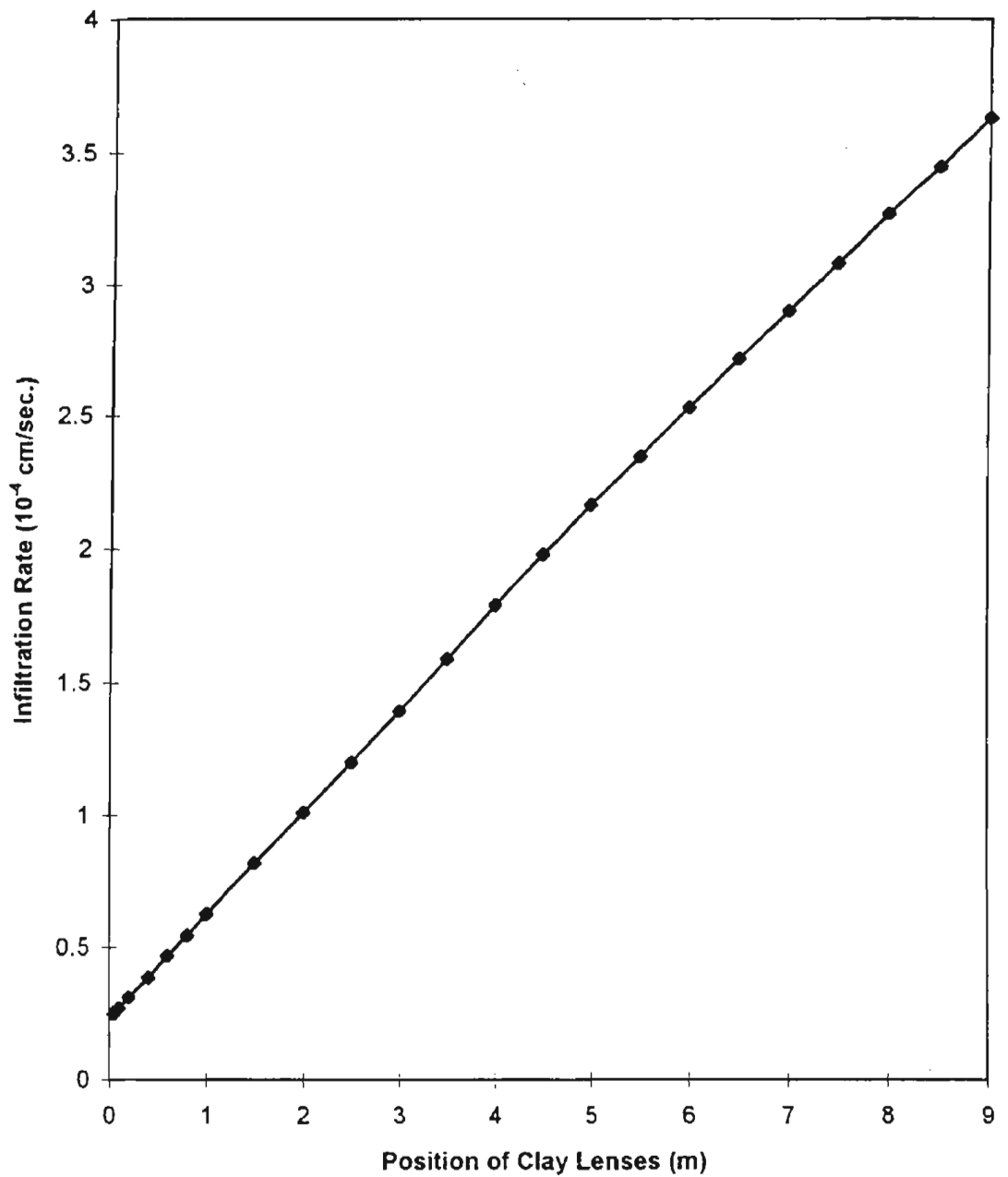


Figure 3-64 1-D Simulation of Sweetwater Soil with Clay Lenses
thickness of clay=10cm, ponding depth=1cm

The effect of lateral extend of the clay layers In order to study the effect of lateral extend of clay lenses, a conceptual model was used for numerical simulations. Assume the pond was elongated and 2-dimensional model was appropriate. Fig 3-65 shows the cross-section of the simulation domain. Figure 3-66 and Figure 3-67 present the steady-state infiltration rate as a function of the opening of the clay lense for North Pond soil and Sweetwater soil respectively. For North Pond soil, the infiltration rate is approximately linear to the opening of the clay lense. For Sweetwater soil, a small opening of 1 m dramatically increased the infiltration rate from 3.37×10^{-5} cm/sec for no opening to 1.21×10^{-3} cm/sec.

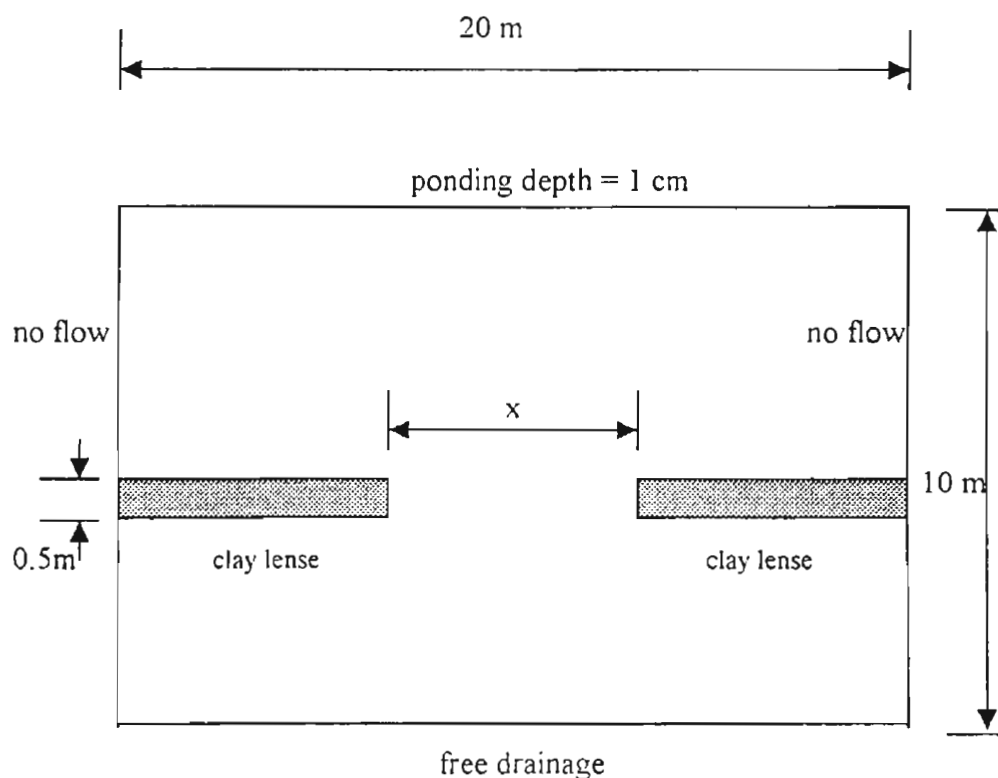


Figure 3-65 Cross-Section of Simulation Domain

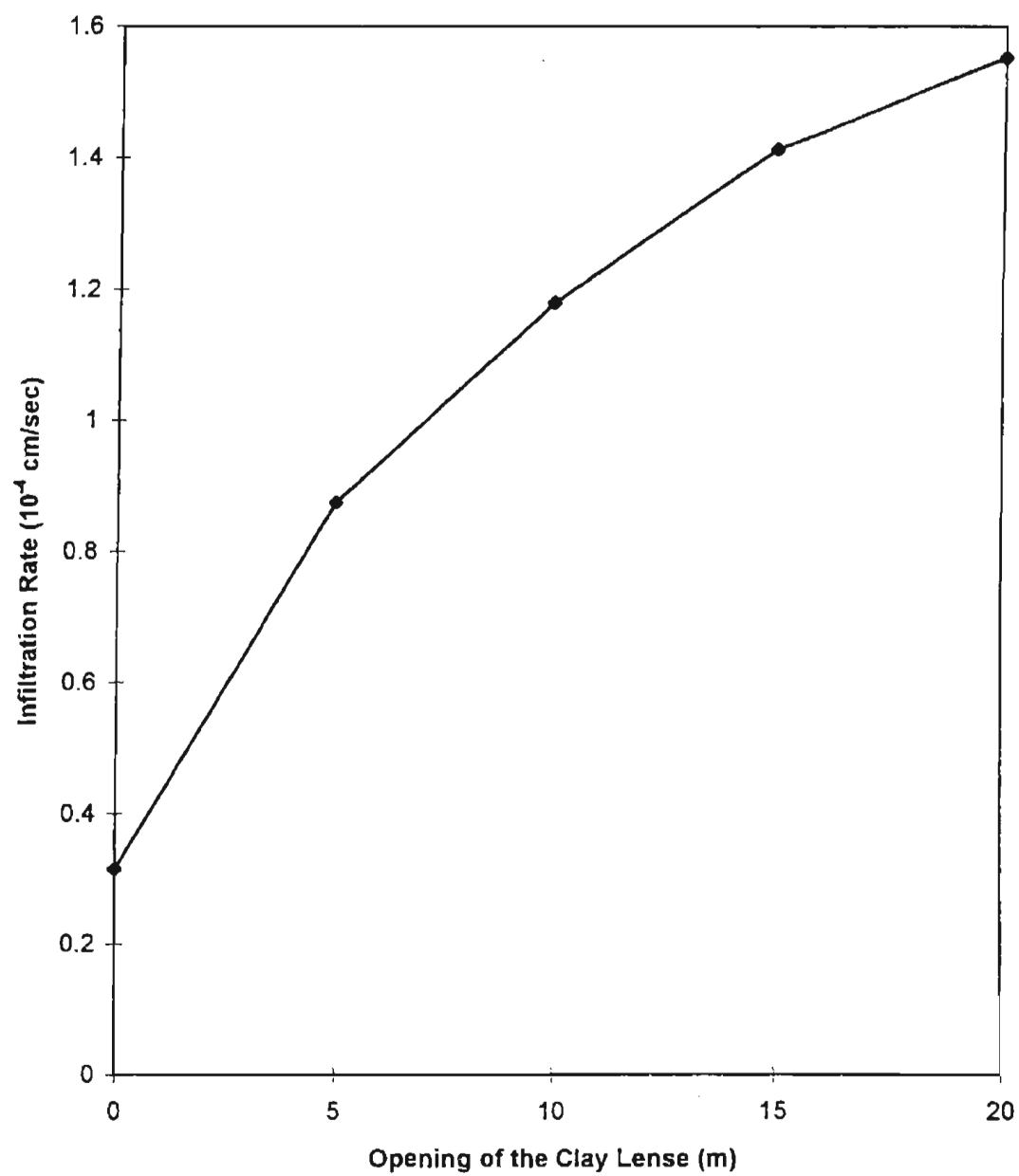


Figure 3-66 2-D Simulation of North Pond Soil with Discontinuous Clay Lense

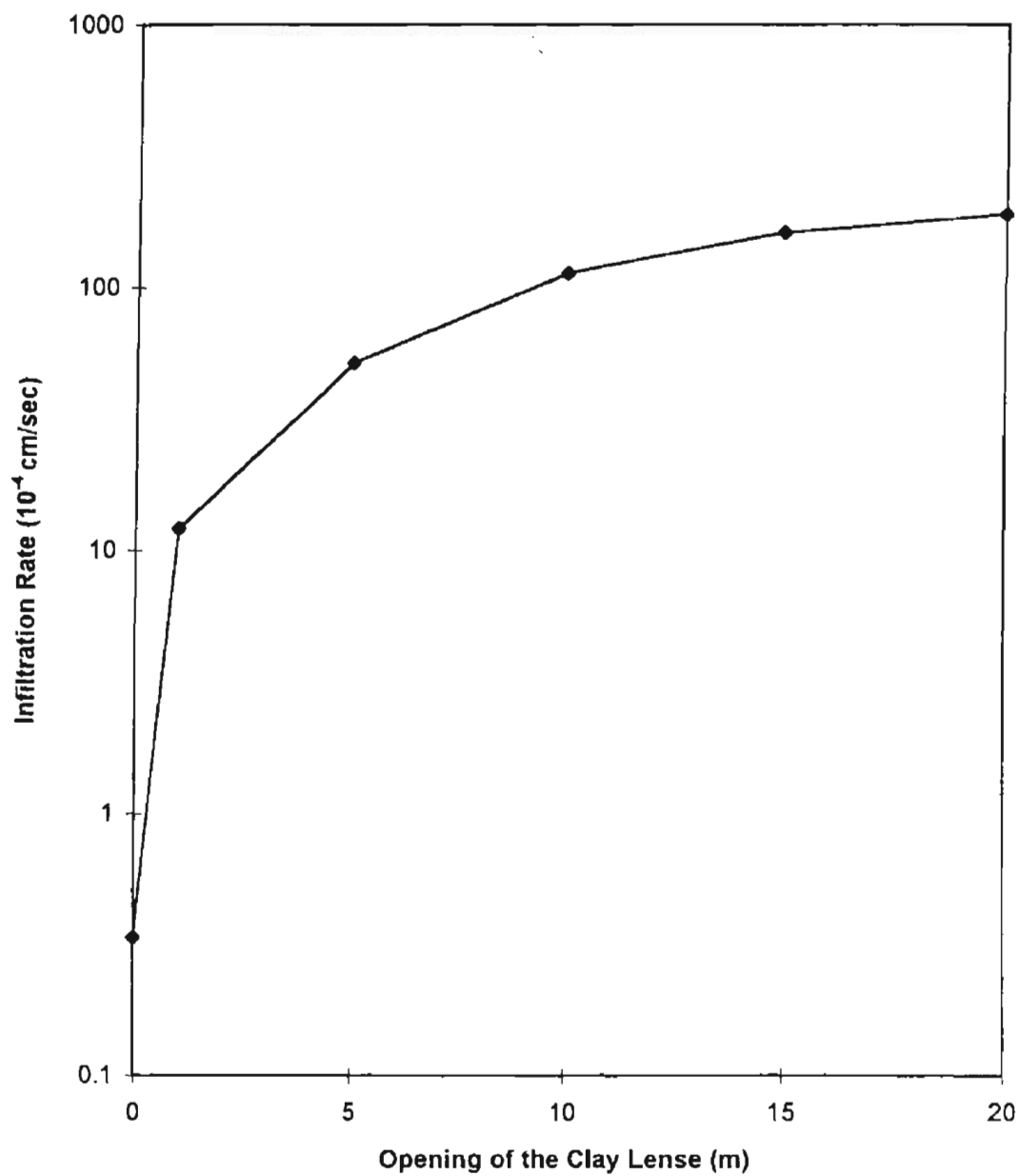


Figure 3-67 2-D Simulation of Sweetwater Soil with Discontinuous Clay Lense

SUMMARY AND DISCUSSION OF SOIL HYDROLOGICAL PROPERTIES FROM FIELD AND COLUMN STUDIES

Infiltration Rate and Hydraulic Conductivity

It has been observed both in laboratory and field tests that infiltration rate during ponded infiltration is initially quite large and decreases with increasing time, finally approaching a constant value. This final condition is usually called steady-state infiltration. Steady-state infiltration rate is an important factor in evaluating maximum SAT system capacity. When the hydraulic gradient is unity, infiltration rate and hydraulic conductivity are the same. Hydraulic conductivity is generally used for the "constant" in Darcy's law relating Darcian velocity to hydraulic gradient. The same form of Darcy's law is used for both saturated and unsaturated conditions, but for unsaturated conditions the hydraulic conductivity is a function of the soil suction. In general, the hydraulic conductivity decreases with increasing soil suction, but at the same time the gradient may go up. Therefore, the infiltration rates tend to be more stable than the hydraulic conductivity. It is believed that the steady-state infiltration rate tend to approach the saturated hydraulic conductivity as far as surface clogging is not concerned. The hydraulic conductivity and infiltration rate from several sources were compared. These included laboratory permeability test, lab infiltration columns, large diameter field columns and field percolation tests. Because the hydraulic gradients for field percolation tests were about one, it was reasonable to compare hydraulic conductivity to infiltration rate. The data are summarized in Table 3-12 below. Results from Greeley and Hansen field percolation basins showed that the difference between the average infiltration rate and saturated hydraulic conductivity was less than a factor of 3 for each of the two sites. In general, reproducibility of hydraulic conductivity of a factor of 2 or 3 is considered fairly normal when comparisons are made on specimen compacted by different operators. In the case of field infiltration rates, there are numerous reasons for differences between these and the laboratory columns. These reasons include decreased degree of saturation in the field compared to the laboratory, some horizontal movement of water, and field soil nonhomogeneity.

Axisymmetric numerical simulation showed that when pond diameter was 10 m, the steady-state infiltration rates was only 14%, 18% and 4% higher than those when pond diameter

was infinite for North Pond soil, Sweetwater soil and Ag. Field soil respectively. It is therefore concluded that when pond diameter is larger than about 10 m, the error from one-dimensional assumption can be neglected.

The numerical simulation of field percolation with clay lenses indicated that if the thickness of the clay layer is the same, the closer the clay layer to the ponding surface, the more significant the impedance to the flow. When the position of the clay layer is fix, the thicker the clay layer, the lower the infiltration rate. When the clay layer is discontinuous, the infiltration rates depend on the opening of the clay layer and the difference of hydraulic conductivity between the clay and background soils.

Table 3-12
Comparison of hydraulic conductivity data

Soil	ASU Lab K_{sat} (ft/day)		ASU Lab Column K (ft/day)	ASU Lg. Column K (ft/day)	U of A Lab Column K (ft/day)	G & H Field Infiltration Rate (ft/day)
	Dist.	Undist.				
Agua Fria	238	N/A	258	N/A	330	N/A
Sweetwater	53.0	N/A	71.0	N/A	68.1	N/A
South Pond	1.96	3.59	1.92	N/A	N/A	2.5
North Pond	0.50	0.65	0.64	0.56	1.64	2.5
Ag. Field	0.01	0.09	0.0048	0.06	N/A	N/A

Hydrological Parameters

Numerical simulation of fluid flow in unsaturated soil requires the knowledge of unsaturated hydraulic conductivity and suction head as a function of water content or degree of saturation. Although there are many models available to be used, the difficulties arise when determining the model parameters. These difficulties are associated with the uncertainty in the measurement of unsaturated conductivity and suction head. However, in comparison with the variability of unsaturated conductivity and soil suction, measured values of infiltration rate and progression of wetting front vary over a much more narrow range. Numerical simulation was conducted using hydrological parameters obtained from measured characteristic curves and fitted to van Genuchten's model. Simulation was also performed using parameters back-calculated from lab column infiltration tests. Simulation results were compared to those from lab columns of

different boundary conditions and those from field percolation tests. It was found that simulations using back-calculated parameters provided more reasonable results than those using parameters from characteristic curves. In view of these findings it is recommended that infiltration tests be performed for every case where prototype infiltration is to be modeled. It is further recommended that those infiltration test results serve as the primary benchmark to which the model is calibrated.

CLOGGING LAYER STUDIES

Historically soil aquifer treatment projects, similar to the one proposed herein, have run into difficulty with a marked decrease in infiltration rate due to the development of a clogging layer at the original ground surface. One aspect of this project has been to investigate the nature and behavior of this impeding layer. The clogging layer is made up of a combination of components which may include some or all of the following:

- Algae growing in the pond that originated in either the soil or the effluent,
- Suspended solids (organic and/or inorganic) filtered from the effluent,
- Dust blown into the pond from surrounding areas by the wind,
- Microbes growing in the soil or the pond that also may have originated in either the soil or the effluent, and
- Salts (including calcium carbonate) precipitated from solution.

As these components accumulate on the bottom of the basin to form the clogging layer, they begin to restrict infiltration. Furthermore, it is suspected that they may be compressed by the seepage force exerted by the infiltrating water. As a result, there appears to be an additional reduction in the governing conductivity and consequently in the infiltration rate as well.

Clogging Layer Model

Surface clogging is an extremely complex process, and a number of mechanisms have been proposed to explain it. These include interception of particulate material to form a sedimentation layer on top of the native soil and filtration of particulate material (which has penetrated below the original ground surface) by the native soil to form a so called filtration layer. The particulates, that are entrained in the native soil of the filtration layer, tend to clog its coarse pore space and produce a corresponding reduction in the hydraulic conductivity. The following working

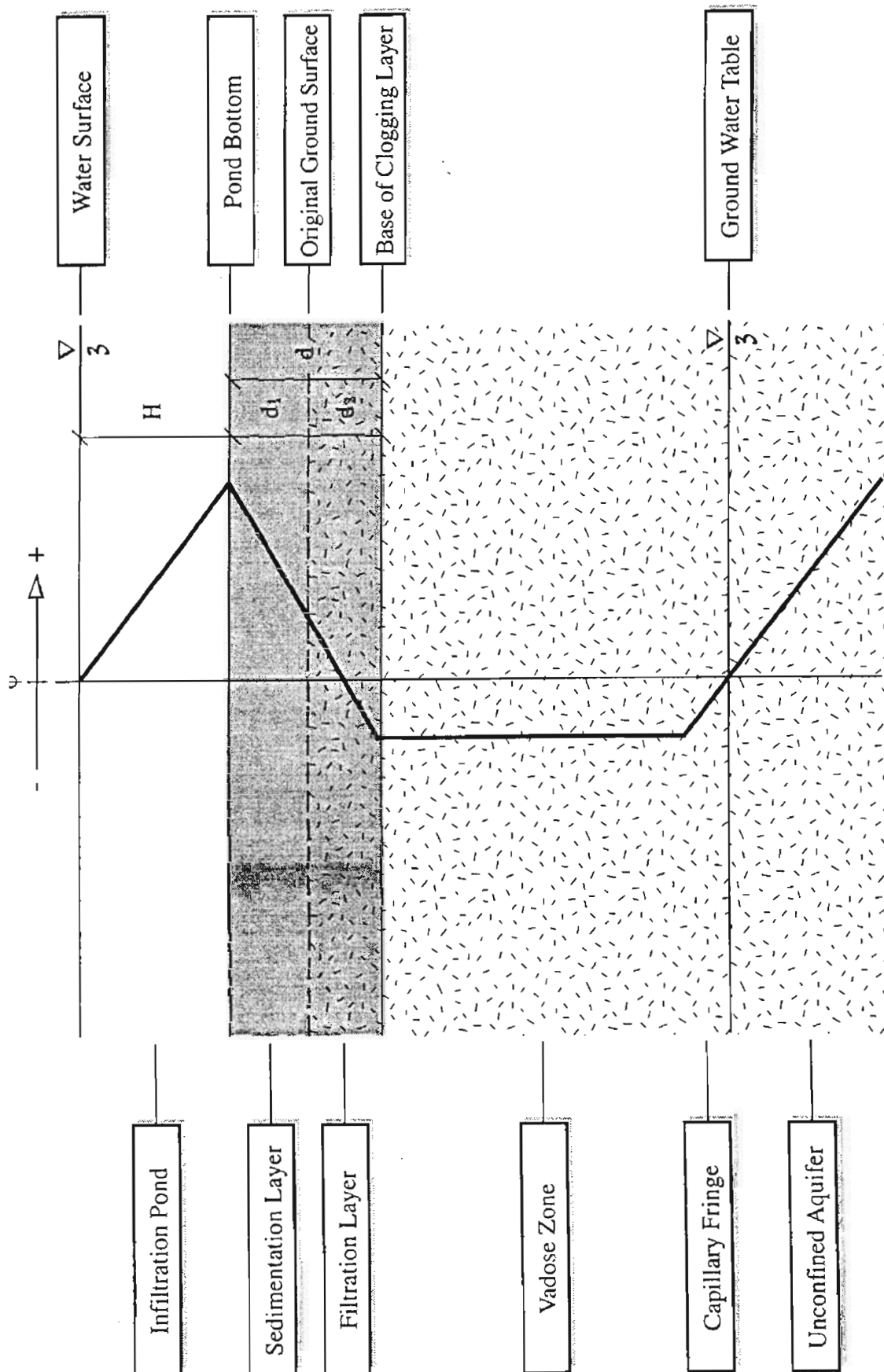
definition of clogging layer is proposed: that zone of material over which a sharp drop in hydraulic head occurs as water infiltrates into a soil profile. This would typically include both the sedimentation and filtration layers, which are shown schematically in Figure 3-68.

Two Layer Approach

Historically, there has been some disagreement regarding the relative importance of the two mechanisms. However, a study of municipal wastewater lagoons by the United States Environmental Protection Agency seems to clarify the issue (USEPA 1987). The EPA was concerned about groundwater contamination from leaky wastewater lagoons, a situation that would be closely analogous to flow through a clogging layer in an SAT infiltration basin. The EPA undoubtedly found a decrease in leakage with the build up of a sludge layer on the bottom of the lagoon, and this would tend to illustrate the importance of the sedimentation layer. However, there were also differences in leakage between lagoons, with sludge layers of similar type and thickness, that were attributed to the character of the underlying soil, and that data seemed to point toward the importance of the filtration layer. Hence, it would appear that both may make significant contributions to the overall hydraulic conductivity of the clogging layer.

In assessing the potential for the clogging layer to undergo consolidation by seepage forces, two things must be evaluated, the stiffness of the material and the magnitude of the effective stress which is tending to cause compression. Typically, most soil profiles tend to exhibit some apparent over consolidation at the very near surface. This means that they have previously experienced some effective stress (called the preconsolidation pressure) that was greater than the effective stress under which they currently exist due to the weight of any overlying soil. Conceptually, overconsolidated material is represented as a soil that was previously buried deeper in the earth, but was unloaded by the erosion of some of the overlying soil. In arid climates, a similar effect can be produced by the capillary forces induced during desiccation by the heat of the sun. The result of overconsolidation is changes in the microstructure of the soil, such that the soil is more stiff (resistant to volume change) until it is loaded to a point that exceeds the preconsolidation pressure.

Figure 3-33 Clogging Layer Schematic



At a minimum, the soil under an SAT basin will have experienced some over consolidation due to desiccation. Additionally, based on informal observations of the construction of the large field percolation basins designed by Greeley and Hansen (Greeley and Hansen 1994), the soil will also have experienced a substantial compactive effort from construction equipment, if similar methods are used in basin construction. As such the native soils themselves should be fairly stiff. Furthermore even assuming a deep pond and a fairly thin clogging layer, the expected stress levels are quite low. Therefore, the native soil, and as a result the filtration layer, seems unlikely to undergo any substantial consolidation under the seepage forces induced by the infiltration; in contrast, the softer newly deposited sedimentation layer might be subject to some compression.

All together, it would appear that the conductivity of the clogging layer should be modeled in two distinct parts. The conductivity of the upper layer, that consists of material which accumulates above the original ground surface, would be governed by consolidation under seepage forces. In contrast, the conductivity of the lower layer, consisting of native soil augmented by entrained organic and inorganic solids, would be controlled by the loss of preferred flow channels due to clogging of the coarse pore space in the native soil.

Model Conceptual Framework

With the above physical picture of the clogging layer, and additionally assuming that the clogging layer is saturated and that flow follows a one-dimensional, vertical path (which seem reasonable for a thin layer immediately beneath a pond of considerable lateral extent), a conceptual model of flow through the clogging layer can be constructed around a fairly fundamental application of Darcy's law.

Given the thickness (d) and hydraulic conductivity (K) of the clogging layer, the water depth (H) and the soil suction at the base of the clogging layer (ψ_b), the flow can be quantified as specific discharge or Darcian velocity (v) as shown below.

$$v = K \frac{(d + H - \psi_b)}{d}$$

To account for the influence of both the sedimentation and filtration layers, a composite hydraulic conductivity, that is applicable over the entire thickness of the clogging layer, can be computed from the properties of the individual parts as follows:

$$K = \frac{d}{\frac{d_1}{K_1} + \frac{d_2}{K_2}}$$

where d_1 , K_1 , d_2 , and K_2 are the thickness and conductivity of the sedimentation and filtration layers respectively.

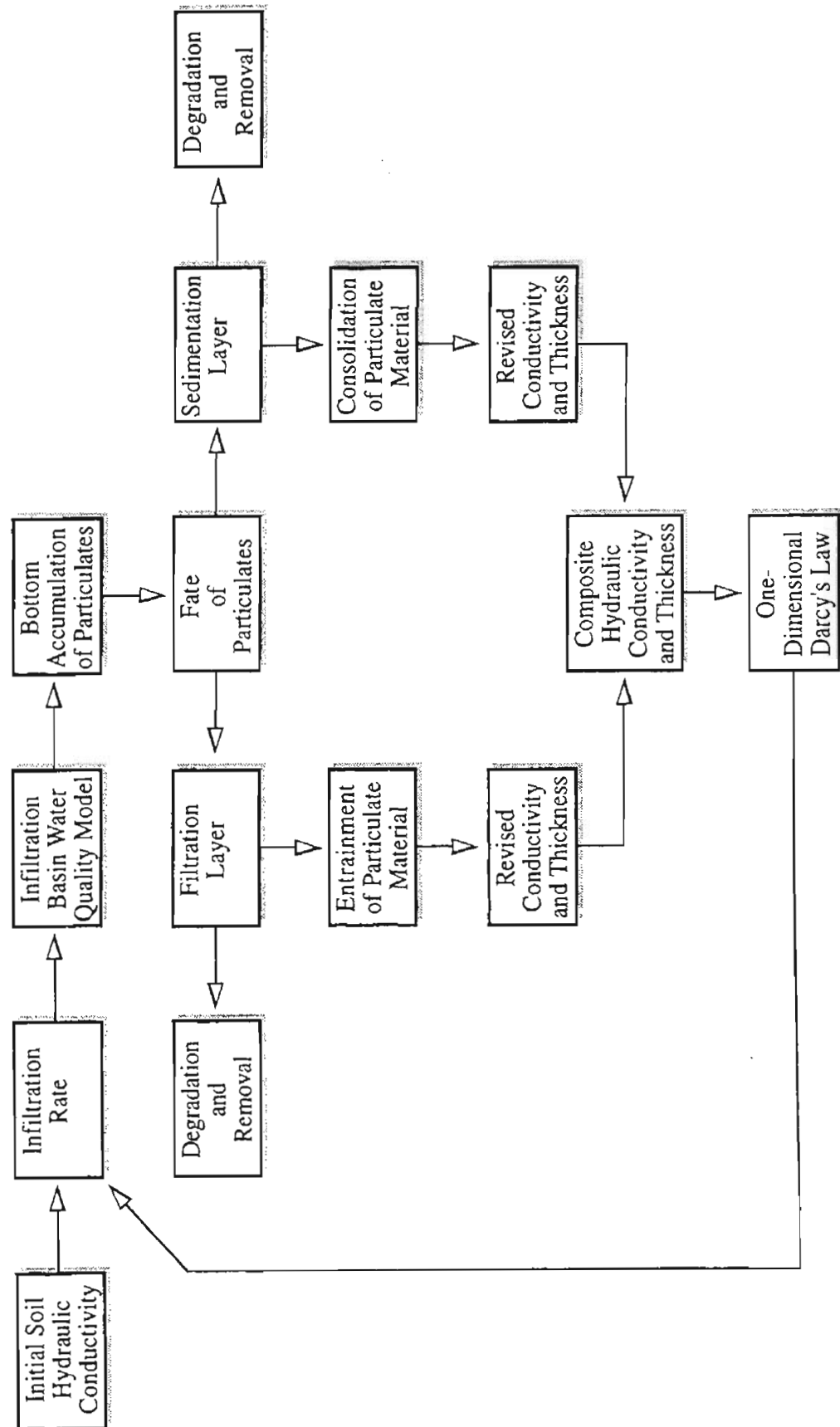
Figure 3-69 illustrates how these two concepts may be incorporated into an overall model of the clogging layer. First, the initial infiltration rate is entered as an input to an ecological model of the infiltration basin. The water quality model then produces an estimate of the particulate matter that reaches the pond bottom. Ultimately, this material has one of three fates; it is either incorporated into the sedimentation layer or the filtration layer or it degrades and is removed from the system. Once the distribution of the particulates is established, revised estimates of the conductivity and thickness of the sub-layers can be made. Then, the composite conductivity is calculated and entered into Darcy's law. This produces a revised estimate of the infiltration rate, which is then applied during the next time increment.

Hydraulic Conductivity and Consolidation Tests

Upon initial inspection, it is not immediately obvious how consolidation theory relates to the problem of surface clogging in groundwater recharge basins. As originally developed by Karl Terzaghi in the early part of this century, consolidation theory is most commonly used to determine the amount and rate of occurrence of settlement that can be expected at the ground surface in response to an additional load on a soil profile, for example from a newly constructed building.

When the stress on a saturated soil is increased because of the added load at the surface, that increase is initially carried by the fluid that fills the voids or pores between the soil grains. This is due to the fact that the water is stiffer, or less compressible, than the soil skeleton. As a result, the pore pressure, that is the pressure of the fluid in the voids, then exceeds the hydrostatic

Figure 3-44 Flow Chart for Hypothesized Clogging Layer Flow Model



pressure, which is that pressure existing solely due to the weight of the overlying fluid. In response to this excess pressure, water begins to flow out of the soil mass. With the expulsion of some of the pore fluid and the resulting decrease in volume, the soil skeleton compresses and begins to accept some of the applied load. As a portion of the load is transferred to the soil skeleton, the excess pressure in the pore fluid is reduced and the flow of water slows. Over time, the applied load will be fully transferred to the soil grains, and all of the excess pore pressure will have been dissipated. The end result is a compression, or decrease in volume, of the soil and a corresponding settlement of the ground surface.

This process is of interest in the study of surface clogging because not only does the decrease in volume and void ratio, which was just described, result in settlement, but it yields a decrease in the hydraulic conductivity of the soil as well. If the material in the clogging layer were subjected to an increase in effective stress, it would also experience consolidation with the resultant decreases in volume and, more importantly, conductivity.

Intuitively, it would be expected that increasing the depth of water in a basin that has experienced some clogging would increase the infiltration rate by increasing the driving hydraulic head. However, studies on similar projects have actually shown the opposite at times; infiltration has been observed to decrease with increased water depth. This phenomena can be attributed to consolidation of the clogging layer, not under gravity loads, but under the action of seepage forces induce by the infiltrating water (Bouwer 1989).

Test Program

A program of consolidation and hydraulic conductivity testing has been conducted with the intent of quantifying the mechanical and hydrologic characteristics of the clogging layer and its individual components. This program includes tests of actual clogging layers, as well as tests of the individual constituents such as soil, algae, wind blown dust and effluent suspended solids.

The clogging layer samples are taken from related infiltration column experiments (that have been operated by other investigators) as material becomes available. The samples are divided into individual specimens for testing; each one represents about a two centimeter increment of depth into the clogging layer. Upon completion of the testing, the specimens are analyzed for total

organic content, which should help to further quantify the make up of the clogging material and to identify the depth to which the particulate matter is entrained in the native soil. The sources of clogging layer samples include the large diameter infiltration columns at the 91st Avenue Wastewater Treatment Plant, which were operated by Arizona State University personnel, and smaller laboratory columns operated by other investigators at the University of Arizona.

The specimens of the unaltered soils were statically recompacted from disturbed bulk samples, to an appropriate dry density and water content in a hydraulic press, to minimize the destruction of soil clods and alteration of the soil structure. However, the results will still have to be corrected for disturbance effects and the influence of large scale nonhomogeneities, that are not captured in testing a small laboratory specimen, before they can be applied to field conditions. The algae specimens were drawn from an algae culture grown at ASU in a nutrient rich broth. Seed for the culture was taken from secondary clarifiers at the 91st Avenue Treatment Plant (that particular effluent stream was also the effluent source for several of the large diameter columns). Samples of wind blown dust will be simulated by separating that fraction of sizes, which is likely to be transported by the wind, and sedimenting it through a water column.

Test Procedures

Because of the range in material types and the variation in the degree to which the soil specimens have experienced clogging, several different test procedures have been employed. These include incremental load and constant rate of strain consolidation testing, as well as concurrent measurement of the hydraulic conductivity.

Incremental load. The governing partial differential equation for consolidation, as most commonly applied in geotechnical engineering, was developed by Karl Terzaghi and presented, with its solution, by Taylor (1948). It is written in terms of the excess pore pressure (u_e) as follows:

$$c_v \frac{\partial^2 u_e}{\partial z^2} = \frac{\partial u_e}{\partial t}$$

where z is depth, t is time and c_v is the coefficient of consolidation. The equation is written slightly differently as applied in water resources. It is based on the hydraulic head (h) and includes

several different parameters α , β , n and K (the compressibility of the water bearing layer, the compressibility of water, the porosity of the soil and its conductivity, respectively):

$$\frac{\partial^2 h}{\partial z^2} = \frac{\rho_w g (\alpha + n\beta)}{K} \frac{\partial h}{\partial t}$$

Noting that the density of water times the acceleration due to gravity ($\rho_w g$) equals the unit weight of water (γ_w), that most often α is much larger than $n\beta$, and that α is also known as the coefficient of volume change, m_v , yields a much used expression for the coefficient of consolidation.

$$c_v = \frac{K}{m_v \gamma_w}$$

When the initial distribution of excess pore pressure (u_0) is constant with depth, the solution to the governing equation for consolidation yields this expression for excess pore pressure in the soil layer at any given depth and time:

$$u_{e,z,t} = \sum_{m=0}^{\infty} \frac{2u_0}{M} \sin\left(\frac{Mz}{H}\right) e^{-M^2 T_v}$$

where:

$$M = \frac{\pi(2m+1)}{2} \text{ and } T_v = \frac{c_v \cdot t}{H^2}$$

Such an initial distribution of excess pore pressure is consistent with a sudden incremental increase in the total stress on the soil, hence the name incremental load consolidation. Note that T_v is a unitless time factor, and H is the length of the drainage path. Terzaghi was able to relate the time factor to the average percent consolidation, and such values have been tabulated for use in consolidation computations. The length of drainage path equals the thickness of the soil when the layer or specimen is singly drained (that is typically freely drained at the top with an impermeable lower boundary).

In conducting an incremental load test, the specimen is confined in a rigid ring, which provides lateral confinement and restricts the strains to the vertical direction. A given load increment is applied suddenly to the soil through the use of dead weights and is held constant for a sufficient period of time for the specimen to reach equilibrium (typically 24 hours). Through out that period, time versus deformation data is recorded manually. Subsequently, the next (larger)

load is applied and another set of time-deformation data is obtained. This continues until the stress range of interest has been covered in sufficient detail.

For each load increment at equilibrium, all of the excess pore pressure has been dissipated, and the total and effective stresses are equal. As such, the average effective stress (σ') can be computed from the applied load (P) and the cross sectional area of the specimen (A):

$$\sigma'_{ave} = \frac{P}{A}$$

Similarly, the average strain (ϵ) is computed from the deformation (ΔH) and the initial height of the specimen (H_0):

$$\epsilon_{ave} = \frac{\Delta H}{H_0}$$

Then, the coefficient of volume change is computed for each increment from that data,

$$m_v = \frac{\Delta \epsilon}{\Delta \sigma'}$$

From a plot of the deformation versus the square root of time for a given increment, Taylor developed a graphical construction to determine the time to ninety percent consolidation (t_{90}). With that known, the coefficient of consolidation for that increment can be computed from the definition of the time factor.

$$c_v = \frac{T_{v_{90}} \cdot H^2}{t_{90}}$$

Finally, hydraulic conductivity can be back calculated as:

$$K = c_v m_v \gamma_w$$

With those three parameters quantified (m_v , c_v and K), the mechanical and hydrologic characteristics of the given material are well defined. The back calculation of conductivity was often augmented by direct measurement as described later. Incremental load consolidation was the test method employed for the algae, and was also used to provide verification of the constant rate of strain test results on the soils.

Constant rate of strain. When possible, consolidation testing was done by a computer-controlled, constant rate of strain (CRS) procedure. This provided two substantial advantages.

The tests were completed much more rapidly than traditional consolidation tests would be, and the acquisition of data was automated.

The theoretical development of constant rate of strain consolidation, from this point forward, is based almost exclusively on work completed at the Massachusetts Institute of Technology in the early 1970s (Wissa et al. 1971). The governing partial differential equation for consolidation, from which CRS consolidation theory begins, is a nearly identical equation to that shown earlier, but due to slightly different assumptions it is written in terms of strain rather than excess pore pressure. Terzaghi assumed that both m_v and K were constant; Wissa assumed only that c_v is constant.

$$c_v \frac{\partial^2 \epsilon}{\partial z^2} = \frac{\partial \epsilon}{\partial t}$$

The solution to the governing equation yields this expression for strain in the soil layer at any given depth and time.

$$\epsilon_{z,t} = rt + \frac{rH^2}{c_v} \left[\frac{1}{6} \left(2 - \frac{6z}{H} + 3 \frac{z^2}{H^2} \right) - \frac{2}{\pi^2} \sum_{n=1}^{\infty} \frac{\cos \frac{n\pi z}{H}}{n^2} e^{-n^2 \pi^2 T_v} \right]$$

In the above equation, the strain is equal to the average strain (rt - the strain rate times the elapsed time) plus some variation from average. The term in the equation, which expresses the variation from average strain, consists of a steady state and a transient portion. The strain distribution within the soil is parabolic. Points, in the soil nearer to the top and its free drainage surface, strain faster than average, while points in the soil nearer to the bottom, which is impermeable, strain slower than average.

From this point there are four different ways to analyze the data, transient and steady-state coupled with either a linear or non-linear assumption regarding the stress strain relationship. If the strain rate is properly selected such that the time factor does not drop below 0.25, the transient part of the strain response is negligible. Also since the analysis is made on an incremental basis, the linear assumption is sufficiently accurate if the increments are made sufficiently small. Of the four, the steady state linear solution is the least computationally intensive, and since those assumptions are often quite acceptable, it is also the most commonly used. The expression for c_v ,

that is shown below, follows from the solution to the governing partial differential equation, under the steady state and linear assumptions:

$$c_v = \frac{H^2}{2u_{e_{\max}}} \frac{d\sigma}{dt}$$

where $d\sigma/dt$ is the time rate of change in total stress, and $u_{e_{\max}}$ is the maximum excess pore pressure (the pressure measured at the base of the specimen).

During a test, the computer controlled apparatus applies an steadily increasing load to the specimen through a pneumatic piston (until a specified maximum is reached), and records the elapsed time, applied load, specimen deformation and maximum excess pore pressure on a specified time interval. Stress-strain data are analyzed as follows. The average strain is computed as the measured deformation divided by the initial height, and the average effective stress is computed as the applied total stress less the average excess pore pressure. For a parabolic distribution, the average excess pore pressure is equal to two thirds of the maximum excess pore pressure.

$$\text{Strain: } \varepsilon_{\text{ave}} = \frac{\Delta H}{H_0}$$

$$\text{Effective Stress: } \sigma'_{\text{ave}} = \sigma - \frac{2}{3} u_{e_{\max}}$$

Then, the coefficient of volume change is computed incrementally from that data,

$$m_v = \frac{\Delta \varepsilon}{\Delta \sigma'}$$

and the coefficient of consolidation is computed as shown earlier.

$$c_v = \frac{H^2}{2 \cdot u_{e_{\max}}} \frac{\Delta \sigma}{\Delta t}$$

Finally, hydraulic conductivity can be back calculated as:

$$K = c_v m_v \gamma_w$$

As with the incremental load test, once those three parameters (m_v , c_v and K) are quantified, the mechanical and hydrologic characteristics of the material are well defined. These test results were also augmented with direct measurement of conductivity. The tests of the clay

and clogging layers from infiltration columns, which were filled with that soil, were tested in this manner.

Successful application of the CRS test requires a small, but measurable, buildup of excess pore pressure. The entire procedure can not be applied when the specimens exhibit a conductivity that is large enough to preclude the generation of sufficient excess pore pressure to be measurable or where the soil is relatively stiff over the stress range of interest. In such a case, the specimen exhibits little volume change, and hence little excess pore pressure build up as well. This is typical of soils in their over consolidated range.

For such cases, the CRS procedure can still be used to evaluate the stress-strain behavior of the soil (including the computation of m_v), but the determination of the time rate of consolidation (specifically c_v) can not be accomplished. In that case a modified version of the CRS consolidation test can be used. In this procedure, the stress-strain behavior of the material will be evaluated as usual, but the test is periodically interrupted to independently measure the hydraulic conductivity. Once the hydraulic conductivity is known and the coefficient of volume change is computed as before, the coefficient of consolidation can then be back calculated as:

$$c_v = \frac{K}{m_v \gamma_w}$$

Again once K , m_v and c_v are known, the properties of the material have been fully characterized and any consolidation type behavior could be readily modeled. This procedure was used for the majority of the soils and clogging layer specimens.

Concurrent permeability testing. Concurrent permeability testing is being run with most of these consolidation tests, either as an integral part of the procedure, as described above, or as a means of augmenting the results of the consolidation tests. The values of conductivity back calculated from the consolidation analyses can be compared with the direct measurements of conductivity values to verify the results. The permeability test procedure was developed such that it could be run in the consolidation apparatus with a minimum of disruption in the consolidation test procedure. The test amounts to a falling head, rising tailwater permeability test with two added complexities. The standpipes can be of different diameters, and an additional gradient can be induced by applying constant pressure to the headwater surface and a constant, but lower,

pressure to the tailwater surface. The additional gradient is only induced when the gravity head is insufficient to give results within a reasonable test duration. The conductivity is computed as:

$$K = \frac{A_{sp1} A_{sp2} L}{A(A_{sp1} + A_{sp2})t} \ln \left(\frac{z_0 + (p_1/\gamma_w - p_2/\gamma_w)}{z + (p_1/\gamma_w - p_2/\gamma_w)} \right)$$

- where: K - hydraulic conductivity
 A - cross sectional area of soil specimen
 A_{sp1} - cross sectional area of headwater stand pipe
 A_{sp2} - cross sectional area of tailwater stand pipe
 L - length of soil specimen
 t - elapsed time since start of test
 z₀ - initial elevation difference between headwater and tailwater
 z - elevation difference between headwater and tailwater
 p₁ - pressure applied above headwater
 p₂ - pressure applied above tailwater

It should be noted that because of the substantially higher flow rates, the observed head differences were corrected for non-negligible head losses in the apparatus during tests of the more pervious soils.

Test Results

Initial hypotheses regarding the behavior of the clogging layer have been based on previous observations made by Bouwer and others. Intuitively, it would be expected that increasing the depth of water in a basin that has experienced some clogging would increase the infiltration rate by increasing the driving hydraulic head. However, their work on similar projects has actually shown the opposite; at times, infiltration has decreased with increased water depth. This phenomena has been attributed to consolidation of the clogging layer, not under gravity loads, but under the action of seepage forces induce by the infiltrating water (Bouwer 1989). The consolidation testing described here was conducted, at least in part, to investigate the significance of this phenomena for the proposed Phoenix SAT site.

Expected order of magnitude of effective stresses. The hydraulic gradient (*i*) across a clogging layer can be approximated as the sum of the thickness of the layer (*d*) and the pond depth (*H*) divided by the thickness, if the soil suction at the base of the clogging layer is ignored.

$$i = \frac{d + H}{d}$$

Then, the seepage force per unit volume (*j*) can be computed as the hydraulic gradient times the unit weight of water.

$$j = i \cdot \gamma_w$$

Although the effective stress at the top of the clogging layer equals zero, the maximum effective stress, at the base of the clogging layer, equals its thickness times the seepage force.

$$\sigma'_{\max} = d \cdot j$$

To determine the order of magnitude of the expected effective stresses, these quantities were evaluated for a range of likely thicknesses (2 to 16 cm or about 1 to 6 inches) and depths (15 to 60 cm or about 6 to 24 inches). The results are presented in Table 3-13 below.

Table 3-13

Maximum effective stress induced by seepage forces

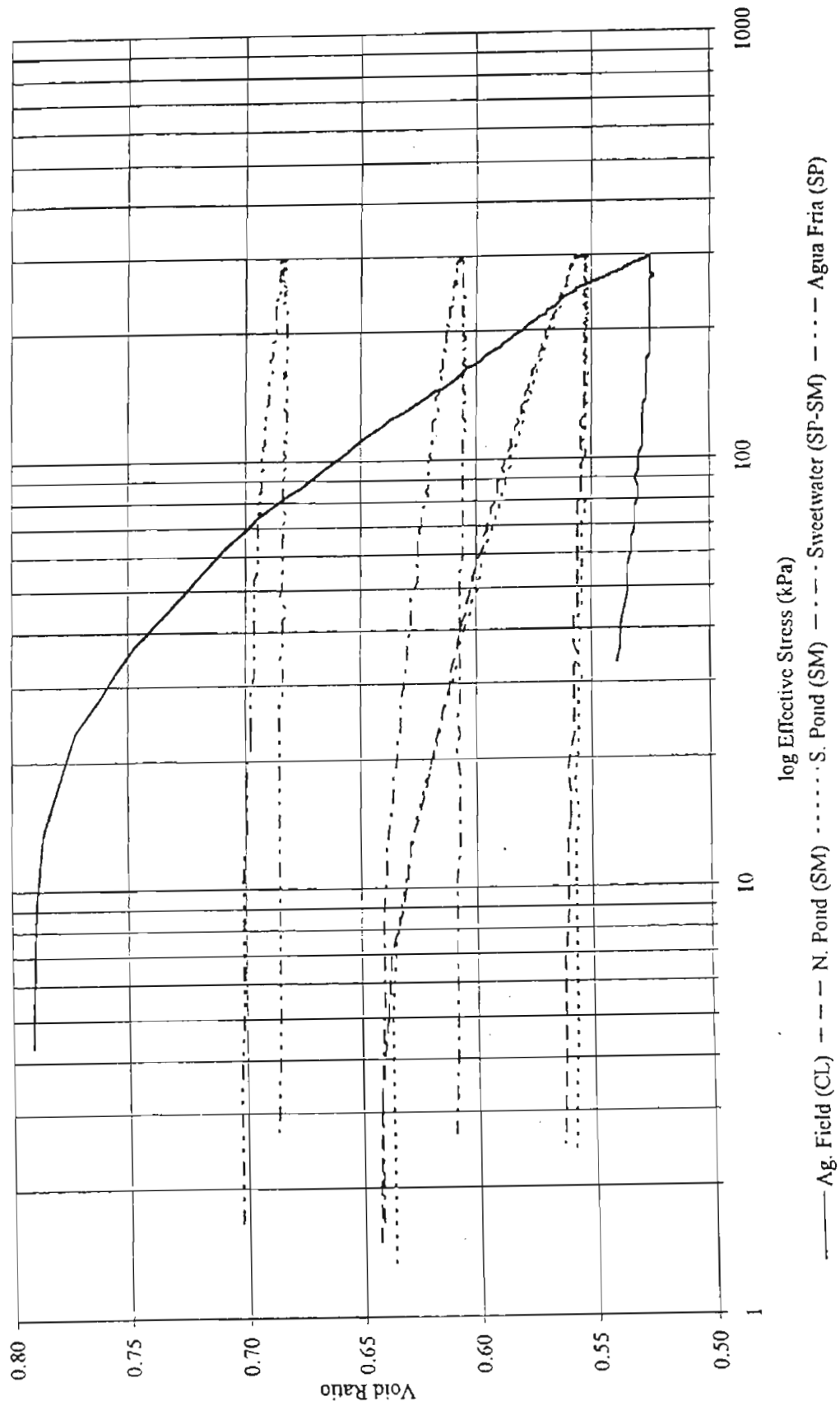
d (cm)	H = 15 cm			H = 30 cm			H = 60 cm		
	i (cm/cm)	j (kN/m ³)	σ' _{base} (kPa)	i (cm/cm)	j (kN/m ³)	σ' _{base} (kPa)	i (cm/cm)	j (kN/m ³)	σ' _{base} (kPa)
2	8.5	83.4	1.7	16.0	157.0	3.1	31.0	304.1	6.1
4	4.8	46.6	1.9	8.5	83.4	3.3	16.0	157.0	6.3
8	2.9	28.2	2.3	4.8	46.6	3.7	8.5	83.4	6.7
16	1.9	19.0	3.0	2.9	28.2	4.5	4.8	46.6	7.5

It should be noted that the stresses range on the order of 1 to 10 kPa.

Soils. CRS testing of the five subject soils was been completed, and their stress-strain behavior is illustrated by Figure 3-70 (the graphs of void ratio versus effective stress). It should be noted that the soils did not begin to exhibit any significant compression until stresses on the order of 10 to 50 kPa were reached.

These results on the unaltered soils indicate that, within the range of stresses which are anticipated from the seepage forces due to infiltration, the soil skeleton will be fairly stiff. As such,

Figure 3-70 CRS Consolidation on SAT Soils



the increase in effective stress due the seepage forces produces little decrease in void ratio, and with little reduction in void ratio, there is little reduction in hydraulic conductivity as well.

Therefore if a consolidation-type phenomena is occurring, as is indicated by the field observed behavior (that is water depth versus infiltration rate data discussed by Bouwer), it takes place in the loose material that accumulates above the original ground elevation and not in the native soil itself. However, tensiometer measurements (taken by others during column infiltration experiments) seemed to indicate that the clogging layer extends below the original ground surface. Based on these data, it would appear that the proposed two-layered conceptual model of the clogging layer is a plausible representation of the physical situation. Both layers contribute to the reduction in infiltration but by different processes. The upper is subject to consolidation and a corresponding reduction in hydraulic conductivity, while the lower experiences a reduction due to the loss of preferred flow paths that results from the entrainment of particulate matter from the overlying basin.

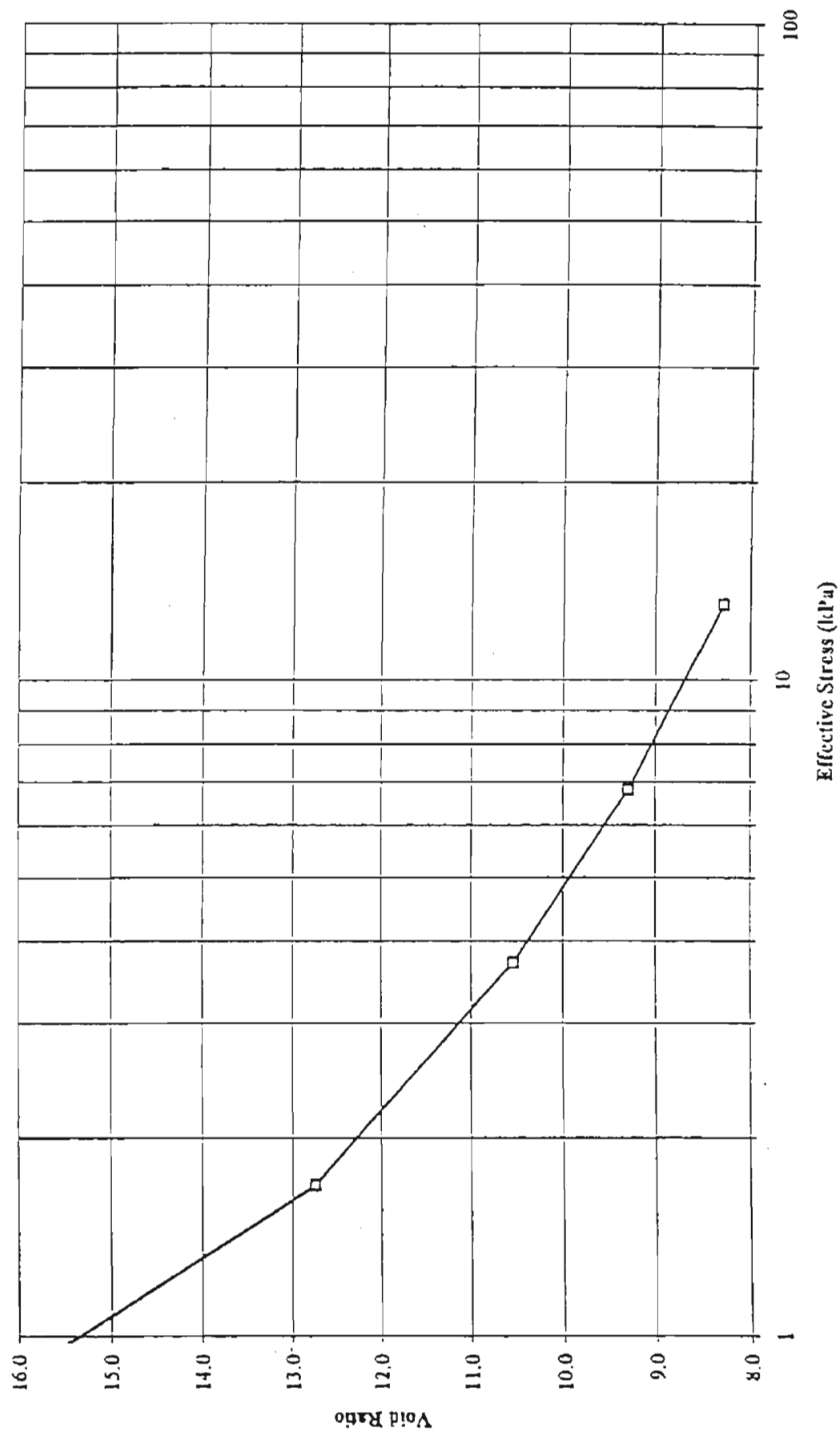
Algae. This conclusion has been further verified by the consolidation testing on the algae. Algae is expected to be a primary component of the upper portion of the clogging layer, and it has exhibited extreme compressibility under very low stresses. This can be seen dramatically in the plot of void ratio versus effective stress (Figure 3-71). With these marked changes in void ratio, corresponding changes in conductivity are also expected and are in fact observed as is illustrated in Table 3-14 below.

Table 3-14
Variation in the conductivity of algae with effective stress

Effective Stress (kPa)	Hydraulic Conductivity	
	(cm/sec)	(ft/day)
1.70	4.79×10^{-3}	13.6
3.71	3.70×10^{-6}	0.0105
6.82	1.65×10^{-6}	0.0047
13.02	2.84×10^{-7}	0.0008

Clogging layers. The results of consolidation testing, as augmented with direct measurements of hydraulic conductivity, on the Ag. Field and North Pond soils are shown below in Tables 3-15 and 3-16 respectively. The first line of data in each table gives the results of a test on a soil specimen that had not been subjected to simulated SAT. The remaining data are for

Figure 3-7| Incrementally Loaded Consolidation Mixed Culture Algae



specimens of the particular soil, that were taken from infiltration columns at the specified depth, after an extended time of simulated SAT operation.

Table 3-15

Results from column with Ag. Field Soil

Sample Depth (cm)	Hydraulic Conductivity		Void Ratio	Porosity	Total Organic Content (%)
	(cm/sec)	(ft/day)			
Soil	1.03E-5	0.0292	0.791	0.442	3.03
0-2	1.20E-6	0.0034	0.988	0.497	2.10
2-4	4.86E-7	0.0014	0.979	0.495	1.92
4-6	2.95E-7	0.0008	0.932	0.482	2.75
8-10	3.80E-7	0.0011	0.809	0.447	2.91

Table 3-16

Results from column with North Pond Soil

Sample Depth (cm)	Hydraulic Conductivity		Void Ratio	Porosity	Total Organic Content (%)
	(cm/sec)	(ft/day)			
Soil	7.09×10^{-4}	2.01	0.641	0.391	1.23
0-2	6.87×10^{-5}	0.20	0.840	0.457	1.63
2-4	4.71×10^{-4}	1.34	0.741	0.426	0.88

The Ag. Field samples did not exhibit any appearance of a distinct clogging layer, while the North Pond samples showed a clearly defined film of organic matter at the top surface of the soil. In each case, the hydraulic conductivity showed a significant reduction below that of the soil which had not been subjected to SAT. However, the samples were still fairly resistant to compression, and as a result they did not experience any substantial additional decrease in conductivity once they were subjected to stress levels equivalent to those expected from the seepage forces due to infiltration.

It should also be noted that the very near surface clogging layer samples experienced a marked increase in void ratio above that to which they were originally compacted in the columns. This can be attributed to several processes acting in concert; soil swelling, loosening and cracking of the clogging layer due to desiccation, and disturbance of the dried material during sampling. An

attempt was made to minimize the effects sample disturbance by rehydrating the samples before they were extruded from their sample tubes and tested. Under other circumstances, a corresponding increase in conductivity would have been expected with such an increase in void ratio. Therefore, the observed decrease in conductivity points toward clogging by a low density, low conductivity material.

For the specimens from the column with the North Pond soil, the conductivity and total organic content seem to be rapidly recovering toward their "unclogged" values with depth. The results from the 2 to 4 centimeter specimen are much closer to those of the plain soil than those of the visibly clogged 0 to 2 centimeter specimen. This would seem to indicate that the clogging layer is fairly thin (something less than 2 centimeters).

RELATIONSHIP BETWEEN COLUMN AND PROTOTYPE HYDRAULICS

There are many factors affecting the relationship between column and field hydraulics. The results from this study show that there is some variability in hydraulic loading rate from column to column and also from column to field. However, none of the data presented are indicative of hydraulic loading-rate difficulties for the Phoenix site soils, with the exception of the clay columns. The column studies indicate that a hydraulic loading rate for effluent of approximately 0.1 to 0.5 ft/day for the silts and 0.5 to 1 ft/day for the Sweetwater and Agua Fria sands could be maintained, even with effluent and surface clogging, by controlling the wetting/drying cycles and through periodic surface scarification of the clogging layer, or at worst periodic removal and replacement of the very near-surface soils. Field tests indicate that the hydraulic loading rates may be expected to be higher than those observed for the columns. The infiltration rates for the large-scale field ponding tests conducted by Greeley and Hansen showed hydraulic loading rates of approximately 2.5 ft/day. Even if a near-surface clay layer does exist in limited regions of the proposed SAT facility, as it appears at the Greeley and Hansen South basin site, it is probable that reasonable hydraulic loading rates could be achieved by creating a series of short sand columns through these layers, thereby preventing water from perching on these lenses. However, when effluent is used as the field permeant, a more flow-restrictive clogging layer may develop. Therefore, assuming a reduced infiltration rate for the prototype, as suggested by Greeley and

Hansen, would be reasonable. The discussion below summarizes the most important factors leading to differences in the observed infiltration rates and hydraulic conductivities for this study.

One difference between the laboratory and the field conditions is that the laboratory columns are typically compacted (repacked) to the average field density. The process of disturbing the soil and then repacking it can change the structure, particularly of the finer-grained soils, tending to decrease the conductivity of the columns compared to the field soil. However, repacking of the soils into the columns had only a minor effect on the measured saturated conductivity for the soils used in this study, except for the clay. The repacked clay exhibited a conductivity approximately one order of magnitude less for the repacked columns compared to the undisturbed samples at the same porosity. Column tests in general are useful for parametric studies and they give some indication of field infiltration rates. However, there are numerous factors which affect the field infiltration rates. These factors, for the most part, tend to make the field infiltration rates higher than those for column studies. For example, the field conditions involve infiltration through a relatively large mass of soil compared to that used in the laboratory. The large mass of soil in the field is likely to contain some features which tend to increase the conductivity, such as preferential flow paths due to natural nonhomogeneities and existence of root holes, cracks, or fissures. In addition, some amount of lateral movement of water occurs in the field, but not in the lab columns. These factors lead to increased field rates compared to the lab.

If a lab column were constructed with a layer of low conductivity soil, such as a clay, sandwiched in the column, flow would be constrained to occur through the clay layer and the infiltration rates would be strongly controlled by the layer of low conductivity. If the exact same profile existed in the field and the depth of the impeding layer were large compared to the basin width (which was the case for the Greeley and Hansen South percolation basin site), then water would simply flow laterally and the infiltration rate as measured at the basin would not be substantially affected adversely. However, if the basin width were large compared to the depth of the low conductivity layer, lateral flow would still occur to some extent, but the infiltration rates measured at the basin would be significantly reduced because of the great lateral distance the water would have to travel under relatively low gradient. If test results from a lab column containing no restricting layer were extrapolated to the field where an impeding layer existed,

then the infiltration rates for wide prototype basins could be significantly less than those indicated by the lab column tests. Differences in geometry and material type must be considered in making extrapolations from lab to field.

In summary, if the material types and geometry in lab column tests are a rather precise match for the field conditions, then experience shows that the field infiltration rates will normally be somewhat higher than the lab column rates due to scale effects. However, if layers or lenses of impeding soil are present in the field and not represented in the lab columns, then the reverse may be true. It should also be noted that the formation of the clogging layer and growth of algae tend to be more fully-developed for field prototype conditions, which also reduces field infiltration rates compared to the lab. For the column studies on uniform soil performed using effluent as a permeant, it appears that the surface clogging layer tended to control infiltration rates after several cycles of wetting, except for the Agua Fria Sand columns.

The presence and location of impeding layers and lenses in the field can be detected by study of carefully obtained boring logs. If the lenses are of small lateral extent, they will not cause much retardation of flow. If they are of wide lateral extent then it is quite probable that significant reduction in hydraulic loading rate can be alleviated by introduction of short sand columns, as cited above. The surface clogging layer, however, must be controlled with wetting-drying cycles, surface scarification, periodic surface soil removal/replacement, or other methods in order to maintain adequate infiltration rates.

REFERENCES

- Bodman, G.B., and E.A. Colman. 1943. Moisture and Energy Conditions during Downward Entry of Water into Soils. *Soil Science Society of America Proceedings*, 8:116-122.
- Bouwer, H., and R.C. Rice. 1989. Effect of Water Depth in Groundwater Recharge Basins on Infiltration. *Journal of Irrigation and Drainage Engineering*, 115(4):556-567.
- Brook, R.H., and A.T. Corey. 1964. *Hydrology Paper No. 3 - Hydraulic Properties of Porous Media*. Fort Collins, CO: Colorado State University.
- Burdine, N.T. 1953. Relative Permeability Calculations from Pore-Size Distribution Data. *Petroleum Transactions of AIME*, 198:71-77.

- Daniel, D.E. 1983. Permeability Test for Unsaturated Soil. *Geotechnical Testing Journal*, 6(2):81-86.
- El-Ehwany, M., and S.L. Houston. 1990. Settlement and Moisture Movement in Collapsible Soils. *Journal of Geotechnical Engineering*, 116(10):1521-1535.
- Environmental Systems and Technologies. *Computer Program - FLOFIT A Program for Estimating Soil Hydraulic and Transport Properties from Unsaturated Flow and Tracer Experiments*. Blacksburg, VA.
- Fredlund, D.G., and H. Rahardjo. 1993. *Soil Mechanics of Unsaturated Soils*. New York, NY: John Wiley and Sons, Inc.
- Freeze, R.A., and J.A. Cherry. 1979. *Groundwater*. Englewood Cliffs, NJ: Prentice-Hall, Inc.
- Greeley and Hansen Engineers. 1994. *City of Phoenix 91st Avenue Wastewater Treatment Plant Reclaimed Water Study Phase II Element B Pilot Percolation Basin Studies*. Phoenix, AZ: Greeley and Hansen Engineers.
- Holtz, R.D., and W.D. Kovacs. 1981. *An Introduction to Geotechnical Engineering*. Englewood Cliffs, NJ: Prentice-Hall, Inc.
- Houston, S.L., R.J. Hong and A. Richardson. 1995. Column and Basin Infiltration Studies on Unsaturated Soils. In *Proceedings of the Seventh Biennial Symposium on Artificial Recharge of Groundwater*. Tempe, AZ: Salt River Project, USDA Agriculture Research Service U.S. Water Conservation Lab, and University of Arizona Water Resources Research Center.
- Jury, W.A., W.R. Gardner and W.H. Gardner. 1991. *Soil Physics*. 5th ed. New York, NY: John Wiley and Sons, Inc.
- Keys, W.S. and L.M. MacCary. 1971. Application Of Borehole Geophysics to Water-Resources Investigations. In *Techniques of the Water-Resources Investigations of the United States Geological Survey*.
- Kool, J.B. and J.C. Parker. 1988. Analysis of the Inverse Problem for Transient Unsaturated Flow. *Water Resources Research*, 24(6):817-830.
- Kool, J.B., J.C. Parker, and M.T. van Genuchten. 1987. Parameter Estimation for Unsaturated Flow and Transport Models — A Review. *Journal of Hydrology*, 91:255-293.

- Kool, J.B., and M.T. van Genuchten. 1991. *Computer Program - HYDRUS*. Riverside CA: USDA Agriculture Research Service U.S. Salinity Laboratory.
- Lambe, T.W., and R.V. Whitman. 1969. *Soil Mechanics*. New York: John Wiley and Sons, Inc.
- Mitchell, J.K. 1976. *Fundamentals of Soil Behavior*. New York: John Wiley and Sons, Inc.
- Mualem, Y. 1976. A New Model for Predicting the Hydraulic Conductivity of Unsaturated Porous Media. *Water Resources Research*, 12(3):512-522.
- Sergent, Hauskins and Beckwith Consulting Geotechnical Engineers. 1992. Logs of Borings and Geotechnical Tests.
- Taylor, D.W. 1948. *Fundamentals of Soil Mechanics*. New York: John Wiley and Sons, Inc.
- USEPA. Office of Municipal Pollution Control. 1987. *Report to Congress - Municipal Wastewater Lagoon Study, Vol. 1*. NTIS PB88-154307. Washington, D.C.: Government Printing Office.
- USEPA. Office of Municipal Pollution Control. 1987. *Report to Congress - Municipal Wastewater Lagoon Study, Vol. 2*. NTIS PB88-154315. Washington, D.C.: Government Printing Office.
- van Genuchten, M.T. 1980. A Closed Form Equation for Predicting the Hydraulic Conductivity of Unsaturated Soils. *Soil Science Society of America Journal*, 44:982-998.
- van Genuchten, R. 1987. *Computer Program - RETC Analysis of Soil Hydraulic Properties*. Riverside, CA: USDA Agriculture Research Service U.S. Salinity Laboratory.
- White, M.D., and W.E. Nichols. 1993. *Computer Program - MSTs*. Richland, WA: Pacific Northwest Laboratory.
- Wissa, A.E.Z., J.T. Christian, E.H. Davis, and S. Heiberg. 1971. Consolidation at Constant Rate of Strain. *Jour. of the Soil Mechanics and Foundations Division*, 97(SM10):1393-1413.
- Yates, S.R., and M.T. van Genuchten. 1992. Analysis of Measured, Predicted, and Estimated Hydraulic Conductivity Using the RETC Computer Program. *Soil Science Society of America Journal*, 56:347-354.

**Soil Properties for the
Soil Aquifer Treatment and Clogging Layer Studies**

Prepared by:

Sandra L. Houston, Co-Investigator

Pete Duryea, Research Associate

Ruijin Hong, Research Associate

Department of Civil Engineering

Arizona State University

26 July 1995

TABLE OF CONTENTS

Introduction	3-129
Physical Properties	3-129
Grain Size Distribution	3-129
Atterberg Limits	3-131
Unified Soil Classification	3-132
Specific Gravity of Soil Solids	3-132
Target Dry Density and Molding Water Content	3-133
Hydrological Properties	3-134
Saturated Hydraulic Conductivity	3-134
Soil Suction	3-135
Moisture Retention Model	3-137
Unsaturated Hydraulic Conductivity Model	3-139
Unsaturated Air Permeability	3-139
Mineralogical and Chemical Properties	3-140
X-Ray Diffraction	3-140
Cation Exchange Capacity	3-141
Total Organic Content	3-141
References	3-142
Test Procedures	3-142

LIST OF TABLES

Table 1: Grain Size Distribution	2	3-
Table 2: Coefficients of Uniformity and Curvature.....	8	3-
Table 3: Atterberg Limits	8	3-
Table 4: Unified Soil Classification	4	3-
Table 5: Specific Gravity of Soil Solids.....	4	3-
Table 6: Target Dry Density and Molding Water Content	5	3-
Table 7: Saturated Hydraulic Conductivity	8	3-
Table 8: Soil Suction.....	8	3-
Table 9: Model Parameters from Program RETC	10	3-
Table 10: Model Parameters from Program FLOFIT	10	3-
Table 11: Air Permeability.....	12	3-
Table 12: Cation Exchange Capacity	13	3-
Table 13: Total Organic Content	13	3-

LIST OF FIGURES

Figure 1: Gradation Curves
Figure 2: Soil Suction versus Water Content
Figure 3: Soil Suction versus Saturation
Figure 4: Soil Water Characteristic Curves
Figure 5: Characteristic Curves with Suction Data
Figure 6: Hydraulic Conductivity Curves
Figure 7: Conductivity Curves with Data
Figure 8: Air Permeability versus Water Saturation
Figure 9: X-Ray Diffraction (minus #200)

INTRODUCTION

As a part of the SAT (Soil Aquifer Treatment) Project, the influence of soil type on water quality and infiltration rate in a ground water recharge facility is to be examined. Also, the Clogging Layer Study will more closely evaluate the behavior of and flow of water through the materials found in the very near surface. To this end, five different soil types have been chosen for study, which cover a broad range of physical, hydrological and chemical properties. This report summarizes the results of the initial background testing of the soils and provides a preliminary characterization of each soil. The soils were sampled at the following locations:

Agua Fria Soil - Agua Fria River Bottom at Camelback Road in Glendale, AZ;
Sweetwater Soil - Sweetwater Groundwater Recharge Site in Tucson, AZ;
South Pond Soil - South Ponding Site for SAT Pilot Percolation Study in Glendale, AZ;
North Pond Soil - North Ponding Site for SAT Pilot Percolation Study in Glendale, AZ;
Ag. Field Soil - Agricultural Field south of South Ponding Site in Glendale, AZ.

PHYSICAL PROPERTIES

The physical properties discussed below include those necessary to classify the soils and those required for mass-volume and degree of saturation calculations.

Grain Size Distribution

The distribution of particle sizes for each soil is reported in Table I as the percent, by weight of the material, which "passes" or is smaller than each respective size. The data actually combine the results of several tests. The percentage of fines, that is the material passing a No. 200 sieve (the silt and clay fraction), was determined by a wet sieve analysis; subsequently, the data for the larger sizes was determined by dry sieving the remaining material. Finally, if the soil had more than 15 percent fines, a hydrometer analysis, which employs Stokes Law to establish the grain size distribution of the fines, was performed on a separate specimen.

Table 1
Grain size distribution

Standard Sieve Size	Particle Size (mm)	Percent Passing by Weight				
		Agua Fria	Sweetwater	South Pond	North Pond	Ag. Field
3/4 in.	19.100			97.6		
3/8 in.	9.520			94.4		
No. 4	4.760	98.8	99.5	93.5	98.5	
No. 8	2.380	96.3		92.1	97.9	99.5
No. 10	2.000		96.1			
No. 16	1.190	88.4		87.5	95.3	98.6
No. 40	0.420	26.9	32.5	62.4	85.9	93.9
No. 100	0.149	1.3	9.0	28.8	53.9	82.3
No. 200	0.074	0.7	5.5	19.2	26.9	73.0
	0.060			7.0		
	0.050				10.1	
	0.042					61.1
	0.036			5.2		
	0.030				7.0	58.3
	0.025				5.5	
	0.022					51.3
	0.021			3.4		
	0.012					39.9
	0.009			2.4		
	0.008				3.6	35.7
	0.006			2.0		31.5
	0.005					27.3
	0.004			1.7		
	0.003					16.5

Figure 1 shows the gradation curves, plots of the log of the particle size versus the percent passing by weight, for each soil. The coefficients of uniformity (C_u) and curvature (C_c) describe the shape of the gradation curves and are used to help classify granular or coarse grained soils. They are defined as follows:

$$C_u = \frac{D_{60}}{D_{10}} \qquad C_c = \frac{(D_{30})^2}{D_{10} * D_{60}}$$

where D is the particle size corresponding to the percent passing that is specified in the subscript. The results for the five subject soils are presented in Table 2.

Table 2
Coefficients of uniformity and curvature

Soil	D ₁₀ (mm)	D ₃₀ (mm)	D ₆₀ (mm)	Coefficient of Uniformity	Coefficient of Curvature
Agua Fria	0.21	0.43	0.73	3.5	1.2
Sweetwater	0.16	0.37	0.81	5.1	1.1
South Pond	0.07	0.15	0.39	5.6	0.8
North Pond	0.05	0.08	0.17	3.4	0.8
Ag. Field	<0.01	0.01	0.04	18.5	0.4

Atterberg Limits

The Atterberg limits tests quantify the relationship between the consistency of a soil and its gravimetric water content and are used to help classify fine grained soils. Although the tests are empirical and the definitions of the liquid and plastic limits somewhat arbitrary, the behavior of a soil can generally be described as follows. At a water content between the liquid and plastic limits, the soil behaves primarily as a plastic solid, but as its water content increases above the liquid limit, the soil begins to behave as a viscous fluid or slurry. The plasticity index is defined as the difference between the liquid and plastic limits; it is the width of the range in water contents over which the soil will tend to behave plastically. The results for the subject soils are given in Table 3.

Table 3
Atterberg limits

Soil	Liquid Limit	Plastic Limit	Plasticity Index
Agua Fria	--	--	NP
Sweetwater	--	--	NP
South Pond	--	--	NP
North Pond	--	--	NP
Ag. Field	33.8	21.7	12.1

NP - Non-Plastic

Unified Soil Classification

The Unified Soil Classification System is commonly used in geotechnical engineering to group soils that exhibit similar engineering properties and behavior. Divisions are made based on grain size distribution and either the Atterberg limits of the soil or its coefficients of uniformity and curvature. The details of the classification system and the specifics of each soil type are discussed thoroughly by Holtz and Kovacs (1981). The soils are classified as shown in Table 4.

Table 4
Unified soil classification

Soil	Description	USCS Designation
Agua Fria	Poorly Graded Sand	SP
Sweetwater	Poorly Graded/Silty Sand	SP-SM
South Pond	Silty Sand	SM
North Pond	Silty Sand	SM
Ag. Field	Low Plasticity Clay	CL

Specific Gravity of Soil Solids

The specific gravity of the actual soil particles themselves varies with soil type depending on the variety and relative proportions of the minerals that constitute the soil. The specific gravity is measured experimentally and is required to analyze the results of the hydrometer test described earlier. It is also required, along with the density and water content of the soil, to calculate its degree of saturation. The results for the specific soils of interest are contained in Table 5.

Table 5
Specific gravity of soil solids

Soil	Specific Gravity
Agua Fria	2.67
Sweetwater	2.63
South Pond	2.73
North Pond	2.74
Ag. Field	2.78

Target Dry Density and Molding Water Content

As noted by Mitchell, many important soil properties, including the hydraulic conductivity, are not only a function of the soil type but also the arrangement of the soils grains, that is the soil fabric (Mitchell 1976). However, this effect is much more pronounced for fine grained soils. The fabric varies with the dry density of the soil, the water content at which the soil is compacted and the method of compaction employed. As a result, it is important to specify a target dry density and molding water content for use in recompacting soil into columns from disturbed bulk samples. This helps to ensure uniform properties among different columns which contain the same soil.

For the Ag. Field, North Pond and South Pond soils, the in-situ density was readily determinable by the sand cone method and/or by measuring the density of an undisturbed Shelby tube sample. As such, a representative value of the in-situ density was selected as the target for the lab columns that are filled with those soils. This should more closely model field conditions in the area of the proposed SAT facility. For the more granular materials (the Sweetwater and Agua Fria soils), a target, that was fairly dense but readily achievable under lab conditions, was selected based on several trial compaction tests. Molding water contents were also selected by trial to be dry of optimum but to be wet enough to allow the target density to be obtained with a reasonable amount of compactive effort. The specifications for each soil are detailed in Table 6.

Table 6
Target dry density and molding water content

Soil	Target Dry Density		Molding Water Content (%)
	(g/cm ³)	(lb/ft ³)	
Agua Fria	1.57	98.0	Air Dry (<1.0)
Sweetwater	1.60	99.8	Air Dry (<1.0)
South Pond	1.66	103.6	2.0
North Pond	1.67	104.2	3.3
Ag. Field	1.59	99.2	9.4

HYDROLOGICAL PROPERTIES

Since the SAT project will, by definition, involve the study of infiltration of fluid into unsaturated soils, the flow regimes will not be adequately characterized by a simple application of Darcy's Law for saturated conditions alone. In addition to the saturated hydraulic conductivity, knowledge of the relationships between pressure head, volumetric water content and unsaturated hydraulic conductivity is required. The following sections detail the experimental and analytical procedures used to evaluate those relationships. For notational convenience, the pressure head is shown as positive for unsaturated conditions.

Saturated Hydraulic Conductivity

For each of the soils with a significant fines content (South Pond, North Pond and Ag. Field), tests were conducted on undisturbed and recompacted specimens. The undisturbed specimens were obtained from the near surface using thin-walled Shelby tube samplers. The recompacted samples were prepared in the lab at the target dry density. All samples were tested in a falling head type permeameter. Due to non-homogeneous conditions in the field, often the dry density of the undisturbed samples, as measured after the test, differed from the selected target dry density. To provide a better basis for comparisons, all conductivity test results have been adjusted to an approximately equivalent value at the target dry density. This adjustment was made by applying the Kozeny-Carmen equation as follows (Lambe 1969):

$$\frac{K_{\text{target}}}{K_{\text{measured}}} = \frac{e_{\text{target}}^3}{e_{\text{measured}}^3} * \frac{1 + e_{\text{measured}}}{1 + e_{\text{target}}}$$

Due to the difficulty in obtaining truly undisturbed samples of granular materials and in measuring their in-situ density, only tests of recompacted specimens at the target dry density were performed on the Agua Fria and Sweetwater soils. It should be noted that little difference was expected for these soils, because experience has shown that granular materials are not particularly

sensitive to changes in fabric. Conductivity tests were also done in a falling head type apparatus, and the results adjusted to the target dry density as above, if the density as measured after the test differed slightly from the target value.

A summary of results is presented below in Table 7. Each reported value is the average of at least two separate tests, and all results have been adjusted to the appropriate target density.

Table 7
Saturated hydraulic conductivity

Soil	Undisturbed Conductivity		Recompacted Conductivity	
	(cm/sec)	(ft/day)	(cm/sec)	(ft/day)
Agua Fria	N/A	N/A	8.4×10^{-2}	238.25
Sweetwater	N/A	N/A	1.9×10^{-2}	53.03
South Pond	1.3×10^{-3}	3.59	6.9×10^{-4}	1.96
North Pond	2.3×10^{-4}	0.65	1.8×10^{-4}	0.50
Ag. Field	3.3×10^{-5}	0.09	3.5×10^{-6}	0.01

Soil Suction

Soil suction, that is the negative pore water pressure which arises in unsaturated conditions, was also determined experimentally. The measurements were made using the filter paper technique. The actual data are summarized in Table 8 for each soil type. Typically, soil suction is related to volumetric water content as shown in Figure 2. However, Figure 3 shows a similar relationship between suction and degree of saturation. The soil suction is reported in pF, which is the base 10 logarithm of negative pore water pressure in centimeters of water.

Table 8

Soil suction

Agua Fria Soil (SP)			Sweetwater Soil (SP-SM)		
Degree of Saturation (%)	Volumetric Water Content (%)	Matric Suction (pF)	Degree of Saturation (%)	Volumetric Water Content (%)	Matric Suction (pF)
10.6	4.5	2.00	11.7	4.7	3.80
22.0	9.1	1.59	18.6	7.4	1.95
30.3	12.6	1.47	26.7	10.6	1.46
41.3	17.0	1.36	33.9	13.6	1.37
50.8	20.9	1.36	45.7	18.3	1.36
60.3	24.8	1.33	54.9	21.8	1.18
70.9	29.1	1.29	64.2	25.4	1.22
81.1	33.4	1.27			
89.8	36.6	1.21			

South Pond Soil (SM)			North Pond Soil (SM)		
Degree of Saturation (%)	Volumetric Water Content (%)	Matric Suction (pF)	Degree of Saturation (%)	Volumetric Water Content (%)	Matric Suction (pF)
11.9	4.7	4.12	30.0	11.3	2.90
17.8	7.1	3.35	41.5	15.7	2.42
25.4	10.4	2.28	48.4	18.6	2.23
32.2	13.0	1.91	57.4	21.9	2.03
40.7	16.5	1.70	70.6	26.8	1.66
49.2	20.2	1.53	80.9	30.7	1.59
52.6	21.5	1.42	91.2	34.6	1.32
78.0	30.9	1.15	~100	37.8	1.16

Ag. Field Soil (CL)		
Degree of Saturation (%)	Volumetric Water Content (%)	Matric Suction (pF)
22.5	9.3	5.78
29.4	12.1	5.23
35.6	14.8	4.77
46.3	17.0	4.42
50.8	20.8	4.02
50.1	20.9	3.91
59.7	25.1	3.67
71.2	29.7	3.40
81.6	34.0	3.17
92.0	38.2	2.74
~100	42.0	2.13

Moisture Retention Model

One important aspect of the SAT project is the development of a computer simulation of the infiltration process using program HYDRUS, which was written by van Genuchten. As such, numerical models of the moisture retention characteristics and unsaturated hydraulic conductivity of the soil are required.

Moisture retention describes the relationship between volumetric water content and pressure head (soil suction). In program HYDRUS, van Genuchten adopts his own moisture retention model, which can be summarized as follows (van Genuchten 1980).

$$\theta = \theta_r + \frac{\theta_s - \theta_r}{\left(1 + (\alpha h)^n\right)^m}$$

where θ - water content

θ_r - residual water content

θ_s - saturated water content

h - pressure head (suction positive)

α , n and m - empirical constants (Note typically $m = 1 - 1/n$.)

To assist in use of this model, van Genuchten has written another program RETC, which will determine θ_r , θ_s , α , n and m from experimental retention and saturated conductivity data, using a least squares optimization technique (van Genuchten 1987). The evaluation of the subject soils is summarized in Table 9, and the RETC-determined characteristic curves are plotted together in Figure 4. It should be noted that these analyses were made for the soils in a recompacted state. Figure 5 is a series of plots that show the characteristic curves individually, along with the laboratory data from which they are derived, for each soil type.

Table 9

Model parameters from program RETC

Soil	θ_r	θ_s	α (cm ⁻¹)	m	n
Agua Fria	0.000	0.427	0.047	0.767	4.297
Sweetwater	0.000	0.394	0.095	0.492	1.968
South Pond	0.058	0.394	0.075	0.456	1.839
North Pond	0.075	0.396	0.033	0.387	1.631
Ag. Field	0.069	0.427	0.001	0.274	1.378

After completion of the initial estimates of the required parameters, an attempt was made to numerically simulate the results of column infiltration tests. The RETC derived parameters did not provide an acceptable level of accuracy in modeling either the progress of the wetted front or of the degree of saturation behind the front. As such, revised estimates of the parameters were developed using an alternative method, program FLOFIT (Kool 1988).

Where as RETC estimated the required parameters by fitting a curve to observed moisture retention data, FLOFIT involves an inverse method of determining the parameters. Those parameters with a distinct physical meaning (K_r and θ_s) are measured independently, and θ_r can be approximated as the air-dried volumetric water content. Then, the remaining parameters are evaluated by assuming the form of the soil moisture and unsaturated conductivity relationships (as presented here in) and back analyzing the results of an infiltration column experiment. The FLOFIT derived parameters for each soil type are listed in Table 10, and the corresponding characteristic curves are also included in Figures 4 and 5.

Table 10

Model parameters from program FLOFIT

Soil	θ_r	θ_s	α (cm ⁻¹)	m	n
Agua Fria	0.000	0.427	0.0180	0.889	8.990
Sweetwater	0.000	0.394	0.0178	0.873	7.875
South Pond	0.010	0.394	0.0101	0.602	2.510
North Pond	0.010	0.396	0.0037	0.614	2.590
Ag. Field	0.080	0.427	0.0029	0.425	1.740

The revised parameters have been found to provide a good numerical representation of the velocity of the wetted front in comparison to the column infiltration tests, but they still tend to overestimate the degree of saturation behind the front.

Unsaturated Hydraulic Conductivity Model

In addition to the moisture retention model discussed previously, HYDRUS also uses the unsaturated conductivity model proposed by Mualem (van Genuchten 1980). As can be seen from the following equation, it employs the same parameters as the retention model.

$$K = K_s * \frac{\left\{ 1 - (\alpha h)^{n-1} * \left[1 + (\alpha h)^n \right]^{-m} \right\}^2}{\left[1 + (\alpha h)^n \right]^{m/2}}$$

where K - unsaturated hydraulic conductivity

K_s - saturated hydraulic conductivity

Figure 6 illustrates the relationship between water content and the logarithm of conductivity for all of the soil types together, whereas Figure 7 is a series of arithmetic plots of conductivity versus water content for each soil type alone. These figures show the curves for each of the two different sets of parameters (RETC and FLOFIT derived). Note that 1 cm/sec is approximately equal to 2835 ft/day. The results of these models have been confirmed for the clayey soil by instantaneous profile testing, which is used to obtain a direct measure of the unsaturated conductivity. These data are shown along with the theoretical curves in Figure 7.

Unsaturated Air Permeability

Because entrapped air can potentially impede infiltration into unsaturated soils, the air permeability of the various soil types was investigated as a function of the water degree of saturation. Results are summarized in Figure 8 and Table 11.

Table 11

Air permeability

Agua Fria Soil (SP)		Sweetwater Soil (SP-SM)	
Degree of Saturation (%)	Air Permeability (m ²)	Degree of Saturation (%)	Air Permeability (m ²)
0.0	1.56E-10	0.0	6.18E-11
15.2	1.77E-10	16.4	7.04E-11
30.5	1.74E-10	32.7	7.03E-11
45.7	1.14E-10	49.1	2.85E-11
61.0	4.61E-11	65.4	6.70E-13

South Pond Soil (SM)		North Pond Soil (SM)	
Degree of Saturation (%)	Air Permeability (m ²)	Degree of Saturation (%)	Air Permeability (m ²)
0.0	1.13E-11	0.0	9.18E-12
19.8	6.07E-12	27.8	1.95E-12
38.7	3.78E-12	51.8	1.37E-12
72.9	1.01E-12	70.3	9.70E-13

Ag. Field Soil (CL)	
Degree of Saturation (%)	Air Permeability (m ²)
0.0	7.53E-12
25.7	1.97E-12
47.6	7.40E-13
74.6	2.76E-14

MINERALOGICAL AND CHEMICAL PROPERTIES

In addition to physical and hydraulic properties, the chemical characteristics of the soil are also of interest, especially in terms of assessing the type and effectiveness of treatment processes.

X-Ray Diffraction

Analysis by x-ray diffraction provides an indication of the types of minerals present in the soil. These results can be particularly helpful in understanding the behavior of the soil. Figure 9 graphically shows the results of tests on the finer grained soils and identifies the minerals present.

These analyses were performed on the fine fraction of the soil; additional tests on the minus 2 micron fraction showed little difference.

Cation Exchange Capacity

The cation exchange capacity is a measure of the soil's affinity for ions. It can be used to assess the adsorptive characteristics of the soil. Results for the five soils are presented in Table 12.

Table 12
Cation exchange capacity

Soil	CEC (meq/100 g of soil)
Agua Fria	2.4
Sweetwater	5.7
South Pond	6.9
North Pond	7.1
Ag. Field	22.3

Total Organic Content

The total organic content of the soil was evaluated according to an ASTM standard procedure in which oven-dried soil is placed in a muffle furnace to incinerate any organic matter present. The percent change in weight is then reported as the organic content. This information is of interest because it helps to quantify the chemical/biological conditions in the soil column prior to the introduction of any effluent for treatment. Results are shown in Table 13.

Table 13
Total organic content

Soil	TOC (% by weight)
Agua Fria	0.32
Sweetwater	0.70
South Pond	0.97
North Pond	1.14
Ag. Field	3.03

REFERENCES

- Holtz, R.D. and W.D. Kovacs. 1981. *An Introduction to Geotechnical Engineering*. Englewood Cliffs, New Jersey: Prentice-Hall, Inc.
- Kool, J.B. and Parker, J.C. 1988. Analysis of the Inverse Problem for Transient Unsaturated Flow. *Water Resources Research*, 24(6):817-830.
- Lambe, T.W. and R.V. Whitman. 1969. *Soil Mechanics*. New York: John Wiley and Sons, Inc.
- Mitchell, J.K. 1976. *Fundamentals of Soil Behavior*. New York: John Wiley and Sons, Inc.
- van Genuchten, M.Th. 1980. A Closed Form Equation for Predicting the Hydraulic Conductivity of Unsaturated Soils. *Soil Science Society of America Journal*, 44:892-898.
- van Genuchten, R. 1987. Manual for *RET C - Analysis of Soil Hydraulic Properties*. Riverside, CA: USDA - Agriculture Research Service U.S. Salinity Laboratory,.

TEST PROCEDURES

- American Society for Testing and Materials. 1987. *ASTM D 2974 Standard Test Methods for Moisture, Ash, and Organic Matter of Peat and Other Organic Soils*.
- Atterberg Limit Tests*. Unpublished Lab Procedure. Berkeley, CA: University of California Department of Civil Engineering.
- Bowles, J.E. 1978. Determination of In-Place Soil Density. In *Engineering Properties of Soil and Their Measurement*. 2nd ed. New York: McGraw-Hill, Inc.
- Bowles, J.E. 1978. Gradation by Sieve Analysis. In *Engineering Properties of Soil and Their Measurement*. 2nd ed. New York: McGraw-Hill, Inc.
- Cation Exchange Capacity*. Unpublished Lab Procedure. Berkeley, CA: University of California Department of Civil Engineering.
- The Determination of the Grain-Size Distribution of a Fine-Grained Soil by the Method of Hydrometer Analysis*. Unpublished Lab Procedure. Berkeley, CA: University of California Department of Civil Engineering.

- Houston, S.L., W.N. Houston and A. Wagner. 1994. Laboratory Filter Paper Suction Measurements. *Geotechnical Testing Journal*, 17(2):185-194.
- Kirkham, D. 1946. Field Method for Determination of Air Permeability of Soil in its Undisturbed State. *Soil Science Society Proceedings*, 93-99.
- Specific Gravity of Soils*. Unpublished Lab Procedure. Berkeley, CA: University of California Department of Civil Engineering.
- U.S. Army Corps of Engineers. 1986. *Engineer Manual No. 1110-2-1906 Laboratory Soils Testing*.
- X-Ray Diffraction Analysis*. Unpublished Lab Procedure. Berkeley, CA: University of California Department of Civil Engineering.

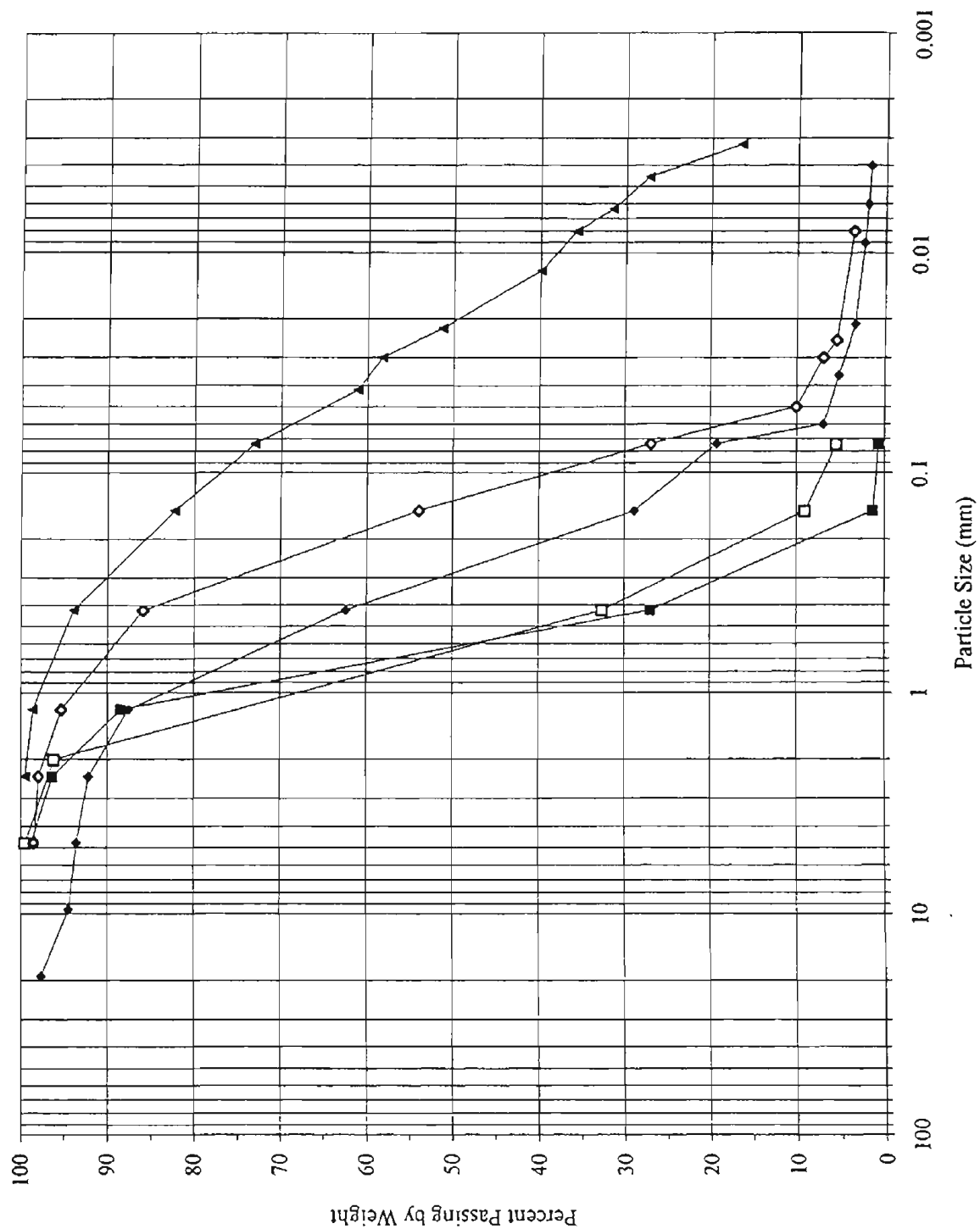


Figure 1 Gradation Curves

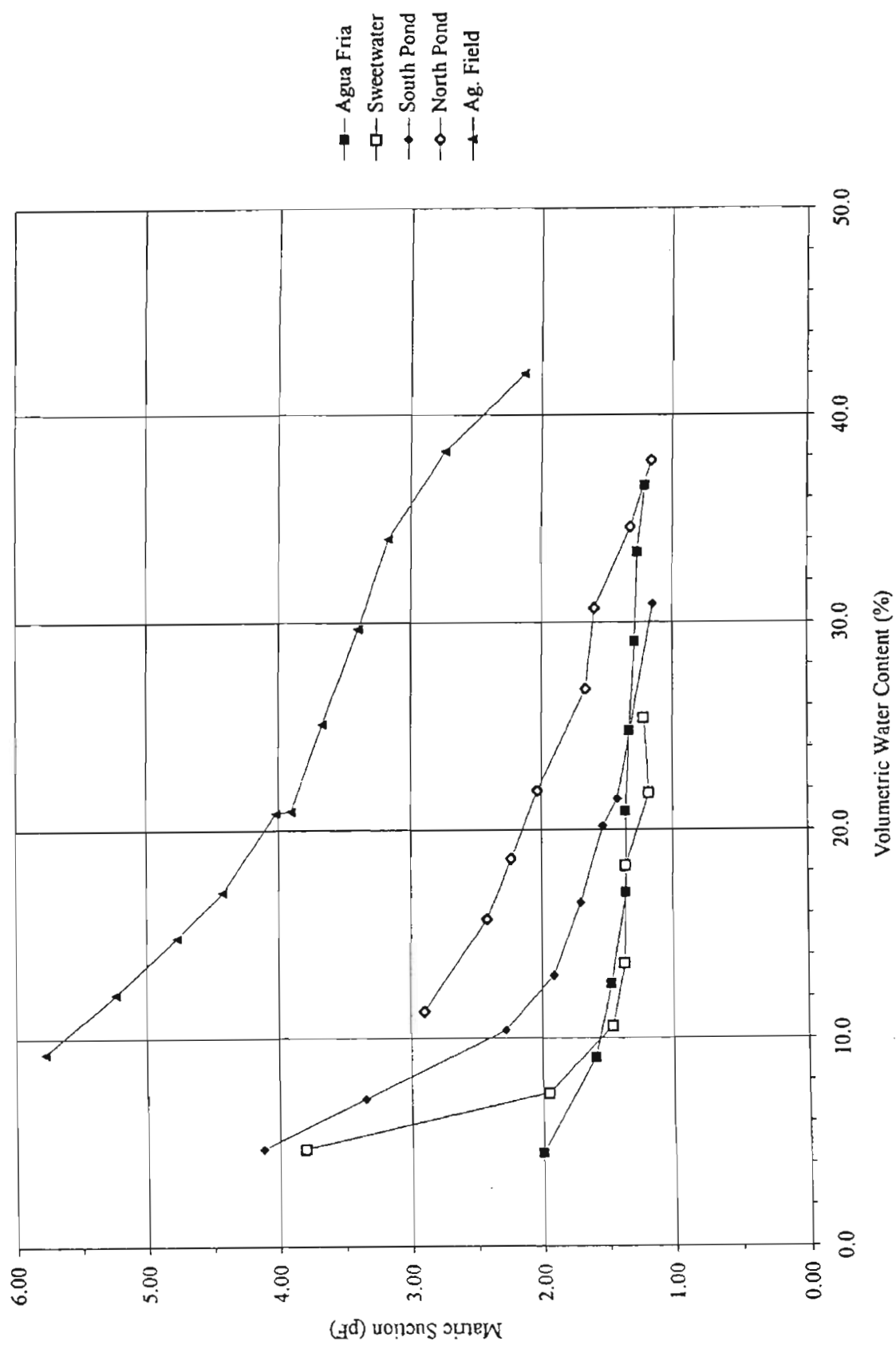


Figure 2 Soil Suction versus Water Content

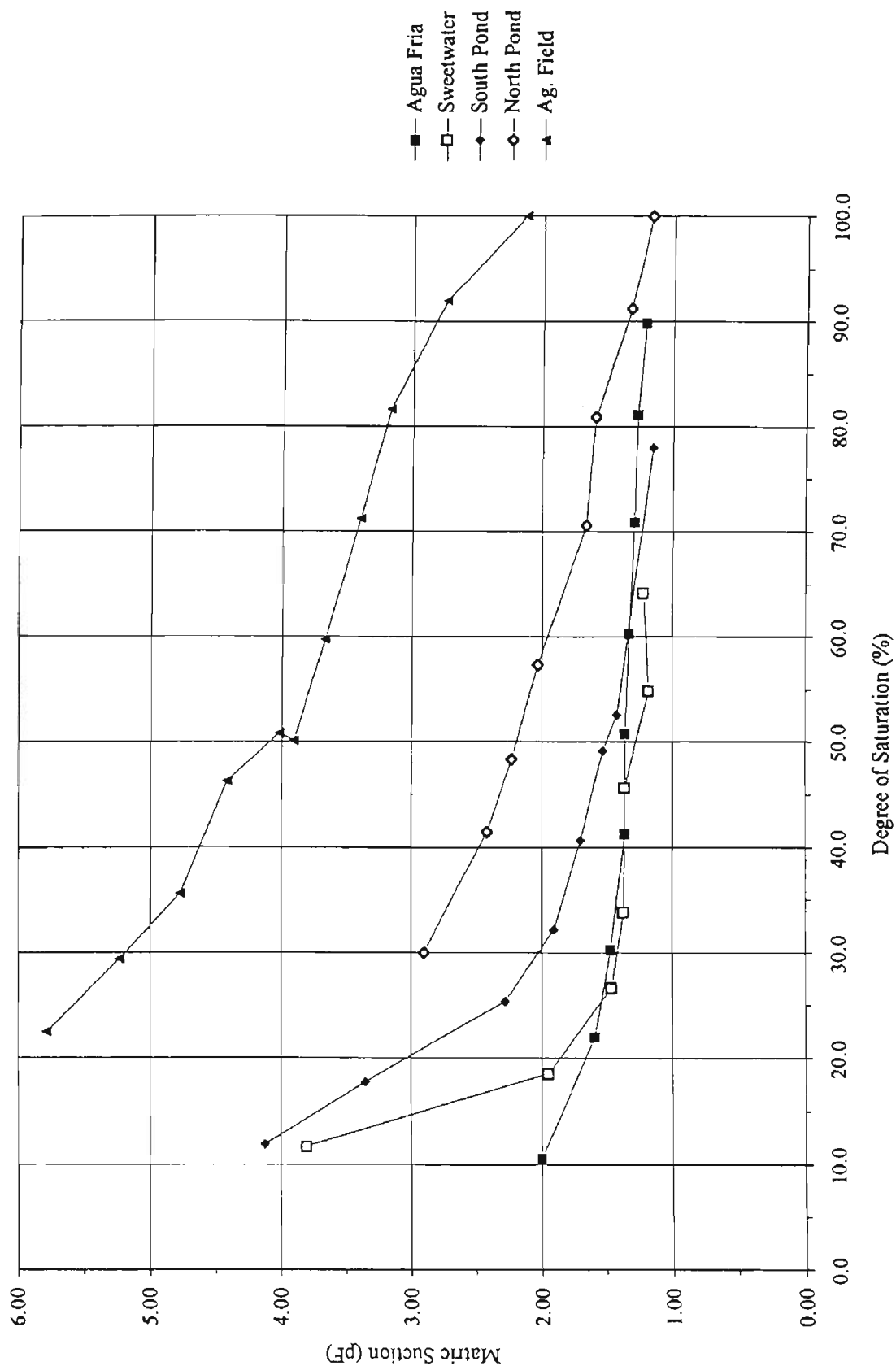


Figure 3 Soil Suction versus Saturation

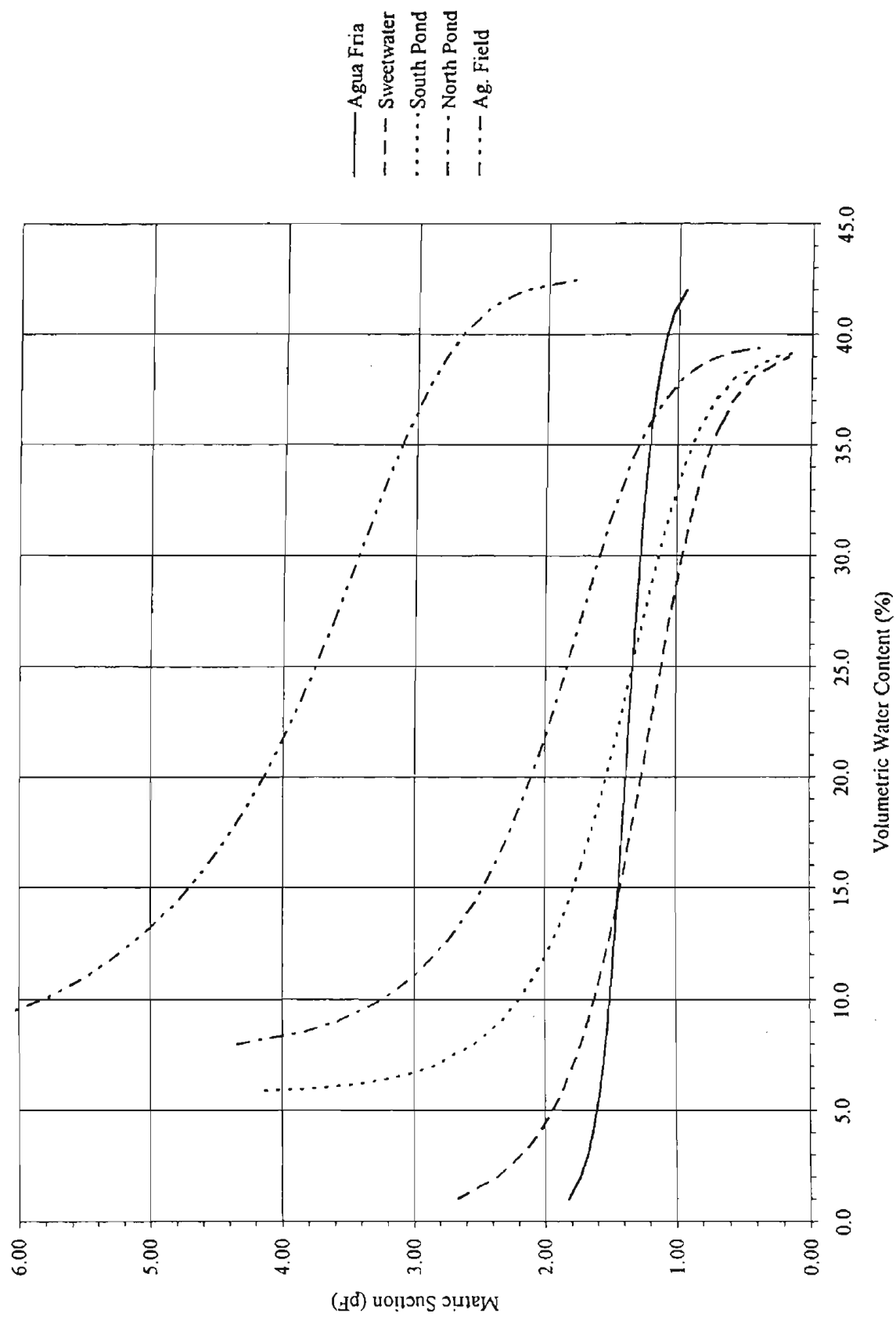


Figure 4a RETC Derived Characteristic Curves

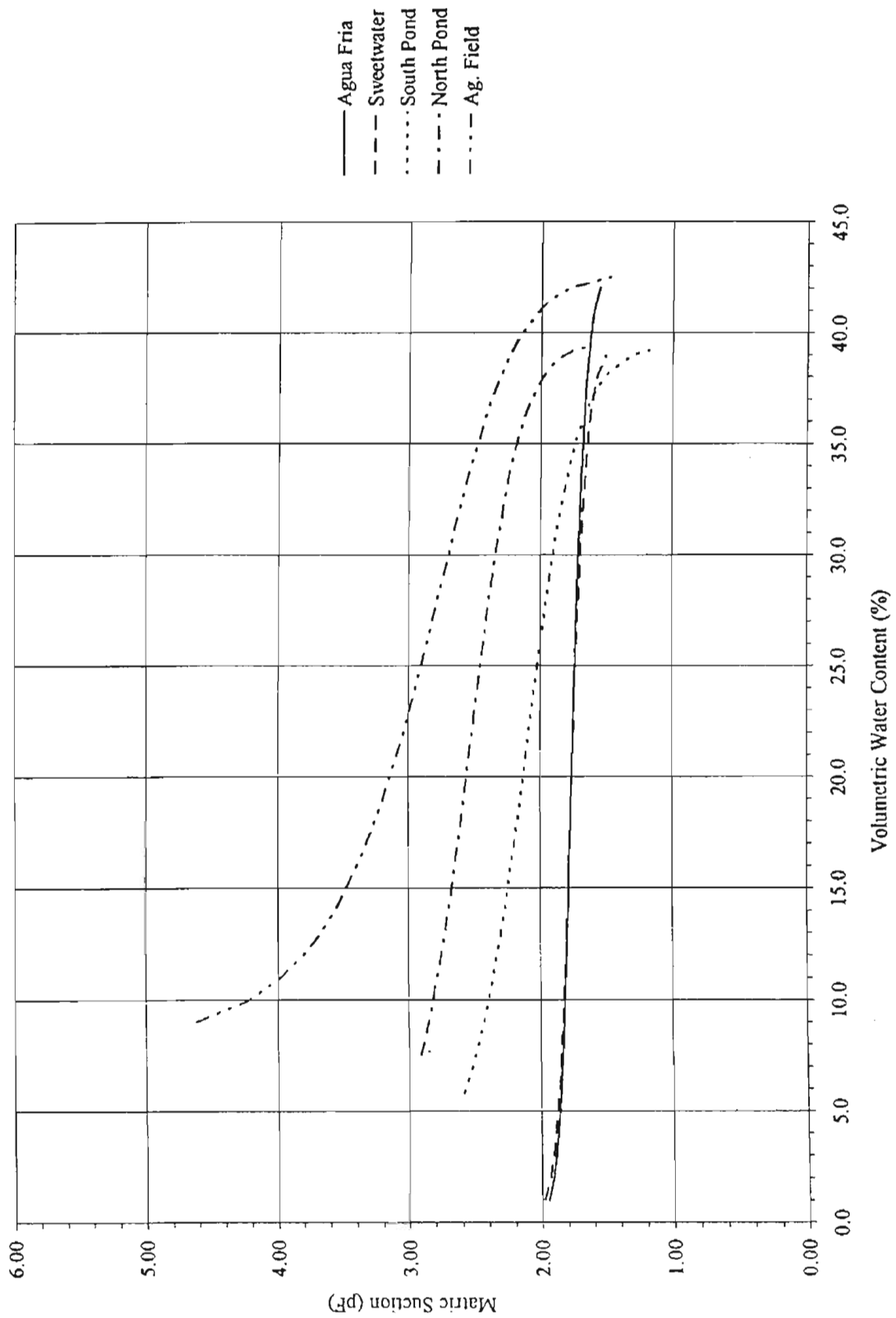


Figure 4b FLOFIT Derived Characteristic Curves

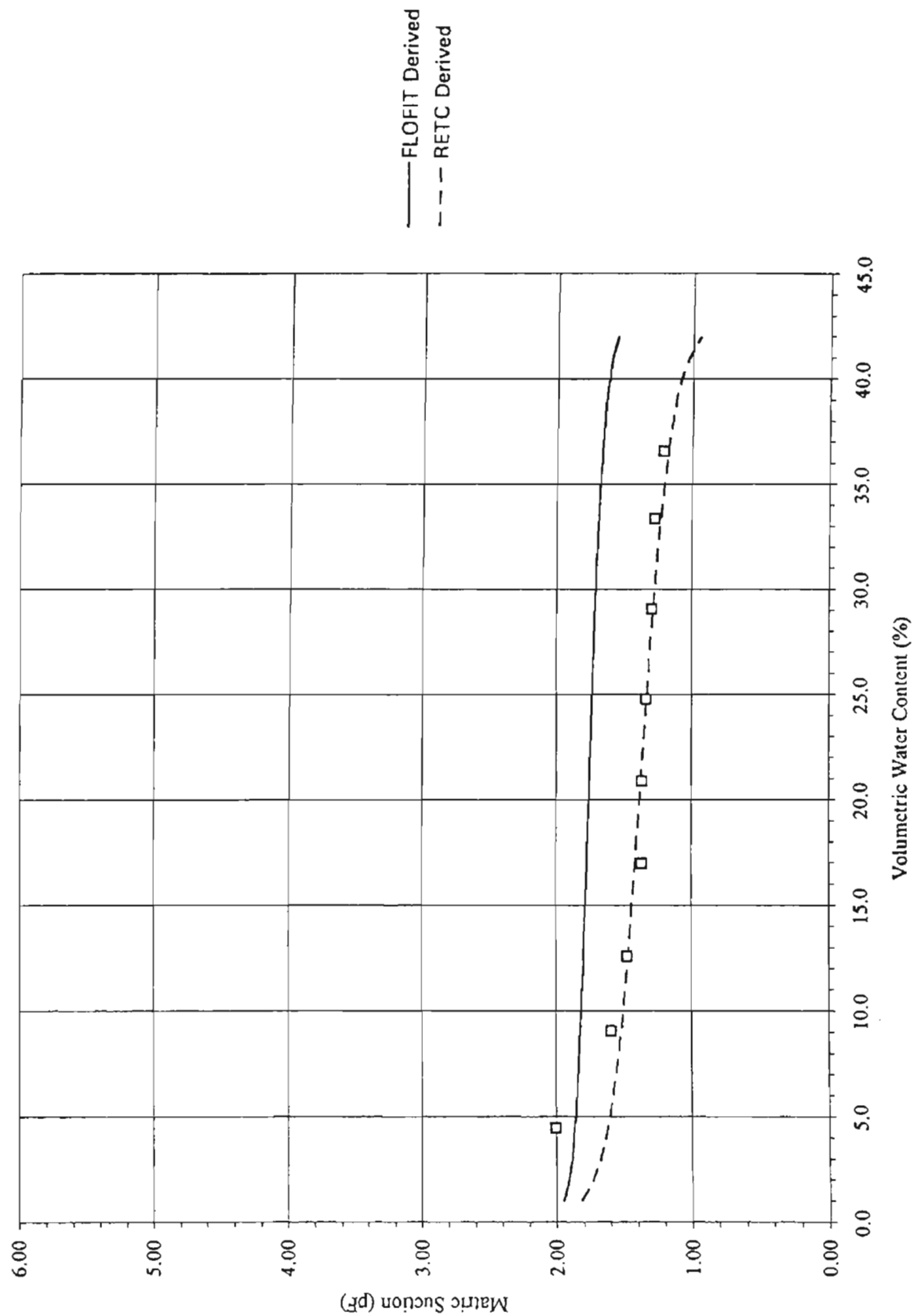


Figure 5a Agua Fria Soil Characteristic Curve with Suction Data

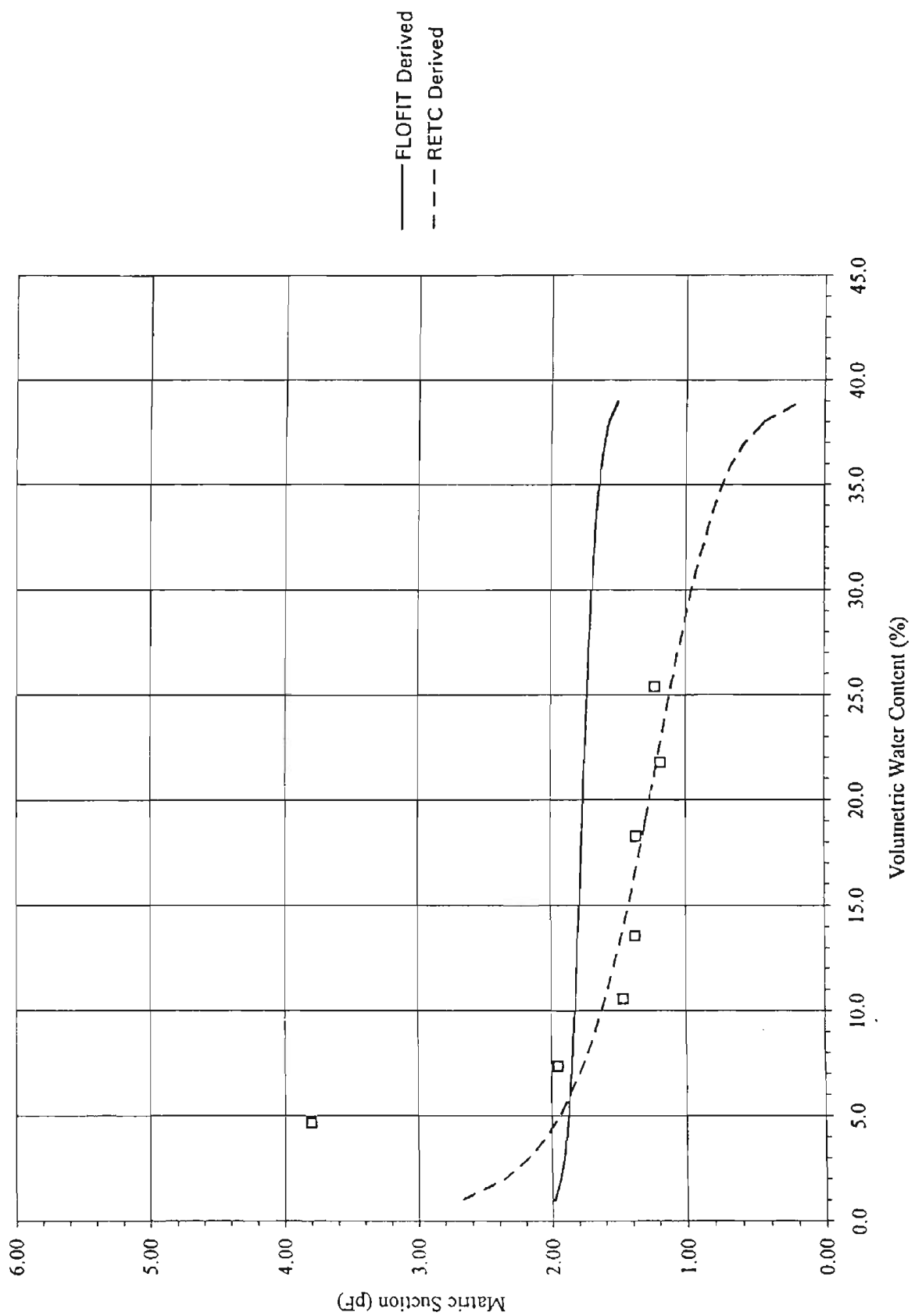


Figure 5b Sweetwater Soil Characteristic Curve with Suction Data

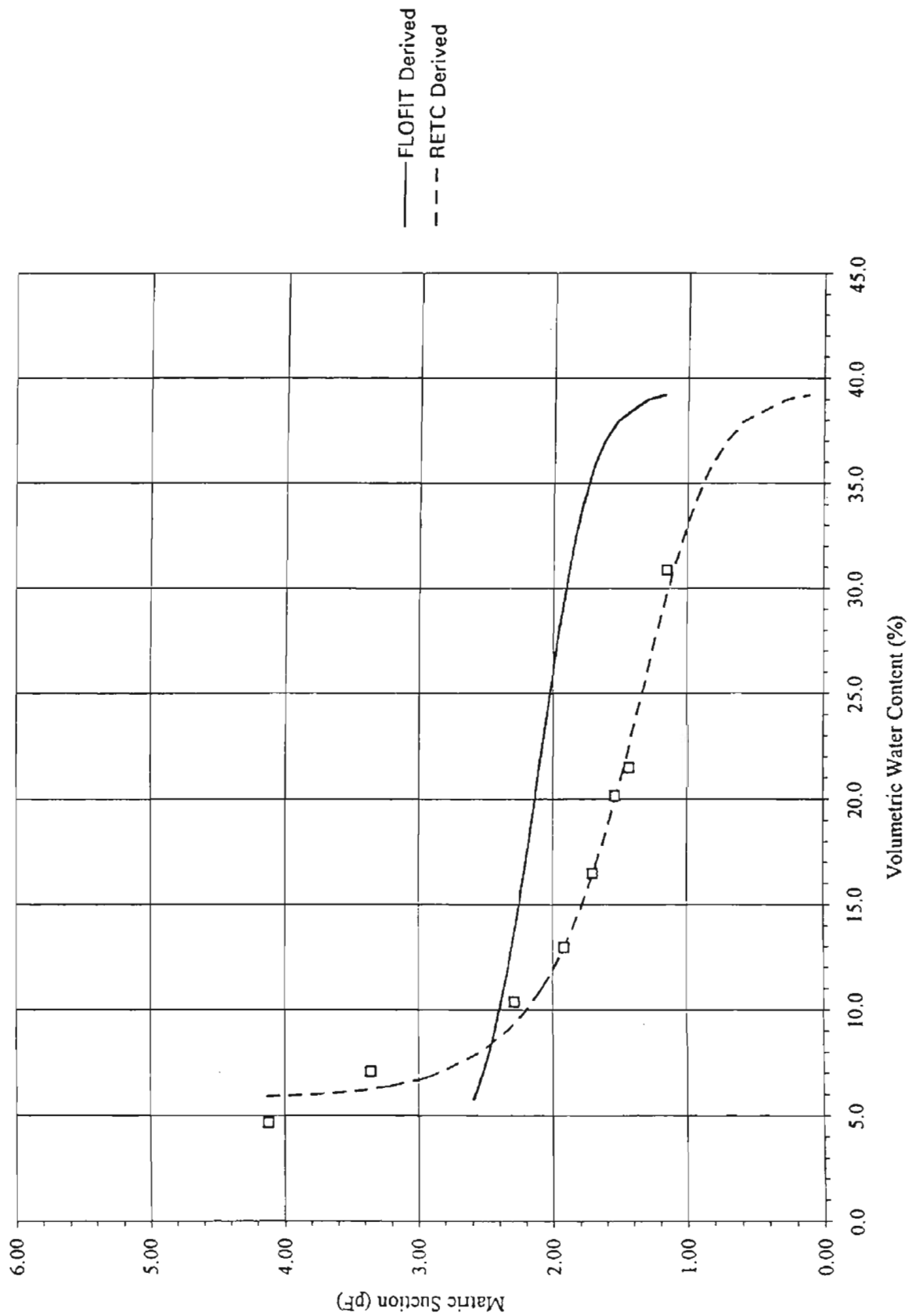


Figure 5c South Pond Soil Characteristic Curve with Suction Data

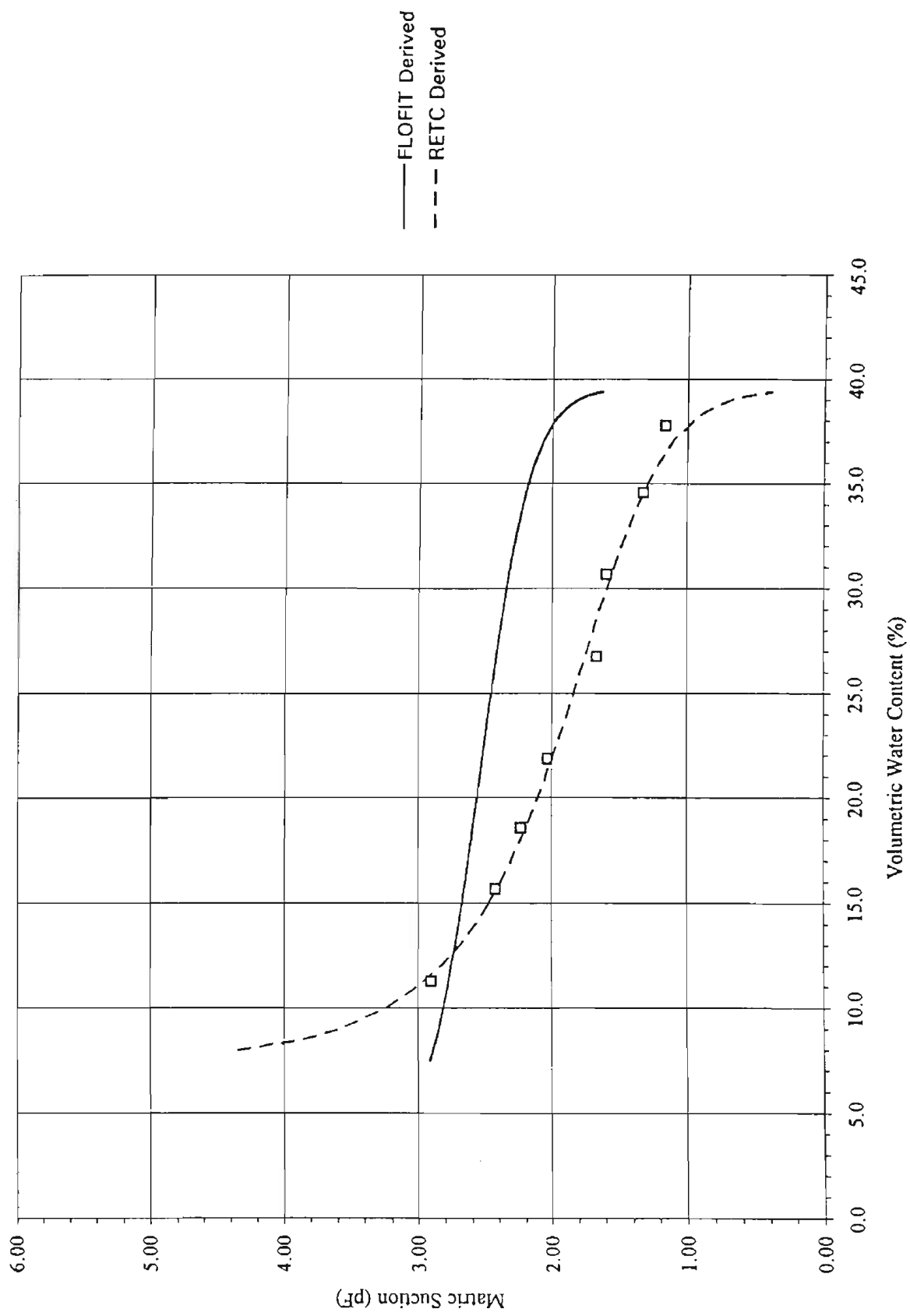


Figure 5d North Pond Soil Characteristic Curve with Suction Data

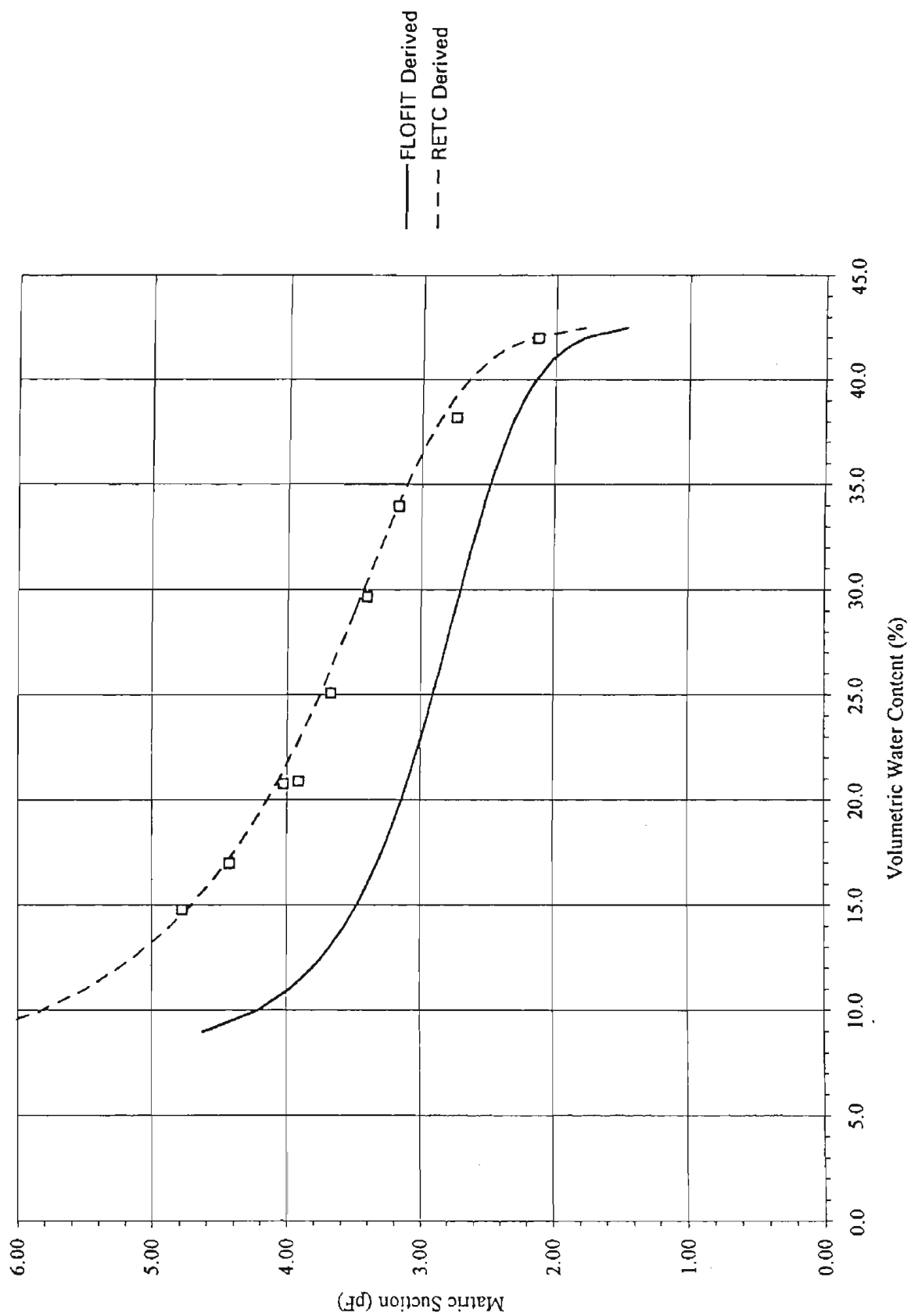


Figure 5e Ag. Field Soil Characteristic Curve with Suction Data

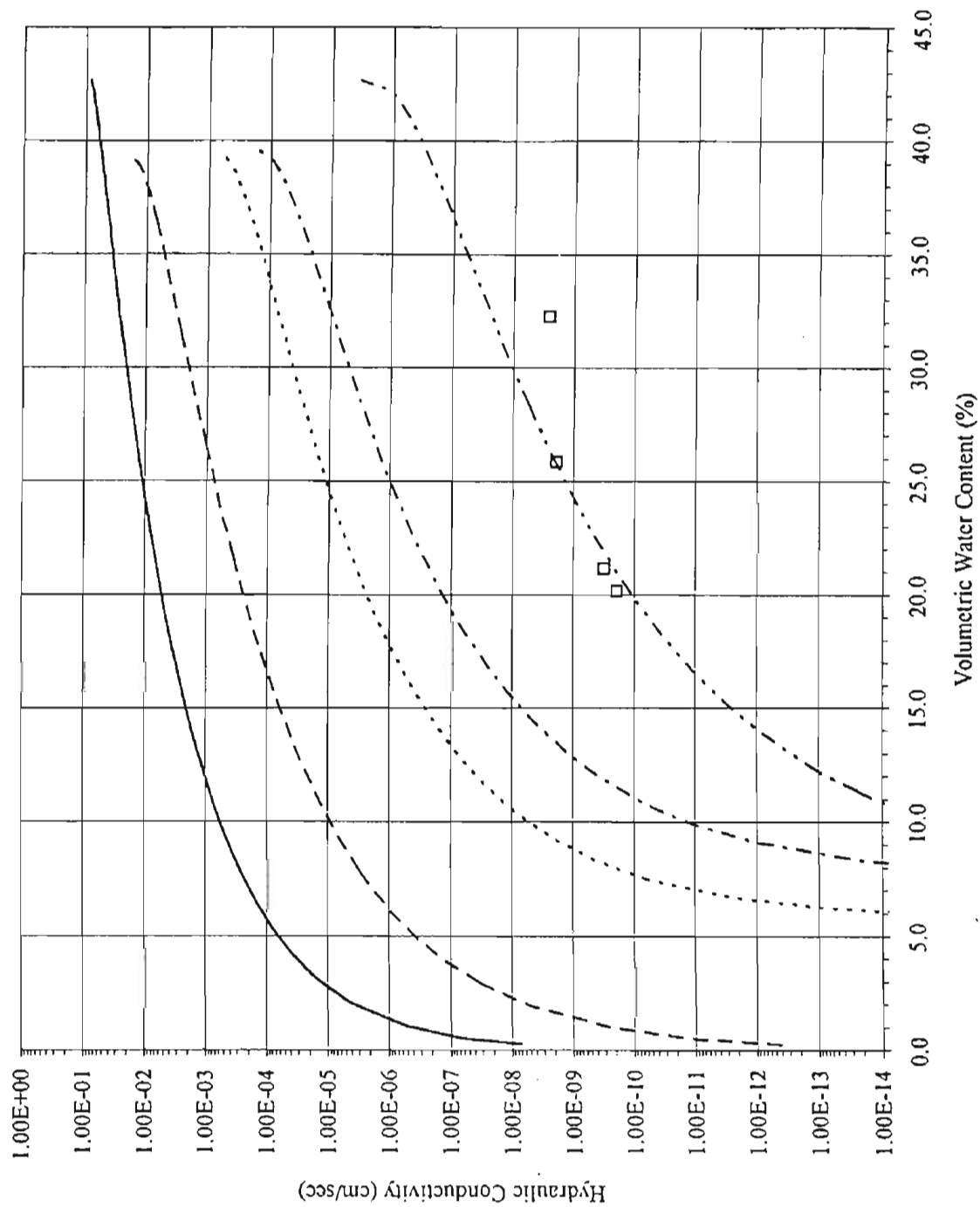


Figure 6a RETC Derived Conductivity Curves

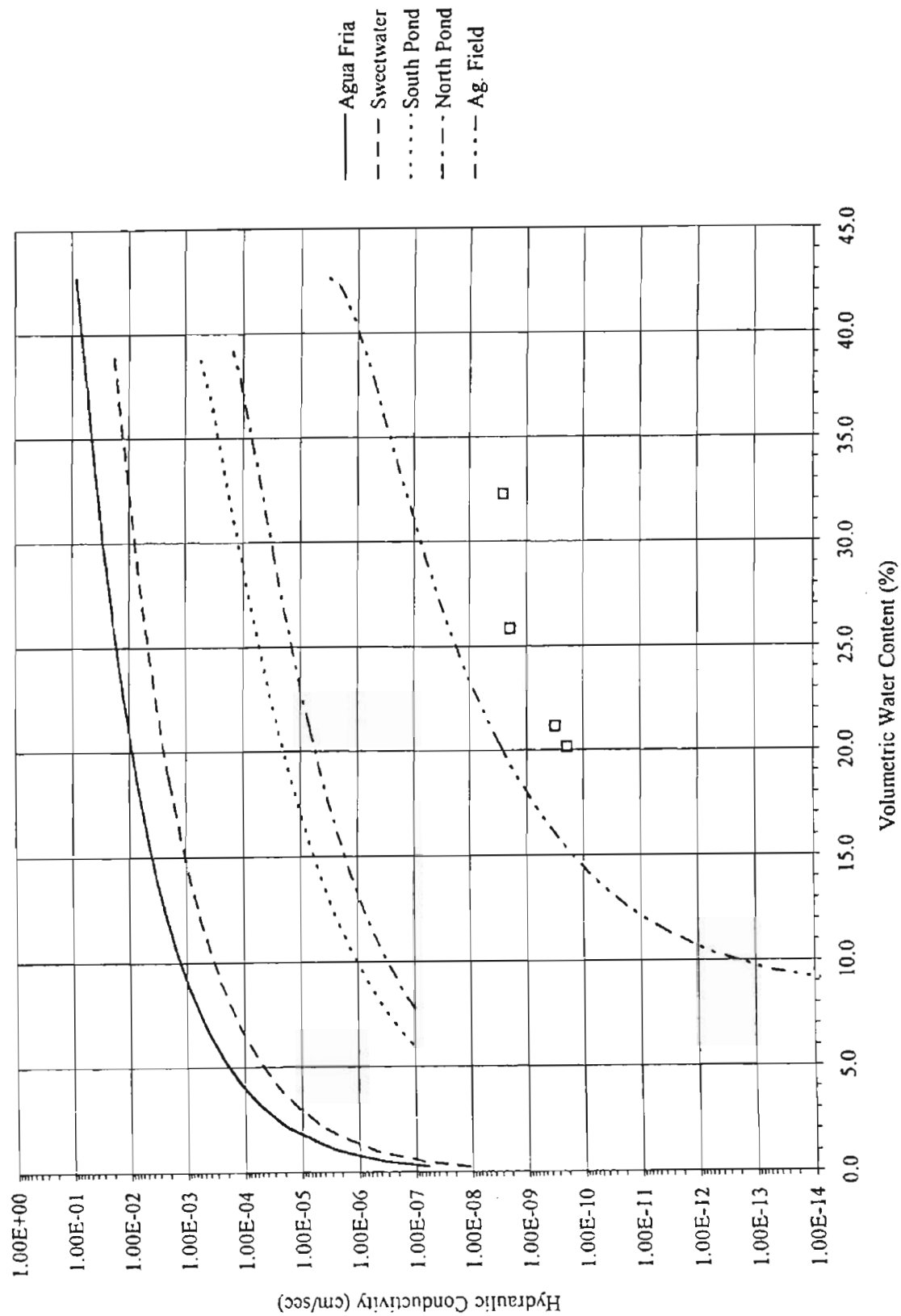


Figure 6b FLOFIT Derived Conductivity Curves

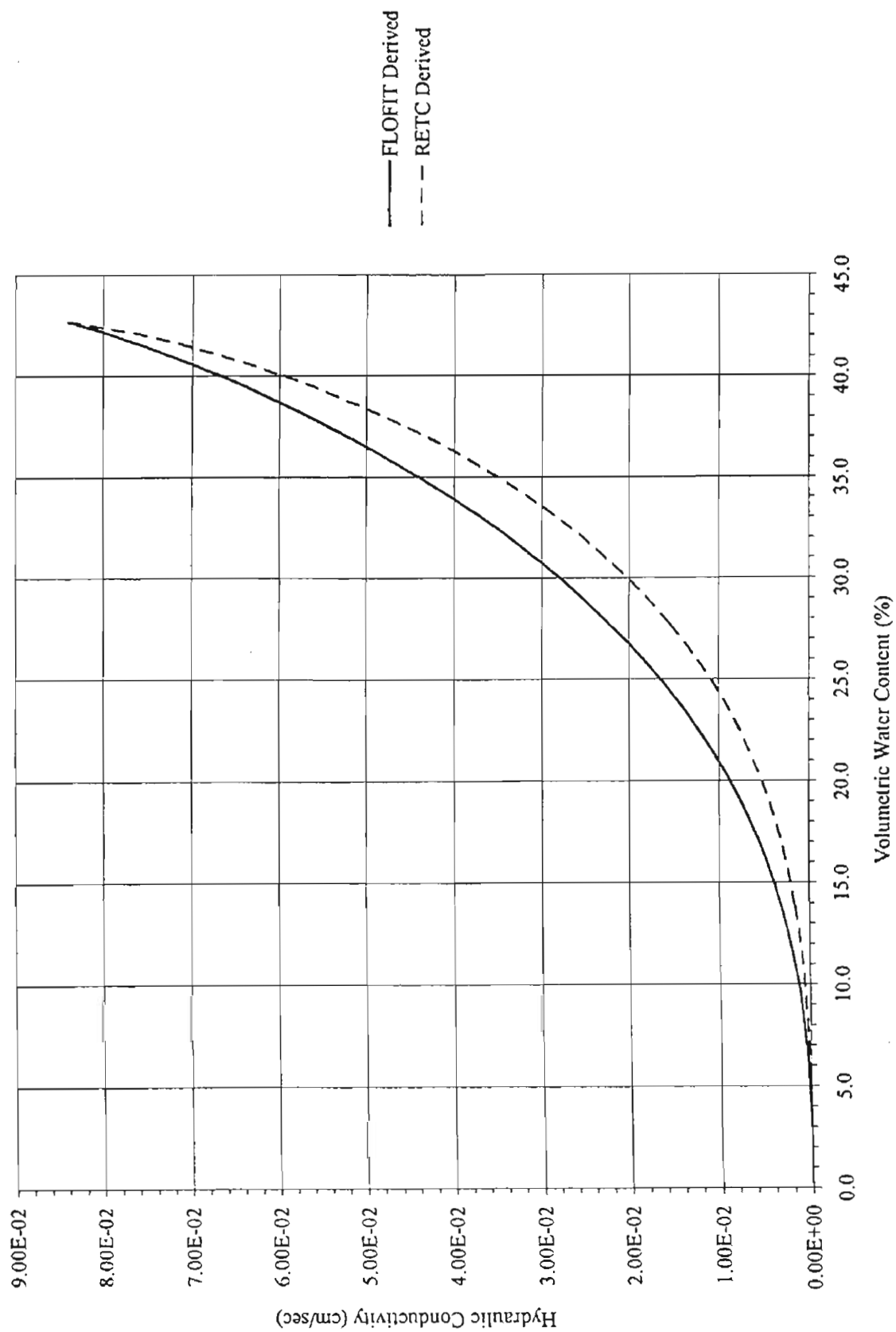


Figure 7a Agua Fria Soil Hydraulic Conductivity

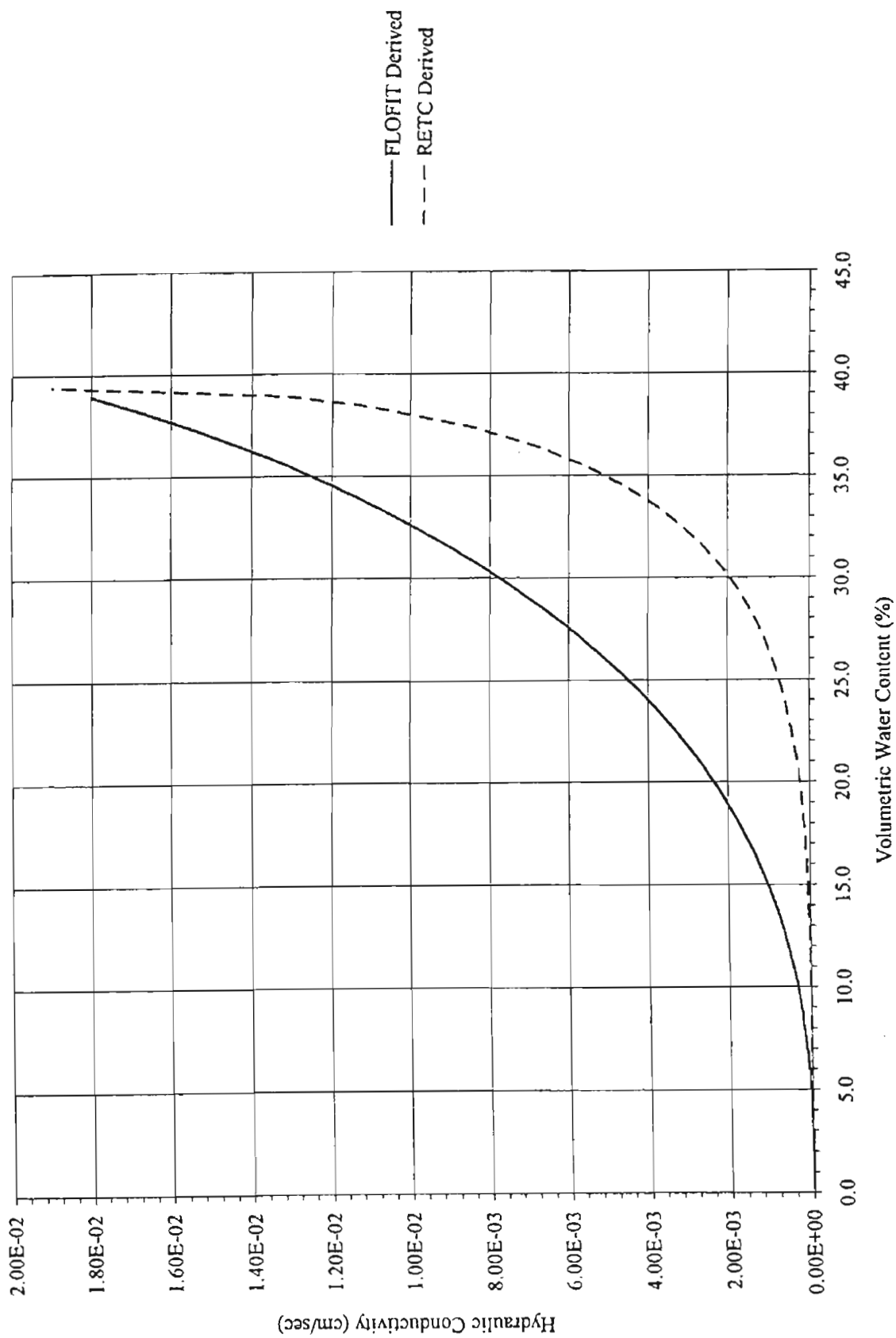


Figure 7b Sweetwater Soil Hydraulic Conductivity

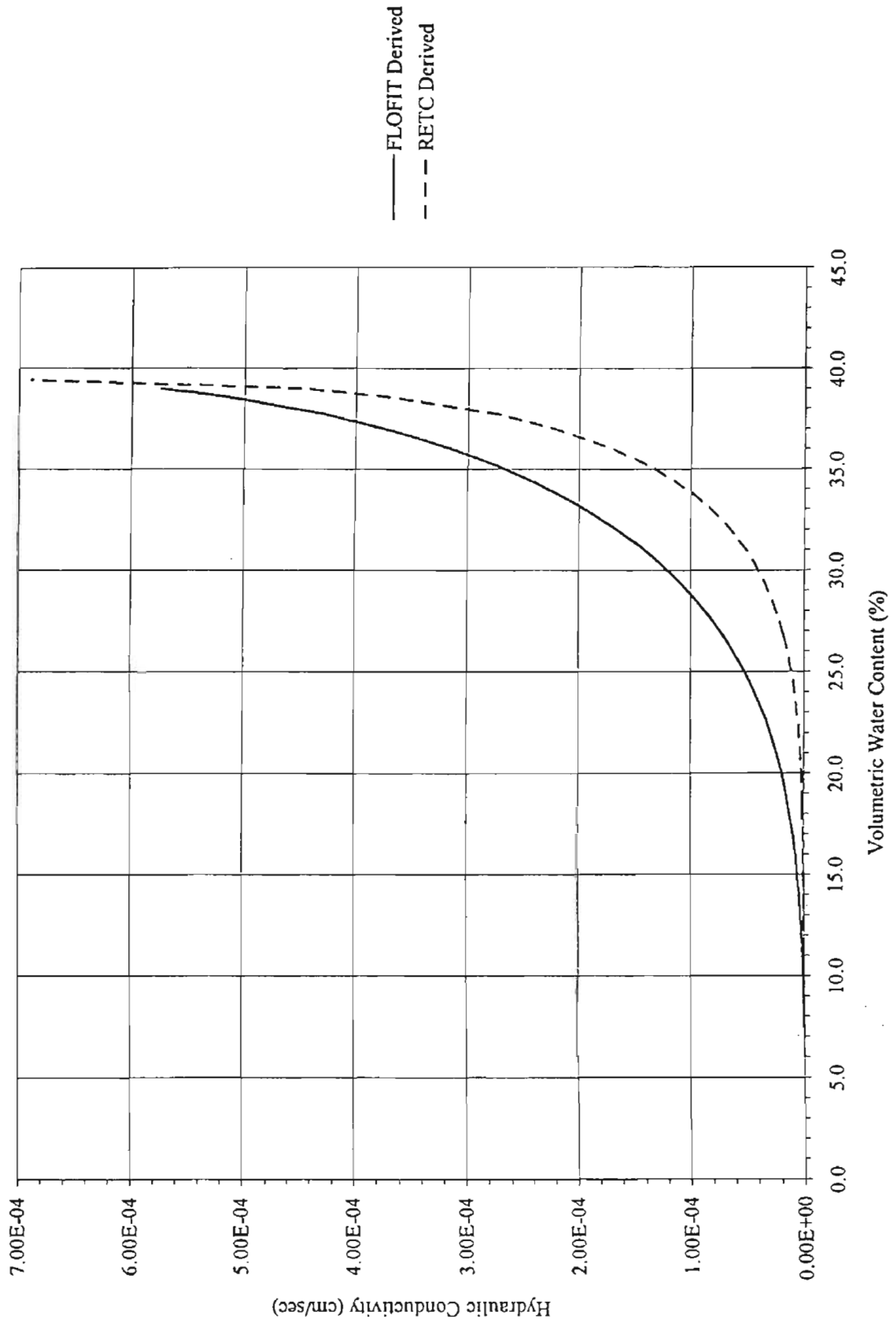


Figure 7c South Pond Soil Hydraulic Conductivity

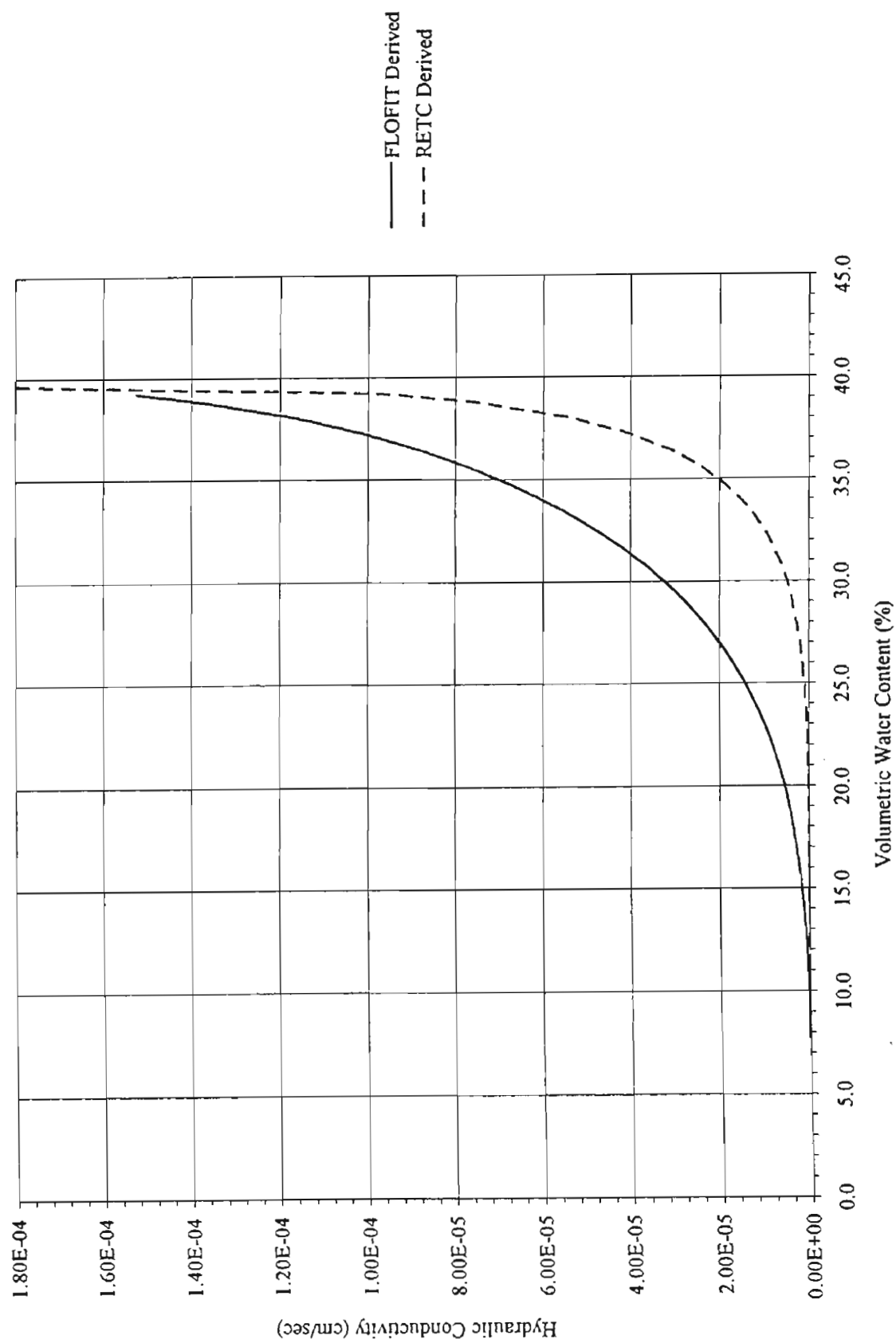


Figure 7d North Pond Soil Hydraulic Conductivity

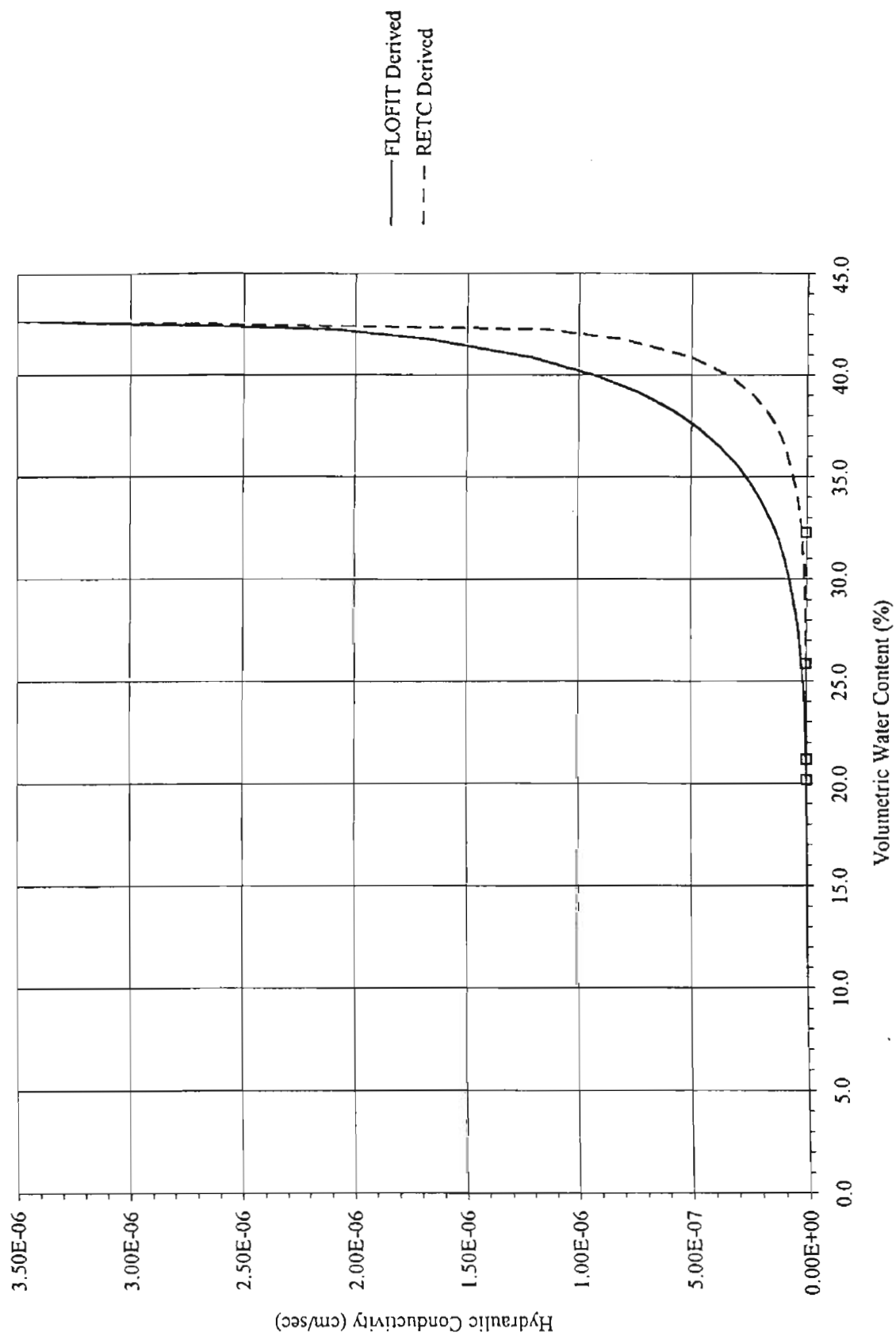


Figure 7e Ag. Field Soil Hydraulic Conductivity

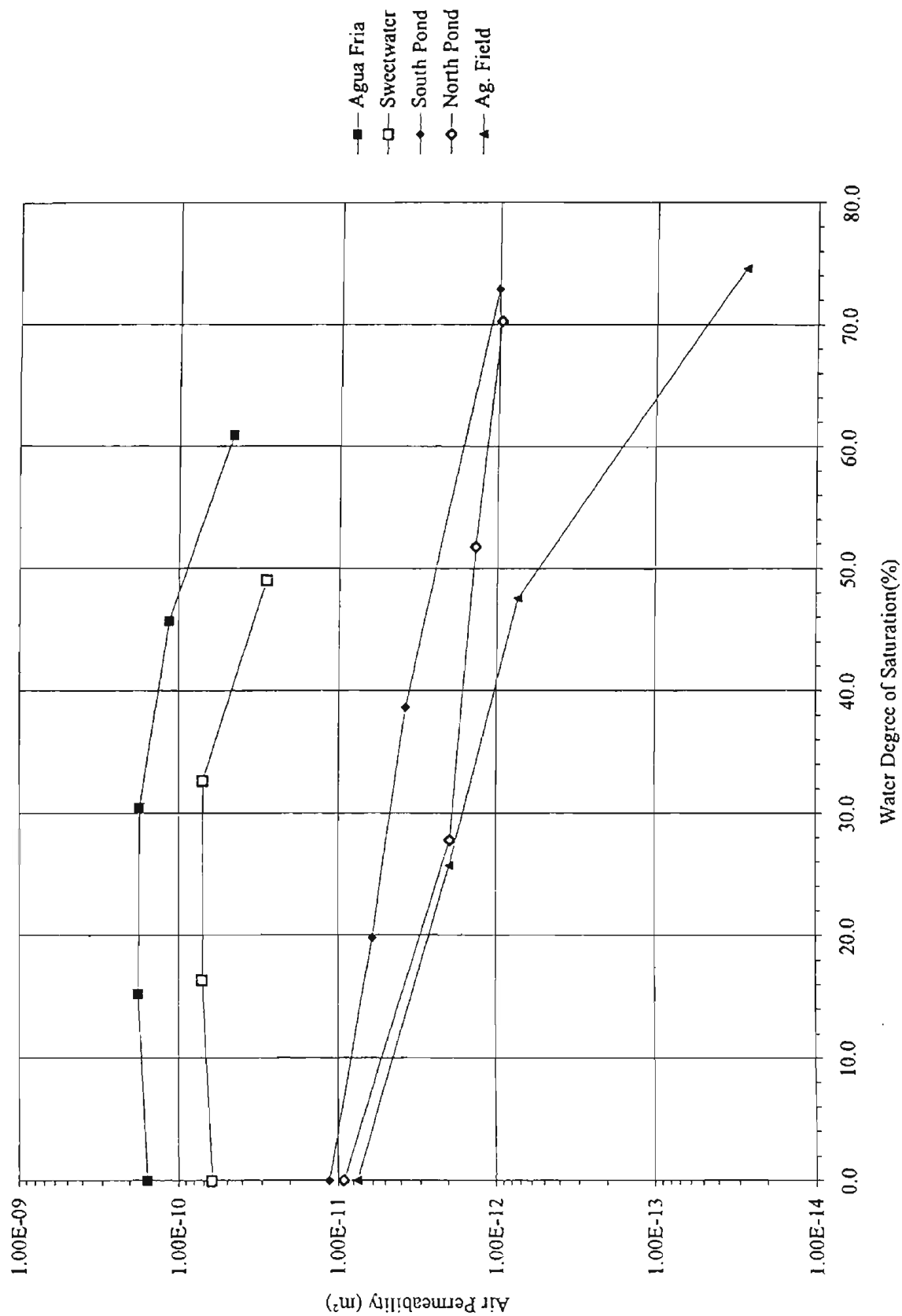


Figure 8 Air Permeability

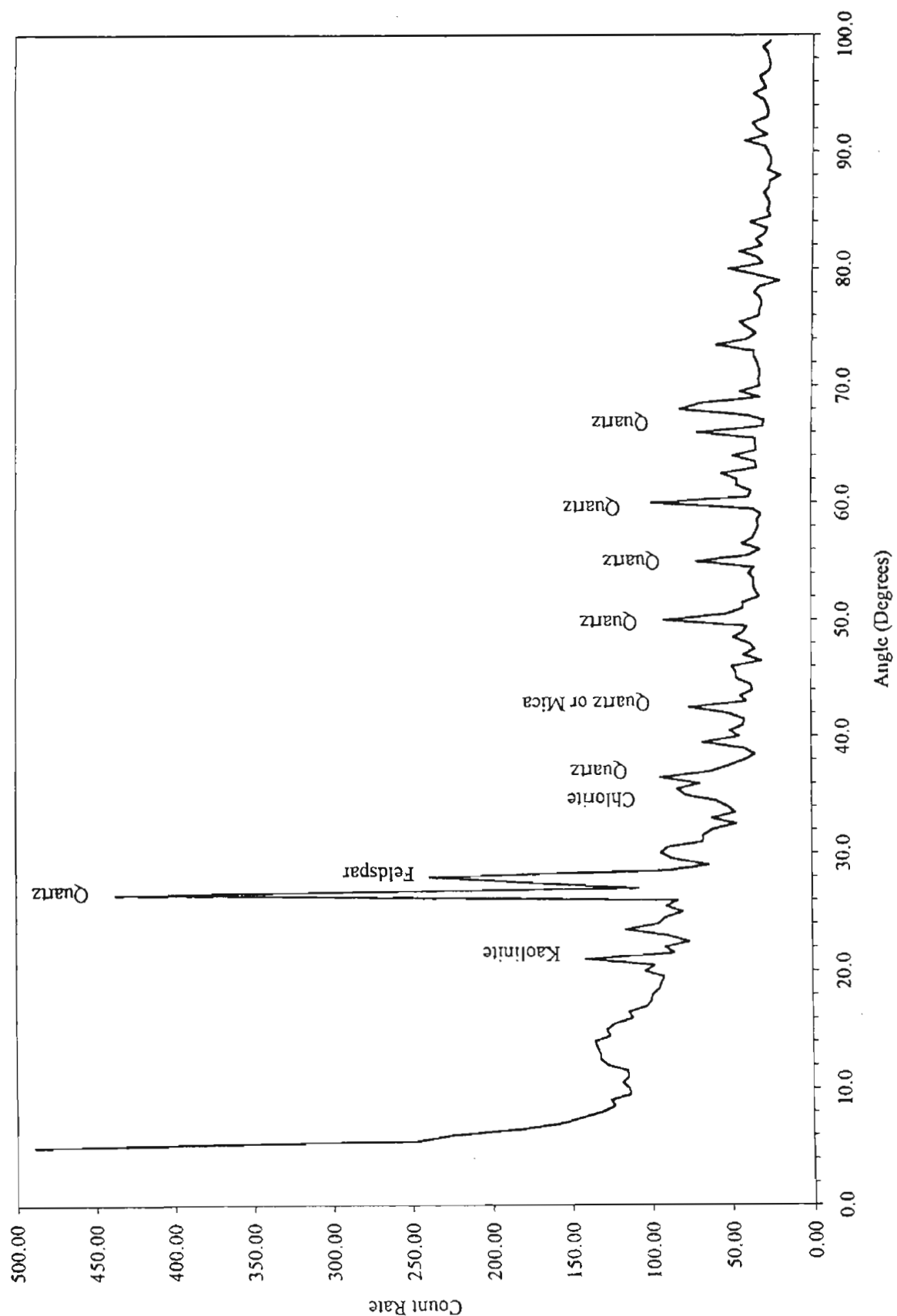


Figure 9a X-Ray Diffraction on South Pond Soil (minus #200)

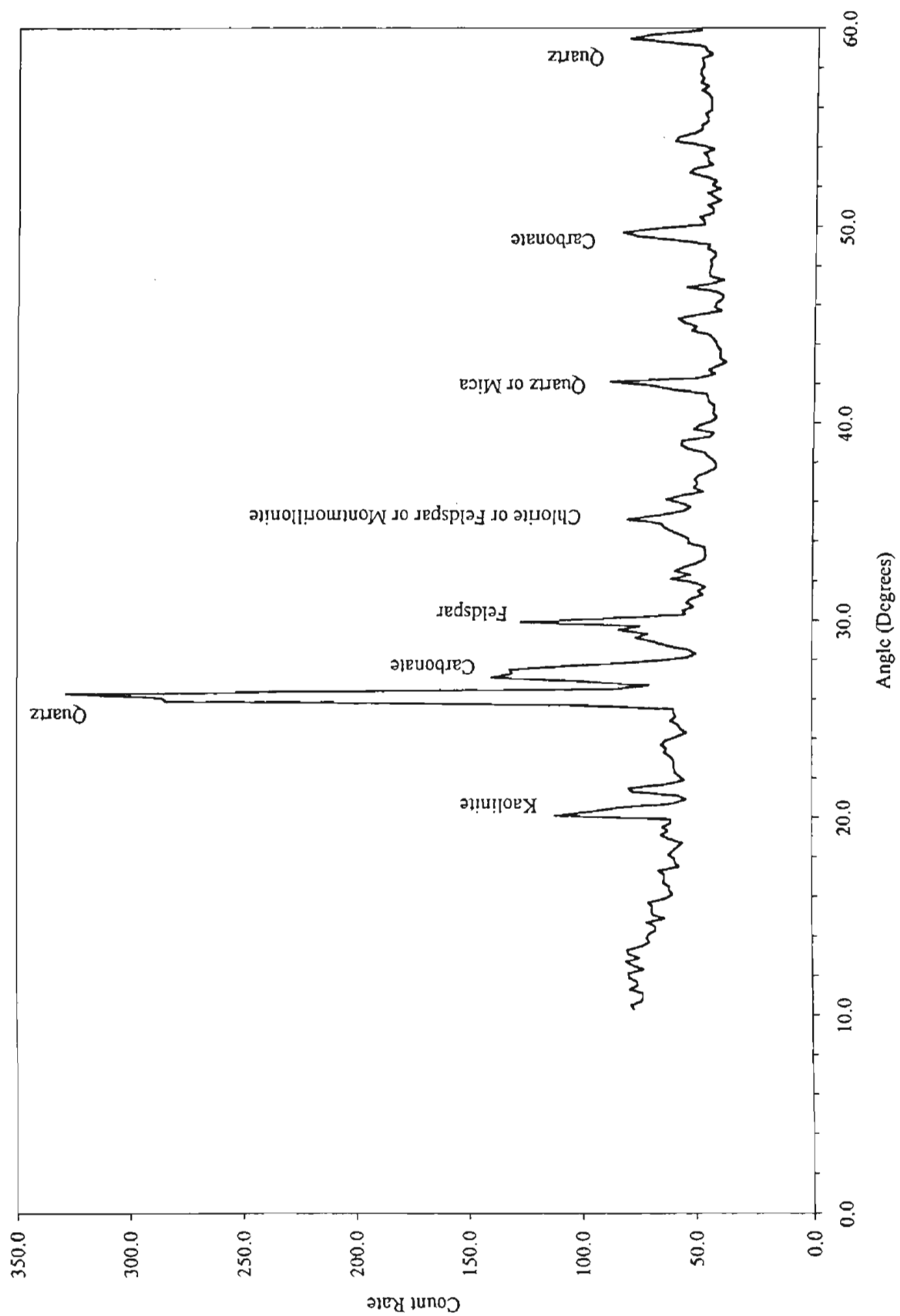


Figure 9b X-Ray Diffraction on North Pond Soil (minus #200)

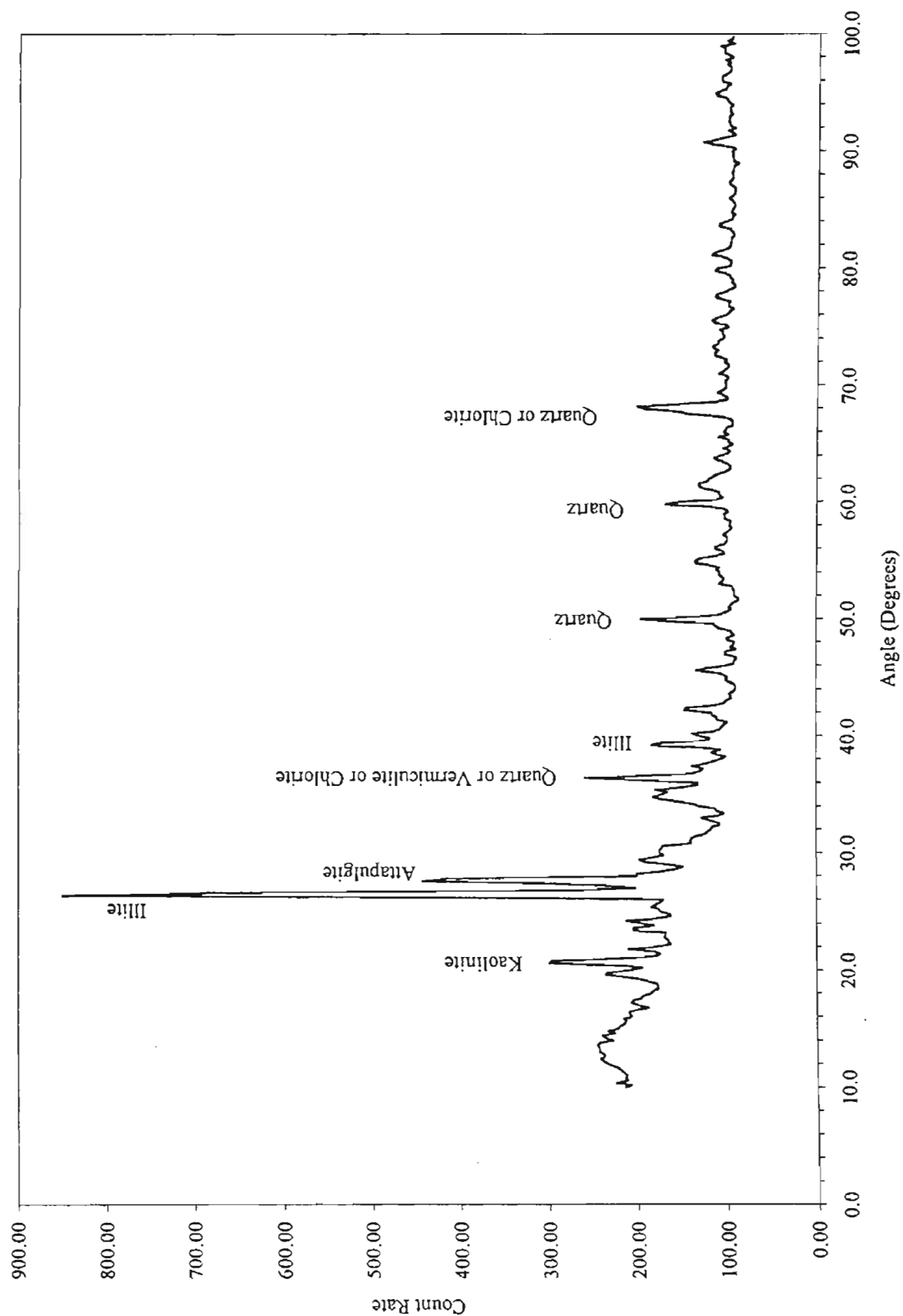


Figure 9c X-Ray Diffraction on Ag Field Soil (minus #200)

CHAPTER 4

THE FATE OF RESIDUAL WASTEWATER ORGANICS DURING SOIL-AQUIFER TREATMENT

OVERVIEW – INTRODUCTION TO THE EXPERIMENTAL DESIGN

Hypotheses

Experiments were designed to test our primary hypotheses that organics removals during SAT are functionally related to soil structure and the degree of above-ground treatment that precedes SAT. Secondary questions surrounded the importance of operational variables (e.g., the length of wet and dry periods that comprise an SAT cycle), oxygen transport and biological activity, etc., to SAT process efficiency and sustainability from the perspective of organics removal. The character and reactivity of persistent organic components with chlorine were also investigated. In the context of this study, it is possible to operationally separate wastewater organics into four broad classes:

- i. those that are essentially always removed during wastewater treatment;
- ii. organics that are not always removed via above-ground wastewater treatment but which are susceptible to biochemical oxidations during soil-aquifer treatment;
- iii. components that frequently survive high-rate biochemical oxidations during above-ground treatment but are removed abiotically, primarily via sorption reactions, during SAT; and
- iv. compounds that are not generally removed via a combination of above-ground treatment and SAT.

Naturally the efficacy of soil-aquifer treatment, in concert with above-ground treatments, is critically dependent on the degree to which wastewater organics fall into categories i-iii and the eventual fate of organics that are removed via chemisorption during SAT (category iii). It is anticipated that reclaimed water that is further polished via soil-aquifer treatment will, as a minimum, be chlorinated prior to reuse for potable purposes, thereby permitting formation of haloorganic compounds such as trihalomethane species and haloacetic acids. Consequently, the nature and

especially the reactivity of the class iv organics (residuals that evade SAT removal mechanisms) with chlorine are important when soil-aquifer treatment leads to potable reuse of reclaimed wastewater.

A number of process variables are available to engineers designing SAT systems for indirect potable reuse of reclaimed water. These include alternative levels of above-ground treatment, travel-time and/or mixing requirements as precursors to reuse, and well-head treatment requirements. Consequently, quantitative representation of process efficiency and costs among contributing processes is a necessary precursor to minimum-cost design of such treatment systems.

Column studies; independent variables

Study independent variables included primarily soil or sediment type and water quality or degree of above-ground treatment that preceded SAT simulations. Due to the excessive number of possibilities, an exhaustive factorial design was abandoned in favor of the select combinations of independent variables indicated in Table 4.1. It is apparent that pre(SAT)-treatments under investigation ranged from primary treatment to ozonated secondary effluent. The type of secondary treatment provided was itself a variable and included both biofilm and suspended growth processes. Effluent from the activated sludge process was further treated via nitrification/denitrification to produce influent for a subset of the SAT simulation experiments.

The effect of soil type on SAT efficiency was investigated by packing column reactors with a series of local soils that ranged in texture from sand to clay. A summary of soil characteristics among the five distinct soil types that were used in these experiments is provided in Chapter 3 to this report. It was hypothesized that the coarse soils would provide relatively favorable hydraulic characteristics and reasonable recharge capacities, while soils with fine grain structure might offer more efficient removal of residual organic material at some cost in the hydraulic capacities of infiltration basins designed for SAT.

Dependent variables

During the two-year length of the project we focussed primarily on changes in water quality that accompany the percolation of wastewater effluent through biologically active surface soils and

Table 4.1

Experimental matrix for column simulations of SAT. Data in the table indicate the combinations of independent variables that were actually studied (e.g., an ozonated secondary effluent was influent to columns packed with Agua Fria sand and Sweetwater sandy loam), the location of the study (University of Arizona vs. Arizona State University) and the type of column used in the simulation (2-meter, 1-meter or 18-cm column length)

pre-treatment level	Agua Fria sand	Sandy loam	North Pond silt	South Pond silt	Field clay
primary		UA: 18-cm ¹ , 1-m ¹			
chlorinated/dechlorinated secondary (trickling filter)	UA: 1-m ^{1,2} , 2-m ¹	UA: 18-cm ¹ , 1-m ¹	UA: 1-m ^{1,2}		UA: 1-m ²
chlorinated secondary (activated sludge)	ASU: 2-m ¹		ASU: 2-m ¹	ASU: 2-m ¹	ASU: 2-m ¹
nitrified/denitrified secondary (activated sludge)	ASU: 2-m ¹		ASU: 2-m ¹	ASU: 2-m ¹	ASU: 2-m ¹
O ₃ -secondary	UA: 1-m ¹	UA: 18-cm ¹ , 1-m ¹			
filtered secondary		UA: 18-cm ¹			

¹repacked homogenized soils

²intact soil cores

representative underlying sediments. To expose possible differences between the performances of repacked and native sediments, a subset of the simulations involved intact sediment cores that were withdrawn from the ground in stainless steel sleeves that were designed for that purpose. Throughout this work, the primary indicators of change in the organic characteristics of treated waters were the concentration of dissolved organic carbon (DOC) and absorbance of ultraviolet light at a wavelength of 254 nm (UVA₂₅₄).

Detention times on the order of hours were employed for SAT simulations. Since theoretical detention times on the order of days to months are characteristic of field operations leading to indirect potable reuse, biodegradable DOC (BDOC) was measured as a more realistic indication of changes in wastewater quality to be expected during SAT under field conditions — i.e., SAT consisting of both percolation through biologically active soils and extended storage in an aquifer prior to withdrawal for reuse. Trihalomethane formation potential (THMFP) was relied upon to indicate the reactivity of residual organics with chlorine at each treatment stage. The test was modified, however, to drastically lower ammonia levels in wastewater effluent prior to THMFP measurements. This modification to standard procedures acknowledges the importance of chlorine dose (as affected by ammonia concentration) as a determinant of trihalomethane development. Organic residuals were characterized in terms of molecular weight signatures before and after several combinations of above-ground treatment and column or BDOC simulations of soil-aquifer treatment.

SUMMARY OF EXPERIMENTAL METHODS AND OBJECTIVES

Reactor design and operation

Several reactor types were used for the simulation of SAT. Column reactors included both one- and two-meter bench and pilot-scale reactors. Columns designed specifically to study reactions in surface soils were only 18 cm in length. A subset of the 1-meter reactors were filled with intact soil cores that were obtained by driving a prefabricated stainless steel sleeve into the ground at select locations for sample withdrawal. The sleeve containing the intact core was then fitted with tensiometers for the depthwise measurement of suction head during the execution of continuous- flow

experiments. Other procedures were identical to those used for SAT simulations involving repacked cores.

It was hypothesized that the uppermost few centimeters of soil eventually form the greatest barrier to infiltration and transport of dissolved organics due to the development of a biologically active surface layer on soils during SAT. This layer is sometimes referred to as *schmutzdecke*. To carry out detailed studies of the *schmutzdecke*, including its respective roles as determinant of basin hydraulic and treatment performances, we designed and built short columns with a total working soil depth of only about 18 cm (7 inches). Instrumentation was concentrated at the top of the column to establish the activity and overall importance of this layer to SAT performance.

Columns were generally operated in two-week cycles – one week wet followed by a dry week to regenerate column hydraulic capacity. During the several cycles that were usually necessary for column acclimation, infiltrating water was initially applied at an approach velocity of 10 ft/d. After ponding was observed, columns were operated at a constant head of approximately 30 cm (12 inches). Routine measurements included influent and effluent DOC and UVA_{254} . Influent and effluent BDOC and THMFP were measured less frequently, and in a few instances these measurements were carried out using fractions derived from molecular weight separations. These and contemporary hydraulic data formed the basis of conclusions regarding the importance of alternative above-ground treatments and soil types on the performance of near-surface soil/sediment strata during SAT.

The mechanism of observed organic removals was also of importance since biological oxidations are considered renewable and hence infinite in capacity whereas water quality improvements due to chemisorption on soil surfaces will eventually exceed the soil capacity and permit chemical breakthrough. In order to set a lower limit on the biochemical contribution to observed SAT-dependent water quality improvements, select columns were operated normally, to establish uninhibited levels of organics removals, after which aerobic microbial activity was restricted by adding inhibitory levels of sodium azide (2.0 mM) to the column influent. The difference in performance efficiencies before and after azide addition was attributed to bacterial respiration.

A complete list of the column reactors used for the simulation of soil-aquifer treatment at the University of Arizona and Arizona State University is provided as Table 4.2. Comments relative to the use of each of the columns over all or portions of the two-year study illustrate how experimental objectives were pursued.

Table 4.2.a

List of long column reactors (1-and 2-meter columns) used at The University of Arizona during SAT situations. A complete description of sorts is provided in Chapter 2. Secondary effluent was obtained from the Roger Road Wastewater Treatment Plant (RRWTP) in Tucson. Primary effluent from RRWTP was filtered through coarse sand prior to use. Microbial amendments were seeded viruses or protozoan pathogens for pathogen-transport experiments. Azide addition was designed to inhibit aerobic respiration. Columns contained either repacked, homogeneous sediments or intact cores

column designation	soil type & structure	soil depth	source water	intended use
1	Agua Fria sand (repacked)	1 m	secondary ¹	biotic
2a	North Pond silt (repacked)	1 m	secondary ¹	biotic
2b	Agricul. Field clay	1 m	secondary ¹	biotic
3	Agua Fria sand (repacked)	1 m	secondary ¹	biotic
4	North Pond silt (repacked)	1 m	secondary ¹	biotic
5	Sweetwater sandy loam (repacked)	1 m	secondary ¹	biotic
6	Sweetwater sandy loam (repacked)	1 m	secondary ¹	biotic/ (O ₂ studies)
7	Agua Fria sand (repacked)	1 m	secondary ¹	microbial amended ²
8	North Pond silt (repacked)	1 m	secondary ¹	microbial amended ²
9	Sweetwater sandy loam (repacked)	1 m	secondary ¹	microbial amended ²
11	Agua Fria sand (repacked)	1 m	secondary ¹	inhibited control
12	North Pond silt (repacked)	1 m	secondary ¹	inhibited control
13	Sweetwater sandy loam (repacked)	1 m	secondary ¹	inhibited control
B-1	Sweetwater sandy loam (repacked)	1 m	filtered primary	biotic (1°)
B-2	Sweetwater sandy loam (repacked)	1 m	filtered primary	biotic (1°)
14	Agua Fria sand,	2 m	secondary ¹	biotic

¹chlorinated/dechlorinated secondary (biotower)

²columns spiked with various pathogens

Table 4.2b

List of column reactors used at Arizona State University during SAT simulations. Source water for all columns was the effluent from the 91st Avenue Wastewater Treatment Plant in Phoenix

column designation	soil type & structure	soil depth	source water	intended use
1SA	Agua Fria sand (repacked)	2-m	secondary ¹	biotic
2SA	Agua Fria sand (repacked)	2-m	secondary ²	biotic
1SMSAC	North Pond silt (repacked)	2-m	secondary ¹	biotic
2SMSAC	North Pond silt (repacked)	2-m	secondary ¹	biotic
3SMSAC	North Pond silt (repacked)	2-m	secondary ²	biotic
1SM	South Pond silt (repacked)	2-m	secondary ¹	biotic
2SM	South Pond silt (repacked)	2-m	secondary ¹	biotic
3SM	South Pond silt (repacked)	2-m	secondary ²	biotic
1CL	Agricul. Field clay (repacked)	2-m	secondary ¹	biotic
2CL	Agricul. Field clay (repacked)	2-m	secondary ²	biotic

¹chlorinated secondary

²nitrified/denitrified secondary

Table 4.2.c

List of short (18-cm) column reactors used at the University of Arizona during SAT simulations. These were designated schmutzdecke columns and used to investigate water quality changes in surface sediments during SAT. Source water for all columns was the RRWTP in Tucson. Ozonation was provided at a level of 1 part O₃ transferred per part DOC as carbon. Tertiary treatment consisted of multi-media filtration. Water from the primary clarifier consisted of a blend of primary and secondary (biotower) effluents since biotower effluents were recycled during routine operations at the RRWTP

column designation	soil type & structure	soil depth	source water	intended use
ASUS	Sweetwater sandy loam (repacked)	18cm	secondary ¹	ASU soil compaction
ASUT	Sweetwater sandy loam (repacked)	18cm	tertiary ²	ASU soil compaction
Sec	Sweetwater sandy loam (repacked)	18cm	secondary ¹	biotic/THM study
O3(1)/Sec2	Sweetwater sandy loam (repacked)	18cm	ozonated secondary ³	biotic/THM study
O3(2)	Sweetwater sandy loam (repacked)	18cm	ozonated secondary ³	biotic/THM study
SC	Sweetwater sandy loam (repacked)	18cm	azide amended secondary ¹	inhibited control
Tert	Sweetwater sandy loam (repacked)	18cm	tertiary ²	biotic
Prim	Sweetwater sandy loam (repacked)	18cm	primary clarifier	biotic
PC	Sweetwater sandy loam (repacked)	18cm	azide amended primary	inhibited control

¹chlorinated/dechlorinated secondary (trickling filter)

²chlorinated/dechlorinated tertiary (sand/carbon filtered secondary)

³1:1 ratio (mgDOC:mgOzone)

Measurements of BDOC were carried out to indicate the extent of biochemical oxidation of organic residuals that could reasonably be expected during an extended period of groundwater storage following the recharge of treated wastewater and to investigate the degree to which alternative above-ground treatments alter the biochemically inert fraction of DOC in wastewater effluent. Although reactor configurations for this work were dissimilar at Colorado University (closed-loop column reactors with recycle) and the University of Arizona (batch reactors), the results of inter-lab calibration efforts showed that the results of BDOC tests at the two universities were comparable. Details of reactor design and operation are provided in Chapter 2 of this report.

Summary of research objectives with respect to organics removals

Use of the reactors and procedures described immediately above permitted us to pursue the following experimental objectives:

- i. Establish the period that was required for evolution of steady column performance during SAT simulations. In this context, steady performance was indicated by a succession of wet/dry cycles in which organics removal efficiencies were statistically indistinguishable.
- ii. Determine through-column removal efficiencies for DOC and UVA_{254} during periods of steady column performance as functions of soil type and degree of above-ground treatment.
- iii. Develop depth-dependent profiles of column (organic) parameters in order to establish the importance of the uppermost, biologically active sediments to overall SAT performance.
- iv. Determine the degree to which biochemical processes contribute to the overall removal of organics during simulated SAT.
- v. Compare performance characteristics in repacked and intact soil columns using the same source material.
- vi. Establish the magnitude of the fraction of residual wastewater organics that is refractory (resistant to removal via sorption or biochemical oxidation) during simulated SAT. It was expected that the refractory fraction would be sensitive to the selection of above-ground treatment options, particularly ozonation.

vii. Estimate the degree to which refractory organics contribute to trihalomethane formation during chlorination of recovered waters following soil-aquifer treatment.

viii. Investigate the probable nature of compounds or classes of compounds that comprise the refractory components of wastewater effluents. This work was pursued using a series of novel analytical procedures at Colorado and Stanford Universities.

RESULTS AND DISCUSSION

Experimental results are organized along the lines of the project research objectives in order to facilitate the display and discussion of pertinent data.

Column maturation. Only representative data are provided. A complete set of experimental results, including those corresponding to periods of column maturation, is appended to this report.

Scatter plots representing organics removal efficiencies (through-column removals of DOC and UVA_{254}) as functions of infiltration rates (not shown) suggest that there is no strong correlation present. Because the mean hydraulic residence time in our column reactors was inversely related to infiltration rate, there is at best only a weak relationship between the residence time and removal efficiency. This somewhat unexpected finding suggests that organics that are removed in the one-meter columns are either very biodegradable in nature or that rapid sorption plays a more important role in organics attenuation than was indicated by previous studies. The mean hydraulic residence time in our columns was on the order of 1 hour at the start of the wet cycles and increased to about 10 hours at the end of a week as infiltration rates decreased. The lack of dependence of organics removals on column infiltration rate (or mean hydraulic retention time) enabled us to lump data obtained over entire cycles for the purpose of subsequent statistical comparisons.

Agua Fria sand

Average through-column removals (percent reduction) of DOC and UVA_{254} for the three one-meter columns packed with Agua Fria sand are given in Table 4.3. Figures 4.1 through 4.3 show mean values with error bars (one standard deviation) for influent and effluent DOC and UVA_{254} for

Table 4.3

Through-column percent reduction for DOC and UVA₂₅₄ for one-meter (UA) columns packed with Agua Fria sand as a function of wet cycle number. Values shown represent averages approximately seven daily measurements for each wet cycle. All columns were fed secondary effluent from the Roger Road Wastewater Treatment Plant in Tucson

Wet Cycle #	Column #					
	#3		#7		#11	
	DOC	UV254	DOC	UV254	DOC	UV254
1	21.7	19.3	21.0	17.4	18.6	13.8
2	31.3	12.7	37.0	18.9	35.6	8.1
3	44.2	23.6	58.8	34.3	46.5	9.3
4	21.3	15.9	48.6	34.6	23.1	4.9
5	19.9	17.4	52.7	27.5	22.7	3.4
6	27.4	25.4	31.7	12.1	34.3	1.5
7	42.8	20.0	34.2	19.2	31.7	5.3
8	43.1	22.6	33.6	15.9	36.5	5.8
9	49.2	25.9	40.6	16.8	48.6	2.77
10	39.6	29.2	28.8	27.8	28.6	11.4
11	39.8	24.7	41.9	20.6	38.6	5.4
12	34.8	11.6	36.8	-	18.5	-
13	44.6	8.9	33.0	10.4	-	-
14	52.3	23.9	21.4	13.3	22.3	8.2
15	44.7	4.1	22.9	-	21.1	30.3
16	43.6	21.8	29.0	9.6	-	10.4
17	52.1	26.0	-	-	35.8	3.8
18	32.9	19.9	69.1	-	2.1	3.2
19	48.9	23.0	-	-	14.9	11.2
20	48.5	12.6	-	-	20.5	4.5
21	44.3	19.3	-	-	-	-

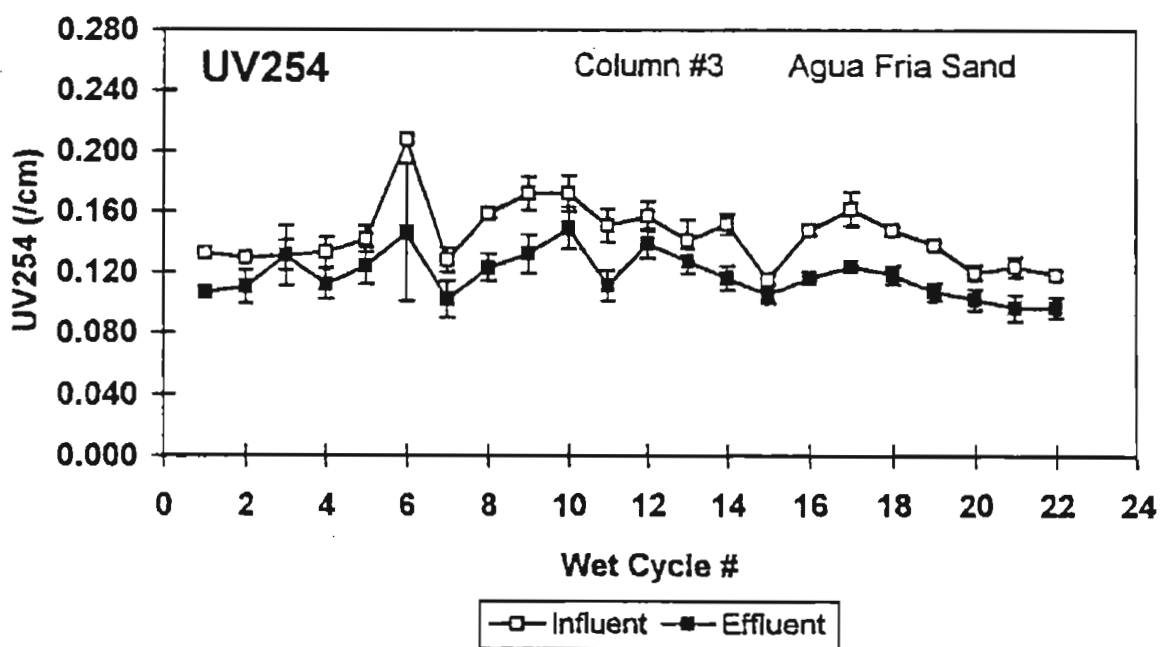
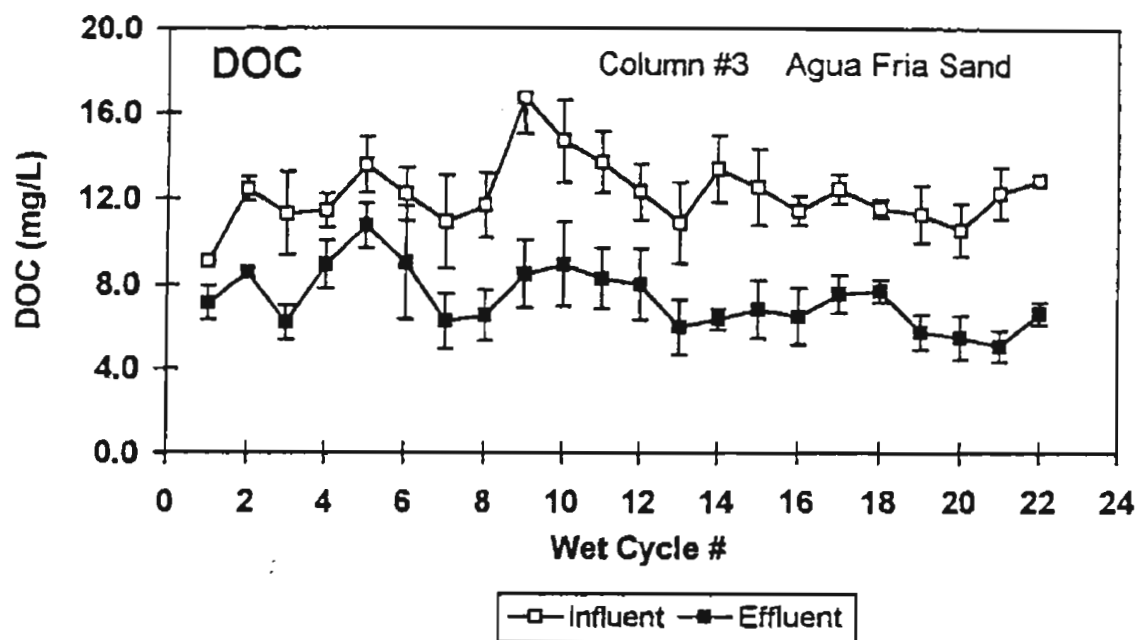


Figure 4.1 Influent and effluent levels of dissolved organic carbon and ultraviolet-absorbing material as functions of cycle # in a one-meter (UA) column (#3) containing Agua Fria sand. The column was fed secondary effluent from the Roger Road Wastewater Treatment Plant in Tucson

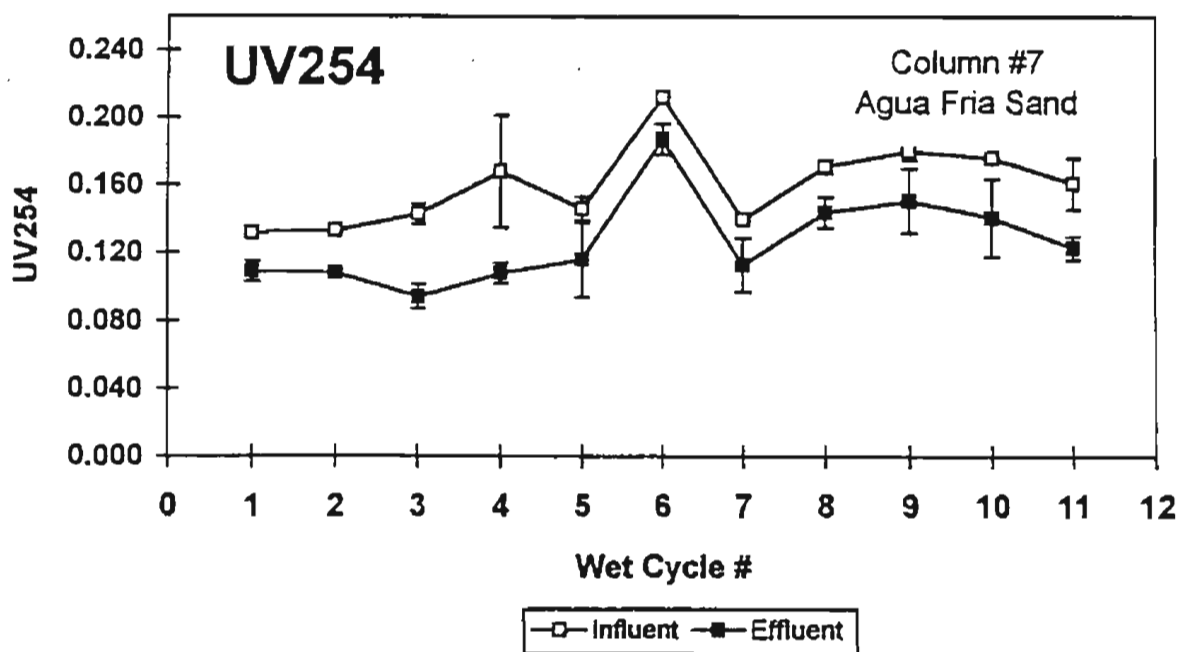
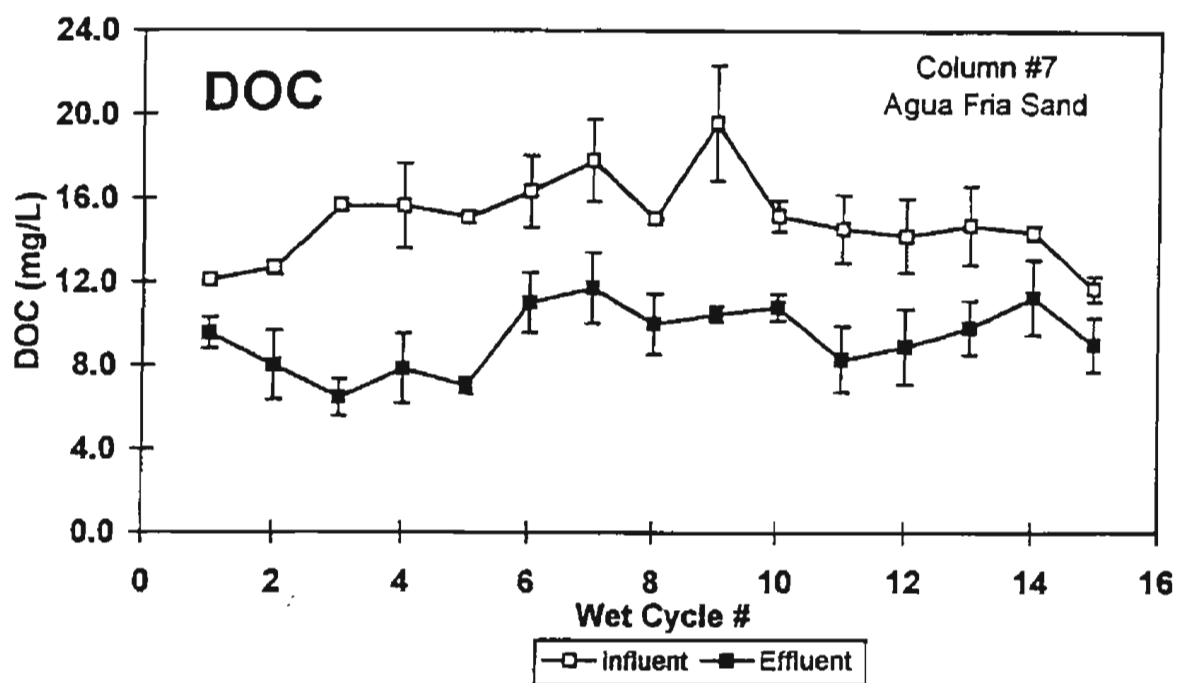


Figure 4.2 Influent and effluent levels of dissolved organic carbon and ultraviolet-absorbing material as functions of cycle # in a one-meter (UA) column (#7) containing Agua Fria sand. The column was fed secondary effluent from the Roger Road Wastewater Treatment Plant in Tucson

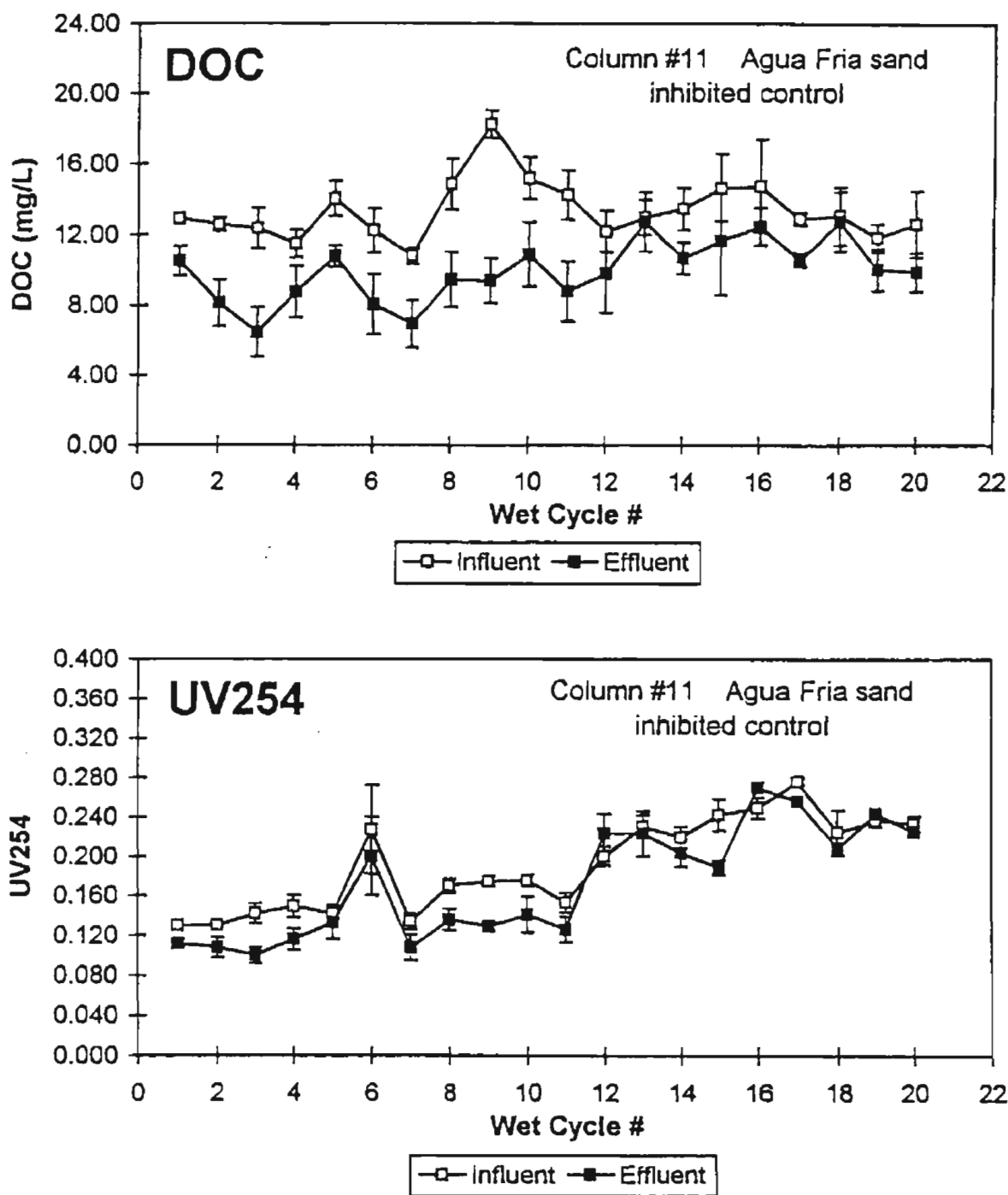


Figure 4.3 Influent and effluent levels of dissolved organic carbon and ultraviolet-absorbing material as functions of cycle # in a one-meter (UA) column (#11) containing Agua Fria sand. The column was fed secondary effluent from the Roger Road Wastewater Treatment Plant in Tucson. Addition of 2.0 mM Na azide was initiated in cycle #12 and continued throughout the remainder of the record shown. Points represent the arithmetic mean of at least seven measurements during individual cycles. Error bars encompass two standard deviations. Where no error bars are visible, a standard deviation lay within the symbol

the three sand columns (#3, 7, and 11) during the first cycles of operation. There appear to be significant increases in removal efficiency of DOC and somewhat less significant increases in removal of UV_{254} .

Time-series analyses (linear regressions) were performed to determine if the soil columns entered a period of "steady" operation during the period of operation shown. Results from time-series analyses for through-column removal of DOC and UVA_{254} are given in Table 4.4. Two regression analyses were performed on each column for each parameter. The first was based on the complete data set (percent reduction values for DOC or UVA_{254}) collected over the period of column operation corresponding to cycles #1-11. A second regression test was performed using a subset of these data, corresponding to the last 3 to 6 cycles of operation for each column (i.e., including only that portion of data over which there appeared to be steady levels of removal, see Figures 4.1 - 4.3). Results of regression analyses indicate that column performances were "steady" in terms of through-column removal of DOC and UV_{254} during the last 3-6 cycles of operation. Periods of operation representing steady behavior for removal of DOC encompass cycles 7 to 11 for column #3 ($P=0.775$), cycles 6-11 for column #7 ($P=0.959$) and cycles 6-11 for column #11 ($P=0.618$). Periods of operation in which removals of UVA_{254} were steady include cycles 7-11 for column #3 ($P=0.967$), cycles 6-11 for column #7 ($P=0.682$) and cycles 6-11 for column #11 ($P=0.965$) (Table 4.4).

Please note that in these statistical tests our null hypothesis was always that the slope of the curve representing cycle- or time- dependent column removal efficiency was zero. The P values reported represent the probability of error if the null hypothesis is rejected. That is, values approaching 1.0 strongly suggest that there is no time dependence in these data. Very small values suggest that values increased or decreased systematically with time.

Sweetwater Sandy Loam

Although infiltration rates typically varied from around 3-4 ft/day to less than 0.5 ft/day during wet cycles in these columns, again there do not appear to be corresponding, infiltration-rate-dependent differences in column efficiency. Average through-column removals (percent reduction) of DOC and UVA_{254} for the three Sweetwater soil columns are given in Table 4.5. Figures 4.4 through 4.6 show mean values with error bars (one standard deviation) for influent and effluent DOC

Table 4.4

Results from time-series analyses for through-column percent removals of DOC and UVA_{254} , for columns containing Agua Fria sand. All columns received secondary effluent from the Roger Road Wastewater Treatment Plant in Tucson. For the regression analyses represented, cycle # was the independent variable and through-column percent removal was the dependent variable. P-values represent the probability of error in rejecting the null hypothesis (percent removal is independent of cycle number).

parameter	average	std. dev.	P-value	R^2	n	cycles tested
column #3						
DOC	34.85	13.91	0.002	0.153	67	1-11
	42.65	9.90	0.775	0.003	33	7-11
UVA_{254}	21.21	10.28	0.306	0.017	64	1-11
	22.61	7.87	0.967	5.6×10^{-5}	32	7-11
column #7						
DOC	40.75	13.64	0.006	0.118	62	1-11
	35.06	11.55	0.959	8.0×10^{-5}	35	6-11
UVA_{254}	22.59	10.03	0.031	0.071	66	1-11
	21.14	6.71	0.682	0.009	21	9-11
column #11						
DOC	35.17	12.03	0.406	0.011	67	1-11
	36.82	10.72	0.618	0.007	39	6-11
UVA_{254}	19.06	8.17	0.778	0.001	66	1-11
	19.84	7.45	0.965	6.5×10^{-5}	33	7-11

Table 4.5

Results from time-series analyses for through-column percent removals of DOC and UV_{254} for columns containing Sweetwater sandy loam

parameter	average	std. dev.	P-value	R ²	n	cycles tested
column #5						
DOC	34.05	13.93	3.8×10^{-5}	0.224	63	1-11
	41.35	13.21	0.875	0.001	37	6-11
UVA_{254}	13.10	8.05	4.1×10^{-7}	0.349	62	1-11
	19.47	6.43	0.589	0.011	29	7-11
column #9						
DOC	46.54	13.61	0.051	0.058	66	1-11
	49.54	15.24	0.575	0.008	38	6-11
UVA_{254}	20.93	9.73	0.001	0.160	64	1-11
	25.51	8.55	0.283	0.039	31	7-11
column #13						
DOC	31.40	13.36	3.3×10^{-11}	0.505	65	1-11
	41.54	9.40	0.509	0.015	31	7-11
UVA_{254}	14.06	7.59	9.5×10^{-6}	0.262	67	1-11
	18.24	7.09	0.250	0.042	33	7-11

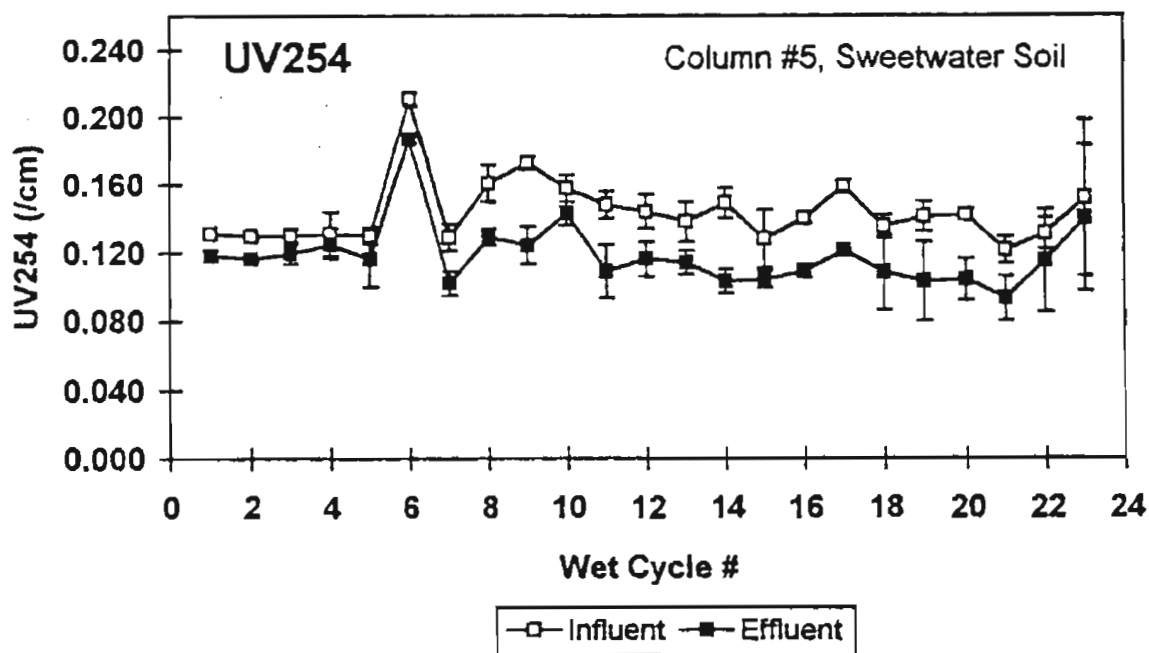
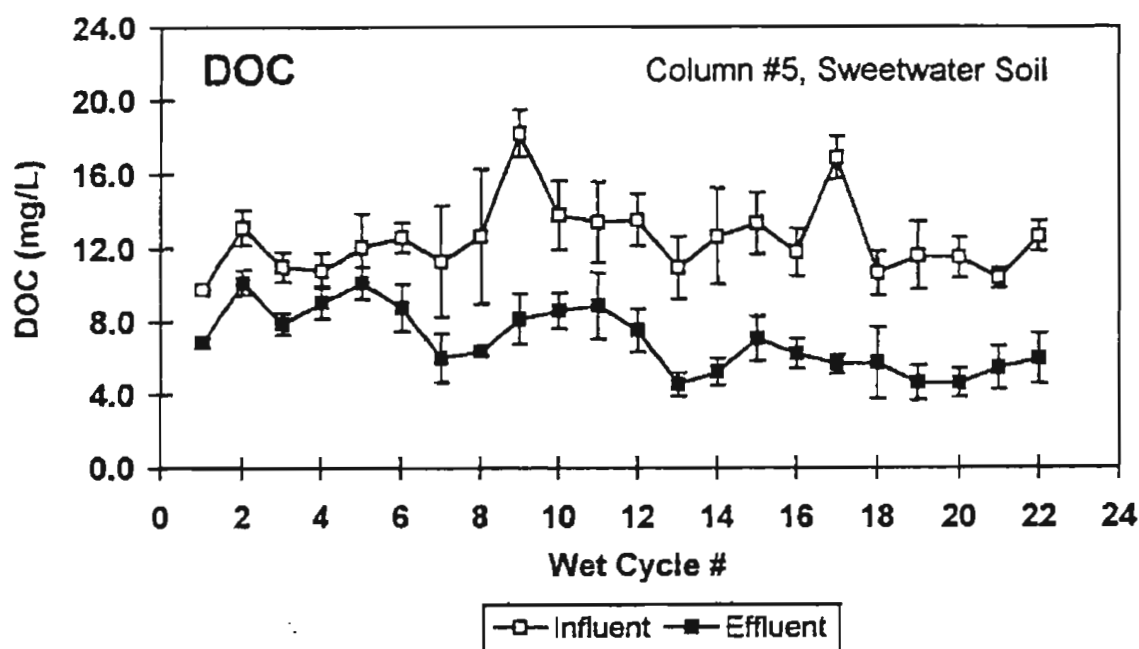


Figure 4.4 Influent and effluent levels of dissolved organic carbon and ultraviolet-absorbing material as functions of cycle # in a one-meter (UA) column (#5) containing Sweetwater sandy loam. The column was fed secondary effluent from the Roger Road Wastewater Treatment Plant in Tucson. Points represent the arithmetic mean of at least seven measurements during individual cycles. Error bars encompass two standard deviations. Where no error bars are visible, a standard deviation lay within the symbol

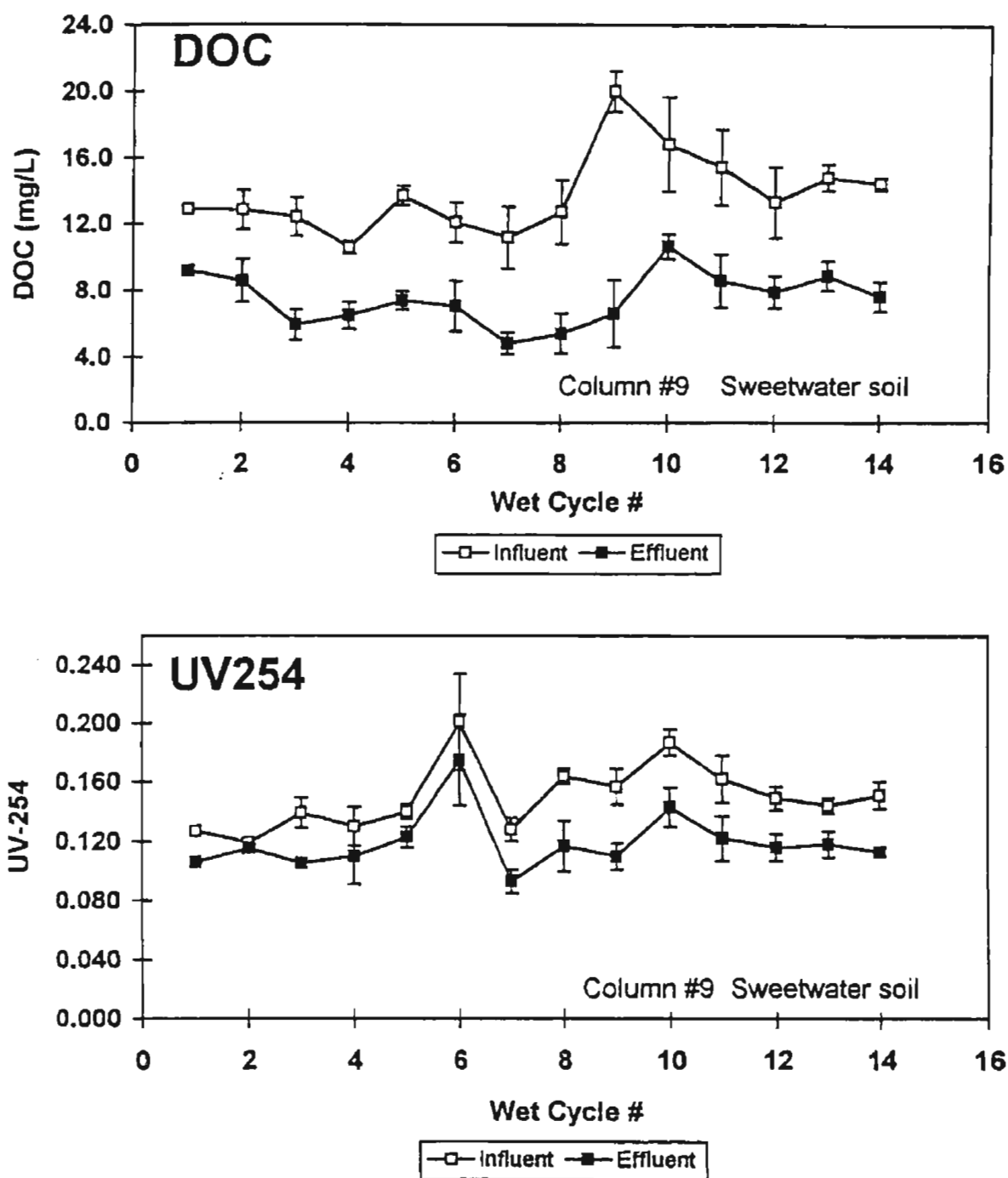


Figure 4.5 Influent and effluent levels of dissolved organic carbon and ultraviolet-absorbing material as functions of cycle # in a one-meter (UA) column (#9) containing Sweetwater sandy loam. The column was fed secondary effluent from the Roger Road Wastewater Treatment Plant in Tucson. Points represent the arithmetic mean of at least seven measurements during individual cycles. Error bars encompass two standard deviations. Where no error bars are visible, a standard deviation lay within the symbol

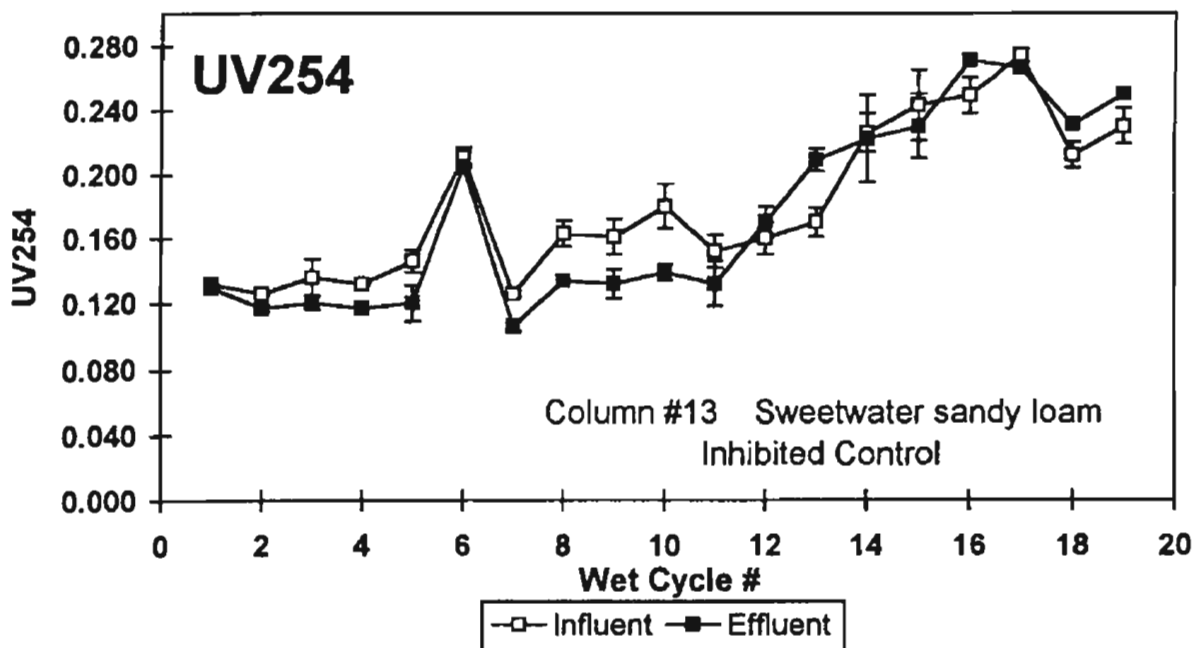
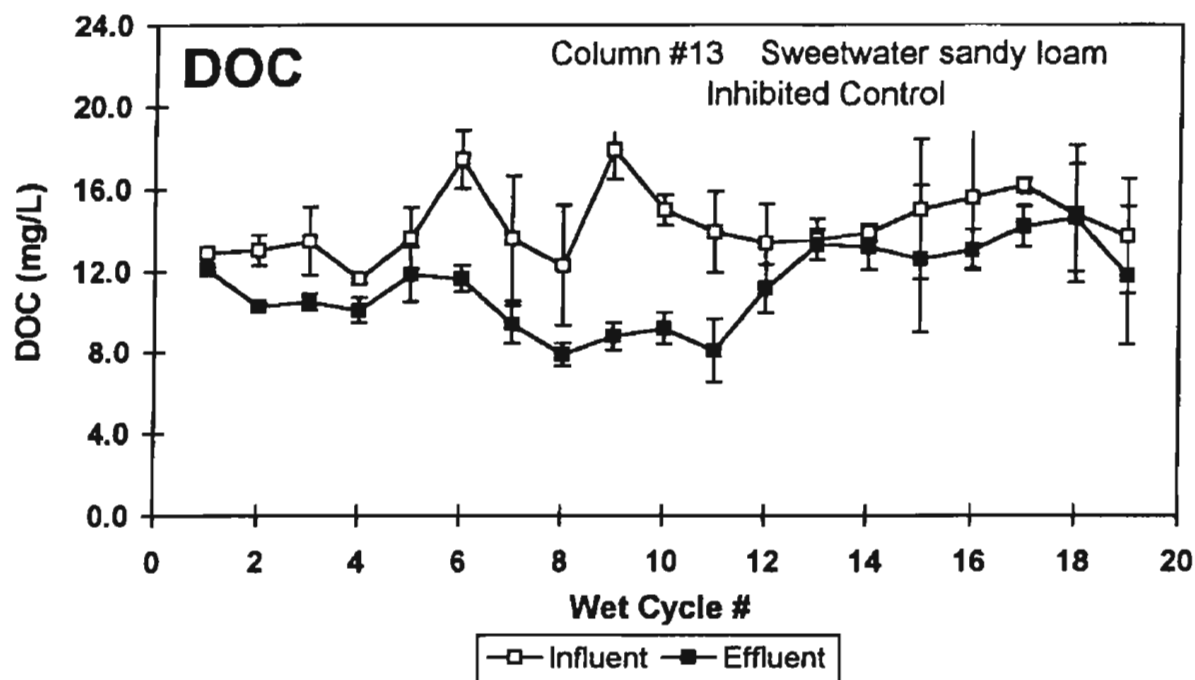


Figure 4.6 Influent and effluent levels of dissolved organic carbon and ultraviolet-absorbing material as functions of cycle # in a one-meter (UA) column (#13) containing Sweetwater sandy loam. The column was fed secondary effluent from the Roger Road Wastewater Treatment Plant in Tucson.

and UVA_{254} for the three Sweetwater soil columns during the first cycles of operation. Removal efficiencies of DOC and UVA_{254} again apparently increased over time when the entire period of data collection is considered (Table 4.5). The increased efficiency of removal may reflect the gradual development of populations of bacteria that are better able to utilize the organic residuals present in secondary effluent or simply increases in bacterial numbers. Results from time-series analyses (performed as described above) indicate that the columns containing Sweetwater sandy loam also entered a period of steady performance for removal of DOC and UVA_{254} (Table 4.5). Periods of operation corresponding to steady performance for removal of DOC are cycles 6 to 11 for column #5 ($P=0.875$), cycles 6-11 for column #9 ($P=0.575$) and cycles 7-11 for column #13 ($P=0.509$). Periods of operation corresponding to steady performance for removal of UVA_{254} are cycles 7 to 11 for column #5 ($P=0.589$), cycles 7-11 for column #9 ($P=0.283$) and cycles 7-11 for column #13 ($P=0.250$).

In summary, statistical analyses of the rather uneven record of early performance by one-meter columns packed with the coarse Agua Fria sand suggest that steady column performance in terms of DOC and UVA_{254} removal efficiencies is not achieved until sometime after the fifth or sixth wet/dry cycle. Column acclimation thus occurred over approximately three months. Selecting column #3 as typical of SAT simulations of this type (admittedly a stretch in some respects), then DOC removals averaged 28.1 percent over the first six cycles of operation and 42.7 percent during cycles 7-11. Corresponding values for UVA_{254} were 19.8 percent and 21.5 percent. The performance of columns packed with the Sweetwater sandy loam was similar. That is, steady performance is evident after perhaps six cycles of operation. Selecting column #5 as typical, DOC removal averaged 24.1 percent in the first six cycles and 42.3 percent in cycles 7-11. Corresponding removal efficiencies for UVA_{254} were 9.6 percent and 19.7 percent.

Acclimation in the (ASU) two-meter columns

There is also clear evidence of column acclimation in the performance records of the 2-meter columns operated at Arizona State University, although time-dependence was not analyzed statistically. Average effluent concentrations of total organic carbon (TOC) and UVA_{254} declined rapidly during the first nine or ten cycles of operation involving both the North Pond and South Pond

silts (Figures 4.7-4.9). This improvement was independent of the source of influent to the columns (nitrified/denitrified versus chlorinated secondary). Since the column effluent concentrations of TOC and UVA_{254} were considerably higher than representative influent values, it is certain that organics were leached from the silts during the first 6 to 7 months of column operation (Figure 4.10). Consequently, observed time-dependent improvements in effluent quality may not have been due to acclimation or growth of microbial populations. There appear to be no differences in effluent quality based on sediment type (North Pond versus South Pond silt) or on column influent quality (chlorinated secondary versus nitrified/denitrified effluent).

Corresponding time-dependent records for the two-meter (ASU) column packed with Agua Fria sand indicate that leaching of organics was minimal (Figure 4.11a&b). Effluent concentrations of TOC and UVA_{254} were relatively steady throughout the period of performance shown. The deterioration of effluent quality that was observed after about cycle #20 was probably related to efforts to create ponding atop the sand columns. At no point, did ponding occur, even at the highest feasible rates of water application, due to the permeability of Agua Fria sand. In pursuit of pond formation, algae were added to the column feed at about cycle #20. Thereafter, deterioration in column effluent organic water quality parameters was probably due to degradation of algae and liberation of soluble organic components. The effluent record appears to be independent of influent quality.

Effluent data from columns packed with Agricultural Field clay indicate that column acclimation was incomplete, even after 15 cycles of operation (Figure 4.11c&d). Due to the poor hydraulic conductivity of these soils and resultant low flow (Chapter 2), the organic character of these effluents was dominated by leaching throughout the period of operation shown. Nothing can be said about the eventual organics removal efficiencies of the clay soils, and they will receive no further consideration in this chapter.

Effect of soil type.

One-meter column studies at the University of Arizona

After selecting periods of column operation in which organic removal efficiency was independent of time based on statistical criteria (column cycles 7-11 in the one-meter columns,

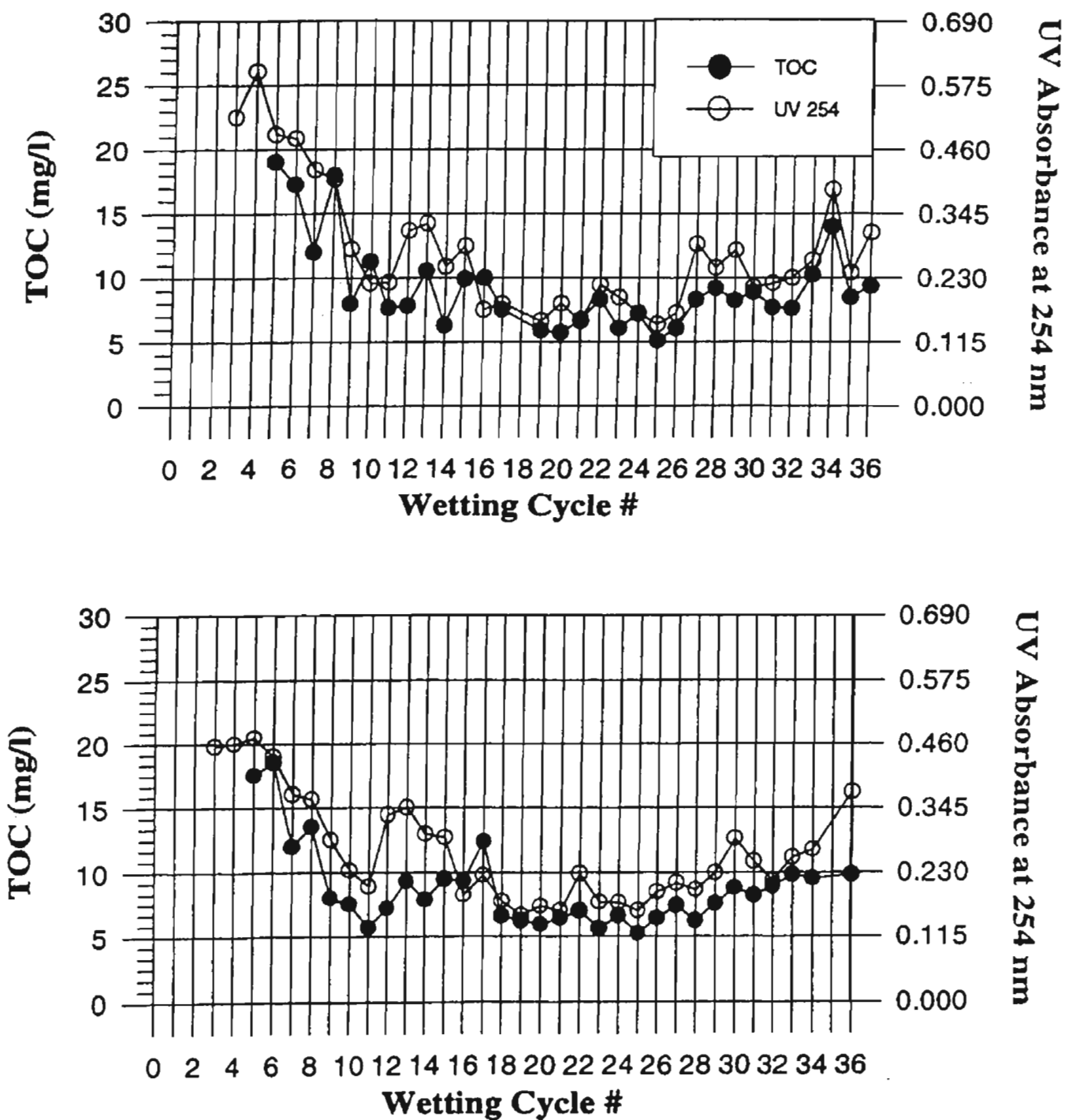


Figure 4.7 Average effluent concentration of TOC and UVA_{254} in (a) North Pond silt and (b) South Pond silt repacked in 2-meter (ASU) columns. Both columns received chlorinated secondary effluent from the 91st Avenue Wastewater Treatment Plant in Phoenix. Column designations correspond to those provided in Table 4.2.b

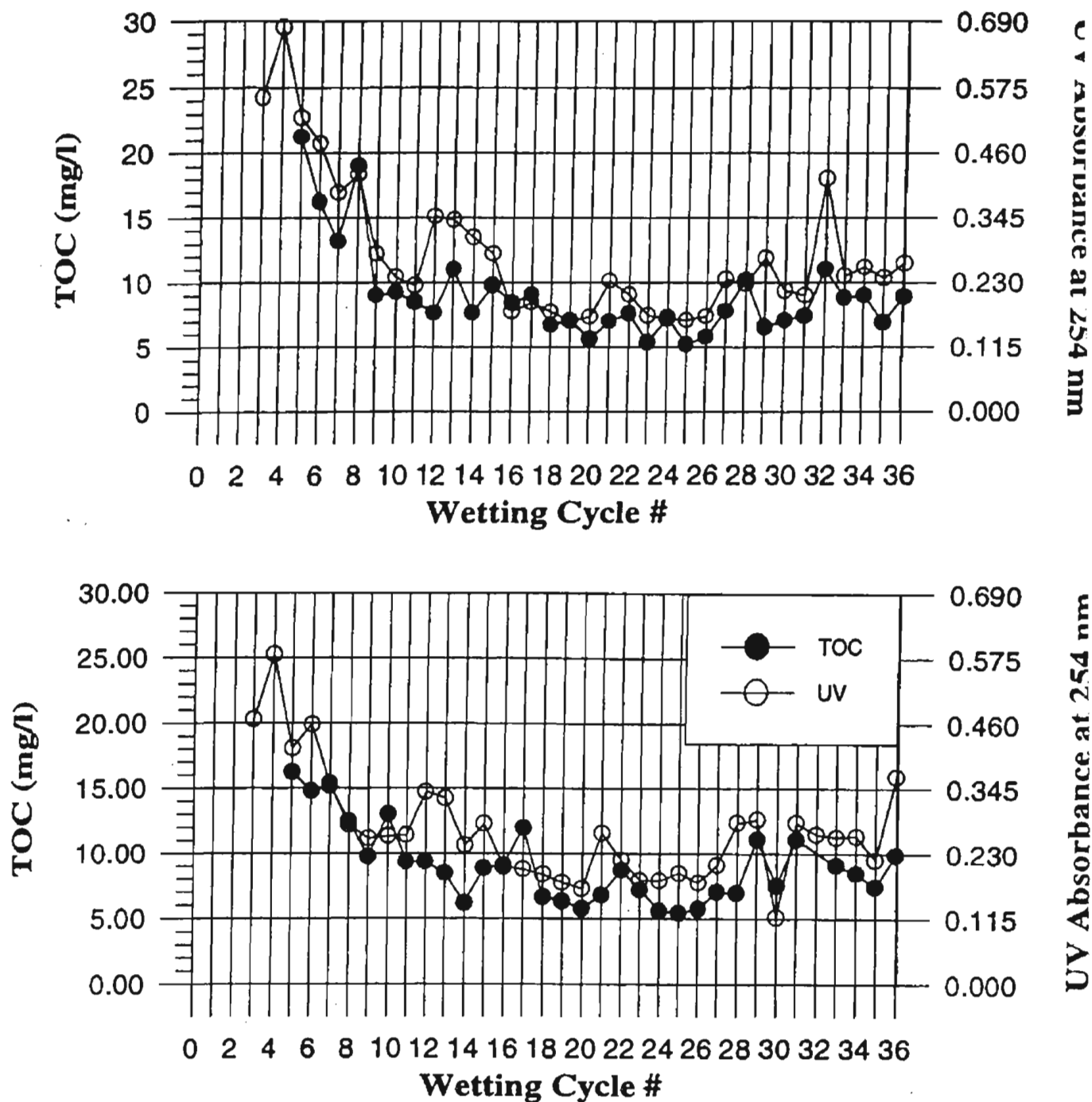


Figure 4.8 Average effluent concentrations of TOC and UVA₂₅₄ in (a) North Pond silt and (b) South Pond silt repacked in 2-meter (ASU) columns. Both columns received chlorinated secondary effluent from the 91st Avenue Wastewater Treatment Plant in Phoenix. Column designations correspond to those provided in Table 4.2

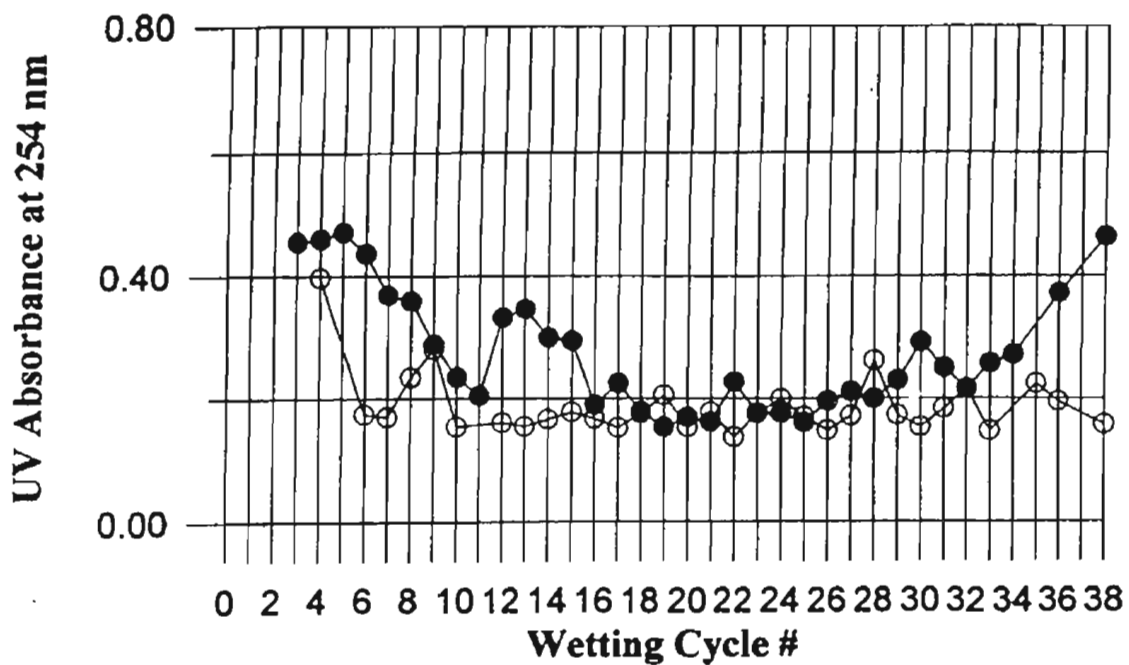
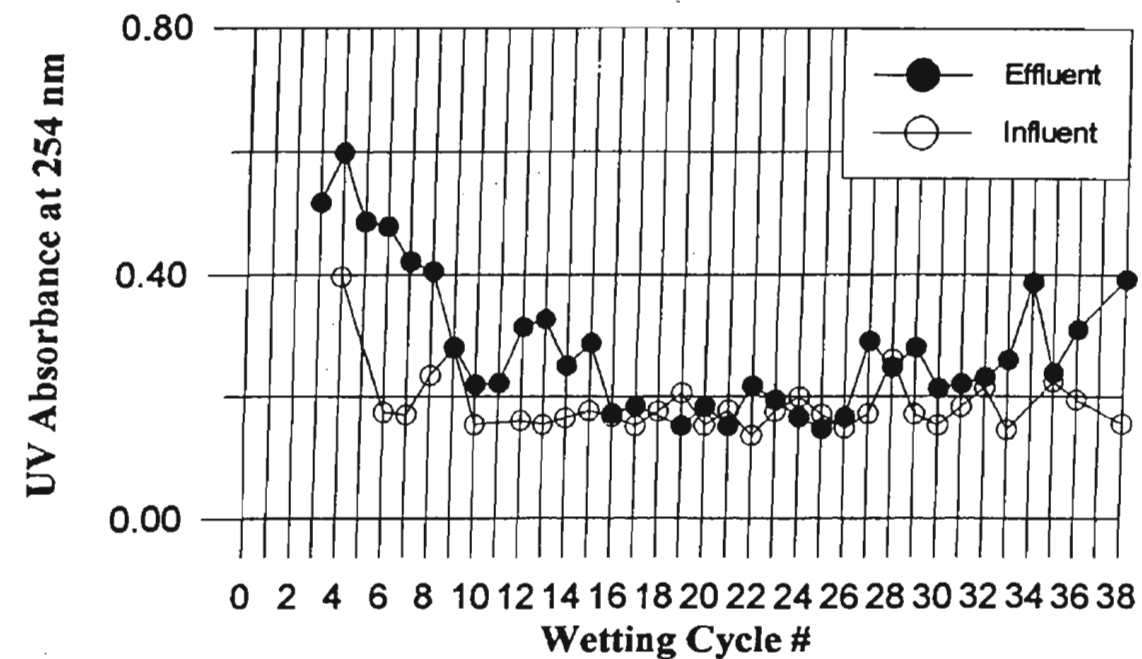


Figure 4.10 Average influent and effluent concentrations of UVA_{254} versus wetting cycle in 2-meter (ASU) columns. Column designations correspond to those assigned in Table 4.2.b. Columns were fed effluents from the 91st Avenue Wastewater Treatment Plant in Phoenix. (a) North Pond silt fed chlorinated secondary effluent. (b) South Pond silt fed chlorinated secondary effluent

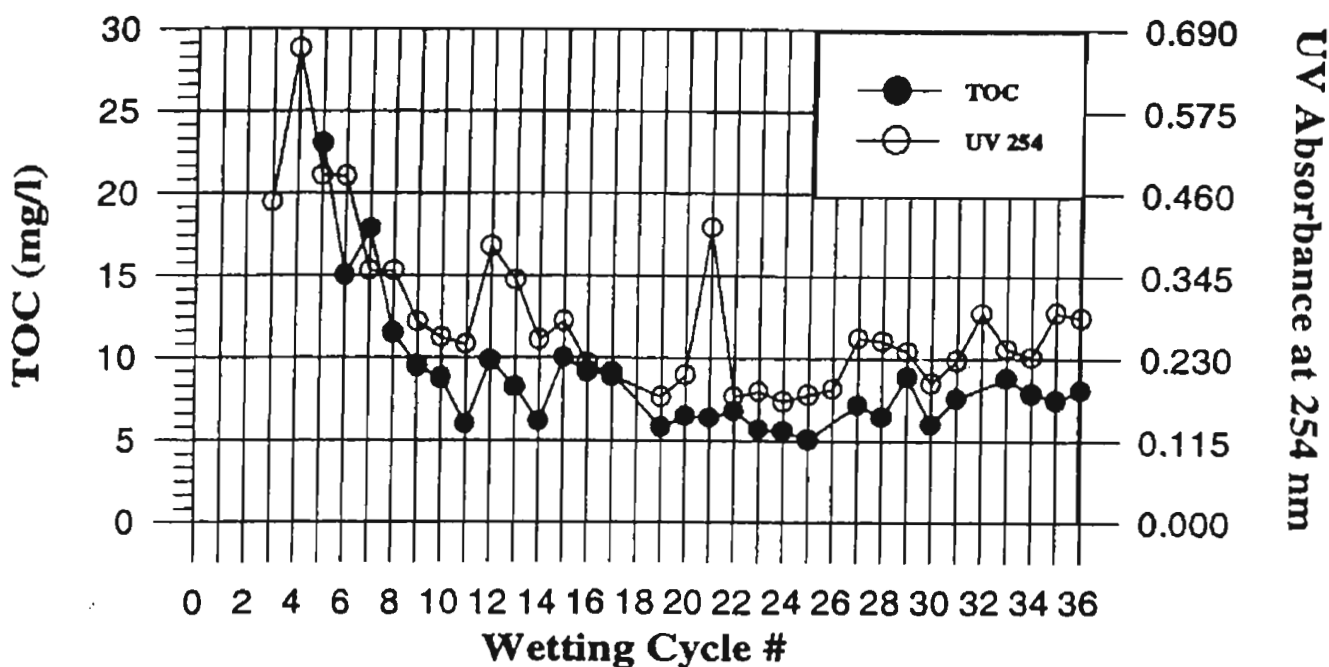
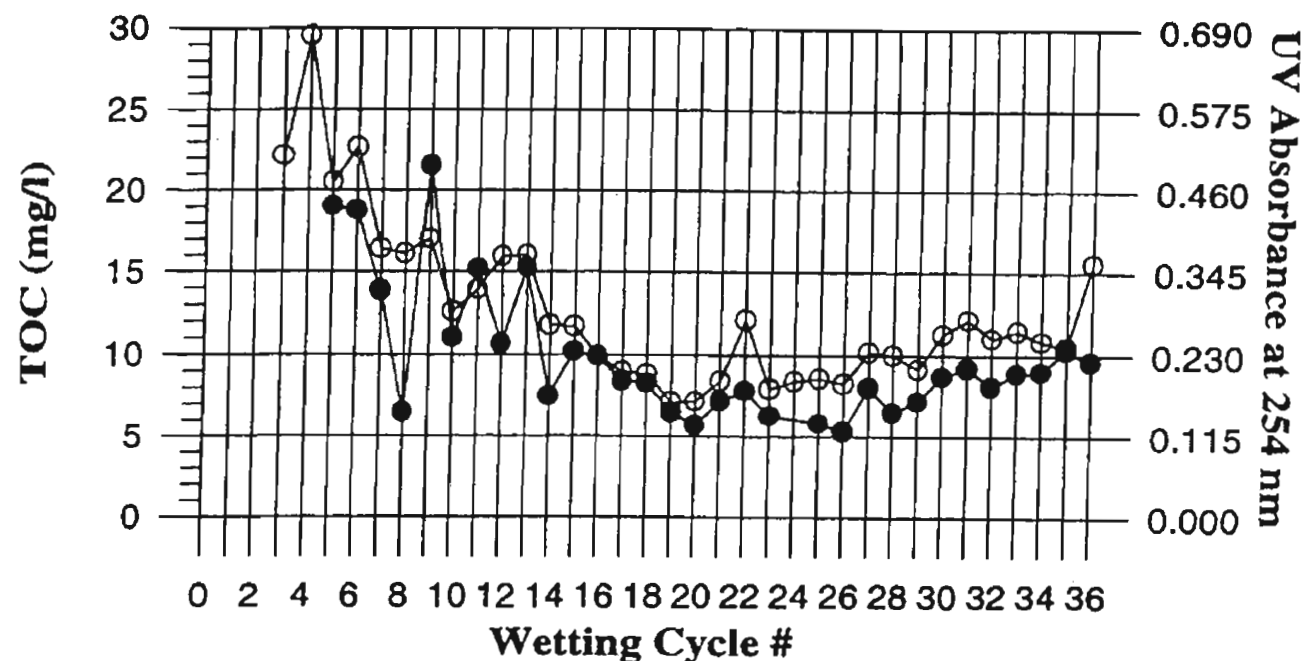


Figure 4.9 Average effluent concentrations of TOC and UVA_{254} in (a) North Pond silt and (b) South Pond silt repacked in 2-meter (ASU) columns. Both columns received chlorinated secondary effluent from the 91st Avenue Wastewater Treatment Plant in Phoenix. Column designations correspond to those provided in Table 4.2.b

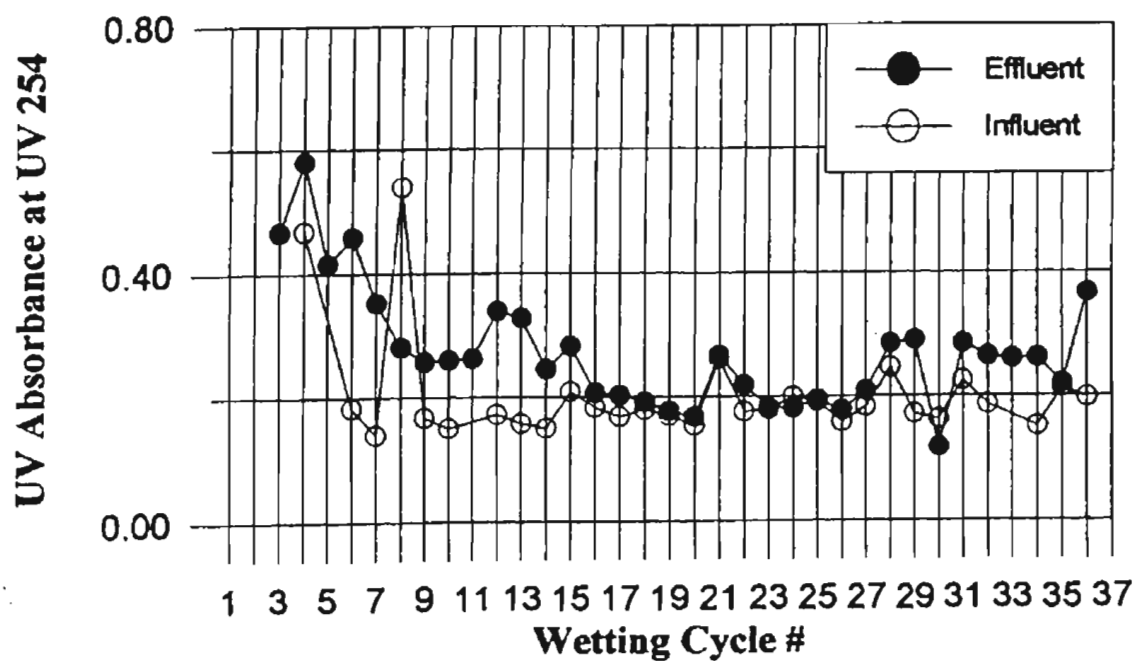
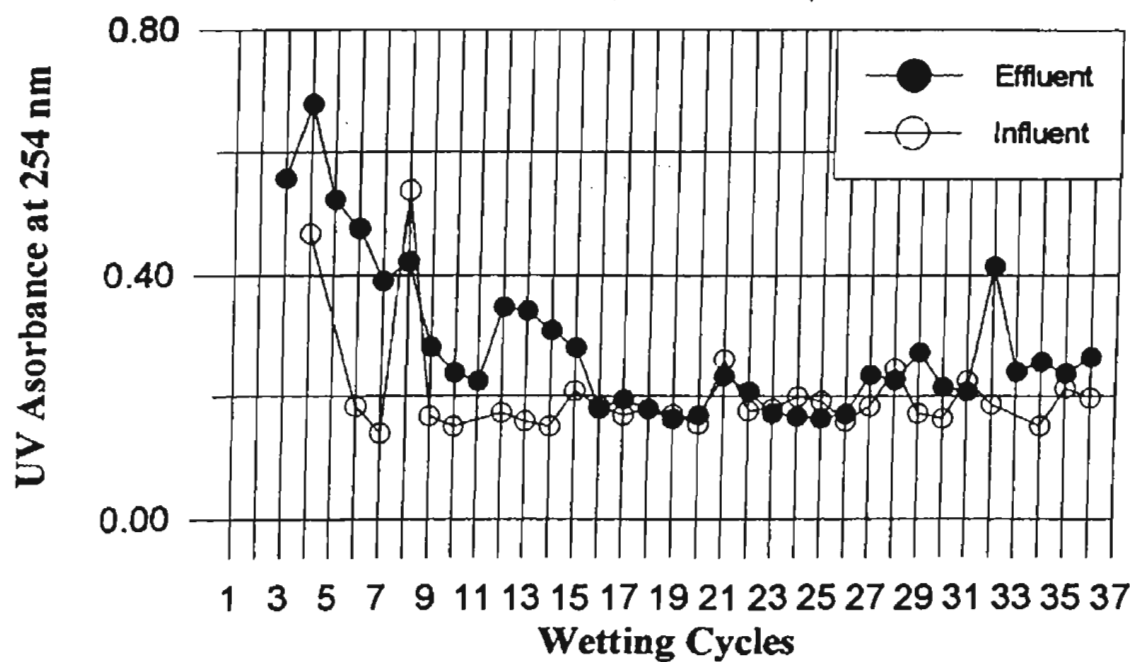


Figure 4.10 (continued) (c) North Pond silt fed chlorinated secondary effluent. (d) South Pond silt fed chlorinated secondary effluent

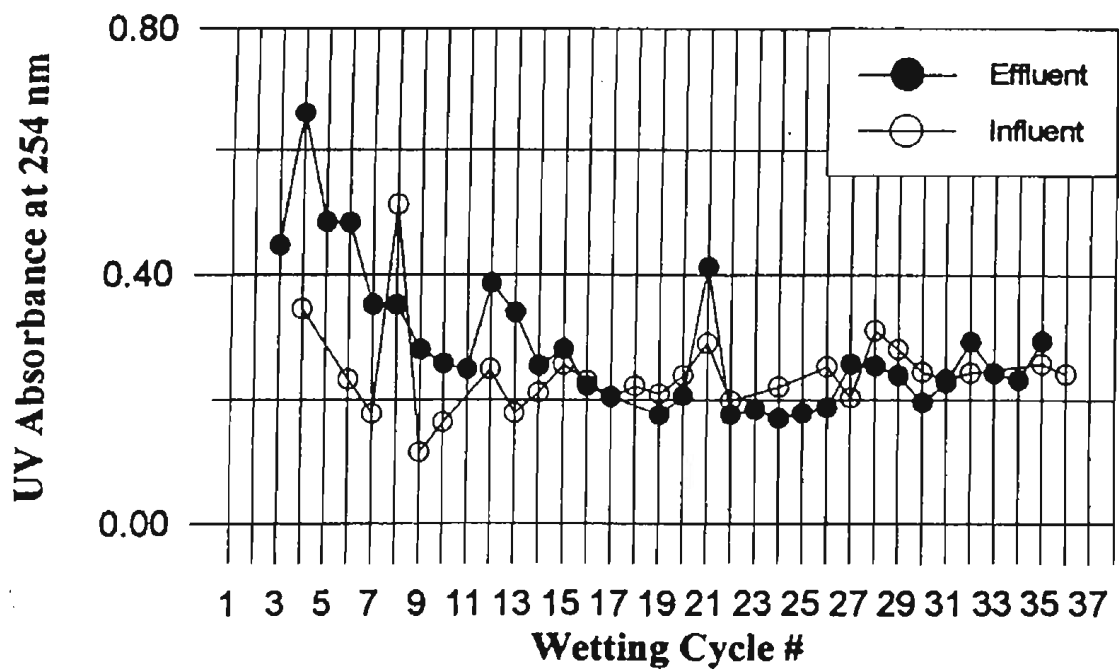
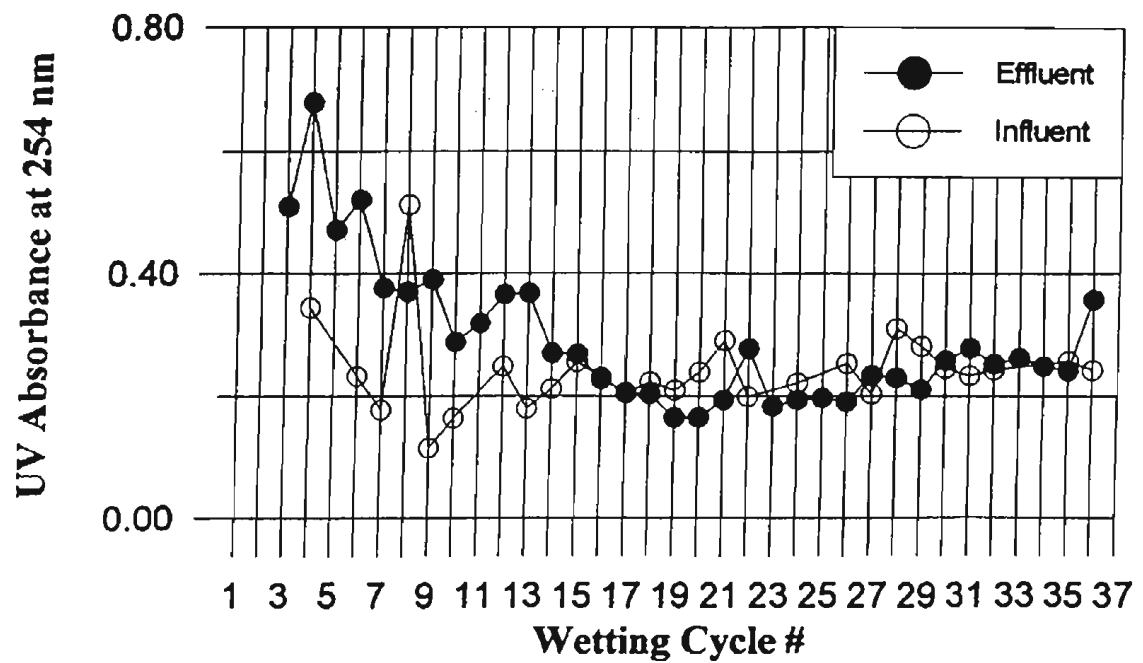


Figure 4.10 (continued) (e) North Pond silt fed nitrified/dentrified effluent. (f) South Pond silt fed nitrified/dentrified effluent

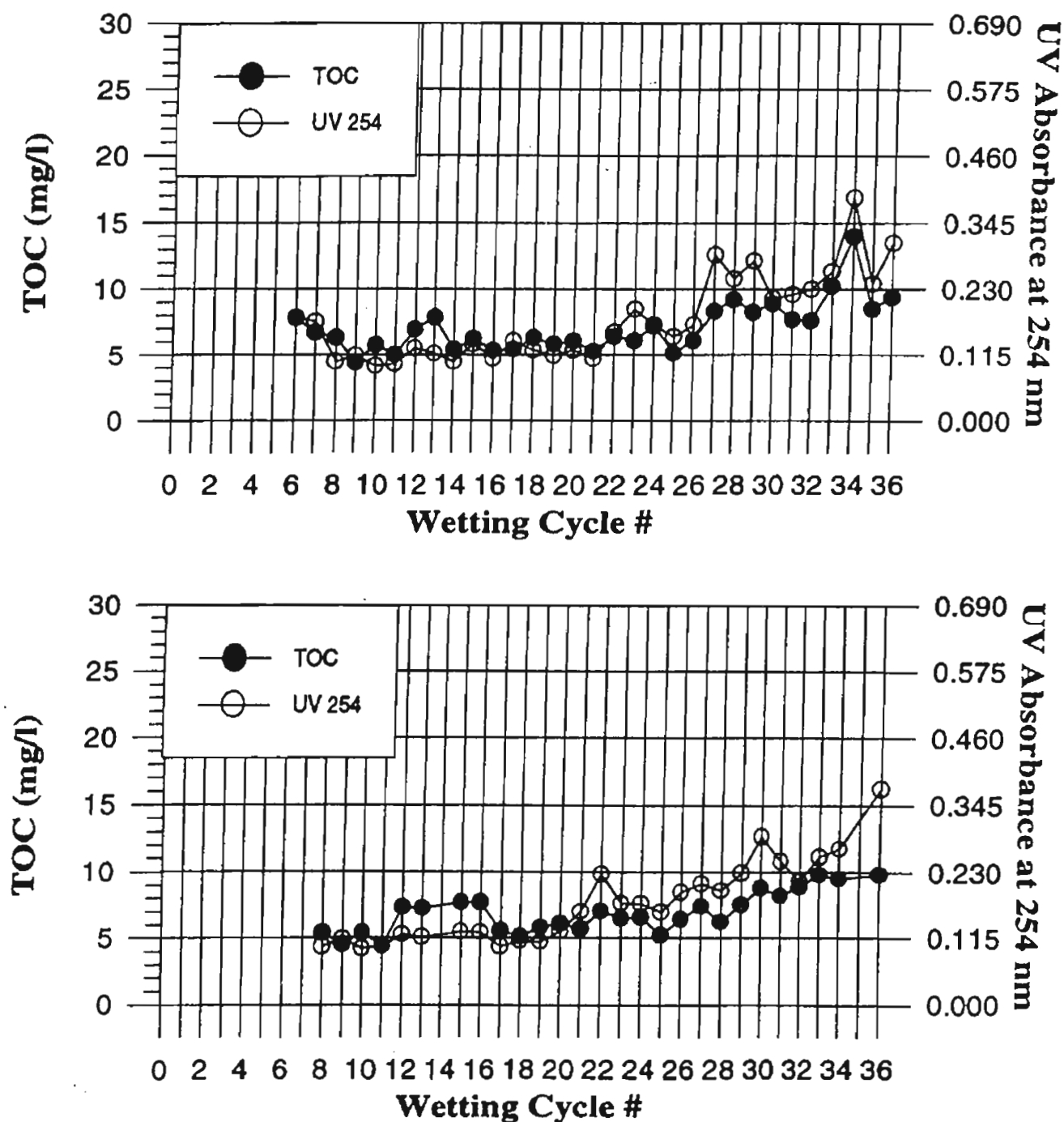


Figure 4.11 Effluent concentrations of TOC and UVA_{254} versus wetting cycle in 2-meter (ASU) columns packed with Agua Fria sand. Column designations correspond to those assigned in Table 4.2.b. (a) Agua Fria sand fed chlorinated secondary effluent. (b) Agua Fria sand fed nitrified/denitrified effluent

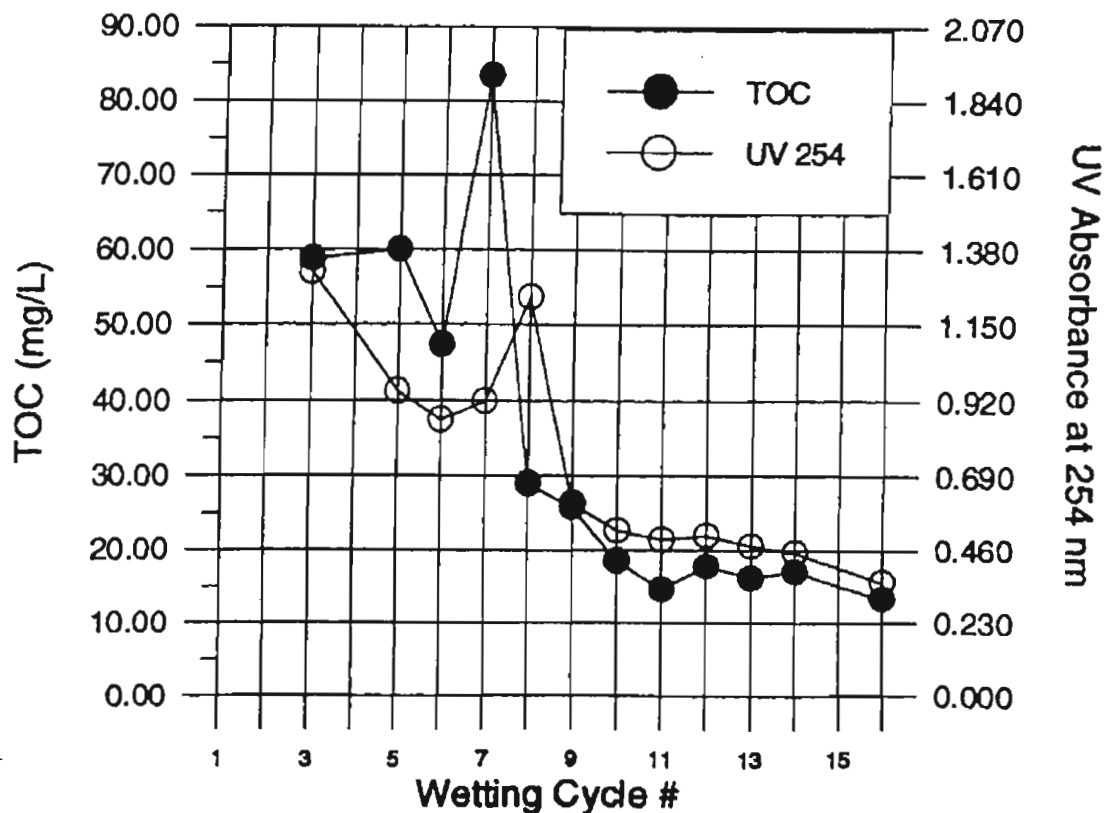
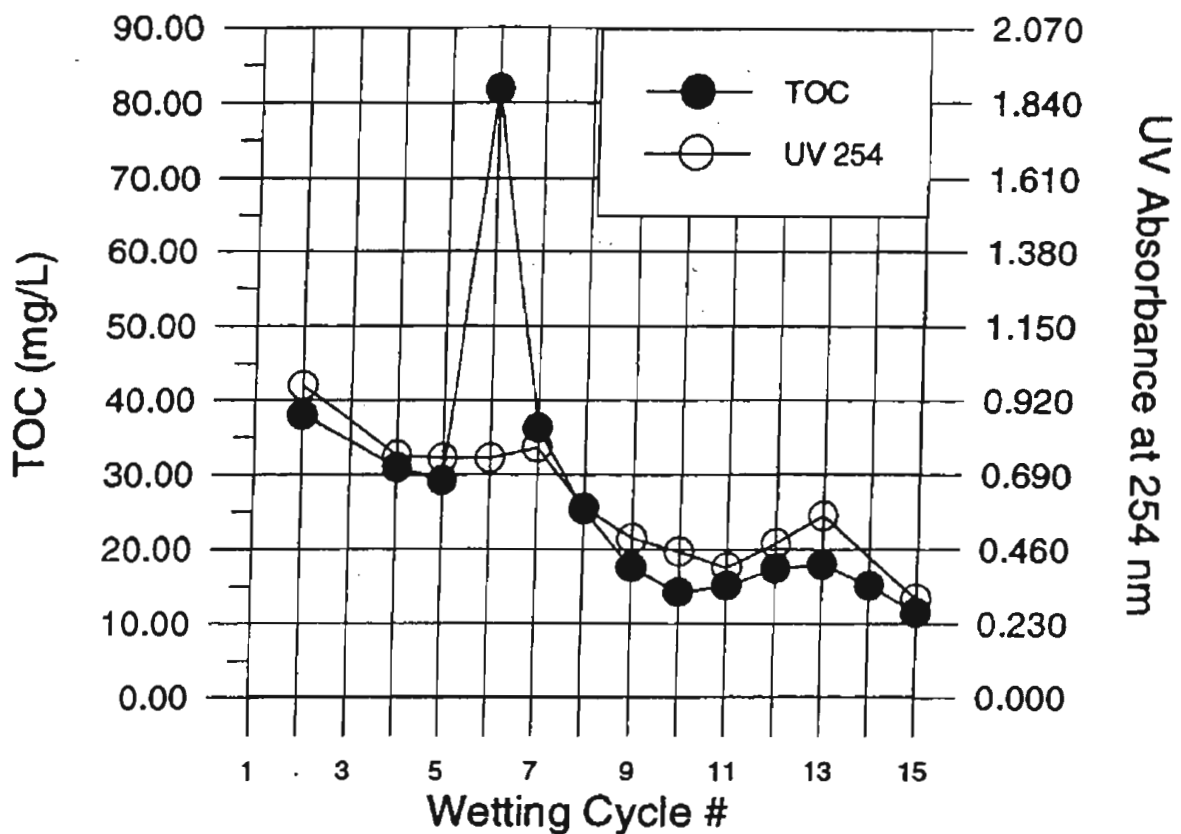


Figure 4.11 Effluent concentrations of TOC and UVA_{254} versus wetting cycle in 2-meter (ASU) columns packed with Agricultural Field clay. Column designations are those assigned in Table 4.2.b. Columns were fed effluents from the 91st Avenue Wastewater Treatment Plant in Phoenix. (c) Clayey soil chlorinated secondary effluent. (d) Clayey soil fed nitrified/dentrified effluent

University of Arizona; see Section 4.3.1) data from that period were lumped in order to analyze differences in carbon removal that were due to soil type. One-way analysis of variance tests (ANOVAs) were performed to determine whether there were significant differences in through-column removals of DOC and UVA_{254} as functions of (i) column #, within soil types, and (ii) soil type. ANOVAs performed for through-column percent reduction of DOC are summarized in Table 4.6. Two of the columns containing sand, #7 and #11, were not significantly different ($\alpha=0.50$; average DOC removals, 35.1 and 36.8 percent, respectively). Likewise two of the columns containing sandy loam, #5 and #13, were not significantly different ($\alpha=0.80$; average DOC removals, 41.4 and 41.5 percent, respectively).

The performances of the two sand columns (#7 and #11) were then compared to those of the two Sweetwater sandy loam columns (#5 and #13). There was a significant difference in removal of DOC ($\alpha = 0.05$; Table 4.6). That is, DOC removals in the columns containing the Sweetwater soil were significantly higher than corresponding removals in columns packed with Agua Fria sand. A similar set of analyses based on measurements of UVA_{254} removal was less conclusive. Differences in the means of through-column removals for UVA_{254} in Agua Fria sand and Sweetwater sandy loam were considerably less reliable ($\alpha=0.20$; see Table 4.7).

One-meter columns containing the North Pond silt were not placed in operation at the University of Arizona until mid-year 1995. As a consequence, their record of performance is less extensive than the record corresponding to other soils (Table 4.8). Statistical analyses designed to establish (i) the equivalence of data separated in time and (ii) differences in soil column performance based on soil type were not carried out using these data. Nevertheless, it is apparent that DOC removals in these columns approached those observed across columns packed with either Agua Fria sand or Sweetwater sandy loam. The average DOC removals over the first 9 cycles of operation of columns with North Pond silt were 48.6 percent (column #4) and 33.8 percent (#12). Through-column attenuation of UVA_{254} decreased over the same period of operation with effluent concentration eventually exceeding influent UVA_{254} (Figure 4.12). These results suggest that organics that contributed to UVA_{254} measurements were leached from the silts and that the concentration of these organics in column effluent increased over time.

Unlike experiments conducted in 2-meter columns, the North Pond silt in one-meter columns at the University of Arizona was flushed with clean water to leach desorbable organic material, as

Table 4.7

Results from one-way analysis of variance tests for through-column percent reduction of UVA_{254} . All columns received chlorinated secondary effluent from the Roger Road Wastewater Treatment Plant in Tucson. Periods of operation tested were based on analyses of time dependence summarized in Tables 4.4 and 4.5. Only data arising from periods in which column performances were independent of cycle number were used. Column designations correspond to those in Table 4.2.a. Only periods of uninhibited operation were used in the comparison.

basis of comparison	F-value	means are significantly different at $\alpha \geq$
sand: col. #3, 7, and 11	0.769	0.40
sandy loam: col. #5, 9, and 13	10.991	0.001
sandy loam: col. #5 and 13	0.520	0.40
sand vs sandy loam: col. #3, 7, 11 and #5, 13	1.482	0.20

Table 4.8

Through-column percent reduction for DOC and UV₂₅₄ for one-meter (UA) columns packed with North Pond silt as a function of wet cycle number. Values shown represent averages of approximately seven daily measurements for each wet cycle. All columns were fed secondary effluent from the Roger Road Wastewater Treatment Plant in Tucson.

Wet Cycle #	Column #					
	#4		#8		#12	
	DOC	UV-254	DOC	UV-254	DOC	UV-254
1	60.8	60.0	44.2	53.8	48.7	38.8
2	54.7	25.2	a*	a*	37.7	22.9
3	58.3	17.9	64.5	2.3	24.3	-11.8
4	65.3	20.2	74.8	a*	74.8	-19.4
5	50.3	14.7	a*	32.0	30.2	-14.7
6	42.9	-18.0	a*	a*	26.3	-9.7
7	45.5	7.2	a*	a*	14.6	-24.8
8	22.8	5.2	a*	a*	22.5	-16.2
9	36.9	-6.9	a*	a*	24.9	-9.3
10	-	-8.3	a*	a*	26.9	-6.8
11	-	-	a*	a*	38.6	-
12	-	-	a*	a*	-	-

a* data not collected for column #8 during this cycle

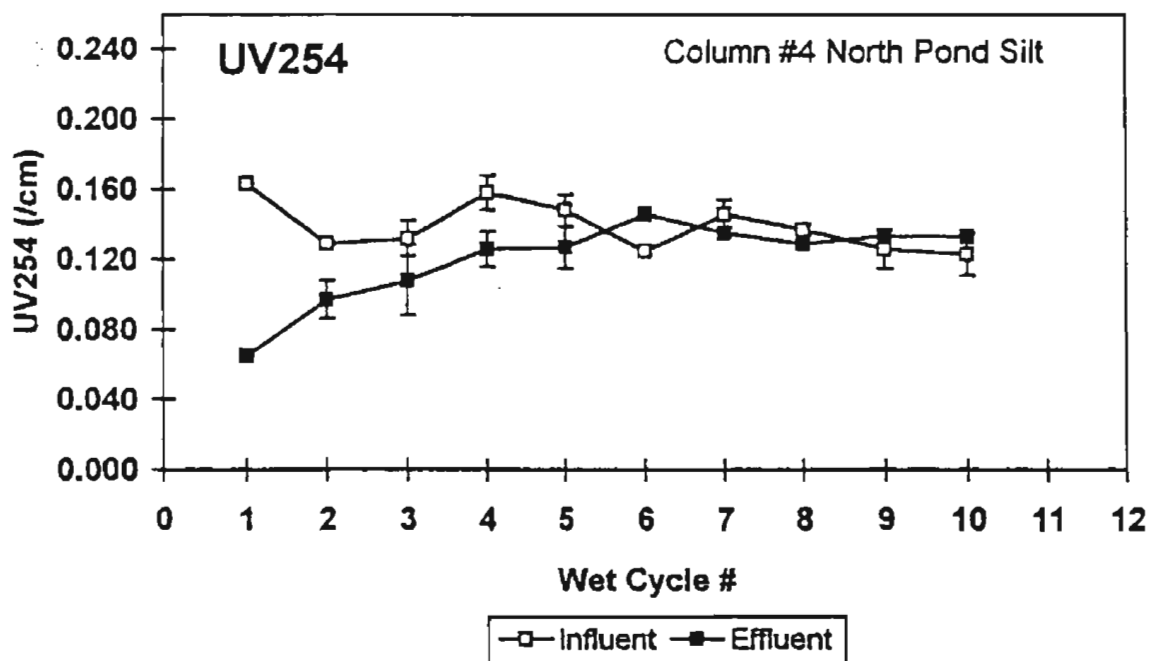
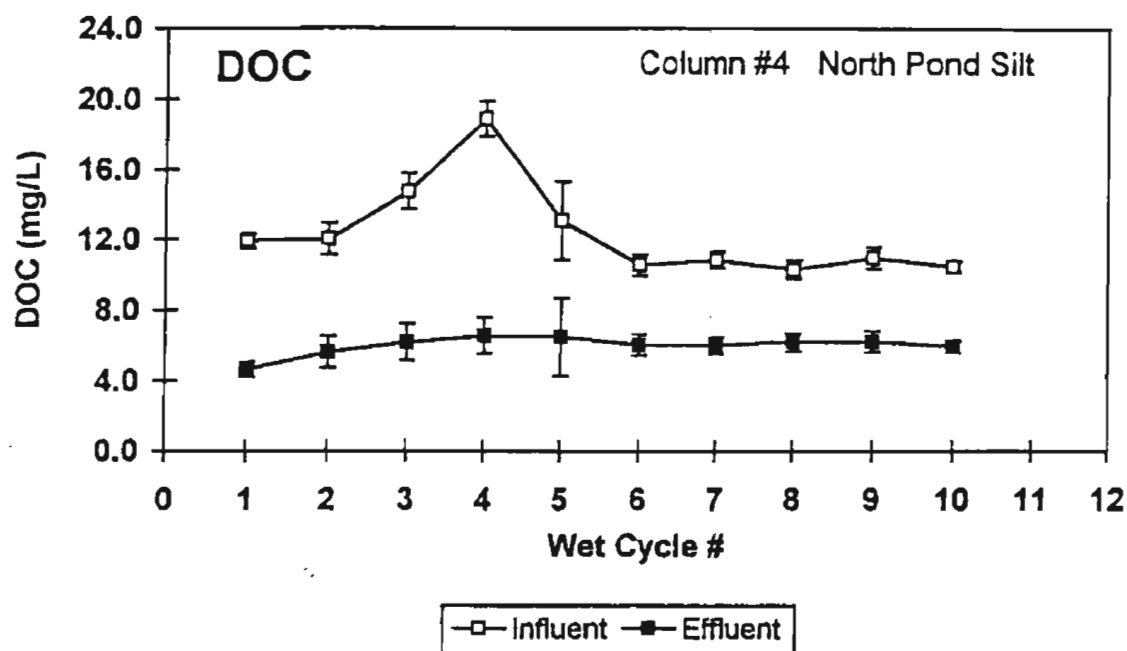


Figure 4.12 Average influent and effluent concentrations of DOC and UVA_{254} in a one-meter (UA) column packed with North Pond silt. The column received chlorinated secondary effluent from the Roger Road Wastewater Treatment Plant in Tucson. Points represent the arithmetic mean of at least seven measurements during individual cycles. Error bars encompass two standard deviations. Where no error bars are visible, a standard deviation lay within the symbol.

measured by UVA_{254} , prior to the collection of through-column data. Despite this soil cleaning procedure, it is evident that leaching of UVA_{254} adsorbing organics from the silts was reestablished during column operation. It is also apparent that cycle-dependent improvements in DOC removal efficiency were due to microbe acclimation or growth, as opposed to reductions in leachable organics over time.

Two-meter column studies at Arizona State University

Four soil types were included in the experimental design for SAT simulations at Arizona State University. Three two-meter columns were packed with North Pond silt. Of these, two received denitrified secondary effluent and a third was fed secondary effluent. The records of total organic carbon (TOC) and UVA_{254} measurements in column effluents (Figures 4.7-4.9) indicate that 15-18 cycles were necessary for column acclimation, after which effluent concentrations of TOC approached 5 mg/l as carbon and UVA_{254} measurements reached about 0.13 (cm^{-1}). Unfortunately, the period of optimal column performance was short-lived. After about 25 cycles of operation, the record indicates a marked deterioration in effluent quality, probably due to the contribution of a persistent organic fraction of algal origin.

A similar picture is evident in the effluent quality records corresponding to the two columns that were packed with sand (Figure 4.11). That is, the best quality column effluent was characterized by TOC concentrations of about 5 mg/l, and effluent quality (in terms of the organic quality parameters that received routine attention) declined noticeably after wetting cycle #20 (Figure 4.11).

In each of the three columns that were packed with North Pond silt, effluent levels of UVA_{254} consistently exceeded corresponding influent concentrations (Figure 4.10), again implying that organic material was added to percolating waters during SAT simulations.

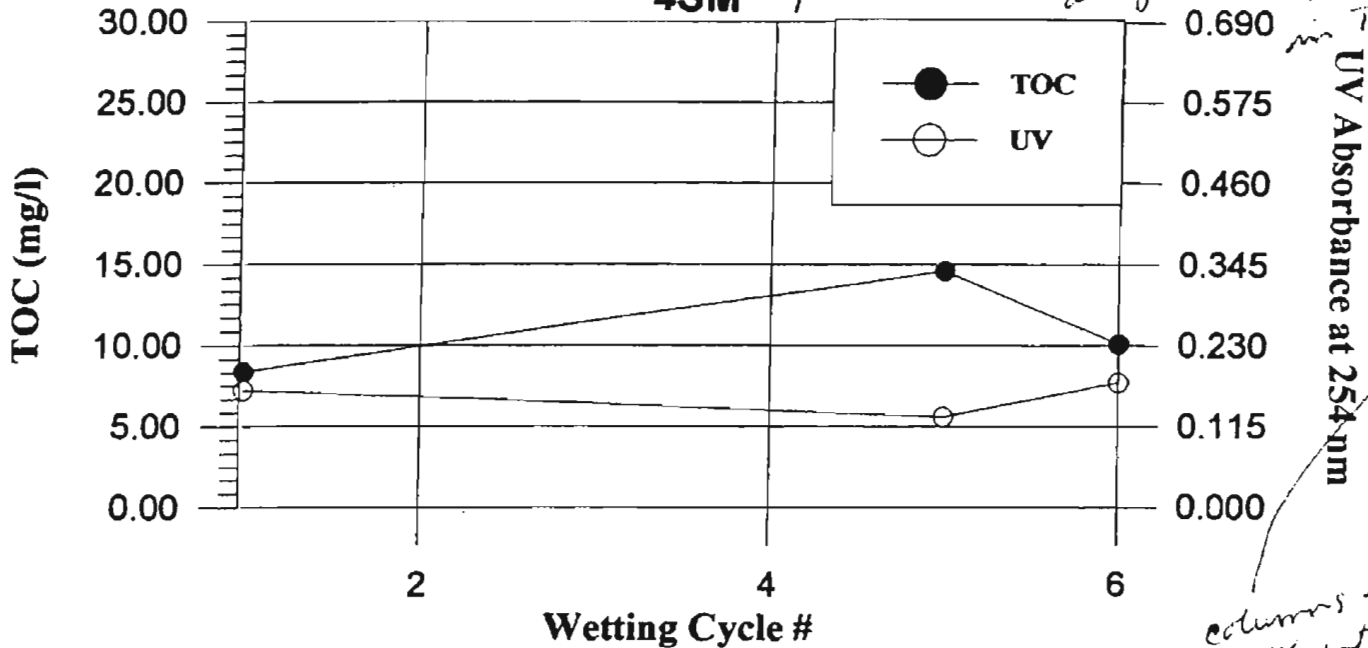
As indicated previously, use of the clay columns was discontinued after about 15 wet/dry cycles due to poor hydraulic performance and our inability to completely leach out soil organic material at the very low infiltration rates in these columns (Figure 4.12). The clay was replaced with South Pond silt (finer-grained than the North Pond silt) midway through the overall experimental period. The necessarily abbreviated period of column performance (Figure 4.13) indicates that we

FIGURE TOC and UV 254 vs Wetting Cycles
Average Effluent Values

Figure 4.13. effluent concentration of TOC and UV₂₅₄ versus wetting cycle in 2-meter columns packed with South Pond silt. Column designations are then assigned in Table 4.26.

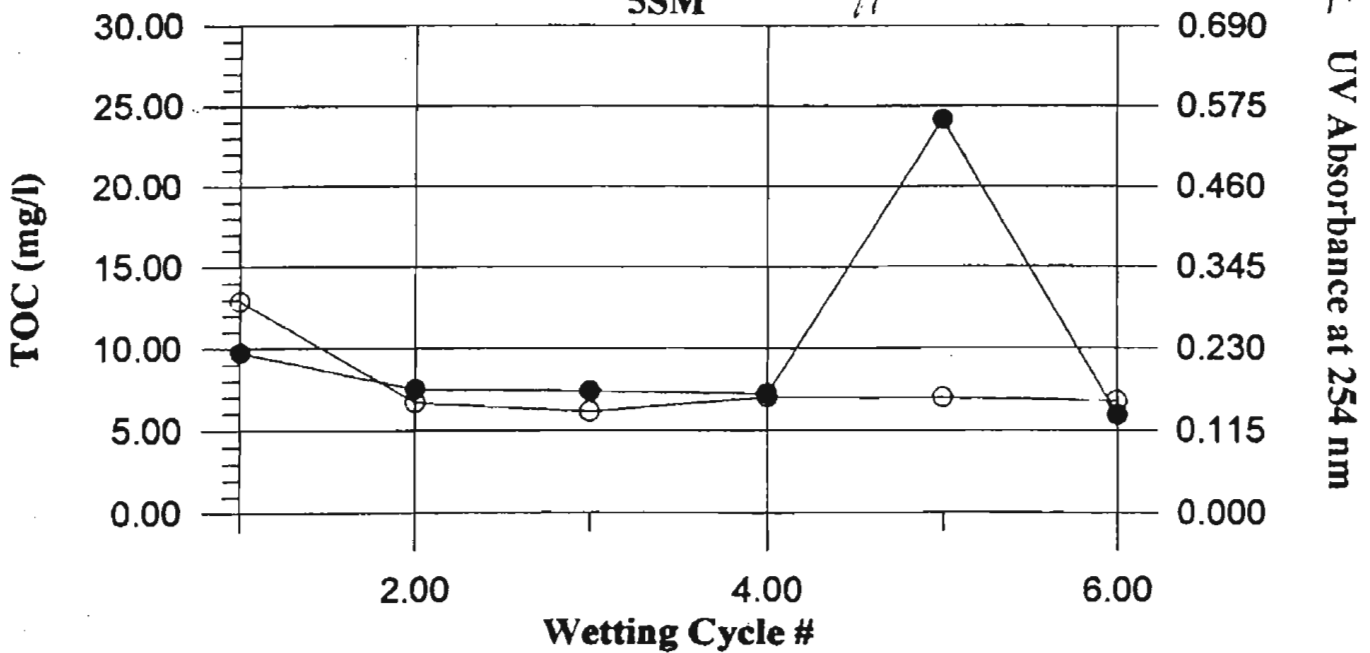
(a) South Pond silt fed chlorinated secondary effluent

4SM



(b) South Pond silt fed nitrified/denitrified effluent

5SM



columns were fed effluents from the 91st Avenue Wastewater Treatment Plant in Phoenix.

should expect a column effluent of no higher quality than 5 mg/l TOC and UVA_{254} values of at least 0.1 (cm^{-1}) in the columns packed with the South Pond silt.

It is therefore evident that, at least in terms of the organic parameters that were routinely measured here, column effluent was essentially independent of soil in 2-meter columns that were operated at Arizona State University. It seems that the 91st Avenue Treatment Plant effluent (the source water for these studies) is generally of sufficient quality to compress soil-dependent differences in SAT efficiencies in short-column simulations. Under optimal conditions for column operation, TOC was reduced from 8-10 mg/l to 5-7 mg/l across the 2-m columns. During the latter stages of column operation, effluent concentrations frequently reached those of the influent, due primarily to the decomposition of algae. Not surprisingly, it proved difficult to see soil-dependent differences in removal efficiency against this rather narrow differential in water quality.

Effects of differences in above-ground treatment processes on post-SAT effluent quality

General

The experimental design called for the use of two different effluent qualities in SAT simulations conducted at Arizona State University -- secondary effluent and nitrified/denitrified secondary effluent. Experiments conducted at the University of Arizona in similar, although shorter (one-meter or 18-cm) columns involved the use of secondary (biotower), filtered secondary (tertiary), ozonated secondary and primary effluents in SAT simulations. The primary effluent study is described in a separate chapter of this report, but a few results are included here for the sake to completeness. Supplementary studies involving ozonated secondary effluents from three western states that were performed at Colorado University are also described here.

Column studies at the University of Arizona

Effluent concentrations of DOC and UVA_{254} that are representative of steady performance in University of Arizona 18-cm and one-meter columns are summarized in Table 4.9. It is evident

Table 4.9a

Average influent and effluent concentrations of DOC and UVA_{254} in short, 18-cm columns packed with Sweetwater sandy loam. All columns received effluents from the Roger Road Wastewater Treatment Plant in Tucson. Ozone was provided at a dosage of one part transferred per part DOC. The secondary control was inhibited with sodium azide. NBDOC was the residual DOC concentration at the conclusion of BDOC tests. NB-254 is the corresponding level of UVA_{254} .

	DOC			UV254		
	influent	effluent	NBDOC	influent	effluent	NB-254
chl. secondary	10.73	8.25	5.0	0.138	0.121	0.115
secondary control	13.86	12.96	n/a	0.357	0.353	n/a
O ₃ secondary	12.63	9.84	4.8	0.120	0.108	0.08
tertiary	11.41	9.53	n/a	0.138	0.127	n/a

Table 4.9b

Average influent and effluent concentrations of DOC and UVA₂₅₄ in one-meter columns. Inhibition was achieved with sodium azide. NBDOC was the residual DOC concentration at the conclusion of BDOC tests. NB-254 is the corresponding level of UVA₂₅₄.

Soil Type	Influent		Effluent		Cycles Tested
	DOC (mg/L)	UV-254 (/cm)	DOC (mg/L)	UV-254 (/cm)	
Agua Fria sand ¹	10.71	0.133	7.67	0.118	6-12
	± 1.44	± 0.006	± 1.13	± 0.013	
North Pond silt ¹	11.98	0.133	5.29	0.129	2-6
	± 1.29	± 0.005	± 0.98	± 0.006	
Agua Fria sand ²	12.16	0.139	6.39	0.112	13-20
	± 1.76	± 0.017	± 0.85	± 0.010	
Sweetwater sandy loam ²	12.41	0.142	5.45	0.108	13-20
	± 2.00	± 0.009	± 0.88	± 0.006	
North Pond silt ²	11.08	0.138	6.24	0.133	4-10
	± 1.02	± 0.014	± 0.22	± 0.007	
Auga Fria sand ³	13.31	0.239	11.37	0.227	13-20
	± 1.01	± 0.018	± 1.21	± 0.028	
Sweetwater sandy loam ³	14.64	0.229	13.21	0.240	13-19
	± 1.00	± 0.033	± 0.95	± 0.023	
North Pond silt ³	11.08	0.160	8.22	0.177	6-11
	± 0.89	± 0.028	± 0.89	± 0.027	

¹intact core

²repacked

³repacked inhibited

that after percolation through even one meter of the Sweetwater soil, effluent organic qualities are fairly close, at least in terms of the parameters listed.

Because the detention times in the one-meter reactors are much shorter than periods available for the oxidation of persistent organics during field operations, BDOC measurements were carried out on column effluents. Organics that survived the five-day period of aerobic treatment were much more likely to resist removal processes that contribute to soil-aquifer treatment in the field. Post-BDOC levels of dissolved organic carbon and UVA_{254} were essentially identical for all the effluents tested, from primary to filtered secondary (Table 4.9), suggesting that water quality in percolated effluents is independent of the level of above-ground treatment provided.

Secondary effluent from the Roger Road Wastewater Treatment Plant in Tucson, Arizona, was ozonated prior to treatment via SAT simulation and the BDOC procedure. These experiments were motivated by expectations that ozonation would render refractory organics significantly more amenable to subsequent biochemical oxidations. Our expectations were premised on observations in the surface water treatment industry, where ozonation contributes to the biodegradability of organic residuals during rapid sand filtration and bacterial regrowth in potable water distribution systems. Results of experiments conducted in the 18-cm schmutzdecke columns (Table 4.9) indicate that, contrary to our expectations, even ozonation at a level of one part ozone transferred per part DOC (as C) had little effect on the size of the organic fraction that was likely to persist beyond SAT under field conditions.

From Figure 4.14, it is apparent that ozonation of secondary effluent can increase effluent DOC, presumably by solubilizing particulate organics. However, (i) differences in pre- and post-ozonation DOC levels in secondary effluent were dramatically reduced via SAT, even in the 18-cm schmutzdecke columns, and (ii) ozonation did little to increase the biodegradability of the residual organic fraction that resists SAT removal processes. The latter observation was strengthened by BDOC measurements (DOC measurements at the conclusion of the BDOC procedure). Organic residuals in ozonated and unozonated effluents were essentially indistinguishable at the end of the 5-day protocol. For one of these ozonated samples, the period of aerobic treatment in the BDOC procedure was extended to approximately six months. At the end of the extended period, approximately 5 mg/l of DOC remained (data not shown). Although long-term BDOC results are at best preliminary and should be reinforced by additional measurements of a similar nature, the data

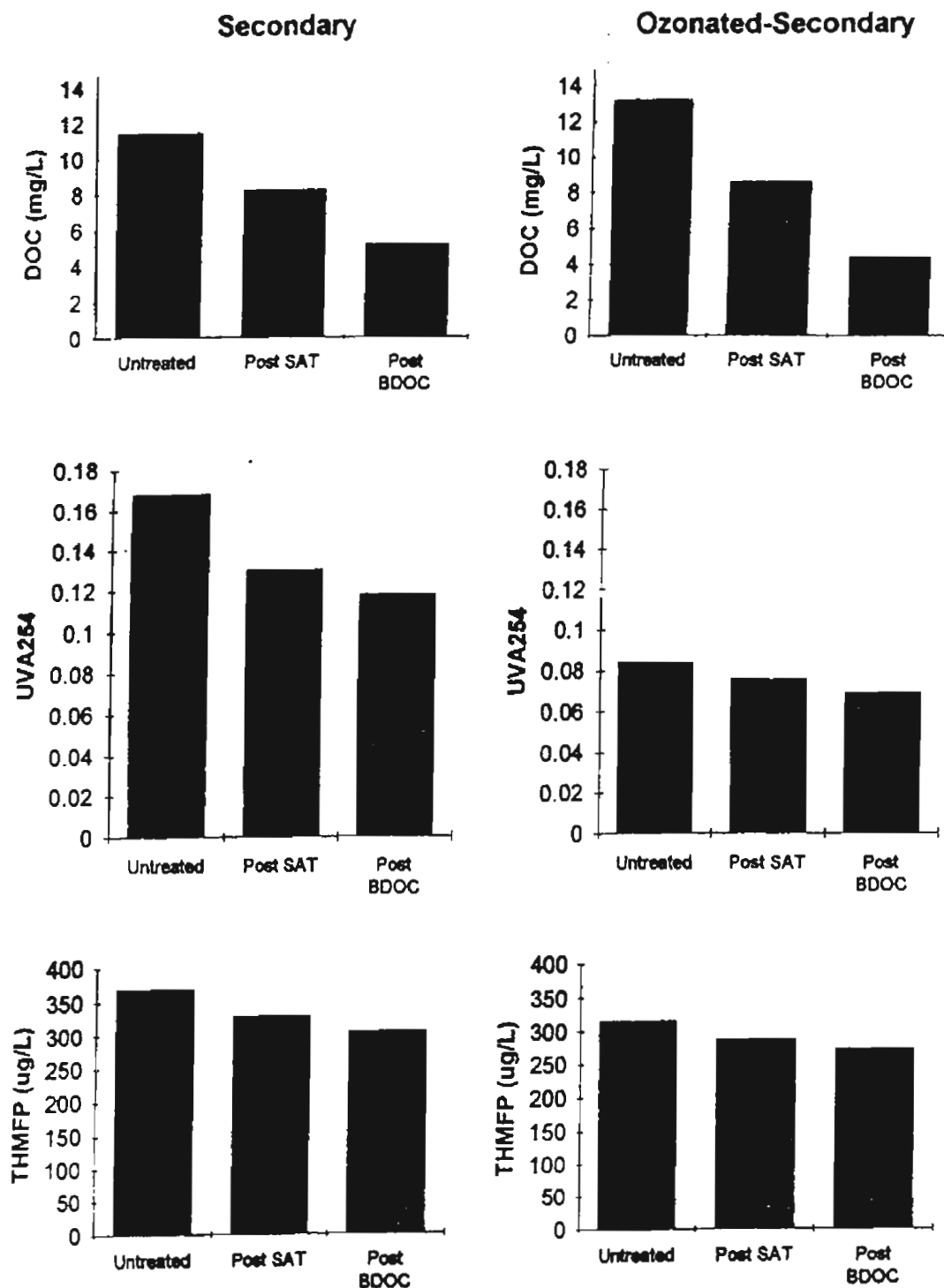


Figure 4.14 Synopsis of simulated SAT and BDOC treatment efficiencies in the removal of DOC, UVA₂₅₄ and THMFP in secondary and ozonated-secondary effluents. Reported data are the results of a single intensive study as opposed to data averages. POST-SAT data represent levels of DOC, UVA₂₅₄ and THMFP in 18-cm schmutzdecke columns. The columns were packed with Sweetwater sandy loam and received secondary effluent from the Roger Road Wastewater Treatment Plant in Tucson.

suggest that secondary municipal effluent has a significant organic fraction that is refractory to aerobic biological treatment. Other experimental findings that contribute to this conclusion include the apparent stability of the residual organic fraction at the five-day mark in BDOC tests (Figure 4.15) and results of special studies involving secondary effluents from a number of western states (see below).

It is also evident from the short-column experiments that organic residuals in ozone-treated secondary effluent are reactive with free chlorine (Figure 4.14). Even the modest reduction in THMFP that accompanied the ozonation of secondary effluent from the Roger Road Wastewater Treatment Plant was partially compensated for during either simulated SAT in the 18-cm schmutzdecke columns or aerobic treatment associated with the BDOC protocol. That is, after extended aerobic treatments designed to biochemically oxidize all biodegradable organics, THMFP measurements in secondary effluents produced results that were hardly distinguishable.

Similar experiments were conducted in the one-meter columns at the University of Arizona with slightly different results. In this case, results are reported as averages of numerous data points as opposed to stand-alone measurements. Once again ozonation increased the DOC concentration in secondary effluent (from 11.5 to 12.2 mg/l as C on average; see Figure 4.16). Unlike previous results, however, post-SAT differences in DOC appeared to be significant (7.2 mg/l as C in secondary versus 5.0 mg/l as C in ozonated secondary effluent). Furthermore, ozonation produced a slightly more biodegradable set of organic residuals, as evidenced by the results of BDOC tests. NBDOC levels in secondary effluent averaged 4.5 mg/l as C (n=3). Corresponding NBDOC measurements in ozonated secondary effluent averaged 3.6 mg/l as C (n=3). These differences were also reflected in UVA_{254} and THMFP measurements carried out for the same waters (Figures 4.16).

Ozonation studies at Colorado University

Our objective here was to evaluate the biodegradability of DOC in several secondary effluents with and without preozonation. Secondary effluents were selected from three western states to represent sources differing in process type, scale, and geographic influence. Ozonation was carried out at 1 part O_3 transferred per part DOC (as C). Wastewaters were subjected to bench-scale five-day BDOC analyses (Mogren, 1990). The biodegradability of effluent organic matter was also

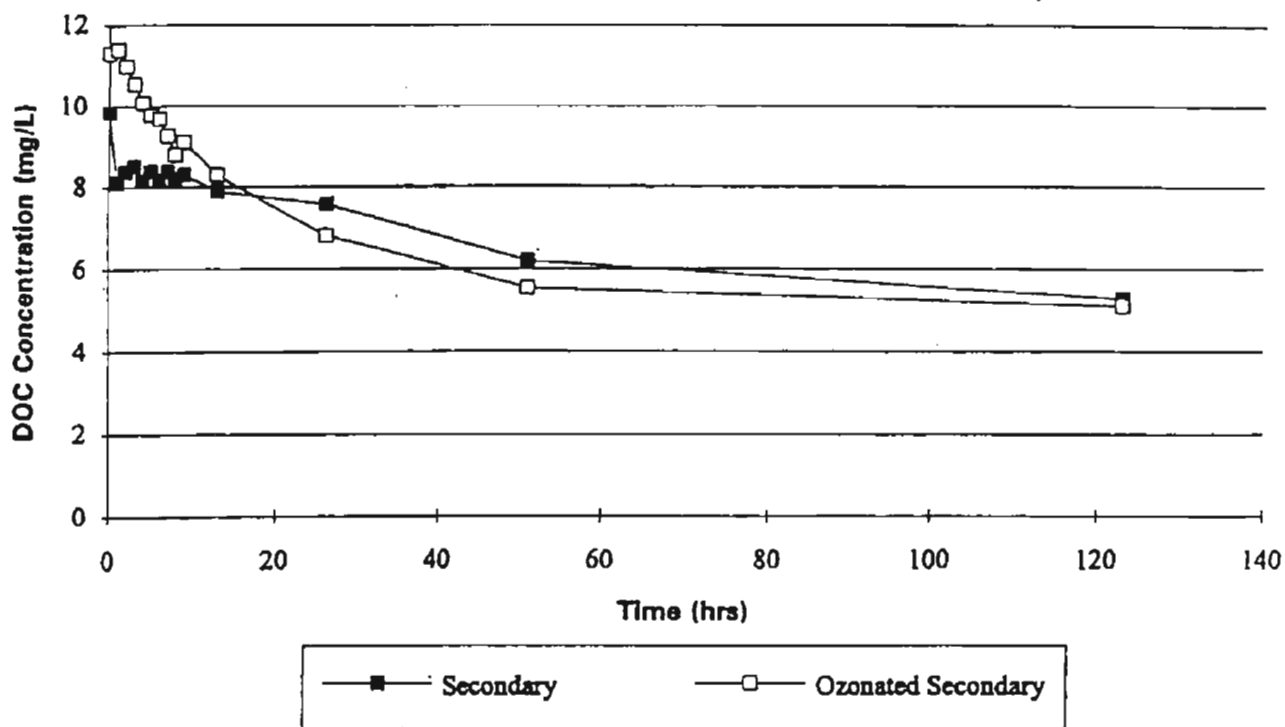


Figure 4.15 Time-dependent concentrations of DOC in BDOC flasks containing acclimated sands and secondary effluents from the Roger Road Wastewater Treatment Plant in Tucson. The ozone dosage was 1 part ozone transferred per part DOC.

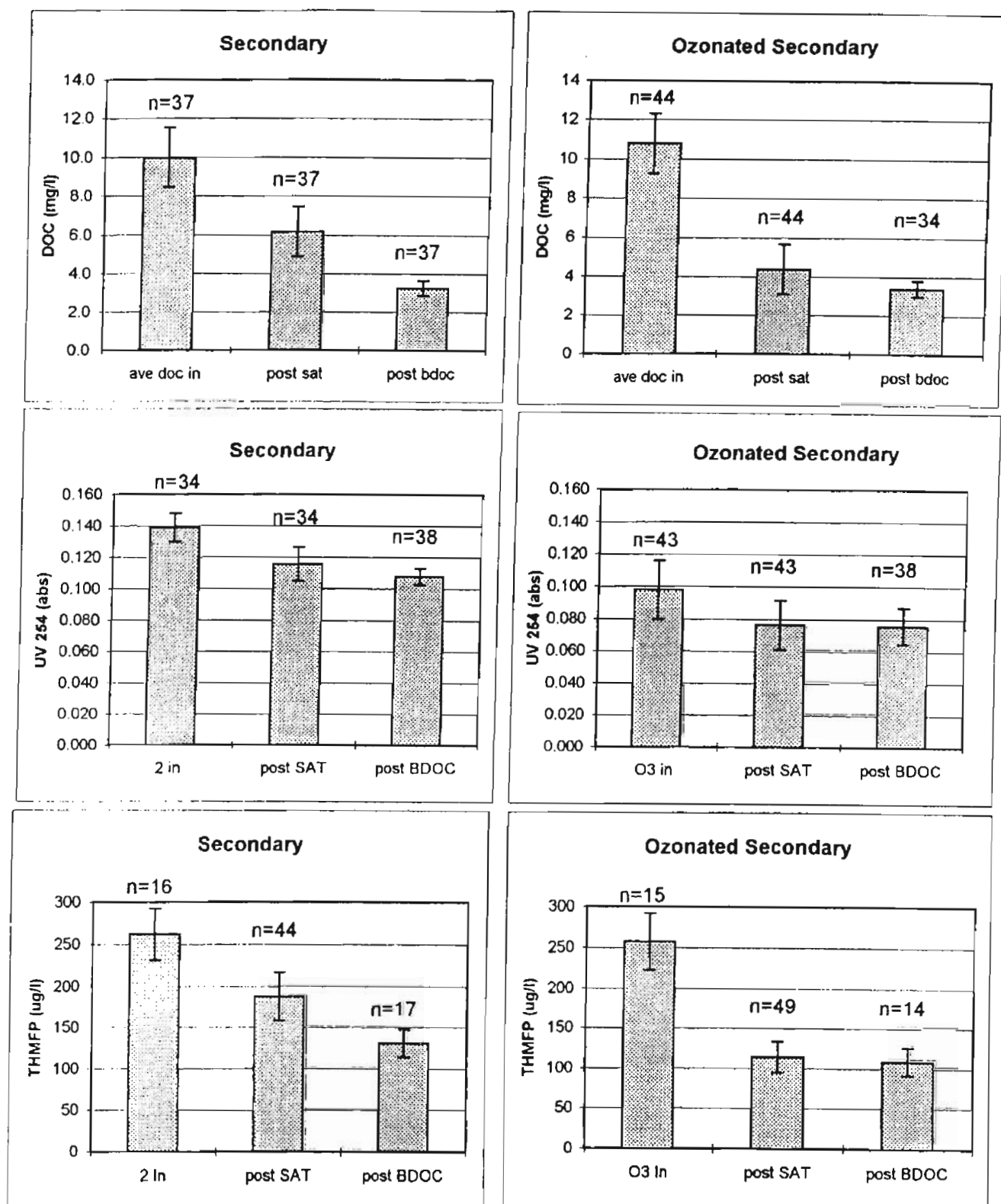


Figure 4.16 Summary of treatment efficiencies during simulated SAT (one-meter columns packed with Agua Fria sand) and BDOC tests. Columns received secondary effluent from the Roger Road Wastewater Treatment Plant in Tucson. Ozone dosage was 1 part O_3 transferred per part DOC or carbon.

compared to that of natural organic matter (NOM). A secondary objective of these studies was to distinguish between biochemical and sorptive removal mechanisms for DOC removal.

Preliminary test results indicate the importance of providing an acclimated bacterial culture for BDOC tests (Figure 4.17). That is, cultures acclimated to surface water organics were initially ineffective agents for the destruction of effluent organic matter. A period on the order of weeks was adequate for acclimation of these cultures to their new substrates. The fraction of DOC removed in sequential BDOC measurements (same sand) increased from 25 to 50 percent within three weeks. No such period of acclimation was necessary when the original BDOC culture was acclimated to wastewater.

The fraction of organics in secondary effluent that was removed via the BDOC procedure did not change as a function of ozone dosage in the range 0-3.0 parts ozone transferred per part DOC as C (Figure 4.18). This is in contrast to ozonation effects in surface waters, which increased the biodegradable fraction of DOC from 10 percent to almost 50 percent at the highest ozone doses.

BDOC results corresponding to the various effluents indicate that in none of the six geographically and treatment-diverse effluents tested did ozonation positively influence the fraction of DOC removed via the BDOC procedure (Figure 4.19). Furthermore, the wastewater organic fraction that proved recalcitrant to biochemical oxidation during BDOC measurements (NBDOC) was between 4.5 and 6.0 mg/l as C for each of the waters tested. One is tempted to speculate that the refractory organic fraction in treated municipal wastewaters is of similar magnitude and composition throughout the study region. Nor does NBDOC appear to be strongly influenced by the type of secondary treatment practiced (Table 4.10). On the other hand, ozonation dramatically decreased the fraction of non-biodegradable DOC in the surface water tested (Figure 4.19). To pursue this apparent difference further, it will be necessary to determine the character of organic residuals in treated wastewaters and surface waters.

Influence on nitrification/denitrification reactions on effluent organics levels

Two-meter columns packed with North Pond silt, South Pond silt, and Agua Fria sand were operated in parallel in order to determine the effect of effluent denitrification on SAT performance. Results, in terms of column effluent TOC and UVA_{254} concentrations (Figures 4.7--4.11) indicate that

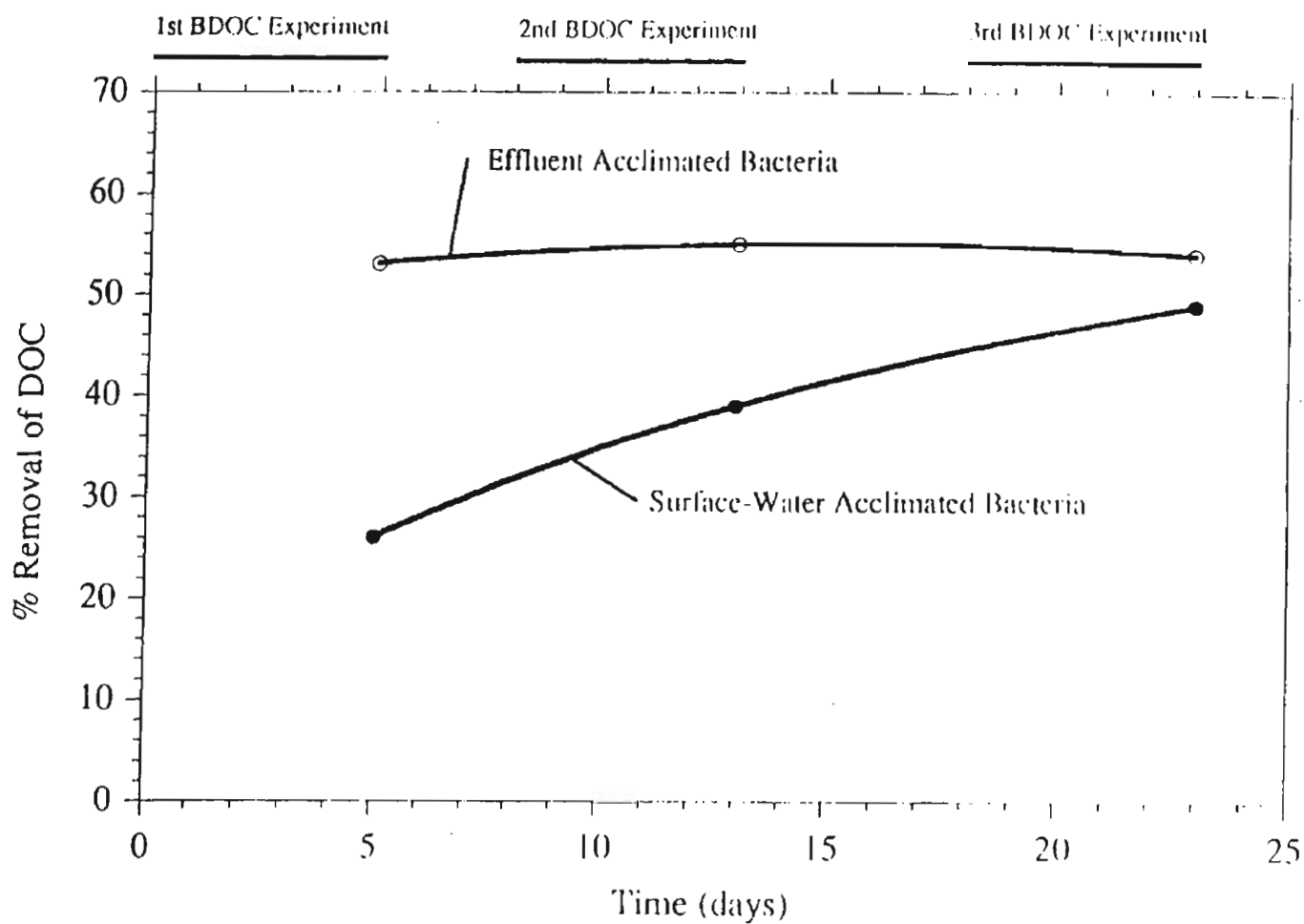


Figure 4.17 Effect of acclimation procedure (surface-water acclimation versus effluent acclimation) on the performance of “acclimated” bacteria during five-day BDOC tests. Data points on each line represent the results of successive tests.

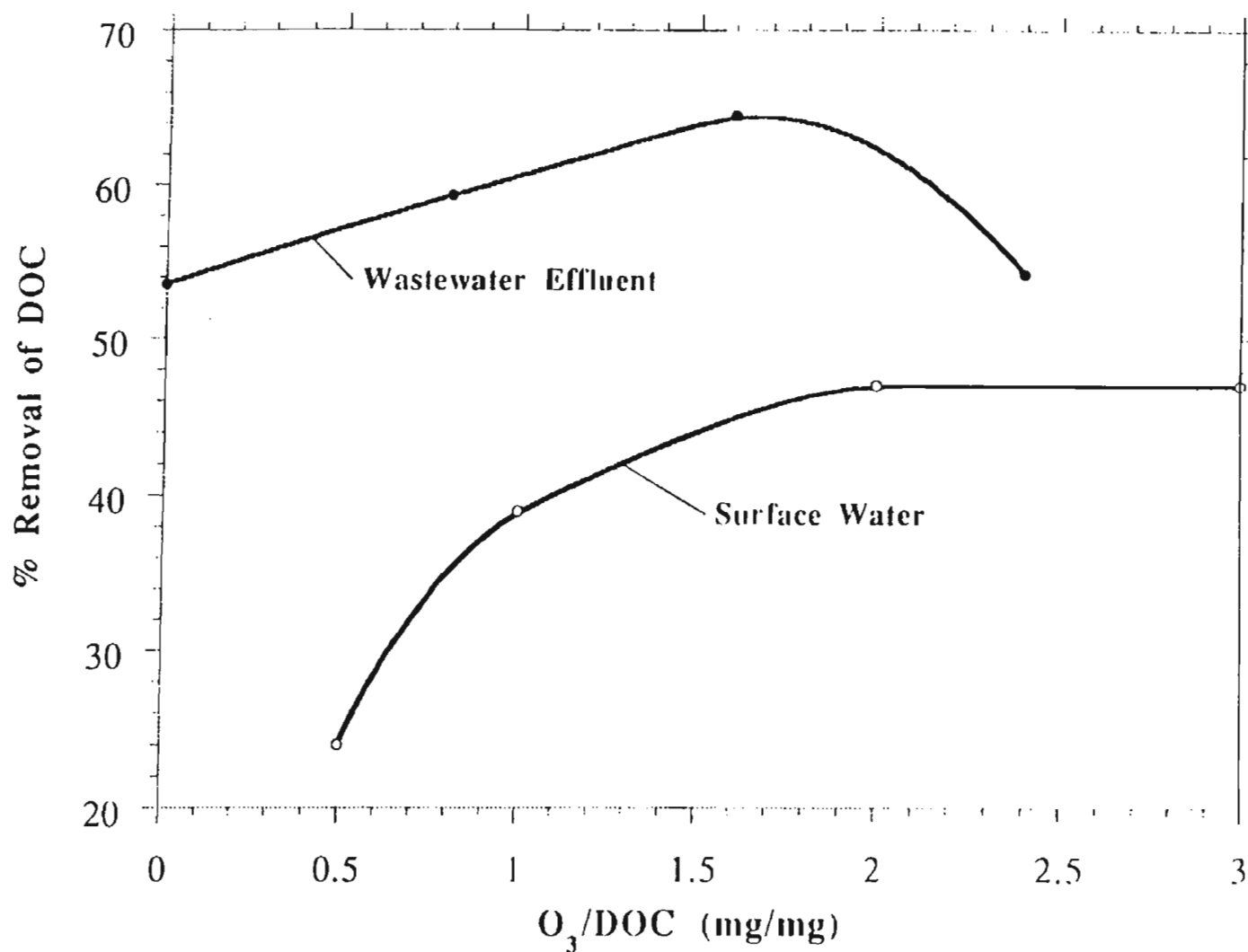


Figure 4.18 Effect of ozone dose in mg O₃ transferred per mg DOC on organics removal during the BDOC test procedure. The wastewater designation (T3) is explained in Table 4.10.

Figure 4.19 Effect of ozonation at 1 part O₃ transferred per part DOC on the biodegradability of dissolved organic residuals in treated wastewaters and a surface water source. Biodegradability was measured in a series of 5-day BDOC tests.

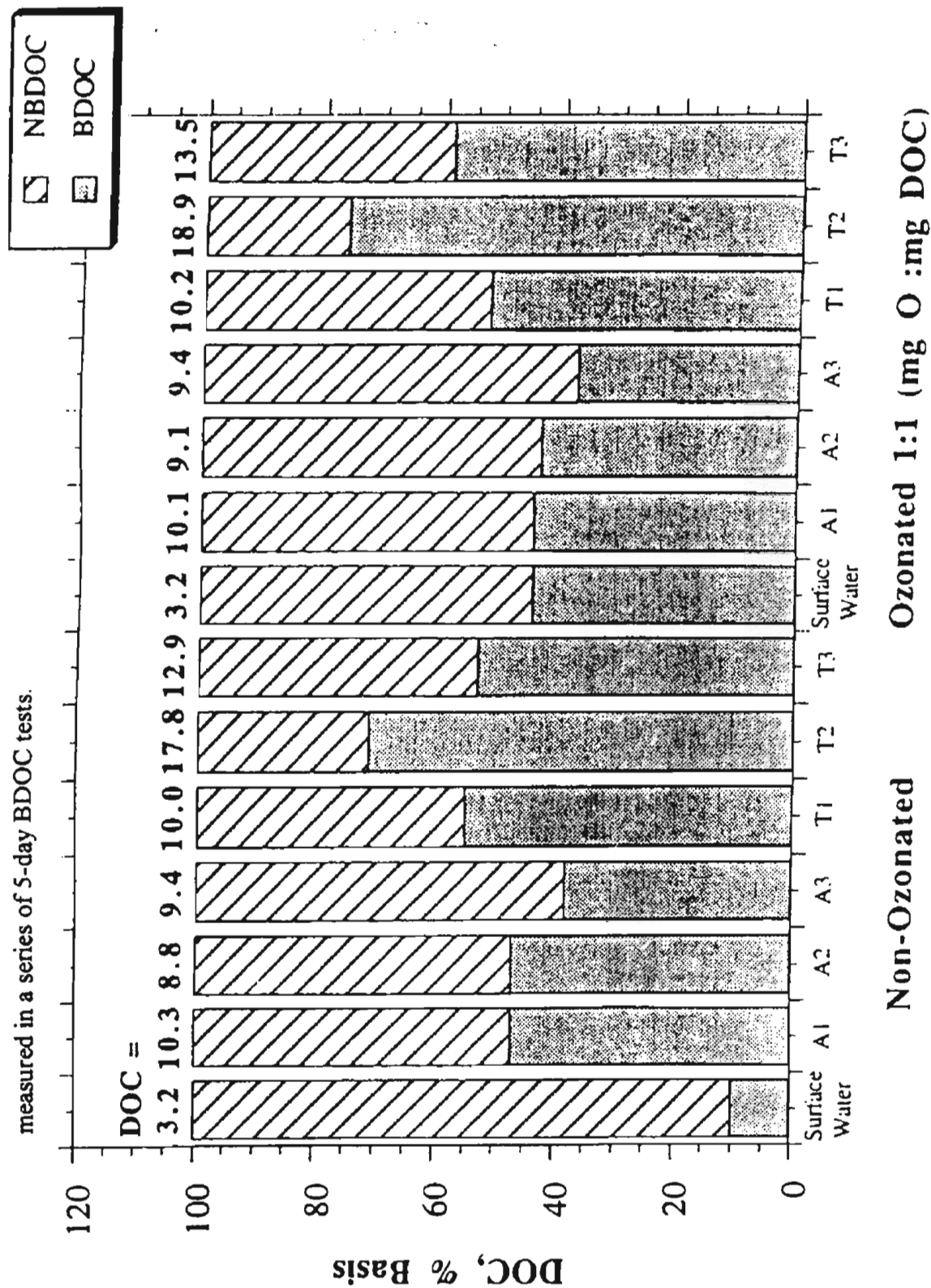


Table 4.10

Summary of water quality characteristics and source parameters in waters and wastewaters used for BDOC tests by the University of Colorado. Designations correspond to those used in Figures 4.18 and 4.19.

Parameters	Silver Lake Source Water	Effluent A1*	Effluent A3*	Effluent T1*	Effluent T3*
DOC (<0.45 μm)	3.2	10.3	9.4	10.0	12.9
UVA ₂₅₄ /DOC	0.052	0.013	0.015	0.028	0.014
BDOC	n/a	4.8	3.6	5.5	6.9
UVA ₂₅₄ /NBDOC	n/a	0.019	0.020	0.028	0.019
BDOC after O ₃ **	1.4	4.5	3.5	5.2	8
UV ₂₅₄ /NBDOC after O ₃	n/a	0.015	0.019	0.020	0.023
Biological Process	n/a	Activated Sludge	Activated Sludge	Trickling Filter	Trickling Filter

*. Effluents designated by state:

- 1- Colorado
- 2- California (BDOC analyses underway)
- 3- Arizona

and by Biological Process:

- A- Activated Sludge
- T- Trickling Filter

**-. Transferred ozone dose 1:1 (mg O₃: mg DOC) except for A3, 0.8:1 (mg O₃: mg DOC)

Wastewater	Column Height			
	18 cm		1 m (#5)	
	% DOC reduced	% UV254 reduced	% DOC reduced	% UV254 reduced
Secondary	23.2 ± 5.3	12.3 ± 6.4	49.1 ± 10.4	21.2 ± 5.7
Ozonated Secondary	22.1 ± 5.7	9.9 ± 4.1	n/a	n/a
Inhibited Control	6.4 ± 3.9	0.9 ± 2.8	9.8 ± 9.5	-4.7 ± 6.2

Table 4.11 Removal comparison of DOC and UV₂₅₄ for different column lengths containing Sweetwater sandy loam.

effluent organic qualities were indistinguishable despite the dissimilarities in column influent quality. See Chapter 2 for a complete description of differences in quality corresponding to secondary effluent and denitrified secondary effluent at the 91st Avenue Wastewater Treatment Plant in Phoenix. Findings reinforce the general idea that differences in influent quality or in the degree of above-ground treatment afforded wastewaters that are earmarked for SAT are of little relevance to post-SAT organic quality characteristics.

Depthwise measurements of organic parameters during SAT simulations

In order to establish the dependence of SAT performance on biologically active surface soils, we carried out depth-dependent measurements of DOC and UVA_{254} in one-meter columns fed secondary effluent from the Roger Road Wastewater Treatment Plant. In anticipation of these efforts, columns were constructed with sampling ports located in relative proximity in the upper portion of each column. The importance of the surface clogging layer, or *schmutzdecke*, to the hydraulic performance of the SAT columns has already been noted.

Depthwise measurements of DOC and UVA_{254} were carried out for one of the columns packed with Sweetwater sandy loam on each day of two consecutive week-long periods of wastewater applications (Figures 4.20 and 4.21). Results are inconclusive regarding the relative importance of the clogging layer in this context. A few, but by no means all, of the profiles shown indicate that organics are rapidly transformed in this layer. On the other hand, almost all the reliable profiles indicate that local DOC values are still declining at the bottom of the one-meter columns. Since no concentrations less than 6 mg/l DOC as C were measured, the biodegradable fraction of residual organics does not appear to be exhausted in these simulations, even at the conclusion of a week-long wet period (when average detention in the column is maximal). See also the results of BDOC measurements, which tend to show that nonbiodegradable levels of DOC in Roger Road effluents are considerably less than 6 mg/l as C.

Variation in depth-dependent DOC and UVA_{254} measurements arise in part from the difficulty that is inherent in such measurements in unsaturated soils. Tensiometer pore sizes were selected to facilitate withdrawal of water samples without exceeding the nominal air entry value for the material (ceramic or stainless steel). Nonetheless, maintenance of even pressure during sample withdrawal

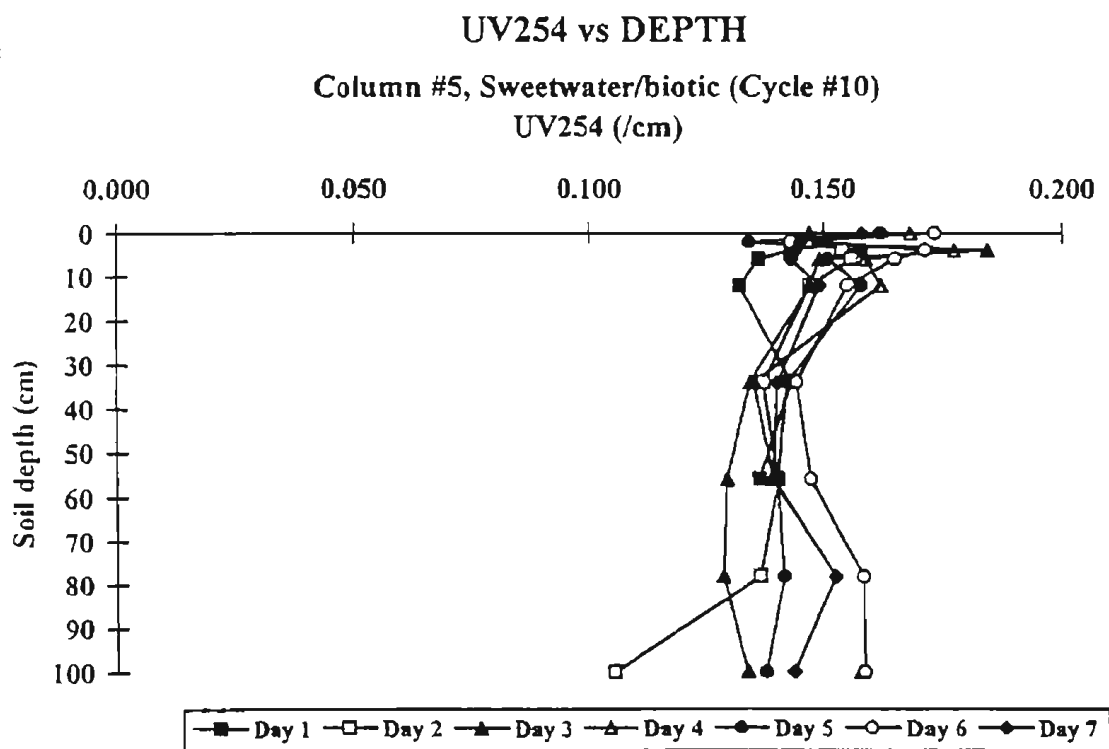
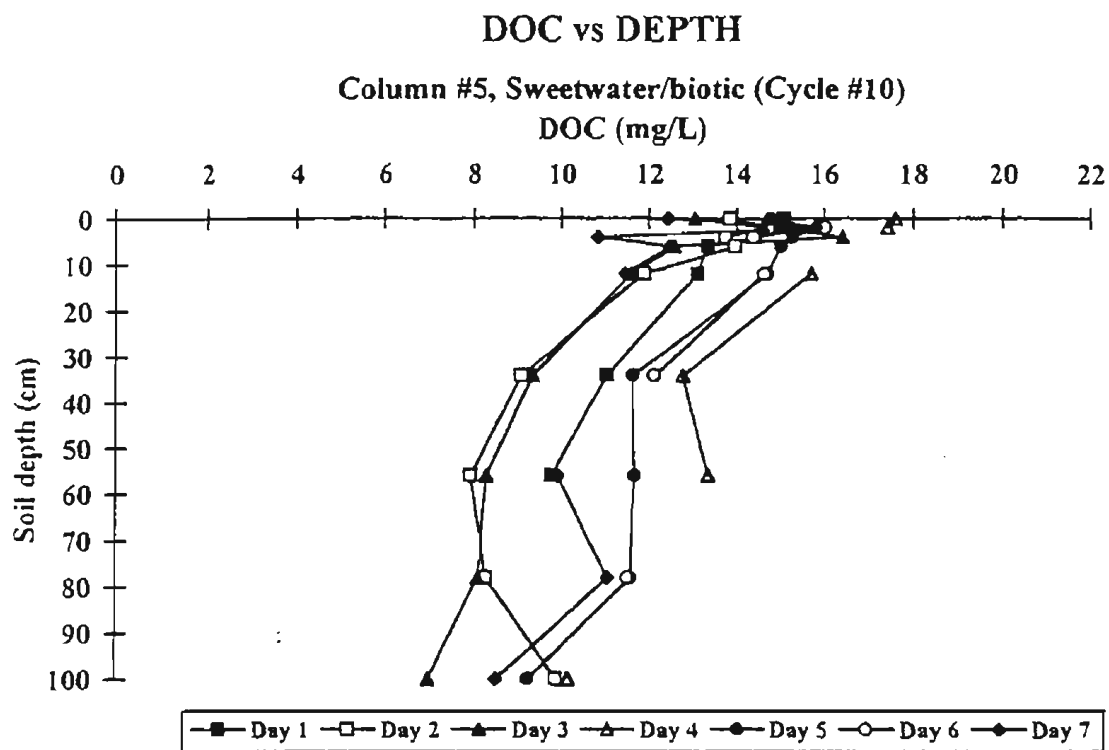


Figure 4.20 Depth-dependent profiles of DOC and UV₂₅₄ concentrations in a one-meter column (#5) packed with Sweetwater sandy loam. Profiles were measured daily during the week long wet period of cycle #10.

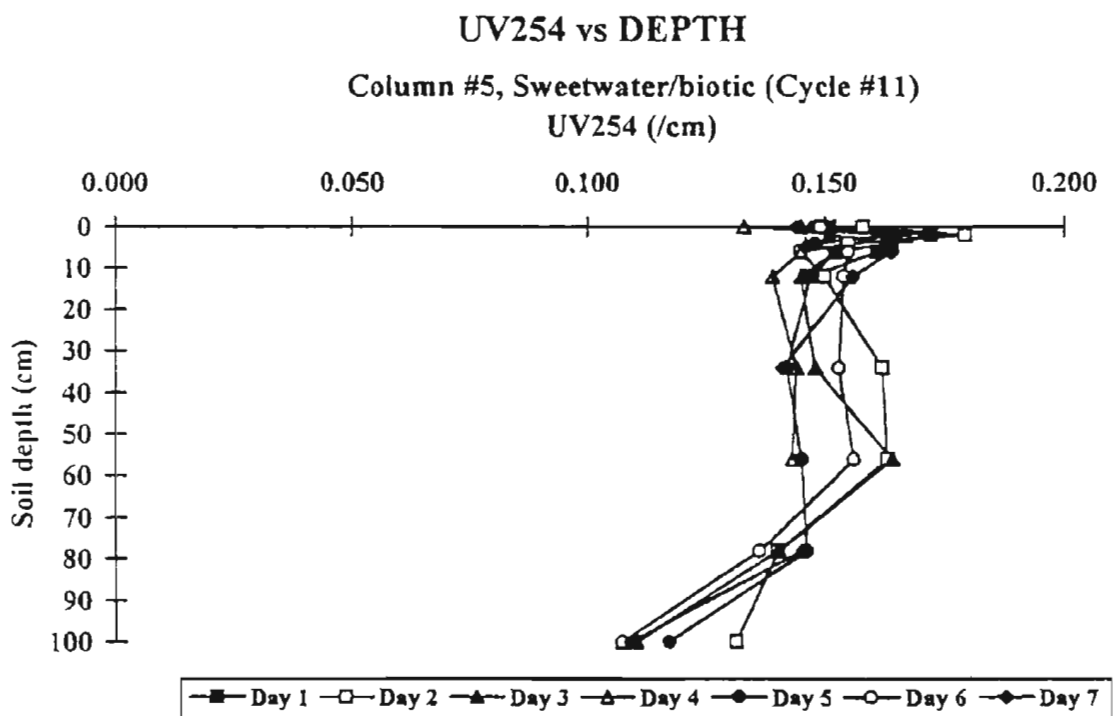
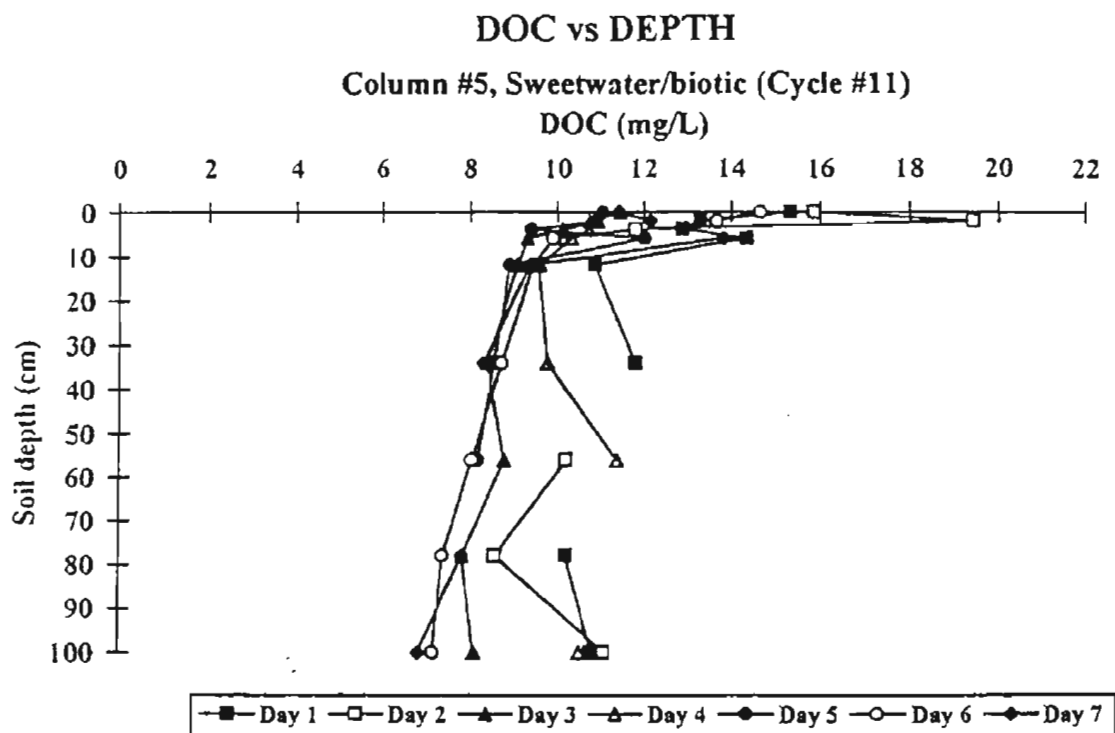


Figure 4.21 Depth-dependent concentrations of DOC and UV₂₅₄ in a one-meter column (#5) packed with Sweetwater sandy loam. Profiles were measured daily during the week long wet period of cycle #11.

and possible deterioration and/or biological growth on the tensiometer during the extensive overall period of column operation contributed to the already significant challenge of obtaining meaningful data in these experiments.

It may be more instructive to compare the through-column performances in similar columns of different lengths in order to develop insight into the role of the schmutzdecke in organics removals during SAT. To this end, it is possible to compare the performances of the 18-cm schmutzdecke columns with those of the one-meter and two-meter columns that were packed with the Sweetwater sandy loam. Representative data (Table 4.11) indicate that loss of DOC in the top 18-cm of the column is approximately what one would expect from the continuous log decay of any organic constituent during advective transport through the column. That is, if we hypothesize that, during transport through soils, organics are governed by a relationship of the form:

$$\ln [(C_0 - C_f)/(C_i - C_f)] = kt,$$

where t is time following the entry of a fluid element into the column reactor,

k is the specific rate constant for loss of organic material,

C is used to represent an organic parameter, e.g., DOC and UVA_{254} , and

C_f is the concentration of the refractory component of a specific organic measure,

then it is possible to estimate the specific rate constant based on depth-dependent values of DOC or UVA_{254} and predict the effluent concentration of that parameter at a distance of 18 cm into the column. When this exercise is carried out and results are compared to measurements obtained in the schmutzdecke columns, measured losses of DOC or UVA_{254} are comparable to computed values. The comparison suggests that organic removals are not in fact dominated by residence time in the schmutzdecke, but proceed in a more or less uniform, first-order manner throughout the entire column.

Comparison of intact and repacked soil column performances.

General

The objective of these experiments was to compare the performances of intact soil columns containing unsorted, nonhomogeneous soils and sediments with those of repacked SAT columns containing media originating from the same locations. A complete description of media preparation for the one- and two-meter repacked SAT reactors is provided in Chapter 3 to this report. The packing process resulted in the loss of large stones and a general homogenation of the soil sample. Columns were packed to achieve the same bulk density as the original sediment. Nevertheless, it may not be assumed that the repacked and intact sediments behave similarly in terms of hydraulic or other SAT performance characteristics due to elimination of natural heterogeneity, preferred infiltration pathways, etc.

The three soils obtained as intact sediment cores were all taken from the Phoenix area in the same locations as the original North Pond silt, Agua Fria sand and Agricultural Field clay. In each case, a stainless steel sleeve (prefitted with ports for the insertion of tensiometers or fittings to provide access for sampling) was driven into the ground and removed with an intact column of soil. The procedure had the advantage of preserving sediment stratification and heterogeneity.

SAT performance in the intact sediment cores

DOC and UVA_{254} removal efficiencies for the repacked columns (Figures 4.22--4.23) indicate that through-column removals of DOC in columns containing the Agua Fria sand and North Pond silt were equivalent to those in corresponding repacked columns. Column acclimation was apparent in the sand column over the first 8-12 cycles of operation, as evidenced by continuously declining effluent DOC concentrations. Although effluent DOC concentrations in the silt column were similar to the NBDOC levels measured at the conclusion of BDOC test procedures, effluent UVA_{254} was indistinguishable from influent levels, suggesting that organics that contribute to the absorbance of ultraviolet light were still being leached from the North Pond silt after five cycles of operation (2

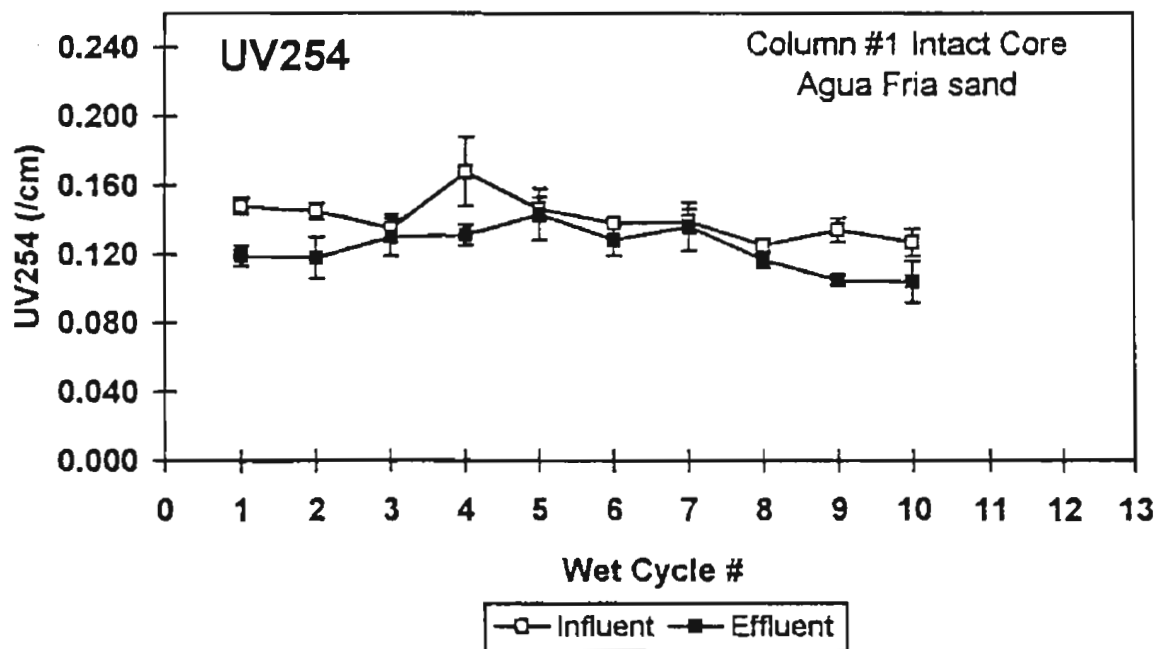
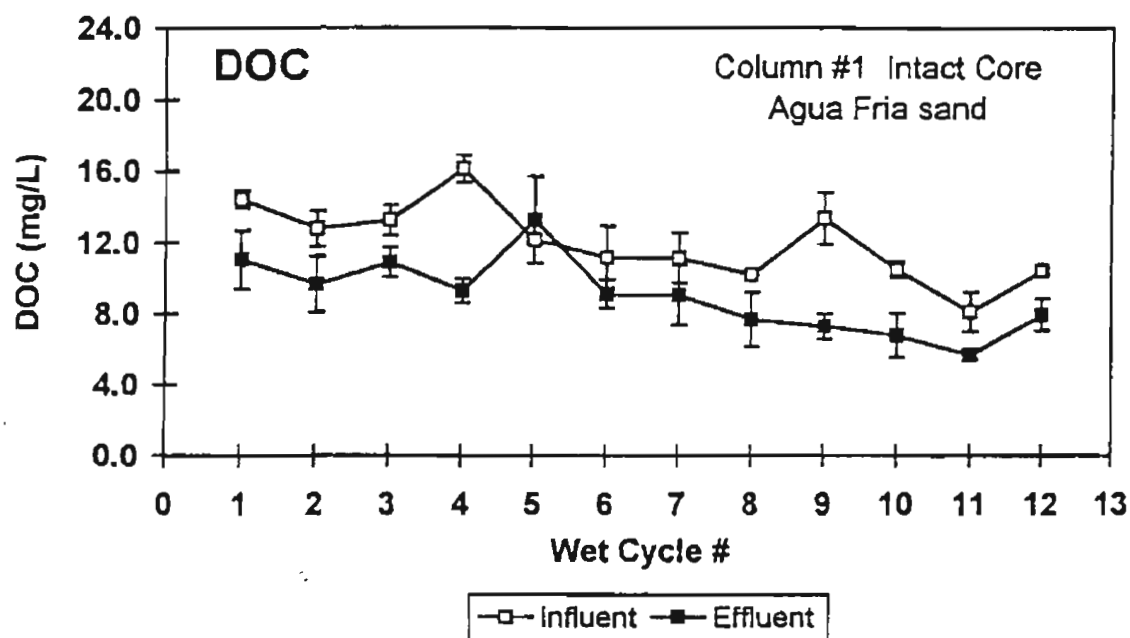


Figure 4.22 Influent and effluent concentrations of DOC and UVA₂₅₄ during simulated SAT in a one-meter columns containing on intact core Agua Fria sand. Column designations correspond to these in Table 4.2a.

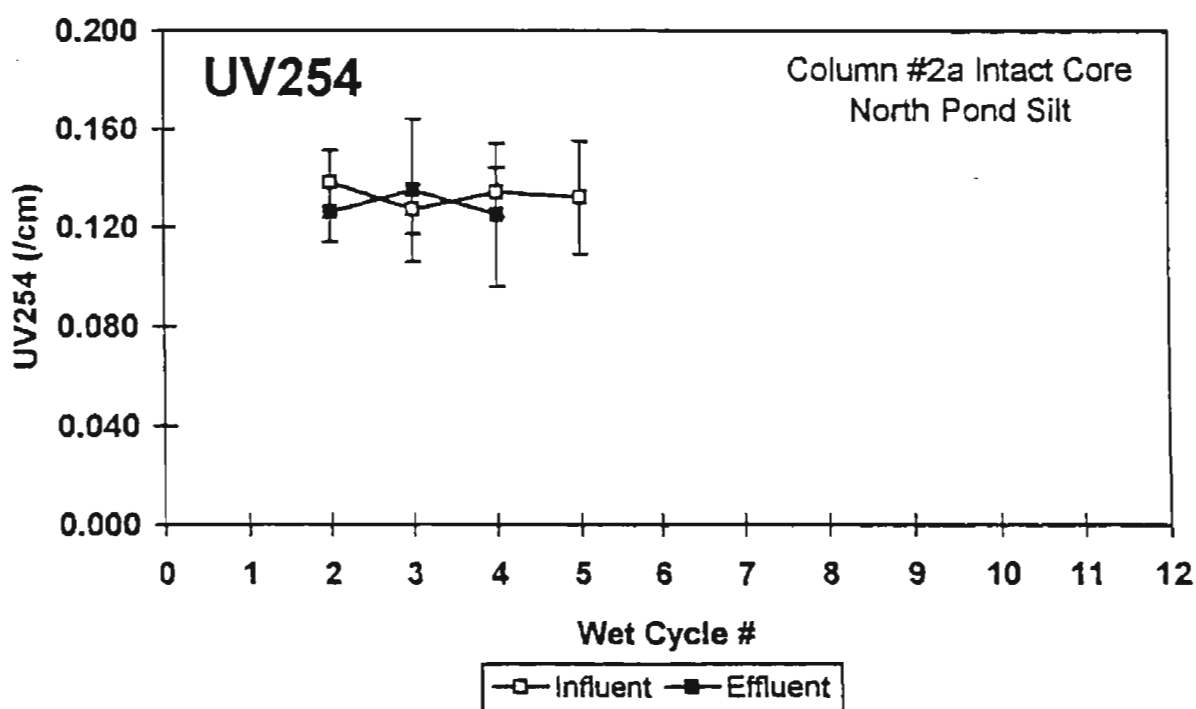
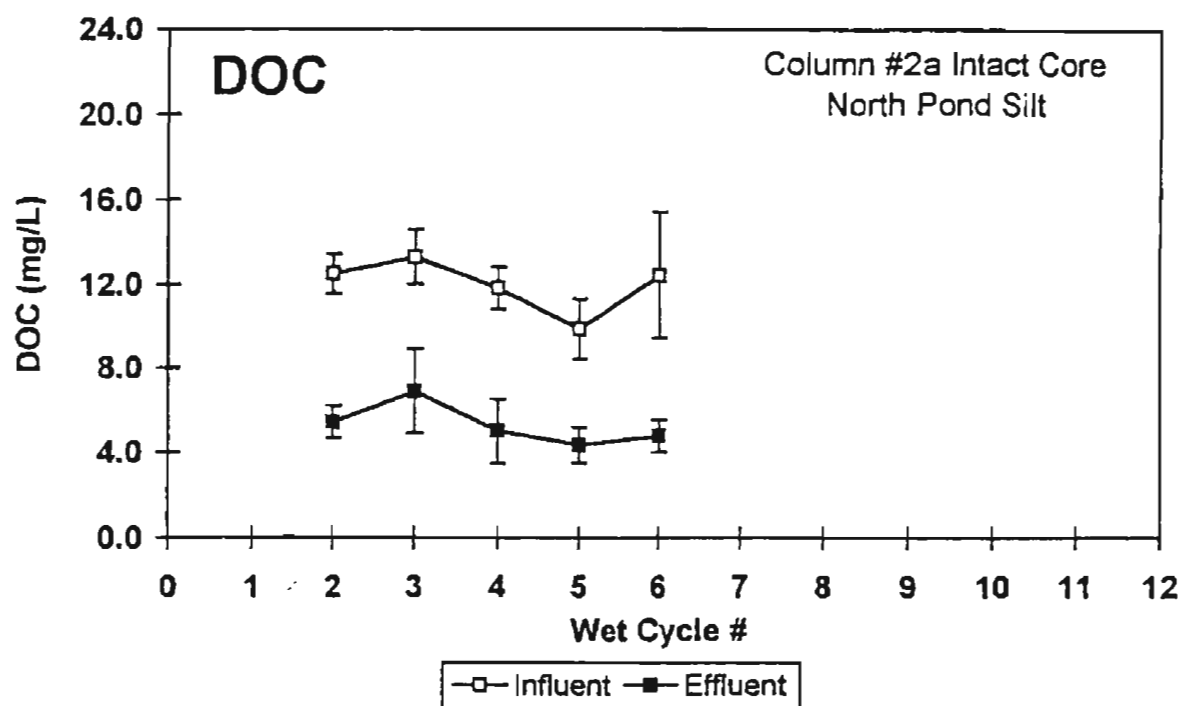


Figure 4.23 Influent and effluent concentrations of DOC and UVA₂₅₄ during simulated SAT in a one-meter column containing an intact core of North Pond silt. Column designations correspond to those in Table 4.2a.

months; Figure 4.23). In terms of organics removals, there is no basis for distinguishing between the performances of intact and repacked columns.

Infiltration rates through the intact clay column were too slow to permit collection of meaningful effluent samples. When clay is present among other soil types at candidate infiltration sites, low infiltration rates will not allow local zones with low permeability to contribute in a meaningful way to the overall quality of infiltrated waters.

Biochemical and abiotic contributions to overall SAT performance.

General

In order to place a lower limit on the importance of biochemical processes to observed improvements in organic parameters during simulated soil-aquifer treatment (and establish an upper limit for the role of abiotic processes) a number of columns were poisoned by continuous addition of 2.0 mM azide with the column feed throughout the wetting period. At that level, azide was able to completely inhibit aerobic respiration in acclimated sediment samples withdrawn from uninhibited columns (data not shown). It was possible or even likely, however, that fermentative activity persisted among the facultative anaerobes in the column. Consequently, residual activities in inhibited columns may be attributable to oxygen-independent biochemical transformations in addition to abiotic processes (primarily sorption).

In a practical sense, the distinction between biochemical and abiotic transformations of organics is extremely important. SAT-derived improvements in water quality that arise due to sorptive removal of organics will eventually exceed the removal capacity of the soil and sediment. Under those circumstances, contaminants will break through to the underlying aquifer and may eventually reach points of ground water withdrawal. On the other hand, biochemical transformations are renewable and essentially infinite in character. The design life of an infiltration basin that is used for SAT will, therefore, depend on the mechanism of organics removal from percolating wastewater effluents.

Azide inhibition in short (schmutzdecke) columns

Representative data are provided for the purposes of comparing organics removals (DOC and UVA_{254}) through the 18-cm schmutzdecke columns (Figures 4.24 and 4.25). Under azide-inhibited and uninhibited conditions. Both columns were packed with Sweetwater sandy loam. Through-column reductions in DOC averaged 25-30 percent over the 50-hour period of operation in the column fed secondary effluent from the Roger Road Wastewater Treatment Plant. Average removal of DOC in the column that received azide-amended secondary effluent was between 5 and 10 percent. The results of UV absorbance measurements over the same period showed about the same thing. That is, reduction of UVA_{254} across the uninhibited column (ignoring the first two readings, which suggested that organics were being leached from the dried soil at the start of the wet period) averaged between 15 and 20 percent. Essentially no UV-absorbing material was removed from the azide-inhibited column. Results suggest that the primary process for removing organics in the short, schmutzdecke columns during SAT simulations was aerobic microbial activity. For reasons explored earlier, it should not be assumed that residual losses of DOC -- those that were observed across the inhibited column -- were due entirely to sorption. However, it is apparent that sorptive losses amounted to no more than about 25 percent of the overall removal of DOC in the short columns.

It should be noted that these experiments offer no clue relative to the eventual fates of organics that are removed via sorptive processes during SAT simulations. That is, such organics could be totally refractory to biological processes, in which case eventual breakthrough and aquifer contamination might be expected. On the other hand, sorbed organics may be destroyed by biochemical or abiotic processes on a timescale that is much longer than the average liquid residence in the columns.

Inhibition experiments in one-meter columns

The role of aerobic respiration as a source of organics removal was also investigated by poisoning specific one-meter SAT columns with 2.0 mM azide. Through-column removals of DOC and UVA_{254} before and after azide addition with the column feed indicate that about 80 percent of the organic carbon and 40 percent of the UVA_{254} removal efficiency in 1-m are attributable to aerobic microbial activity (Figures 4.26-4.27). Residual changes in these parameters, observed in the presence of the inhibitor, may have been due to abiotic (primarily sorptive) or O_2 -independent

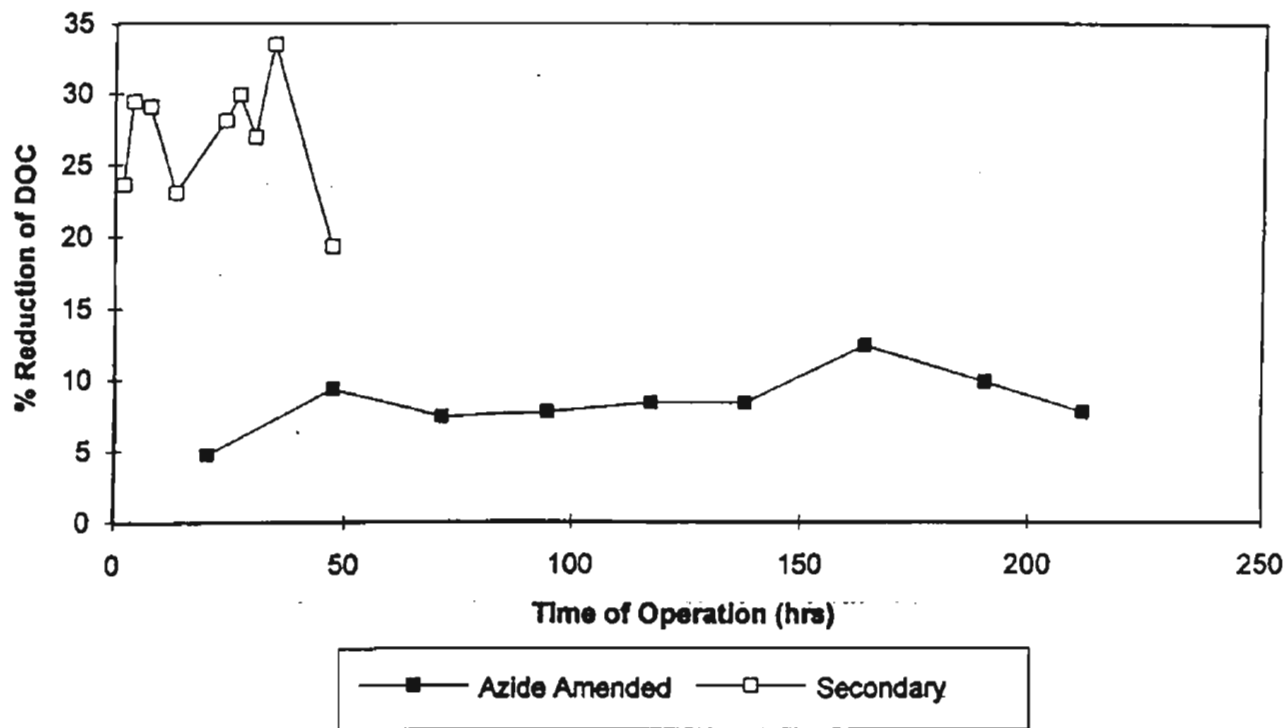


Figure 4.24 Percent Reduction of DOC for Azide-amended (Secondary Control) and Secondary Columns. Columns were the short, schmutzdecke reactors. Reductions were influent-to-effluent, over the 6-7 inch reactor depth.

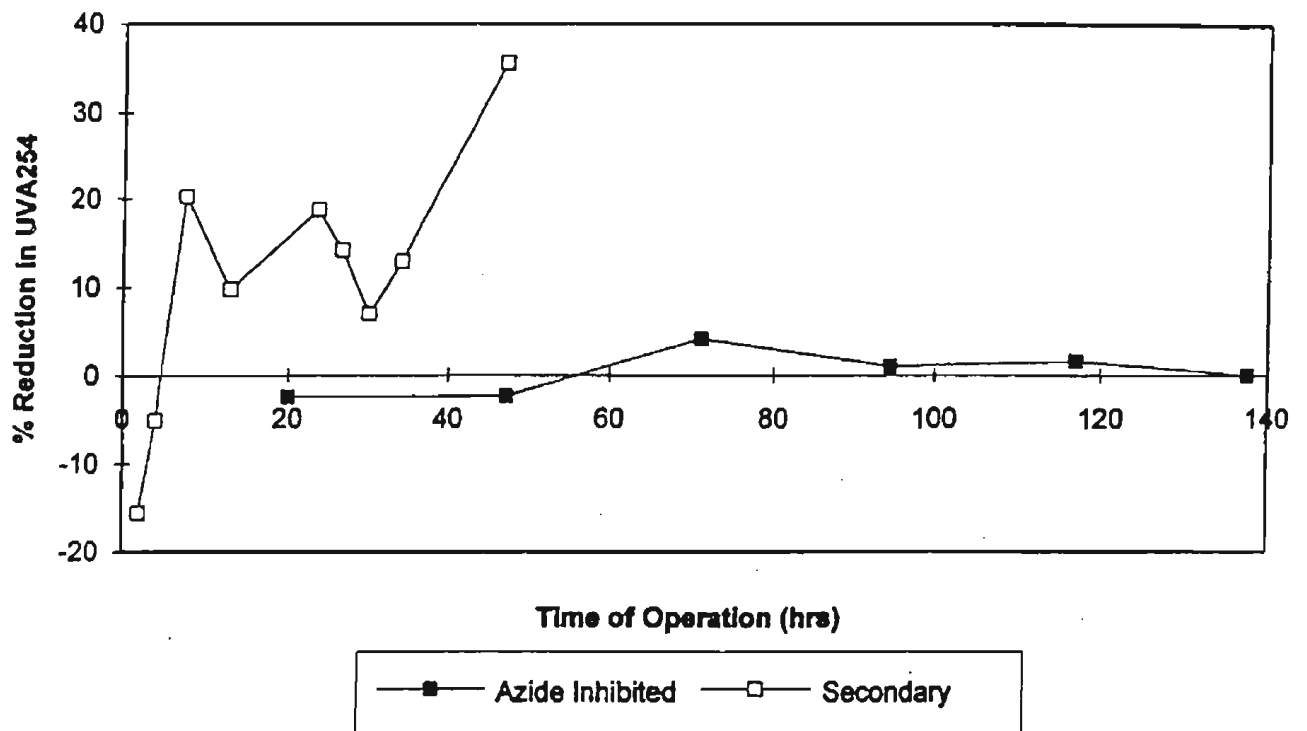


Figure 4.25 Percent reduction in UVA₂₅₄ for Azide-Amended (Secondary Control) and Secondary Columns. Columns were the short, schmutzdecke reactors. Reductions were influent-to-effluent, over the 6-7 inch reactor depth.

biochemical activities. Results suggest that a large percentage of the organic removal capacity of SAT sediments is biochemical in nature, and therefore sustainable. A higher percentage of those compounds that contribute to UVA_{254} is presumably removed via abiotic processes including sorption. Essentially nothing is known about the eventual fate of organics sorbed in this fashion. They may be degraded on a time scale much longer than that of fluid retention in our column reactors (hours) or even the BDOC reactors (days). The sorptive capacity of sediments for biorefractory compounds, however, is finite, and sorbed organics may eventually break through to local groundwaters and extraction wells. Additional study is warranted in this area.

Nature of organic compounds that survive SAT simulations

General

As indicated previously, ozonation at 1 part O_3 transferred per part DOC had little effect on the biodegradability of residual organics. This result was in stark contrast to previous observations in the water treatment industry, where ozonation of surface waters at much lower dosages generally increase the degradability of organic components. Differences may arise from the natures of the organics themselves or from differences in the inorganic compositions of the waters. Since very little is known about the nature of organics that survive secondary wastewater treatment, environmental researchers at Stanford University were asked to produce a detailed chemical representation of residual organic components in pre- and post-SAT waters.

The Stanford University Water Quality Research Laboratory has developed a suite of chemical analyses with which to identify residuals in reclaimed wastewater and groundwater recharged with water of wastewater origin (Fujita *et al.*, 1995). These methods were used to identify/measure specific compounds or classes of compounds in selected wastewaters effluents from processes designed to simulate SAT and groundwater samples from a recharge site. All the waters analyzed were derived within the overall SAT project, from the Phoenix and Tucson areas. Analytical procedures and parameters measured are summarized in Table 4.12.

The goals of this investigation were to (1) test the analytical approach, (2) obtain preliminary information on the composition of DOC in selected wastewater and groundwater samples, (3)

Table 4.12

Summary of analytes and analytical procedures

	Methods	Detection Limits
DOC	Combustion@680°C	0.1 mg/L
Anions NO ₃ ⁻ , NO ₂ ⁻ , SO ₄ ⁻² , Br ⁻	Ion Chromatography	0.4 mg/L 0.5 mg/L
Polyhydroxyaromatics (PHA) (Plus amino acids and peptides)	Modified Lowry Method/Colorimetric Standard: phenol	0.1 mg-C/L
Wastewater Indicators EDTA, NTA, APEC, NDC	Derivatization- GC/MS	0.1 µg/L
Biotransformation By-Products Polyfunctional carbonyls	Derivatization- GC/MS	0.1 µg/L

NTA: Nitrilotriacetic acid.

NDC: Naphthalene dicarboxylic acid.

APEC group: Alkylphenol polyethoxycarboxylates, metabolites of alkylphenol polyethoxylates.

measure changes in water quality during percolation through surface soils, and (4) compare the organic composition of Arizona wastewaters to those of another geographic area (Orange County, California). Due to financial constraints, the scope of the study was highly circumscribed and replication of analyses was not feasible.

Methods of sample collection and analytical procedures are described in depth in Appendix _____. Concentrations of specific organics were determined semi-quantitatively by comparison with machine (GC/MS) response to an internal standard. It was assumed that the response factors of the internal standard and the analyte were the same.

Results

Table 4.13 summarizes data derived from wastewaters provided by the University of Arizona. Since only one sample set was analyzed, only preliminary interpretation of the data is possible. Comparing the influent and effluent column data (one-meter columns) indicates that DOC and polyhydroxy aromatic material (PHA) are breaking through to a significant extent. Through-column attenuation was approximately 50 percent. Similarly, the trace organics used as wastewater indicators appear to pass through the columns with little attenuation. Compared to the column effluent, the concentrations in Well 199A, located immediately below the operational Sweetwater infiltration basin in Tucson, were much lower. It was previously supposed that this groundwater was dominated by wastewater effluent that was spread locally. The reasons for this apparent attenuation are not yet clear.

The group of APEC compounds (alkylphenol polyethoxycarboxylates and their metabolites) are ubiquitous in wastewaters and can sometimes be traced far away from the source. The APEC compounds are typically present as a complex mixture. Only total values are reported here. In the Tucson SAT columns, these compounds appear to break through with little apparent attenuation, a finding that merits further investigation. Recent research at Stanford (Fujita and Reinhard, unpublished) has shown that APEC compounds can be transformed under groundwater conditions.

Short-chain polyfunctional carbonyls and acids, classified as biotransformation by-products, were present in the influent and effluents with few exceptions. The fate and significance of these compounds is not yet understood.

Table 4.13

Concentrations of DOC, PHA, anions and specific organics in column influent, effluents and groundwater from Tucson

SAT column sampling date: 5/3/95, Field sampling date: 7/26/95

	Influent (dechlorinated)	Effluent- Agua Fria Sand (Column#3)	Effluent- Sweetwater Sandy loam (Column#5)	Field Sample Well#199A
DOC (mg-C/L)	13.8	6.8	5.9	0.9
PHA (mg-C/L)	8	5.6	3.1	0.1
Nitrate (mg/L)	16	3.6	2.3	28
Nitrite (mg/L)	n.d.	n.d.	n.d.	n.d.
Sulfate (mg/L)	110	120	110	100
Bromide (mg/L)	n.d.	n.d.	n.d.	n.d.
<u>Wastewater Indicator</u>				
($\mu\text{g/L}$)				
EDTA	63	51	42	2.1
NTA	0.1	0.4	1.8	n.d.
NDC	2.7	3.2	5.4	0.4
APEC group	35	43	22	0.1
<u>Biotransformation By-</u>				
<u>Products ($\mu\text{g/L}$)</u>				
Methyl glyoxal	0.2	n.d.	17	n.d.
Glyoxylic acid	6.5	7.6	22	3.1
Glyoxal	1.3	1.7	3.8	n.d.
Other carbonyls	4.6	5.4	32	3.8
Unknown amino acid	0.2	n.d.	250	28

PHA: Polyhydroxy aromatic material

NTA: Nitrilotriacetic acid

NDC: Naphthalene dicarboxylic acid

APEC group: Alkylphenol polyethoxycarboxylates, metabolites of alkylphenol polyethoxylates.

An unidentified amino acid was detected. The concentration of this unknown acid was especially high in the effluent of the Sweetwater sandy loam column. This compound was also found in river water and groundwater of wastewater origin in Orange County, as indicated in Table ^{4.14}~~4.13~~. Its origin and significance remain to be investigated.

EDTA is generally difficult to degrade and thought to be mobile in groundwater. Therefore, it has been proposed to serve as a wastewater indicator in artificially recharged aquifers. It was found in distant wells in aquifers recharged with water of wastewater origin (Ding *et al.*, 1995 and Fujita *et al.*, 1995).

X Table ^{4.15}~~4.14~~ summarizes the Phoenix data (two-meter columns operated by Arizona State University). As in the Tucson case, only one sample set was analyzed, and only preliminary interpretation of the data is possible. The contaminant concentrations and removals are similar to those observed in Tucson. The DOC and PHA appear to break through the two-meter columns with perhaps 50% attenuation. The wastewater indicator compounds show little apparent attenuation during column percolation with the possible exception of NTA. The short-chain polyfunctional carbonyls and acids were present in column influent and effluent with few exceptions.

In Table ^{4.14}~~4.13~~, the occurrence and concentrations of specific organics in different waters are compared. The data clearly indicate that, with respect to the wastewater indicator and biotransformation by-products patterns, the organic compositions of the three effluents are similar. This finding is significant. It means that knowledge and treatment technologies developed at one site will be applicable in other geographical areas.

Summary

The following statements are supported by data obtained in this study and comparison to results obtained previously:

1. DOC and wastewater indicators break through the experimental SAT columns. More data are needed to quantify the degree of attenuation.
2. Polyfunctional carbonyls believed to be biotransformation by-products were found in all the samples analyzed. The significance of these contaminants is unknown.

Table 4.14

Comparison of specific organics in reclaimed wastewater from three locations

	Phoenix WTP- Effluent (7/6/95)	Tucson WTP- Effluent (5/3/95)	Tucson Groundwater Well#199A	OCWD WTP- Effluent (8/15/95)	SAR@ River Rd (8/15/95)	OCWD Groundwater (8/15/95)
EDTA	+++	++++	++	++++	+++	+
NTA	+	+	-	++	-	-
NDC	++	++	+	+++	++	-
APEC groups (total)	+++	+++	+	++++	++	-
Methyl glyoxal	+	+	-	-	++	-
Glyoxylic acid	+++	++	++	+++	+++	++
Glyoxal	++	++	-	++	++	-
Other carbonyls	+++	++	-	+++	+++	++
Unknown amino acid	+	+	+++	++	++++	+++

SAR@River Rd.: The Santa Ana River water sampled at River Rd. sampling site.

++++: greater than 50 µg/L,

+++ : 10 - 50 µg/L,

++ : 1-10 µg/L,

+ : smaller than 1 µg/L,

- : not detected.

Table 4.15

Concentrations of DOC, PHA, and specific organics in column influent and effluent from Phoenix

SAT column sampling date: 7/6/95

	Influent (dechlori/denitrified)	Effluent- (Column2SA)
DOC (mg-C/L)	7.0	4.8
PHA (mg-C/L)	3.9	2.2
<u>Wastewater Indicator</u> ($\mu\text{g/L}$)		
EDTA	37	53
NTA	0.4	n.d.
NDC	4.4	7.9
APEC group	34	12
<u>Biotransformation By-Products</u> ($\mu\text{g/L}$)		
Methyl glyoxal	0.6	n.d.
Glyoxylic acid	14	9.1
Glyoxal	1.9	1.0
Other carbonyls	14	9.2
Unknown amino acid	0.5	5.1

PHA: Polyhydroxy aromatic material

NTA: Nitrilotriacetic acid

NDC: Naphthalene dicarboxylic acid

APEC group: Alkylphenol polyethoxycarboxylates, metabolites of alkylphenol polyethoxylates.

3. Small concentrations of EDTA ($2.1 \mu\text{L}$) and APECs ($0.1 \mu\text{L}$) were detected in a groundwater sample taken from monitoring well WR-199A. The extent of dilution with clean groundwater during travel from the infiltration point to the observation well must be known to interpret this finding.
4. The analysis of wastewater characteristics in reclaimed wastewater from three different geographical areas, Phoenix, Tucson and Orange County, indicated a similar DOC composition. This suggests that research results obtained in one area should be applicable to recharge operations in other geographical areas.

DISCUSSION

Despite the inclusion of interpretive information at various points within the results section, a few additional points require discussion. Referring to the original experimental objectives as set forth in Section 4.2.2:

i. Length of acclimation period required to establish steady column performance

Statistical analysis of the experimental record (DOC and UV absorbance) in the one-meter columns operated at the University of Arizona indicated that six or seven wet/dry cycles were necessary to establish steady operating conditions. In this context, steady performance was defined by the onset of similar through-column removal efficiencies in successive wet/dry cycles of operation. Beyond the sixth or seventh cycle of operation, there was no discernible time-dependent change in the efficiency of one-meter SAT column operations. Throughout the overall period of operation, there was essentially no relationship between column flow rate (or reactor detention time) and through-column organic removal efficiency. The constant-head mode of operation resulted in approach velocities on the order of 10 ft/d at the start of a wet period, and flow rates generally decreased by an order of magnitude or more during the week-long wet period. Nonetheless, through-column removals of DOC and UVA_{254} were remarkably stable and permitted us to lump data from each wet period for statistical analyses.

Acclimation of the two-meter columns operated by Arizona State University followed a different course. In the case of the sand columns, ponding of effluent on the soil surface was never

possible, even when influent was applied at a constant rate of $>10\text{ft/d}$. Consequently, it is probable that steady conditions representing field operations were not achieved during the period of experimentation. Our inability to maintain standing water on the soil surface may have been related to the very low levels of organics and ammonia nitrogen in the 91st Avenue Wastewater Treatment Plant effluent. Steady operation was apparent in the columns packed with North Pond silt although not until fifteen cycles of operation had been concluded. The primary barrier to steady operation, however, seems not to have been column acclimation but the necessity to leach organics from the soil. By the thirtieth cycle of column operation, effluent organic levels exceeded those in the influent, presumably due to contribution of algal decomposition and, again, the very low levels of influent organics.

Based on these observations, we speculate that there will be a relatively long period at the onset of infiltration basin operations--six months to a year--during which SAT efficiency through the top few meters of soil and sediment will improve from initially low values. It is less certain that the contribution of algal organics to post-SAT effluent quality will be of practical importance. For one thing, it is not clear that algae had a significant effect on effluent organic levels in the one-meter columns. When algal organics are apparent in effluent from the two-meter columns, the eventual fate of those organics during SAT is not known. That is, mineralization of organic material of algal origin might be expected during percolation through a longer sediment column and extended aquifer storage pending withdrawal for use.

ii. Through-column removals of DOC and UVA_{254} . In combination, the results of the one-meter column studies and BDOC measurements conducted at the University of Arizona indicate that most of the non-refractory organic material (BDOC) present in the Roger Road Wastewater Treatment Plant effluent is removed in the top meter of soil or sediment during SAT. Of the 7-8 mg/l DOC that remained in the post-SAT effluent, perhaps another 2-3 mg/l is biodegradable or otherwise removed during the extended aeration period that comprises the BDOC test. It is probable that under field conditions post-SAT organic water quality parameters will be essentially independent of the level of above-ground treatment provided. The observation is based on the results of laboratory SAT simulations using wastewaters differing substantially in organic character--from primary to filtered secondary effluent--and on the results of BDOC tests involving the same influent waters. Soil-aquifer

treatment offers a viable mechanism with which to assure the production of a high quality, low organic carbon water prior to withdrawal for potable or non-potable uses.

It is probable that 4-5 mg/l DOC is not amenable to biological treatment on the time scale required for percolation of wastewater effluent through the vadose zone (hours to days). There are indications from past field studies in local (Tucson) infiltration basins that such residuals are further attenuated during field SAT operations. Levels of organics in aquifers that underlie the infiltration basins consistently reached 1 mg/l, even at the end of the infiltration season, when local waters should have been dominated by wastewater effluent. The mechanism by which residual organics were removed is not completely known, but probably involved an initial sorption step.

UV₂₅₄ was not removed to the same extent as DOC in the one-meter column studies at the University of Arizona. Results suggest that UV-absorbing organics, which have frequently been equated with aromatic or humic substances, are on average more difficult to remove than other components of DOC. The statement applies to effluent from the Roger Road Wastewater Treatment Plant and may not be true in effluents with a lower DOC, such as that from the 91st Avenue Wastewater Treatment Plant (source water for the Arizona State 2-meter columns).

On the basis of comparative removal efficiencies in columns packed with Agua Fria sand and North Pond silt, it seems probable that in this range of sediment classes, sediment structure is not a strong determinant of organic removal efficiencies during soil-aquifer treatment. The post acclimation performances of both the sand and silt suggested that most biodegradable organics are removed within a few meters in either material. Hydraulic considerations should be afforded preference in designing infiltration basins that will serve large metropolitan needs.

iii. **Role of the schmutzdecke in overall SAT performance.** Comparison of organic (DOC and UV₂₅₄) removals in short (7-in.) and meter-length columns at the University of Arizona indicates that, although the schmutzdecke is biochemically very active, the removal of biodegradable organics from wastewater is spread over the top several meters of sediment. Data are reasonably well represented by a continuous log-decay model in which a single decay coefficient can be used to represent the disappearance of BDOC in that region. Depthwise measurements of DOC and UVA₂₅₄ in the 1-meter columns are consistent with such a picture, as are time-dependent DOC measurements within a single wetting period. The latter show that the development of the schmutzdecke, as indicated by loss of hydraulic conductivity and an increase in head loss in the top few centimeters of

the column, does not noticeably improve the overall column performance in terms of organics removal efficiency.

iv. Contribution of biochemical processes to overall organics removal efficiencies.

Comparison of DOC and UVA₂₅₄ measurements in effluents from azide-inhibited and uninhibited columns indicate that most organics removals are biochemical in origin during SAT. Such activity should be considered renewable and thus completely sustainable. The mechanism of DOC loss from azide-inhibited columns is less certain. The azide-inhibited columns remained biologically active, as indicated by direct cell counts (data not shown) although it is probable that azide completely inhibited biochemical O₂ utilization. Nonetheless, non-oxygen-dependent biological processes may have contributed to column performance. These would include, for example, fermentative activity and oxidations linked to anaerobic respirations. It has been shown that O₂-independent respiration can occur in the presence of a suitable inhibitor of aerobic electron transport. It is probable that a substantial portion of the DOC removed in azide-inhibited columns is also biochemical in nature and therefore completely sustainable.

Removal of UV-absorbing material was completely eliminated by azide addition. It is possible that oxygenases, which are frequently credited with initiating the breakdown of aromatic organics, are efficiently inhibited by azide.

v. Comparison of soil SAT efficiencies in repacked and intact columns. In terms of organics removal efficiency, there is no clear basis for distinguishing between the performances of intact and repacked columns containing Agua Fria sand and North Pond silt. The DOC removal efficiencies of the intact columns were at least equivalent to those of corresponding repacked reactors. It remains possible, however, that preferred flow pathways that are available to channel flow under field conditions cannot be reproduced in an intact vertical soil core.

vi. Levels of refractory organics in post-SAT effluents. A number of virtually independent lines of inquiry (column reactors, BDOC studies and ozonation studies involving a variety of secondary effluents) indicated that a significant fraction of residual organics in secondary effluent resist further biochemical transformation during SAT simulations. That fraction consistently contributes 4-5 mg/l (as C) to the overall DOC. The stability of those organics is emphasized by their resistance to biochemical oxidations even after treatment with O₃ at 1 part ozone transferred per part

DOC. Since ozone has been used successfully to increase the biodegradability of low levels of organics in surface water supplies, its lack of effect on wastewater residuals is surprising.

It remains possible, however, that organic residuals sorb to soil or sediment particles during SAT, thereby permitting their eventual biodegradation at locally enhanced concentrations in biofilms. This remains an entirely speculative explanation for field observations of DOC levels, however, pending additional study.

The reactivity of these seemingly refractory organics with free chlorine is a source of additional concern. Results of THMFP measurements indicate that care must be taken to minimize DOC levels at points of chlorine addition if post-chlorination levels of THMs are to reliably satisfy federal drinking water standards. Our THMFP measurements are significantly higher than THM levels that would be expected at chlorination points in the field. Mitigation should arise from (i) the very conservative nature of the THMFP procedure, (ii) transport, storage or dilution-related reductions in DOC residuals ahead of withdrawal points, and (iii) transformation of ammonia nitrogen via nitrification reactions prior to chlorination. Ammonia losses will facilitate addition of breakpoint levels of chlorine for achievement of free chlorine targets at much lower overall chlorine dosages. Presumably concentrations of THMs formed in the process will also be lower. This is, however, another area in which additional study is warranted.